DEVELOPMENT IN THE FEMALE FLOWERS/FRUIT OF THE DWARF MISTLETOE *ARCEUTHOBIUM AMERICANUM* (VISCACEAE): REPRODUCTIVE DEVELOPMENT, VISCIN TISSUE DEVELOPMENT, AND CYTOGENETIC ANALYSIS OF TISSUE REGIONS WITHIN THE FRUIT.

by:

Cynthia Marie Ross

A thesis
submitted in partial fulfillment
of the requirements for the degree of
Doctor of Philosophy
in the ***Department of Botany***
The University of Manitoba
August 26, 2002

THE UNIVERSITY OF MANITOBA

FACULTY OF GRADUATE STUDIES

*****

COPYRIGHT PERMISSION PAGE

DEVELOPMENT IN THE FEMALE FLOWERS/FRUIT OF THE DWARF MISTLETOE *ARCEUTHOBIUM AMERICANUM* (VISCACEAE): REPRODUCTIVE DEVELOPMENT, VISCIN TISSUE DEVELOPMENT, AND CYTOGENETIC ANALYSIS OF TISSUE REGIONS WITHIN THE FRUIT

BY

CYNTHIA MARIE ROSS

A Thesis/Practicum submitted to the Faculty of Graduate Studies of The University

of Manitoba in partial fulfillment of the requirements of the degree

of

Doctor of Philosophy

Development in the Female Flowers/Fruit of the Dwarf Mistletoe *Arceuthobium americanum* (Viscaceae): Reproductive Development, Viscin Tissue Development, and Cytogenetic Analysis of Tissue Regions within the Fruit.

By: Cynthia Marie Ross

Arceuthobium americanum (dwarf mistletoe) is a parasitic angiosperm that attacks *Pinus banksiana* (jack pine) in Manitoba. Reproductive development in the female flowers/fruit was documented from anthesis in April to explosive pseudoseed discharge in August of the second summer (seventeen months after anthesis). Two megasporocytes developed in the reduced, ategmic ovular structure (the placental-nucellar complex or PNC). Megasporogenesis was bisporic; only one functional megaspore completed megagametogenesis. The egg apparatus arose at the lower pole of the embryo sac. Following double fertilization, cell wall material was deposited at the interfaces among all embryo sac cells. A caecum (outgrowth) emanated from the lower side of the fertilized central cell, which permitted endosperm to develop below the zygote. Endosperm development was cellular. Embryogenesis followed the Asterad-type, *Penaea* variation. Fruit differentiation occurred over the second summer, during which the endocarp and lower mesocarp became tannin-filled to form the pseudoseed coat. The upper three-quarters of the mesocarp developed into viscin tissue, which was comprised of an inner uniseriate layer of elongated, mucilaginous viscin cells and an outer region containing three to four layers of vesicular cells. Cytochemical staining and lectin probing indicated that the viscin cell mucilage resulted from organellar secretion and was comprised of carbohydrates, proteins, and some lipid, although the proportions of these components changed throughout development. Biochemical assays for carbohydrates and proteins showed that the mucilage in the nearly mature fruit was composed of approximately 62% neutral carbohydrates, 37% uronic acids, and 12% proteins (dry weight/dry weight mucilage). By the examination of fine-scale ovular features, it was determined that *Arceuthobium* likely share a common ancestry with the Santalaceae. Cytogenetic techniques coupled with a novel application of image analysis were used to determine ploidy levels of the different tissue regions within the fruit. The endosperm was verified to be triploid with 3n=42 chromosomes. The viscin cells were confirmed to be diploid with 2n=28 chromosomes. The cap (a tissue situated above the embryonic radicular apex) was determined to be triploid with 3n=42 chromosomes; the triploid status of the cap supported anatomical observations that had indicated an endosperm origin for the cap.

TABLE OF CONTENTS

LIST OF ABBREVIATIONS

A	= antipodal (cell)
ABB	= aniline blue black stain
ai	= aborted individual (either an unfertilized flower or aborted fruit)
am	= amyloplast membranes
apm	= antipodal plasma membrane
ATPase	= adenosine triphosphate phosphohydrolase
br	= bract
C	= Celsius
c	= caecum (pouch); can also refer to the first endosperm cell of the caecum resulting from division of the primary endosperm nucleus and cytokinesis
cap	= cap of endosperm cells (resides above the embryo)
cap_l	= in the case of twin embryos and endosperms, refers to a cap lagging in development
cap_t	= in the case of twin embryos and endosperms, refers to a cap at a typical stage of development for the time of year
cep	= crushed epidermal cells of the placental-nucellar complex
cct	= counterclockwise tier of primarily anticlinally-dividing endosperm cells
ch	= chromosomal material
C.I.	= colour index (for a stain)
cl	= chloroplast
cp	= cell plate
cs	= chromosome (seen during mitosis)
ct	= cotyledon (rudimentary)
CV	= crystal violet stain
cve	= cis Golgi vesicle
cw	= cell wall
cw_1	= a transverse cell wall arising from zygotic division; the cell wall separating the two cells of the two-celled embryo
cw_2	= each longitudinal cell wall arising from division of each cell in the two-celled embryo; found in the four-celled embryo
cwt	= clockwise tier of primarily anticlinally-dividing endosperm cells
des	= degenerating embryo sac
DNA	= deoxyribonucleic acid
dn_c	= primary endosperm daughter nucleus in the caecum
dn_z	= primary endosperm daughter nucleus in the vicinity of the zygote
dp	= digitate protuberance
DS	= degenerating synergid (cell)
dscm	= degenerating synergid cytoplasmic margin

$\underline{E}$	= east
E	= egg cell
ec	= caecum endosperm cell(s)
ed	= endocarp or cells of the endocarp
ed+me	= region where the endocarp has become confluent with the mesocarp
en	= endosperm cell(s) of undetermined origin or simply the endosperm
en_l	= in the case of twin embryos and endosperms, refers to an endosperm lagging in development
en_t	= in the case of twin embryos and endosperms, refers to an endosperm at a typical stage of development for the time of year
ep	= epidermis
epm	= egg cell plasma membrane
eq	= equator of a dividing cell
er	= endoplasmic reticulum
esw	= embryo sac wall
ew	= viscin cell end (cell) wall
exi	= inner region of the exocarp or cells of the inner exocarp
exo	= outer region of the exocarp or cells of the outer exocarp
ey	= embryonic cell(s) or simply the embryo
ey_l	= in the case of twin embryos and endosperms, refers to an embryo lagging in development
ey_t	= in the case of twin embryos and endosperms, refers to an embryo at a typical stage of development for the time of year
ez	= endosperm cell(s) in the vicinity of the zygote or those endosperm cells derived from endosperm cells initially in the vicinity of the zygote
f	= funiculus
fa	= filiform apparatus
fb	= fibrillar material
FCC	= fertilized central cell
fccpm	= fertilized central cell plasma membrane
fm	= functional megaspore
foml	= first outer mesocarp layer (undifferentiated)
fr	= mature, ripe fruit in the second summer of development
gb	= Golgi body
gm	= ground meristem
h	= helical secondary cell wall material; refers to the secondary cell wall
hr(s).	= hour(s) material in a xylem vessel element
HS	= Hoechst stain (DNA-specific)
i	= inner or single integument
iml	= (undifferentiated) inner mesocarp layer
l	= lower pole of a megasporocyte, megaspore, or embryo sac

lat	= lateral flower
ld	= lower dyad
ls	= lower side of a megasporocyte, megaspore, or embryo sac
m	= megasporocyte
me	= mesocarp or cells of the mesocarp
min.	= minute(s)
ml	= middle lamella
mp	= micropyle
MPV	= mean pixel value
ms	= megaspore (whether the megaspore is functional has not been determined)
mt	= mitochondrion
mu	= (viscin cell) mucilage
N	= north
n	= nucleus
nc	= nucellus/nucellar tissue
ne	= nuclear envelope
nfd	= nonfunctional dyad
NIH	= National Institute of Health
nl	= nucleolus
ob	= osmiophilic body
oi	= outer integument
oml	= (undifferentiated) outer mesocarp layer(s); may or may not include the first outer mesocarp layer
ov	= ovarian tissues
ow	= ovary wall (pericarp)
p	= pedicel
pa	= plasmodesma
paf	= pre-anthesis flower; refers to incipient, pre-meiotic flowers in the summer prior to the first spring of development
PAS	= Periodic Acid - Schiff's (PAS) treatment/stain
PATCH	= Periodic Acid - Thiocarbohydrazide - Silver Proteinate treatment/stain
pc	= procambium
pd	= protoderm
pg	= (chloroplast) plastoglobuli
pl	= pole of a dividing cell
plc	= placenta (ovarian)
pm	= plasma membrane
pmu	= periplasmic (viscin cell) mucilage
PNC	= placental-nucellar complex
PNA	= peanut agglutinin (lectin)

PS	= persistent synergid (cell)
psc	= pseudoseed coat or cells of the pseudoseed coat
pspm	= persistent synergid plasma membrane
pt	= pollen tubes
ra	= radicular apex
rbcL	= chloroplast ribulose-1,5-bisphosphate carboxylase large chain; used in reference to DNA sequence
RF	= relative frequency (histogram)
RNA	= ribonucleic acid
RPM	= revolutions per minute
S	= south
s	= stigma
SBB	= Sudan Black B stain
Sctn.	= section in a township
sec.	= second(s)
sg	= starch grain
sh	= shoot (pedicel) tissue or cell
sp	= space (separating the middle lamellar mucilage of two adjacent viscin cells)
SSU rDNA	= small subunit ribosomal DNA sequence
st	= style/stylar canal
sw	= viscin cell side (cell) wall
SYa, SYb	= synergid (cells); cannot differentiate between persistent and degenerating synergids, but can distinguish the presence of two synergids
SY	= synergid material (an amalgamation of two crushed synergids)
t	= tannin-like material
te	= tepal
ter	= terminal flower
th	= threadlike materials
TB	= Toluidine blue O stain
tp_1	= Type 1 endosperm cells (large and vacuolate)
tp_2	= Type 2 endosperm cells (small and cytoplasmic)
TPV	= total pixel value
tn	= (vacuolar) tonoplast
TTC	= 2, 3, 5-triphenyl tetrazolium chloride (viability stain)
tve	= trans Golgi vesicle
ty	= (chloroplast) thylakoid membrane
u	= upper pole of a megasporocyte, megaspore, or embryo sac
UA/LC	= uranyl acetate/lead citrate stain
UCC	= unfertilized central cell

uccpm = unfertilized central cell plasma membrane
ud = upper dyad
us = upper side of a megasporocyte, megaspore, or embryo sac
v = vacuole
vc = vesicular cell(s) of the viscin tissue
ve = vesicle
VFA = *Vicia faba* agglutinin (lectin)
vg = vacuolar ghost
vi = viscin cell(s) of the viscin tissue
vs = vegetative shoot
v/v = volume/volume
W = west
w/v = weight/volume
x = xylem tissue
xve = xylem vessel element
yfr = young, immature fruit from the first summer of development
Z = zygote
zw = original bounding cell wall of the zygote; also forms the boundary of the embryo after zygotic division
zpm = zygote plasma membrane

* = electron opaque deposit
! = cell wall material

LIST OF FIGURES

If a figure represents a micrograph, the micrograph depicts a longitudinal section unless stated otherwise. If a figure represents a light micrograph, the stain is CV unless stated otherwise. Similarly, if a figure represents an electron micrograph, the stain is UA/LC unless stated otherwise.

Page

Chapter Three Figures

Chapter Four Figures

Chapter Five Figures

Chapter Six Figures

All figures represent images of or data from nearly mature fruit sampled from early August of the second summer of development.

ACKNOWLEDGEMENTS

I wish to gratefully acknowledge the guidance provided to me by my advisor, Dr. Michael J. Sumner. It was a pleasure working with Dr. Sumner, who was always available to help me with both the researching and the writing process, and who was always very supportive of my work. I am also very grateful for the financial assistance Dr. Sumner contributed to the project. I would also like to thank the other members of my advisory committee: Dr. G. Murray Ballance, Dr. Jeannie Gilbert, and Dr. David Punter. My committee was comprised of extremely talented scientists, and their ideas and suggestions were always useful. I also graciously thank Dr. Clyde Calvin from the Department of Biology at Portland State University for agreeing to serve as my external examiner. I also thank Dr. Carol A. Wilson from the Department of Biology at Portland State University for her helpful comments. I thank all members of my committee for the time they spent reading my thesis; apparently, a picture (micrograph) really is worth a thousand words.

Special thanks to the three (!) electron microscope technicians I worked with over the (long!) course of my Ph.D.: Mr. Garry Burgess, Mrs. Lynn Burton, and Ms. Karen Sereda. I learned a lot from each technician. In addition, I would like to gratefully acknowledge the assistance and lab space I acquired from the Ballance Lab in the Department of Plant Sciences at the University of Manitoba in order to perform general biochemical analyses of viscin cell mucilage. Particularly, I would like to recognize the guidance I received from Dr. G. Murray Ballance, Mr. Ralph Kowatsch, and Ms. Pat Kenyon in the Department of Plant Sciences during the general biochemical analyses. I also wish to graciously thank Dr. Dan Nickrent from the Department of Plant Biology and Center for Systematic Biology, Southern Illinois University (Carbondale) and Dr. Valéry Malécot from the Laboratoire de Paléobotanique, Paris, France for permission to use their phylogeny of Santalales found in Figure 4.79 of this thesis.

The Department of Botany at the University of Manitoba is an excellent department, both academically and collegially, and I wish to thank fellow students, instructors, professors, and technicians in the department for their support over the years. Thank you to Department Head Dr. David Punter for providing me with the opportunity to be a graduate student in Botany (and for providing the beautiful macro lens

photographs seen in Figures 4.1, 4.54, and 4.70). A special thank you to Dr. Tom Booth for the help and encouragement he provided. I also thank Dr. Larry Van Caeseele for graciously sharing his knowledge with me. Special thanks to current and former Botany Department members Dr. Sam Badour, Dr. Olaf Bakke, Ms. Alex Bourne, Mr. André Dufrense, Ms. Melissa Day, Ms. Kerry Dust, Ms. Barb Dyck, Mr. Mark Elliot, Dr. Bruce Ford, Ms. Carol Graham, Dr. Ed Groot, Dr. Georg Hausner, Dr. Leonard Hutchison, Ms. Sharon Inch, Dr. Cheryl Jerome, Mr. Narindar Kalkat, Dr. Norm Kenkel, Ms. April Kiers North, Ms. Jen Line, Mr. Richard Martin, Ms. Lisa Matthias, Dr. Rhonda McDougal, Dr. D.A. Ross McQueen, Dr. James Reid, Dr. Sylvie Renault, Dr. Darren Robinson, Ms. Karen Sereda, Ms. Jen Mustard, Mrs. Margaret Smith, Mr. Keith Travis, Dr. Dave Walker, Dr. Isobel Waters, and Ms. Vera Williams.

I also wish to acknowledge the support and encouragement I received from the Department of Biology at the University of Manitoba, and for the teaching experience I obtained through that department. Special thanks to current and former Biology Department members Ms. Pat Gutoski, Mrs. Deanne Jabs, Ms. Maria Kuraszko, Mr. Michael Shaw, Dr. Michael Sumner, and Mr. Rick Yunyk. In addition, I would like to thank Ms. Marilyn Fabris for her encouragement. She is missed.

I also thank my sister Kelly Anne for her friendship and support throughout my life. I must thank her profusely for the help she provided me with tissue preparation over one summer (sorry about that allergy to Propylene Oxide...). I also thank Brian Swail for his love, patience, and understanding. In addition, I am extremely grateful to my parents, Paul and Rose Anne, and to my Grandma, for their support. Thanks to the whole Swail family for their encouragement toward my endeavors. I also thank my friends not previously mentioned, Ms. Brenna Beaulieu, Dr. Lorraine Hamiwka, and Ms. Gayle Stilkowski, for their support over the years. I should also acknowledge the comforting presence of my cat, Bonnie, who sat beside me during the majority of the writing process.

Finally, I thank the Natural Sciences and Engineering Research Council of Canada for providing me with two post-graduate student scholarships. I also thank the Alumni Association, the Faculty of Graduate Studies, the Faculty of Science, and the Graduate Students Association at the University of Manitoba for travel funding I received throughout this study.

ABSTRACT

Arceuthobium americanum (dwarf mistletoe) is a dioecious flowering plant that is parasitic on *Pinus banksiana* (jack pine) in Manitoba. The purpose of this thesis was to elucidate reproductive developmental processes occurring in the female flowers and fruit of *A. americanum* in Manitoba using techniques of microscopy and image analysis. Reproductive development in the female flowers/fruit was documented from anthesis in early April to explosive discharge of the dispersal unit (ategmic seed or pseudoseed) at the end of August, seventeen months after anthesis. At anthesis, the ategmic reduced ovular structure, which was defined as a placental-nucellar complex (PNC), was fully developed, and two obliquely oriented hypodermal megasporocytes were evident in the tenuinucellate PNC. Multiple pollen tubes were already present in the style and around the base of each megasporocyte, and so synergids were not needed for pollen tube attraction in *A. americanum.* Both megasporocytes were capable of completing megasporogenesis. Megasporogenesis was bisporic, and the upper dyad from each megasporocyte (the dyad distal to the base of the PNC) became a functional megaspore. Only one functional megaspore was capable of completing megagametogenesis to form an unfertilized mature seven-celled embryo sac; the other functional megaspore degenerated.

The unfertilized mature seven-celled embryo sac possessed an egg apparatus (two synergids and an egg cell) at the lower pole of the embryo sac, three antipodals at the upper pole, and a central cell that occupied the remainder of the embryo sac. The two polar nuclei in the central cell fused shortly after their formation. One of the two synergids began to degenerate almost immediately after it was formed. Cell wall material was lacking at the interface between the unfertilized central cell and unfertilized egg apparatus. The unfertilized egg cell was attached to the upper side of the embryo sac, above and to the side of the two synergids. Only one pollen tube penetrated the mature embryo sac, entering via the degenerating synergid. Following double fertilization, cell wall material was deposited at the interfaces among all cells of the embryo sac. The egg cell and central cell become more metabolically active following fertilization, as evidenced by a loss of vacuolation and increase in organellar content. Instead of

immediately degenerating, the antipodals and persistent synergid also became more metabolically active following fertilization.

A few days after fertilization, a caecum (pouch-like outgrowth) began to develop from the lower side of the central cell; this was aided by vacuole formation. Division of the primary endosperm nucleus then occurred, preceding division of the zygote. Following division of the primary endosperm nucleus, one endosperm daughter nucleus migrated into the caecum and the other remained near the zygote. A cell wall formed at the mouth of the caecum, separating the two nuclei; endosperm development was *ab initio* cellular. Caecum formation, initial net downward displacement of endosperm cells, and the fact that the egg cell was originally attached to the upper side of the embryo sac permitted endosperm to develop below the zygote, even though the unfertilized central cell was initially morphologically higher than the unfertilized egg cell.

Although endosperm development had a net downward displacement, two upwardly-developing tiers of endosperm cells achieved encirclement of the zygote, which had earlier initiated dislodgment from the embryo sac wall. The endosperm cells that developed above the zygote were called cap cells. At the end of the first summer, the endosperm had undergone only limited development. During late endosperm development in the second summer, cells at the base of the endosperm and in the cap became highly vacuolate, endowing the endosperm with a vase-shaped appearance. Starch grains, protein bodies, and lipids were common storage forms within the endosperm, although the peripheral endosperm cells and cells adjacent to the embryo retained starch-free transfer zones throughout most later phases of development. Chlorophyll was found in the endosperm; the discharged pseudoseed was albuminous.

Embryogenesis followed the Asterad-type, *Penaea* variation. The embryo was only a small, undifferentiated globe of cells by the end of the first summer. The majority of embryo development took place over the second spring and summer. The protoderm was the first embryonic tissue to differentiate, followed by the radicular apex at the upper pole of the embryo, the procambium, the rudimentary shoot apex (with two rudimentary cotyledons) at the lower pole of the embryo, and the ground meristem. Prior to explosive discharge, the radicle of the embryo elongated, compressing the cells of the cap. The embryo possessed the same storage forms as the endosperm, and similarly possessed

chlorophyll. The presence of large and varied nutrient stores within the embryo and endosperm as well as the presence of chlorophyll in these two tissues suggested that the process of germination requires a high input of energy.

At the end of the first summer, the three fruit zones (the endocarp, mesocarp, and exocarp) were evident but unspecialized. Fruit differentiation occurred over the second spring and summer. During fruit differentiation, the endocarp and lower mesocarp became crushed and tannin-filled, forming the pseudoseed coat. The upper three-quarters of the mesocarp (above the radicular pole of the embryo) developed into viscin tissue, which was comprised of an inner uniseriate layer of elongated, mucilaginous viscin cells and an outer region containing three to four layers of vesicular cells. The mature exocarp was comprised of two layers: an inner and an outer exocarp. Two vascular traces were found within the inner exocarp, and the vascular traces appeared to be comprised solely of xylem tissue. All vessel elements in the xylem tissue of the fruit had helical secondary thickenings, but a few vessel elements possessed cytoplasm at maturity. The cytoplasmic vessel elements possibly represented flange-type parenchyma cells.

The discharged pseudoseed was comprised of the embryo, endosperm, remnants of the PNC, pseudoseed coat, and viscin cells. Viability of the dispersed pseudoseed persisted in the field. Moreover, it was concluded that the scoring of pseudoseed viability should encompass not only the viability of the embryo, but also the viability of other pseudoseed components, particularly the endosperm tissue in the vicinity of the embryo.

By compiling fine-scale, pre-fertilization ovular characteristics of *Arceuthobium* that were elucidated in this thesis and those of other Santalalean families that have been described in the literature, major phylogenetic trends in the order were exposed. One major phylogenetic trend supported the idea that *Arceuthobium* likely share a relatively recent common ancestry with the tribe Santaleae of the family Santalaceae.

The viscin tissue (mucilaginous viscin cells and vesicular cells) of *Arceuthobium americanum*, a tissue that plays a role in explosive discharge (both cell types) and adhesion of the pseudoseed to its host (viscin cells), was examined in detail. During development, the viscin cells had elongated uniformly, not via tip growth. Not all viscin cells within a young fruit were at the same relative stage of development; only in the nearly mature fruit did the viscin cells reach the same relative stage of development.

Both plastids and chlorophyll were found in the viscin cells prior to explosive discharge; this suggested that light was able to penetrate the fruit exocarp and that the viscin cells could have possibly photosynthesized even while inside the fruit exocarp. Evidence from cytochemical and general biochemical analyses suggested that the viscin cell mucilage was composed of a large proportion of neutral and acidic carbohydrates, some glycoproteins, and a small proportion of lipids throughout most stages of development; non-glycosylated proteins were rare. Cytochemistry supplemented with fluorescence microscopy, enzymatic digests, and lectin probing suggested that the neutral soluble carbohydrate component of the mucilage was primarily represented by Calcofluor-positive hemicelluloses (some of which were apparently somewhat fibrillar), Calcofluor-negative hemicelluloses, and carbohydrate moieties of glycoproteins. The uronic acid component of the mucilage was primarily represented by granular pectic acids.

Organelles including endoplasmic reticulum, Golgi bodies, and plastids were required for the assembly and secretion of viscin cell mucilage components. Rough endoplasmic reticulum likely assembled the protein moieties of the mucilage. The Golgi bodies were responsible for granulocrine secretion of assembled glycoproteins and pure carbohydrate mucilage components into the periplasmic space, whereas plastids likely secreted the small amount of lipids present in the mucilage in an ecrine fashion. Throughout intense periods of mucilage secretion, mucilage accumulated in the periplasmic space, although most mucilage materials ultimately passed through the viscin cell wall to reach the middle lamella or became incorporated into the non-cellulosic viscin cell wall matrix. Amorphous materials crossed the viscin cell wall as clusters, whereas the fibrillar components crossed the cell wall as more dispersed fibrils.

Notable compositional changes occurred in the viscin cell mucilage throughout development. Firstly, there was a breakdown of the Calcofluor-positive hemicellulose(s) just prior to explosive discharge, which likely triggered explosive discharge. Secondly, there was solubilization and loss of most remaining pure carbohydrate material as well as a large proportion of glycoproteins from the mucilage following explosive discharge. Consequently, after explosive discharge, only some insoluble glycoproteins and lipids remained in the mucilage, and so the post-dispersal mucilage had a proportionately large proteinaceous component.

Cytochemical analysis and polarizing microscopy showed that the viscin cell wall was largely cellulosic. The viscin cell wall underwent two thickening events. As the thickening events primarily occurred via the elongation of helically-arranged cellulose fibrils, the viscin cell wall remained a primary cell wall. Many of the mucilage materials remained associated with the viscin cell wall as non-cellulosic matrix materials, even after compositional changes had taken place in the mucilage, as the cellulose acted as a strong polar attractant for matrix materials. Therefore, matrix materials were likely retained in the viscin cell wall even following explosive discharge.

Prior to explosive discharge, tannins accumulated in the viscin cell cytoplasm, pseudoseed coat, and inner exocarp cells. The presence of hydrophobic tannins in these regions likely ensured that the bulk of water was directed toward the viscin cell mucilage. Only the viscin cell nuclei and potentially the plastids remained active in the viscin cell cytoplasm after explosive discharge. The lipid-filled, thin-walled vesicular cells were not explosively-discharged with the viscin cells, but likely aided in the retention of water within the viscin cell mucilage prior to explosive discharge. Thin-walled vesicular cells also represented a weak point that permitted abscission and explosive discharge.

The ploidy levels of certain tissues within the *Arceuthobium americanum* fruit were determined with classical cytogenetic techniques coupled with image analysis involving the DNA-specific Hoechst dye. A novel method was developed so that dividing and non-dividing tissue regions could be compared. Using these techniques, the endosperm of *A. americanum* was verified to be triploid with $3n = 42$ chromosomes, substantiating that fertilization of the central cell had occurred, and strongly indicating that a second fertilization had also led to the creation of the diploid zygote and embryo. The viscin cells were confirmed to be diploid with $2n = 28$ chromosomes. This finding supported the anatomical observations, which indicated that the viscin cells were derived from maternal diploid ovarian tissues (mesocarp). The cap was determined to be triploid with $3n = 42$ chromosomes. This finding strongly supported the anatomical observations, which indicated that the cap was derived from the triploid endosperm.

CHAPTER ONE - THESIS INTRODUCTION

I. GENERAL INTRODUCTION

1. The Study Organism, *Arceuthobium americanum*, and the Genus *Arceuthobium*

The study organism for this Ph.D. thesis was *Arceuthobium americanum* Nuttall *ex* Engelmann. The genus *Arceuthobium* (formerly the genus *Razoumofskya*) belongs to the dicotyledonous family Viscaceae and includes approximately forty species (Hawksworth and Wiens, 1996). *Arceuthobium* species are perhaps better known as the dwarf mistletoes, which are small (generally less than twenty centimetres tall) flowering plants. As dwarf mistletoes, *Arceuthobium* species belong to the larger assemblage of flowering plants called mistletoes.

Mistletoes belong to the families Viscaceae, Eremolepidaceae, Misodendraceae (Myzodendraceae), and Loranthaceae of the primarily parasitic order Santalales (Bhatnagar and Johri, 1983). Aside from three root parasitic Loranthaceous genera, mistletoes are aerial parasites. All mistletoes contain chlorophyll, are dependent on their host for water and mineral nutrients, and undergo some degree of secondary growth (Bhandari and Vohra, 1983). A few mistletoes, including *Arceuthobium*, also obtain substantial assimilates from their hosts (Coetzee and Fineran, 1989). All mistletoes lack true seed coats derived from integuments, and thus the dispersal unit liberated from the mistletoe fruit is not a true seed (Bhandari and Vohra, 1983). The dispersal unit of dwarf mistletoes is explosively discharged from the fruit, whereas that of other mistletoes is ingested and dispersed by birds. Families comprising the remainder of the order Santalales are the Olacaceae, Opiliaceae, and Santalaceae, which are primarily parasitic on roots and often herbaceous (Judd *et al*, 1999).

Arceuthobium hosts include members of the coniferous families Pinaceae and Cupressaceae (Hawksworth and Wiens, 1996). *Arceuthobium* species are the most invasive mistletoes, as they develop an extensive endophytic haustorial system that is often seriously pathogenic to their hosts. *Arceuthobium* species are of immense economic importance because they are the most destructive pathogen of commercially-valuable coniferous timber trees in several regions of Mexico, western Canada, western

United States, and parts of Asia (Bakshi and Puri, 1971; Hawksworth and Shaw, 1984; Zakaullah and Badshah, 1977).

Arceuthobium americanum is also known as the lodgepole pine dwarf mistletoe. It is a New World species, and has the most extensive distribution of any *Arceuthobium* species in North America (Hawksworth and Wiens, 1996). *A. americanum* is found in Canada (British Columbia, Alberta, Saskatchewan, and Manitoba) as well as in the United States (Washington, Idaho, Montana, Oregon, California, Utah, Wyoming, and Colorado). The principal hosts are *Pinus contorta* Douglas ex Louden var. *latifolia* Engelmann and *P. contorta* var. *murrayana* (Greville and Balfour) Engelmann (the lodgepole pines), and *Pinus banksiana* Lambert (jack pine). In Canada, *A. americanum* is found primarily on *P. contorta* in British Columbia and Alberta, on *P. contorta* x *banksiana* (lodgepole pine/jack pine hybrids) in Alberta and Saskatchewan, and on *P. banksiana* in Alberta, Saskatchewan and Manitoba (Hawksworth and Wiens, 1996). In Manitoba, *Arceuthobium americanum* seriously degrades both the potential yield of commercial *Pinus banksiana* stands and the aesthetic appeal of resort areas on the southern shores of Lake Winnipeg where *P. banksiana* is the dominant tree species on sandy soils (Gilbert, 1988).

2. Rationale for the Study

Since *Arceuthobium americanum* has pathogenic characteristics, it is important to understand all aspects of its biology. Control of these pathogens has been hampered by inadequate knowledge of their basic biological characteristics (Hawksworth and Wiens, 1996). More importantly, it is necessary to specifically examine the events in the female reproductive flowers/fruit of *Arceuthobium*, as the female reproductive organs ultimately produce the units of infection. Although some work has been done on reproductive development in *Arceuthobium* species, no study fully encompasses the powers of all levels of microscopy. In addition, studies of most mistletoes have been primarily limited to Old World species (Zaki and Kuijt, 1995). In general, studies of flowering plants as a group have been riddled with inconsistencies (Reiser and Fischer, 1993): a thorough study of reproductive development in the female tissues of *A. americanum* would

contribute to the body of knowledge regarding the reproductive biology of flowering plants.

Characteristics of reproductive development are very important: plant families can often be recognized by a single reproductive character (Johri, 1963b). In addition, suites of reproductive and other morphological characters have been used to reconstruct phylogeny for various hierarchical levels within the flowering plants (Judd *et al.*, 1999). Notably, reproductive and morphological characters have been used to organize phylogenetic relationships among families in the order Santalales, although the relationships described by different authors do not always agree (see Kuijt, 1969; Wiens and Barlow, 1971; Bhatnagar and Johri, 1983). Reproductive characters used for such phylogenetic reconstructions are usually relatively large-scale, broad traits: for example, the general type of endosperm development. It is very likely that finer-scale reproductive characters in the female flowers, including the degree of ovular reduction, the number of cells in the archesporium, the type of megasporogenesis, and the final organization of the embryo sac, could be particularly useful in understanding evolutionary derivation. If such fine scale characteristics could be elucidated for *Arceuthobium* and compared to corresponding fine-scale reproductive features described for other families in the Santalales, it is very likely that a basic series of evolutionary derivation could be constructed for the order. Molecular characters ascertained from nuclear small subunit (SSU) ribosomal (r) DNA sequences and chloroplast ribulose-1,5-bisphosphate carboxylase large chain (rbcL) DNA sequences have also been used to reconstruct phylogeny in the order Santalales (Nickrent and Franchina, 1990; Nickrent and Malécot, 2001a, b). The phylogeny of the Santalales based on molecular techniques could be compared to the evolutionary series of the Santalales determined by fine-scale reproductive characters in order to determine if the two reconstructions support each other.

Several studies have examined the viability of the embryo in the *Arceuthobium* dispersal unit with 2,3,5-triphenyl tetrazolium chloride (TTC: Scharpf and Parmeter, 1962; Robinson, 1995; Jerome, 2001). In these studies, the viability testing has either been performed on dispersal units that had been stored in the laboratory for various time periods at various temperatures (Scharpf and Parmeter, 1962; Jerome, 1995) or on

dispersal units that had been recently collected (Robinson, 1995). Although Gilbert (1988) stressed the importance of examining dispersal units in the field, no study has examined the changes in 2,3,5-TTC-tested viability of naturally discharged dispersal units left in the field for several months. Moreover, only the embryo is typically scored for viability; no study has examined the viability of other components in the dispersal unit. In this study, the viability of various components in the *A. americanum* dispersal unit left in the field for up to three months were examined with 2,3,5-TTC. The information obtained from such an examination may aid researchers wishing to maintain dwarf mistletoe dispersal units for infectivity and for germination experiments.

Although the dispersal unit of mistletoes lacks an integument-derived seed coat, the dispersal unit is most visibly enveloped by a mucilaginous, viscid layer frequently called "viscin" (Hawksworth and Wiens, 1996). In all mistletoes, viscin is extremely important for adhering the discharged dispersal unit to the host. In *Arceuthobium*, viscin is also important in generating the hygroscopic force required for explosive discharge while the dispersal unit is within the fruit (Paquet *et al.*, 1986). It is likely that the viscin of typical mistletoes is different from that of dwarf mistletoes, as the viscin of typical mistletoes does not play a role in the generation of an explosive force. Thus, while there have been some studies on mistletoe viscin (Bhandari and Nanda, 1968a; Bhandari and Indira, 1969; Paquet, 1975; Paquet *et al.*, 1986; Gedalovich and Kuijt, 1987; Gedalovich *et al.*, 1988; Gedalovich-Shedletzky *et al.*, 1989; Sallé, 1983), only those of Bhandari and Nanda, 1968a, Paquet, 1975, Paquet *et al*, 1986, and Gedalovich-Shedletzky *et al.*, 1989 examined the viscin of *Arceuthobium* species. Even so, these studies were cursory: Bhandari and Nanda (1968a) did not perform either biochemical or cytochemical analysis, Gedalovich-Shedletzky *et al.* (1989) focused on biochemical analysis, and Paquet (1975) as well as Paquet *et al.* (1986) focused on cytochemical analysis.

For the most part, mistletoe viscin is believed to be a tissue that is comprised at least partially of elongated cells (Gedalovich and Kuijt, 1986; Sallé, 1983). Authors do not agree upon the cellular structure of the tissue. The ontogeny of the cells in the viscin tissue has only been briefly examined in a few mistletoes (Gedalovich and Kuijt, 1987; Gedalovich *et al.*, 1988; Gedalovich-Shedletzky *et al.*, 1989; Sallé, 1983; Bhandari and Nanda, 1968a; Bhandari and Indira, 1969). Only Bhandari and Nanda's (1968a) study

examined an *Arceuthobium* species, although the study was limited, as it only primarily examined the organization of the viscin tissue as a whole.

Although an extremely important feature of the viscin tissue is mucilage, believed to specifically impart the functional properties to the tissue, the origin and composition of the mucilage is poorly understood. One study by Gedalovich and Kuijt (1987) attempted to clarify the origin of the viscin mucilage, but their study was performed on a Loranthaceous mistletoe. Only a few studies have examined viscin mucilage in mature fruit (Paquet, 1975; Paquet *et al.*, 1986; Gedalovich and Kuijt, 1987; Gedalovich *et al.*, 1988; Gedalovich-Shedletzky *et al.*, 1989; Sallé, 1983). No study has examined the mucilage either biochemically or cytochemically for potential compositional changes during development, and no study has employed lectin cytochemistry or fluorescence microscopy to examine the viscin mucilage. As the viscin tissue is crucial to the dissemination of *Arceuthobium*, the value of an examination of the ontogeny, arrangement, and composition of this tissue in an *Arceuthobium* species using modern techniques is evident. It is similarly important to note compositional changes of the viscin cell mucilage that may occur over development.

A cytogenetic and ploidy level analysis of various tissue regions within the fruit of *Arceuthobium americanum* will validate anatomical observations. Ploidy level is defined as the number of haploid (n) chromosome sets in a genome (Purves *et al.*, 1998). *Arceuthobium* species are diploid (2n) organisms with 2n = 28 chromosomes (Wiens, 1968). If the endosperm of *A. americanum* could be determined to be triploid (3n) with 3n = 42 chromosomes, support for the process of double fertilization would be provided. Moreover, some regions in the *Arceuthobium* fruit have an obscure origin. Notably, one of these regions is a cap of tissue that sits above the radicular pole of the embryo. Although not a root cap, workers have suggested that this cap is either maternal tissue (Johnson, 1888; Bhandari and Nanda, 1968a) or endosperm tissue (Thoday and Johnson, 1930; Cohen, 1963). In conjunction with anatomical studies, ploidy level analysis would be an obvious method by which to determine the origin of the cap. If the endosperm could be confirmed to be triploid, and the cap is also determined to be triploid, an endosperm origin for the cap is likely. If the endosperm is triploid, but the cap is determined to be diploid, the endosperm could be ruled out as the source of the cap.

These ploidy level techniques could impart objective measures to what would otherwise be only qualitative observations. New techniques in conjunction with image analysis may need to be developed in order to determine ploidy level in *A. americanum* fruit tissue regions.

II. THESIS GOALS

The present study provides an integrated approach to the study of reproductive developmental features in the female flowers and fruit of *Arceuthobium americanum* using techniques of light microscopy, fluorescence microscopy, and electron microscopy. Modern techniques of cytochemistry will be used to elicit detailed information regarding the chemical nature of structures observed during development. The study encompasses three major goals.

The first goal is to elucidate basic stages of reproductive development in the female reproductive tissues of *Arceuthobium americanum*. Specifically, developmental events pertaining to the ovule, the megasporocytes, megasporogenesis, megagametogenesis, the unfertilized embryo sac, pollination, the fertilized embryo sac, embryogenesis, endosperm development, fruit development, and the discharged dispersal unit will be examined. New terminology may be needed to describe certain events and structures. In addition, the viability of various discharged dispersal unit components will be examined during maturation in the field. Finally, fine-scale, pre-fertilization female reproductive events and characteristics of *A. americanum* will be used to illustrate the evolutionary position of *Arceuthobium* within the Santalales.

The second goal is to describe the ontogeny, development, cellular arrangement, and mechanism of mucilage formation in the viscin tissue of *Arceuthobium americanum*. General biochemical techniques will be used to determine the general composition of the mucilage in the nearly mature fruit, while cytochemical techniques will be used to monitor changes in the viscin mucilage and other viscin components over the course of development.

The third goal is to use cytogenetic techniques, ploidy analysis, and image analysis to provide quantitative support for the occurrence of double fertilization in *Arceuthobium americanum* and to clarify the origin of different tissue regions observed within the nearly mature *A. americanum* fruit.

CHAPTER TWO - LITERATURE REVIEW

I. REPRODUCTIVE DEVELOPMENT IN THE FEMALE STRUCTURES OF TYPICAL FLOWERING PLANTS, *ARCEUTHOBIUM AMERICANUM*, AND RELEVANT TAXA

1. Seasonal Reference Points and Definition of Reproductive Development Used in This Thesis

1A. Salient features of the reproductive phase of *Arceuthobium* species and seasonal reference points used to describe these features in *Arceuthobium americanum*

Before aspects of reproductive development in *Arceuthobium* species can be described, some salient features of the reproductive phase in the *Arceuthobium* life cycle must be clarified. Firstly, *Arceuthobium* species are either direct flowering species or indirect flowering species (Hawksworth and Wiens, 1996). In a direct flowering species, both female and male flower buds become evident immediately prior to anthesis (flower opening). In an indirect flowering species, both female and male flower buds become evident about five to eight months prior to anthesis. Most *Arceuthobium* species, including *A. americanum* and *A. pusillum* (the two *Arceuthobium* species found in Manitoba) are indirect flowering species: in these two species, flower buds become evident in August/September, but anthesis does not occur until April/May of the following spring. Fruits of *Arceuthobium* species then either mature within seventeen months of anthesis (for example, *A. americanum*) or within five months of anthesis (for example, *A. pusillum*). At fruit maturity, which is around August/September for both *A. americanum* and *A. pusillum*, the dispersal unit is explosively discharged, overwinters, and germinates in April/May of the following spring (Gilbert, 1988).

Thus, seasonal reference points can be used where relevant in order to describe the timing of reproductive developmental events in the female flowers/fruit of *Arceuthobium americanum*. These seasonal reference points are generally useful for *A. americanum* growing anywhere in North America. Spring will be defined as the months of March, April, and May, summer as June, July and August, fall as September, October, and November, and as December, January, and February. The spring in which anthesis

occurs will be called the first spring of development, and reproductive developmental events in the female flowers/fruit will be primarily documented from anthesis in the first spring to explosive discharge late in the second summer.

1B. General definition of reproductive development used in this thesis

In this thesis, "reproductive development in the female structures" will be defined as any developmental events occurring within the female structures that either lead to reproduction or are a consequence of reproduction. In the flowering plants, this will include descriptions of the carpels, the ovule(s), the megasporocyte(s), megasporogenesis, megagametogenesis, the unfertilized embryo sac (unfertilized megagametophyte), the fertilized embryo sac (fertilized megagametophyte), embryogenesis, endosperm development, and aspects of fruit development. Aspects of pollination may be addressed in this context or separately. Where reproductive development in the female structures of gymnosperms is referred to, there will obviously be no reference to carpels, embryo sacs, endosperm, or fruit. It is realized that the phrase "female structures" should specifically refer to carpellary/ovular tissue (gynoecium tissues) of flowering plants and to the ovular tissue of gymnosperms. However, the phrase "female structures" will usually be more broadly applied to include entire female reproductive organs, such as the female flowers of dioecious flowering plants or entire female cones of gymnosperms. When comparisons with gymnosperms are not an issue, reproductive development in the female structures of dioecious flowering plants will simply be synopsized as "reproductive development in the female flowers/fruit". "Female development", on the other hand, refers specifically to those events concerning the unfertilized megagametophyte and processes leading to its formation as well as to development of specific female tissues, including the carpellary/ovular tissues of flowering plants and the ovular tissues of gymnosperms.

There is a need for additional study on reproductive development in the female flowers/fruit of *Arceuthobium americanum*. Earlier work on this in *Arceuthobium* and related genera lack detail and agreement. Moreover, previous studies have typically been limited to the light level of microscopy (Hudson, 1966; Bhandari and Nanda, 1968a, b).

Following are definitions of the various aspects of reproductive development in the female flowers/fruit of flowering plants, along with descriptions of the work that has been done on *Arceuthobium*, related taxa, and relevant (usually Santalalean) parasitic plants. The same taxa may not necessarily be described in every section, since reproductive developmental studies of parasitic plants in general are not always comprehensive and because specific descriptions of certain parasitic plants may not be particularly pertinent.

2. Ovules

2A. Typical flowering plants

A typical ovule consists of three basic structures: the nucellus (megasporangium), one or two integuments, and the funiculus (Mauseth, 1988). The archesporium, representing the cell(s) that give rise to the megasporocyte(s), is found in the nucellus. The integument(s) envelop the nucellus. Ovules with two integuments (an inner and an outer integument) are called bitegmic ovules, and ovules with one integument are called unitegmic ovules. Ovules that lack integuments are called ategmic ovules. The funiculus is a narrow stalk that attaches the nucellus and integuments to the ovary wall (pericarp). The special thickened portion of the pericarp where the ovules originate and remain until maturity is called the placenta (Reiser and Fischer, 1993). Types of ovules pertinent to this thesis will be **illustrated** in Figures 4.78 and 4.80 of Chapter Four, section III. Discussion - 2B and 2C.

There are differences in the placentation of ovules. Only two types of placentation that are pertinent to *Arceuthobium* and relevant taxa will be defined here. In free central placentation, the ovules are borne on a central column of placental tissue arising from the base of the ovary (Raven *et al.*, 1999). In basal placentation, a single ovule occurs at the base of the ovary. Ovules that show free central placentation may be either pendulous (descending) or erect (ascending). In pendulous ovules, the funiculus is directed down from the placenta, toward the base of the ovary. In erect ovules, the funiculus is directed up from the placenta, away from the base of the ovary (Geesink *et al.*, 1981). Ovules that show basal placentation are always erect. Of the ovules that show

free central placentation, generally only pendulous types will be encountered in this thesis.

A pore in the integument(s) can be found at the free end or apex of the ovule, and this pore is called the micropyle (Mauseth, 1988). Thus, the presence of a micropyle is dependent upon the presence of at least one integument. The chalaza is the region extending from the base of the integuments to the point of attachment of the funiculus (Esau, 1977), and essentially represents the base of the ovule. As in the case of the micropyle, the usage of the term "chalaza" is dependent upon the presence of at least one integument. The mature ovule displays a polarity with respect to the axis from the micropyle to the chalaza (Reiser and Fischer, 1993). Commonly, the micropyle is considered to be morphologically higher than the chalaza. Thus, micropylar regions are considered higher than chalazal regions. However, problems in ascribing meaning to the micropylar/chalazal polarity potentially arise if the ovule is ategmic, as neither the micropyle nor chalaza is present in an ategmic ovule.

Various arrangements of the funiculus and nucellus of an ovule are also possible (Fahn, 1967). If the funiculus and the nucellus are arranged in a straight line, the ovule is orthotropous (atropous or straight). If the funiculus is bent approximately 180 degrees, the ovule is anatropous (curved). There are also intermediary conditions.

Both orthotropous and anatropous ovules can be either pendulous or erect if they show free central placentation. In an orthotropous pendulous ovule showing free central placentation, the ovular apex projects down toward the base of the ovary (orthotropous erect ovules showing free-central placentation will not be encountered in this thesis, and will not be described). In an anatropous, pendulous ovule showing free central placentation, although the funiculus is initially directed down toward the base of the ovary, the anatropous curvature to the ovule ensures that the ovular apex projects away from the base of the ovary. In an anatropous, erect ovule showing free central placentation, although the funiculus is initially directed away from the base of the ovary, the anatropous curvature ensures that the ovular apex projects down toward the base of the ovary (this type of ovule will be encountered only once in this thesis). A further important distinction exists regarding free-central, anatropous ovules (both pendulous and erect) pertaining to whether the ovule curves inward so that the bulk of the ovule lies

between the placenta and the funiculus, or outward, so that the funiculus lies between the placenta and the bulk of the ovule. The literature describing these two conditions are contradictory (Geesink *et al.*, 1981; Radford *et al.*, 1974; Watson and Dallwitz, 1992). Thus, the condition where the bulk of the free-central anatropous ovule lies between the placenta and the funiculus will be defined here as "in-turned" and the condition where the funiculus lies between the placenta and the bulk of the free-central anatropous ovule will be defined as "out-turned." Of the ovules showing basal placentation (and are thus erect), only orthotropous types will be encountered here.

2B. *Arceuthobium* and relevant taxa

Integumentary reduction to the unitegmic or ategmic condition is a feature of parasitic plants (Bouman, 1984; Judd *et al.*, 1999). Typically, the integumentary reduction is concomitant with nucellar and funicular reduction; this results in an overall ovular reduction.

Varying degrees of ovular reduction are evident in the primarily parasitic order Santalales, an order that is comprised of the families Eremolepidaceae, Loranthaceae, Misodendraceae (Myzodendraceae), Olacaceae, Opiliaceae, Santalaceae, and Viscaceae (Bhandari and Vohra, 1983; Nickrent and Franchina, 1990). The Eremolepidaceae have not been universally granted family status, as their genera have been placed with the Viscaceae (Kuijt, 1969) and the Santalaceae (Nickrent and Malécot, 2001a, b). Nonetheless, for this thesis, they will be considered a family after Bhandari and Vohra (1983). The Olacaceae have bitegmic, unitegmic, and ategmic members, and the ovules possess both a funiculus and a placenta (Reed, 1955; Bouman, 1984). Olacaceae with bitegmic ovules tend to be non-parasitic, whereas Olacaceae with unitegmic and ategmic ovules tend to be parasitic. Ovules in the Olacaceae show free-central placentation, are pendulous, anatropous, and in-turned.

The nucellus in the primarily parasitic family Opiliaceae is more reduced than in the members of the Olacaceae, but like the Olacaceae, a placenta and funiculus are still discernible (Bouman, 1984). Ovules in the Opiliaceae are unitegmic (*Cansjera*, *Opilia*) and ategmic (some *Agonandra*), and are similar to the Olacaceae in all other ways.

Ovules of the primarily parasitic family Santalaceae are more reduced than those of the Opiliaceae and Olacaceae, as the placenta and funiculus are present but much insignificant (Bouman, 1984). However, like the Opiliaceae, the Santalaceae have unitegmic and ategmic ovules. The Santalaceae are comprised of five tribes: the Comandreae, the Osyrideae, the Anthoboleae, the Thesieae, and the Santaleae (Johri and Bhatnagar, 1960; Watson and Dallwitz, 1992). The Comandreae (including the genus *Comandra*) and the Thesieae (including the genus *Thesium*) have unitegmic ovules (Bouman, 1984). In the Comandreae, the unitegmic ovules show free central placentation, are pendulous, anatropous, and out-turned (Johri and Bhatnagar, 1960). Interestingly, the placental column in the Comandreae is twisted. In the Thesieae, the unitegmic ovules show free central placentation, are pendulous, and orthotropous. As in the Comandreae, the placental column in the Thesieae is twisted. The Osyrideae (including the genus *Osyris*), the Anthoboleae (including the genus Exocarpus), and the Santaleae (including the genus *Santalum*) have ategmic ovules in which differentiation into nucellus and integument is lacking (Bouman, 1984). In the Osyrideae, the ategmic ovules show free central placentation on a typical, non-twisted placenta, are pendulous, anatropous, and out-turned (Johri and Bhatnagar, 1960). In the Anthoboleae, a single ategmic, erect, orthotropous ovule shows basal placentation. In the Santaleae, the ategmic ovules show free central placentation on a typical, non-twisted placenta, are pendulous, and orthotropous. Although the parasitic family Misodendraceae (Myzodendraceae) has not been well studied, studies of *Misodendrum puntulatum* and *M. quadrifolum* show that the family has ovules that are very similar to those of the tribe Santaleae in the family Santalaceae (Skottsberg, 1913; Davis, 1966).

Members of the parasitic families Viscaceae and Loranthaceae possess ovules that are even more reduced than those of the Opiliaceae or Santalaceae (Maheshwari, 1950; Bouman, 1984). In the Viscaceae and Loranthaceae, the "ovules" lack a conventional placenta, funiculus, and integuments. In most Viscaceae and many Loranthaceae, a dome-shaped protuberance in the centre of the ovary arises from the base of the ovarian cavity, and this protuberant structure represents a vestigial placenta or placental-ovular complex (Bhandari and Vohra, 1983). Although this protuberant structure lacks a discrete funiculus, it still has the appearance of an orthotropous ovule, since the

protuberant structure emerges directly from the base of the ovary and lacks curvature. The protuberant structure has been called a naked ovule (Kuijt, 1969), an ategmic ovule (Judd *et al.*, 1999), a "mamelon" (Calder, 1983) and a "papilla" (Bhandari and Nanda, 1968a, b; Bhandari and Indira, 1969; Bhandari and Vohra, 1983; Bhatnagar and Johri, 1983). In the Viscaceae, the protuberant structure is always unlobed (Bhandari and Vohra, 1983), whereas in the Loranthaceae, the protuberant structure may be unlobed or have three or four lobes (Bhatnagar and Johri, 1983). However, in *Viscum* and *Notothixos* of the Viscaceae (Bhandari and Vohra, 1983) and in *Helixanthera*, *Barathranthus*, *Dendrophthoe falcata*, *Scurrula*, *Moquiniella*, *Tapinanthus*, *Taxillus*, and *Tupeia* of the Loranthaceae, neither the nucellus nor the ovarian loculus fully differentiates, and the archesporium/megasporocyte(s) develop hypodermally at the base of the ovary. Nonetheless, a better name for the typical Viscaceous and Loranthaceous protuberant "ovule" is necessary. Moreover, some understanding of the evolutionary derivation of this "ovule" should be attempted.

The parasitic family Eremolepidaceae has not been well studied. However, studies of *Eubrachion ambiguum* (Bhandari and Indira, 1969) indicate that the "ovular" structure is similar to an unlobed protuberant structure observed in most Viscaceae and some Loranthaceae. As only one member of the Eremolepidaceae has been well examined (*Eubrachion ambiguum*), any further references made to *Eubrachion ambiguum* in this thesis will typically refer to the genus without stipulation of the specific epithet.

The Balanophoraceae were once considered to be in the Santalales, but due to the information garnered from molecular phylogenetic techniques, the Balanophoraceae have been placed in the order Balanophorales (Nickrent and Franchina, 1990). Nonetheless, in most Balanophoraceae (-ales), the unlobed protuberant "ovule" is similar to that observed in most Viscaceae, some Loranthaceae, and studied members of the Eremolepidaceae, although the similarity is likely a result of convergent evolution. In *Balanophora* of the Balanophoraceae (-ales), ovular reduction is extreme, as the "ovular" structure is very similar to the extremely reduced condition observed in *Viscum* and *Notothixos* of the Viscaceae as well as to that observed in *Helixanthera*, *Barathranthus*, *Dendrophthoe falcata*, *Scurrula*, *Moquiniella*, *Tapinanthus*, *Taxillus*, and *Tupeia* of the Loranthaceae.

Again, the similarities of *Balanophora* to these Viscaceous and Loranthaceous members are likely due to convergence.

3. The Female Archesporium

3A. Typical flowering plants

The (female) archesporium of an ovule is found within the nucellar tissue and is typically unicellular (Reiser and Fischer, 1993). The single (female) archesporial cell is found immediately interior to the nucellar epidermis and is thus a hypodermal cell. The archesporial cell is typically larger than the neighboring cells, has a larger nucleus, and a denser cytoplasm. In about two hundred families, the archesporial cell undergoes a mitotic division to form a primary parietal cell and a primary sporogenous cell. The sporogenous cell will then function as a megasporocyte. The primary parietal cell and surrounding nucellar cells undergo divisions, and thus the nucellus grows between the epidermis and the megasporocyte, causing the megasporocyte to become deeply buried in the nucellar tissue. This results in a crassinucellate ovule. Less frequently, in about one hundred families, the archesporial cell functions directly as the megasporocyte, preparing for meiosis immediately (Davis, 1966). In such a case, the megasporocyte remains adjacent to the nucellar epidermis, and the ovule is said to be tenuinucellate. As the archesporium is typically unicellular, only one megasporocyte forms in an ovule, whether it is crassinucellate or tenuinucellate.

Rarely, however, a single archesporial cell does not represent the female archesporium, and in these species, the archesporium is said to be multicellular (Kennell and Horner, 1985; Sumner and Van Caeseele, 1988; Mauseth, 1988). In these plants, each archesporial cell typically functions directly as a megasporocyte, resulting in tenuinucellate ovules with more than one megasporocyte per ovule (Mauseth, 1988). Multicellular female archesporia are found in Casuarinaceae, Rosaceae, Asteraceae, Rubiaceae, Apiaceae, Liliaceae, Crossomataceae, Paeoniaceae, (Tilton, 1980), and, as will be elucidated shortly, most Loranthaceae, all Viscaceae (Maheshwari, 1950), *Eubrachion* of the Eremolepidaceae (Bhandari and Indira, 1969), and Santalaceae (Ram, 1959). However, although a female archesporium may be multicellular and have the potential to produce multiple megasporocytes, not every archesporial cell necessarily

develops into a megasporocyte. In addition, no matter how many megasporocytes are produced, typically only one megasporocyte per ovule is ultimately capable of successfully continuing with all processes of megasporogenesis, megagametogenesis, and fertilization.

3B. *Arceuthobium* and relevant taxa

Number of cells in the female archesporium

In most Viscaceae, the female archesporium is multicellular, as two hypodermal archesporial cells develop, each one obliquely oriented to the long axis of the "ovule". A two-celled archesporium is described for *Arceuthobium oxycedri* (Johnson, 1888), *A. pusillum* (Thoday and Johnson, 1930; Tainter, 1968), *Phoradendron* spp. (Billings, 1933), *Korthalsella* spp. (Rutishauser, 1935, 1937), *A. douglasii* (Jones and Gordon, 1965; Bhandari and Nanda, 1968b), *A. minutissimum* (Bhandari and Nanda, 1968a), *A. campylopodum* (Cohen, 1970), and *Notothixos* (Bhandari and Nanda, 1983). However, whereas Dowding (1931) reported that the female archesporium of *A. americanum* possesses more than two archesporial cells, Hudson (1966) stated that the female archesporium has a similar cell number and appearance as was reported for all other *Arceuthobium* species. Therefore, the number of cells making up the archesporium in *Arceuthobium americanum* needs to be re-examined.

The female archesporium of *Viscum album* and *V. articulatum* (Steindl, 1935; Schaeppi and Steindl, 1945) as well as *Eubrachion* (Bhandari and Indira, 1969) possesses three rather than two archesporial cells, while that of *V. minimum* possesses between five and eight (Zaki and Kuijt, 1995). Similarly, a female archesporium with more than two archesporial cells seems to be a nearly ubiquitous feature among the Loranthaceae. In those Loranthaceae with lobed protuberant ovular structures, each lobe may possess one to four archesporial cells (Bhatnagar and Johri, 1983), and thus a given three to four-lobed ovular structure could possess between three and sixteen archesporial cells. In those Loranthaceae with unlobed protuberant ovular structures or in which the archesporium develops hypodermally at the base of the ovary, as many as forty archesporial cells may develop (Johri *et al.*, 1957; Bhatnagar and Johri, 1983). The

Santalaceae typically possess about three archesporial cells (Ram, 1959). All Balanophoraceae studied have a unicellular archesporium (Maheshwari, 1950).

Crassinucellate or tenuinucellate pathway

According to Bhandari and Vohra (1983), the archesporial cells of most Viscaceae enlarge and function directly as megasporocytes, resulting in the tenuinucellate condition, as would be expected for species with multicellular archesporia (Mauseth, 1988). However, reports regarding some *Arceuthobium* species are variable, as both the tenuinucellate condition and the crassinucellate condition have been documented in the genus. In *A. minutissimum* (Bhandari and Nanda, 1968a), the two hypodermal archesporial cells develop directly into megasporocytes without cutting off any parietal cells, leading to the tenuinucellate condition. Conversely, however, Johnson (1888) reported that each of the two archesporial cells of *A. oxycedri* cuts off several parietal cells, leading to the crassinucellate condition. Reports for *A. americanum* are also conflicting. Dowding (1931) reported that each archesporial cell of the many-celled (more than two-celled) archesporium of *A. americanum* cuts off parietal cells (leading to the crassinucellate condition), although only two megasporocytes are ultimately formed. However, Hudson (1966) stated that the two archesporial cells of *A. americanum* develop directly into megasporocytes (leading to the tenuinucellate condition). The fate of the archesporium of *A. americanum* needs to be re-examined. Nonetheless, Dowding (1931) and Hudson (1966) did agree that two megasporocytes were ultimately formed in *A. americanum*; Calvin (1996) also indicated that two megasporocytes were ultimately formed in *A. americanum*.

Although *Eubrachion* (Eremolepidaceae) has a many-celled archesporium, no parietal cells are cut off; this leads to the tenuinucellate condition (Bhandari and Indira, 1969). Out of the approximately three archesporial cells, one to three cells become mature megasporocytes. In *Viscum minimum*, which has an archesporium with more than two archesporial cells (as has other *Viscum* species but not other Viscaceae), division of each of the five to eight archesporial cells results in the formation of a primary parietal cell and a primary sporogenous cell, leading to the crassinucellate condition (Zaki and Kuijt, 1995). Consequently, about five to eight primary sporogenous cells function as

megasporocytes. In the Loranthaceae, regardless of the appearance of the ovular structure, several of the archesporial cells in the many-celled archesporium function directly as megasporocytes (Bhatnagar and Johri, 1983), leading to the tenuinucellate condition; the other archesporial cells degenerate. It is not particularly clear as to how many megasporocytes do develop in a given ovular structure, but the number apparently averages four (Johri *et al.*, 1957; Maheshwari *et al*, 1957; Dixit, 1958, 1961; Narayana, 1958a, b; Prakash, 1960, 1963; Raj, 1970). In the Santalaceae, typically only one of the three archesporial cells functions directly as a megasporocyte, leading to the tenuinucellate condition; the other archesporial cells do not generally produce megasporocytes (Ram, 1959).

4. Megasporogenesis

4A. Typical flowering plants

Megasporogenesis is the meiotic process by which a diploid megasporocyte divides to form haploid megaspores (Mauseth, 1988). In all flowering plants, megasporogenesis involves the two nuclear divisions of meiosis: meiosis I and meiosis II. However, the two meiotic divisions may or may not be accompanied by cytokinesis and thus megasporogenesis among the flowering plants is variable. There are three basic types of megasporogenesis: the monosporic type, the bisporic type, and the tetrasporic type (Maheshwari, 1950).

Monosporic. In monosporic megasporogenesis, cytokinesis accompanies both meiosis I and meiosis II (Maheshwari, 1950). Each of the two cells resulting from meiosis I may be called a dyad, and the four cells that are formed upon the completion of meiosis are called megaspores. Three of the four megaspores, however, will immediately degenerate, leaving only one uninucleate haploid functional megaspore. The functional megaspore will continue with megagametogenesis. The position of the functional megaspore relative to the degenerative megaspores and the micropyle has been used in further categorizing monosporic development. However, in almost all flowering plants undergoing monosporic development, the functional megaspore is usually the chalazal-most (the lowest) megaspore.

Bisporic. In bisporic megasporogenesis, cytokinesis follows meiosis I, leading to the formation of two cells, and, as in monosporic megasporogenesis, each cell formed following meiosis I is called a dyad (Mauseth, 1988). After meiosis I, one dyad typically degenerates without undergoing meiosis II, and can be referred to as the nonfunctional dyad (Maheshwari, 1950). The nucleus of the other dyad then completes meiosis II, but meiosis II is not followed by cytokinesis and thus a binucleate cell with two haploid nuclei results. This binucleate cell is the functional megaspore, and the megagametophyte that will develop from the functional megaspore will be a chimeral mixture of two types of nuclei. The position of the functional megaspore relative to the nonfunctional dyad as well as to the micropyle has been used to differentiate different types of bisporic development. However, in almost all flowering plants undergoing bisporic development, the functional megaspore usually arises from the chalazal (lower) dyad.

Tetrasporic. In tetrasporic megasporogenesis, neither meiosis I nor meiosis II is accompanied by cytokinesis, resulting in a tetranucleate cell with four haploid nuclei (Maheshwari, 1950). This tetranucleate cell acts as the functional megaspore. The megagametophyte that will develop from the functional megaspore will be a chimeral mixture of four types of nuclei.

In all types of megasporogenesis, the functional megaspore has also been called the immature embryo sac or immature megagametophyte (Maheshwari, 1950), although this terminology has not been widely accepted (Reiser and Fischer, 1993).

4B. *Arceuthobium* and relevant taxa

Before megasporogenesis or subsequent stages of reproductive development in female tissues can be described for *Arceuthobium* and relevant taxa, a polarity to the axis of the ovule (or ovular structure) should be defined so that integumented (tegmic) and ategmic ovules can be compared equally. If an ovule is bitegmic or unitegmic, a micropyle is therefore present at the apex of the ovule. Thus, as implied earlier, ovular regions near the micropyle will be considered to be morphologically higher than ovular regions further from the micropyle and closer to the chalaza (ovular base); this is a fairly standard topographical orientation (Reiser and Fischer, 1993). However, some of the

taxa described possess ategmic ovules. In those taxa, the apex of the ovular structure, where the micropyle could be presumed to exist if the ovule possessed integument(s), can be considered morphologically higher than the base of the ovular structure. In an ategmic ovular structure, the base of the ovular structure represents the region where the nucellus is attached to the funiculus. In a particularly reduced ategmic ovular structure, the base of the ovular structure represents the region where the ovular structure is attached to or confluent with the placenta or ovary wall. The terms "higher, "lower", "upward", and "downward" can be used with regard to this polarity in order to describe orientation within any given ovular structure, whether or not it is tegmic.

In those taxa that possess ovules displaying free central placentation, such as some Santalaceae, the polarity cannot be readily applied to the longitudinal axis of the flower. However, in those taxa that possess erect, orthotropous "ovules" displaying basal placentation in which the ovular apex projects directly away from the ovarian base (as in the Viscaceae, Loranthaceae, Eremolepidaceae, Balanophoraceae, and some Santalaceae), the polarity can be extended to the longitudinal axis of the flower. In these taxa, regions distal to the pedicel can be considered morphologically higher than regions proximal to the pedicel.

In the Viscaceae, it is believed that all megasporocytes are capable of undergoing megasporogenesis (Bhandari and Vohra, 1983), although this has not been well established. Megasporogenesis has been described as being bisporic in most Viscaceae including *Arceuthobium*. Specifically, bisporic megasporogenesis has been described for *Arceuthobium oxycedri* (Johnson, 1888), *Ginalloa* (Rutishauser, 1937), *Viscum album* (Steindl, 1935; Schaeppi and Steindl, 1945), *V. articulatum* (Steindl, 1935), *Korthalsella dacrydii*, *K. opuntia* (Rutishauser, 1935, 1937; Schaeppi and Steindl, 1945), *Notothixos* (Bhandari and Vohra, 1983), *A. pusillum* (Thoday and Johnson, 1930; Tainter, 1968), *A. americanum* (Dowding, 1931; Hudson, 1966), *A. minutissimum* (Bhandari and Nanda, 1968a), and *A. campylopodum* (Cohen, 1970). Although Jones and Gordon (1965) described the megasporogenesis of *A. douglasii* as tetrasporic, Bhandari and Nanda (1968b) reinvestigated and described the megasporogenesis as bisporic in this species as well. Hudson (1966) further stated that megasporogenesis in *A. americanum* takes place in late May of the first spring of development, whereas D.A.R. McQueen (pers. comm.,

1995) believed that megasporogenesis takes place in mid April of the first spring. The timing of megasporogenesis will be re-examined in *A. americanum*.

Of the two dyads formed per megasporocyte following meiosis I in the above Viscaceous genera, the upper dyad becomes the functional megaspore, while the lower dyad undergoes varying degrees of development in the different species, but is ultimately nonfunctional. Unfortunately, few papers provide adequate detail, and thus a re-examination of megasporogenesis in a Viscaceous species such as *A. americanum* is needed. In addition, as it is the lower ("chalazal") dyad that becomes functional in most flowering plants (Mauseth, 1988), these aforementioned Viscaceae are somewhat atypical in this regard. Bisporic development has also been reported in *Eubrachion* (Bhandari and Indira, 1969). However, as opposed to most Viscaceae, the lower rather than the upper dyad formed from each megasporocyte following meiosis I proceeds through meiosis II to become the functional megaspore, whereas the lower dyad becomes nonfunctional. This is more in accordance with typical flowering plants.

Although most Viscaceae are described as having bisporic megasporogenesis, this is not true for all members. Monosporic development has been noted in *Korthalsella lindsayi* and *Korthalsella salicornoides* (Stevenson, 1934), although no indication was given as to which megaspore becomes the functional megaspore. Also, Billings (1933) described tetrasporic development for *Phoradendron flavescens*, and although Bhandari and Vohra (1983) considered this observation doubtful, it has not been disproved. Interestingly, the latest report of megasporogenesis for a Viscaceous mistletoe, *Viscum minimum*, implies that this species undergoes monosporic megasporogenesis (Zaki and Kuijt, 1995). For each of the five to eight megasporocytes that develop in *V. minimum*, the lowermost megaspore apparently becomes the functional megaspore, as would be expected, although Zaki and Kuijt (1995) did not explicitly state this. Megasporogenesis is also occasionally bisporic in *V. minimum*. The discrepancies among descriptions of megasporogenesis in several Viscaceous species suggest that a reinvestigation of *Arceuthobium americanum* is necessary.

Monosporic megasporogenesis is more characteristic of the Loranthaceae, Santalaceae, and Balanophoraceae (-ales) than the Viscaceae (Johri, 1963a). Each of the approximately four megasporocytes in the Loranthaceae is capable of undergoing

megasporogenesis, with the lowermost megaspore from each megasporocyte becoming functional (Bhatnagar and Johri, 1983), as would be expected in a typical flowering plant. Similarly, the single megasporocyte present in most Santalaceae undergoes monosporic megasporogenesis, and the lowermost megaspore becomes functional (Ram, 1959; Johri and Bhatnagar, 1960). The single megasporocyte in *Balanophora* (Fagerlind, 1945a) and *Langsdorffia* (Fagerlind, 1945b) of the Balanophoraceae undergo monosporic development. From looking at Fagerlind's (1945a, b) diagrams, it is apparent that the uppermost megaspore becomes the functional megaspore in these Balanophoraceae. This is opposite to the condition found in typical flowering plants.

5. Megagametogenesis and General Organization of the Unfertilized Mature Embryo Sac (Megagametophyte)

5A. Typical flowering plants

In the flowering plants, megagametogenesis is the mitotic process by which the functional megaspore develops into the mature embryo sac (mature megagametophyte) (Mauseth, 1988). The typical flowering plant embryo sac has eight haploid nuclei and seven cells. The first part of megagametogenesis involves production of a four-nucleate, coenocytic (multinucleate but unicellular) immature embryo sac (Russell, 1993). The functional megaspore/immature embryo sac derived from a tetrasporic species already possesses four haploid nuclei upon its inception. However, in a monosporic or bisporic species, the functional megaspore/immature embryo sac will acquire four haploid nuclei via mitotic divisions that are not followed by cytokinesis. A functional megaspore derived from a monosporic species needs to undergo two mitotic divisions to form the four-nucleate embryo sac, while a functional megaspore derived from a bisporic species only needs to undergo one mitotic division to form the four-nucleate embryo sac.

During continued megagametogenesis from the four-nucleate stage, regardless of how the four-nucleate embryo sac arose, two nuclei migrate to one pole of the embryo sac, and two nuclei migrate to the other pole (Russell, 1993). After nuclear migration, a final mitotic division takes place, but this mitotic division is followed by cell plate formation. Three uninucleate haploid cells become organized at one pole of the embryo sac, three uninucleate haploid cells become organized at the other pole of the embryo sac,

and the remaining central region of the embryo sac becomes a binucleate cell that possesses two haploid nuclei. Exceptions do occur (Mauseth, 1988).

The three cells at one pole of the embryo sac represent one egg cell and two synergids (Mauseth, 1988). The egg cell and synergids show a triangular arrangement and share common surfaces, forming the structure known as the egg apparatus. The egg cell and synergids remain anchored to the embryo sac wall, which represents the original cell wall of the functional megaspore. The three cells at the other pole of the embryo sac represent the three antipodal cells (or simply antipodals), which also remain anchored to the embryo sac wall. The binucleate cell in the center of the embryo sac represents the central cell, and its two nuclei are called polar nuclei. Cell wall development of the egg cell, synergids, and antipodals may not be entirely complete along the boundary of the central cell and in regions near the central cell. The mature embryo sac wall contains cellulosic material, but plasmodesmata are not frequent (Willemse and van Went, 1984; Han *et al.*, 2000).

The micropylar/chalazal concept of polarity is nearly ubiquitously ascribed to embryo sacs (Reiser and Fischer, 1993). In almost all flowering plants studied in which the ovules possess integuments, the egg apparatus develops at the micropylar, or upper, pole of the embryo sac, and the antipodals develop at the chalazal, or lower, pole. As the micropylar/chalazal concept is problematic with regard to embryo sacs of ategmic ovules, the predefined polarity of upper and lower will be used for ategmic ovules of the taxa examined here.

5B. *Arceuthobium* and relevant taxa

General problems with the literature

Neither megagametogenesis nor the arrangement of the unfertilized mature embryo sac has been particularly well examined in *Arceuthobium* or other related taxa. Moreover, nearly all the taxa investigated in this regard belong to Asiatic genera. In the numerous taxa of the New World and Africa, megagametogenesis remains largely unexplored (Zaki and Kuijt, 1995). No report deals specifically with the processes of embryo sac cellularization and cell wall formation. The timing of megagametogenesis has not been well established in any *Arceuthobium* species.

Ability of a functional megaspore to produce a mature embryo sac

In the Viscaceae, it has not been validated whether the two (or more) functional megaspores that form from the two (or more megasporocytes) are capable of undergoing megagametogenesis to form a mature embryo sac. In *Arceuthobium americanum* (Hudson, 1966), *A. pusillum* (Tainter, 1968), and *A. minutissimum* (Bhandari and Nanda, 1968a), it is believed that megagametogenesis is typically more rapid in one of the two functional megaspores that develops from each megasporocyte. In *A. americanum*, the lagging functional megaspore will be arrested at the four-nucleate stage, and will degenerate (Hudson, 1966; Calvin, 1996). The other functional megaspore will complete megagametogenesis, forming a mature embryo sac. This needs to be confirmed, since reports for *A. pusillum* (Tainter, 1968), *A. minutissimum* (Bhandari and Nanda, 1968a), and *A. douglasii* (Jones and Gordon, 1965; Bhandari and Nanda, 1968b) imply that both functional megaspores complete megagametogenesis to form two mature embryo sacs. Moreover, it was stated that the degenerative embryo sac of *A. pusillum* (Tainter, 1968), *A. minutissimum* (Bhandari and Nanda, 1968a), and *A. douglasii* (Jones and Gordon, 1965; Bhandari and Nanda, 1968b) was not fertilized, whereas the non-degenerative embryo sac in these species underwent double fertilization; this should be validated. Reports for *A. oxycedri* (Johnson, 1888) and *A. campylopodum* (Cohen, 1970) do not describe the process of megagametogenesis at all.

In bisporic *Viscum album*, each of the one to three functional megaspores that forms is capable of undergoing megagametogenesis to produce a mature embryo sac (Steindl, 1935; Schaeppi and Steindl, 1945). Each mature embryo sac may then be fertilized, as polyembryony occasionally occurs in this species, but typically excess embryo sacs degenerate (Steindl, 1935; Schaeppi and Steindl, 1945). All of the five to eight functional megaspores of monosporic *V. minimum* are capable of undergoing megagametogenesis to form five to eight mature embryo sacs; polyembryony is frequent (Zaki and Kuijt, 1994). In bisporic *Eubrachion*, each of the one to three functional megaspores that forms per megasporocyte will produce a mature embryo sac; however, only one embryo sac will be fertilized, and the others will degenerate (Bhandari and Indira, 1969). Unlike most Viscaceae (but like *V. minimum*), polyembryony tends to be a feature of the Loranthaceae (Bhatnagar and Johri, 1983). In monosporic Santalaceae

(Ram, 1959; Johri and Bhatnagar, 1960) and studied members of the monosporic Balanophoraceae, including *Balanophora* and *Langsdorffia* (Maheshwari, 1950), there is only one megasporocyte, and only one functional megaspore and mature embryo sac is formed.

General arrangement of the mature embryo sac

The unfertilized embryo sac(s) of most Viscaceae, including *Viscum album* (Steindl, 1935; Schaeppi and Steindl, 1945), *V. articulatum* (Steindl, 1935), *Korthalsella dacrydii* and *K. opuntia* (Rutishauser, 1935, 1937; Schaeppi and Steindl, 1945), *A. pusillum* (Thoday and Johnson, 1930; Tainter, 1968), *A. minutissimum* (Bhandari and Nanda, 1968a), and *A. douglasii* (Bhandari and Nanda, 1968b), will have eight nuclei prior to cellularization. The lowermost quartet of nuclei in these species organize themselves into the egg apparatus and one polar nucleus, while the uppermost quartet of nuclei will organize themselves into the three antipodals and the other polar nucleus. Since the Viscaceous "ovule" has been described as being erect, orthotropous, and showing basal placentation (Bhandari and Vohra, 1983), the positioning of the egg apparatus at the lower pole of the embryo sac is unusual because the egg apparatus arises at the upper pole of the embryo sac in typical flowering plants (Reiser and Fischer, 1993). Thus, there is an apparent inversion in the arrangement of the embryo sac in the Viscaceae when compared to typical flowering plants.

However, there are some conflicting reports regarding A*rceuthobium americanum* and other *Arceuthobium* species. Dowding (1931) stated that the mature unfertilized (non-degenerative) embryo sac of *A. americanum* only has seven nuclei, but Hudson (1966) said that the embryo sac is eight-nucleate. Nonetheless, both Dowding (1931) and Hudson (1966) agreed that the egg apparatus is found at the lower pole of the embryo sac, and that the three antipodals are found at the upper pole. Cohen (1970) stated that there were only seven nuclei in the mature embryo sac of *A. campylopodum.* Moreover, Cohen (1970) could not tell where the egg apparatus of *A. campylopodum* was relative to the antipodal cells, but he believed that either a synergid or an antipodal cell was lacking, as he did note two polar nuclei in the central cell. Johnson (1888) thought that the egg apparatus of *A. oxycedri* was at the upper pole of the embryo sac and that the antipodal

cells were at the lower pole of the embryo sac. These conflicting reports for *Arceuthobium* species indicate that further study is needed.

The report for megagametogenesis in the bisporic *Eubrachion* (Bhandari and Indira, 1969) is lacking in detail, as were the reports for most Viscaceae. Like most Viscaceae (aside from the disputed cases), the embryo sac that is formed in *Eubrachion* has eight nuclei and seven cells. However, unlike most Viscaceae but like typical flowering plants, the egg apparatus of *Eubrachion* organizes at the upper pole of the embryo sac, adjacent to the degenerating dyad, whereas the antipodals organize at the lower pole.

Only Zaki and Kuijt (1994) have produced an ultrastructural report regarding megagametogenesis and arrangement of the unfertilized mature embryo sac in the Viscaceae, and the report deals specifically with the monosporic *Viscum minimum*. Thus, ultrastructural work should definitely be performed on a bisporic Viscaceous member. In *V. minimum*, each of the five to eight functional megaspores that develop from the lowermost megaspore from each of the five to eight megasporocytes enlarges rapidly and acquires an elongated shape (Zaki and Kuijt, 1994). All embryo sacs apparently reach the eight-nucleate stage following the third mitotic division. Each mature embryo sac has the egg apparatus at the upper pole, adjacent to the three nonfunctional, degenerated megaspores, and the antipodals at the lower pole. Therefore, the polarity of the embryo sac is similar to *Eubrachion* and typical flowering plants.

In the monosporic Loranthaceae, each mature embryo sac is the typical eight-nucleate, seven-celled type (Bhatnagar and Johri, 1983). The egg apparatus is found at the upper pole of the embryo sac, adjacent to the three degenerating megaspores, and the three antipodals are found at the lower pole. The arrangement is essentially the same as in typical flowering plants. The final embryo sac organization in most Santalaceae is similar to that observed in *Eubrachion V. minimum*, and the Loranthaceae (Johri and Bhatnagar, 1960). Thus, the embryo sac arrangement in *V. minimum*, Loranthaceae, and Santalaceae is essentially the same as the arrangement in typical flowering plants.

In the studied members of the Balanophoraceae, including *Balanophora* and *Langsdorffia*, the arrangement of the embryo sac, which is derived from the uppermost megaspore of the single megasporocyte (Maheshwari, 1950), is nearly identical to that

observed in most Viscaceae, aside from the fact that typical antipodals do not develop (Maheshwari, 1950). The egg apparatus arises at the lower pole of the embryo sac; this is atypical with regard to the flowering plants.

6. Details Regarding the Cells of the Unfertilized Mature Embryo Sac

6A. Unfertilized egg cell

Typical flowering plants

The great variation in the characteristics of the egg cell makes it difficult to find common denominators among the flowering plants (Raghavan, 1986; Zaki and Kuijt, 1994). However, some common features do exist. The egg cell is usually larger than the synergids, and is typically the second-largest cell of the embryo sac after the central cell (Mauseth, 1988). The egg cell is polarized, with the nucleus and the bulk of its cytoplasm found adjacent to the central cell. Most of the cytoplasm and plastids are aggregated around the nucleus (Russell, 1987). A large vacuole is found adjacent to the embryo sac wall (Reiser and Fischer, 1993). The few ultrastructural studies of egg cells have suggested that the egg cell is a rather inactive cell, possessing few ribosomes, plastids, or other organelles. The egg cell wall is usually complete only in the regions that are near the embryo sac wall, and is either absent or has extensive gaps in regions that are near the central cell (Kapil and Bhatnagar, 1981). The egg cell lies adjacent to the two synergids (often at the same level as the synergids), and is separated from the synergids by either partial cell walls or plasma membranes alone (Reiser and Fischer, 1993).

Arceuthobium and relevant taxa

Whereas Cohen (1970) could not clearly identify the egg cell of *Arceuthobium campylopodum*, Bhandari and Vohra (1983) stated that the egg cell of the Viscaceae is easily recognizable as the largest and most prominent cell in the embryo sac. Although not agreeing that the egg cell is the largest cell of the embryo sac, Zaki and Kuijt (1994) stated that the egg cell of *Viscum minimum* extends further into the central cell than do the synergids. Hudson (1966) did not comment on possible size differences between the egg cell and the synergids in *A. americanum*, but did report that the egg cell lies above

and to the side of the synergids; this should be confirmed. Hudson (1966) suggested that cell walls form around five of the eight nuclei of the embryo sac in *A. americanum*, leaving the egg and two polar nuclei within the same cell. Hudson (1966) did not mention if double fertilization could trigger cell wall formation.

Zaki and Kuijt (1994) provided a detailed examination of the egg cell of *Viscum minimum* at the ultrastructural level. The egg cell of *V. minimum* features a large vacuole that occupies a significant portion of its volume along with numerous small vacuoles. The large nucleus encloses a prominent nucleolus and is surrounded by a small amount of cytoplasm. The cytoplasm possesses a range of organelles including plastids of various shapes and sizes, underdeveloped mitochondria, and lipid bodies within both the cytoplasm and plastids. Zaki and Kuijt (1994) believed that these lipid bodies might represent a type of reserve for the developing egg cell. The absence of polysomes, endoplasmic reticulum, Golgi bodies, and well-developed mitochondria suggests that the egg cell possesses a low level of activity.

The relative disposition of the nucleus and the vacuole of the egg cell of *Arceuthobium minutissimum* (Bhandari and Nanda, 1968a) and of *Viscum minimum* (Zaki and Kuijt, 1994) does not conform to that characteristic of other flowering plants. In most flowering plants, the cytoplasm and nucleus are adjacent to the central cell, but in *A. minutissimum* (Bhandari and Nanda, 1968a) and *V. minimum* (Zaki and Kuijt, 1994), the cytoplasm and nucleus are adjacent to the embryo sac wall. The egg cell of the Loranthaceae, however, has the typical disposition in which the cytoplasm and nucleus are found adjacent to the central cell (Bhatnagar and Johri, 1983).

6B. Pre-fertilization synergids

Typical flowering plants

In the mature embryo sac, the majority of the synergid cytoplasm and organelles (including the nucleus) is located adjacent to the embryo sac wall (Kapil and Bhatnagar, 1981). Note that this configuration is opposite to the polarization of an egg cell in a typical flowering plant. The synergids are typically more metabolically active than the egg cell, due to the relative abundance and variety of organelles of the synergid compared to the egg cell. The synergids possess numerous organelles, including endoplasmic

reticulum, ribosomes, plastids, and mitochondria, which are suggestive of a high metabolic rate. Like the egg cell walls, the synergid cell walls are usually complete only in the regions adjacent to the embryo sac wall, and are either absent or have extensive gaps in the regions near the central cell.

Synergids are considered to be transfer cells (Mauseth, 1988). A transfer cell has cell walls with irregular ingrowths or labyrinthine protuberances that project into the cell (Jensen, 1965). These ingrowths greatly increase the area of inner surface. Because the plasma membrane is appressed to all the contours of the ingrowths, the plasma membrane also has a large surface area that presumably allows it to have more molecular pumps. In the synergids, the embryo sac wall and the cell wall between the two synergids are modified into transfer cell walls that are collectively called the filiform apparatus. While mitochondria play an important part in providing energy to initiate and establish new membrane extensions around the filiform apparatus, both Golgi bodies and endoplasmic reticulum participate in this process by producing precursors for the cell wall components of the filiform apparatus (Zaki and Kuijt, 1994). Although there is much variation in the filiform apparati of flowering plants, as some are merely thick pads of cell wall material, all filiform apparati appear to play a role in short distance apoplastic transport (Raghavan, 1986).

The synergids might play roles in development of the embryo sac prior to and following fertilization (Reiser and Fischer, 1993). Synergids possibly produce an attractant for the pollen tube, ensure the delivery of the sperm into the egg and central cell, and/or absorb nutrients from the nucellus for transport into the egg and central cell. Typically, one synergid begins to degenerate soon after pollination has taken place but before the pollen tube has reached the embryo sac (Raven *et al.*, 1999). This synergid, which will ultimately receive the pollen tube, is referred to as the degenerate synergid, whereas the other synergid is referred to as the persistent synergid.

Arceuthobium and relevant taxa

Very little literature exists on the synergids of Viscaceae in general, and the presence or absence of a filiform apparatus is not mentioned in many reports. Moreover, the categorization of synergids as degenerate or persistent has not been attempted. Cohen

(1970) could not even distinguish synergids in *Arceuthobium campylopodum*. The synergids of *Eubrachion* lack filiform apparati (Bhandari and Indira, 1969). The synergids of *Viscum minimum* possess a thick, fibrillar filiform apparatus (Zaki and Kuijt, 1994). The synergids of Loranthaceae do have a filiform apparatus and usually degenerate soon after fertilization (Bhatnagar and Johri, 1983). The synergids of *A. americanum* have not been examined in any detail.

Only Zaki and Kuijt (1994) have described the ultrastructure of the synergids in a mistletoe. The two synergids of *Viscum minimum* appear structurally identical, each containing a large nucleus and dense cytoplasm near the central cell, which is the opposite configuration to typical flowering plant synergids. The synergids of *V. minimum* possess numerous small vacuoles distributed throughout the cytoplasm, and the cytoplasm appears dense due to the large amounts of ribosomes and polysomes. In contrast with the egg cell of *V. minimum*, Golgi bodies are abundant in the cytoplasm and are associated with numerous small vesicles. The latter are dispersed throughout the synergids. Rough endoplasmic reticulum, polysomes, lipid bodies, plastids, and well-developed mitochondria are also observed in the cytoplasm. The fibrillar filiform apparatus gradually thins toward the central cell where only a thin cell wall separates the synergids from the egg cell.

6C. Pre-fertilization antipodals

Typical flowering plants

The antipodals show the greatest variation in structure, shape, number, and Golgi body content among the cells of the embryo sac, but little work has been done with regard to these cells (Reiser and Fischer, 1993). This great variation raises questions about the significance and function of antipodals in the embryo sac. Although no specific function has been attributed, the antipodals, like synergids, might be involved in the import of nutrients to the embryo sac. The antipodals also appear to have high metabolic rates, as they possess numerous ribosomes and plastids, as well as a large amount of endoplasmic reticulum. However, the antipodal cell walls are usually complete, even in regions near the unfertilized central cell.

Arceuthobium and relevant taxa

As was the case for most flowering plants, the antipodals of Viscaceae, including *Arceuthobium*, are not well described in the literature. Cohen (1970) could not positively identify the antipodals in *Arceuthobium campylopodum*. The antipodals of *A. pusillum* are persistent and are delimited by rather substantial crosswalls (Tainter, 1968). However, the antipodals of *A. minutissimum* are not persistent and degenerate shortly after their development (Bhandari and Nanda, 1968a). The antipodals of *Eubrachion*, like *A. pusillum*, are persistent (Bhandari and Indira, 1969). The antipodals of *Viscum minimum* show various stages of degeneration among the three cells: while one antipodal appears healthy and metabolically active, the other two show various stages of degeneration (Zaki and Kuijt, 1994). In *V. minimum*, the crosswalls delimiting the antipodals from each other as well as the cell walls separating the antipodals from the central cell appear to be made of fibrillar material, and are quite substantial (Zaki and Kuijt, 1994), as were the antipodal crosswalls of *A. pusillum* (Tainter, 1968). The antipodals of *A. americanum* remain to be examined.

Ultrastructural work has only been performed on the antipodals of one mistletoe, *Viscum minimum* (Zaki and Kuijt, 1994). In this species, the antipodals have prominent, centrally located nuclei that possess evenly distributed chromatin. The cytoplasm of the one healthy antipodal contains vacuoles, plastids, mitochondria, Golgi bodies, and endoplasmic reticulum. Lipid bodies are also seen in the cytoplasm of the one healthy antipodal along with some starch grains in the plastids. The other two antipodals lack these organelles, suggesting that they are less physiologically active than the healthy one.

6D. Unfertilized central cell

Typical flowering plants

The central cell, usually the largest cell of the typical flowering plant embryo sac, is also rich in organelles and appears to be the site of much synthesis (Mauseth, 1988). In the cytoplasm, large plastids, endoplasmic reticulum, ribosomes, starch, lipid bodies, and mitochondria are found in abundance. The engagement of the central cell in high synthetic activity and accumulation of reserves in the form of starch and lipid bodies may be necessary if the central cell plays a significant physiological role in the nourishment of

the egg cell (Zaki and Kuijt, 1994). The embryo sac wall bordering the unfertilized central cell typically possesses transfer cell wall ingrowths that aid in the uptake of materials for synthetic activity (Reiser and Fischer, 1993). Most of the cytoplasm lies near the egg apparatus, whereas a large vacuole occupies the remainder of the central cell. Polar nuclei are generally found in the middle of the central cell, although in some flowering plants, the polar nuclei may be closer to the egg apparatus. The central cell wall is either absent or has extensive holes where it lies in contact with the cells of the egg apparatus.

The unfertilized central cell of some species may send out projections called caeca (pouches; singular: caecum) or haustoria that invade surrounding tissues (Mauseth, 1988). These will be described in section I - 11 of this chapter.

Arceuthobium and relevant taxa

There are a few reports regarding the unfertilized central cells of mistletoes, and none of these refer to *Arceuthobium* species. In fact, aside from statements suggesting that the two polar nuclei of *Eubrachion* (Bhandari and Indira, 1969) and of *Viscum minimum* (Zaki and Kuijt, 1994) are almost equal in size, the mistletoe literature makes no significant reference to the unfertilized central cell. Central cell caeca will be described in section I - 11 of this chapter.

Only Zaki and Kuijt (1994) further discuss the central cell and polar nuclei of a mistletoe at the ultrastructural level. The central cell of *Viscum minimum* surrounds a major part of the egg apparatus, particularly the egg cell, and extends to the lower pole of the embryo sac where it borders the antipodals (Zaki and Kuijt, 1994). The central cell occupies the major portion of the embryo sac, is highly vacuolated, and is the largest cell of the embryo sac, as would be expected. Most cytoplasm of the central cell lines the periphery as a thin layer and contains small vacuoles, lipid bodies, mitochondria, and endoplasmic reticulum. A small amount of cytoplasm also surrounds the two polar nuclei and contains a range of organelles including small vacuoles, starch-containing plastids, mitochondria, endoplasmic reticulum, lipid bodies, free ribosomes, and polysomes. The organellar composition of both the peripheral and nucleus-associated cytoplasm in the

central cell of *V. minimum* indicates the high cellular activity of the central cell, which is confirmed by the presence of starch and lipid bodies.

The two polar nuclei of *Viscum minimum* occupy a central position in the embryo sac, but lie slightly closer to the egg apparatus at the upper pole of the embryo sac (Zaki and Kuijt, 1994). The two polar nuclei have dispersed chromatin and large prominent nucleoli. The two nuclei appear identical, and once they meet prior to fertilization, it is difficult to distinguish one nucleus from the other because portions of their outer nuclear membranes are closely appressed to each other, and no cytoplasm can be seen between the two outer membranes. However, there is no sign of actual fusion between the nuclei.

7. Pollination and Pollen Tube Growth

7A. Typical flowering plants

The process whereby the pollen is transferred to the stigma is called pollination (Raven *et al.*, 1999). The surface of many stigmas is essentially glandular or secretory tissue that secretes a sugary solution or exudate, and this exudate facilitates the process of pollen entrapment. Once in contact with the stigma, the pollen grains take up additional water and are said to germinate. In the process of pollen germination, which is possibly also facilitated by the stigmatic exudate, the tube cell grows through one of the pollen grain wall apertures, forming a pollen tube (Mauseth, 1988). Typically, all of the tube cell cytoplasm moves into the pollen tube, carrying the tube nucleus as well as the generative cell or the two sperm cells with it. If the generative cell has not already divided, it soon does so, forming the two sperm. Many species, especially the wind pollinated ones, are polysiphonous, where each pollen grain may produce up to fourteen separate tubes or where individual tubes are bifurcated (branched). Only one pollen tube will have the tube nucleus and sperm cells, and yet all pollen tubes will be capable of growth.

The pollen tube penetrates into the stigma and grows down through the style (Raven *et al.*, 1999). The style is modified both structurally and physiologically to facilitate the growth of the pollen tube. Most styles have a central region called the stylar canal, which is comprised of transmitting tissue. This tissue consists of specialized thin-walled cells, connects the stigmatic tissue to the ovules, and serves as a path for the

growing pollen tubes. The pollen tube typically makes its way between the cells of the transmitting tissue, and not through them, thus causing little disturbance (Maheshwari, 1950).

Typically only one pollen tube is ultimately capable of penetrating the ovule (Maheshwari, 1950). As a pollen tube grows toward an ovule, it possibly absorbs nutrients from the surrounding transmitting tissue, although the pollen tube itself does not produce much cytoplasm (Mauseth, 1988). Instead, all of the cytoplasm continues to move with the pollen tube tip, whereas the older regions become filled with large vacuoles. Callose plugs are deposited periodically, sealing off the vacuolated areas, and callose is also typically present in the pollen tube cell wall. The pollen tube grows intrusively by tip growth; lateral walls do not slide through the transmission tissue but rather remain where they are deposited. Different opinions have been expressed as to the factors directing the growth of the pollen tubes (Fahn, 1967). Some workers have suggested that there is a chemotropic attraction between the pollen tube and the embryo sac, with the chemical attractant emanating from the filiform apparatus between the synergids, whereas other workers have suggested that the structure and arrangement of the transmitting tissue guide the pollen tube. Once inside the ovary loculus, the pollen tube(s) contacts the ovule, and then one usually grows through the micropyle (porogamy) toward the egg apparatus. There is no term to correctly describe the penetration of an ategmic ovule.

The synergid that is to receive the pollen tube begins to degenerate soon after pollination has taken place but before the pollen tube has reached the embryo sac (Raven *et al.*, 1999). Upon reaching the egg apparatus, a pore is formed in the pollen tube, and the cytoplasm, tube nucleus, and sperm cells are discharged into the degenerating synergid via the filiform apparatus (Cass and Jensen, 1970). The tube cytoplasm and the degenerating synergid cytoplasm do not mix; instead, they remain distinct, even when the tube cytoplasm also begins to degenerate.

7B. *Arceuthobium* and relevant taxa

Pollination studies in the Viscaceae have typically been confined to the determination of pollination vectors (Gilbert, 1988). In *Arceuthobium*, both wind and

insects are believed to aid pollination (Hawksworth and Wiens, 1996), although it would be useful to see if there are any other characteristics of *A. americanum* that could indicate its method of pollination. Pollen in *A. americanum* forms in August or September, prior to the first spring, but the pollen is not dispersed until late March of the first spring (Hudson, 1966; Gilbert, 1988; D.A.R. McQueen, pers. comm., 1995).

Multiple pollen tubes have been observed in the styles of *Arceuthobium* species (Johnson, 1888; Hudson, 1966; D.A.R. McQueen, pers. comm., 1995), as is typical for a flowering plant (Maheshwari, 1950). However, it has not been determined if more than one pollen tube can enter the ovular tissues of any member of the Viscaceae, although D.A.R. McQueen (pers comm., 1995) believed that more than one pollen tube entered the ovular tissues of *A. americanum*. Moreover, D.A.R. McQueen (pers. comm., 1995) thought that the pollen tubes had bifurcated tips.

Hudson (1966) and D.A.R. McQueen (pers. comm., 1995) observed the pollen tubes in the stylar canal of *A. americanum* in early April of the first spring. Hudson (1966) believed it took two months for the pollen tube(s) to grow through the stylar canal and ovular tissues before reaching a functional megaspore, after which the pollen tube(s) would wait for megagametogenesis to complete. In slight contrast, D.A.R. McQueen (pers. comm., 1995) believed that it took only one month for the pollen tubes to grow before reaching a megasporocyte, after which the pollen tubes would wait for both megasporogenesis and megagametogenesis to occur. In *A. oxycedri,* a species that undergoes anthesis in the fall, the pollen tubes apparently overwinter in contact with the embryo sac (Johnson, 1888). Obviously, the timing of pollen tube growth and, as mentioned, megasporogenesis should be re-examined in an *Arceuthobium* species, specifically *Arceuthobium americanum.*

Hudson (1966) further stated that in *Arceuthobium americanum,* megagametogenesis, the formation of a mature embryo sac, and double fertilization (to be described in section I - 8 of this chapter) is not completed until mid June of the first summer. D.A.R. McQueen (pers. comm., 1995) believed that megasporogenesis, megagametogenesis, the formation of a mature embryo sac, and double fertilization is not completed until the end of May of the first spring. Therefore, the time between pollination (late March) and double fertilization (the end of May to mid June) in *A.*

americanum is about two to two and a half months. Hudson's (1966) and D.A.R. McQueen's (pers. comm., 1995) observations on the interval between pollination and fertilization in *A. americanum* disagree with Dowding's (1931) report that fertilization in *A. americanum* occurs within a few days of pollination. Hudson's (1966) and D.A.R. McQueen's (pers. comm., 1995) assertions are also in marked contrast to observations for *A. douglasii* (Jones and Gordon, 1935) and *A. pusillum* (Tainter, 1968) in which the interval between pollination and fertilization is said to be only a few days. Moreover, such a long interval between pollination and fertilization as observed in *A. americanum* (Hudson, 1966; D.A.R. McQueen, pers. comm., 1995) is inordinately long for a flowering plant, since in most flowering plants, the time between pollination and double fertilization is usually about 48 hours (Maheshwari, 1950). Very long intervals between pollination and fertilization are more characteristic of the gymnosperms than the flowering plants (Raven *et al.*, 1999).

Since pollen tube(s) of *Arceuthobium americanum* will reach a megasporocyte (D.A.R. McQueen, pers. comm., 1995) or a functional megaspore (Hudson, 1966) rather than a mature embryo sac, the role of the synergids in pollen tube attraction must be re-examined. Other possible mechanisms of pollen tube attraction that do not involve synergids must be determined. Even if more than one pollen tube or pollen tube tip reaches a megasporocyte (or megaspore/embryo sac), it does not necessarily follow that more than one pollen tube tip will actually penetrate and fertilize the embryo sac when it is formed. Furthermore, in *Arceuthobium*, it has not been determined where the pollen tube discharges into the embryo sac. Hudson (1966) reported that the egg cell of *A. americanum* lies above and to the side of the synergids and stated that this arrangement of the egg apparatus may preclude the normal process of pollen tube discharge into the (degenerating) synergid. It has not been conclusively shown that pollen tube discharge does not occur in some region of the embryo sac that is not adjacent to the egg apparatus.

8. Double Fertilization

8A. Typical flowering plants

After the two (uninucleate haploid) sperm cells are discharged into the degenerate synergid of a typical flowering plant, the two sperm cells begin to migrate toward the

areas of the egg apparatus near the central cell where the cell wall is absent (Russell, 1993). At the interface of the degenerating synergid with the egg cell in a wall-less area, one sperm cell sheds its cell wall (if present), and the plasma membrane of that sperm cell fuses with the plasma membrane of the egg cell. The plasma membrane of the degenerate synergid cannot interfere with this fusion process, as it has degenerated as well. Upon fusion of the sperm cell's plasma membrane with the egg cell plasma membrane, the haploid sperm nucleus enters the egg cell via exocytosis. Similarly, at the interface of the degenerate synergid with the central cell in a wall-less area, the second sperm cell sheds its cell wall (if present), the sperm cell's plasma membrane fuses with the central cell plasma membrane, and the haploid sperm nucleus is exocytosed into the central cell. Entry of a sperm nucleus into the egg cell is believed to precede entry of a sperm nucleus into the central cell (Steffen, 1963).

After one sperm nucleus has entered the egg cell, that haploid sperm nucleus will migrate toward the haploid egg nucleus and fuse with it, forming a diploid nucleus, and thus accomplishing fertilization of the egg cell (Russell, 1993). The fertilized egg cell with the diploid nucleus is now called the zygotic cell or simply the zygote. The low phase of activity associated with the unfertilized egg cell is replaced by a period of high cellular activity immediately following fertilization (Schulz and Jensen, 1968). The unicellular zygote essentially reinstates the sporophytic generation and will develop into the multicellular embryo (Maheshwari, 1950).

Inside the central cell, the second haploid sperm nucleus will migrate towards the two haploid polar nuclei of the typical eight-nucleate, seven-celled embryo sac (Bhatnagar and Sawhney, 1981). The polar nuclei may have already fused to each other, forming a diploid fusion nucleus, or the two polar nuclei may remain unfused. Wide variations in the time of fusion of the two polar nuclei have been observed in various species of flowering plants (Raghavan, 1986). The second sperm nucleus will fuse with the two polar nuclei, producing the triploid primary endosperm nucleus, and thus accomplishing fertilization of the central cell. The process by which the sperm nucleus fuses with the two polar nuclei can also be called triple fusion. The fertilized central cell represents the first cell of the nutritive endosperm tissue, although the endosperm will

develop in different ways in different species. As implied, the egg cell is typically fertilized before the central cell (Steffen, 1963).

As two sperm nuclei are involved in the fertilization process, and both the egg cell and the central cell are fertilized, the fertilization process in flowering plants is called double fertilization (Raven *et al*, 1999). However, only true fertilization involves syngamy, which is the fusion of the sperm nucleus and the egg nucleus. After double fertilization, the embryo sac, which is held within the nucellus, can be called a fertilized embryo sac and the ovule then conventionally called a seed (Reiser and Fischer, 1993). The integuments, if present, will begin to differentiate into a protective seed coat. In addition, the pericarp begins to develop into the fruit after double fertilization. The endosperm and embryo develop within the confines of the original embryo sac wall, which gradually expands to accommodate this growth. The endosperm usually develops before the embryo.

8B. *Arceuthobium* and relevant taxa

Very few detailed accounts exist with regard to double fertilization in *Arceuthobium* and relevant taxa, although the process is said to be common to all Viscaceae (Bhandari and Vohra, 1983). The time when degeneration of the unsuccessful embryo sac(s) occurs relative to double fertilization is clear for only a few *Arceuthobium* species. Fertilization of the egg cell via one sperm nucleus occurs before fertilization of the polar nuclei and endosperm formation in *A. minutissimum* (Bhandari and Nanda, 1968a) as well as *A. pusillum* (Tainter, 1968) and *Eubrachion* (Bhandari and Indira, 1969). Double fertilization has not been conclusively observed in *A. americanum* or in *A. douglasii*.

There is apparently interspecific variation as to how the triploid endosperm comes into being in the Viscaceae. In *Korthalsella*, *Ginalloa* (Rutishauser, 1935; 1937) *Viscum articulatum* (Steindl, 1935), and *Phoradendron flavescens* (Billings, 1933), the two polar nuclei and the male nucleus fuse simultaneously. In *Viscum album* (Steindl, 1935), *Arceuthobium minutissimum* (Bhandari and Nanda, 1968a), and *Eubrachion* (Eremolepidaceae) (Bhandari and Indira, 1969), the sperm nucleus fuses with one of the polar nuclei and the resulting diploid nucleus becomes confluent with the second polar

nucleus to accomplish triple fusion. In *A. pusillum* (Tainter, 1968) and *A. campylopodum* (Cohen, 1970), the two polar nuclei form a secondary or fusion nucleus before the sperm nucleus fuses with it. Zaki and Kuijt (1994) state that because the two polar nuclei of *V. minimum* are appressed to each other but not fused at the nuclear envelope, formation of a secondary or fusion nucleus does not take place, but the mechanism of triple fusion is not explicitly stated. There is little knowledge regarding fertilization in the Loranthaceae (Bhatnagar and Johri, 1983).

9. The Fertilized Embryo Sac

9A. The zygote, its quiescence, and the ending of quiescence

Typical flowering plants

Immediately following fertilization of the egg cell, cell wall material becomes deposited in the region where the egg cell contacts the fertilized central cell (Mogensen and Suthar, 1979). The cell wall in this region was previously absent or had extensive gaps. The zygotic cell wall becomes further thickened by the deposition of a highly cellulosic cell wall over the entire cell boundary (Natesh and Rau, 1984). Thus, a cell wall will completely encircle the newly formed zygote, although the zygote will typically still share a common cell wall with the embryo sac wall. The zygote may vary in size and form not only within a genus but even in the same species (Crété, 1963). However, the overall shape of the zygote is believed to be similar to that of the unfertilized egg cell. Following fertilization, the major change in the cytoplasmic organization of the zygote involves the aggregation of the free ribosomes into polysomes (Diboll, 1968; D'Alascio-Deschamps, 1981). Other typical post-fertilization changes in the cell cytoplasm include the accumulation of starch, lipids, and protein (Raghavan, 1986). The cytoplasm assumes a fairly homogeneous nature, increasing in volume to a certain extent (Maheshwari, 1950). In addition, the large vacuole originally typically present at the pole of the unfertilized egg cell at the embryo sac wall gradually disappears, and thus the cytoplasmic polarity of the egg cell is lost in the zygote. All of these events indicate a shift to a more metabolically active state.

The zygote typically goes into a non-dividing stage called the quiescent period (Mauseth, 1988). The term is somewhat misleading, as metabolic activity is greater than

that observed in the unfertilized egg cell. In a few flowering plants, the zygote may divide once immediately after fertilization, forming a two-celled proembryo, but then the proembryo will not divide again for some time and enters the quiescent period. Nonetheless, during the quiescent period, the primary endosperm nucleus divides and the endosperm develops. The quiescent period of the zygote varies with different species and is to some extent dependent on environmental conditions (Maheshwari, 1950).

Arceuthobium and relevant taxa

In *Arceuthobium* species and most Viscaceae, almost no information exists regarding the changes that occur in the egg cell after it is fertilized to become the zygote. Most changes in an egg cell of a flowering plant following fertilization would take place at the ultrastructural level (Schulz and Jensen, 1968). There is just one report of post-fertilization changes in the egg cell in a Viscaceous species at the electron microscope level. The major change in cytoplasmic organization following fertilization of the egg cell of *Viscum minimum* involves the aggregation of free ribosomes into polysomes in the zygote (Zaki and Kuijt, 1994), as is typical for flowering plants (Diboll, 1968; D'Alascio-Deschamps, 1981). Regarding the Loranthaceae, it has been mentioned that the zygote maintains the same distribution of the vacuole and the cytoplasm that the unfertilized egg cell had (Bhatnagar and Johri, 1983), instead of losing the vacuole, as is typical for flowering plants.

The zygote of most Viscaceae including *Viscum album* (Pisek, 1923; Steindl, 1935), *Korthalsella dacrydii*, *K. opuntia* (Rutishauser, 1935), *Arceuthobium pusillum* (Tainter, 1968), *A. campylopodum* (Cohen, 1970) and *Eubrachion* (Eremolepidaceae) (Bhandari and Indira, 1969), does not undergo its first division until the endosperm has developed to a considerable extent. Therefore, upon formation, the zygote of most Viscaceae immediately enters a quiescent period. The length of the quiescent period of the zygote is not known for most Viscaceae, although Pisek (1923) stated that it is about two months in *Viscum album*. The zygote of both *A. americanum* (Hudson, 1966) and *A. minutissimum* (Bhandari and Nanda, 1968a) is said to divide once after being surrounded by the endosperm in all planes, forming a two-celled proembryo before entering the true quiescent period. No indication is given as to how the zygote/proembryo could become

detached from the embryo sac wall in order to become surrounded by endosperm. Hudson (1966) stated that the two-celled proembryo remained quiescent for three to six weeks before it began to divide, whereas Bhandari and Nanda (1968a) do not describe the length of the quiescent period in *A. minutissimum*. Little is known regarding any changes that might induce the zygote (or two-celled proembryo) of *Arceuthobium* species or relevant taxa to end the quiescent period and divide. It is known that prior to division, the zygote of Loranthaceae elongates considerably (Bhatnagar and Johri, 1983).

9B. Post-fertilization synergids and antipodals

Typical flowering plants

Very little work has been done with regard to changes that occur in the synergids and antipodals of typical flowering plants after double fertilization, except to state that both the synergids and antipodals typically fully degenerate and become crushed (Reiser and Fischer, 1993).

Arceuthobium and relevant taxa

With regard to the other cells of the embryo sac following fertilization, both synergids of *Arceuthobium minutissimum* (Bhandari and Nanda, 1968a) and *A. pusillum* (Tainter, 1968) are said to be ephemeral and fully degenerate at the time of double fertilization. The synergids of *Eubrachion*, however, are said to be persistent (Bhandari and Indira, 1969), although no indication is given as to how long the synergids persist or if there are differences between the two synergids. The post-fertilization antipodals of Viscaceae and Loranthaceae have not been described.

9C. Fertilized central cell

Typical flowering plants

After fertilization, the central cell becomes denser as more organelles are formed (Briarty *et al.*, 1979). The vacuole is believed to dissipate (Folsom and Cass, 1992). As was noted for the unfertilized central cell of some species, the fertilized central cell of certain species may send out caeca/haustoria that invade surrounding tissues (Mauseth, 1988). These will be described in section I - 11 of this chapter.

Arceuthobium and relevant taxa

There has been no work regarding the anatomy or changes in the central cell immediately following its fertilization in *Arceuthobium* and relevant taxa, aside from descriptions of central cell caeca (Hudson, 1966; Tainter, 1968) and reports of fertilized central cell division (Hudson, 1966; Tainter, 1968; Bhandari and Nanda, 1968a). Central cell caecum formation and central cell division will be described in section I - 11 of this chapter. The ultrastructure of the fertilized central cell in *Arceuthobium* remains completely unexplored.

10. Embryo Development (Embryogeny)

10A. Typical flowering plants

Zygotic division, the proembryo, the embryo proper, and suspensors

The embryo develops from the zygote after it exits the quiescent period and initiates division (Crété, 1963). Each zygote typically produces only one embryo (Maheshwari, 1950). The division of the zygote always involves cytokinesis, creating a two-celled proembryo (Crété, 1963). Johansen (1950) stated that, aside from a very few species, the zygotic division is transverse to the long axis of the zygote, as the cell wall that forms is a transverse wall. Of the two embryonic cells formed via a transverse division, the cell that lies toward the interior of the embryo sac is called the terminal or apical cell. The other cell, which is proximal and attached to the embryo sac wall, is called the basal cell. Subsequent divisions of the two-celled proembryo may occur in a variety of patterns (Maheshwari, 1950).

A proembryo typically gives rise to the embryo proper and the suspensor, if present (Crété, 1963). The new sporophyte is derived only from the embryo proper. The suspensor usually consists of just a few cells that push the embryo proper into the endosperm (Mauseth, 1988). Typically, only dicotyledonous species (dicots) form suspensors. In species that do not form suspensors, the proembryo directly gives rise to the embryo proper. Suspensors are most often rather small and inconspicuous, but can range from being virtually absent, which is the common condition, to being well developed and conspicuous, which is rare (Wardlaw, 1955). The suspensor, if present, completes its development early, when the embryo proper consists of only a few cells.

As the embryo grows, the suspensor begins to degenerate, and at embryo maturity, the suspensor has become completely crushed by the growth of the embryo.

Johansen's (1950) embryogeny classification system

Johansen (1950) developed a classification system of embryogeny in which the nature of the orientation of the zygotic division as well as of subsequent divisions allowed for the categorization of six basic embryogeny types. Johansen's (1950) embryogeny classification system also depended upon knowledge of the fate of the young embryonic cells. Each embryogeny type was named for the genus it was first observed in, and usually characterizes the family of that genus, although a given type is not exclusive to the family of the genus in which it was first observed. Occasionally, the embryogeny of a genus may deviate slightly from a given type, in which case the embryogeny is called a variation of the type. Each type can be associated with one or more variations. The types and variations are useful for summarizing early divisions. Following is a list of some of the more important embryogeny types and variations relevant to this thesis, and the genera that best represent these types.

Asterad-type. The Asterad-type is characteristic of the family Asteraceae. In the Asterad-type of embryogeny, the zygotic division is transverse and gives rise to the typical two-celled proembryo with a terminal and basal cell (Johansen, 1950). The division in the terminal cell is longitudinal (the division in the basal cell may vary). Both the terminal and basal cell contribute to the construction of the embryo proper as well as the suspensors. In the *Penaea* variation, both the terminal and basal cell contribute to the construction of the embryo proper, but a suspensor does not differentiate, and thus the terminal and basal cell of the two-celled "pro"embryo essentially represent the embryo proper or simply the embryo.

Solanad-type. The family Solanaceae presents this type of embryogeny, but it also occurs in the Hydnoraceae (Johansen, 1950). In the Solanad-type, the zygotic division is transverse and gives rise to the typical two-celled proembryo with a terminal and basal cell. Each division in the terminal cell and basal cell is also transverse, and thus the Solanad type is based on the formation of a linear four-celled proembryo. The derivatives of the basal cell do not take part in the organization of the embryo proper, as

the embryo proper is mostly derived from the terminal cell. The basal cell gives rise to the suspensor, which can become quite long.

Piperad-type. The Piperad-type is officially characteristic of the Piperaceae, Loranthaceae, Balanophoraceae, and Dipsacaceae (*Scabiosa*) (Johansen, 1950; Bhatnagar and Johri, 1983). The Piperad-type includes all those instances where the zygote undergoes a longitudinal (vertical) or longitudinally-oriented oblique division. In the true Piperad type, division of each cell that resulted from zygotic division is also in the longitudinal plane, but at right angles to the plane of the zygotic division, resulting in four elongated embryonic cells. In the *Dendrophthoe* variation, the early divisions are characteristic of the type, but the suspensor becomes greatly elongated. In the *Balanophora* variation, division of each cell that resulted from zygotic division is also in the longitudinal plane, but the walls that are formed are curved and attached at both ends to the first longitudinal wall, and no suspensor forms. In the *Scabiosa* variation, division of each cell that resulted from zygotic division is in the transverse plane, and the suspensor is rudimentary or absent.

Globular stage of embryo development

Regardless of the type of embryogeny, when the embryo proper (henceforth referred to as the embryo) is eight-celled, it has a ball-like appearance (Maheshwari, 1950). At this point, the embryo is said to have reached the globular stage. The globular embryo is small relative to the many-celled endosperm (endosperm will be described in section I - 11 of this chapter). When the embryo reaches the globular stage, subsequent cell divisions are typically described as being either periclinal, in which cell walls form parallel to the outer bounding surface of the embryo, or anticlinal, in which cell walls form perpendicular to the outer bounding surface of the embryo (Mauseth, 1988). Often, the transition from the eight-celled to the sixteen-celled stage occurs by periclinal cell wall formation and establishes the protoderm. The protoderm is the outermost layer of meristem that later develops into the epidermis.

Once the protoderm has formed, the embryo becomes divided into two distinct populations of cells, an outermost layer of protoderm and an inner population of cells (Mauseth, 1988). The protoderm subsequently develops by anticlinal divisions, while the

inner population of cells divides in all planes. Due to the cell divisions in the protoderm and inner population of cells, the embryo will begin to lengthen.

Heart stage of embryo development

In most dicots, two areas of the embryo begin to protrude into the region where the embryo lies in contact with the endosperm (distal to the initial point of attachment of the embryo to the original embryo sac wall) (Mauseth, 1988). At this time, the embryo is said to have moved into the heart stage. The pole of the embryo where these two protuberances develop is called the cotyledonary pole, as these two protuberances represent the future cotyledons. In a monocotyledon (monocot) embryo at a comparable stage in development, only one protuberance is formed.

Torpedo and cotyledonary stages of embryo development

With continued growth, the embryos of both dicots and monocots become elongated, and enter the torpedo stage (Mauseth, 1988). At this stage, the innermost population of cells that became established during the globular stage differentiate into the procambium (the part of the meristem that gives rise to vascular tissue) and the ground meristem (the part of the meristem that gives rise to the bulk of the plant body). At the cotyledonary pole, the shoot apical meristem typically differentiates and the cotyledon(s) become further developed. At the pole of the embryo opposite from the cotyledonary pole (proximal to the initial point of attachment to the original embryo sac wall), the root apical meristem typically differentiates and the radicle (embryonic root) becomes established. The pole where the radicle differentiates is called the radicular pole. The hypocotyl encompasses the region between the radicular pole and cotyledonary pole, and the cotyledon(s) are attached to the hypocotyl. The embryonic shoot apical meristem typically produces a small amount of embryonic shoot, or epicotyl. Often, when the cotyledons and epicotyl become fully established, the embryo is said to have moved into the cotyledonary stage.

Nutrient reserves of the mature embryo

The cells of the embryo often develop nutrient reserves (Bewley and Black, 1978; Lott, 1981; Parker, 1984a; Parker, 1984b). Starch grains in amyloplasts and protein

bodies are predominant storage forms within the embryo. The method of transfer of nutrients from the endosperm into the embryo is not known, especially considering that plasmodesmata between the embryo and endosperm are lacking (Dute *et al.*, 1989). However, the enzymes adenosine triphosphate phosphohydrolase (ATPase), sucrose synthase, and invertase, which are believed to be involved in the active transport of assimilates, is found in high concentrations over the entire surface of the embryo (Wittich and Willemse, 1999; Van Caeseele *et al.*, 1996). Therefore, the whole surface may be absorptive. Chlorophyllous embryos are not common, being found in only about one-third of all flowering plants (Dahlgren, 1980).

10B. *Arceuthobium* and relevant taxa

Johansen's (1950) embryogeny types: zygotic division, early embryonic divisions, and attainment of the globular stage

Differing observations exist with regard to the plane of zygotic division and thus the type of embryogeny that occurs in the Viscaceae as well as in *Arceuthobium* species. Cohen (1963) ascribed the embryogenesis of *A. douglasii* (Jones and Gordon, 1965), *A. campylopodum*, and *A. pusillum* (Tainter, 1968) to the *Penaea* variation of the Asterad type. Embryogenesis in *Viscum* has been also been ascribed to the *Penaea* variation of the Asterad type (Johansen, 1950). In contrast, because the division of the zygote in *A. minutissimum* was thought to be longitudinal, embryogeny of *A. minutissimum* was said to conform to the *Scabiosa* variation of the Piperad type (Bhandari and Nanda, 1968a). Johansen (1950) himself stated that the embryogeny of *Arceuthobium* conforms to the *Scabiosa* variation of the Piperad type, although no particular species were identified. Embryogenesis in *Korthalsella* of the Viscaceae has similarly been ascribed to the *Scabiosa* variation of the Piperad type (Johansen, 1950). As implied by both putative embryogeny types, no suspensors form in these Viscaceae, and any embryonic cells that develop represent the embryo proper. However, the orientation of the zygotic division and resultant embryogeny type in *A. americanum* has not been documented. It should be noted that *Eubrachion* (Eremolepidaceae) follows the Solanad type (Bhandari and Indira, 1969) and develops long suspensors.

The two-celled embryo resulting from zygotic division is rather poorly characterized in the Viscaceae including most *Arceuthobium* species. The relative sizes and shapes of the first two embryonic cells of *Arceuthobium* species have not been described except in *A. pusillum*, in which the two cells were said to be of equal size and of a hemispherical shape (Tainter, 1968). Bhandari and Nanda (1968a) also implied that the two embryonic cells of *A. minutissimum* are of equal size, although this was not explicitly stated. Relative timing of the early divisions has not been well documented in most *Arceuthobium* species. In *A. pusillum*, division in the two embryonic cells is asynchronous, as the terminal cell divides before the basal cell (Tainter, 1968). Hudson (1966) provided no details regarding the early embryonic divisions of *A. americanum*. Embryos of *A. pusillum* (Tainter, 1968), *A. minutissimum* (Bhandari and Nanda, 1968a), and *A. americanum* (Hudson, 1966) were said to reach the globular stage after the four-celled embryo undergoes further divisions. Hudson (1966) mentioned that the globular stage of *A. americanum* is reached by the end of the first summer. There are no other detailed reports on early embryonic divisions for any other *Arceuthobium* species.

Globular to torpedo stages of embryo development and concurrent tissue differentiation

Embryonic differentiation and the timing of differentiation with regard to the endosperm or season have not been well described for any *Arceuthobium* species. Some information exists for *A. pusillum* (Tainter, 1968) and *A. minutissimum* (Bhandari and Nanda, 1968a). After the embryo of *A. pusillum* reaches the globular stage, periclinal divisions decrease in frequency and the cells in the outermost layer begin dividing anticlinally to keep pace with the internal embryonic growth (Tainter, 1968). This outermost uniseriate layer of cells is then recognizable as embryonic protoderm and forms a continuous, discrete tissue on the upper (future radicular) pole of the embryo (recall the orientation of upper and lower described in section I. - 4B of this chapter). Similarly, the onset of repeated anticlinal divisions in the outer cells of the globular embryo of *A. minutissimum* marks the differentiation of the protoderm and the central group of meristematic cells (Bhandari and Nanda, 1968a). As in *A. pusillum* (Tainter, 1968), the protoderm in *A. minutissimum* (Bhandari and Nanda, 1968a) is continuous at

the upper (future radicular) pole and a conspicuous cuticle lines the protoderm at the upper pole.

Shortly after the uniseriate protoderm is distinguishable in *Arceuthobium pusillum*, the radicular apex differentiates, and continued cell divisions at the radicular pole cause the embryo to appear ovoid to torpedo-shaped (Tainter, 1968). Likewise, further divisions in *A. minutissimum* result in a bipolar, torpedo-shaped embryo with a distinct radicular apex (Bhandari and Nanda, 1968a). In *A. pusillum*, repeated anticlinal divisions of meristematic cells just inside of the protoderm will then give rise to ground meristem, which will appear as a file of cells (Tainter, 1968). Thus, the heart-shaped stage is bypassed in the development of an *Arceuthobium* embryo as proper cotyledons are said to be absent or nearly so (Hawksworth and Wiens, 1996). In *A. pusillum*, only traces of the two vestigial cotyledons were observed, appearing as slight depressions on the lower (coteledonary) pole of the torpedo-shaped embryo (Thoday and Johnson, 1930; Tainter, 1968). Similarly, in *A. minutissimum*, two coteledonary initials originate from the lower pole (cotyledonary) of the embryo, leading to the formation of two small cotyledons on the torpedo-shaped embryo. The presence of rudimentary cotyledons in *A. americanum* has not been validated.

If procambium differentiates in *Arceuthobium* species, it is the last tissue to begin differentiation. Just prior to explosive discharge, anticlinal divisions of cells in the innermost core of cells in the longitudinal axis of the embryo of *Arceuthobium pusillum* differentiates into embryonic procambium (Tainter, 1968). Kuijt (1960) and Cohen (1963) reported a distinct procambial strand and even differentiation of vascular strands in the mature embryo of *A. americanum*, *A. campylopodum* and *A. douglasii*, but Bhandari and Nanda (1968a) did not observe any distinct procambium in *A. minutissimum*.

Mature embryo

The shape and overall appearance of the mature embryo in *Arceuthobium* species and relevant taxa has been described, but little information regarding the ultrastructure, cytochemistry, or nutrient stores of any Viscaceous or Loranthaceous embryo is available. Hudson (1966) mentions that the embryo is mature and ready for

dissemination by late August of the second summer, approximately twenty-four months after floral inception, although the embryo is not specifically described. Although uncommon in flowering plants (Dahlgren, 1980), Viscaceous members (Bhandari and Vohra, 1983) and Loranthaceous members (Bhatnagar and Johri, 1983) are said to possess chlorophyllous embryos. The mature *Arceuthobium* embryo is rod-shaped, and only several millimetres long (Hawksworth and Wiens, 1996). The mature embryo in *Eubrachion* is cylindrical and straight, and the cells of the embryo, except at the radicular end, are said to contain abundant starch grains (Bhandari and Indira, 1969). The mature embryo of the Loranthaceae is three to four mm long and occupies almost two-thirds of the length of the endosperm (Bhatnagar and Johri, 1983). The cells of the Loranthaceous embryo are densely cytoplasmic.

Proper cotyledons are absent or nearly so in *Arceuthobium* species (Hawksworth and Wiens, 1996). Two well-developed cotyledons are, however, present in most other Viscaceae (Bhandari and Vohra, 1983; Sallé, 1983), as well as in *Eubrachion* (Bhandari and Indira, 1969) and Loranthaceae (Bhatnagar and Johri, 1983). The shoot apical meristem is deemed insignificant and undeveloped in all of the Viscaceae (including *Arceuthobium* species), Loranthaceae, and in *Eubrachion* (Eremolepidaceae).

The mature embryo of both Viscaceous and Loranthaceous species reveals a well-developed hypocotyl (Bhandari and Vohra, 1983). The "radicle" of Viscaceous and Loranthaceous embryos is not a true radicle, but instead is a hypocotyledonary extension showing endarch, collateral bundles (Johri and Ambegaokar, 1984). Moreover, the swollen, meristematic "radicular" apex lacks a root cap. Similarly, in *Eubrachion*, no true radicle is formed (Bhandari and Indira, 1969). However, as the hypocotyledonary extension will develop into a haustorial process that superficially resembles a root, it makes more sense to continue to refer to this structure as radicular, and to refer to the upper pole of the embryo as the radicular pole (Kuijt, 1969).

The embryos of Viscaceae, Loranthaceae, and *Eubrachion* are essentially reduced or rudimentary embryos (Bhandari and Nanda, 1968a; Bhandari and Indira, 1969; Hawksworth and Wiens, 1996), lacking a notable shoot apex, true radicle, and coteledonary development.

Potential and realized polyembryony

In the Viscaceae (Bhandari and Vohra, 1983) and in *Eubrachion* (Bhandari and Indira, 1969), neither polyembryony nor polyendospermy (composite endosperm) is definitive of the family (Johri, 1963b). However, in the Loranthaceae (Bhatnagar and Johri, 1983) as well as in *Viscum minimum* (Zaki and Kuijt, 1994), the multiple embryo sacs frequently give rise to multiple embryos and endosperms, although only one embryo usually matures/germinates. Nonetheless, polyembryony in *Arceuthobium* species, although rare, has been recorded (Hawksworth and Wiens, 1996). Hudson (1966) noted one instance in which two embryos were found within the same dispersal unit of *A. americanum*. Similarly, Tainter (1968) occasionally observed two embryos in the dispersal unit of *A. pusillum*. Hawksworth (1961) also observed rare polyembryony in *Arceuthobium* species, reporting that only about 1% of the dispersal units of *A. americanum* and *A. vaginatum* subsp. *cryptopodum* contained two embryos and two endosperms. Weir (1914) found somewhat higher levels of polyembryony in *A. vaginatum* subsp. *cryptopodum* (15%) and *A. douglasii* (13%). In addition, more than one embryo as well as more than one endosperm could occasionally be found in *Viscum album* (Sallé, 1983).

11. Embryo Sac Expansion and Endosperm Development

11A. General comments regarding embryo sac expansion, embryo sac caeca, and endosperm caeca

Embryo sac expansion takes place in all flowering plants, as the unfertilized embryo sac is usually larger than any of the surrounding cells (Reiser and Fischer, 1993). Such expansion is extreme in few Viscaceous genera (Rutishauser, 1935, 1937; York, 1913); Rutishauser, 1937; Billings, 1933; Zaki and Kuijt, 1994), but this phenomenon is more characteristic of the Loranthaceae (Bhatnagar and Johri, 1993) and *Eubrachion* (Bhandari and Indira, 1969). In these taxa, the extreme elongation and expansion is a pre-fertilization event, as elongation begins at the four-nucleate stage and continues within the central cell of the unfertilized embryo sac.

Such expansion via elongation seen in some Viscaceae and all Loranthaceae is not to be confused with embryo sac expansion via the formation of caeca that can emanate

from one or more cells of the embryo sac in flowering plants. Again, vacuolar expansion is believed to aid in caecum formation (Maheshwari, 1950). These caeca may emanate from (a) given cell(s) of the embryo sac prior to double fertilization, or form as a result of double fertilization (Mikesell, 1990). As implied earlier, embryo sac caeca most commonly originate from the central cell. As it is sometimes difficult to determine if fertilization has taken place, it can be equally difficult to determine if formation of a caecum is a pre- or post-fertilization phenomenon. Although the caeca are believed to function in general embryo sac expansion, some caeca have been credited with having haustorial function (and called "haustoria"), despite the fact that haustorial function has not necessarily been validated. If the unfertilized or fertilized central cell contributes to the formation of an embryo sac caecum, endosperm nuclei or cells may proliferate in the caecum, and the embryo sac caecum can also be called an endosperm caecum or haustorium (endosperm will be described in section I - 11B of this chapter). Some caeca do not form immediately after double fertilization but do so from a more well-developed endosperm. These caeca are also called endosperm haustoria, although again, haustorial properties have not been proven (Mikesell, 1990). Overall, about 76% of flowering plant families have unfertilized embryo sac caeca, fertilized embryo sac caeca, and/or endosperm caeca.

11B. Endosperm development in typical flowering plants

Types of endosperm development

The fertilized central cell with its primary endosperm nucleus represents the first cell of the nutritive endosperm tissue (Maheshwari, 1950). Following fertilization, the primary endosperm nucleus begins one of three possible types of development: nuclear endosperm development, cellular endosperm development, or helobial endosperm development. Endosperm development typically begins before embryo development. Different species follow different patterns of development.

Nuclear endosperm development. Nuclear endosperm development is the most common type of endosperm development, occurring in almost two hundred families of both dicots and monocots (Mauseth, 1988). In nuclear endosperm development, mitotic nuclear divisions are not accompanied by cytokinesis, at least not initially, and the

endosperm grows as a coenocyte (multinucleate entity) within the fertilized central cell. These mitotic nuclear divisions are often synchronous. The cytoplasm and organelles tend to accumulate along the periphery of the central cell, and a large vacuole forms in the centre. The endosperm may remain in a coenocytic condition until maturity. More typically, though, each nucleus becomes enclosed within a cell after the coenocytic endosperm reaches a certain size.

Cellular endosperm development. Cellular endosperm development occurs in about seventy families (Mauseth, 1988). Except for the Araceae and the Lemnaceae, these families are all dicots. Often, plants with bisporic megasporogenesis also undergo cellular endosperm development. In cellular endosperm development, mitosis is typical: the first mitotic division of the primary endosperm nucleus is followed immediately by cytokinesis, and the first two endosperm cells are established. All of the subsequent mitotic divisions are typical, as all mitotic nuclear divisions are accompanied by cytokinesis. Cellular endosperm development is also called *ab initio* cellular development because the endosperm is cellular from its initiation and throughout all of its development. Very few studies have dealt with the cytochemistry and ultrastructure of cellular endosperm (Vijayaraghavan and Prabhakar, 1984).

Helobial endosperm development. Helobial endosperm development is rare, occurring in only seventeen families, fourteen of which are monocots (Mauseth, 1988). Helobial endosperm development is essentially a combination of nuclear and cellular endosperm development in which part of the endosperm remains nuclear, and part remains cellular.

Endosperm maturation

The nature of endosperm development (nuclear, cellular, or helobial) does not appear to influence the distribution of reserves and organelles in the endosperm (Mauseth, 1988). Starch, the most common storage material, can be found in amyloplasts, and these amyloplasts become more numerous throughout development (Bewley and Black, 1978). Protein (Lott, 1981) and lipid bodies (Bewley and Black, 1978) may accumulate. Mitochondria increase in number and swell, presumably due to greater biochemical activity (van Went, 1970). The endosperm of some species may

become quite chlorophyllous and appear very green, such as the endosperms of Viscaceae (Calder, 1983), *Coffea* (Carvalho *et al.*, 1991), and some Brassicaceae (Yoffe, 1952). However, the presence of chlorophyll in endosperm has not been well documented in the literature.

In the developing endosperm of some species, zonation may occur (Mauseth, 1988). For example, in most flowering plants, there is a starch-free zone near the embryo due to the likely absorption of these materials by the embryo. The developing endosperm forms a rather large mass with a smooth contour (Maheshwari, 1950). The growing endosperm completely crushes the remainder of the nucellus, and it is believed that the increased amount of storage materials within the endosperm is a result of the consumption of the nucellus by the endosperm (Norstog, 1974; Pacini *et al.*, 1975). However, the mechanism by which the nucellus is possibly consumed is not known. Typically, no nucellar tissue remains when the seed is fully developed (Maheshwari, 1950).

At maturity, the cells of the endosperm are usually isodiametric and store large quantities of food reserves (Maheshwari, 1950). In most plant families, the mature endosperm appears to consist of living cells, although in some cases it consists of both living and dead cells, as in Poaceae and Fabaceae. Just as no nucellar tissue remains in the fully-developed seed, in many cases, no endosperm remains in a mature seed, and this type of seed is called an exalbuminous, or non-endospermous seed (Jacobsen, 1984). Exalbuminous seeds are much more common in dicots than in monocots. In albuminous, or endospermous seeds, large amounts of endosperm are present at seed maturity.

11C. Caecum formation and endosperm development in *Arceuthobium* and relevant taxa

Caecum formation and first division of the primary endosperm nucleus

Some type of embryo sac caecum formation is believed to occur in *Arceuthobium* species. For the most part, formation of the embryo sac caecum is related to endosperm development, although specific reference to the role of the central cell in caecum formation is rarely made. It is not clear as to which cell(s) of the embryo sac contribute to the caecum, and where known for certain species, these are not necessarily consistent

with observations made for other species. There are differences of opinion as to whether a caecum forms from both embryo sacs, if the embryo sac underwent double fertilization prior to caecum formation, if any cell or nuclear division took place before caecum formation, and if partitioning of the embryo sac occurred prior to caecum formation. All authors studying *Arceuthobium* (Thoday and Johnson, 1930; Jones and Gordon, 1965; Tainter, 1968; Bhandari and Nanda, 1968a, b; Cohen, 1970) stated that the caecum has a haustorial function, although this was not validated. Similarly, these authors all believed that the caecum reached the base of the ovary.

Thoday and Johnson (1930) stated that a caecum emanated from the upper pole of the embryo sac of *Arceuthobium pusillum*, and noted that the antipodals, which would be situated at the upper pole of the embryo sac, were found within the caecum. However, no indication was given as to whether the embryo sac had undergone (double) fertilization, or if both embryo sacs could produce a caecum.

Tainter's (1968) observations on caecum formation in *Arceuthobium pusillum* contrast with Thoday and Johnson's (1930) observations. Tainter (1968) stated that following double fertilization but prior to nuclear division and caecum formation, a transversely-oblique cell wall segregated the embryo sac into two chambers: an upper chamber that contained the zygote and degenerating synergids and a lower chamber that included the primary endosperm nucleus and degenerating antipodals. These observations are odd for two reasons. Firstly, cell wall formation does not typically precede nuclear division. Secondly, in most *Arceuthobium* species (including *A. pusillum*) the egg apparatus arises at the lower pole of the embryo sac while the antipodals arise at the upper pole, so it is unclear how a lower chamber could contain the antipodals. Nonetheless, Tainter (1968) went on to state that a lateral caecum emerged from the lower chamber, and that the primary endosperm nucleus migrated into the caecum. The fact that double fertilization occurred prior to caecum formation in *A. pusillum* suggested that only one embryo sac formed a caecum, since the other embryo sac was believed to degenerate prior to double fertilization (Tainter, 1968). After its migration into the caecum, the primary endosperm nucleus divided: one endosperm daughter nucleus remained in the caecum, while the other daughter endosperm nucleus migrated back into the region near the zygote. A cell wall then formed at the mouth of

the caecum (the point where the caecum is attached to the embryo sac), cutting off the daughter nucleus in the caecum from the rest of the embryo sac. This effectively resulted in the formation of a two-celled endosperm: the caecum was one endosperm cell and the cell in the vicinity of the zygote was the other.

A similar situation in which a transversely-oblique cell wall partitioned the embryo sac following double fertilization but prior to nuclear division and lateral caecum formation also occurred in *Arceuthobium campylopodum* (Cohen, 1970). It cannot be stated if only one embryo sac was capable of forming a caecum, since the production of successful embryo sacs was not described in *A. campylopodum*. Cohen (1970) suggested that the transversely-oblique cell wall partitioned the embryo sac of *A. campylopodum* into a lower chamber that contained only the antipodals (Cohen thought there were only two antipodals) and an upper chamber that contained the zygote, the primary endosperm nucleus, and the synergids. Thus, the same problem that was noted for *A. pusillum* is also evident in *A. campylopodum* with regard to the antipodals residing in a lower chamber. However, Cohen (1970) could not ascertain where the egg apparatus was relative to the antipodals in the unfertilized embryo sac of *A. campylopodum*, so his comments regarding embryo sac partitioning are questionable. Cohen (1970) then stated that a lateral caecum emerged from the upper chamber, but did not mention whether the primary endosperm nucleus of *A. campylopodum* migrated into the caecum as it did in *A. pusillum* (Tainter, 1968). Cohen (1970) did not provide any more information on caecum development or the primary endosperm nucleus.

A transversely-oblique cell wall was also believed to partition the embryo sac following double fertilization but prior to nuclear division and lateral caecum formation in *Arceuthobium douglasii* (Jones and Gordon, 1965; Bhandari and Nanda, 1968b) and *A. americanum* (Hudson, 1966). As in *A. pusillum* (Tainter, 1968), only one embryo sac of *A. douglasii* (Jones and Gordon, 1965; Bhandari and Nanda, 1968b) and *A. americanum* (Hudson, 1966; Calvin, 1996) was believed to undergo (double) fertilization, and thus only one embryo sac would have produced a caecum. However, in *A. americanum* (Hudson, 1966) and *A. douglasii* (Jones and Gordon, 1965; Bhandari and Nanda, 1968b), it was the lower chamber rather than the upper chamber that contained the zygote and the synergids, while the upper chamber contained the antipodals and the primary endosperm

nucleus. Thus, the fertilized embryo sac apparently maintained the same polarity as an unfertilized embryo sac, with the egg apparatus at the lower pole and the antipodals at the upper pole. In *A. americanum* (Hudson, 1966) and *A. douglasii* (Jones and Gordon, 1965; Bhandari and Nanda, 1968b), the lateral caecum emerged from the upper chamber. The primary endosperm nucleus did not migrate into the caecum in either *A. douglasii* (Jones and Gordon, 1965; Bhandari and Nanda, 1968b) or *A. americanum* (Hudson, 1966) as it did in *A. pusillum* (Tainter, 1968). Rather, in these two species, the primary endosperm nucleus divided in the vicinity of the zygote, after which one endosperm daughter nucleus migrated into the caecum, while the other endosperm daughter nucleus remained in the vicinity of the zygote. A cell wall then formed between the two daughter endosperm nuclei at the mouth of the caecum, as was described for *A. pusillum* (Tainter, 1968).

As described for the species above, double fertilization also preceded the formation of a lateral caecum in *A. minutissimum* (Bhandari and Nanda, 1968a). In *A. minutissimum*, one embryo sac was believed to degenerate prior to double fertilization (Bhandari and Nanda, 1968a), and thus only one embryo sac develops a caecum. As in *A. douglasii* and *A. americanum*, there was no apparent reversal in the polarity of the unfertilized as compared to the fertilized embryo sac. Unlike the other *Arceuthobium* species, however, there was no partitioning of the embryo sac prior to nuclear division and lateral caecum formation in *A. minutissimum* (Bhandari and Nanda, 1968a). Rather, the lateral caecum originated from the embryo sac just below the level of the zygote and approximately diagonally opposite to and prior to division of the primary endosperm nucleus. Like *A. douglasii* and *A. americanum*, the primary endosperm nucleus of *A. minutissimum* divided in the vicinity of the zygote. One endosperm daughter nucleus migrated into the caecum, while the other endosperm daughter nucleus remained in the vicinity of the zygote. Moreover, as in *A. pusillum* (Tainter, 1968), *A. douglasii* (Jones and Gordon, 1965; Bhandari and Nanda, 1968b) and *A. americanum* (Hudson, 1966), a cell wall formed between the two daughter endosperm nuclei, resulting in a two-celled endosperm.

Interestingly, no embryo sac caeca occur in *Eubrachion* (Bhandari and Indira, 1969) or *Viscum minimum* (Zaki and Kuijt, 1994). No information is available regarding

caecum formation in any other Viscaceae. Although the Loranthaceae all show embryo sac elongation, formation of a lateral caecum of the embryo sac occurs only in *Nuytsia* and *Atkinsonia* (Bhatnagar and Johri, 1983). The development of the caecum in these species is quite different from that observed in *Arceuthobium*.

Early endosperm development

Division of the primary endosperm nucleus in studied *Arceuthobium* species is followed by cell wall formation between the two endosperm daughter nuclei, and as further divisions of endosperm nuclei are (generally) followed by cell wall formation, endosperm development in *Arceuthobium* is cellular (Hawksworth and Wiens, 1996). Likewise, endosperm development in all other members within the order Santalales is cellular (Bhandari and Vohra, 1983; Bhatnagar and Johri, 1983). Division of the primary endosperm nucleus in *Arceuthobium* species generally precedes division of the zygote (Jones and Gordon, 1965; Hudson, 1966; Tainter, 1968; Bhandari and Nanda, 1968a, b; Calder, 1996), and therefore the endosperm develops before the embryo, as is typical of flowering plants (Maheshwari, 1950). However, there are some differences of opinion regarding endosperm divisions in the caecum as well as in the vicinity of the zygote in *Arceuthobium* species.

Bhandari and Nanda (1968a) stated that no divisions occurred in the caecum of *Arceuthobium minutissimum*, and that the caecum remained uninucleate due to the presence of the undivided primary endosperm daughter nucleus. However, in both *A. pusillum* (Tainter, 1968) and *A. douglasii* (Jones and Gordon, 1965; Bhandari and Nanda, 1968b), the primary endosperm daughter nucleus in the caecum underwent cellular divisions, filling the caecum with a uniseriate file of endosperm cells. The primary endosperm daughter nucleus in the caecum of *A. americanum* apparently underwent several rounds of free-nuclear divisions prior to cellularization and formation of a uniseriate file (Hudson, 1966). Calvin (1996) illustrated the presence of a uniseriate caecum in *A. americanum* and *A. cyanocarpum*, although he did not specify if cellular or free-nuclear divisions preceded the formation of the uniseriate caecum. Hudson (1966) further stated that the caecum of *A. americanum* did not remain uniseriate, but that tiers of cells then formed within the caecum, which persisted throughout embryogenesis.

In all *Arceuthobium* species in which endosperm development has been studied, the endosperm proper (or simply endosperm) apparently developed from the cell containing the primary endosperm daughter nucleus that resided (or came to reside) in the vicinity of the zygote (Hawksworth and Wiens, 1996). From this first endosperm daughter cell near the zygote, cellular endosperm proliferated and apparently surrounded the zygote/embryo (Calder, 1996). As implied earlier, no indication was given as to how the zygote became detached from the embryo sac wall in order to permit envelopment by the endosperm. In *A. pusillum*, the endosperm cell divisions in the vicinity of the zygote were anticlinal with respect to the outer surface of the zygote, and thus produced a uniseriate layer of cells that surrounded the zygote (Thoday and Johnson, 1930; Tainter, 1968). Similarly, a uniseriate plate-like layer of endosperm cells formed around the zygote of *A. americanum* (Hudson, 1966). Hudson (1966) added that large triangular to rectangular endosperm cells encircled the zygote in both a clockwise and a counterclockwise fashion. Hudson (1966) further stated that after the zygote had been encircled by the endosperm cells in one plane, the large triangular endosperm cells underwent anticlinal and periclinal divisions to completely surround the zygote in all planes. Drawings of the two-celled embryo of *A minutissimum* also clearly show that a small amount of cellular endosperm surrounded the young embryo (Bhandari and Nanda, 1968a). However, it was not clear whether the cellular endosperm of *A. minutissimum* (Bhandari and Nanda, 1968a) initially surrounded the zygote in a uniseriate layer, as it did in *A. pusillum* (Thoday and Johnson, 1930; Tainter, 1968) and *A. americanum* (Hudson, 1966).

Little is known about early endosperm development in *Eubrachion* (Bhandari and Indira, 1969), and the authors made no mention of endosperm surrounding the zygote or embryo. Loranthaceae are known to have a uniform development of endosperm that is considerably different from that of the Viscaceae (Bhatnagar and Johri, 1983), although again there is no mention of the endosperm surrounding the zygote or embryo. In the Loranthaceae, multiseriate cellular endosperm development occurs in each of the many embryo sacs (typically four) that form. Eventually, all the endosperms developing in the same ovary fuse to form a composite tissue. The inner region of the endosperm will eventually be crushed as the composite endosperm grows.

Continued endosperm development

By means of repeated periclinal and anticlinal divisions, the cellular endosperm of *Arceuthobium* species will grow larger, and by the time the zygote undergoes limited development, the endosperm will have grown to a sizable mass (Hawksworth and Wiens, 1996; Calvin, 1996). There is little information regarding the seasonal timing of events of the developing embryo and endosperm, or regarding relative rates of growth between the endosperm and the embryo. Moreover, the fate of the endosperm cells in the caecum has not been well addressed. Hudson (1966) stated that the growing endosperm displaced and crushed the ovular structure of *A. americanum*. Calvin (1996) also indicated that the growing endosperm crushed the ovular structure of *A. americanum* and *A. cyanocarpum*.

In *Arceuthobium* species requiring two summers for development, growth of the endosperm ceases in September of the first summer, remains in a resting state throughout winter, and resumes growth in the second spring (Hawksworth and Wiens, 1996). Endosperm development in these *Arceuthobium* species is complete by the middle of the second summer. In *Arceuthobium* species that only require one summer to develop, the endosperm reaches its full size by mid-summer.

Problems in interpreting the appearance of the embryo and endosperm

It is important to note that in *Arceuthobium* species in which the embryo sac has been studied, the position of the embryo relative to the endosperm does not mirror the position of the egg cell relative to the central cell in the unfertilized embryo sac. In all cases, the embryo is found at a higher position than the endosperm within the mature dispersal unit. In most *Arceuthobium* species studied, however, the unfertilized egg cell was found at a lower position than the unfertilized central cell, as the egg cell typically arose at the lower pole of the unfertilized embryo sac. In *A. pusillum* (Thoday and Johnson, 1930; Tainter, 1968) and in *A. campylopodum* (Cohen, 1970), there was an apparent and unexplained reversal of the polarity of the embryo sac immediately following double fertilization by which the zygote assumed a higher position than the primary endosperm nucleus. In *A. douglasii* (Jones and Gordon, 1965; Bhandari and Nanda, 1968b), *A. americanum* (Hudson, 1966), and *A. minutissimum* (Bhandari and Nanda, 1968a), there was no reversal in the polarity of the embryo sac immediately

following double fertilization, and the zygote remained morphologically lower than the fertilized central cell. Yet, in a mature dispersal unit, the embryo will come to lie at a position higher than the endosperm. A similar phenomenon of reversal apparently occurs in some Viscaceae (Rutishauser, 1935, 1937; York, 1913; Billings, 1933; Steindl, 1935). No similar reversals occurred in *Eubrachion* (Bhandari and Indira, 1969), *Viscum minimum* (Zaki and Kuijt, 1994), or the Loranthaceae (Bhatnagar and Johri, 1983), as the unfertilized egg cell was higher than the unfertilized central cell, and the embryo is similarly higher than the endosperm.

Another problem arises in explaining the appearance of the embryo and endosperm in the mature dispersal unit of *Arceuthobium* species. In all figures depicting the mature embryo embedded in the endosperm, the endosperm surrounds three-fourths of the lower part of the embryo, while the swollen upper pole (the radicular apex) appears to lie outside the endosperm (Sallé, 1983). Bhandari and Nanda (1968a) explicitly made this observation for ripe fruit of *A. minutissimum*. Therefore, it should be determined how the mature embryo, which at a younger stage was completely surrounded by endosperm cells, apparently comes to partially lie outside of the endosperm.

Maturing and mature endosperm

The mature Viscaceous endosperm is vase-like in *Arceuthobium* (Hawksworth and Wiens, 1996), forms a vertically compressed disc in *Phoradendron, Korthalsella, Ginalloa,* and *Viscum* (Bhandari and Vohra, 1983), and is columnar in *Dendrophthora* (York, 1913). No explanation is given as to how the Viscaceous endosperm attains these forms. The endosperm is top-shaped in *Eubrachion*, and resulted from unequal growth in the lower region of the endosperm (Bhandari and Indira, 1969). The vascular zone of Loranthaceae determines the general shape or contour of the composite endosperm (Bhatnagar and Johri, 1983).

The dispersal units of Viscaceae (Bhandari and Vohra, 1983), *Eubrachion* (Bhandari and Indira, 1969), and Loranthaceae (Bhatnagar and Johri, 1983) are albuminous. The mature Viscaceous endosperm is chlorophyllous (Bhandari and Vohra, 1983), whereas the mature Loranthaceous endosperm, except for *Lysiana*, is achlorophyllous (Bhatnagar and Johri, 1983). The cells of the mature endosperm of all

Arceuthobium species are packed with starch grains (Hawksworth and Wiens, 1996). However, there was no mention of any type of endosperm zonation. Endosperm zonation was referred to in *Eubrachion*, as the cells of the mature endosperm near the embryo lack starch grains, while the other cells of the endosperm distal to the embryo contain many starch grains (Bhandari and Indira, 1969). Endosperm zonation was also described for the Loranthaceae, in which three regions of endosperm were distinguished (Bhatnagar and Johri, 1983). The outermost layer, or epidermis, comprised small, densely cytoplasmic cells with prominent nuclei. The middle region consisted of large polygonal cells filled with starch, and some cells in this region also contained tannin. In *Atkinsonia* and *Nuytsia*, the middle endosperm cells were also loaded with fatty material. The inner layer was not described.

12. Fruit (Pericarp) Development

12A. Typical flowering plants

After double fertilization, the pericarp begins to develop, thus transforming the ovary into a fruit (Mauseth, 1988). Many mature pericarps have three zones. The innermost zone is called the endocarp and may be stony or fleshy. The middle zone is called the mesocarp and represents the "flesh" of the fruit. The outermost zone is called the exocarp (epicarp or ectocarp) and represents the "skin" or "peel" of the fruit. Vascular tissue may be found in any of these zones. These zones do not necessarily indicate the origin of tissues relative to the immature pericarp, but simply reflect the different appearances in the layers. Thus, fruits often have few homologous layers but many analogous ones. However, if zones become evident in a younger pericarp, and a distinctive region (such as a mucilaginous layer) differentiates from a given zone, fruit zones can be useful in describing tissue ontogeny.

Fruit types may be characterized by the appearance of the fruit zones (Mauseth, 1988). There are two fruit types relevant to this thesis. The first of these is the berry. A berry is a fleshy fruit containing one or more seeds. The endocarp, mesocarp, and exocarp of a berry are easily distinguishable, and are all fleshy. The second relevant fruit is the drupe. A drupe is like a berry, except that a drupe is typically one-seeded.

Moreover, the endocarp of the drupe is especially thick, hard, and commonly adherent to the seed.

Fruits must protect the ovule during its development into a seed, but then allow for seed release and subsequent germination (Fahn, 1967). Fruits are typically either dehiscent or indehiscent. In a dehiscent fruit, the fruit opens while still on the plant, and thus the seed is the dispersal unit. In an indehiscent fruit, the seed remains within the fruit upon fruit dispersal, and thus the function of seed dispersal is transferred to the fruit. A seed is released from an indehiscent fruit only after the fruit has been dispersed.

12B. *Arceuthobium* and relevant taxa

Mature fruit

While descriptions of the developing fruit of *Arceuthobium* and relevant taxa are rare, descriptions of the mature fruit are relatively more easily acquired. For this reason, the mature fruit of *Arceuthobium* and relevant taxa will be described first. In addition, if the overall topography of the mature fruit of *Arceuthobium* and related taxa is explained first, the rare accounts of fruit development will be more comprehensible. Obviously, though, more studies of fruit development in Viscaceae are required.

The fruit in the Viscaceae, *Eubrachion*, and Loranthaceae is said to be a pseudoberry, as a primarily fleshy pericarp encloses the embryo(s) and endosperm(s), but lacks a seed coat derived from integumentary tissue (Calder, 1983; Bhandari and Indira, 1969; Bhandari and Vohra, 1983). The usage of both the terms "pseudo" and "berry" are worth examining in the context of *A. americanum.* In contrast, the fruit in the Santalaceae and Olacaceae is a pseudodrupe (Ram, 1959).

The pericarp of the Viscaceae (Bhandari and Vohra, 1983) and *Eubrachion* (Bhandari and Indira, 1969) is differentiated into three fruit zones. The innermost zone is the parenchymatous endocarp. In most cases, the endocarp is believed to be entirely persistent, even when the fruit is mature. Sallé (1983) specifically stated that the endocarp of *Viscum album* is adherent to the embryo and endosperm. However, in *Arceuthobium minutissimum*, most of the endocarp, aside from a so-called cap at the radicular pole of the embryo, is said to be crushed and rendered nonexistent by the developing endosperm (Bhandari and Nanda, 1968a). A similar crushing of the endocarp

and retention of a cap of endocarp is believed to also occur in *Eubrachion* (Bhandari and Indira, 1969). This crushing of the endocarp is not described for other Viscaceae.

The second Viscaceous fruit zone is the mesocarp, and lies just outside of the endocarp (Bhandari and Vohra, 1983) or endosperm, in those species in which the endocarp is believed to be rendered nonexistent (Bhandari and Nanda, 1968a; Bhandari and Indira, 1969). The mesocarp is generally considered to be entirely comprised of viscin tissue, although this is not always the case. For the most part, viscin tissue is described as a layer of elongated mucilaginous viscin cells, although the number of cell layers comprising the tissue has not been clarified. Sallé (1983) believed that vesicular cells, described as isodiametric cells lying at the outer perimeter of the viscin tissue, were also part of the viscin tissue (and thus mesocarp) of *Viscum album*. Bhandari and Indira (1969) observed a layer of degenerate cells lying at the outer perimeter of the viscin tissue of *Eubrachion*, and stated that these cells were part of the mesocarp (although not part of the viscin tissue proper). Moreover, in *Arceuthobium minutissimum* (Bhandari and Nanda, 1968a) and *Eubrachion* (Bhandari and Indira, 1969), a region of compact, tannin-filled cells lying immediately inside of the viscin tissue and adjacent to the endosperm was called the crest. As the endocarp was believed to have been rendered non existent in these two organisms, the crest was considered to be part of the mesocarp (although not part of the viscin tissue proper).

The outermost zone in the Viscaceous fruit is the leathery exocarp (Bhandari and Vohra, 1983). The exocarp of *Arceuthobium minutissimum* (Bhandari and Nanda, 1968a) and of *Eubrachion* (Bhandari and Indira, 1969) consists of about six to eight layers of parenchymatous cells. In *A. minutissimum,* a cuticle covers the epidermis, and some of the cells of the exocarp cells are filled with a tannin-like substance (Bhandari and Nanda, 1968a). However, the exocarp has not been further characterized.

The Viscaceous fruit contains vascular tissue (Bhandari and Vohra, 1983). In most Viscaceae including *Arceuthobium* (as well as *Eubrachion*), the vascular tissue is present only in the exocarp, although the vascular tissue in the Viscaceous tribes Phorodendrae and Visceae is present in both the exocarp and the endocarp. However, the number of vascular traces present in Viscaceous fruits has not been explicitly stated. There are apparently two vascular traces in *A. minutissimum* (Bhandari and Nanda,

1968a) and *Eubrachion* (Bhandari and Indira, 1969). The general composition of the vascular tissue has also not been well described in any Viscaceous fruit, although helical (spiral) and reticulate xylem vessel elements have been observed (Bhandari and Vohra, 1983). In addition, Wilson and Calvin (1996) suggested that the tracheary elements in the fruit of *Arceuthobium* species were mainly graniferous tracheary elements. Graniferous tracheary elements are either vessels or tracheids that are dead at maturity and that possess numerous small and/or one to a few large granules (Fineran *et al.*, 1978; Wilson and Calvin, 1996).

The mature Loranthaceous fruit is said to have four distinct zones (Bhatnagar and Johri, 1983). Like most Viscaceae, these zones include an exocarp, viscid mesocarp, and endocarp. However, the vascular tissue of the Loranthaceae, found internal to the endocarp and appressed to the endosperm, is considered to be a fourth zone.

The external appearances of Viscaceous fruits vary. The ripe fruit of *Viscum album* has a uniformly round and whitish appearance (Sallé, 1983), whereas the ripe fruit of *Arceuthobium* species is ovoid or cylindrical, recurved, and olive green to dark brown (Hawksworth and Wiens, 1996). The colour of the *Arceuthobium* fruit is not uniform, but shows demarcation near its equator by a slight variation in colour that divides the fruit into its upper and lower halves (Hawksworth and Wiens, 1996; Wilson and Calvin, 1996). The fruit of *Eubrachion* (Bhandari and Indira, 1969) has an external appearance that is very similar to the fruit of *Arceuthobium*. Loranthaceous fruit are typically larger more colorful than Viscaceous fruits (Bhatnagar and Johri, 1983).

Fruit development

As implied earlier, there are only a few reports detailing fruit development in *Arceuthobium* and relevant taxa. Moreover, there is little information regarding the timing of when the fruit zones become evident relative to the developing embryo and endosperm. Additionally, there is some controversy among the few reports as to the specific ontogeny of the fruit zones and as to how certain structures arise. Aside from a study on viscin tissue development (Gedalovich-Shedletzky *et al.*, 1989), there are no detailed studies on the fruit development in *A. americanum*.

The only detailed studies in fruit development in *Arceuthobium* species and related taxa have been provided by Bhandari and Nanda (1968a) on *A. minutissimum* and by Bhandari and Indira (1969) on *Eubrachion*. The pericarp of *A. minutissimum* is twelve to fourteen cells thick when the embryo sac is fully formed (Bhandari and Nanda, 1968a), while that of *Eubrachion* is eighteen to twenty layers thick (Bhandari and Indira, 1969). In both *A. minutissimum* (Bhandari and Nanda, 1968a) and *Eubrachion* (Bhandari and Indira, 1969), the young pericarp is parenchymatous and already encompasses the two vascular traces.

In *Arceuthobium minutissimum* (Bhandari and Nanda, 1968) and *Eubrachion* (Bhandari and Indira, 1969), a two to three layered meristematic zone arises interior to the vascular region of the pericarp and divides to form six to eight layers of parenchymatous cells. The innermost two to three layers of parenchymatous cells become endocarp, the middle one to two layers become the so-called crest, and the outer one to three layers become viscin tissue in the upper part of the fruit. In *Eubrachion* (Bhandari and Indira, 1969), an outermost single layer of parenchymatous cells becomes a non-differentiating, degenerate layer. In both *A. minutissimum* and *Eubrachion*, the regions of the pericarp containing and outside of the vascular region become exocarp. As development proceeds in both *A. minutissimum* and *Eubrachion*, the endocarp becomes obliterated, and only the degenerated remains of the endocarp persist as a cap on the radicular end of the embryo in a ripe fruit.

13. Seed Release, Dispersal, and Germination

13A. Typical flowering plants

In dehiscent fruits, seed release is usually accomplished by the formation of an abscission layer, and may be aided by explosive discharge (Mauseth, 1988). Explosive seed discharge from a dehiscent fruit usually disperses the seeds a fair distance away from their source (species exhibiting explosive discharge and mechanisms of explosive discharge will be addressed in much more detail in Chapter Five, section III. Discussion). Other vectors by which a dehisced seed or an indehiscent fruit containing seeds may be dispersed include wind, water, and animals, and combinations thereof (Mauseth, 1988).

In indehiscent fruits, the seed(s) may be released from the fruits via animal activity of some form or another.

If the timing and location is correct, seeds germinate (Fahn, 1967). During germination of albuminous seeds, the endosperm may be totally degraded as the embryo expands. After radicle emergence, the epicotyl will typically emerge. In some species, the hypocotyl and cotyledon(s) will emerge as well. If all goes well, the process of germination will establish the new sporophytic generation.

13B. *Arceuthobium* and relevant taxa

General aspects

Arceuthobium species possess one of the most effective hydrostatically controlled, explosive mechanisms of dispersal known in flowering plants (Hinds *et al.*, 1965). The mucilage in the viscin tissue is hygroscopic, and allows pressure to continually increase throughout fruit development. At fruit maturity, an abscission layer in the pedicel is formed, and explosive discharge of the dispersal unit occurs (Toth and Kuijt, 1978). The typical *Arceuthobium* dispersal unit contains the embryo enveloped by endosperm, which is in turn said to be surrounded by endocarp (Bhandari and Vohra, 1983) or mesocarpic crest with an endocarpic cap (Bhandari and Nanda, 1968a; Bhandari and Indira, 1969). The endocarp/crest has not been adequately clarified as the tissue that surrounds the embryo and endosperm. The endocarp/crest/(and potentially other tissues) of the *Arceuthobium* dispersal unit are in turn surrounded on the upper three-quarters (the radicular end) by viscin tissue. The cellular composition of the discharged viscin tissue has not been described. Notably, the *Arceuthobium* fruit is not truly a dehiscent fruit, as some fruit tissues are included with the discharged dispersal unit.

In this thesis, the dispersal unit of *Arceuthobium* (as well as all Viscaceae, Loranthaceae, and *Eubrachion*) will be referred to as a pseudoseed, following the logic of Calder (1983) who described the pseudoberry. The use of this terminology will be further addressed in Chapter Four, section III - 10G. Likewise, the endocarp/crest/unknown non-viscid tissues that envelop the embryo and endosperm will be referred to as a pseudoseed coat, and the reason for the use of this terminology will be similarly addressed in Chapter Four.

Regardless of how the pseudoseed of Viscaceae, Loranthaceae, or *Eubrachion* is dispersed (*Arceuthobium* and *Korthalsella* are the only mistletoe genera with explosive fruits), the viscin tissue mucilage plays an important role in adhering a pseudoseed to its respective host (Bhandari and Vohra, 1983; Hawksworth and Wiens, 1996). Regarding *Arceuthobium* species, host conifer needles typically intercept *Arceuthobium* pseudoseeds immediately after discharge in the fall (Roth, 1959). Rains moisten the *Arceuthobium* viscin mucilage, and the pseudoseed slides to the base of upward-pointing needles. The mucilage will then dry, and the *Arceuthobium* pseudoseed will become fastened to the host periderm. "Germination" of the *Arceuthobium* pseudoseed will take place in the following spring whereby the green "radicle" (hypocotyledonary structure) will emerge from the pseudoseed coat/dried residual viscin. Following germination, the *Arceuthobium* radicle will continue to elongate, displaying neutral geotropism, negative phototropism, and positive thigmotropism (Hawksworth and Wiens, 1996). The tip of the elongating radicle will contact the host periderm, after which the radicular tip will form a holdfast structure and penetrate the host periderm.

Viability testing and germination success

Naturally discharged pseudoseeds of *Arceuthobium* have been examined for germination potential by treatment with 2,3,5-triphenyl tetrazolium chloride (TTC), a chemical commonly used for viability tests (Smith, 1951; Scharpf and Parmeter, 1962). Red staining of the embryo after treatment with 2,3,5-TTC indicates viability and hence germination potential. With 2,3,5-TTC, Scharpf and Parmeter (1962) tested the viability of the embryos from naturally discharged *Arceuthobium campylopodum* pseudoseeds that had been stored at various but constant temperatures for up to approximately five months. Up to 96% of the pseudoseeds tested immediately with 2,3,5-TTC were deemed viable. At 2° Celsius (C), viability ranged from 94% after storage for one month to 66% after storage for five months. At 13° C, viability ranged from 81% after storage for one month to 9% after storage for five months. At 25° C, viability ranged from 1% after storage for one month to 0% after storage for five months. Viability was limited after about three months in storage, and the higher temperatures were more detrimental. Similarly, Robinson (1995) and Jerome (2001) used 2,3,5-TTC to test the viability of embryos from

naturally discharged *A. americanum* pseudoseeds that had been collected in the Manitoba fall. Robinson (1995) found embryo viability percentages that ranged from approximately 88% to 93%, while Jerome (2001) found embryo viability percentages that ranged from approximately 33% to 67%. Differences between Robinson's (1995) and Jerome's (2001) values were likely due to the fact that Robinson (1995) tested pseudoseeds for viability immediately after returning to the lab, whereas Jerome (2001) tested pseudoseeds for viability after the pseudoseeds had been stored for a few days at 4° C. In either case, the values obtained by Robinson (2001) and Jerome (2001) correspond to the values determined by Scharpf and Parmeter (1962).

All authors determined that actual germination rates were lower than the viability tests had indicated (Scharpf and Parmeter, 1962; Robinson, 1995; Jerome, 2001). No authors have looked at the viability of all components of the naturally discharged pseudoseed of *Arceuthobium*, and although Gilbert (1988) stressed the importance of examining the fate of naturally discharged pseudoseeds in the field, no author has examined how the 2,3,5-TTC-tested viability of naturally discharged pseudoseed left *in campo* changes over time.

II. THE VISCIN TISSUE OF MISTLETOES

1. Definition of Viscin Tissue

Viscin is a unique tissue found in the fruit of mistletoes (Bhandari and Vohra, 1983; Bhatnagar and Johri, 1983). An overall mucilaginous appearance as well as a generally adhesive nature characterizes the viscin tissue. The viscin tissue is believed to be a cellular tissue that is derived from a portion of the pericarp (Gedalovich and Kuijt, 1987). In the Viscaceae and *Eubrachion*, viscin tissue is typically found interior to the vascular region, whereas in the Loranthaceae, viscin tissue is found exterior to the vascular region (Bhandari and Vohra, 1983; Bhatnagar and Johri, 1983). However, literature on the viscin tissue is extremely sparse and not typically current.

In all mistletoes, the viscin tissue is at least partially comprised of elongated, mucilaginous viscin cells. The lengths of the viscin cells are rarely explicitly indicated at any stage of development. Viscin cells have been described as being highly organized fibrillar cylinders that are immersed in a mucilage (Gedalovich-Shedletzky, *et al.*, 1989), although those of *Eubrachion* are apparently filled with and not enveloped in mucilage (Bhandari and Indira, 1969). The fibrillar cylinder essentially represents a cellulosic viscin cell wall and lumen, and the viscin cell mucilage is sometimes simply referred to as viscin. More details on the likely composition of these viscin cell constituents and contents of the lumen will be addressed in parts 3 and 4 of this chapter. The viscin cells of all mistletoes are believed to be closely associated with the dispersal unit (pseudoseed), even after the pseudoseed has been released from the fruit exocarp (Bhandari and Vohra, 1983; Bhatnagar and Johri, 1983). Thus, the viscin cells primarily serve to fasten the pseudoseed to a new host surface. When examined with the naked eye, the viscin tissue of all mistletoes typically appears whitish and slimy due to the presence of the viscin cells.

In addition to viscin cells, the viscin tissue of the Loranthaceae is also comprised of non-mucilaginous, highly vacuolate vesicular cells (Gedalovich-Shedletzky *et al.*, 1989). These vesicular cells possibly play a role in providing nutrients for an avian disseminator. In contrast, Gedalovich-Shedletzky *et al.* (1989) believed that vesicular cells are absent from the Viscaceae, specifically citing *Arceuthobium americanum,*

Korthalsella dacrydii, and *Phoradendron californicum*. Typically, descriptions of viscin tissue in the Viscaceae mention only the viscin cells, although vesicular cells have been observed in *Viscum album* (Sallé, 1983). Apparently, no vesicular cells have been observed in *Eubrachion* (Bhandari and Indira, 1969).

2. Origin/Development of Viscin Tissue and Secretion of Mucilage by Viscin Cells

2A. Origin of the viscin tissue

Accounts of viscin tissue origin are rare. In *Arceuthobium minutissimum* (Viscaceae), a two to three layered meristematic zone found interior to the vascular region of the pericarp divides to form six to seven layers of parenchymatous cells (Bhandari and Nanda, 1968). The innermost two to three layers of parenchymatous cells become endocarp, the middle one to two layers become the so-called crest, and the outer two to three layers become viscin tissue (comprised only of viscin cells) in the upper part of the fruit. Therefore, the viscin tissue in this species is potentially two to three cell layers in thickness, is bordered on its inner layer by the crest, and is bordered on its outer layer by exocarp. The viscin tissue as well as the crest is morphologically representative of mesocarp. In the lower part of the fruit, no viscin tissue will develop, and the outer two to three layers of parenchymatous cells (the layers that form viscin tissue in the upper part of the fruit) contribute to the crest. However, no data were provided with regard to timing of these and other changes (such as viscin cell elongation) in the fruit relative to embryo/endosperm development.

A similar but not identical pathway for viscin tissue (viscin cell) ontogeny was detailed for *Eubrachion* (Bhandari and Indira, 1969). In *Eubrachion*, a two to three layered meristematic zone found interior to the vascular region of the pericarp divides to form six to eight layers of parenchymatous cells. The innermost two to three layers of parenchymatous cells become endocarp, the middle two to three layers become the crest, a single layer immediately outside of the crest becomes viscin tissue in the upper part of the fruit, and the outermost single layer becomes a non-differentiating, degenerate layer. No vesicular cells were said to develop. The cell layer that becomes viscin tissue (viscin cells) possesses dense cytoplasm, few vacuoles, and large nuclei, and development begins when the cells of the layer begin to elongate radially, but it is not know if this occurs

simultaneously in all developing viscin cells. Elongation occurs at the pre-globular stage of the embryo. It can be deduced that the viscin tissue in this species is probably one cell layer in thickness, is bordered on its inner portion by the crest, and is bordered on its outer portion by the degenerate layer. The viscin tissue along with the crest and degenerate layer would all be morphologically representative of mesocarp. In the lower part of the fruit, no viscin tissue develops, and here the outer two layers of parenchymatous cells contribute to the crest. Although the timing of when the viscin cells become fully elongated was not clearly indicated, it was mentioned that the viscin cells enlarge further radially, become more vacuolated, and maintain relatively large nuclei at the globular stage of embryo development.

2B. Development (maturation) of the viscin tissue and secretion of the viscin cell mucilage

A somewhat detailed account of viscin tissue development/maturation was provided for *Phthirusa pyrifolia*, a member of the Loranthaceae (Gedalovich and Kuijt, 1987). When the fruits of *P. pyrifolia* are one-third of their final length and green, a region of slightly elongated cells became evident in the pericarp (Gedalovich and Kuijt, 1987). The exact location of this region in the pericarp was not specified, and it is not clear how many cell layers make up the young region. The elongated cells of this region had ultrastructural characteristics of immature cells and develop into viscin tissue composed of viscin and vesicular cells.

When *Phthirusa pyrifolia* fruits are one-half to two-thirds of their final length and green, the two cell types of the viscin tissue in *Phthirusa pyrifolia* begin to diverge in an obvious manner (Gedalovich and Kuijt, 1987). The viscin cells begin to secrete mucilage, whereas the vesicular cells do not. The nascent viscin cell mucilage of *P. pyrifolia* is apparently principally represented by what Gedalovich and Kuijt (1987) call the compound middle lamella, a region where no clear distinction between the middle lamella and the primary cell wall of the viscin cells was discernable. Gedalovich and Kuijt (1987) believed that the organelles seen in the viscin cell cytoplasm, including Golgi bodies and associated vesicles, rough and tubular endoplasmic reticulum, ribosomes, and mitochondria play a role in mucilage secretion. Many spherical

vacuoles/vesicles containing Periodic Acid - Thiocarbohydrazide - Silver Proteinate (PATCH)-positive fibrillar materials were embedded in the central vacuole, and these spherical vacuoles were also implicated in mucilage secretion, as they were often open to the outside of the cell and their membranes continuous with the plasma membrane. The spherical vacuoles stained pink with Toluidine Blue, and thus contained some pectic materials. Therefore, both Golgi-derived vesicles and embedded spherical vacuoles were believed to be depositing mucilage components into the periplasmic space. However, no indication was given as to how the mucilage materials then traversed the cell wall to become a part of the compound middle lamella/mucilage. At this stage in development, the vesicular cells were somewhat elongated, possessed thin walls, a large central vacuole, and a very small amount of dark peripheral cytoplasm.

When *Phthirusa pyrifolia* fruits are two-thirds of their final length to full sized but still green, the viscin cells have reached their final length of approximately 760 μm and the viscin cell walls become greatly thickened with cellulosic microfibrils (Gedalovich and Kuijt, 1987). Highly PATCH-positive membranous vesicles are seen embedded within the microfibrils of the cell wall. These vesicles, likely carrying mucilage materials, presumably originated from the highly PATCH-positive plasma membrane, but become buried in the cell wall as the intense synthesis of the microfibrils proceeds. At this stage in development, the vesicular cells also reach their final length of about 630 μm, but do not change in appearance.

When *Phthirusa pyrifolia* fruits are full sized and orange (mature), the viscin cell walls are extremely thick (Gedalovich and Kuijt, 1987). The compound middle lamella/mucilage appears swollen and moves adjacent viscin cells further away from each other, although no indication was given as to how this was accomplished. The viscin cell cytoplasm had apparently degenerated. Likewise, the vesicular cells seemed to be partially collapsed and their cytoplasm disintegrated. More details on the composition of the mature viscin cell constituents and contents of the lumen of this and other species will be addressed in the following sections.

3. General Organization of Mature Viscin Tissue in the Mistletoe Fruit

3A. Viscaceae (and *Eubrachion*)

In *Arceuthobium minutissimum*, the viscin tissue (viscin cells) forms a continuous dome-shaped structure in the upper half of the fruit, distal to the pedicel or base and represents a portion of the fruit mesocarp (Bhandari and Nanda, 1968a). Although the number of cell layers making up the mature viscin tissue was not explicitly stated, ontogenetic descriptions implied that the viscin tissue is possibly two to three cell layers in thickness, bordered on its inner layer by the crest and its outer layer by exocarp.

In *Phoradendron flavescens*, the viscin tissue was illustrated as a continuous dome in the upper half of the fruit composed of five to seven cell layers (Billings, 1933). In *P. californicum*, the viscin tissue was illustrated as a continuous dome that nearly completely encircles the embryo and endosperm within the fruit, aside from a portion near the base of the fruit (Gedalovich *et al.*, 1988). The ontogeny of the viscin tissue in these species was not described. Gedalovich *et al.* (1988) implied that the viscin tissue in *P. californicum* is only one cell layer in thickness and stated that the outer border of the viscin tissue layer is formed by the inner tissue of the exocarp. There was no explanation of what tissue specifically formed the inner border of the viscin cells, although an illustration provided implied that it is the endosperm. However, the viscin cells as delineated by the microfibrillar cylinders do not extend all the way to the exocarp and only mucilage on the outer portion of the viscin cell layer contacts the inner tissue of the exocarp. In *Viscum articulatum*, the viscin tissue is distinguishable into inner and outer regions separated by a narrow band of cells (Steindl, 1935), although the number of cell layers comprising each band was not indicated, the viscin tissue was not referred to as mesocarp, and no ontogeny was described.

The viscin tissue of *Viscum album* has been fairly well described by Sallé (1983), and was specifically referred to as mesocarp, although no ontogeny was described. In contact with the endocarp, the inner part of the mesocarp is composed of elongate viscin cells, although the number of viscin cell layers was not indicated. Spherical, highly vacuolate, and thin walled vesicular cells form the outer part of the mesocarp, being found just beneath the exocarp as well as among the viscin cells. The number of vesicular cell layers was not indicated.

In *Eubrachion*, the viscin cells are not continuous but rather form an annular zone around the upper part of the endocarp at the apex of the fruit, apparently representing a portion of the mesocarp (Bhandari and Indira, 1969). Bhandari and Nanda (1969) implied that the viscin tissue is only one cell layer in thickness, although this was not explicitly stated. The viscin cell layer is bordered on its inner portion by the crest and on its outer portion by the degenerate layer.

The orientation of the viscin cells and vesicular cells relative to the long axis of the fruit is not addressed in any article pertaining to the Viscaceae or *Eubrachion*.

3B. Loranthaceae

Viscin tissue is the most prominent zone of the Loranthaceous pericarp (Bhatnagar and Johri, 1983). The viscin tissue in the Loranthaceae is believed to be comprised of both viscin cells and vesicular cells (Gedalovich-Shedletzky *et al.*, 1989), although most authors rarely distinguish between the two cell types, and the number of cell layers making up the viscin tissue is not typically addressed. There are no instances in which the Loranthaceous viscin tissue is specifically referred to as mesocarp; ontogeny is rarely addressed and the tissues immediately bordering the viscin tissue are not typically identified. Whereas the viscin tissue in the Viscaceae is more prominent in the upper portions of the fruit (distal to the pedicel), the viscin tissue in the Loranthaceae is more prominent in the basal portions of the fruit (proximal to the pedicel).

The viscin tissue shows much variation in the Loranthaceae. It is confined to the base of the fruit in *Amylotheca dictyophleba* (Raj, 1970), *Lepeostegeres gemmiflorus* (Dixit, 1958), and *Peraxilla tetrapetala* (Prakash, 1960). The viscin tissue is quite prominent in the basal region and directly abuts the vascular zone in *Barathranthus axanthus* (Prakash, 1963). In the upper portion of the *B. axanthus* fruit, however, viscin tissue is not so conspicuous and surrounds the parenchymatous zone (a zone somewhat analogous to endocarp). In *Lysiana exocarpi*, the viscin tissue covers the parenchymatous zone in the basal region, and shows six vertical strands in the upper portion (Narayana, 1958a). In *Nuytsia floribunda*, the viscin tissue is constricted around the parenchymatous zone (Narayana, 1958b). In *Helicanthes elastica* (Johri *et al*, 1957), *Tolypanthus involucratus* (Dixit, 1961), and *T. lagenifer*, the parenchymatous zone is

completely covered by the viscin tissue. This is also true of *Phthirusa pyrifolia* (Kuijt, 1969; Gedalovich and Kuijt, 1987) and *Struthanthus quercicola* (Kuijt, 1969).

Gedalovich and Kuijt (1987) further described the organization of the viscin and vesicular cells in the viscin tissue of *Phthirusa pyrifolia*, stating that the vesicular cells primarily make up the top portion of the fruit, and the viscin cells the basal part of the fruit. However, thin walled vesicular cells can be found between the viscin cells and vice versa, and the transition from areas occupied mainly by one cell type to areas where the second type is dominant is gradual. Although not explicitly stated, the elongated viscin cells in the mature fruit appear to be one cell layer in thickness, whereas the vesicular cells, which are also fairly elongated, occupy one to two cell layers.

The orientation of the viscin cells and vesicular cells relative to the long axis of the Loranthaceous fruit is only briefly addressed in two articles. Gedalovich and Kuijt (1987) specifically stated that the viscin cells and vesicular cells of *Phthirusa pyrifolia* are tangentially/diagonally/obliquely placed. Singh (1952) also showed that the viscin cells of *Dendrophthoe falcata* are tangentially/diagonally/obliquely placed (the vesicular cells were not mentioned).

4. Structure and Cytochemistry of Mature Viscin Tissue (Specifically Viscin Cells)

4A. Problems with the literature

The relevant literature pertaining to vesicular cells has already been detailed in section III - 1 to 3 of this chapter, as no thorough examination of the structure and cytochemistry of the vesicular cells at any stage of their development has been reported. The remainder of this review will focus on the mature viscin cells. Published descriptions are not always clear as to the stage of development or maturity of the given viscin cells, or whether then cells are being examined within the fruit or after the pseudoseed has been released from the fruit exocarp.

4B. Viscin cell walls

Cytochemistry and structure

Viscin cell walls of all mistletoes are widely believed to be cellulosic (Gedalovich-Shedletzky, *et al.*, 1989). In *Arceuthobium tsugense* (Viscaceae), mature viscin cell walls are positive for the Periodic Acid - Schiff's (PAS) treatment for

carbohydrates and the zinc-chlor-iodide reaction for cellulose, providing the first cytochemical evidence that the mature viscin cell walls are cellulosic (Paquet, 1975). Similarly, the viscin cells of *Viscum album* possess a cell wall that stains with both Congo red and the sulfuric acid-iodine reaction, indicating a cellulosic cell wall (Sallé, 1983). Using solid-state spectroscopic analysis, Azuma *et al.* (2000) confirmed that the viscin cell walls of *V. album* contain cellulose. The viscin cell walls of the Viscaceous *Phoradendron californicum* (Gedalovich *et al.*, 1988) and of the Loranthaceous *Phthirusa pyrifolia* (Gedalovich and Kuijt, 1987) possess well-organized, highly birefringent microfibrils that are all oriented in a uniform direction. The microfibrils are PATCH-positive, which suggest that they are cellulosic (Gedalovich and Kuijt, 1987). The mature viscin cell walls of *Phthirusa pyrifolia* were further described as being extremely thickened, and having furrowed inner boundaries facing the narrow cell lumen and smooth outer boundaries facing the mucilage (Gedalovich and Kuijt, 1987). Whereas Paquet (1975) believed the viscin cell walls in *A. tsugense* to be primary, Gedalovich and Kuijt (1987) believed those in *P. pyrifolia* to be secondary cell walls.

Question of helical substructure

Paquet (1975) described the mature viscin cells walls of *Arceuthobium tsugense* as having a helical substructure. Peirce (1905) also noted a helical viscin cell wall in *A. occidentale,* as did Heinricher (1915) in *A. oxycedri*, and Gedalovich *et al.* (1988) in *Phoradendron californicum.* Sallé (1983) and Gjokic (1896) also reported a helical cell wall in *Viscum album* (Viscaceae). The viscin cells of *Eubrachion* were described as being spirally twisted (Bhandari and Indira, 1969), although it is not clear if the phrase "spiral twisting" referred to a viscin cell wall or to the appearance of several viscin cells spirally-twisted around each other.

Gedalovich and Kuijt (1987), however, believed that the viscin cell walls of Loranthaceous mistletoes do not have a helical substructure, citing a single species, *Phthirusa pyrifolia*, as an example. In contrast, Singh (1952) suggested that the viscin cells of the Loranthaceous *Dendrophthoe falcata* are spirally twisted; again, though, the exact meaning of the phrase "spirally twisted" is unclear. Gedalovich and Kuijt (1987) were not convinced that the helical nature of the viscin cell wall seen in some Viscaceae is not an artifact.

4C. Viscin cell mucilage

The mucilage in the mature viscin cells of *Arceuthobium tsugense* is positive for the PAS treatment for carbohydrates and the hydroxylamine-ferric chloride reaction for pectins, but not for the zinc-chlor-iodide reaction for cellulose (Paquet, 1975). Thus, Paquet (1975) suggested that the mucilage is rich in pectic acid. In *Viscum album*, the mucilage stains with ruthenium red, also indicating a pectic nature (Sallé, 1983). Under high magnification, the mucilage of *Phoradendron californicum* (Viscaceae) appears to be built up of distinct PATCH-positive loops to which linear branched PATCH-positive segments are attached; larger dense clusters of polysaccharides are also present (Gedalovich *et al.*, 1988). However, the types of carbohydrates being localized with PATCH were not clarified. The mucilage surrounding each viscin cell of *P. californicum* evidently has a distinct boundary separating the mucilage of one cell from that of another, and this boundary is believed to be a thin middle lamella. In *Phthirusa pyrifolia*, the mature mucilage contains loosely and irregularly arranged PATCH-positive fibrillar material, which uniformly envelops each viscin cell (Gedalovich and Kuijt, 1987). Again, the nature of the carbohydrates stained with PATCH was not specified, although the mature mucilage also stained pink for Toluidine Blue, which suggested that the mucilage had a pectic component.

4D. Fate of the viscin cells

The fate and state of viscin cells at maturity or after release from the fruit exocarp has only been addressed in a cursory manner in the literature. Both Kuijt (1960) and Paquet (1975) believed that the elongate viscin cells of *Arceuthobium tsugense* are dead at maturity. Paquet (1975) suggested that, in a natural setting, the viscin cell mucilage of expelled pseudoseeds would be degraded by naturally-occurring factors. Sallé (1983) believed that the mature viscin cells of *Viscum album* are degenerate. Likewise, only cytoplasmic remnants were observed in the mature viscin cells of *Phoradendron californicum* (Gedalovich *et al.*, 1988) and *Phthirusa pyrifolia* (Gedalovich and Kuijt, 1987). No viability testing on whole viscin cells was performed in any instance, however.

5. General Biochemistry of Viscin Cell Mucilage

5A. General observations

Some biochemical analyses on the mucilage of mistletoes have been performed for the Viscaceous members *Arceuthobium tsugense* (Paquet, 1975; Paquet *et al.*, 1986), *A. americanum* (Gedalovich-Shedletzky *et al.*, 1989), and *Phoradendron californicum* (Gedalovich *et al.*, 1988; Gedalovich-Shedletzky *et al.*, 1989) as well as for the Loranthaceous member *Phthirusa pyrifolia* (Gedalovich-Shedletzky *et al.*, 1989). For the most part, the fruit were deemed "mature", although this was never really clarified.

Paquet (1975) and Paquet *et al.* (1986) determined that each fruit of *Arceuthobium tsugense* produces about 1 mL of hydrated mucilage, although the dry mass of the mucilage was not determined. Gedalovich *et al.* (1988) and Gedalovich-Shedletzky *et al.* (1989) did not determine the volume of hydrated mucilage per mistletoe fruit, but instead reported the dry mass of viscin mucilage as a percentage of the total dry mass of the fruit examined in each species. This was easily reconverted to an absolute value of viscin mucilage dry mass. Thus, the dry mass of the viscin mucilage per fruit is approximately 360 μg in *Arceuthobium americanum* (Gedalovich-Shedletzky *et al.*, 1989), 3.36 mg in *Phoradendron californicum* (Gedalovich *et al.*, 1988; Gedalovich-Shedletzky *et al.*, 1989), and 2.21 mg in *Phthirusa pyrifolia* (Gedalovich-Shedletzky *et al.*, 1989).

5B. Neutral soluble carbohydrate analyses

Gedalovich-Shedletzky *et al.* (1989) assayed the viscin cell mucilage of *A. americanum*, *Phoradendron californicum*, and *Phthirusa pyrifolia* for neutral soluble carbohydrates using the method of Dubois *et al* (1956). Gedalovich-Shedletzky *et al.* (1989) reported these carbohydrate estimations as mg of carbohydrate per gram total dry mass of an ethylenediamine tetraacetic acid-extracted mucilage fraction and of a sodium carbonate-extracted mucilage fraction per species. For simplicity, a conversion was made that expresses the dry mass of the neutral carbohydrate as a percentage of the total mucilage dry mass per species. Ideally, it would have also been useful to express the amount of neutral soluble carbohydrates per mL of hydrated mucilage in each species,

but this could not be achieved, as no volumetric values of hydrated mucilage were provided.

Soluble neutral carbohydrates account for approximately 46% of the viscin mucilage dry material of *Arceuthobium americanum*, weight/weight (w/w) (Gedalovich-Shedletzky *et al.*, 1989). Similarly, soluble neutral carbohydrates account for approximately 48% of the viscin mucilage dry material of *Phoradendron californicum* w/w. Using chromatography, it was determined that xylose and arabinose are the most abundant neutral soluble carbohydrates in the viscin cell mucilage of *A. americanum* and *P. californicum*, and most of the xylose and arabinose is found in highly branched xylans and arabinans. Soluble neutral carbohydrates account for approximately 17% of the viscin mucilage dry material of *Phthirusa pyrifolia* w/w. Non-cellulosic glucose is the most abundant neutral soluble carbohydrate in the viscin cell mucilage of *P. pyrifolia*, although the potential forms of the glucose were not indicated.

5C. Uronic acid analyses

Paquet (1975) and Paquet *et al.* (1986), using the carbazole method of Bitter and Muir (1962), determined that there is110 µg of (hexa)uronic acids per mL of mucilage (and thus per fruit) of *Arceuthobium tsugense*. Using chromatography, Paquet (1975) and Paquet *et al.* (1986) determined that only oligo-D-galacturonic acids are present in the mucilage of *A. tsugense*.

Gedalovich-Shedletzky *et al.* (1989), using a method of Blumenkranz and Asboe-Hansen (1973), determined the uronic acids content in the two separate viscin mucilage fractions in *Arceuthobium americanum*, *Phoradendron californicum*, and *Phthirusa pyrifolia*. Again, data from the two fractions have been compiled for each species (as they were for the neutral soluble carbohydrate analyses) and have been converted to a dry mass of uronic acids expressed as a percentage of the total dry mass mucilage per species. Uronic acids account for approximately 18% of the viscin mucilage dry material of *A. americanum* w/w, approximately 19% of the viscin mucilage dry material of *Phoradendron californicum* w/w, and approximately 7% of the viscin mucilage dry material of *Phthirusa pyrifolia* w/w.

5D. Protein analyses

Using thin layer chromatographic amino acid analysis, Gedalovich-Shedletzky *et al.* (1989) determined the protein content in two viscin cell mucilage fractions from *Arceuthobium americanum*, *Phoradendron californicum*, and *Phthirusa pyrifolia*. Compiling the data as was done for neutral carbohydrates and uronic acids, proteins accounted for approximately 17%, 20%, and 24% of the dry viscin mucilage material w/w in *A. americanum*, *P. californicum*, and *P. pyrifolia*, respectively. In all three species, glycine is the most abundant amino acid, there is a large amount of histidine, and hydroxyproline is present in small amounts. Gedalovich *et al.* (1988) had also analyzed two viscin cell mucilage fractions of *P. californicum* for proteins using the method of Bradford (1976), but believed that not all proteins had solubilized in the assay reagent due to polyphenolic interference.

5E. Analyses for other components in the mucilage

Paquet (1975) and Paquet *et al.* (1986), using lipid analysis of Ways and Hanahan (1964), examined the lipid content in the viscin cell mucilage of *Arceuthobium tsugense*. No results pertaining to lipids are provided in either the 1975 or the 1986 reports.

Although lipids were not examined, Gedalovich-Shedletzky *et al.* (1989), using a method of Mapson *et al.* (1963), determined the ortho-di-phenolic content in two separate viscin mucilage fractions of three mistletoe species. Phenols are a potential component of the viscin cell mucilage; Salatino *et al.* (1993) found that tannins in the adult fruit of the Loranthaceous *Struthanthus vulgaris* are localized in the viscin tissue, although no specific reference was made to which cell type or cell component possessed the tannins. The ortho-di-phenol assay results of Gedalovich-Shedletzky *et al.* (1989) have been compiled as they were for their other analyses. Ortho-di-phenol accounts for approximately 2% of the viscin mucilage dry material of *Arceuthobium americanum* w/w, approximately 7% of the viscin mucilage dry material of *Phoradendron californicum* w/w, and approximately 5% of the viscin mucilage dry material of *Phthirusa pyrifolia* w/w.

Gedalovich-Shedletzky *et al.* (1989) believed that a certain component of the mucilage of the three mistletoe species examined is not accounted for by neutral soluble

carbohydrates, uronic acids, proteins, or ortho-di-phenol. Compiling the results as before, approximately 16%, 6%, and 42% of the viscin mucilage dry material w/w in *Arceuthobium americanum, Phoradendron californicum*, and *Phthirusa pyrifolia* is unidentified, respectively. These unknown materials constitute a substantial proportion of the viscin mucilage dry material, and thus all biochemical results need to be re-examined.

III. CYTOGENETIC AND PLOIDY LEVEL ANALYSES

1. Definition of Cytogenetics and Ploidy Level

Cytogenetic studies are those in which the appearance and "behavior" of chromosomes are examined (Purves *et al.*, 1998). As cytogenetic studies deal with chromosomes, these studies are also relevant to examinations of ploidy level. Ploidy level is defined as the number of haploid (n) chromosome sets in a genome. When a genome has two sets of haploid chromosomes, its ploidy level is referred to as being diploid, or 2n. Similarly, when a genome has three sets of haploid chromosomes, its ploidy level is referred to as being triploid, or 3n, and so forth.

2. Cytogenetic Examination and Determination of Ploidy Level

2A. Cytogenetic examination

For cytogenetic study, chromosomes must be evident in the cells being examined. In order for chromosomes to be visible, cells must be actively undergoing cell division (Jones and Luchsinger, 1986). Meiotic cells in flower buds and mitotic cells in root tips are common sources of plant material used for cytogenetic study. Usually, cells are treated with DNA-specific stains (such as the Feulgen staining treatment or acetocarmine stain) in order to make the chromosomes visible to the examiner. Moreover, it is common for whole mounts, as opposed to sectioned material, to be used for examination of chromosomes.

2B. Determination of ploidy level

Overview and general concepts: direct and indirect ploidy analysis

Ploidy level can be measured directly by counting condensed chromosomes, or indirectly by performing photometry on stained nuclei (Jones and Luchsinger, 1986). As with cytogenetic studies, chromosome counting is limited to regions of active cell division. Determination of ploidy level by photometry makes use of DNA-specific stains. The amount of visible spectrum information being absorbed or emitted (reflected) by the stain ("photo-") is proportional to the amount of DNA and can be measured ("-metry"). The measurement of DNA can then be translated into ploidy level, which is of

course proportional to the amount of DNA. If the visible spectrum information is emitted light from fluorescence, the term "fluorometry" may also be used. Photometry (including fluorometry) can be applied to squashes of all tissues of the plant, dividing and non-dividing, to determine the ploidy level, although the resulting data must be critically interpreted with regard to the phases of the cell cycle.

Measuring the intensity of staining during photometric (including fluorometric) ploidy analysis

Several photometric (or fluorometric) methods exist to measure the intensity of nuclei stained with DNA-specific stains. For absolute measurements of the amount of DNA, an internal standard, such as chicken erythrocyte nuclei with known amount of DNA values, is needed for calibration (Berlyn and Miksche, 1976). Relative measurements, however, can use nuclei of a known ploidy as a standard for the basis of ploidy determination. In relative measurement, the amount of DNA is never determined absolutely, but relative ploidy levels of different tissues can be obtained. In all cases, however, whole mounts as opposed to sectioned material should be used, since all DNA must be included in the measurements.

Microspectrophotometry, also known as microdensitometry, is the oldest method used to measure the amount of stained material in a sample (Gahan, 1984). Determination of the amount of DNA present in nuclei with microspectrophotometry is accomplished through absorbance measurements of nuclei stained with DNA-specific, absorbant stains (such as the Feulgen staining treatment). The microspectrophotometer detects absorption at a given wavelength via a monochromator and a photomultiplier tube fixed to a light microscope. In a small field of view, or "plug", delimited by a measuring diaphragm so that only a nucleus is visible, the absorbance is measured. The volume of the nucleus must be estimated, and the absorbance is then converted to the total amount of DNA using Beer's law. Aside from problems with estimating the volume of a nucleus, this technique also suffers from absorptive distributional error, which occurs if the stain is not evenly dispersed throughout the nucleus. Distributional error can be overcome in a more sophisticated scanning integration system, in which plugs even smaller than the nucleus being examined are collected and averaged (Gahan, 1984).

Unfortunately, objects of arbitrary shape, including nuclei, are not accurately measured by a microspectrophotometer, as the limiting diaphragm assigns a rigid circular border to the object of interest (Gahan, 1984). However, objects of arbitrary shape can be measured by computerized digital image analysis. As in the determination of ploidy level by microspectrophotometry, DNA-specific stains are employed in the determination of ploidy level by image analysis. Moreover, because either reflected/emitted light or absorbed light can be measured via image analysis, all types of DNA-specific stains may be used, including fluorescent stains. A computerized image analysis system stores digitized data of a specimen, which can subsequently be operated on by numerical methods (Bradbury, 1989). The system can either be a dedicated machine or a personal computer with additional software and hardware.

Digitized data are obtained by scanning in micrographs from a flatbed scanner by capturing images from a video camera attached to the microscope (Bradbury, 1989). When an image has been digitized, it becomes represented by array of numbers, each number denoting the optical density at a particular x-y co-ordinate in the array. The digitized image can be stored on magnetic media, processed numerically, or displayed on a video monitor by converting each number in the array to a pixel of corresponding brightness or colour. For example, a number ranging from 0 (corresponding to pure black) to 255 (corresponding to pure white) commonly represents grey level. The resolution of the digitized image is hardware dependent and subject to continuous improvement. Computerized image analysis systems have an immense number of functions to process an image for analysis and their applications are explained in accompanying technical manuals. Functions relevant to image analysis for the determination of ploidy level include the subtraction of background images, elimination of irrelevant detail, delimitation of the nuclear outlines, report of the total brightness (reflectance, fluorescence)/absorbance of each nucleus, and the calculation of ploidy. The major advantages of a computerized image analysis system is the rapidity of analysis due to the automation of tasks, and the flexibility to accommodate various types of measurements and analyses. The field of image analysis advances rapidly.

Overall, fluorescent stains such as Hoechst are better suited to ploidy analysis than absorptive stains such as achieved by the Feulgen reaction, which generally takes

longer than fluorescence staining. Firstly, the use of fluorescent stains is an advantage over absorptive stains because reflectance/emission measurements do not suffer from distributional error (Gahan, 1984). Also, the use of fluorescent stains usually results in a higher signal-to-noise ratio than with absorptive stains. Additionally, the Hoechst dyes do not bind to either single-stranded DNA or to RNA, so specific hydrolyzations need not be undertaken as controls for Hoechst staining as they need to be for the Feulgen reaction (Arndt-Jovin and Jovin, 1989).

Examples of the use of photometric (and fluorometric) ploidy analysis in the literature

There are several examples of ploidy analysis via photometry in the literature. The Feulgen reaction in conjunction with microspectrophotometry has been used to determine seasonal variations in DNA content of balsam fir cambia (Mellerowicz *et al.*, 1989), and to assess polyploidy in the cotyledons of developing canola embryos (Silcock *et al.*, 1990). The DNA-specific fluorescent Hoechst dye #33258 in conjunction with fluorometry via image analysis has been used in the determination of ploidy in Mitchell petunia protoplasts (Kamo and Griesbach, 1989). Similarly, Hoechst dye #33342 was used in conjunction with fluorometry via image analysis to determine ploidy of isolated carrot nuclei by flow cytometry (Coutos-Thevenot *et al.*, 1990). Flow cytometry, a very rapid process that encompasses a large population of nuclei, was made possible because, as mentioned, reflectance measurements do not suffer from distributional error. Groot (1992) also used Hoechst dye #33342 and fluorometry via image analysis to determine that the aleurone layer in canola seed is a triploid rather than a diploid tissue.

3. Cytogenetic Studies and Ploidy Level in Mistletoes

Although there have been several studies on the general chromosomal morphology in many Viscaceae (including *Arceuthobium*) and Loranthaceae (Wiens, 1968), these studies have all focused on either the mitotic diploid tissue of the stem or the meiotic diploid tissue (microsporocytes) in anthers. There have been no cytogenetic studies performed with regard to female tissues, embryonic material, or endosperm.

The Viscaceae have base chromosome numbers that range from 10 to 17, and the base number for the family is likely 14 (Watson and Dallwitz, 1992). Therefore, the

lowest haploid chromosome number of n = 10 in the Viscaceae is best interpreted as the lower end of a decreasing aneuploid series from 14 to 10 in *Viscum*. *Arceuthobium* has a base chromosome number of 14 and polyploidy is unknown (Wiens, 1968). The base number of 14 also characterizes the other New World genera of Viscaceae (*Dendrophthora* and *Phoradendron*), as well as *Korthalsella,* a widely distributed genus occurring in East Africa, southern Asia, and Oceania as far east as Hawaii. *Notothixos* is karyologically distinct with a base number of 12. The chromosomes of *Ginalloa* are unstudied (Hawksworth and Wiens, 1996). If polyploidy were involved in the evolution of 14 as a base chromosome number in Viscaceae, then its origin was certainly ancient (Hawksworth and Wiens, 1996). Under any circumstances, however, the chromosome systems in *Arceuthobium* (including *A. americanum*) and other genera of Viscaceae clearly operate as functional diploids. Therefore, in *A. americanum*, the haploid chromosome number is 14 and the diploid (2n) chromosome number is 28.

Eubrachion of the Eremolepidaceae has a haploid chromosome number of n = 13, and in the Eremolepidaceae, which contains four genera, haploid chromosome numbers range from n = 10 to n = 13 (Watson and Dallwitz, 1992). It has not been determined whether or not these haploid numbers represent true base numbers, or if polyploidy has occurred. The Loranthaceae have base numbers of chromosomes that range from 8 to 12. Polyploidy has not been documented, and thus the range in the base chromosome numbers (Watson and Dallwitz, 1992) represents the range in the haploid chromosome numbers.

CHAPTER THREE - GENERAL MATERIALS AND METHODS

I. THE STUDY AREA

Sampling of *Arceuthobium americanum* in Manitoba was performed in Grand Beach Provincial Park, which is located 75 km north of Winnipeg on Provincial Trunk Highway 59 (Figure 3.1 - found on the following page). The study area was located at 50° 35' latitude and 96° 35' longitude. The entire study area, found in Township 18, included the northwestern portion of Section 26, the northeastern portion of Section 27, the southeastern portion of Section 34, and the southwestern portion of Section 35. The study area had jack pine (*Pinus banksiana*) stands that were heavily infested with *A. americanum*. Not all trees were infected, however. Lichens, mosses, and *Arctostaphylos uva-ursi* (L.) Spreng provided the greatest cover in the herb layer while *Vaccinium angustifolium* Alt. predominated in the shrub layer (Gilbert, 1988).

The study area did not have a completely uniform topography, so three sites possessing differing topographies were chosen from the study area (Figure 3.1); this provided a range in the stages of reproductive development in the *Arceuthobium americanum* female flowers/fruit. Sites were approximately 50 m by 50 m in area. Descriptions of the three sites are as follows, although topographical observations of the three sites were of a qualitative nature only.

Site 1 or the "Datalogger Site" straddled Sections 26 and 27, and was located approximately 100 m west of Highway 59 where The Manitoba Department of Natural Resources had labeled the area "the Dwarf Mistletoe Disease Management Area". In previous studies, the CSI Model 21X Datalogger monitored this site. Site 1 had a hummocky topography and was fairly well-drained. No standing water was ever observed.

Site 2 or the "KD Site" was located on the northwestern side of Section 26. A rock with the graffiti "KD" helped in the identification of this site. Site 2 was found on the east side of Highway 59, approximately 100 m northeast of Site 1. Site 2 was fairly flat and very well drained. No standing water was ever observed. The density of trees

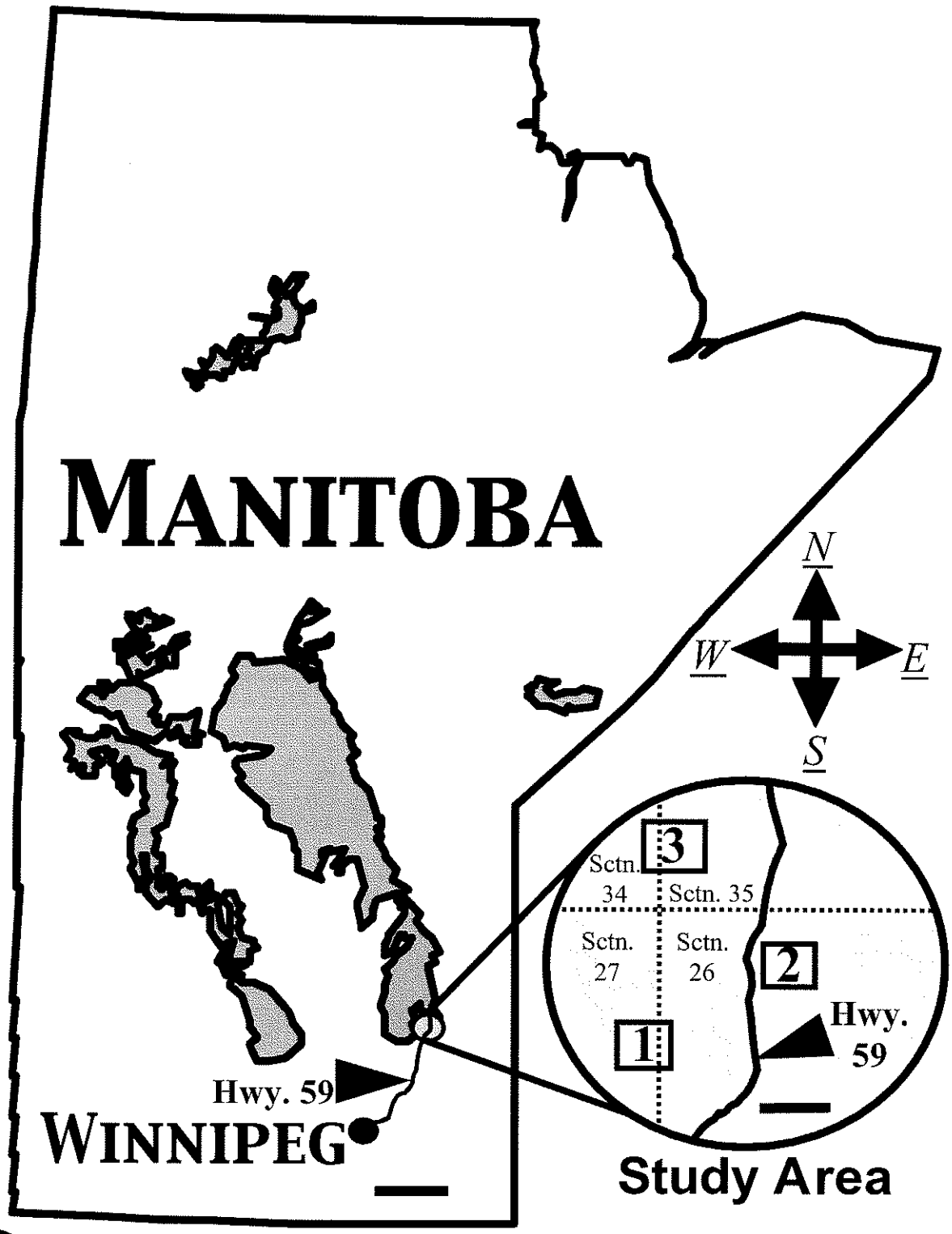

3.1 Map of Manitoba highlighting the study area in Grand Beach Provincial Park. The three study sites are labeled 1, 2, and 3. The boundaries of the four Sections (Sctn.) 26, 27, 34, and 35 of the study area inTownship 18 are indicated by hatched lines. The 1 cm scale bar for the main map = 50 km, and the 1 cm scale bar in the inset = 50 m.

(both infected and non-infected) appeared to be lower than that observed at Site 1.

Site 3 or the "Love Site" straddled Sections 34 and 35. A rock with valentine heart graffiti helped in the identification of this site. Site 3 was located 50 m west of Highway 59, 150 m northeast of Site 1, and 100 m northwest of Site 2. Site 3 appeared to be in a slough compared with Sites 1 and 2, and occasionally had standing water. This site possessed the greatest density of trees (both infected and non-infected).

After sampling of *Arceuthobium americanum* for this project was completed, the Manitoba Department of Natural Resources cleared the area of many infected jack pine trees, including trees that had been used in this study.

II. SELECTION OF INFECTED TREES AND SAMPLING OF *ARCEUTHOBIUM AMERICANUM*

1. Selection of Infected Trees for *Arceuthobium americanum* Sampling

To encompass within-site variability in *Arceuthobium americanum* female development, three infected jack pine trees per site were selected for sampling. Infected trees were those with witches' brooms, and because this study focused on female development, the witches' brooms needed to display female (pistillate) *A. americanum* shoots. One witch's broom typically results from an infection by one *A. americanum* individual (Hawksworth and Wiens, 1996).

A simplified uniform sampling design was used to select the three infected trees within each site starting at a centrally located arbitrary landmark. In each site, one witch's broom at eye level on a tree infected with female *Arceuthobium americanum* was chosen at distances of 5, 15, and 25 m away from the arbitrary landmark along a visual transect lying perpendicular to Highway 59. Therefore, a total of (three trees x three study sites =) nine witch's brooms were selected for sampling.

2. Manner and Timing of the Sampling of Female Individuals of *Arceuthobium americanum*

2A. Sampling to obtain a representative group of female flowers and/or fruits at various stages of development

From each of the nine *Arceuthobium americanum* female individuals, five female shoots were collected. Each female shoot contained at least fifteen female flowers and/or fruits. Fixation was performed in the field (see section III. - 1 of this chapter). In 1995, *A. americanum* female shoots were sampled from April to October from all three sites. Sampling was performed on Wednesday and Sunday of each week. In 1996, *A. americanum* female shoots were sampled from mid June to October on a weekly basis from all three sites. From November 1996 to March 1997, *A. americanum* female shoots were sampled every three weeks from all three sites in order to determine if any development occurred over the winter. Finally, in 1997, sampling occurred once a week

from April to October in Site 1 only, as it had been determined that the among-site variability was not consequential.

Although *Arceuthobium americanum* female shoot samples from each of the different sites, trees, and sampling dates were all kept track of, the data from samples collected from all trees and sites at a given date of the month over all sampling years were pooled. This was achieved by careful observation, note-taking, and photographic documentation, and permitted reasonable conclusions to be made regarding the overall pattern of development. Over five hundred female flowers/fruit from each given date of the month were examined, allowing for the among- and within-site variability as well as the yearly variation to be encompassed in the anatomical observations without fear that some variation was unaccounted for. Labeled specimens from each tree, site, and date are located at the University of Manitoba, Winnipeg, Manitoba, Canada.

2B. Sampling to obtain pseudoseeds

Artificially discharged pseudoseeds from nearly mature fruit

At least twenty *Arceuthobium americanum* shoots with nearly mature fruits were collected in a paper bag in the first week of August, 1998 (August 5), prior to explosive discharge. In the lab, the fruits were plucked off the shoots and lightly squeezed so that the pseudoseeds could be aimed at and discharged into a 6 mL glass vial. Each vial was filled to one-quarter full (at least fifty pseudoseeds) per vial. Artificially discharged pseudoseeds from nearly mature fruit were not fixed but immediately examined. This method for collecting pseudoseeds was modified after Hawksworth and Wiens (1996), in which paper bags containing shoots with fruit are shaken to induce discharge, and pseudoseeds picked off the paper bags.

Again, although the artificially discharged *A. americanum* pseudoseeds from each of the different trees and sites in this study were all kept track of, the data from samples collected from all trees and sites were pooled, allowing for the encompassment of variability. About one five hundred pseudoseeds were collected in this fashion.

Naturally discharged pseudoseeds from ripe, mature fruit

In 1998, pseudoseeds that had been naturally discharged from the ripe, mature fruit exocarp were obtained. In Manitoba, explosive discharge of *Arceuthobium americanum* can occur as early as the second week of August (Gilbert, 1988), so it was important to be prepared to obtain naturally discharged pseudoseeds prior to that date. In the first week of August, 1998 (circa August 1), cheesecloth (fine weave Sofwipe, Grade 40, 24 x 20 threads/ square inch) was loosely wrapped around branches of witch's brooms that were heavily laden with mature fruit. Six cheesecloth wraps were placed on each of the nine trees.

The cheesecloth wraps were then successively removed after the approximate time of explosive discharge. Eighteen cheesecloth wraps (two from each tree) were removed from the brooms on August 25m September 9, and October 1 (1998).

In the lab, naturally discharged pseudoseeds that had adhered to the cheesecloth were picked off by hand. These pseudoseeds were either immediately examined or were placed into 6 mL vials of fixative (see section III. - 1 of this chapter). This method of pseudoseed collection from cheesecloth wraps was also described in Hawksworth and Wiens (1996). Pseudoseeds from the three cheesecloth wrap sampling times were examined separately.

III. PREPARATION OF *ARCEUTHOBIUM AMERICANUM* PLANT MATERIAL FOR LIGHT MICROSCOPY, FLUORESCENCE MICROSCOPY, AND TRANSMISSION ELECTRON MICROSCOPY

All treatment was at room temperature (22° Celsius [C]) unless otherwise noted. All solutions, either weight/volume (w/v) or volume/volume (v/v) were aqueous, unless otherwise noted. Vinyl gloves were worn at all times during the handling of noxious substances, even in the field.

1. Fixation

A modified Karnovsky's fixative composed of 4% (w/v) paraformaldehyde/5% (w/v) glutaraldehyde in 0.015 M potassium phosphate (KPO_4) at pH 6.8 was used for all fixation. Slips of paper with pencil labeling were inserted into 6 mL glass vials, and fixative was added to the vials. The labeling remained highly legible. Plastic reusable caps were used to seal the vials.

Glass vials containing freshly prepared fixative were taken into the field for the collection of five female shoots from each of the nine trees. Prior to the insertion of the shoots into the vials, the flowers and fruits were lightly scored with a razor blade in order to facilitate the infusion of the fixative. Using a dissecting microscope and under a fume hood, the female flowers and/or fruits were detached from the shoot with a pair of forceps (#5) and a fine scalpel (11 blade). The detached flowers and fruits were returned to the vials containing the fixative, vacuum aspirated, and left overnight (14 hours [hr.]).

Approximately fifty naturally discharged pseudoseeds obtained from each cheesecloth wrap were fixed in the lab in a similar fashion. However, there was no need to score or vacuum aspirate the pseudoseeds.

After the fixation period, the vials were either processed for sectioning or transferred into the cold room at 4° C for storage. Some samples of nearly mature fruit (collected from the first week of August, circa August 5) that had been stored in fixative would not be processed for sectioning and would instead be used in the fluorometric ploidy analysis of the tissue regions within the fruit (see sections III. - 8B, III - 10D of this chapter, and Chapter Six, section II). Likewise, a proportion of the naturally discharged

pseudoseeds that had been fixed and stored in fixative would not be processed for sectioning and would instead be examined for their general whole appearance under the dissecting microscope (see section III. - 8A of this chapter).

2. Post-Fixation of Some Samples with Osmium Tetroxide and Pre-Dehydration Wash during Processing for Sectioning

A proportion of the fixed materials to be processed for sectioning was post fixed in osmium tetroxide. After fixation in the modified Karnovsky's fixative, the samples were rinsed 3 times each for 10 min. with 0.05 M KPO_4 buffer and were then post-fixed in 2% (w/v) osmium tetroxide in 0.025 M KPO_4 (pH 6.8) for 5 hr. This step was performed at room temperature in order to facilitate penetration of the samples by osmium tetroxide. The samples were then washed 3 times each for 10 min. with distilled, deionized water.

A proportion of the samples fixed in the modified Karnovsky's fixative was washed 3 times each for 10 min. in distilled, deionized water.

3. Dehydration in Preparation for Sectioning

All washed samples, including those that were post-fixed with osmium tetroxide, were dehydrated by an ascending series of ethanol in water solutions containing increasing proportions (v/v) of ethanol. The ethanol dehydration series was as follows: 30%, 50%, 70%, 90%, 95% (20 min. for each concentration) and 100% (3 times at 10 min.). Samples that had been post-fixed in osmium tetroxide were further dehydrated in an ascending series of propylene oxide in 100% ethanol solutions containing increasing proportions of propylene oxide as follows: 50% (10 min.), and 100% propylene oxide (3 times, each 10 min.).

4. Infiltration and Embedding for Sectioning

4A. Spurr's epoxy resin

Infiltration

Dehydrated samples that had been post-fixed with osmium tetroxide were infiltrated with Spurr's epoxy resin (Spurr, 1969). During infiltration, the vials were

continuously rotated to ensure adequate infiltration. This was accomplished by attaching the specimen vials to a barbecue rotisserie set up in the fume hood. The dehydrated samples were passed through a series of solutions containing increasing proportions (v/v) of Spurr's epoxy resin in 100% propylene oxide as follows: 50% Spurr's epoxy resin, 75% Spurr's epoxy resin (48 hr.), and 100% Spurr's epoxy resin (3 times in 12 days, 96 hr. each time). The infiltration times were longer than usual to infiltration of the relatively large fruit samples. Spurr's accelerator was added only in the last change of 100% Spurr's epoxy resin in order to prevent premature polymerization.

Polymerization and embedding

For polymerization and embedding of the samples infiltrated with Spurr's epoxy resin, the samples plus 100% Spurr's epoxy resin were evenly distributed in 44 mm aluminum weighing dishes (Fisher Scientific) with a toothpick. Polymerization of Spurr's epoxy resin is not impeded by oxygen. Spurr's embedding typically takes place at 70° C in 14 hr., but a lower temperature and longer polymerization time (48° C for 72 hr.) was used in order to preserve reactive sites that might otherwise have been damaged by the higher temperature (Newman *et al.*, 1982).

4B. L.R. White resin

Infiltration

Dehydrated samples that had not been post-fixed with osmium tetroxide were infiltrated with L.R. White (Polysciences) acrylic resin (hard grade). The general method is outlined in the Polysciences specification sheet. As with Spurr's epoxy resin, the vials were continuously rotated during infiltration. Infiltration of L.R. White resin into the sample tissue is facilitated by 100% ethanol. The dehydrated samples were passed through a series of solutions containing increasing proportions (v/v) of L.R. White resin in 100% ethanol as follows: 30% L.R. White, 60% L.R. White (24 hr.), and 100% L.R. White (3 times in 6 days, 48 hr. each time). Care was taken not to fill the vials too full with 100% L.R. White, as premature polymerization would occur.

Polymerization and embedding

Samples were evenly distributed in 44 mm aluminum weighing dishes (Fisher Scientific) with a toothpick. To create an oxygen-free environment for L.R. White polymerization, an empty aluminum weighing dish was placed on top of each dish that contained samples and L.R. White so that no air was in contact with the L.R. White. The dishes were then placed in an oven at 48^{o} C, and left 14 hr. to polymerize.

5. Mounting of Samples for Sectioning

Cubes containing an embedded flower, fruit, or naturally discharged pseudoseed, were cut out from the plastic discs of hardened Spurr's epoxy and L.R. White resin with a small hand saw. The cubes were then mounted onto blanks of hardened Spurr's epoxy resin Beem capsules with 5-min. epoxy (Lepage's), forming a block. The mounting of the cubes was achieved in various orientations so that longitudinal sections, cross sections, and oblique sections could be obtained. The block was then rough trimmed using a Dremel grinder and fine trimmed into a trapezoidal face with a Reichert-Jung TM-60 Trimmer.

6. Sectioning of Samples

Throughout this thesis, anatomical descriptions are of median longitudinal sections unless otherwise stated.

6A. Sectioning for light and fluorescence microscopy

Sectioning for Spurr's epoxy resin-embedded samples and L.R. White resin-embedded samples was performed in the same manner. Only Spurr's-embedded samples were used for fluorescence microscopy.

Sections were cut 5 at a time on a Sorvall, Porter-Blum JB-4 microtome with a glass knife equipped with a water trough (Fisher, 1968). For most cases, 2 μm sections were an ideal thickness for both the Spurr's-embedded and the L.R. White-embedded samples. For the examination of chromosomes for ploidy analysis, sections were made as thick as 5 μm (see Chapter Six, section II). All sections were transferred from the surface of the water in the water trough to a drop of distilled, deionized water on a gelatin-coated

glass slide using a glass microprobe. Slides had been coated with 0.5% (w/v) gelatin adhesive (Jensen, 1962). Up to 10 separate drops of sections and water were placed on to a single slide. The slides were placed on a slide warmer (at 65° C) under xylene vapour to dry and flatten the sections, as well as to ensure proper section adhesion to the slide.

6B. Sectioning for transmission electron microscopy

Both Spurr's-embedded samples and L.R. White-embedded samples were sectioned for electron microscopy. Sections were cut on a Reichert-Jung Ultracut ultramicrotome with a DuPont diamond knife; 60-90 nm (pale gold interference colours) sections seemed to be the ideal thickness. The ribboned sections floating on the surface of the water in the diamond knife boat were absorbed on the shiny side of nickel 200 hex grids. The grids were placed section side up on Whatman #1 filter paper in a Petri dish and the grids were allowed to air dry overnight (14 hr.).

7. Light Microscopy Stains for Sections and Whole Mounts

7A. Stains for Spurr's-embedded sections

Crystal violet

Crystal violet stain (colour index [C.I.] 42555, Fisher) was used to outline basic morphology of the sectioned samples embedded in Spurr's epoxy resin. The stain is a basic, cationic dye which binds to acidic groups (Pease, 1964). Crystal violet stain was made by dissolving 2g crystal violet in 20 mL of 95% (v/v) ethanol and mixing with 0.8 g ammonium oxalate dissolved in distilled water (Gerhardt *et al.*, 1981). The stain was filtered twice through Whatman #1 filter paper. The stain was dispensed onto slide-mounted sections through a 0.45 μm filter. Spurr's sections were stained 45 seconds (sec.) on a slide warmer at 65° C, and rinsed under running distilled water to remove excess stain. Slides were dried with a stream of filtered air, and mounted in 70% (w/v) sucrose. The cytoplasm stains violet; good contrast is provided. Lipid components not disturbed by the dehydration procedure have a tendency to stain greenish-grey to grey (Sumner, 2001; personal communication).

Periodic Acid - Schiff's (PAS) Treatment

The Periodic Acid - Schiff's (PAS) treatment was used to localize insoluble polysaccharides (carbohydrates) by the method outlined by O'Brien and McCully (1981). According to Jensen (1962), the PAS reaction is the most important histochemical technique available for the localization and identification of carbohydrate polymers. Periodic acid oxidizes vicinal 1,2 glycol groups (hydroxyl groups at the 2^{nd} and 3^{rd} carbon) into dialdehydes and breaks the carbon-carbon bond (Sumner, 1988). Schiff's reagent, a colourless reagent, binds to dialdehyde groups and gives a pink/dark pink/magenta colour when combined with dialdehydes. Thus, pink colour indicates a PAS-positive reaction.

Compounds can be PAS-negative when the hydroxyl groups are not attached to vicinal carbon atoms. This occurs when the glycol group is substituted with a sulfate, in the case of sulfated polysaccharides, or with phosphate, in the case of nucleic acids. This is also the case when one of the vicinal carbons is involved in linkages such as β 1-3 glucans (i.e. calloses). Carbohydrates such as cellulose, hemicellulose, pectic compounds, oligosaccharide side chains of glycoproteins, and starch should all be PAS-positive. However, cellulose can also produce a PAS-negative reaction. O'Brien and McCully (1981) speculated that stearic hindrance may block the available vicinal glycol groups in tightly-packed cellulose cell wall microfibrils.

Certain compounds, other than carbohydrates, will also exhibit a PAS-positive reaction. These include the amino acids serine, threonine, and hydroxylysine, which have vicinal hydroxy-amino groups that can be oxidized to dialdehydes.

The slides with Spurr's sections were blocked for endogenous aldehyde by incubating in saturated 2,4 dinitrophenyl hydrazine (DNPH) in 15% (v/v) acetic acid for 30 min. and rinsed 10 min. in distilled water. After incubation for 30 min. in 1% (w/v) periodic acid in distilled, deionized water and rinsing for 10 min. in distilled water, they were stained for 45 min. in Schiff's reagent (Fisher Scientific). The slides were rinsed for 10 min. in distilled running water, blown dry with a stream of filtered air, and mounted in 70% (w/v) sucrose. A control procedure was also employed in which water was substituted for periodic acid.

Aniline blue black (ABB)

Aniline blue black (ABB) stain, an anionic dye, was used to localize protein after the methods outlined by O'Brien and McCully (1981). Slides with Spurr's sections were placed in Copland jars containing 1% (w/v) ABB (C.I. 20470, Polysciences) in 7% (v/v) acetic acid for 15 min. at 65° C. The slides with sections were briefly rinsed in 7% (v/v) acetic acid at room temperature to remove excess stain and then mounted in glycerol containing 5% (v/v) acetic acid. A positive reaction results in a bright to dark blue stain, whereas a negative reaction results in no colour. ABB was occasionally used to stain sections that had previously been treated with PAS.

The Yeung procedure

The Yeung procedure is a cytochemical test that helps to verify results obtained by other cytochemical tests, and is particularly good for distinguishing lipids from phenolics in osmicated tissue (tissues that have been post-fixed in osmium tetroxide). The procedure is after Yeung (1990). Slides with Spurr's sections were immersed in 0.5% (w/v) periodic acid in distilled, deionized water for 20 min. The slides were rinsed in slow running water for 5 min. and transferred to three successive baths of 0.5% (w/v) solutions of sodium metabisulfite in a 1% (v/v) dilution of concentrated hydrochloric acid for 2 min. each time. The slides were then rinsed in slow running water for 5 min. Next, counterstaining was achieved by dispensing large drops of 0.5% (w/v) Toluidine Blue O in 2.5% (w/v) sodium carbonate at a basic pH (pH 10.9) onto slide-mounted sections through a 0.45 μm filter. The slides were placed on a slide warmer at 65° C for 5 min. The basic pH and the increased time of Toluidine Blue staining allowed the water soluble Toluidine blue to penetrate the hydrophobic Spurr's resin. Finally, the slides were rinsed with tap water at room temperature for 1 min. by flooding the slide, and the slides were dried on the slide warmer at 65° C. Sections were mounted in 70% (w/v) sucrose. Cell walls and starch grains appear red, lipid materials/bodies appear grayish-blue, cytoplasm and nuclei appear pinkish-blue to purple, carbohydrates appear pink as per the PAS reaction, and phenolics appear greenish-blue.

7B. Stains for L.R. White-embedded sections

Toluidine blue O (TB) stain

A Toluidine blue O (also simply "Toluidine Blue" [TB]) stain (C.I. 52040, Polysciences) was used to outline general morphology as well as to provide cytochemical information. TB is a basic, cationic, metachromatic dye which binds to acidic groups. If the acid groups are less dense, the substances will stain blue. However, if the acid groups are arranged close together, the substances will appear purple or red in an aqueous environment (Sumner, 1988). A 0.05% (w/v) solution of TB was prepared in benzoate buffer (0.25 g of benzoic acid and 0.29 g of sodium benzoate in 200 mL of water) at a pH of 4.4. A 1% (w/v) solution of TB (unbuffered) at a pH of 2.2 was also prepared. L.R. White sections were covered with either TB solution, incubated on a slide warmer at 65° C for 1.5 min., rinsed under distilled water for 15 sec., dried with a stream of filtered air, and mounted in 70% (w/v) sucrose. With TB staining at pH 4.4, phenolics stain metachromatic greenish-blue, nucleic acids and proteins stain metachromatic purple due to the presence of phosphate groups, and pectic and alginic acids stain pink due to the presence of carboxyl groups. At pH 2.2, the carboxyl groups are no longer ionized and thus do not stain with TB. Therefore, TB at the lower pH acted as a control for the staining of carboxyl groups. However, where TB was used simply to outline basic morphology, the solution at the higher pH was used.

Sudan Black B (SBB)

Lipid materials and lipid bodies were localized with saturated Sudan Black B (SBB, C.I. 26150, Sigma) used according to Bronner (1975) with some modifications. A saturated solution (about 0.3% w/v) of SBB in 70% (v/v) ethanol was warmed at 37° C overnight (14 hr.) and filtered twice through Whatman #1 filter paper just prior to use. Slides with L.R. White sections were preincubated in 70% ethanol for 2 min., and stained in the SBB solution at 55° C for 1 hr. They were rinsed one min. in 70% (v/v) ethanol, and differentiated for 15 min. in 80% (v/v) ethanol at room temperature. Slides were rinsed briefly in running distilled water, blown dry with a stream of filtered air, and mounted in 70% (w/v) sucrose. A positive reaction, indicative of lipids, results in dark grey to black staining. Tannins and polyphenolics also display a slightly positive

reaction, in which grey staining is observable. However, as a dehydration process was used to infiltrate L.R. White resin into the tissues, it is realized that some of the lipids may have been lost during the dehydration process. Nonetheless, as the L.R. White infiltration process did not require dehydration with the very hydrophobic propylene oxide, it is believed that at least some lipid material/bodies would be retained and stained with SBB.

7C. Vital staining of whole, unfixed material with 2,3,5-triphenyl tetrazolium chloride (2,3,5-TTC)

To test the viability of naturally discharged pseudoseed components, pseudoseeds were picked off the cheesecloth wraps and immediately soaked in distilled water for 24 hr. Pseudoseeds were then bisected longitudinally, placed in sterile Petri plates, and submerged in 1% (w/v) 2,3,5-triphenyl tetrazolium chloride (2,3,5-TTC) in the dark for 72 hr. (Smith, 1951; Scharpf and Parmeter, 1962). A general red staining, visible to the naked eye and under the dissecting microscope, indicated viability of the given pseudoseed component. In order to examine the embryo more effectively, pressure was applied to the middle of the pseudoseed with forceps (#3) so that the embryo was forced from the endosperm. If the embryo stained red, it was assumed that the pseudoseed had germination potential. The staining reaction of the viscin cells was also examined at the light microscope level (see section III. - 10B of this chapter).

8. Fluorescence Microscopy Stains for Sections and Whole Mounts

8A. Stains and relevant procedures for Spurr's-embedded sections

Resin extraction

Prior to the examination of Spurr's epoxy resin-embedded sections with stains for fluorescence microscopy, the resin, which is autofluorescent, was extracted following a procedure outlined by Sutherland and McCully (1976). Slides containing the Spurr's-embedded sections were immersed in a saturated solution of potassium hydroxide in 95% ethanol for 2 min., immersed in 2 successive changes of 95% ethanol for 5 min. each, and

then immersed in deionized, distilled water for 5 min. The slides were carefully blown dry with a stream of filtered air.

Calcofluor White M2R ("Calcofluor")

Calcofluor White M2R ("Calcofluor", C.I. 40622, Polysciences) was used to localize ß 1-4 glucans, such as cellulose and hemicellulose, as demonstrated by Wood and Fulcher (1978), although Calcofluor also has the ability to bind to β 1-3 glucans (Krishnamurthy, 1999). After the resin extraction, the sections on the slides were covered in 0.01% (w/v) Calcofluor for 5 min., and rinsed under distilled water for 30 sec. The slides were dried with a stream of filtered air, and mounted in 70% (w/v) sucrose. When viewed with ultraviolet illumination, Calcofluor positive regions show blue fluorescence.

Enzymatic digests in conjunction with Calcofluor staining

Since both cellulose and hemicellulose will fluoresce in the presence of Calcofluor, enzymatic digests were used to clarify whether cellulose or hemicellulose predominated in viscin tissue cell walls and mucilage (concerns regarding the specificity of the enzymes will be addressed in Chapter Four - III. Discussion). Glass slides in which the sections had the resin removed (see the first paragraph in section III - 8A of this chapter) were treated with several combinations of digestive enzymes from *Aspergillus niger* (Sigma):

(1) Cellulase alone. The enzyme is an endo-ß 1-4 glucanase that cleaves unbranched molecules, and will digest cellulose, which is never branched (Krishnamurthy, 1999). This particular enzyme (product # C1184; lot # [MDL] MFCD00081510) is 99.9% pure (single band on an electrophoretic gel), but does show some ß 1-3 glucanase activity. The cellulase is prepared as1 mg enzyme/ mL 0.5 M KPO_4, pH 6.8. Cellulase alone would be expected to digest cellulose but leave hemicellulose largely undigested.

(2) Hemicellulase alone. The enzyme is primarily an endo-ß 1-4 glucanase that cleaves branched molecules, and thus will digest any hemicellulose (which are almost always branched molecules) with a large number of ß 1-4 linked glucosyl units in the backbone (Joseleau and Ruel, 1985). This particular enzyme (product # H2125; lot # [MDL] MFCD00131279), although considered crude (it displays some cellulase activity and ß 1-

3 glucanase activity), has measured xyloglucanase activity. The hemicellulase is prepared as1 mg enzyme/ mL 0.5 M KPO_4, pH 6.8. Hemicellulase alone would be expected to digest hemicelluloses with ß 1-4 linked glucosyl units in the backbone but leave cellulose largely undigested.

(3) Both cellulase (1 mg enzyme/ mL 0.5 M KPO_4, pH 6.8) and hemicellulase (1 mg enzyme/ mL 0.5 M KPO_4, pH 6.8), which, in combination, would be expected to remove both cellulose and hemicelluloses with ß 1-4 linked glucosyl backbone units, respectively.

(4) 0.5 M KPO_4, pH 6.8 alone, which acted as a control for the digestive enzyme treatments; cellulose and hemicellulose should remain undigested.

Slides were immersed in Copland jars containing the three treatments and the control at 37° C for 6 hr. and subsequently stained with Calcofluor. The amount of fluorescence emanating from the cell walls and the mucilage of viscin cells was visually estimated in order to determine the relative abundance of cellulose and hemicellulose.

Aniline Blue

Aniline blue is a fluorescent stain thought to be specific for ß 1-3 glucans, such as callose (O'Brien and McCully, 1981). Callose is a cell wall carbohydrate composed of linear ß 1,3 glucans that cannot be located using the Periodic Acid - Schiff's treatment since the vicinal hydroxyl groups are not available due to the 1-3 linkage at the polymers.

Slides with sectioned material in which the resin was removed were stained for 5 min. in a solution of 0.05% (w/v) aniline blue (C.I. 42755, Polysciences) in 0.01 M KPO_4 buffer (pH 6.8). The sections were then mounted in the same buffered stain and viewed under ultraviolet illumination. When viewed with ultraviolet illumination, the aniline blue positive regions show pale blue fluorescence.

8B. Hoechst staining of non-embedded, whole fixed material for fluorometric ploidy analysis

Pre-staining treatment

Ten nearly mature fruit samples that had been collected in early August (circa August 5), fixed in the modified Karnovsky's fixative, and stored in the fixative at 4° C

(review section III. - 1 of this chapter) were used for fluorometric ploidy analysis (see Chapter Six, section II). The fruit were stored for six months without obvious degradation. Immediately prior to use, the fruit samples were washed 3 times in 30 min. (10 min. each time) in distilled, deionized water. The fruits were examined under a dissecting microscope (see section III. - 10A of this chapter), the various specific fruit components were separated from each other (see Chapter Six, section II), and specific fruit samples were affixed to gelatin-coated glass slides (also see Chapter Six, section II).

Hoechst staining

The Hoechst dyes are specific for DNA, binding to the major groove (Arndt-Jovin and Jovin, 1989). A 100 μg/mL stock solution of Hoechst dye #33342 (C.I. B 2261, Sigma) in distilled, deionized water was prepared and stored at 4° C in the dark, as this dye is light sensitive. When ready for use, the Hoechst dye was freshly diluted to 1 μg/ml distilled water. For staining, two drops of the diluted Hoechst dye were applied to each sample that had been affixed to the slides. The slides were then placed in the dark for 4 min. After the staining time, the slides were transferred to Copland jars containing fresh distilled water for 2 min. in order to wash away excess stain. The washing step was also performed in the dark. The slides were then dried with a stream of filtered air and the specimen was mounted in 0.5M KPO_4 buffer (pH 6.8). Examination of the slides was immediate. Nuclei fluoresce blue-white under ultraviolet illumination, and condensed chromosomal material fluoresces especially brightly.

9. Transmission Electron Microscopy Stains

9A. Stains for Spurr's-embedded sections

Osmium tetroxide

Osmium tetroxide, in addition to acting as a secondary fixative, acts as a lipophilic stain for electron microscopy (O'Brien and McCully, 1981).

Uranyl Acetate/Lead Citrate (UA/LC)

Uranyl acetate and lead citrate (UA/LC) were used together and in conjunction with osmium tetroxide to provide contrast within the tissues and outline the

ultrastructural morphology. The staining procedure for UA/LC is after Reynolds (1963). Saturated uranyl acetate in 50% (v/v) methanol was dispensed into the wells of a ceramic plate through a 0.2 μm syringe filter. The nickel grids containing the sections on the shiny side were floated shiny side down on the stain for 30 min. in the dark, as uranyl acetate is light sensitive. The grids were dipped briefly in 50% (v/v) methanol and rinsed 30 min. in distilled, ultrafiltered water. A Petri dish was lined with Parafilm, and a small dish of wetted potassium hydroxide was placed inside to absorb carbon dioxide. After 5 min., large drops of lead citrate were dispensed through a 0.2 μm syringe filter onto the Parafilm. Grids were floated shiny side down on the drops for 10 min. The grids were dipped for 10 sec. in boiled (degassed) water, blotted with filter paper, and laid on a silicone rubber mat to dry overnight (14 hr.).

9B. Stains for L.R. White-embedded sections

Periodic Acid - Thiocarbohydrazide - Silver Proteinate (PATCH)

Periodic Acid - Thiocarbohydrazide - Silver Proteinate (the PATCH procedure) was used to localize carbohydrate polymers at the ultrastructural level. This procedure works on the same basis as the PAS reaction for light microscopy except that it employs an electron-dense marker for use with electron microscopy. Again, the periodic acid oxidizes vicinal glycol or glycol-amino groups to a dialdehyde, but each aldehyde is then condensed with a molecule of thiocarbohydrazide (TCH) to produce two thiocarbohydrazones, which are strong reducing agents. Each pair of thiocarbohydrazone molecules is then the binding site for one molecule of silver proteinate. When silver proteinate combines with a pair of thiocarbohydrazone molecules, reduced silver is deposited over the reaction site. Krishnamurthy (1999) stated that the PATCH procedure is somewhat specific for hemicellulose. Hemicellulose has a greater number of potential reaction sites than pectic acids (in which the silver proteinate molecules, unlike the Schiff's molecule, may be unstable; Owen and Thomson, 1991) or cellulose (which is crystalline and stearically hinders the binding of TCH and/or the silver proteinate; O'Brien and McCully. 1981). Like PAS, though, oligosaccharide side chains of glycoproteins would likely be positive for PATCH if vicinal hydroxyl groups are

available. However, cellulose can be identified with PATCH staining, as cellulose microfibrils that are enveloped in hemicellulose can be visualized (Krishnamurthy, 1999).

The procedure after Thiéry (1967) was followed. The entire staining process was carried out in a high humidity chamber, which consisted of a partially water-filled Tupperware vessel. Grids were immersed in 1% (w/v) periodic acid for 30 min. In the case of grid immersion, grids were not floated but instead were sunk to the base of staining wells with the shiny- or section-side of the grid up. The grids were then rinsed in distilled water three times (10 min. each), immersed in 0.2% (w/v) thiocarbohydrazide in 20% (v/v) acetic acid for 5 hr., and then rinsed in 10%, 5%, and 1% (v/v) acetic acid 20 min. each time. Next, the grids were rinsed in distilled water for 3 times, 20 min. each time. The grids were blotted dry and left on a silicone mat overnight (14 hr.). The grids were immersed in 1% (w/v) silver proteinate for 30 min. in the dark, as silver proteinate is light-sensitive, rinsed in distilled water 3 times (1 hr. each time), blotted on filter paper, and air dried overnight (14 hr.) on a silicone mat. Electron opaque deposits identify carbohydrates containing 1,2 glycol groups or dialdehyde groups. A control procedure was also employed in which water was substituted for periodic acid. The PATCH positive regions show grainy electron opaque deposits.

Lectins

Lectins are proteins or glycoproteins that are able to bind to specific carbohydrate moieties of complex carbohydrates (Goldstein and Hayes, 1978; Damjanov, 1987). Lectins can be readily labeled with electron-opaque markers such as colloidal gold or ferritin and these labeled lectins can be used in transmission electron microscopy as probes to localize carbohydrate moieties of various tissues and cells (Horisberger, 1985; Damjanov, 1987).

Two lectins were purchased from Sigma as conjugates with electron-opaque markers. The first lectin was *Vicia faba* agglutinin (VFA), a lectin conjugated with a colloidal gold label. VFA localizes α/β-D-mannosyl and α/β-D-glucosyl carbohydrate moieties (Roth, 1983). VFA was purchased as a conjugate with 20 nm colloidal gold. The second lectin was peanut agglutinin (PNA), which localizes ß-D-galactosyl-(1,3)-NAc-galactosyl and ß -D-galactosyl carbohydrate moieties (Roth, 1983). PNA was

purchased as a conjugate with 20 nm colloidal gold as well as with ferritin. Other purchased lectins gave inconclusive results.

All lectin cytochemistry was performed on Parafilm (Fisher). Grids with sections were always floated section-side down on 2 mL drops of the appropriate solution. The protocol was as follows:

a). Blocking. Grids were treated with 5% (w/v) bovine serum albumin (BSA) (Sigma) in 0.15 M potassium phosphate-buffered saline (PBS), pH 6.8 for 30 min.

b). Washing. Grids were washed 3 times in 0.5% (w/v) BSA in 0.15 M PBS (pH 6.8), 10 min. each time.

c). Lectin-Marker Probing. Each lectin-marker was diluted from 1 in 5 to 1 in 250 (v/v) with PBS buffer. The dilutent buffer consisted of 0.5% (w/v) BSA and 0.1% (w/v) Tween 20 (Sigma) in 0.15 M PBS (pH 6.8). For controls, a second set of lectin dilutions was prepared in which 0.1 M of the appropriate inhibitory sugar was included. For VFA, the inhibitory sugar was D-glucose (mixed anomers) (Roth, 1983). For PNA, the inhibitory sugar was β-D-galactose (Roth, 1983). Treatment and control dilutions were left in microcentrifuge tubes (Fisher) for 30 min. prior to incubation of the grids. This was to allow time for the inhibitory sugars in the controls to bind with the lectins. Grids were left in the treatment and control lectin dilutions for 5 hr.

d). Final Washing and Drying. Grids were washed 3 times in 0.5% (w/v) BSA in 0.15 M PBS (pH 6.8), 10 min. each time, and then washed 3 times in water. Grids were allowed to dry overnight section side up on Whatman # 1 filter papers (Fisher) in covered Petri dishes (Fisher).

Electron-opaque colloids (gold) or grains (ferritin) identify appropriate carbohydrate residue binding sites. Previewing with electron microscopy determined that the lectin dilution that showed the least background binding in the control in all cases was the 1 in 25 dilution. Occasionally, uranyl acetate/lead citrate staining was used after lectin treatment to enhance morphology, even though lectin-treated sections had been infiltrated and embedded in L.R. White.

10. Manipulation, Viewing and Image Capture of Sections and Whole Materials

10A. Light microscopy with a dissecting microscope

A Wild Leitz M5A dissecting microscope equipped with a Wild Leitz Microscope Transformer light source was used for routine dissections, including the detachment of flowers and/or fruit from the shoot and the separation of various fruit components. In all cases, the Wild Leitz was used with epiillumination and a clear base. Images were not captured during these routine dissection processes, although general observations were made.

In order to examine and photograph whole, naturally discharged pseudoseeds (fixed and unfixed) for their general structure, to examine extracted viscin cell mucilage (see section IV - 2 of this chapter) for cellular contaminants, and to examine those naturally discharged pseudoseeds for their general staining reaction with 2,3,5-TTC, an Olympus SZH DFplan dissecting microscope equipped with an Intralux Volpi 150H light source was employed. Epiillumination and a white stage base proved most useful. Photomicrography was possible with this microscope, and was performed as described in section III. - 10E of this chapter.

10B. Brightfield light microscopy with a compound microscope

All sections of flowers, fruit, and naturally discharged pseudoseeds were viewed on a Nikon Optiphot compound light microscope. Wherever possible, high quality glycerol immersion objective lenses (10X and 40X) were employed. Photomicrography was performed as described in section III. - 10E of this chapter. Whole viscin cells from naturally discharged pseudoseeds stained with 2, 3,5-TTC were also examined with the compound light microscope. Additionally, for the purpose of counting chromosomes in ploidy analysis, photomicrography as well as video capture with a framegrabber (described in Chapter Six, section II) was performed with the compound light microscope.

10C. Polarizing and interference-contrast microscopy

Whole viscin cells of unfixed, artificially discharged pseudoseeds from nearly mature fruit were examined with polarizing optics and differential interference-contrast

light microscopy. Extracted viscin cell mucilage (see section IV - 2 of this chapter) was also examined with polarizing optics. Observations were made using a Leitz Orthoplan compound microscope equipped with two polarizing filters (the polarizer and the analyzer), and, in the case of the interference-contrast microscopy, two modified Wollaston prisms. For both polarizing and interference-contrast microscopy, whole viscin cells dissected from the artificially discharged pseudoseeds as well as extracted mucilage samples were mounted on glass slides with 0.5 M KPO_4 buffer (pH 6.8) and viewed immediately. Photomicrography was performed as described in section III. - 10E of this chapter.

10D. Fluorescence microscopy

For fluorescence microscopy, the Nikon Optiphot compound light microscope was fitted with a Nikon "EF" episcopic fluorescence attachment containing a 50 W high pressure mercury vapour lamp.

Ultraviolet illumination was used to view sections stained with Calcofluor, and aniline blue, as well as whole fruit components stained with Hoechst. For observation under ultraviolet excitation, an excitation filter transmitting 330-380 nm, a dichroic mirror DM 400, and a barrier filter transmitting above 420 nm were used.

Blue illumination was used to examine whole viscin cells from unfixed pseudoseeds that were either artificially or naturally discharged from nearly mature or fully mature fruit, respectively. The blue illumination induces chlorophyll autofluorescence in the red end of the visible light spectrum. The whole viscin cells were mounted on glass slides with 0.5 M KPO_4 buffer (pH 6.8) and viewed immediately. For observation under blue illumination, an excitation filter transmitting 410-485 nm and a barrier filter transmitting above 515 nm were used.

Photomicrography for all fluorescence microscopy was performed as described in section III. - 10E of this chapter. For fluorometric ploidy analysis of Hoechst-stained fruit tissues, photomicrography as well as video capture with a framegrabber (described in Chapter Six, section II) was performed.

10E. Photomicrography for dissecting microscopy, brightfield microscopy, polarizing microscopy, interference-contrast microscopy, and fluorescence microscopy

Photomicrographs from the types of microscopy listed above (dissecting, brightfield, polarizing, interference-contrast, and fluorescence) were recorded using a Nikon Microflex AFX photomicrographic attachment. Phototube magnification was between 5X and 10X. Colour slide photomicrographs were recorded on 35 mm Ektachrome 160 T professional film (for dissecting, brightfield, polarizing, and interference-contrast microscopy) and on 35 mm Ektachrome 400 Daylight film (for fluorescence microscopy). The film was developed by the Ektachrome procedure into colour slides at Don's Photo (261 Vaughan Street, Winnipeg, Manitoba, Canada).

10F. Transmission electron microscopy

All sections were viewed on a Hitachi Model H-7000 transmission electron microscope and electrons were accelerated at an operating voltage of 75 kilovolts. Electron images were recorded on Kodak electron microscope film, ESTAR thick base. Electron microscope negatives were developed using Kodak D-19 developer.

11. Landscape Photography and Macrophotography

Photography of landscapes, although not incorporated into the thesis plates, was essential to obtaining an overall perspective of the *Arceuthobium americanum* study area. Landscape photography was performed with a Minolta Maxxum 7000i camera equipped with a program back (PB-7) and a 90 mm (ϕ 52) 1:2.5 Tamron lens with macrophotographic capability. For macro lens photography of *A. americanum* female shoots containing flowers and fruit, the same system was equipped with a Minolta Maxxum Macro (Ring) Flash 1200 AF. All landscape and macro lens photographs were colour slide photographs recorded on 35 mm Ektachrome 400 Daylight film. The film was developed into colour slides at Don's Photo (Ektachrome procedure).

12. Digitization of Colour Slides and Electron Microscope Negatives for the Purposes of Plate Making

Colour slides were digitally captured using a Polaroid Sprint Scan 35/LE slide scanner in conjunction with Adobe PhotoShop 5.0.2 and PolaColor Insight 3.5 imaging software installed on a Macintosh G3 computer. Electron microscope negative images were digitally captured and made positive through a UMAX Astra 3450 Flatbed scanner in conjunction with Adobe PhotoShop 5.0.2 and UMAX VistaScan imaging software installed on the G3. Images were saved as 1200 DPI (dots per inch) JPEG (Joint Photographic Experts' Group) files, which could be compressed to a manageable size of about 900 K (kilobytes) per image. Aside from the enhancement of contrast, brightness, colour balance, and orientation, images were not typically digitally altered. Occasionally, spot blurs, sharpens, and erasures were used to enhance the appearance of the image without altering the anatomical information. Images were arranged into plates and labeled using the Adobe Illustrator 9 program. Computer-assisted drawings were also composed in the Adobe Illustrator 9 program. The plates were arranged in the CMYK (Cyan-Magenta-Yellow-Black) colour mode, although either the RGB (Red-Green-Blue) mode or the Lab Colour mode would have been acceptable. Plates were printed with an Epson 900 Colour inkjet printer onto Office Depot high gloss photo-quality paper. Caution was taken to ensure that the images would not deteriorate. Electronic compact disc backups will become the property of the University of Manitoba.

IV. GENERAL BIOCHEMICAL ANALYSIS OF THE VISCIN CELL MUCILAGE OF ARTIFICIALLY DISCHARGED PSEUDOSEEDS FROM THE NEARLY MATURE FRUIT OF *ARCEUTHOBIUM AMERICANUM*

1. Procurement of Viscin Cell Mucilage

Some unfixed artificially discharged pseudoseeds from nearly mature fruit (sampled from early August, circa August 5) were prepared for the procurement of viscin cell mucilage so that the general biochemical properties of the mucilage could be determined. To obtain mucilage, thirty pseudoseeds at a time were placed on Nylon 66 membrane (47 mm diameter, 0.20 μm pores, Sigma), wetted with 2 mL of KPO_4 (pH 6.8), and bundled. Each bundle was then placed in a microcentrifuge tube so that the lid closed on the bundle and suspended the pseudoseeds near the middle of each tube. Tubes were centrifuged for 2 min. at a low speed of 500 revolutions per minute (RPM). The hydrated viscin cell mucilage accumulated at the bottom of tubes, whereas the remaining cellular components were retained within the Nylon membrane and discarded. Some mucilage was removed from the centrifuge tubes with pipettes so that it could be visually assessed for cellular contaminants (see section III. - 10A) or viewed with polarizing microscopy (see section III. 10C).

2. Preliminary Assessments of the Viscin Cell Mucilage

In order to determine the amount of hydrated mucilage per pseudoseed in mL, the total amount of hydrated mucilage obtained was divided by the number of pseudoseeds used to obtain that hydrated mucilage (mucilage removed for microscopical observation was accounted for). In order to determine the amount of dry mucilage material (in μg) per mL of hydrated mucilage, a known volume of hydrated mucilage was placed in a 44 mm aluminum weighing dish and placed overnight (14 hr.) in a vacuum drying oven at 48^{o} C. After drying, the oven was allowed to reach room temperature before the vacuum was released. The mass of the dried mucilage was then obtained immediately, and was divided by the total known volume of hydrated mucilage.

3. Preparation for Biochemical Assays

Distilled, deionized water was used for all biochemical analyses, and all solutions were aqueous, unless otherwise noted. In order to ensure that the viscin mucilage being analyzed fell within the optimal range of detection for the quantification of either carbohydrates, uronic acids, or proteins, the hydrated mucilage was diluted to 10% mucilage, 5% mucilage, and 2% mucilage (v/v). The 10% mucilage dilution was beyond the range of detection for all three assays, and so it was not used in further estimations.

Mucilage was assayed for total carbohydrates (against a galactose standard), total uronic acids (against a galacturonic acid as well as against a glucuronic acid standard), and total proteins (against a bovine serum albumin [BSA] standard). For each assay, a standard curve was generated in which the concentrations of the proper standard were known. In order to generate the standard curve, each standard substance first was dried in a vacuum drying oven at 48^{o} C. After drying, the oven was allowed to reach room temperature before the vacuum was released. Each substance was weighed immediately so that a precise known concentration of each standard could be made. Then, a series of dilutions was made for each standard (0, 20, 40, 60, 80, and 100 μg/mL). The standard curve would represent a straight line with the formula $y = mx + b$. In the formula, y = absorbance measured at the proper wavelength for the particular standard component (carbohydrate, uronic acid, or protein), m = the slope of the line, x = the known concentration of the standard in μg/mL, and b = the ordinate intercept). The m and b parameters were calculated with DataDesk 4.0 Statistical software. Thus, when determining the unknown concentration of carbohydrate, uronic acid, or protein for a viscin mucilage dilution, y would represent the absorbance measured at the proper wavelength for the given viscin mucilage dilution, and one would solve for x using the m and b parameters from the standard curve formula.

4. Neutral Soluble Carbohydrate Assay

The neutral soluble carbohydrate assay was after Dubois *et al.*, 1956. 1 mL of Phenol Reagent was added to 1 mL of each mucilage sample dilution and to 1 mL of each galactose standard dilution in test tubes. The test tubes were vigorously vortexed. To

each test tube, 5 mL of concentrated sulfuric acid was delivered rapidly and directly to the surface of the liquid in each of the test tubes with great caution. The reactions started at room temperature (22° C), but the addition of sulfuric acid caused the evolution of heat. The digests were incubated for 10 min., and were then allowed to cool to room temperature. The absorbances were read with the Zeiss Spectrophotometer in the Department of Plant Sciences at the University of Manitoba at a wavelength of 490 nm (the proper wavelength for absorbance by Phenol-treated hexose sugars; Dubois *et al.*, 1956). A test tube containing the reagents and 0 μg galactose/mL acted as a blank.

The neutral soluble carbohydrate concentration (x) in each of the 5% and the 2% viscin mucilage dilutions was calculated from the measured absorbance (y) and the m and b parameters derived from the standard curve using the formula $y = mx + b$. The calculated neutral soluble carbohydrate concentration for each dilution was then converted to the mass of carbohydrate in 1 mL of 100% undiluted mucilage (as equivalent sugar monomers), and the two results were averaged.

5. Uronic Acid Assay

For the estimation of uronic acids, the carbazole method after Bitter and Muir (1962) was used. All reactions were performed at 4° C (on ice). 3 mL of 0.025 M sodium tetraborate in concentrated sulfuric acid was added to 0.5 mL of each mucilage sample dilution and to 0.5 mL of each galacturonic or glucuronic standard dilution in test tubes. The test tubes were capped with Teflon-lined caps, mixed gently, and then vortexed vigorously while keeping the tubes on ice (10 min.). Then the test tubes were heated at 100° C for 10 min. and cooled to room temperature. 0.1 mL of 0.125% (w/v) carbazole in 95% (v/v) ethanol was added to each of the test tubes and vortexed. The test tubes were heated at 100° C for 15 min., and then cooled to room temperature. The absorbances were read with a Zeiss Spectrophotometer at a wavelength of 530 nm (Bitter and Muir, 1962). A test tube containing the reagents and 0 μg uronic acid/mL acted as a blank.

The uronic acid concentration (x) in each of the 5% and the 2% viscin mucilage dilutions was derived from the galacturonic acid standard curve as well as the glucuronic

acid standard curve using the formula y = mx + b from each standard. The calculated uronic acid concentration for each standard at each dilution was then converted to the mass of uronic acids in 1 mL of 100% undiluted mucilage (as equivalent sugar monomers), and the four results were averaged.

6. Protein Assay

The protein assay was after Lowry *et al.* (1951). 1 mL of 1% (w/v) cupric sulfate was combined with 1 mL of 2% (w/v) sodium-potassium tartrate, and to these 2 mL, 98 mL of 2% (w/v) sodium carbonate in 0.1 N sodium hydroxide was added, forming 100 mL of the Lowry Mixture. 5 mL of the Lowry Mixture was added to 1 mL of each mucilage sample dilution and to 1 mL of each BSA standard dilution in test tubes. The test tubes were allowed to incubate for 10 min. Phenol Reagent 2N Solution-Folin-Ciocalteau (Fisher) was diluted to 50% (v/v). To each test tube, 0.5 mL of the diluted Phenol Reagent was added. The tubes were vortexed vigorously and allowed to incubate for a further 30 min. The absorbances were read at wavelengths of 500 nm and 660 nm on a Zeiss Spectrophotometer. The 500 nm wavelength is better for detecting a small amount of protein (5-25 micrograms), whereas the 660 nm wavelength is better for detecting larger amounts of proteins (Lowry *et al.*, 1951). The test tube containing the reagents and 0 μg BSA/mL acted as the blank.

The protein concentration (x) in each of the 5% and the 2% viscin mucilage dilutions was derived from the standard curve using the formula y = mx + b for each wavelength. The mass of protein in 1 mL of 100% undiluted mucilage was derived as for soluble carbohydrates and uronic acids.

CHAPTER FOUR - REPRODUCTIVE DEVELOPMENT IN THE FEMALE FLOWERS/FRUIT OF *ARCEUTHOBIUM AMERICANUM*

I. INTRODUCTION

1. Questions and Controversies Regarding Reproductive Development in Female Flowers/Fruit of *Arceuthobium americanum*

Although there have been several studies regarding reproductive development in *Arceuthobium* species, few of these studies have been performed at the ultrastructural level. For this reason, a study on reproductive development in a species of *Arceuthobium*, such as *A. americanum*, is warranted. Several papers have been published on megasporogenesis, embryogeny, general endosperm formation, and endosperm caecum development, but there is little agreement among these investigations. Light microscopy used in conjunction with both fluorescence and electron microscopy may help to clarify some of the more poorly understood aspects of reproductive development in *Arceuthobium*. Moreover, some of the information garnered for *A. americanum* may be relevant to reproductive development in flowering plants in general.

One of the more interesting features of the *Arceuthobium* female flower is the absence of a typical ovule: specifically, the nucellar tissues are continuous with the placenta and integuments are lacking (Kuijt, 1969). This structure has been called several different names, although none adequately describe it. While the archesporium of *Arceuthobium* is believed to be multicellular, there are discrepancies regarding the number of archesporial cells initially present (see Dowding, 1931; Hudson, 1966), and it has not been established whether the development in the *Arceuthobium* ovular structure follows a crassinucellate (Dowding, 1931) or tenuinucellate (Hudson, 1966) pattern of development.

Several aspects of pre-fertilization events in the female flower of *Arceuthobium* are unclear. Megasporogenesis has generally been described as being bisporic (Cohen, 1963; Hudson, 1966, Tainter, 1968, Bhandari and Nanda, 1968a, b), there are exceptions (Jones and Gordon, 1965). The position of the functional megaspore relative to the polarity of the ovular structure needs to be clarified. Although two megasporocytes are

believed to form in most *Arceuthobium* species regardless of the number of cells initially present in the archesporium (Dowding, 1931; Hudson, 1966; Calvin, 1996), the number of functional megaspores and successful embryo sacs that form has not been established. The general arrangement of the cells in the unfertilized embryo sac needs further clarification, especially with regard to the location of the egg apparatus in the embryo sac relative to the polarity of the ovular structure. When these pre-fertilization features in *Arceuthobium* have been clarified, they can be compared with similar features in other Santalalean families and compiled with general ovular data to infer phylogenetic relationships among the Santalalean families.

The ultrastructure of an unfertilized mistletoe embryo sac has only been described for *Viscum minimum* (Zaki and Kuijt, 1994), and further study in another mistletoe, such as *Arceuthobium americanum* may be illuminating. In particular, the structure of cell walls and distribution of organelles in the embryo sac cells should be examined, as such details are lacking in flowering plants in general (Reiser and Fischer, 1993). The structure of the *Arceuthobium* egg apparatus should be scrutinized: filiform apparati have not been observed in *Arceuthobium* species, and Hudson (1966) suggested that the egg cell of *A. americanum* lies above and to the side of the synergids. Hudson (1966) believed that this positioning might preclude the normal discharge of the pollen tube into the degenerate synergid. Consequently, the general processes of pollination and pollen tube growth in *Arceuthobium* also need examination, particularly since these events are believed to take place before an embryo sac is even formed (Hudson, 1966; D.A.R. McQueen, pers. com., 1995). As synergids are believed to be required for the pollen tube growth in typical flowering plants (Reiser and Fischer, 1993), the absence of synergids should be discussed in relation to pollen tube growth. The number of pollen tubes that can enter the ovular structure of *Arceuthobium* should be noted: typical flowering plants usually only permit one pollen tube to enter the ovule (Maheshwari, 1950), but typical flowering plants do not usually have the ability to potentially produce more than one embryo sac.

Immediate post-fertilization changes that occur in the embryo sacs of typical flowering plants have not been well described (Mauseth, 1988). Therefore, in order to contribute to the knowledge of flowering plants in general as well as to *Arceuthobium*

species, the ultrastructure of the post-fertilization embryo sac in *A. americanum* should be described. In order to be able to compare the ultrastructure of the fertilized *A. americanum* embryo sac with the unfertilized embryo sac, the same features that were examined in the unfertilized embryo sac, including cell wall formation and organellar composition, should be examined in the fertilized embryo sac.

Features of early embryogenesis have only been cursorily examined in *Arceuthobium* species. Reports conflict with regard to how long quiescence lasts in the zygote, and whether there is a true quiescent period (Hudson, 1966; Bhandari and Nanda, 1968a). It has not been established whether the zygote undergoes any changes that indicate imminent division, and there have been several contradictory reports regarding the type of embryogenesis that occurs in *Arceuthobium* species. Cohen (1963) believed the embryogenesis in *Arceuthobium* conformed to the Asterad-type, *Penaea* variation, whereas Bhandari and Nanda (1968a) believed the embryogeny was of the Piperad-type, *Scabiosa* variation. Obviously, then, clarification is required. Furthermore, although some general descriptions of embryonic meristem ontogeny exist for *Arceuthobium* (Cohen, 1963; Tainter, 1968; Bhandari and Nanda, 1968a), similar observations have not been made for *A. americanum*, especially with regard to the concurrent state of the developing endosperm. Finally, as the cytochemistry of the *Arceuthobium* embryo has not been examined for any species, cytochemistry should definitely be performed for the *A. americanum* embryo during development.

Endosperm development in *Arceuthobium* has been examined in several species (Thoday and Johnson, 1930; Cohen, 1963; Hudson, 1966, Tainter, 1968, Bhandari and Nanda, 1968a; Calvin, 1996), but there is little agreement among the findings. Although it has generally been determined that the endosperm development is cellular, and that an embryo sac caecum is involved in endosperm development, the observations dealing with caecum development differ. Clarification is needed as to whether a caecum forms from both embryo sacs, if the embryo sac undergoes double fertilization prior to caecum formation, if any cell or nuclear division takes place before caecum formation, if partitioning of the embryo sac occurs prior to caecum formation, and which cell(s) of the embryo sac contribute to the caecum. The function of the caecum is also worth contemplating, as a haustorial function has been postulated for many caeca (Mikesell,

1990). In addition, as caeca of some sort form in 76% of flowering plants, it is worth examining caecum formation in *A. americanum*, as this information would be useful to those workers studying the formation of caeca.

There are other concerns regarding endosperm development in *Arceuthobium*. Firstly, although endosperm is believed to completely surround the zygote/embryo (Hudson, 1966; Tainter, 1968, Bhandari and Nanda, 1968a; Calvin, 1996), no indications have been given as to how this can occur, especially considering that the zygote originally shares a common wall with the embryo sac wall. Also, there are some problems regarding the relative position of the embryo and endosperm in the mature pseudoseed. In all *Arceuthobium* pseudoseeds, the embryo is found at a morphologically higher position than the endosperm, while in the embryo sacs of many *Arceuthobium* species, the egg cell is found at a morphologically lower position than the central cell. The mechanism by which this reversal is obtained must be examined. The fate of the endosperm that surrounded the upper portion of the zygote must be determined, as the embryo in the ripe, mature *Arceuthobium* fruit appears to lie outside the endosperm (Sallé, 1983; Bhandari and Nanda, 1968a). Concerns regarding the presence of endosperm zonation, the possible "consumption" of the nucellus by the endosperm, and the final shape of the endosperm must be addressed. As very few studies have dealt with the cytochemistry of cellular endosperm (Vijayaraghavan and Prabhakar, 1984), this should be examined in *A. americanum* in order to contribute to the knowledge of flowering plants.

The mature fruit has been described for several *Arceuthobium* species (Cohen, 1963; Hudson, 1966; Tainter, 1968; Bhandari and Nanda, 1968a), although no thorough cytochemical studies have been performed on the fruit tissues. Thus, cytochemistry should be performed on the fruit tissues in *A. americanum* as they develop. Moreover, regarding fruit tissue development, there are still problems concerning the origin of certain fruit zones. Notably, the fate of the endocarp has not been determined. Sallé (1983) believed the endocarp of Viscaceous species was persistent, whereas Bhandari and Nanda (1968a) thought that the endocarp of *A. minutissimum* became almost entirely obliterated except for a persistent cap of endocarp tissue above the radicular pole of the embryo. Perhaps the cap described by Bhandari and Nanda (1968a) does not represent

endocarp but instead represents endosperm, as endosperm initially envelops the zygote in most *Arceuthobium* species; this needs investigation.

The mesocarp of *Arceuthobium* and related species is ill defined as well. The mesocarp has been said to be comprised of viscin cells alone (Gedalovich-Shedletzky, 1989), both viscin cells and vesicular cells (Sallé, 1983), both viscin cells and crest tissue (Bhandari and Nanda, 1968a), or viscin cells, crest tissue, and a degenerate layer (Bhandari and Indira, 1969). The exact origin of the tannin-filled layer immediately appressed to the embryo and endosperm (the pseudoseed coat) needs further clarification: Sallé (1983) believed the tannin-filled layer was solely endocarp, whereas Bhandari and Nanda (1968a) believed the tannin-filled layer was part of the (mesocarpic) crest. The precise layers of fruit that are discharged with the embryo and endosperm need to be clarified.

The exocarp of the *Arceuthobium* fruit needs further examination, as it has only been cursorily examined in most species. Specifically, the presence, number of traces, and appearance of the vascular tissue should be better described since the vascular tissues of many mistletoes have been shown to possess novel cell types, especially in regions of transfer (see Fineran *et al.*, 1978; Fineran, 1985; Fineran, 1996, 1998; Wilson and Calvin, 1996; Fineran and Calvin, 2000). The whole fruit needs to be examined to determine if it is truly a berry, and if the term "pseudoberry" (Calder, 1983) is appropriate. Likewise, use of the terms "pseudoseed" and "pseudoseed" coat should be scrutinized with regard to the literature to ensure that the terms adequately describe the dispersal unit of *Arceuthobium*.

Although viability of the embryo in naturally-discharged pseudoseeds has been tested in several *Arceuthobium* species using 2, 3, 5-TTC (Scharpf and Parmeter, 1962; Robinson, 1995; Jerome, 2001), these workers have not tested the viability of the embryo in pseudoseeds that have been left in the field for several months. It would be useful to test pseudoseeds that have aged in the field, as the viability rates of these pseudoseeds would best approximate the natural viability rate. Information garnered from this might in turn aid those workers wishing to store discharged pseudoseeds. In addition, perhaps more than just the embryo should be tested for viability, as other components may be important in determining the overall germination potential. Pertinent characteristics and

discoveries regarding reproductive development in female flowers/fruit of *Arceuthobium* should be related to the ultimate process of germination, as all preparation within the female flowers/fruit leads to this particular event. Any salient characteristics of reproductive development that appear to be congruent with the host conifer should be elaborated upon, as development in the parasite may be controlled by (or controlling) development in the host.

2. Objectives for this Study

This study is relevant, as the literature regarding reproductive development in the female tissues of *Arceuthobium* species is contradictory. There are four major objectives to be accomplished in this part of the project. The first objective is to describe aspects of reproductive development in the female flowers/fruit of *A. americanum* using modern techniques of light, fluorescence, and electron microscopy, applying cytochemical procedures wherever relevant. The second objective is to answer some questions and resolve some controversies evident in the literature of *Arceuthobium* with regard to reproductive development in the female tissues. The third objective is to clarify some of the terminology used for describing reproductive development in the female tissues of *Arceuthobium*, coining new terminology where necessary. Along with the third objective is the desire to perform simple viability tests on pseudoseeds left in natural conditions in order to contribute information to those wishing to store and germinate pseudoseeds. The fourth objective is to use information garnered from the study as well as from the literature so that phylogenetic relationships among the Santalales can be illustrated, congruencies between the parasite and host can be better understood, and knowledge can be contributed to the study of flowering plants in general.

All materials and methods used to achieve these objectives are as described in Chapter Three of this thesis.

II. RESULTS

1. Timeline for Reproductive Developmental Events in the Female Flowers/Fruit of *Arceuthobium americanum* in Manitoba

As outlined in Chapter Two, section II. - 1A, seasonal reference points were used in order to describe the timing of reproductive events in female flowers/fruit of *Arceuthobium americanum* in North America, and these same reference points were used to describe timing of reproductive events in Grand Beach Provincial Park, Manitoba. The timing was similar in all years of the study. Young female flowers (buds) became evident by the middle of August, prior to the first spring of development, and anthesis of the female flowers (as well as the male) typically occurred in early April of the first spring. Fruit maturation and explosive discharge took place in late August of the second summer, about seventeen months following anthesis.

2. General External Morphology of Female Shoots, Inflorescences, and Flowers Prior to And Immediately Following Double Fertilization

The female shoots and inflorescences of *Arceuthobium americanum* in Grand Beach Provincial Park observed in mid April (circa April 14) during the first spring of development possessed a verticillate branching pattern (Figure 4.1). The floral arrangement was complex, but each inflorescence was essentially a raceme of typically three-flowered cymes (Figures 4.1 and 4.2a). Each three-flowered cyme consisted of a central terminal flower that was flanked by two lateral flowers. A cup-like bract consisting of two fused leaflike appendages subtended the three flowers of a cyme. Each flower possessed an extremely reduced pedicel (Figures 4.2b and 4.2c) that was attached to the peduncle where the bract enveloped the three flowers (Figure 4.2a). Each flower possessed a flattened oval shape when viewed from the side (Figures 4.2a and 4.2c), but appeared heart-shaped in face view (Figure 4.2b). Thus, each flower was bilaterally flattened and bilaterally symmetrical, and the three flowers were arranged in the cyme so that their flattened faces were aligned with each other (Figures 4.1 and 4.2a). It was not unusual, however, for members of the cyme to remain vegetative and capable of elongation into a new shoot (stem) segment (Figure 4.1).

A typical female flower observed in mid April (circa April 14) during the first spring of development, prior to megasporogenesis, was greenish and drab (Figure 4.1). Each flower had either two sepals or two petals, but because the origin of these parts was not determined, they were called tepals (Figure 4.2b). Each flower possessed a single, punctate yellow stigma (Figure 4.1), and the obvious protrusion of the stigma through the tepal envelope indicated that anthesis had occurred in these minute female flowers (Figures 4.1, 4.2a, 4.2b, and 4.2c). At this time, each stigma was coated in an exudate (Figure 4.1). Each flower was narrowest at its base at the pedicel (Figures 4.2b and 4.2c). In face view, each flower was broadest near its apex, which was distal to the pedicel and in the region of the stigma (Figure 4.2b). In side view, the flower was thickest at a position halfway between the pedicel and the stigma (Figures 4.2a and 4.2c). Thus, a typical flower was approximately 1 mm in length (Figures 4.2b and 4.2c), 0.2 mm in breadth at its base, 3 mm in breadth at its broadest point (Figure 4.2b), and 1 mm in thickness (from flattened side to flattened side) (Figure 4.2c).

Young flowers maintained this general external appearance as well as these dimensions throughout the processes of megasporogenesis as well as megagametogenesis, and into the period immediately following double fertilization (Figures 4.1, 4.2a, 4.2b, and 4.2c). However, the stigmatic exudate (Figure 4.1) disappeared just before the onset of megasporogenesis. There were no immediate distinctive changes in external morphology to verify whether double fertilization had taken place. Approximately two months after double fertilization took place, the fertilized flower or immature fruit lost the bilateral flattening.

3. Orientation

The polarity to the axis of the ovular structure as outlined in Chapter Two, section I. - 4B will be used to describe reproductive development in *Arceuthobium americanum*. The apex of the ovular structure will be considered to be morphologically higher than the attached part of the ovule (the base). As it will be shown that *A. americanum* possessed an erect orthotropous ovular structure displaying basal placentation in which the ovular apex projects directly away from the ovarian base, the polarity can be extended to the longitudinal axis of the female flower/fruit. Therefore, regions distal to the pedicel can

be considered to be morphologically higher than regions proximal to the pedicel. The terms "higher/upper", "lower", "upward", and "downward" were used with respect to this polarity, which was defined for orientation and descriptive purposes only.

4. The Unfertilized Female Flower and the Placental-Nucellar Complex (PNC)

Figure 4.3 depicts a near median longitudinal face view section of a representative unfertilized female flower sampled from mid April of the first spring (circa April 14). Figure 4.2b, while showing the female flower in face view, also gives a diagrammatic interpretation of the internal structures seen in Figure 4.3. A single inferior ovarian loculus was evident within the ovarian tissues of the carpel at the base of the flower (Figures 4.2b and 4.3). The ovarian loculus was a product of two connate fused carpels. At this time, a single, ategmic, erect ovular structure lacking a discrete funiculus and displaying basal placentation occupied the entire cavity of the ovarian loculus. As the ovular structure lacked integuments and a discrete funiculus, only the nucellar portion of the ovule actually existed. However, because the base of the nucellus was continuous with the ovarian placenta, no concrete distinction could be made between the placenta and the nucellus. Thus, the ategmic ovular structure was more aptly called a placental-nucellar complex (PNC), and the generic term "sterile PNC cells" was used to describe the non-archesporial cells of either the nucellus or placenta without specifically distinguishing between these two regions. The PNC was orthotropous and teardrop shaped with the broad base of the PNC being proximal to the pedicel, and the apex or tip of the PNC being distal to the pedicel. Since the section in Figure 4.3 was not median, only the sterile PNC cells were captured, whereas the fertile cells (the two megasporocytes) were slightly out of the plane of section. Two vascular traces, apparently comprised solely of xylem tissue, were found embedded in the ovarian tissues on either side of the PNC (Figures 4.2b and 4.3). No obvious phloem tissue was observed in the vascular traces. Along with xylem parenchyma, the xylem tissue appeared to be primarily represented by vessel elements that often appeared empty and that possessed helical secondary wall thickenings (evident in Figure 4.3). The cell walls of the young vessel elements stained purplish with crystal violet.

Most of the sterile PNC cells were non-vacuolate and possessed fairly dense cytoplasm (Figure 4.3). However, some of the sterile PNC cells were vacuolate, especially at the periphery and the base of the PNC. The vacuoles were not stained, and thus the vacuolate cells appeared to be empty. All sterile PNC cells had thick cell walls that were similar in thickness to the cell walls of the surrounding ovarian tissue.

5. The Two Megasporocytes

Figure 4.4 depicts a median section of a female flower at the same stage of development as seen in Figures 4.1, 4.2, and 4.3, sampled in mid April of the first spring (circa April 14). In this median section, two elongate megasporocytes could be observed in the hypodermal layer of the PNC (Figure 4.4). Thus, only one layer of sterile cells (the epidermis of the PNC) separated each megasporocyte from the ovarian tissue on either side of the PNC, and consequently, the PNC was tenuinucellate. Accordingly, each of the two megasporocytes was presumed to have developed directly from an archesporial cell. The two megasporocytes were at least twice as large as any surrounding sterile PNC cell, although no crushed cells were noted. Each megasporocyte was obliquely oriented to the long axis of the PNC. Hence, the upper poles of the two megasporocytes were separated from each other by about one to two layers of sterile PNC cells, whereas the lower poles of the two megasporocytes were separated from each other by about three to four layers of sterile PNC cells. Also as a result of the oblique orientation, each elongate side of a megasporocyte could be designated as either being an upper side (adjacent to the epidermis of the PNC) or a lower side (near the centre of the PNC).

Each of the two megasporocytes possessed a dense and granular cytoplasm that was distinctive from the fairly dense but agranular cytoplasm of the sterile PNC cells (Figure 4.4). At the lower pole of each megasporocyte, a single large nucleus was observed to occupy nearly 50% of the cell. Each megasporocyte appeared to be in prophase I of meiosis as the nuclei lacked nucleoli, the nuclear envelopes were not completely intact, and the chromosomal material was in a state of condensation. It was common for megasporocyte nuclei to be seen in prophase I of meiosis, since meiosis had actually initiated in the unopened female flower buds during the fall preceding the first spring (not shown).

6. Megasporogenesis

6A. Meiosis I

By early May of the first spring (circa May 4), each of the two megasporocytes had completed meiosis I and cytokinesis to create two uninucleate dyads per megasporocyte (Figure 4.5). The cell wall that formed between the two dyads from each megasporocyte was transverse relative to the long axis of the original megasporocyte. For a given pair of dyads that arose from a megasporocyte, the original megasporocyte wall formed the majority of each dyad's boundary, and the newly-formed transverse cell wall comprised the remainder of each dyad's boundary. Meiosis I had been simultaneous in the two megasporocytes (not shown). Of the two dyads that arose from a megasporocyte, the upper dyad was larger than the lower dyad and possessed a larger nucleus (Figure 4.5 and further verified by serial sectioning - not shown). The nucleus of the upper dyad appeared to be in a period of transient interkinesis, because the nucleolus and nuclear envelope had not reformed. The nucleus in the lower dyad appeared to be dark and degenerating. Some of the vacuoles in the vacuolate sterile PNC cells were lined with a darkly stained tannin-like material.

6B. Meiosis II

By mid May of the first spring (circa May 17), meiosis II had occurred simultaneously in each upper dyad (one from each megasporocyte), but meiosis II, unlike meiosis I, was not followed by cytokinesis (Figures 4.6, 4.7, and 4.8). Following meiosis II, each upper dyad became binucleate and represented a functional megaspore or immature binucleate embryo sac. The majority of the original megasporocyte wall still formed the boundary of each functional megaspore, although the lower boundary of each functional megaspore was represented by the transverse cell wall that had formed following meiosis I. Thus, where necessary, the bounding walls of a functional megaspore (immature embryo sac) will now be referred to as the embryo sac wall.

The lower dyads (one from each megasporocyte) did not undergo meiosis II and remained uninucleate. The cytoplasm was more darkly stained than that of a functional megaspore, indicating that the lower dyad was in the process of degeneration. Each lower dyad thus represented a nonfunctional dyad, and would eventually completely

degenerate. Therefore, megasporogenesis in *Arceuthobium americanum* was deemed to be of the bisporic type. The remnants of the nonfunctional dyad could be recognized for a considerable period after megasporogenesis was complete. There was no apparent difference in the products of megasporogenesis from the two megasporocytes.

The two nuclei of a functional megaspore appeared to be fairly similar in size and relatively large (Figures 4.7 and 4.8). The nuclei possessed homogeneous nucleoplasm, distinct nucleoli, and discrete nuclear envelopes, all of which indicated that meiotic division was complete. Occasionally, cytokinesis would follow meiosis II in an upper dyad in one of the two megasporocytes, leading to anomalous monosporic megasporogenesis (Figures 4.9 and 4.10). Figures 4.9 and 4.10 are serial sections, and the serial sections allow for both nuclei that resulted from meiosis II in the upper dyad to be observed. In this anomalous monosporic megasporogenesis, a cell wall that was transverse to the long axis of the megasporocyte separated the two nuclei in an upper dyad. This cell wall was more tenuous than the cell wall that resulted from cytokinesis following meiosis I. The nucleus in each anomalous uninucleate megaspore possessed a prominent nucleolus and a discrete nuclear envelope.

Although many of the sterile PNC remained fairly densely cytoplasmic, more sterile PNC cells became highly vacuolate after meiosis II took place (Figures 4.7, 4.8, 4.9, and 4.10). Most of the vacuoles were either lined with or completely filled with a darkly staining tannin-like material.

A section of a female flower at a similar stage of development as seen in Figures 4.6, 4.7, and 4.8, sampled from mid May of the first spring (circa May 17) was subjected to aniline blue fluorescence microscopy (Figure 4.11). Both megasporocytes had undergone typical bisporic megasporogenesis. The functional megaspore and nonfunctional dyad from each megasporocyte were visible. In the presence of the aniline blue stain, pale blue fluorescence could be observed in the cell walls of the functional megaspores and the nonfunctional dyads, indicating the presence of callose in those cell walls. However, the pale blue fluorescence was particularly effulgent in the lower side of each functional megaspore and in the cell walls of each nonfunctional dyad. No notable fluorescence was detected in the cell walls of the PNC or ovarian tissues except at pinpoints in the cell walls. Also, strong pale blue fluorescence could be detected in the

region of the style, as well as at the base of each nonfunctional dyad. This strong fluorescence was associated with the callosic cell walls of pollen tubes.

7. Megagametogenesis and the Unfertilized Mature Seven-Celled Embryo Sac

Megagametogenesis was a very rapid process that occurred between mid May (circa May 17) and late May (circa May 25) of the first spring. Only one of the two functional binucleate megaspores was capable of completing megagametogenesis to form a mature seven-celled embryo sac (megagametophyte). The second embryo sac did not progress beyond the four-nucleate stage (not shown), after which it degenerated. The remnants of the abortive, degenerative embryo sac could be seen in the PNC along with the seven-celled embryo sac (Figure 4.12). An unfertilized mature seven-celled embryo sac consisted of two synergids and one egg cell (the egg apparatus) at the lower pole of the embryo sac; three antipodals at the upper pole of the embryo sac; and a central cell residing in the centre of the embryo sac (Figures 4.12 and 4.13; Figure 4.13 is a diagrammatic representation of the unfertilized mature seven-celled embryo sac seen in Figure 4.12). The unfertilized central cell was at a morphologically higher position than the egg cell. It was also the largest cell of the embryo sac (average median diameter of 24 μm), followed by the egg cell (average median diameter of 18 μm). The two synergids had average median diameters of 14 μm, and the antipodals were the smallest cells of the embryo sac, with average median diameters of 11 μm.

Using fluorescence microscopy with Calcofluor staining, it was possible to discern that the antipodals were delineated from each other and the unfertilized central cell by thin cell walls (Figure 4.14). However, the three cells of the egg apparatus were delineated by cell walls only in the regions proximal to their point of attachment to the embryo sac wall. These cell walls were extremely tenuous, and no cell wall delineated the unfertilized central cell from the three cells of the egg apparatus.

At both the light microscope level (Figure 4.12) and the electron microscope level (Figures 4.15, 4.17, and 4.23), one synergid could be seen to be in the process of degeneration, as indicated by the very darkly stained cytoplasm. This synergid represented the degenerating synergid. The other, persistent synergid appeared to be healthy (Figures 4.12, 4.15, 4.17, and 4.21). The mature seven-celled embryo sac

(Figures 4.12 and 4.13) maintained the oblique angle of the original megasporocyte (Figure 4.4). The nonfunctional dyad could be seen below the level of the egg apparatus (Figure 4.12).

A single nucleus was observed within the egg cell (Figure 4.18), each of the two synergids (Figure 4.12), each of the three antipodals, and the central cell. At no time were two polar nuclei observed within the central cell, and thus the two polar nuclei had coalesced into a fusion nucleus prior to double fertilization. Therefore, a functional binucleate megaspore would have undergone two rounds of mitosis in the process of megagametogenesis. Following is a more detailed description of the seven cells of unfertilized mature embryo sacs and the interfaces among the seven cells as observed in late May of the first spring (circa May 25). No plasmodesmata were observed among any of the seven cells of the embryo sac, or between any cell of the embryo sac and sterile PNC cells.

7A. Pre-fertilization egg apparatus: General appearance, configuration, plasma membranes, and cell walls

The three cells of the egg apparatus shared common interfaces with each other, the unfertilized central cell, and the embryo sac wall at the lower pole of the embryo sac (Figures 4.12, 4.13, 4.15, 4.16a, and 4.16b). Figures 4.16a and 4.16b are diagrammatic interpretations of the egg apparatus as it would appear if it had been cross-sectioned along the dotted lines labeled 16a and 16b seen in Figure 4.13. Notably, the base of the pear-shaped egg cell was attached to the upper side of the embryo sac at the lower embryo sac pole (Figures 4.12, 4.13, and 4.15). The two synergids occupied the rest of the embryo sac wall boundary at the lower pole. The bases of the two synergids, however, were primarily attached to the embryo sac wall at its lowest position in the embryo sac. Thus, the majority of the egg cell was always found at a position that was above and to the side of both synergids, relative to the longitudinal axis of both the embryo sac and the PNC. One synergid shared a common interface with the upper side of the embryo sac, and the other synergid shared a common interface with the lower side of the embryo sac. Either synergid could occupy either position (Figure 4.13): in Figures 4.12 and 4.17, the persistent synergid interfaced with the lower side of the embryo sac,

and the degenerating synergid interfaced with the upper side of the embryo sac. Conversely, in Figure 4.15 the degenerating synergid interfaced with the lower side of the embryo sac, and the persistent synergid interfaced with the upper side of the embryo sac.

The persistent synergid, the egg cell, and the unfertilized central cell were each bounded by a plasma membrane (Figures 4.19 and 4.20). Prior to its degeneration, the degenerating synergid was also bounded by a plasma membrane, but the plasma membrane had deteriorated (Figures 4.20 and 4.23). Thus, the degenerating synergid boundary was represented by its cytoplasmic margin. The interface of the unfertilized central cell with the egg cell and with the persistent synergid was essentially a contact of two plasma membranes (Figure 4.19), as cell wall material at this interface was typically absent (Figures 4.14 and 4.19). Electron opaque deposits were present between the plasma membranes at this interface (Figure 4.19). Similarly, the interface of the unfertilized central cell with the degenerating synergid lacked cell wall material (Figures 4.14 and 4.23), and the interface consisted of a contact between the unfertilized central cell plasma membrane and the cytoplasmic margin of the degenerating synergid (Figure 4.23). Electron opaque deposits were, nonetheless, present between the unfertilized central cell plasma membrane and the cytoplasmic margin of the degenerating synergid.

Scant cell wall material was present at the interfaces among the three cells of the egg apparatus (Figures 4.14, 4.19 and 4.20). The presence of blue fluorescence at these interfaces under Calcofluor fluorescence microscopy indicated that the cell wall material was of a cellulosic and/or hemicellulosic nature (Figure 4.14). The cell wall material was scantiest in regions in the vicinity of the central cell (Figures 4.14, 4.19 and 4.20). Where the egg cell contacted the persistent synergid, scant cell wall material was found between the egg cell plasma membrane and the persistent synergid plasma membrane (Figures 4.19 and 4.20). Where the degenerating synergid contacted the egg cell and persistent synergid, scant cell wall material was found between the degenerating synergid cytoplasmic margin and the egg cell plasma membrane as well as between the degenerating synergid cytoplasmic margin and the persistent synergid plasma membrane (Figure 4.20). No electron opaque deposits were observed at the interfaces among the three cells of the egg apparatus (Figures 4.19 and 4.20).

However, the cell wall material between the two synergids was particularly copious at the embryo sac wall, and the embryo sac wall itself was thickened at that point (Figures 4.14 and 4.20). These cell wall thickenings constituted the so-called filiform apparatus. In the persistent synergid, a portion of the filiform apparatus contorted the plasma membrane (Figure 4.20). Also, some of the filiform apparatus could be seen to affect the egg cell plasma membrane at the embryo sac wall where the three cells of the egg apparatus intersected at the embryo sac wall. The filiform apparatus, however, did not have true digitate filiform transfer cell wall ingrowths, but was instead a thick pad of cell wall material.

7B. Unfertilized egg cell: Cytology and ultrastructure

The pear-shaped egg cell extended further into the central cell than either synergid, and featured a large vacuole that occupied a significant portion of the egg cell volume (Figures 4.12, 4.15, and 4.18). The large vacuole of the egg cell was found at a position that was closer to the central cell than to the embryo sac wall at the lower pole of the embryo sac. The nucleus (Figure 4.18) and cytoplasm of the egg cell (Figures 4.15 and 4.18), however, were more proximal to the embryo sac wall at the lower pole of the embryo sac. The cytoplasm was most notable in the region surrounding the nucleus (perinuclear cytoplasm) and at the periphery of the embryo sac (peripheral cytoplasm) (Figure 4.18). Numerous small vacuoles could be seen in the cytoplasm (Figures 4.15 and 4.18).

The nucleus possessed a prominent nucleolus and a distinct nuclear envelope (Figure 4.18). A large amount of the chromosomal material appeared to be condensed, although not to the point that one would consider the egg nucleus to be preparing to divide. Homogeneous, large osmiophilic bodies were infrequently seen within the egg cell cytoplasm viewed with electron microscopy (Figure 4.18). These bodies stained greyish-light blue (not blue-purple) when stained with crystal violet and viewed with light microscopy (not shown). Also, smaller, heterogeneous organelles representing mitochondria (as evidenced by the their electron translucent matrices) were also rare but evident in the egg cell cytoplasm viewed with electron microscopy (Figure 4.20). Starch

grains were not observed in the unfertilized egg cell (Figures 4.18 and 4.20), although proplastids had been observed in the unfertilized egg cell (not shown).

7C. Pre-fertilization synergids: Cytology and ultrastructure

The two elongate, crescent-to triangular-shaped synergids of the unfertilized embryo sac had a fairly similar appearance to each other at the light level of microscopy (Figure 4.12). Both synergids possessed fairly darkly stained cytoplasm, although the degenerating synergid cytoplasm was more darkly stained than the persistent synergid. Also at this level, the nucleus of the degenerating synergid was less conspicuous than the nucleus of the persistent synergid, although both were fairly darkly stained. Differences between the persistent synergid and the degenerating synergid were more obvious at the electron level of microscopy.

The persistent synergid was fairly cytoplasm-rich (non-vacuolate), and the cytoplasm occupied a large portion of the cell (Figures 4.21 and 4.22). Only a few smallish vacuoles could be observed within the persistent synergid cytoplasm. Like the egg nucleus (Figure 4.18), the persistent synergid nucleus possessed a prominent nucleolus, a distinct nuclear envelope, and condensed chromosomal material (Figures 4.15 and 4.17). Unlike the egg cell nucleus (Figure 4.18), the persistent synergid nucleus was found at a position that was closer to the central cell than to the embryo sac wall at the lower pole of the embryo sac (Figure 4.17). The persistent synergid cytoplasm possessed many mitochondria (Figures 4.20 and 4.22). In addition, osmiophilic bodies were common in the persistent synergid (Figures 4.20, 4.21, and 4.22). These bodies stained greyish-blue when stained with crystal violet and viewed with light microscopy (not shown). Starch grains, however, were only rarely observed in the persistent synergid (Figure 4.20), although proplastids were seen (not shown). Plasmolysis occurred occasionally in the persistent synergid at the embryo sac wall (Figure 4.21) and at the tenuous interface with the central cell (Figure 4.22).

The degenerating synergid was never captured in a non-degenerative state, so degeneration must have occurred almost immediately after the synergid was formed (Figures 4.15, 4.17, 4.22, and 4.23). Figure 4.15 depicts a slightly earlier stage of synergid degeneration and membrane lysis, as certain organelle fragments, including the

silhouette of the nucleus and vacuolar ghosts, could still be discerned. As in the persistent synergid, the nucleus of the degenerating synergid was found in a position that was closer to the unfertilized central cell than to the embryo sac wall (also see Figures 4.12 and 4.13). Figures 4.17, 4.22, and 4.23 depict a slightly later stage of degeneration, as it was difficult to identify internal membranous structures. Starch grains in the degenerating synergid, however, were relatively well preserved during all stages of degeneration, even though the amyloplast membranes had deteriorated (Figures 4.15, 4.22, and 4.23). Plasmolysis occurred occasionally in the degenerating synergid at the embryo sac wall (Figure 4.21). The degenerating synergid in Figure 4.23 may have just received a pollen tube, as a tube is visible in the vicinity of the degenerating synergid. For all purposes, the embryo sac is unfertilized, though, as the typical post-fertilization changes have not become evident.

7D. Pre-fertilization antipodals

The three oval- to triangle-shaped antipodals shared common interfaces with each other, the central cell, and the embryo sac wall (Figures 4.12, 4.13, and 4.24). The three antipodals were each bounded by a plasma membrane (Figure 4.24). Cell wall material was found at the interface of the unfertilized central cell with the three antipodals (Figures 4.14 and 4.24), between the plasma membrane of the unfertilized central cell and the plasma membranes of the antipodals (Figure 4.24). Cell wall material was also found at the interfaces among the three antipodals, between the antipodal plasma membranes (Figures 4.14 and 4.24). The interfaces among the antipodals contained an amount of cell wall material similar to that seen at the interface of the central cell with the antipodals. Among the interfaces of the antipodals, the amount of cell wall material in regions near the central cell compared to regions nearer the embryo sac wall did not differ (Figure 4.24). The presence of blue fluorescence at all antipodal interfaces under Calcofluor fluorescence microscopy indicated that the cell wall material was of a cellulosic and/or hemicellulosic nature (Figure 4.14).

Electron-opaque deposits were present at the interface of the unfertilized central cell with the antipodals (Figure 4.24), just as they were seen at the interface of the

unfertilized central cell with the egg apparatus (Figures 4.19 and 4.23). Electron opaque deposits were not present at the interfaces among the three antipodals (Figure 4.24).

At the light level of microscopy, the three antipodals generally appeared similar to each other, as each possessed a darkly stained nucleus and a fairly darkly stained cytoplasm (Figure 4.12). Interestingly, at the light level of microscopy, the antipodals appeared very similar to the persistent synergid, although the antipodals were slightly smaller than the synergids in average median diameter. At the electron level of microscopy, it was apparent that the antipodals (Figure 4.24) were slightly less cytoplasm-rich (and thus more vacuolate) than either synergid (Figures 4.20, 4.21, and 4.22). The egg cell and the antipodals shared features, including relative positioning of the cytoplasm as well as a distinct nuclear envelope and moderately condensed chromosomal material (Figures 4.15, 4.17, and 4,18). Like the persistent synergid (Figures 4.20, 4.21, and 4.22), the cytoplasm of the antipodals contained many mitochondria and numerous large osmiophilic bodies (Figure 4.24). These bodies stained greyish-blue when stained with crystal violet and viewed with light microscopy (not shown). Proplastids but not starch grains were observed in the antipodal cytoplasm (Figure 4.24). Similarly, starch grains were only rarely observed in the persistent synergid cytoplasm (Figure 4.20).

7E. Unfertilized central cell

The original embryo sac wall, which was relatively thick, formed the major boundary of the unfertilized central cell. There was no evidence of transfer cell wall ingrowths in the embryo sac wall of the central cell (Figures 4.12 and 4.25). The unfertilized central cell was highly vacuolate (Figure 4.25). The central cell possessed a single fusion nucleus with an average median diameter of approximately 12 μm (Figures 4.12 and 4.25), and was approximately 2 times larger than any other nucleus of the embryo sac. The fusion nucleus was in close proximity to the vacuolate end of the egg cell at the lower pole of the embryo sac and to the lower side of the embryo sac (Figures 4.12 and 4.25). The fusion nucleus possessed a prominent nucleolus, a distinct nuclear envelope, a dense nucleoplasm, and moderately dispersed chromosomal material (Figure 4.25).

The very large vacuoles of the unfertilized central cell contained tannin-like debris and threadlike materials (Figure 4.25). The threadlike materials represented remnants of trans-vacuolar cytoplasmic strands. Sterile PNC cells surrounding the central cell appeared crushed, as enlarging vacuoles within the unfertilized central cell were causing it to expand. The central cell cytoplasm was found only in a thin perinuclear layer and as a thin layer along the periphery of the central cell. There did not appear to be a difference in organelle composition of the perinuclear cytoplasm when contrasted to the peripheral cytoplasm. The scant cytoplasm contained small vacuoles (Figures 4.17 and 4.25), which appeared to be confluent with the large central vacuole of the central cell. It also contained starch grains in amyloplasts, osmiophilic bodies (Figure 4.25), and proplastids (not shown). The osmiophilic bodies stained greyish-blue when stained with crystal violet and viewed with light microscopy (not shown). Mitochondria were also observed, and were most obvious in Figures 4.21 and 4.23.

8. Pollen Tubes

Pollen tubes were observed in the style and at the lower pole of both megasporocytes, prior to megasporogenesis, as early as mid April (circa April 14) (not shown; D.A.R. McQueen, pers. comm., 1995). More than one pollen tube could enter the PNC, and more than one pollen tube could reach a megasporocyte (not explicitly shown, but see Figure 4.11). However, it could not be determined if the multiple pollen tubes originated from a single pollen grain (polysiphony), if multiple pollen grains germinated, or if a combination of polysiphony and multiple pollen grain germination occurred. The multiple pollen tubes became bifurcated in the vicinity of the megasporocytes (D.A.R. McQueen, pers. comm., 1995). Additionally, pollen tubes were observed throughout the process of megasporogenesis at both original megasporocytes, below the level of the nonfunctional dyad (Figure 4.11). After megagametogenesis had taken place, pollen tubes could be seen at the lower pole of the unfertilized, mature, seven-celled embryo sac and at the lower pole of the second, degenerating embryo sac in late May, circa May 25 (not shown). These pollen tubes possessed typical spongiform cell walls and could be observed within a mature seven-celled embryo sac in the vicinity of the degenerating synergid (Figure 4.23). The pollen tube segment was typically observed between the

embryo sac wall and the cytoplasmic margin of the degenerating synergid (i.e. within a periplasmic space), but above the level of the nonfunctional dyad. The pollen tubes disintegrated shortly after double fertilization (not shown).

9. Double Fertilization and the Fertilized Embryo Sac

Double fertilization was a very rapid process that occurred at the end of May in the first spring of development (circa May 30). The most obvious sign that the embryo sac had undergone double fertilization was the formation of distinct cell walls (Figures 4.26 and 4.27). Distinct cell walls delimited the three antipodals (Figures 4.26 and 4.27), the fertilized central cell, the persistent synergid, the degenerating synergid, and the newly formed zygote (Figures 4.28 and 4.30). Another sign that the embryo sac had undergone double fertilization was the fact that the newly formed zygote (Figure 4.28) had lost the large vacuole that had characterized the unfertilized egg cell (Figure 4.12, 4.15, and 4.18). After syngamy, the zygote attained a more rounded-triangular appearance (Figures 4.28, 4.29a, and 4.29b) compared to the pear shape of the unfertilized egg cell (Figures 4.12, 4.15, and 4.18). The rounded zygote, with an average median diameter of 27 μm, had increased in size by about 1.5 times (Figure 4.28) in comparison with the average median diameter of the unfertilized egg cell (18 μm; review Figure 4.12). Similarly, the post-fertilization persistent synergid attained a more rounded appearance (Figures 4.28, 4.29a, and 4.29b) compared to the elongated shape of the persistent synergid prior to double fertilization (Figures 4.12, 4.17, and 4.18). The post-fertilization persistent synergid, with an average median diameter of 20 μm, had also increased in size by about 1.5 times (Figure 4.28) in comparison with the average median diameter of the persistent synergid prior to double fertilization (14 μm; review Figure 4.12). As a consequence of enlargement of both the zygote and the persistent synergid, the degenerating synergid had become crushed and much reduced (Figures 4.29a, 4.29b, and 4.31). Moreover, the central cell, upon fertilization (Figure 4.31) lost the very large vacuole that the unfertilized central cell had possessed (review Figure 4.25). The nonfunctional dyad could still be seen after double fertilization (Figure 4.28). Just as the unfertilized central cell was at a morphologically higher position than the egg cell (Figures 4.12 and 4.13), the fertilized central cell was at a morphologically higher

position than the zygote (Figures 4.28, 4.29a, and 4.29b). Following is a more detailed description of the seven cells of fertilized embryo sacs and the interfaces among the seven cells as observed at the end of May in the first spring (circa May 30).

9A. The newly-formed zygote and post-fertilization synergids: General appearance, configuration, plasma membranes, and cell walls

As either synergid could occupy either synergid position prior to double fertilization (review Figure 4.13), fertilized embryo sacs with both synergid configurations were observed (Figures 4.26, 4.28, 4.29a, 4.29b, and 4.31).

Cell wall material was now present at the interface of the fertilized central cell with the three cells of the fertilized egg apparatus (Figures 4.27, 4.30 and 4.31), whereas it had been absent prior to double fertilization (review Figures 4.14, 4.19, and 4.23). The presence of blue fluorescence at this interface under Calcofluor fluorescence microscopy indicated that the cell wall material was of a cellulosic and/or hemicellulosic nature (Figure 4.27). This cell wall material was found between the fertilized central cell plasma membrane and the zygote plasma membrane (Figure 4.30), between the fertilized central cell plasma membrane and the persistent synergid plasma membrane (Figures 4.30 and 4.31), and between the fertilized central cell plasma membrane and the cytoplasmic margin of the very reduced degenerating synergid (Figure 4.31). Electron opaque deposits were no longer present at these interfaces (Figures 4.28, 4.30, and 4.31).

In addition, cell wall material had become more abundant at the interfaces among the three cells of the fertilized egg apparatus (Figures 4.27, 4.30 and 4.31) than it had been prior to double fertilization (review Figures 4.14, 4.19 and 4.20). The presence of blue fluorescence at these interfaces under Calcofluor fluorescence microscopy indicated that the cell wall material was still of a cellulosic and/or hemicellulosic nature (Figure 4.27). This cell wall material was found between the zygote plasma membrane and the persistent synergid plasma membrane (Figure 4.30), between the persistent synergid plasma membrane and the degenerating synergid cytoplasmic margin (Figure 4.31), and between the zygote plasma membrane and the degenerating synergid cytoplasmic margin (not shown). All cell walls were of a uniform thickness, and were comparable in thickness to the interface at the fertilized central cell. Aside from where the zygote

shared a common cell wall with the upper side of the embryo sac, the cell walls bounding the zygote could also be collectively referred to as the zygote wall.

The filiform apparatus could still be seen at the interface between the two synergids at the embryo sac wall (Figures 4.28, 4.29a, 4.29b, 4.30, and 4.31). However, within the persistent synergid at the embryo sac wall, the filiform cell wall material had become even more substantial (Figures 4.29a, 4.29b, and 4.30), and now possessed vesicles with threadlike materials (Figure 4.30). Vesicles could also be seen within the persistent synergid cytoplasm near the filiform apparatus. Moreover, the filiform apparatus within the persistent synergid had become more digitate than it was prior to double fertilization (review Figure 4.20), although it was still primarily a thick pad of cell wall material (Figures 4.29a, 4.29b and 4.30). These digitate protuberances were suggestive of digitate filiform transfer cell wall ingrowths, and the persistent synergid plasma membrane appeared to closely follow the contours of the protuberances (Figure 4.30). However, the filiform apparatus was not observed to affect the zygote cell plasma membrane (Figure 4.30) as it had affected the unfertilized egg cell plasma membrane (review Figure 4.20).

9B. The newly-formed zygote: Cytology and ultrastructure

Although the newly formed zygote had lost the large vacuole (Figure 4.28) that the unfertilized egg cell had possessed (review Figures 4.12, 4.15, and 4.18), the zygote cytoplasm still possessed a number of small vacuoles (Figure 4.28). The distinct polarity of the vacuole and the cytoplasm in the unfertilized egg cell (review Figures 4.15 and 4.18) was lost in the newly formed zygote (Figures 4.28 and 4.30). In the zygote, the nucleus occupied a more central location (Figures 4.29a, 4.29b, and 4.30), and the cytoplasm was distributed more uniformly (Figures 4.28 and 4.30) than in the unfertilized egg cell (review Figure 4.18). Osmiophilic bodies and mitochondria, which were uncommon in the unfertilized egg cell (review Figures 4.18 and 4.20) could be now observed with more frequency in the zygote (Figure 4.28). As in the unfertilized egg cell, the osmiophilic bodies in the zygote stained greyish-blue when stained with crystal violet and viewed with light microscopy (not shown). Starch grains in amyloplasts, which were

not observed in the unfertilized egg cell (review Figures 4.18 and 4.20), could now be easily seen in the zygote (Figure 4.28).

9C. Post-fertilization synergids: Cytology and ultrastructure

After double fertilization, the prominent nucleus of the persistent synergid migrated to a more central location (Figures 4.28, 4.29a, and 4.29b) while maintaining a distinct nucleolus and a discrete nuclear envelope (Figures 4.26 and 4.28). However, the chromosomal material became more dispersed (Figures 4.26 and 4.28) than it was prior to fertilization (review Figures 4.15 and 4.17). The cytoplasm remained fairly darkly stained (Figure 4.28). After double fertilization, mitochondria and starch grains were commonly observed in the cytoplasm of the persistent synergid. In addition, the persistent synergid maintained a few small vacuoles post double fertilization. In contrast, osmiophilic bodies, which appeared the same as they did in the pre-fertilization persistent synergid, were fewer in number.

Following double fertilization, starch grains were observed in the darkly stained cytoplasm of the degenerating synergid (Figure 4.31).

9D. Post-fertilization antipodals

After double fertilization, more cell wall material was observed at the interface of the fertilized central cell and the three antipodals (Figures 4.27 and 4.32). The electron opaque deposits that were seen at this interface prior to double fertilization (review Figure 4.24) were no longer visible (Figure 4.32). Notably, one of the major changes in the antipodals was the deposition of large amounts of cell wall material at the interfaces among the three antipodals (Figures 4.27 and 4.32), between the antipodal plasma membranes (Figure 4.32). These thick cell walls possessed fibrillar materials and electron opaque deposits (Figure 4.32), which were not seen in the antipodals prior to double fertilization (review Figure 4.24). The antipodal plasma membranes were slightly contorted by the thickenings (Figure 4.32). The presence of blue fluorescence at all of the antipodal interfaces under Calcofluor fluorescence microscopy indicated that the cell wall material was of a cellulosic and/or hemicellulosic nature (Figure 4.27).

The nuclei, cytoplasm, vacuolar content, and overall size of the post-fertilization antipodals (Figures 4.26 and 4.32) were very similar to the post-fertilization persistent synergid (review Figure 4.28). Like the persistent synergid nucleus (Figures 4.26 and 4.28), each antipodal nucleus possessed a distinct nucleolus and a discrete nuclear envelope (Figure 4.26). Also similar to the persistent synergid (Figures 4.26 and 4.28), the chromosomal material in the antipodal nucleus became more dispersed after double fertilization (Figure 4.26). Like the persistent synergid nucleus (review Figure 4.28) and the zygote nucleus (review Figure 4.30), the antipodal nuclei had assumed a more central location post double fertilization (Figures 4.26, 4.29a, and 4.29b). The antipodals had become more cytoplasm-rich following double fertilization, and the cytoplasm was more darkly stained (Figure 4.32) than it was prior to double fertilization (review Figure 4.24). Thus, the cytoplasm of the post-fertilization antipodals (Figure 4.32) closely resembled the post-fertilization persistent synergid. Moreover, the cytoplasm of the antipodals was no longer found primarily in the perinuclear and peripheral regions (Figure 4.32) as it was found prior to double fertilization (review Figure 4.24). Like the zygote (review Figure 4.28), the antipodals had lost the highly vacuolated region in the vicinity of the central cell (Figure 4.32) that was observed prior to double fertilization (review Figure 4.24). However, some vacuoles remained in the antipodal cytoplasm (Figure 4.32).

Although the pre-fertilization antipodal cytoplasm had contained many mitochondria (review Figure 4.24), as did the pre-fertilization persistent synergid cytoplasm (review Figures 4.20 and 4.22), more mitochondria became evident in the antipodal cytoplasm following double fertilization (Figure 4.32). A similar increase in mitochondria occurred in the persistent synergid following double fertilization (review Figures 4.28 and 4.30). However, osmiophilic bodies, which were observed in the antipodals prior to double fertilization (Figure 4.24) and had stained greyish-blue with crystal violet (not shown), could no longer be easily observed in the antipodal cytoplasm (Figure 4.32). This was similar to the loss of osmiophilic bodies in the persistent synergid post double fertilization (review Figures 4.28 and 4.30). No new organelles appeared in the cytoplasm, and starch grains were not observed in the antipodal cells at any time in development. The antipodals showed no signs of degeneration immediately post-fertilization (Figure 4.32).

9E. Fertilized central cell: Configuration, plasma membranes, cell walls, cytology, and ultrastructure.

Obvious at both the light level (Figure 4.26) and the electron microscope level (Figure 4.31) was the very large primary endosperm nucleus (average median diameter of 20 μm; also see Figures 4.29a and 4.29b). The primary endosperm nucleus was approximately 1.5 times larger than the unfertilized central cell fusion nucleus (review Figures 4.12 and 4.25). Similarly, the primary endosperm nucleus (Figures 4.26 and 4.31) was larger than any other nucleus in the fertilized embryo sac (review Figures 4.26, 4.28, and 4.30). However, similar to the fusion nucleus of the unfertilized central cell (review Figure 4.25), the primary endosperm nucleus (Figure 4.31) possessed a distinct nuclear envelope, a prominent nucleolus, and dispersed chromosomal material. The primary endosperm nucleus was typically found at a position that was closer to the lower pole than to the upper pole of the embryo sac, and was typically seen in the vicinity of the lower side of the embryo sac (Figures 4.29a, 4.29b, and 4.31). Thus, the primary endosperm nucleus (Figures 4.29a, 4.29b, and 4.31) was found in a similar location to the fusion nucleus of the unfertilized central cell (review Figures 4.12 and 4.25).

The fertilized central cell had become much less vacuolate (Figure 4.31) than the highly vacuolate unfertilized central cell (review Figure 4.25). However, small vacuoles were still evident in the cytoplasm (Figure 4.31). The overall amount of cytoplasm and the amount of pre-existing subcellular structures (review Figures 4.17, 4.21, 4.23, and 4.25) had increased substantially (Figure 4.31). Mitochondria, which were most obvious in Figures 4.21 and 4.23, were now abundant in the fertilized central cell and were found in peripheral clusters (Figures 4.28 and 4.31). This increase in mitochondria was similar to the increase noted in the post-fertilization persistent synergid (Figures 4.28 and 4.30) and in the post-fertilization antipodals (review Figure 4.32). In the fertilized central cell, the clusters of mitochondria were found proximal to the embryo sac wall and to the primary endosperm nucleus (Figures 4.28 and 4.31). Starch grains in amyloplasts and osmiophilic bodies, which were both present in the unfertilized central cell (review Figures 4.17, 4.21, 4.23, and 4.25), became even more plentiful in the fertilized central cell cytoplasm (Figure 4.31). As in the unfertilized central cell, the osmiophilic bodies in

the fertilized central cell stained greyish-blue when stained with crystal violet and viewed with light microscopy (not shown).

10. Post Fertilization Central Cell Caecum Formation and Concurrent Events in the Embryo Sac and the PNC

10A. Initiation of the caecum

In early June of the first summer of development (circa June 1), after double fertilization but prior to division of the primary endosperm nucleus, a lateral projection or caecum (pouch) began to develop from the fertilized central cell on its lower side at the embryo sac wall (Figures 4.33 and 4.35). Figure 4.35 is a composite drawing of the lower portion of the embryo sac and caecum shown in Figure 4.33, and the upper portion of the same embryo sac seen in Figure 4.34. The growth of the young caecum was directed toward the base of the PNC and facilitated the expansion of the fertilized central cell (Figures 4.33 and 4.35). Large vacuole formation within the lower region of the fertilized central cell (in the vicinity of the fertilized egg apparatus) as well as within the caecum aided both the expansion of the fertilized central cell and the intercellular growth of the caecum (Figure 4.33).

Peripheral clusters of mitochondria, which were seen in the fertilized central cell prior to caecum initiation (review Figures 4.28 and 4.31), persisted (Figure 4.33). There was no evidence of transfer cell wall ingrowths in the cell wall of the caecum during any time during its development, although peripheral clusters of mitochondria were also present in the caecum (not shown). Due to the overall enlargement of the fertilized central cell, the persistent synergid became crushed, and could no longer be distinguished from the original degenerating synergid (Figures 4.33 and 4.35). The two crushed synergids (Figures 4.33 and 4.35) and the nonfunctional dyad (Figure 4.33) could be seen as vestiges at the lower pole of the embryo sac. Starch grains in amyloplasts persisted in these degenerated cells (Figure 4.33), although the filiform apparatus could no longer be discerned (Figure 4.33 and 4.35). Cytoplasm of the sterile PNC cells displayed a preponderance of mitochondria in regions adjacent to the fertilized central cell and caecum (Figure 4.33).

During caecum initiation, the zygote remained at the lower pole of the embryo sac, attached to the upper side of the embryo sac (not captured in Figure 4.33 but indicated in Figure 4.35). The primary endosperm nucleus within the fertilized central cell (not captured in Figure 4.33 but indicated in Figure 4.35) remained in the same position that it was found in prior to caecum initiation (review Figure 4.31), above the caecum, in the vicinity of the zygote and crushed synergids (Figure 4.35), and near the point where the caecum had originated (the mouth of the caecum) (Figure 4.35). No cell wall partitioned the fertilized central cell prior to the division of the primary endosperm nucleus.

Unlike the lower region of the fertilized central cell (review Figure 4.33), the upper region (in the vicinity of the antipodals) remained relatively non-vacuolate (Figure 4.34) during caecum initiation, as it had been immediately post-fertilization, prior to caecum formation (review Figure 4.31). Mitochondria, osmiophilic bodies, small vacuoles, and starch grains in amyloplasts, which were seen in the fertilized central cell prior to caecum formation (review Figures 4.28 and 4.31), could still be observed in the upper portion of the fertilized central cell following caecum formation (Figure 4.34). Unlike the persistent synergid (review Figures 4.33 and 4.35), the antipodals did not begin to degenerate during caecum initiation and early caecum growth (Figures 4.34 and 4.35). The antipodals maintained the same organellar composition (Figure 4.34) they had possessed immediately following double fertilization, containing many mitochondria and relatively few osmiophilic bodies (review Figure 4.32).

10B. Full elongation of the caecum

The caecum, exhibiting intercellular growth, reached the base of the PNC in early June of the first summer, circa June 3, only a few days after its inception (Figures 4.36, 4.37, and 4.38). The primary endosperm nucleus remained undivided (Figures 4.36 and 4.38). Figure 4.38 is a drawing of the embryo sac and caecum at the same stage of development as seen in Figures 4.36 and 4.37. By this time, the antipodals were crushed as a result of overall expansion of the fertilized central cell (Figures 4.36 and 4.38), and sterile PNC cells became crushed as a result of the intercellular growth of the caecum (Figure 4.36). The thick-walled zygote, however, was rounded and prominent at the

lower pole of the embryo sac, where the zygote shared a common wall with the original embryo sac wall on the upper side (Figures 4.36 and 4.38). The primary endosperm nucleus did not change position and was located in the vicinity of the zygote and crushed synergids at the mouth of the caecum, above the level of the caecum. The primary endosperm nucleus possessed a prominent nucleolus, a discrete nuclear envelope, and moderately dispersed chromosomal material (Figure 4.36), as it had possessed prior to caecum formation (review Figure 4.31). The crushed nonfunctional dyad was still visible below the level of the crushed synergids (Figure 4.36).

A section of tissue with a fertilized embryo sac and caecum at a similar stage in development as seen in Figures 4.36 and 4.38 was subjected to aniline blue fluorescence microscopy (Figure 4.37). Only the cell wall on the lower side of the embryo sac showed a pale blue fluorescence. The caecum cell wall did not fluoresce.

11. First Division of the Primary Endosperm Nucleus Followed by Cytokinesis and the Relative Repositioning of the Zygote

11A. Division of the primary endosperm nucleus and cytokinesis

The primary endosperm nucleus underwent division in mid June of the first summer, circa June 16, a few weeks after the caecum reached the base of the PNC (Figures 4.39, 4.40, and 4.41). Figure 4.41 is a composite drawing of the serial sections of the embryo sac shown in Figures 4.39 and 4.40. One primary endosperm daughter nucleus remained in the same position that the primary endosperm nucleus had occupied, residing within the original confines of the fertilized central cell in the vicinity of the zygote and crushed synergids (Figure 4.39 and 4.41). The other primary endosperm daughter nucleus migrated into the caecum (Figures 4.39, 4.41, and 4.42). Cytokinesis had taken place immediately, and the two primary endosperm daughter nuclei had become separated by a slightly curved cell wall, which formed at the mouth of the caecum (Figures 4.39 and 4.41). This cell wall was longitudinally (vertically) oblique relative to the long axis of the PNC and to the long axis of the embryo sac. Cell wall formation effectively created the first two endosperm cells; one endosperm cell was delimited by the original confines of the fertilized central cell in the vicinity of the zygote. The other endosperm cell was the entire caecum (Figures 4.39, 4.40, 4.41, and

4.42). The crushed antipodals remained visible at the upper pole of the embryo sac (Figures 4.39, 4.40, and 4.41), and the nonfunctional dyad could still be seen below the level of the crushed synergids (Figures 4.39 and 4.40).

The primary endosperm daughter nucleus of the endosperm cell in the vicinity of the zygote was stained more darkly than the primary endosperm daughter nucleus in the caecum (Figure 4.39). Also, the primary endosperm daughter nucleus in the vicinity of the zygote (Figure 4.39) possessed moderately dispersed chromosomal material and a prominent nucleolus, like the undivided primary endosperm nucleus had possessed (review Figure 4.31). Conversely, the primary endosperm daughter nucleus in the caecum possessed moderately condensed chromosomal material (Figures 4.39 and 4.42). The primary endosperm daughter nucleus in the caecum possessed a fairly distinct nuclear envelope (Figure 4.42), as had the undivided primary endosperm nucleus (review Figure 4.31). The endosperm cell in the vicinity of the zygote was moderately vacuolated, especially in its lower region, and more cytoplasm-rich in its upper region, near the crushed antipodals (Figure 4.39), as was the original fertilized central cell during caecum initiation (review Figures 4.33 and 4.34). The caecum (endosperm cell) was highly vacuolate (Figures 4.39, 4.40, and 4.42). The base of the caecum, which lay near the base of the PNC, was distended (Figures 4.39, 4.40, and 4.41). Some perinuclear cytoplasm that was rich in mitochondria could be seen (Figure 4.42).

11B. Appearance of the zygote and its modified positioning relative to the endosperm

At the time of the division of the primary endosperm nucleus in mid June of the first summer (circa June 16), the zygote could be seen to predominate within the embryo sac (Figures 4.39, 4.40, and 4.41). This predominance was partially due to the fact that the antipodals and synergids had degenerated and become crushed. However, relative to the size of the zygote when it was first formed (average median diameter 27 μm; review Figure 4.28), the zygote had also increased in size (average median diameter now 35 μm) and had become rounder. The zygote cell wall was thickened (Figures 4.39 and 4.40), although the zygote still shared a common cell wall with the upper side of the embryo sac (Figures 4.39, 4.40, and 4.41). The zygote cytoplasm maintained some degree of

vacuolation, and its nucleus was large and prominent (Figure 4.40). The zygote nucleus contained two nucleoli.

The unfertilized central cell was originally at a morphologically higher position than the unfertilized egg cell (review Figures 4.12 and 4.13), and prior to caecum formation, the fertilized central cell was originally at a morphologically higher position than the zygote (review Figures 4.28, 4.29a, and 4.29b). However, development of the caecum in a downward direction (review Figures 4.35 and 4.38) coupled with the migration of a primary endosperm daughter nucleus into the caecum permitted cellular endosperm to develop below the level of the zygote (Figures 4.39, 4.40, and 4.41). This, in addition to the fact that the zygote was attached to the upper side of the embryo sac, established that the zygote (and therefore, ultimately the embryo) would develop at a morphologically higher position than the endosperm.

12. Early Cellular Endosperm Development and the Initiation of the Dislodgment of the Zygote from the Embryo Sac Wall

12A. Cellular endosperm development in one plane below the zygote

The endosperm cell in the vicinity of the zygote and the caecum endosperm cell began to undergo further cellular divisions at approximately the same time in the first summer, circa June 26 (Figure 4.43). Cytokinesis always followed nuclear division, and thus there was never a free-nuclear condition in the endosperm developing either in the vicinity of the zygote or in the caecum.

The first two or three divisions of the endosperm cell(s) in the vicinity of the zygote were anticlinal with respect to the lower surface of the zygote, and were thus restricted to the plane of the zygote (Figure 4.43). The endosperm cells were displaced in a downward direction, and therefore approximately three endosperm cells developed in one plane below the level of the zygote. These endosperm cells were held within the original but expanded confines of the fertilized central cell. The zygote possessed several small vacuoles. The endosperm cells in the vicinity of the zygote were triangular to rectangular shaped and possessed prominent vacuoles. Remnants of the synergids, antipodals, and nonfunctional dyad could still be observed.

The first two or three divisions of the caecum endosperm cell(s) were transverse with respect to the long axis of the caecum, and formed a uniseriate file of approximately four cells within the original but expanded confines of the caecum (Figure 4.43). The endosperm cells in the caecum were more rectangular than the endosperm cells in the vicinity of the zygote. Nuclei and a few large vacuoles were observed in the caecum endosperm cells (Figures 4.43 and 4.44). Cytoplasm was typically found in peripheral and perinuclear locations. The lowermost caecum endosperm cells were particularly vacuolate. It was not uncommon for the nucleus in the lowermost endosperm cell of the caecum to degenerate (Figure 4.44).

12B. Cellular endosperm division in more than one plane below the zygote

By mid July of the first summer, circa July 12, the endosperm cells in the vicinity of the zygote (Figures 4.45 and 4.46) and in the caecum (Figure 4.47) began to divide in all planes. At this stage, the zygote was still easily recognizable as a prominent, rounded cell that possessed a particularly thick cell wall (Figure 4.45).

The endosperm cells in the vicinity of the zygote began to proliferate in a cup that enveloped the lower portion of the zygote (Figure 4.45). No endosperm cells were found above the level of the zygote, as the upper part of the zygote remained attached to the embryo sac wall. Portions of the crushed antipodals (Figure 4.46) and crushed synergids (Figures 4.45 and 4.46) were still visible.

The endosperm cells in the vicinity of the zygote had well-defined cell walls and the cytoplasm contained an assortment of subcellular structures including mitochondria, osmiophilic bodies, and starch grains in amyloplasts (Figure 4.46). Small to medium-sized vacuoles, some of which appeared to be filled with tannin-like substances, were common to these endosperm cells. The nuclei of these endosperm cells were large relative to the size of the endosperm cells and possessed distinct nucleoli.

Simultaneously, the endosperm cells in the caecum began to divide in all planes (Figure 4.47 and further verified by serial sectioning - not shown). However, the lowermost two or three cells at the base of the caecum remained in a uniseriate file (Figure 4.47 and further verified by serial sectioning - not shown).

12C. Initiation of the dislodgment of the zygote from the embryo sac wall

A zygote at a similar stage of development as seen in Figure 4.45, sampled in mid July of the first summer (circa July 12), was captured at the electron microscope level (Figure 4.48). Although the zygote still shared a common cell wall with the embryo sac (Figure 4.45), the zygote was seen to be in the process of dislodging from the embryo sac wall (Figure 4.48). Where the zygote shared a common cell wall with the embryo sac, the plasma membrane could be seen to be pulling away from the embryo sac wall. In the region between the zygote cell plasma membrane and the embryo sac cell wall (the periplasmic space), vesicles lined with electron dense materials could be seen. Thus, the zygote was synthesizing its own cell wall that would allow for complete detachment of the zygote from the embryo sac wall. The zygote cytoplasm still contained clusters of mitochondria, as well as several small vacuoles. The zygote nucleus contained regions of very condensed chromosomal material intermixed with regions of dispersed material.

13. Zygotic Division and Initiation of the Encirclement of the Two-Celled Embryo by Endosperm Cells

13A. Zygotic division forming the two-celled embryo

The zygote underwent its first division in late July of the first summer, circa July 20 (nearly two months after double fertilization) to form a two-celled (pro)embryo (Figures 4.49 and 4.50). As it will be later shown that both embryonic cells contribute to the embryo proper, and that a suspensor is not formed, the proembryo will simply be referred to as the embryo. However, it was extremely difficult to ascribe an orientation to the zygotic division, as cellular endosperm development had distorted the original boundary of the embryo sac. In addition, because the zygote had become more rounded (review Figure 4.45) than the unfertilized egg cell (review Figure 4.18), it was hard to establish a reference point to gauge the orientation of zygotic division. However, relative to the point where the two-celled embryo was anchored to (although dislodging from) the upper side of the embryo sac (review Figure 4.45), the cell wall that separated the two embryonic cells (and thus zygotic division) appeared to be transverse (Figure 4.50).

The two embryonic cells that resulted from zygotic division were equal in size and hemispherical (Figures 4.49 and 4.50). They were held within the boundary of the

original zygote wall, which was thicker than the newly formed transverse wall (Figure 4.50). The two cells had a similar appearance to the undivided zygote (review Figures 4.28 and 4.45), and possessed prominent nuclei that each contained a distinct nucleolus. The second, abortive, degenerative embryo sac could still be seen at this stage (Figure 4.49).

13B. Initiation of the encirclement of the two-celled embryo by endosperm cells

After the zygote had divided during late July of the first summer, circa July 20, dividing endosperm cells that were initially within the vicinity of the undivided zygote began to encircle the two-celled embryo above the level of the embryo (Figures 4.49 and 4.50). Two tiers of primarily anticlinally-dividing upwardly-developing endosperm cells, one advancing clockwise and the other counterclockwise, began to encircle the two-celled embryo. These two encircling tiers were in the same plane as the two-celled embryo, and the encirclement was aided by the fact that the zygote had earlier begun to dislodge from the embryo sac wall (review Figure 4.48). Below the level of the embryo, endosperm cells originally derived from those endosperm cells in the vicinity of the zygote continued to divide in all planes (Figure 4.50). Evidence for this consisted of a view of endosperm cells lying outside of the plane of the two tiers seen in partial section below the embryo. The majority of the caecum endosperm cells, which were also continuing to divide in all planes, were not captured in Figures 4.49 and 4.50, although two distended caecum endosperm cells could be seen at the very base of the PNC (Figure 4.49). As was observed prior to zygotic division (review Figure 4.47) these two lowermost caecum endosperm cells remained in a uniseriate file (Figure 4.49). PNC cells were becoming crushed and displaced on all sides of the expanding endosperm (Figures 4.49 and 4.50). Originally, the embryo sac had been separated from the ovarian tissue on one side by the epidermis of the PNC (review Figures 4.12 and 4.26). However, due to the growth of the embryo and mass of endosperm cells as a tissue, the epidermis of the PNC adjacent to the embryo and endosperm became crushed. Thus, the embryo and endosperm came to lie outside of the PNC, and essentially in direct contact with the ovarian tissue on that side (Figures 4.49 and 4.50).

14. Formation of a Four-Celled Embryo, Complete Encirclement of the Embryo by the Endosperm, Continued Endosperm Development Leading to the Formation of the Cap, and the Initiation of Fruit Tissue Development

14A. Formation of the four-celled embryo

At the end of July of the first summer (circa July 31), each cell of the two-celled embryo underwent simultaneous division (Figure 4.51). The division in each of the two embryonic cells was perpendicularly-oriented relative to the division of the zygote, leading to the formation of a round, four-celled embryo. As the division of the zygote was transverse (review Figures 4.49 and 4.50), the division of each cell of the two-celled embryo was therefore longitudinal (vertical) (Figure 4.51). The four resulting embryonic cells were all in the same plane, possessing a similar appearance to each other and to the original zygote (review Figures 4.28 and 4.45). The original zygote cell wall remained thicker than the newly formed partitioning cell walls (Figure 4.51).

14B. Complete encirclement of the embryo by the endosperm cells

When the embryo reached the four-celled stage, the two primarily anticlinally dividing tiers of endosperm cells that had begun to encircle the two-celled embryo and that had arisen from endosperm cells in the vicinity of the zygote (review Figures 4.49 and 4.50) completely encircled the four-celled embryo (Figure 4.51). Therefore, endosperm cells were now found above the level of the embryo in primarily one plane, and this encirclement effectively separated the embryo from the embryo sac wall. It was not uncommon for either the clockwise-advancing tier or the counterclockwise advancing tier to be the tier that predominately aided in the separation of the embryo from the embryo sac wall. In Figure 4.51, the counterclockwise-advancing tier was the predominant tier, but there were other examples in which the clockwise-advancing tier was the predominant tier, and still other examples in which both tiers participated equally in the complete encirclement of the four-celled embryo (not shown). The majority of the endosperm cell divisions in the endosperm cell tiers above the level of the embryo were in the plane of the embryo (Figure 4.51). Occasional endosperm cell divisions outside of the plane of the embryo took place above the level of the embryo, as endosperm cells that lay outside of the plane of the encircling tiers could also be seen in partial section above

the embryo. Below the level of the embryo, endosperm cells originally derived from those endosperm cells in the vicinity of the zygote continued to regularly divide in all planes, as endosperm cells that lay outside of the plane of the embryo could also be seen in partial section. Caecum endosperm cells continued to divide in all planes except at the uniseriate base (not shown).

14C. Formation of the cap and initiation of fruit tissue development

After the four-celled embryo had been completely encircled by endosperm cell tiers in primarily one plane above the embryo and had completely detached from the embryo sac wall (review Figure 4.51), the endosperm cells above the embryo began to regularly proliferate in all planes circa August 5 (Figure 4.52). The original encircling tiers of endosperm cells could no longer be distinguished, and the mass of endosperm cells that resided above the level of the embryo was called the cap. Thus, the endosperm cells in the cap had ultimately been derived from endosperm cells in the vicinity of the original undivided zygote. However, aside from those endosperm cells in the cap, endosperm cells that had originated in the vicinity of the zygote could no longer be distinguished from those that had originated in the caecum (review Figures 4.39 and 4.43). This was because all endosperm cells were regularly dividing in all planes so that endosperm cells below the level of the embryo began to intermingle (Figure 4.52): it was no longer possible to distinguish the presence of a caecum, except at the uniseriate base (not shown).

As endosperm cells divided, more of the PNC cells had become crushed and displaced to the side containing remnants of the second, abortive, degenerative embryo sac (Figure 4.52). No PNC cells remained above the cap or where the endosperm had come into direct contact with the ovarian tissue, as the epidermis of the PNC that had been in contact with the endosperm had been crushed and obliterated. The ovarian tissue displayed signs of cell division and cell enlargement, and thus the ovarian tissue was beginning to develop. However, no differentiation of the ovarian tissue into specific fruit zones was observed at this point. Because fruit tissue had begun to develop, at this stage the fertilized flower could be more aptly called a young fruit.

15. Formation of the Globular Embryo and Continued Development of the Endosperm and Fruit Tissue

After further proliferation of the endosperm cells and growth of the endosperm as a tissue, the embryo began to divide in all planes to form a small, undifferentiated globe of about eight to sixteen cells in mid August of the first summer, circa August 14 (Figure 4.53). The embryo had reached the globular stage, but no suspensor was formed. The dividing endosperm cells had displaced almost all of the PNC to the side containing the abortive, degenerating embryo sac, and were proceeding to downwardly crush the sterile PNC cells. The base of the endosperm (the original base of the caecum) remained uniseriate and dilated. The ovarian cells continued to divide and enlarge, but there was no differentiation into the specific fruit zones.

16. External Morphology and Internal Anatomy of the Young Fruit at the End of the First Summer of Development

16A. External morphology of the young fruit at the end of the first summer of development

By late August of the first summer (circa August 20), the young fruit now had a more rounded appearance (Figure 4.54), and had lost the bilateral flattening that characterized the unfertilized flower (review Figures 4.1, 4.2a, 4.2b, and 4.2c). The lower three-quarters of each fruit, proximal to the pedicel within the bract, were dark green, and the upper quarter was yellowish-green (Figure 4.54). Each stigma had turned red. The young fruit was now approximately 4 mm in length (a gain of about 3 mm), 1 mm in breadth at its base (a gain of about 0.8 mm), and 3 mm in thickness (a gain of at least 1 mm). The loss of the bilateral flattening was primarily due to the development of fruit tissue, but the enlargement of both the endosperm and the embryo also contributed to the overall increase in the size of the fruit. At this stage, incipient, pre-meiotic, pre-anthesis flowers (buds) developing in the summer prior to the predefined first spring of development (when anthesis occurs) could also be observed on the shoots (not shown).

16B. Appearance of the embryo and endosperm at the end of the first summer of development

Young fruit of a similar stage in development as seen in Figure 4.54, sampled from late August in the first summer (circa August 20), were sectioned (Figures 4.55 and 4.56). At this time, the globular embryo was comprised of about sixty to one-hundred cells, and had an average median diameter of about 60 μm. Specific tissues had not differentiated. The cells of the embryo were less vacuolate than the cells of the endosperm (Figure 4.56). As the embryo had grown due to an increase in cell number and cell size, some of the endosperm cells adjacent to the expanding embryo had become compressed.

The endosperm, also growing by an increase in cell number and cell size, had completely crushed all of the cells of the PNC, and these crushed cells could be seen at the base of the endosperm (Figures 4.55 and 4.56). The endosperm had a length of about 300 μm. The base of the endosperm, which had previously represented the uniseriate base of the original caecum (review Figure 4.53), finally became multiseriate (Figures 4.55 and 4.56). Although outer peripheral endosperm cells were undergoing predominantly anticlinal divisions in order to keep pace with the expanding mass of endosperm, many of the peripheral cells had become slightly compressed due to the pressure of the continued overall growth of the endosperm (Figure 4.56).

16C. First evidence of the three fruit zones at the end of the first summer of development

By the end of August in the first summer of development (circa August 20), three fruit zones could be distinguished within the young fruit (Figures 4.55 and 4.56). The innermost zone, or endocarp, was immediately adjacent to the endosperm, completely enveloped the endosperm on all sides (Figure 4.55), was about five to ten cell layers in thickness, and was primarily comprised of isodiametric, empty-looking, highly vacuolate cells (Figures 4.55 and 4.56). However, tannin-like materials were present in the vacuoles in some of these endocarp cells; these cells had a rather sporadic distribution within the endocarp.

The mesocarp was the next fruit zone immediately outside of the endocarp, and completely enveloped the endocarp on all sides (Figure 4.55). The mesocarp was about four to five cell layers in thickness, but the cells of the mesocarp were much smaller in median diameter relative to the cells of the endocarp. All cells of the mesocarp were slightly elongated, had prominent nuclei that were large relative to the volume of a mesocarp cell, and represented the progenitors of the viscin tissue; viscin tissue would develop in the second spring and summer and would be comprised of two cell types.

Outside of the mesocarp was the outermost fruit zone, or exocarp, which was about ten to fourteen cell layers in thickness and enveloped nearly all of the mesocarp aside from the regions below the level of the endosperm where the exocarp became confluent with the pedicel tissues (Figure 4.55). The cells of the exocarp were larger in median diameter than the cells of the mesocarp, as were the cells of the endocarp. The exocarp was divided into two separate regions. The inner exocarp, immediately adjacent to the mesocarp, possessed five to seven layers of vacuolate cells, and embedded the vascular tissues. The outer exocarp (the outer layer of the fruit) also possessed five to seven layers of darkly stained cells, and the cell walls of these cells were considerably thicker than those of inner exocarp cells. There would be no further changes in the number of cell layers in the fruit tissues.

16D. The resting period

Late in the first summer (circa August 20) the young embryo and endosperm within the fruit had ceased developing, and had entered a resting period. This was confirmed by sampling throughout the winter. Young fruits sampled in mid winter, circa December 20 had a similar external morphology (not shown) and internal anatomy (Figure 4.57) to fruits sampled in late summer, circa August 20 (review Figures 4.54, 4.55, and 4.56). The only change of note was an accumulation of tannin-like materials in the vacuoles of the upper peripheral cells of the endocarp (Figure 4.57). Cells with tannin-like material had a more sporadic distribution within the endocarp prior to the winter period (review Figure 4.55).

17. Resumption of Development in the Second Spring: Differentiation of the Inner Layer of Mesocarp into Viscin Cells (The First Cell Type of the Viscin Tissue)

Development within the fruit of *Arceuthobium americanum* resumed in mid May (circa May 17) of the second spring. The appearance and size of the embryo and endosperm (Figure 4.58) had not changed since late in the first summer, circa August 20 (review Figures 4.55, 4.56, and 4.57). However, the innermost uniseriate layer of the mesocarp to one side of the endocarp in the upper quarter of the fruit was beginning to elongate and secrete a mucilage (Figure 4.58). Hence, this cell layer was beginning to differentiate into viscin cells, the first of the two cell types that would comprise the viscin tissue. Viscin cells would not divide once they began to elongate. The young viscin cells were elongating bi-directionally at an oblique angle to the long axis of the fruit so that they were elongating down toward the endocarp, and up toward the undifferentiated mesocarp and exocarp.

The elongation process was beginning to compress cells of both the endocarp and the inner exocarp in the vicinity of the elongating viscin cells (Figure 4.58). However, the undifferentiated three to four mesocarp cell layers lying between the elongating viscin cells and the compressed areas of the inner exocarp were not affected by viscin cell elongation. Tannin-like materials, which had begun to accumulate in the large vacuoles of the upper peripheral cells of the endocarp in mid-winter, circa December 20 (review Figure 4.57), had now accumulated in the majority of the upper endocarp cells (Figure 4.58). Endocarp cells compressed by the elongating viscin cells were particularly prone to accumulate tannin-like materials in their vacuoles, although these endocarp cells were still found in a sporadic distribution amongst the entire endocarp (Figure 4.58), as they had been prior to the winter period (review Figure 4.57). Tannin-like materials were also beginning to accumulate within the vacuoles of the both inner and outer exocarp cells, particularly in the compressed cells of the inner exocarp (Figure 4.58). Remnants of the crushed PNC could still be seen at the base of the endosperm.

18. Enlargement of the Embryo and Endosperm, and Further Differentiation of the Inner Layer of Mesocarp into Viscin Cells

18A. Enlargement of the embryo and endosperm

By mid June of the second summer (circa June 16), both the embryo and endosperm had enlarged via cell divisions and cell enlargement (Figure 4.59). The embryo had increased in cell number from approximately one hundred cells (review Figures 4.55, 4.56, 4.57, and 4.58) to approximately two hundred cells (Figure 4.59), and accordingly had increased in median diameter from 60 μm (review Figures 4.55, 4.56, 4.57, and 4.58) to 130 μm (Figure 4.59). However, the embryo was still globular in shape, as its general appearance had not changed, and no embryonic differentiation had occurred (Figure 4.59).

Also at this time, the endosperm, with a length of 670 μm, had more than doubled in length via cell divisions and cell enlargement (Figure 4.59) compared to the length observed previously (300 μm - review Figures 4.55, 4.56, 4.57, and 4.58). Two different zones could now be distinguished within the endosperm with regard to cell size and appearance (Figure 4.59). The first zone was essentially the base of the endosperm, and contained large cells with large vacuoles (Type 1 endosperm cells). The second zone comprised the remainder of the endosperm and contained smaller, cytoplasmically-rich cells with small vacuoles (Type 2 endosperm cells). At this time, the second zone also included the cells of the cap. More of the endosperm cells adjacent to the embryo had become compressed to accommodate the growth of the embryo (not shown). Remnants of the crushed PNC could still be seen at the base of the endosperm (Figure 4.59).

18B. Changes in the fruit tissues including further differentiation of the inner layer of mesocarp into viscin cells

To account for endosperm growth at this time in mid June of the second summer (circa June 16), the endocarp cells adjacent to the expanded endosperm had become compressed (Figure 4.59). Below the level of the endosperm, all endocarp cells became completely compressed, confluent with the mesocarp, and tannin-filled. Also at this time, the innermost uniseriate layer of mesocarp on all sides of the endocarp in the upper half of the fruit had developed into viscin cells, which were elongating and secreting

mucilage. Tannin-like material could be seen within some of the viscin cells. The elongation process continued to compress the cells of both the endocarp and the inner exocarp in the vicinity of the elongating viscin cells. Therefore, the endocarp cells were being compressed in one direction by the expanding endosperm, and in the opposite direction by the elongating viscin cells.

18C. Cytochemistry of the young embryo, endosperm, and fruit tissues using aniline blue black (ABB)

A section of a fruit at approximately the same stage of development as seen in Figure 4.59 was treated with aniline blue black (ABB) stain (Figure 4.60). All nuclei and cell walls stained blue, indicative of the ubiquitous presence of protein in these components. Cytoplasmic regions had a tendency to stain blue, indicating the proteinaceous nature of cytoplasm, whereas vacuolar contents tended to be negative for blue staining with ABB. The cells of the young, undifferentiated, globular embryo generally acquired more stain than the cells of the endosperm, since the cells of the young embryo were more cytoplasm-rich overall when compared to the relatively more vacuolate cells of the endosperm. Blue stained globules represented protein bodies, which could be seen within the embryo, although there was no pattern to their location. Protein bodies were also seen in the endosperm cells, but were more common in Type 2 endosperm cells (including the cells of the cap) than in Type 1 endosperm cells.

Protein bodies were present but rare within the cells of the endocarp and exocarp (Figure 4.60) and essentially negative for blue staining with ABB. These cells appeared colourless if there were no tannin-like materials in the vacuoles, or greyish-black if tannin-like materials were present. Viscin cell mucilage stained blue, whereas viscin cell contents were negative for blue staining with ABB. Most viscin cell contents were colourless, but sometimes the viscin cell contents stained greyish-black, indicating the presence of tannin-like materials in their vacuoles. The cells of the mesocarp that had not differentiated into viscin tissue of either cell type contained relatively large nuclei, and because the proteinaceous nuclei were stained blue, these undifferentiated cells appeared quite blue relative to the cells of the endocarp and exocarp.

19. Differentiation of the Embryonic Protoderm, Change in the Cap Cells, and the Completion of Differentiation of the Inner Layer of Mesocarp into Viscin Cells

19A. Differentiation of the embryonic protoderm and change in the appearance of the cap cells

By late July of the second summer (circa July 20), the embryo had doubled in length (265 μm - Figure 4.61) compared to the length of the embryo at mid June (circa June 16) of the second summer (130 μm - review Figure 4.59). The width of the embryo had also increased to about 200 μm (Figure 4.61) from 130 μm (review Figure 4.59). Many cell divisions had occurred, and the cells in the inner region of the embryo had become slightly vacuolate and enlarged (Figure 4.62). The outer layer of embryonic cells remained cytoplasm-rich, and had undergone anticlinal divisions to form the uniseriate protoderm. Consequently, the embryo was more ovoid than spherical, and had progressed beyond the simple globular stage (Figures 4.61 and 4.62). However, because the embryo had not developed cotyledons, it could not be said to be at the heart stage of development. Therefore, the embryo was at an undefined post-globular stage of embryo development. Compressed endosperm cells continued to be observed adjacent to expanding embryo (Figure 4.62). The size of the endosperm had increased, but it was apparent that the rate of endosperm growth was slowing relative to that of the embryo (Figure 4.61). The cells in the cap (Figures 4.61 and 4.62) had become more vacuolate (Figure 4.62) and had increased in size so that they looked more like the cells at the base of the endosperm (Figure 4.61). In other words, the cells in the cap had changed from Type 2 cells (cytoplasm-rich and small) to Type 1 cells (vacuolate and large). The crushed PNC could still be observed (Figure 4.61).

19B. Changes in the fruit tissues including the continued differentiation of the inner layer of mesocarp into viscin cells

Along with the change in the cap cells in late July of the second summer (circa July 20), the growing endosperm, as well as the enlarging embryo, continued to compress endocarp cells adjacent to the endosperm (Figure 4.61). The innermost uniseriate mesocarp layer on all sides of the endocarp in the upper two-thirds of the fruit had developed into elongated, mucilaginous viscin cells. The elongation process had

continued to compress the cells of the endocarp and inner exocarp in the vicinity of the elongating viscin cells, and so the endocarp continued to be compressed from all directions. Tannin-like materials continued to accumulate in the vacuoles of even more cells of the endocarp and exocarp, particularly in those cells that had been compressed.

19C. Cytochemistry of the young embryo with a protoderm, endosperm, and fruit tissues using the Periodic Acid - Schiff's (PAS) treatment

A section of fruit at approximately the same stage of development as seen in Figures 4.61 and 4.62 was subjected to the Periodic Acid - Schiff's (PAS) treatment (Figure 4.63). All cell walls stained pink, indicating the presence of carbohydrates in the cell walls. Pink stained granules represented starch grains in amyloplasts. Starch grains could be seen within the embryo, where they appeared to be limited to the lower peripheral regions of the embryo. In the endosperm, starch grains were only common in the Type 2 endosperm cells. However, Type 2 endosperm cells in the vicinity of the embryo (enveloping the lower two-thirds of the embryo) appeared to lack starch grains. Endosperm cells in the cap and at the base of the endosperm, which were all Type 1 cells, contained only a few starch grains. All of the peripheral cells of the entire endosperm (comprised of both Type 1 and Type 2 cells and including the peripheral cells of the cap) appeared to be completely devoid of starch grains.

A few endocarp cells also contained starch grains (Figure 4.63). Nonetheless, the contents of the highly vacuolate endocarp, inner exocarp (Figure 4.63), and outer exocarp cells (not shown) were essentially negative for the PAS treatment. These cells appeared colourless if there were no tannin-like materials in the vacuoles, or greyish if tannin-like materials were present (Figure 4.63). The viscin cell mucilage stained pink, and there were apparently a few starch grains in the viscin cells. Overall, the cell contents of most viscin cells were colourless and thus also negative for the PAS treatment. However, tannin-like materials in a few of the viscin cells stained greyish. The contents of the undifferentiated mesocarp cells remained colourless. Controls for PAS treatment (not shown) revealed no pink staining in any of the regions that had stained pink with PAS treatment (Figure 4.63) at this and all other subsequent stages of development (not shown). Similarly, controls for PAS treatment (not shown) also revealed reduced greyish

staining in all of the regions that had stained greyish with the PAS treatment (Figure 4.63) at this and all other subsequent stages of development (not shown). The remaining greyish staining was likely due to the presence of osmium tetroxide.

20. Differentiation of the Embryonic Radicular Apex, Appearance of the Endosperm, Differentiation of the Outer Layers of Mesocarp into Vesicular Cells (The Second Cell Type of the Viscin Tissue), Complete Compression of the Endocarp, and Occurrence of Twins

20A. Differentiation of the embryonic radicular apex, appearance of the maturing endosperm, and cytochemistry of the embryo and endosperm using the PAS treatment

By early August of the second summer (circa August 5), the embryo, which was still undergoing cell divisions, had reached its maximum girth but had continued to expand in an upward longitudinal direction, obtaining an elongated ovoid appearance (Figures 4.64 and 4.65). Figure 4.65 depicts a PAS-treated section of the embryo and endosperm at approximately the same stage of development as seen in Figure 4.64. Starch grains could be seen within the embryo, where they were limited to the lower peripheral regions of the embryo (Figure 4.65), as was previously observed (review Figure 4.63). The majority of the cells in the inner region of the embryo remained vacuolate (Figure 4.65), as they had been previously (review Figure 4.62), but a cluster of cells at the upper pole of the embryo had become cytoplasm-rich (Figure 4.65), as they had differentiated into the radicular apex. The protodermal cells (Figure 4.65) maintained their cytoplasm-rich appearance (review Figure 4.62).

At this time, the endosperm acquired a vase-like appearance because the vacuolate Type 1 cells both at the base of the endosperm (Figure 4.64) and in the cap region (Figures 4.64 and 4.65) had enlarged further via their expanding vacuoles. The Type 1 cells no longer appeared to be dividing, whereas mitotic figures could still be seen in the Type 2 cells (see Chapter Six, Figures 6.3, 6.5, 6.6, and 6.7). The crushed remnants of the PNC could still be observed at the base of the endosperm (Figure 4.64). Although starch grains were previously absent from Type 2 endosperm cells enveloping the lower two-thirds of the embryo (review Figure 4.63), they had now accumulated in these Type

2 endosperm cells (Figure 4.65). As was previously observed (review Figure 4.63), Type 1 endosperm cells of the cap region (Figure 4.65) and at the base of the endosperm (not shown) contained only a few starch grains. Moreover, although starch grains were previously absent from all peripheral endosperm cells (review Figure 4.63), a few starch grains were now present in these cells (Figure 4.65). The starch grains of the endosperm were relatively larger than the starch grains in the embryo (Figure 4.65). Cells of the endosperm, notably those cells in the cap immediately adjacent to the radicular pole of the embryo, continued to be compressed in order to accommodate the upward growth of the embryo.

20B. Differentiation of the outer cell layers of mesocarp into vesicular cells, complete compression of the endocarp, and the genesis of the pseudoseed coat

At this time in early August of the second summer (circa August 5), all of the cells in the innermost uniseriate layer of mesocarp in the upper three-quarters of the fruit had developed into viscin cells (Figure 4.64). The viscin cells had elongated to their fullest extent but continued to secrete mucilage. Also, the remaining outer three to four cell layers in the upper three-quarters of the mesocarp had differentiated into the second cell type of the viscin tissue; namely, the enlarged, isodiametric vesicular cells.

As a result of the viscin cell elongation and enlargement of the vesicular cells, as well as a result of the enlargement of the endosperm and embryo, all of the endocarp cells had become compressed and their vacuoles filled with a tannin-like material (Figure 4.64). The lower quarter of the mesocarp, including the portion of mesocarp below the endosperm that had previously become confluent with the endocarp and tannin-filled (review Figure 4.59), would not differentiate into viscin tissue of either cell type (Figure 4.64). Instead, the entire lower quarter of the mesocarp had become tannin-filled and confluent with the compressed endocarp (Figure 4.64). The compressed, tannin-filled endocarp, along with the tannin-filled lower quarter of the mesocarp, comprised the tanniferous pseudoseed coat. The term pseudoseed coat was used because the compressed endocarp and lower mesocarp fulfilled the role of a typical seed coat as it

was directly appressed to and enveloped the embryo and endosperm. Unlike a true seed coat, the pseudoseed coat was not derived from integuments.

Cells of the inner exocarp immediately adjacent to the now evident vesicular cells had all been fully compressed and their vacuoles had all become filled with tannin-like materials (Figure 4.64). Additionally, more cells of both the inner exocarp and the outer exocarp were continuing to accumulate tannin-like materials in their vacuoles, although not to the extent of the compressed cells of the inner exocarp. To account for the overall increase in the size of the fruit due to viscin cell elongation and enlargement of the embryo and endosperm, anticlinal cell divisions had taken place at the base of the exocarp in the non compressed regions.

20C. Cytochemistry of the maturing embryo, endosperm, and fruit tissues using ABB

Non-median sections of fruit at approximately the same stage of development as seen in Figures 4.64 and 4.65 were treated with ABB (Figures 4.66 and 4.67). As these sections were non-median, the embryo and cap appeared to have a smaller volume (Figures 4.66 and 4.67) than they truly possessed (review Figures 4.64 and 4.65). There was no change in the general distribution of the ABB stain in the embryo, endosperm, and viscin cells (Figures 4.66 and 4.67) from what was seen earlier in development in mid June of the second summer, circa June 16 (review Figure 4.60). As before, protein bodies were more common in Type 2 endosperm cells than Type 1 endosperm cells (not indicated). As such, because the cap cells had changed from Type 2 endosperm cells (review Figure 4.60) to Type 1 endosperm cells (review Figures 4.61, 4.62, 4.64, and 4.65), there now appeared to be fewer protein bodies in the cap (Figure 4.67). The vesicular cells were negative for blue staining with ABB (Figure 4.66). As before (review Figure 4.60), tannin-like materials had a tendency to appear greyish-black in the presence of the ABB stain (Figures 4.66 and 4.67). Because all cells of the pseudoseed coat and many cells of the exocarp (especially the compressed cells of the inner exocarp) had accumulated tannin-like materials in their vacuoles, these areas had a tendency to appear greyish-black overall and thus remained negative for the blue staining with ABB

(Figures 4.66 and 4.67). If protein bodies remained in the exocarp or endocarp (now the majority of the pseudoseed coat), the greyish-black staining obscured them.

20D. Cytochemistry of the maturing embryo, endosperm, and fruit tissues using Toluidine blue O (TB)

A non-median section of fruit at approximately the same stage of development as seen in Figures 4.64, 4.65, 4.66, and 4.67 was also treated with the metachromatic stain Toluidine blue O (TB) at pH 4.4 (Figure 4.68). As the section was non-median, the embryo and the cap appeared to have a smaller volume (Figure 4.68) than they truly possessed (review Figures 4.64 and 4.65). The embryo as a whole stained purple, indicating the presence of proteins and possibly nucleic acids (Figure 4.68). The endosperm also stained generally purple, although vacuolate Type 1 endosperm cells, including those in the cap, stained less purple than the cytoplasm-rich Type 2 endosperm cells. All peripheral cells of the endosperm (comprised of both Type 1 and Type 2 cells and including the peripheral cells of the cap) stained notably purple. Tannin-like materials that had accumulated in vacuoles of the pseudoseed coat cells and in exocarp cells stained greenish-blue. The viscin cell mucilage stained pink, indicating the presence of pectic acids, whereas the majority of the viscin cell contents did not take up the TB stain, although tannin-like materials previously seen in the viscin cells (review Figures 4.59, 4.61, and 4.66) stained greenish-blue (Figure 4.68). Starch grains were also observable in the viscin cells, although the starch grains were unstained and thus recognizable only by their shape and appearance (Figure 4.68). The enlarged vesicular cells were essentially negative for the TB stain (Figure 4.68). Staining with TB at a lower pH of 2.2 acted as a control for carboxylic acid staining, and the regions that had stained pink with TB at a pH of 4.4 (Figure 4.68) did not stain pink with TB at a pH of 2.2 (not shown).

20E. Occurrence of twins

Notably, a fruit at approximately the same stage of development as seen in Figures 4.64, 4.65 4.66, 4.67, and 4.68 was sectioned, and showed the presence of two embryos, or "twins" (Figure 4.69). Each embryo was found in its own endosperm. Out

of the hundreds of fruits sectioned at various ages, this was the only case of twins seen. Thus, polyembryony and polyendospermy must be extremely rare in *Arceuthobium americanum*. There was only one region where crushed PNC cells could be observed, so it could be assumed that each embryo and endosperm had been conceived in the same PNC. Also, because the two embryos and their endosperms were placed side-by-side, both of the two original megasporocytes must have had the capacity to produce functional embryo sacs that were each capable of undergoing double fertilization.

One embryo and its endosperm (Figure 4.69) had a similar appearance to a typical embryo and endosperm observed circa August 5 of the second summer (review Figure 4.64). The typical embryo (Figure 4.69) possessed a radicular apex with cytoplasm-rich cells, a protoderm with cytoplasm-rich cells, and an inner region with relatively vacuolate cells, as would be expected for a typical embryo observed circa August 5 of the second summer (review Figure 4.65). The endosperm associated with the typical embryo possessed Type 1 endosperm cells at the endosperm base, and Type 2 endosperm cells in the central region of the endosperm (Figure 4.69), as would also be expected for an endosperm observed circa August 5 of the second summer (review Figure 4.65). The cap cells of this typical endosperm had developed from Type 2 endosperm cells into Type 1 cells (Figure 4.69), as would be expected. The second embryo and its endosperm, however, appeared to be at a less advanced stage of development (Figure 4.69). No differentiation had occurred in the embryo. This lagging embryo and endosperm were smaller than the typical embryo and endosperm. Although the two types of endosperm cells were visible in the endosperm, the cap cells of the lagging endosperm had not become vacuolate and thus had not developed from Type 2 cells into Type 1 cells. Therefore, the lagging embryo and its endosperm (Figure 4.69) had an appearance more in accordance with an embryo and endosperm sampled from mid June of the second summer, circa June 16 (review Figures 4.59 and 4.60). However, the viability of either twin embryo (Figure 4.69) could not be determined. The fruit tissues, including the pseudoseed coat, viscin cells (Figure 4.69), vesicular cells (not shown), and exocarp enveloping the two embryos and endosperms (Figure 4.69) had a similar appearance to the typical fruit tissues sampled at this time in early August, circa August 5 (review Figures 4.64, 4.66, and 4.68).

21. External Morphology and Internal Anatomy of the Ripe Fruit at the End of the Second Summer of Development, Prior to Explosive Discharge

21A. External morphology of the fruit at the end of the second summer of development

By late August in the second summer (circa August 20), the fruits had reached their maximum size and ripeness (Figure 4.70). Along with the ripe fruit ready to discharge their contents, young first year fruits were also evident on the same shoot. Additionally, incipient, pre-meiotic, pre-anthesis flowers (buds) developing in the summer prior to the predefined first spring of development (when anthesis occurs) could also be observed (review part 1 of these results). In the ripe, mature fruit, the yellow pedicels had elongated to about 2 mm in length, and could be seen outside of the cup-like bract. The pedicels were recurved, and thus the fruits were somewhat droopy. The lower three-quarters of each fruit, proximal to the pedicel, were still dark green, and the upper quarter was still yellowish-green. Each stigma was still reddish. Originally, each cyme held up to three flowers (review Figures 4.1 and 4.2a), and accordingly, there were typically up to three ripe fruits in a cyme (Figure 4.70). However, it was not uncommon to see aborted individuals in the cyme alongside ripe fruit, which were either flowers that had undergone meiosis and anthesis but had failed to be fertilized, or were flowers that had been fertilized but had failed to mature into ripe fruit. Sometimes it was apparent that a fruit had prematurely dropped out of the cyme, as there were some bracts in which the pedicel could no longer be observed. In typical fruit dehiscence, the pedicel would remain, but if a fruit had prematurely dropped, no pedicel was evident. At its maximum ripeness, just prior to explosive discharge, a fruit was approximately 6 mm in length (not including the pedicel), 2 mm in breadth at its base where it was attached to the pedicel, and 4 mm in thickness.

21B. Appearance of the mature dispersal unit (the pseudoseed) within the ripe fruit at the end of the second summer of development and cytochemistry as observed with the Yeung procedure

Ripe fruit of a similar stage in development as seen in Figure 4.70 was sectioned and stained with the Yeung procedure (Figure 4.71). The mature embryo, the endosperm (including the cap), the crushed remnants of the PNC, the pseudoseed coat, and the

elongated viscin cells would comprise the dispersal unit (pseudoseed) that would be forcibly ejected from the fruit at the end of the second summer of development. The vesicular cells would not be ejected from the fruit, and were thus not part of the pseudoseed.

The main components of the pseudoseed held within the fruit can be seen in Figure 4.71, aside from the PNC and the lower portion of the endosperm. The embryo had elongated at its radicular pole, attaining a torpedo-like appearance, and had crushed but not obliterated the cells of the cap (Figure 4.71). The cells of the previously differentiated embryonic protoderm and radicular apex (review Figure 4.65) remained cytoplasm-rich (Figure 4.71). Although cells in the inner region of the embryo had been fairly vacuolate since late July of the second summer (review Figures 4.62 and 4.65), three to four files of cells in the central column of the upper two-thirds of the embryo had reverted to a cytoplasm-rich state (Figure 4.71). These cell files represented the newly differentiated procambium, and in different views (not shown), the procambium appeared to consist of two distinct strands. The remainder of the embryonic cells lying between the procambium and the protoderm represented the differentiating cells of the ground meristem (Figure 4.71), which remained vacuolate (review Figures 4.62 and 4.65). Starch grains stained pink with the Yeung procedure. The ground meristem possessed most of the starch grains of the embryo (Figure 4.71). Rudimentary cotyledons could be seen at the lower pole of the embryo, which represented the rudimentary shoot apex. Chlorophyll was also present within the embryo, as embryos examined in whole ripe fruit were entirely green (not shown).

Starch grains were now extremely abundant in the endosperm (Type 2 cells) surrounding the lower two-thirds of the embryo (Figure 4.71). Like the embryo, endosperm examined in whole ripe fruit was green and thus contained chlorophyll (not shown). The crushed cap cells stained pink from the Yeung procedure, indicating the presence of carbohydrates. Similarly, the viscin cell mucilage stained pink (Figure 4.71) as it did with TB (review Figure 4.68). For the most part, the viscin cell contents remained colourless after treatment with the Yeung procedure (Figure 4.71), as they did upon staining with TB (review Figure 4.68), although, as with TB (review Figure 4.68), the tannin-like materials within a few of the viscin cells stained greenish-blue (Figure

4.71). As with TB (review Figure 4.68), all cells of the pseudoseed coat stained greenish-blue with the Yeung procedure (Figure 4.71). Cell divisions were no longer ongoing in any region within the fruit.

21C. Appearance of the mature pseudoseed within the fruit the end of the second summer of development and cytochemistry as observed with the Sudan Black B (SBB)

A section of fruit at a similar stage in development as seen in Figures 4.70 and 4.71 was treated with Sudan Black B (SBB) stain (Figure 4.72 - a montage). Staining of the pseudoseed components are featured. Cell walls, nuclei, and starch grains were essentially negative for staining with SBB, although the cell wall boundary around the radicular apex of the embryo appeared to be stained quite black, indicating a lipid component. Within the embryo, most cells of the procambium as well as a few cells of the ground meristem in the area of the rudimentary shoot apex were completely filled with a very darkly stained material, and thus these cells had a lipid component.

Type 2 endosperm cells enveloping the lower two-thirds of the embryo (Figure 4.72) and Type 1 endosperm cells (not shown) contained a few black globules, which were most likely lipid bodies, but these were not as large as the lipid components seen within the procambium and ground meristem of the embryo (Figure 4.72). The crushed endosperm cells in the cap appeared to be negative for the SBB stain. The cells of the pseudoseed coat were positive for the stain, especially in the regions adjacent to the crushed cap, but the positive staining reaction was most likely a reaction with the tannin-like materials in these cells as opposed to a reaction with lipid components. The viscin cell mucilage and cell contents were essentially negative for the stain (not shown). The staining of the vesicular cells with SBB will be discussed in Chapter Five. The exocarp, although not part of the discharged pseudoseed, stained differentially with SBB: the cell walls of the outer exocarp reacted positively with SBB (especially in regions proximal to the pedicel), whereas the cell walls of the outer exocarp were essentially negative for SBB (not shown).

21D. Appearance of the vascular traces in the exocarp

Two vascular traces in fruit at a similar stage in development as seen in Figures 4.70, 4.71, and 4.72 were observed in cross section (Figure 4.73). The two traces, each of which was about five to eight cells in diameter, were found within the inner exocarp (just outside of the compressed cells of the inner exocarp), and appeared to be comprised entirely of xylem tissue, since no obvious phloem tissue was observed. The xylem tissue appeared to be comprised primarily of xylem vessel elements and xylem parenchyma. Graniferous tracheary elements were apparently absent. A xylem vessel element from a vascular trace in a fruit at a similar stage in development as seen in Figures 4.70, 4.71, 4.72, and 4.73 was examined in longitudinal section at the electron microscope level (Figure 4.74). The cell wall of the vessel element displayed characteristic secondary wall thickenings, which appeared to represent the helical type. This was confirmed by serial sectioning (also review Figure 4.3). As in the young flowers (review Figure 4.3), the cell walls of vessel elements in the ripe fruit (Figure 4.73) stained purplish with crystal violet. Commonly, vessel elements in the ripe fruit possessed cytoplasm as well as organelles, and thus appeared viable (Figure 4.74 and other examples - not shown). The elongated nucleus of the vessel element could be seen in Figure 4.74, and it possessed fairly condensed chromosomal material. The cytoplasm of the vessel element was relatively dark staining, and contained a large number of mitochondria as well as a few small osmiophilic bodies.

22. Explosive Discharge and the (Naturally) Discharged Pseudoseed

22A. Manner and timing of explosive discharge

Discharge of the pseudoseed resulted from the formation of an abscission layer (not shown) that developed between the lowermost cells of the pseudoseed coat (specifically the region where endocarp was confluent with lower quarter of mesocarp - review Figure 4.64) and the region where exocarp was confluent with the tissues of the pedicel (review Figure 4.55). In all study years (1995 through 1998), explosive discharge took place around the third week to the fourth week in August at the end of the second summer of development. Only a few shoots still held ripe fruit around the first week in September, and no ripe fruit was typically seen after the third week in September.

22B. The (naturally discharged) pseudoseed

Discharged pseudoseeds captured in cheesecloth wraps all had the same external appearance (Figure 4.75), regardless of when the cheesecloth wraps were collected from the fourth week of August (August 25) to the first week of October (October 1). The mucilaginous, nacreous but slightly green viscin cells enveloped the tanniferous brown pseudoseed coat (Figure 4.75), within which could be found the green endosperm and green embryo (not shown). Figure 4.75 depicts a specimen that was preserved in modified Karnovsky's fixative; unfixed material had essentially the same appearance (not shown). No vesicular cells were observed in the discharged pseudoseed.

Discharged pseudoseeds sectioned parallel to their long axes (Figure 4.76) had similar internal appearances regardless of the cheesecloth wrap collection time. Moreover, a discharged pseudoseed (Figure 4.76) had nearly the same appearance as it did when it was still inside the exocarp of the fruit prior to explosive discharge (review Figures 4.71 and 4.72). However, the cells of the embryonic protoderm found above the radicular apex had now become highly vacuolate (Figure 4.76), despite the fact that these cells had been cytoplasm-rich throughout all previous stages of embryonic development (review Figures 4.62, 4.65, and 4.71). In addition, the entire endosperm of a discharged pseudoseed had contracted so that the endosperm had lost some length and gained some width (Figure 4.76). Moreover, the endosperm tissue also appeared to possess more intercellular spaces (Figure 4.76), especially in the region of the Type 2 endosperm cells (review Figures 4.59, 4.61, and 4.64). The cells near the base of the endosperm representing the vacuolate Type 1 cells (review Figures 4.59, 4.61, and 4.64), now appeared to be filled with a brown (unstained), tannin-like material (Figure 4.76). The rudimentary cotyledons of the rudimentary shoot apex were just out of the plane of section in Figure 4.76. Changes in the viscin cells will be discussed in Chapter Five.

22C. Viability of the discharged pseudoseed components

Figure 4.77 depicts a representative discharged pseudoseed containing an embryo that had stained red in the presence of 2, 3, 5-triphenyl tetrazolium chloride (2, 3, 5-TTC). The red staining implied viability and thus this embryo would have been deemed viable. 8, 8, and 10 out of 15 pseudoseeds removed from cheesecloth wraps collected

during the fourth week in August (August 25) during the second week of September, (September 9), and during the first week of October (October 1), respectively, had embryos that stained red with 2, 3, 5-TTC. The germination potentials for the 15 pseudoseeds from each cheesecloth wrap collection time were thus 53%, 53%, and 67%, respectively. The germination potential was relatively high and consistent, as there was no significant difference among the three values. The overall, cumulative germination potential was 27 out of 45, and the average germination potential was 58% plus or minus 2%.

The other components of the pseudoseeds aside from the embryo were qualitatively evaluated for viability in the presence of 2, 3, 5-TTC. The viscin cells had a faint red tinge after staining, so it was possible that certain constituents of these cells were viable (Figure 4.77). The tannin-filled pseudoseed coat cells were not red stained and thus were deemed nonviable. Only the upper portion of the endosperm in the regions that were adjacent to the embryo were red stained (Figure 4.77), and thus only Type 2 endosperm cells were potentially viable (review Figures 4.59, 4.61, 4.64 and 4.76). Due to the dissection process, cells in the cap could not be readily observed in the discharged pseudoseed, and thus the viability of the cap cells in the discharged pseudoseed was not determined (Figure 4.77). However, cap cells examined with 2, 3, 5-TTC in whole fruits appeared to stain faintly red (not shown), even after they became crushed by the elongating embryo circa August 20 (review Figures 4.71 and 4.72). There were no changes in the results regarding the viability of the various pseudoseed components over three cheesecloth wrap collection times in August, September and October at the end of the second summer of development.

Figure 4.1 Figure 4.1 is a macro lens photograph of the female inflorescences of *Arceuthobium americanum* as they would appear on jack pine (*Pinus banksiana*) in mid April of the first spring of development (circa April 14), prior to the onset of megasporogenesis. The inflorescences were essentially racemes of three-flowered cymes (encircled). A cup-like bract (br) enveloped each cyme. Occasionally, a member of the cyme remained vegetative and elongated into a vegetative shoot segment (vs). Exudate was seen on the stigmas (arrowheads). Aside from a loss of the exudate, young female flowers maintained this appearance throughout the process of megasporogenesis into the period immediately following double fertilization. 1 cm scale bar = 2 mm.

Figures 4.2a, 4.2b, and 4.2c Figures 4.2a, 4.2b, and 4.2c are computer-assisted drawings of a cyme and the female flowers seen in Figure 4.1. The location of the stigma (s) is shown in all Figures 4.2a, 4.2b, and 4.2c.

Figure 4.2a depicts how the three flowers of a cyme, each seen in side view, were aligned via their flattened faces and enveloped by the bract (br). The terminal flower (ter) was flanked on either side by a lateral flower (lat).

Figure 4.2b depicts a single female flower seen in a median face view section. The two tepals (te), which can only be effectively seen in face view, are shown. Also, the relative positions of the placental-nucellar complex (PNC) within the ovarian loculus, the ovarian tissues (ov), and the two vascular traces apparently comprised solely of xylem tissue (x) are indicated. The location of the pedicel (p), which would typically be obscured by the bract, is shown.

Figure 4.2c depicts a single female flower seen in side view. The location of the pedicel (p), which would be typically obscured by the bract, is given. 1 cm scale bar = 200 μm.

Figure 4.3 Figure 4.3 is a light micrograph depicting a near median longitudinal face view section of a female flower at the same stage of development as seen in Figures 4.1 and 4.2. The relative positions of the stigma (s), pedicel (p), and 2 tepals (te) are given. The PNC occupied the entire cavity of the ovarian loculus within the ovarian tissues of the carpel (ov). Two vascular traces, each apparently comprised solely of xylem tissue (x), were embedded in the ovarian tissue and flanked the PNC on either side. The xylem appeared to be primarily represented by vessel elements (not specifically indicated) that had an empty appearance and that possessed helical secondary wall thickenings. The cell walls of the xylem vessel elements stained purplish. The majority of the sterile PNC cells possessed fairly dense cytoplasm (small closed arrowhead), although some near the base and periphery of the PNC were more vacuolate (large open arrowhead). The two megasporocytes are out of the plane of section. Stain = CV. 1 cm scale bar = 100 μm.

Figure 4.4 Figure 4.4 is a light micrograph depicting a median longitudinal face view section of a female flower at the same stage of development as seen in Figures 4.1, 4.2, and 4.3. A large arrow points in the direction of the stigma. Regions distal to the pedicel were deemed to be morphologically higher than regions proximal to the pedicel. Two megasporocytes (m) were visible in the hypodermal layer of the PNC. The epidermis (ep) of the PNC was the only layer of sterile PNC cells that separated the megasporocytes from the surrounding ovarian tissue (ov). The two megasporocytes were obliquely oriented relative to the long axis of the PNC. The upper (u) and lower (l) pole as well as the upper side (us) and lower side (ls) of each megasporocyte is designated. A large nucleus (arrowhead) was present at the lower pole of each megasporocyte. The nuclei appeared to be in prophase I of meiosis as the nuclei lacked nucleoli, the nuclear envelopes were not completely intact, and the chromosomal material was highly condensed. The pedicel (p) and one tepal (te) are visible. Stain = CV. 1 cm scale bar = 40 μm.


br
vs
4.1

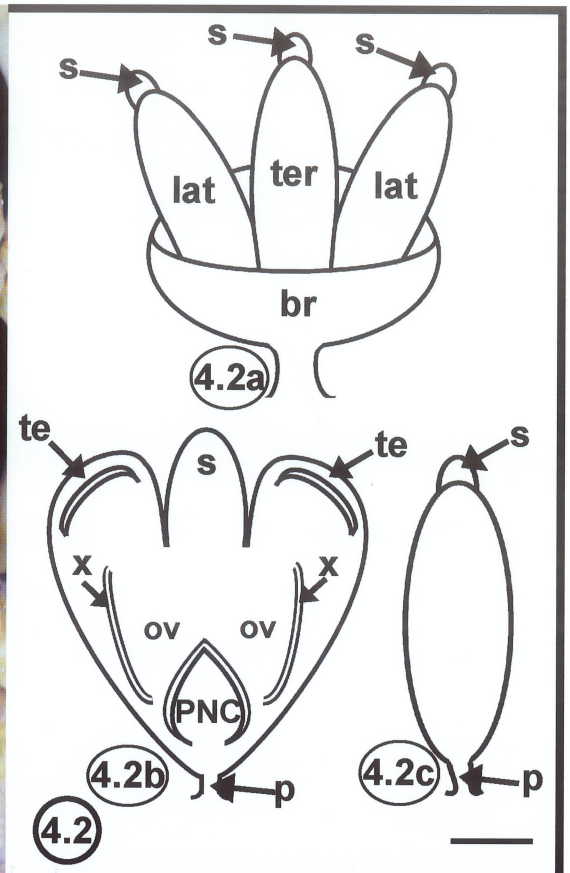
s
s
s
lat
ter
lat
br
4.2a
te
s
te
x
x
ov
ov
PNC
4.2b
p
s
4.2c
p
4.2

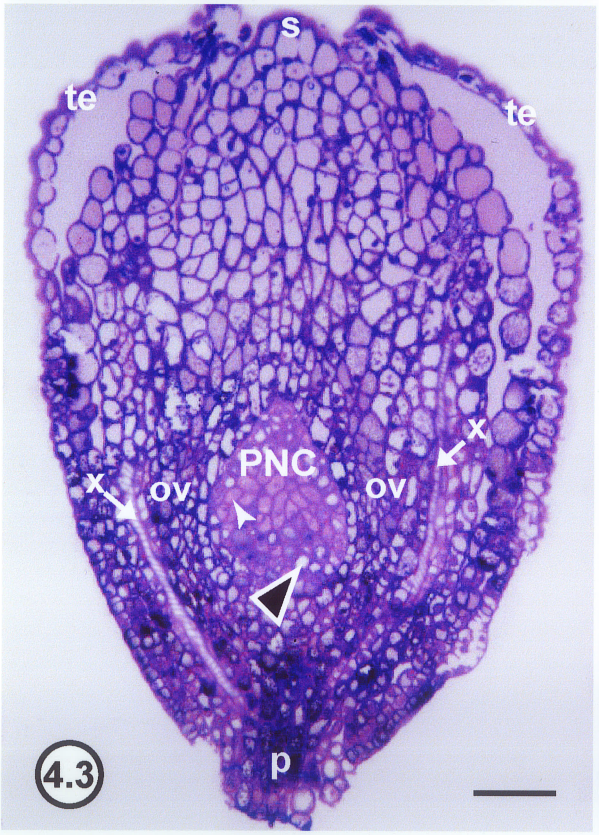
s
te
te
PNC
x
x
ov
ov
p
4.3

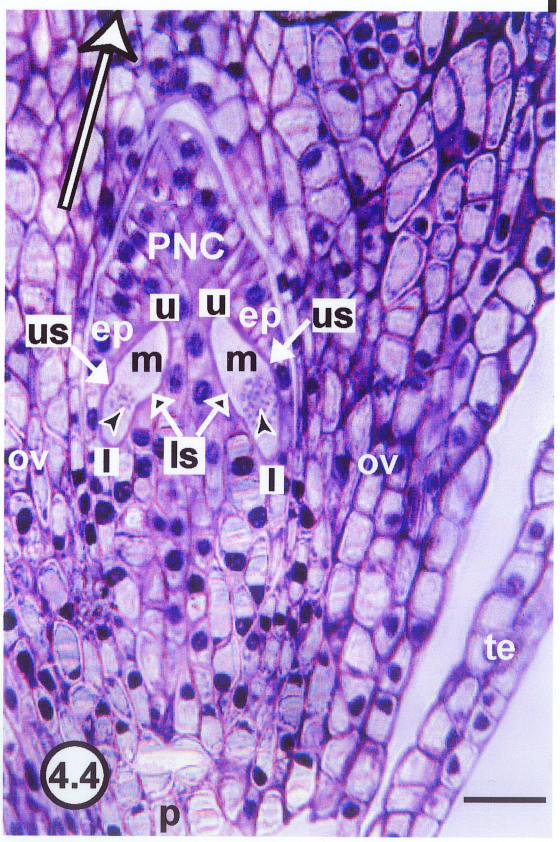
PNC
u
u
ep
us
us
ep
m
m
ov
l
ls
l
ov
te
4.4
p

For the remaining Figures 4.5 through 4.77, as in Figure 4.4, the large unlabeled arrow points in the direction of the stigma, as the stigma represents the morphologically highest region in the flower and fruit. The location of the upper (u) and lower poles (l) of the megasporocyte, dyad, or embryo sac (if present) can be easily derived from the large arrow. Where necessary, the orienting symbols and topography outlined in Figure 4.4 will be used for the remaining Figures 4.5 through 4.77: ep = epidermis, ov = ovarian tissue, ls = lower side, and us = upper side.

Figure 4.5 Figure 4.5 is a light micrograph of a median longitudinal face view section of a female flower sampled in early May of the first spring (circa May 4). Each megasporocyte had undergone meiosis I and cytokinesis, but not meiosis II. Visible within the hypodermal layer of the PNC, just underneath the epidermis (ep) of the PNC, were an upper dyad (ud) and a lower dyad (ld) derived from one of the two megasporocytes as seen in Figure 4.4. The cell wall (cw) that separated the upper dyad from the lower dyad was transversely oriented relative to the long axis of the original megasporocyte. The nucleus (n) in the upper dyad lacked a nucleolus and discrete nuclear envelope. The nucleus (n) in the lower dyad was dark and degenerating. Some of the vacuoles (v) in the vacuolate sterile PNC cells had become lined with a darkly stained tannin-like material (t). Stain = CV. 1 cm scale bar = 12 μm.

Figure 4.6 Figure 4.6 is a light micrograph of a median longitudinal face view section of a female flower sampled in mid May of the first spring (circa May 17). The functional megaspore and nonfunctional dyad from both megasporocytes could be seen in Figure 4.6. Meiosis II without cytokinesis had occurred in each upper dyad forming a binucleate functional megaspore (fm) (one per megasporocyte). Meiosis II did not occur in the lower dyad, which represented a uninucleate nonfunctional dyad (nfd) (one per megasporocyte). Arrowheads indicate the two nuclei in each functional megaspore. The epidermis (ep) of the PNC separated each functional megaspore and nonfunctional dyad from the ovarian tissue (ov). Stain = CV. 1 cm scale bar = 50 μm.

Figure 4.7 Figure 4.7 is a light micrograph depicting a magnified view of one functional megaspore (fm) above a nonfunctional dyad (nfd) from Figure 4.6. The transverse cell wall (cw) that originated during meiosis I separated the functional megaspore and the nonfunctional dyad. The two nuclei (n) of a functional megaspore appeared to be fairly similar in size and relatively large. The nuclei possessed homogeneous nucleoplasm, distinct nucleoli (small closed arrowheads), and discrete nuclear envelopes (large open arrowheads). The nucleus (n) in the nonfunctional dyad was dark and degenerating. Vacuoles in sterile PNC cells were either lined with or completely filled with a tannin-like material (t). Stain = CV. 1 cm scale bar = 18 μm.

Figure 4.8 Figure 4.8 is a light micrograph depicting a magnified view of the other functional megaspore (fm) and nonfunctional dyad (nfd) from Figure 4.6. Observations are the same as for Figure 4.7, illustrating the similarity between the products of megasporogenesis from the two megasporocytes. cw = cell wall, n = nucleus, t = tannin-like material. Stain = CV. 1 cm scale bar = 18 μm.

Figure 4.9 Figure 4.9 is a light micrograph of a median longitudinal face view section of a female flower sampled in mid May of the first spring (circa May 17). Meiosis I and meiosis II were complete. Figure 4.9 depicts a case of anomalous monosporic megasporogenesis in which cytokinesis followed meiosis II in an upper dyad from one of the two megasporocytes. In this anomalous case, the two nuclei that resulted from meiosis II in the upper dyad became separated by a transverse cell wall (cw), resulting in the formation of two uninucleate megaspores (ms) instead of a single binucleate functional megaspore. The degenerating, uninucleate nonfunctional dyad (nfd) was found below the two uninucleate megaspores. A nucleus (n) was seen in the lower of the two megaspores. The nucleus possessed a prominent nucleolus (small closed arrowhead) and a discrete nuclear envelope (large open arrowhead). Tannin-like material (t) was observed in the vacuoles of sterile PNC cells. Stain = CV. 1 cm scale bar = 25 μm.

Figure 4.10 Figure 4.10 is a light micrograph of a median longitudinal face view section of a female flower and is serial to the section depicted in Figure 4.9. Observations were as in Figure 4.9, but in Figure 4.10, a nucleus (n) was seen in the upper of the two megaspores (ms). Like the nucleus in the lower megaspore seen in Figure 4.9, the nucleus in the upper megaspore in Figure 4.10 possessed a prominent nucleolus (small closed arrowhead) and a discrete nuclear envelope (large open arrowhead). cw = cell wall, nfd = nonfunctional dyad, t = tannin-like material. Stain = CV. 1 cm scale bar = 25 μm.

Figure 4.11 Figure 4.11 is a fluorescence micrograph of a median longitudinal face view section of a female flower at a similar stage of development as seen in Figures 4.6, 4.7, and 4.8. This section was subjected to aniline blue fluorescence microscopy. Typical bisporic development had taken place in both megasporocytes, and the functional megaspore and nonfunctional dyad from each megasporocyte could be seen below the epidermis (ep) of the PNC. Pale blue fluorescence could be observed in the bounding cell walls of each functional megaspore (fm) and each nonfunctional dyad (nfd), indicating the presence of callose in these cell walls. The pale blue fluorescence was particularly effulgent in the lower side of each functional megaspore and in all the visible cell walls of each nonfunctional dyad. No notable fluorescence was detected in the cell walls of the PNC or the ovarian tissue (ov) except at pinpoints in the cell wall (arrowheads). Also, pale blue fluorescence was detected in the region of the style (st), as well as at the base of each nonfunctional dyad. This strong pale blue fluorescence was associated with the callosic cell walls of pollen tubes (pt). Stain = aniline blue. 1 cm scale bar = 50 μm.

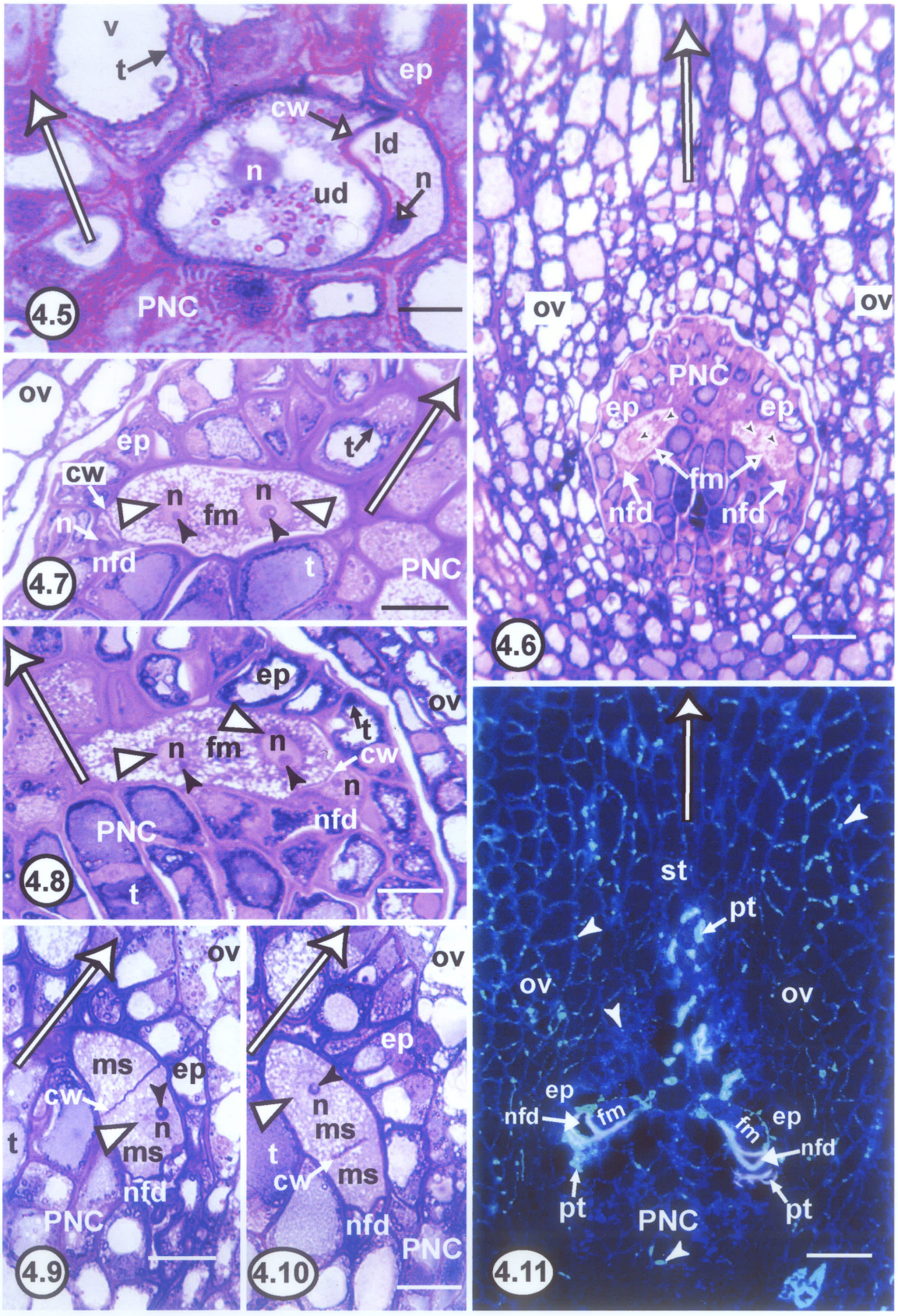
v
t
ep
cw
ld
n
ud
n
4.5
PNC
ov
ov
PNC
ep
ep
fm
nfd
nfd
4.6
ov
ep
t
cw
n
n
fm
n
nfd
t
4.7
PNC
ep
ov
t
n
fm
n
cw
n
nfd
PNC
4.8
t
st
pt
ov
ov
ms
ep
cw
n
t
ms
nfd
PNC
4.9
ov
ep
n
ms
t
cw
ms
nfd
PNC
4.10
ep
nfd
fm
fm
ep
nfd
pt
pt
PNC
4.11

Figure 4.12 Figure 4.12 is a light micrograph depicting a near median longitudinal face view section of a female flower sampled from late May in the first spring of development (circa May 25). A mature, unfertilized seven-celled embryo sac was evident in the PNC, below the epidermis (ep) of the PNC. All seven cells shared a common cell wall with the embryo sac wall (esw). The seven cells of the embryo sac included: three antipodals (A) at the upper pole of the embryo sac; the egg cell (E), persistent synergid (PS), and degenerating synergid (DS) at the lower pole of the embryo sac; and the unfertilized central cell (UCC) residing in the centre of the embryo sac. The two synergids and egg cell constituted the egg apparatus. The base of the egg cell was attached to the upper side of the embryo sac at the lower pole, and the two synergids occupied the rest of the embryo sac wall boundary at the lower pole. The bases of the two synergids, however, were primarily attached to the embryo sac wall the lowest position in the embryo sac. The persistent synergid shared an interface with the lower side of the embryo sac, whereas the degenerating synergid shared an interface with the upper side of the embryo sac. The majority of the degenerating synergid was out of the plane of section. A portion of the filiform apparatus (fa) was visible as a thickening of the embryo sac wall at the persistent synergid. The antipodals and the synergids possessed fairly darkly stained cytoplasm and generally appeared similar. However, the degenerating synergid cytoplasm was slightly more darkly stained than the persistent synergid cytoplasm. A large vacuole (v) was seen in the pear-shaped egg cell, adjacent to the unfertilized central cell. Large vacuoles could also be seen in the unfertilized central cell. A nucleus (arrowhead) could be seen within each of the seven cells except for the egg cell (the egg cell nucleus was out of the plane of section here; it was captured in Figure 4.18). The nuclei in the antipodals and synergids appeared similar to each other and were fairly darkly stained, although the nucleus in the degenerating synergid was not very distinct. The nucleus in the unfertilized central cell represented the fusion nucleus, and it was seen close to the vacuolate end of the egg cell at the lower pole of the embryo sac. A second, degenerating embryo sac (des) was also observed in the PNC where there originally was a second functional megaspore (and megasporocyte). The nonfunctional dyad (nfd) was seen below the lower pole of the embryo sac. Stain = CV. 1 cm scale bar = 15 μm.

Figure 4.13 Figure 4.13 is a computer-assisted drawing of an unfertilized, mature seven-celled embryo sac, similar to that seen in Figure 4.12. This figure displays the spatial organization of the seven cells bounded by the embryo sac wall (esw). The three antipodals (A), seen at the upper pole of the embryo sac, shared common interfaces with the unfertilized central cell (UCC) and each other. The hatched interface of two antipodals indicates where the third antipodal would obscure the interface. The egg cell (E) and two synergids (SYa and SYb) were seen at the lower pole of the embryo sac. The unfertilized central cell was at a morphologically higher position than the egg cell. The three cells of the egg apparatus shared common interfaces with the unfertilized central cell and each other. The base of the egg cell was attached to the upper side of the embryo sac, and the two synergids occupied the rest of the embryo sac wall boundary at the lower pole. The bases of the two synergids, however, were primarily attached to the embryo sac wall at the lowest position in the embryo sac. Thus, the egg was located above and to the side of the two synergids. As either the persistent or the degenerating synergid could occupy either synergid position, no distinction has been made between the two synergids. The hatched interface of the two synergids indicates where the egg cell would obscure the interface. The filiform apparatus (fa), located at the interface of the two synergids at the embryo sac wall, is indicated. The unfertilized central cell (UCC) occupied the central region of the embryo sac. The relative positioning of each nucleus (n) within the seven cells is given, and the hatched portion of a nucleus indicates where another cell would obscure that portion of the nucleus. The egg nucleus was closer to the embryo sac wall at the lower pole of the embryo sac than either synergid nucleus. Each dotted line (labeled 16a and 16b) cross-sections the egg apparatus, and the cross-sectional views are provided in Figures 4.16a and 4.16b. 1 cm scale bar = 7 μm.

Figure 4.14 Figure 4.14 is a fluorescence micrograph of a section serial to the section containing the unfertilized seven-celled embryo sac seen in Figure 4.12. In Figure 4.14, the embryo sac was subjected to Calcofluor fluorescence microscopy. The location of the seven cells is as was seen in Figure 4.12, although due to the serial sectioning, the base of the degenerating synergid was now out of the plane of section. Strong blue fluorescence was seen at the cell walls of the PNC, the nonfunctional dyad (nfd), and the embryo sac, indicating the presence of cellulosic and/or hemicellulosic cell wall material. Additionally, weak blue fluorescence was seen at the interface of the unfertilized central cell (UCC) with the three antipodals (A) (small closed arrowheads) as well as at the interfaces among the three antipodals (large closed arrowheads). The fluorescence indicated the presence of cellulosic and/or hemicellulosic cell wall material. Very weak blue fluorescence was seen at the interface of the egg cell (E) with the persistent synergid (PS) and at the interface of the egg cell with the degenerating synergid (DS) in the regions proximal to the lower pole of the embryo sac (large open arrowheads). The fluorescence at these interfaces became attenuated in the regions near the unfertilized central cell, indicating that the cell wall material was scantier in these regions. No fluorescence was detectable at the interface of the unfertilized central cell with the three cells of the egg apparatus. Very strong fluorescence was seen at the filiform apparatus (fa). Stain = Calcofluor. 1 cm scale bar = 12 μm.

Figure 4.15 Figure 4.15 is an electron micrograph depicting a section of the lower pole of an unfertilized mature seven-celled embryo sac at approximately the same stage of development as seen in Figures 4.12, 4.13, and 4.14. The degenerating synergid (DS), egg cell (E), persistent synergid (PS), and unfertilized central cell (UCC) were visible in the embryo sac. The arrangement of the egg apparatus was as in Figure 4.13. Note that the degenerating synergid shared an interface with the lower side of the embryo sac and the persistent synergid shared an interface with the upper side of the embryo sac (compare to Figure 4.12 in which the two synergids have the opposite arrangement). The majority of the persistent synergid and the filiform apparatus (fa) were out of the plane of section. Electron opaque deposits (*) were seen at the interface of the unfertilized central cell with the three cells of the egg apparatus. A large vacuole (v) was seen in the egg cell in a region close to the unfertilized central cell, distal to the embryo sac wall at the lower pole of the embryo sac. The majority of the egg cell cytoplasm was confined to regions proximal to the lower pole of the embryo sac. The persistent synergid cytoplasm was fairly darkly stained. The nucleus (n) of the persistent synergid possessed a distinct nucleolus (nl), a discrete nuclear envelope (ne), and condensed chromosomal material (ch). Small vacuoles (v) could be seen in both the persistent synergid and the egg cell cytoplasm. The degenerating synergid cytoplasm was darkly stained, although the degeneration was at a fairly early stage as membrane fragments could be observed. The remnants of the nucleus (n) and vacuolar ghosts (vg) could still be observed within the degenerating synergid. Starch grains (sg) were most notable in the degenerating synergid, although the amyloplast membranes had disintegrated. A large vacuole (v) was seen in the unfertilized central cell, whereas the scant cytoplasm of the central cell was confined to its periphery. The nonfunctional dyad (nfd) was also captured in partial section. ob = osmiophilic body. Stain = UA/LC. 1 cm scale bar = 3 μm.

Figures 4.16a and 4.16b Figures 4.16a and 4.16b are computer-assisted drawings of the three cells an egg apparatus from an unfertilized embryo sac at the same stage of development as seen in Figures 4.12, 4.13, 4.14, and 4.15. In both 4.16a and 4.16b, the egg apparatus depicted in Figure 4.13 is seen in cross section, and in both 4.16a and 4.16b, the hatched interface of the two synergids indicates where the egg cell in Figure 4.13 obscured the interface.

Figure 4.16a cross-sections the egg apparatus along the dotted line labeled 16a in Figure 4.13, and captures the portion of the egg apparatus that lies in the vicinity of the unfertilized central cell. The egg cell (E) and the two synergids (SYa and SYb) shared common interfaces with each other and the embryo sac wall (esw). The two synergid nuclei (n), which were found in the vicinity of the central cell, were captured in cross section 16a. The hatched portion of each nucleus indicates where those portions of the nuclei were obscured by the egg cell in Figure 4.13.

Figure 4.16b cross-sections the egg apparatus along the dotted line labeled 16b in Figure 4.13, and captures the portion of the egg apparatus that lies in the vicinity of the embryo sac wall near the lower pole of the embryo sac. The egg cell is seen attached to the upper side of the embryo sac. The egg nucleus, which was found in the vicinity embryo sac wall at the lower pole of the embryo sac, was captured in cross section 16b. 1 cm scale bar = 5 μm.

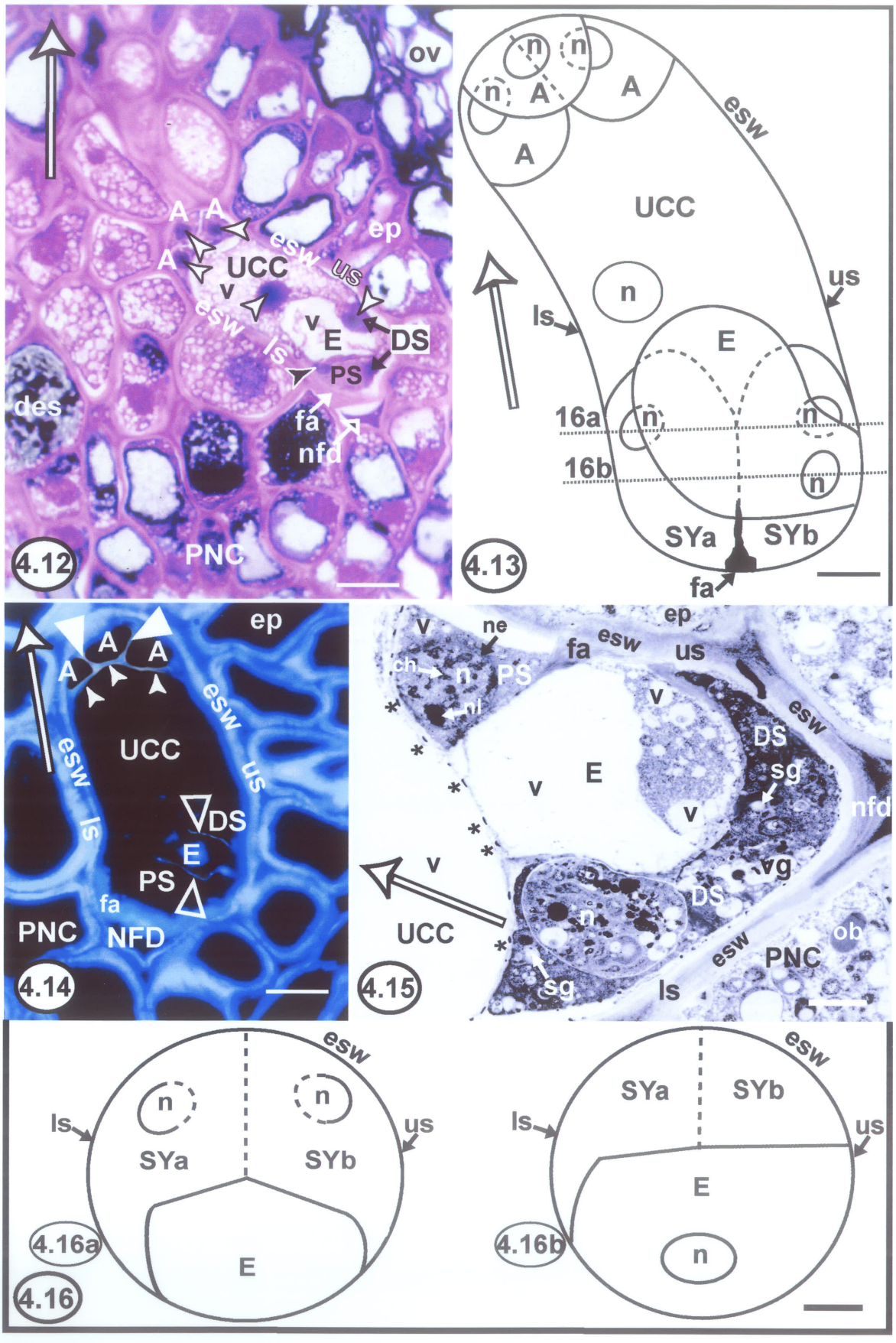
ov
A
A
esw
ep
A
UCC
us
v
esw
v
E
DS
ls
PS
des
fa
nfd
4.12
PNC
n
n
n
A
A
A
esw
UCC
n
us
ls
E
16a
n
n
16b
n
SYa
SYb
fa
4.13
ep
A
A
A
esw
esw
UCC
us
ls
DS
E
PS
fa
PNC
NFD
4.14
v
ne
ep
fa
esw
us
ch
n
PS
nl
v
esw
DS
sg
E
v
v
nfd
v
vg
UCC
DS
n
ob
esw
PNC
sg
ls
4.15
esw
n
n
ls
us
SYa
SYb
E
4.16a
4.16
esw
SYa
SYb
ls
us
E
n
4.16b

Figure 4.17 Figure 4.17 is an electron micrograph depicting a section of the lower pole of an unfertilized mature seven-celled embryo sac at approximately the same stage of development as seen in Figures 4.12, 4.13, 4.14, 4.15, and 4.16. The egg cell (E), persistent synergid (PS), degenerating synergid (DS), and unfertilized central cell (UCC) were visible in the embryo sac. The arrangement of the egg apparatus is as was seen in Figure 4.13, and the synergids were positioned as in Figure 4.12. The majority of the degenerating synergid was out of the plane of section. The filiform apparatus (fa) could be seen as a thickening of the wall between the two synergids at the embryo sac wall. Electron opaque deposits (*) were seen at the interface of the unfertilized central cell and the cells of the egg apparatus. Figure 4.17 highlights the persistent synergid, its nucleus, and the positioning of the nucleus. The nucleus (n) of the persistent synergid was found in close proximity to the unfertilized central cell, and possessed a distinct nucleolus (nl), a discrete nuclear envelope (ne), and condensed chromosomal material (ch). Small vacuoles (v) could be seen in the persistent synergid cytoplasm and as well as the egg cell cytoplasm. Osmiophilic bodies (ob) were seen in the persistent synergid cytoplasm, the egg cell cytoplasm, and the unfertilized central cell cytoplasm. A large vacuole (v) was seen in the unfertilized central cell, and its cytoplasm was confined to the periphery. Small vacuoles (v) in the central cell cytoplasm were confluent with the large vacuole. A large vacuole (v) was seen in the egg cell adjacent to the central cell. A small portion of a nucleus (n) could be seen in the egg cell. The degenerating synergid cytoplasm was very dark. The lack of membrane fragments within the degenerating synergid suggested that it was at a slightly later stage of degeneration than seen in Figure 4.15. Stain = UA/LC. 1 cm scale bar = 3 μm.

Figure 4.18 Figure 4.18 is an electron micrograph depicting a serial section to the portion of an unfertilized mature seven-celled embryo sac and egg apparatus at the lower pole of the embryo sac as seen in Figure 4.17. The observations in Figure 4.18 are similar to those in Figure 4.17, although Figure 4.18 features the egg cell (E), its nucleus (n), and the positioning of its nucleus. In the egg cell, the large vacuole (v) was seen at a position adjacent to the unfertilized central cell (UCC). The egg cell nucleus (n) was found at a region proximal to the lower pole of the embryo sac. The egg cell nucleus possessed a distinct nucleolus (nl), a discrete nuclear envelope (ne), and condensed chromosomal material (ch). The egg cell cytoplasm was confined to regions proximal to the lower pole of the embryo sac, to the perinuclear regions, and to the periphery of the egg cell. In the persistent synergid, n = nucleus, ch = chromosomal material. Other abbreviations: * = electron opaque deposit, fa = filiform apparatus, ob = osmiophilic body, v = vacuole. 1 cm scale bar = 3 μm.

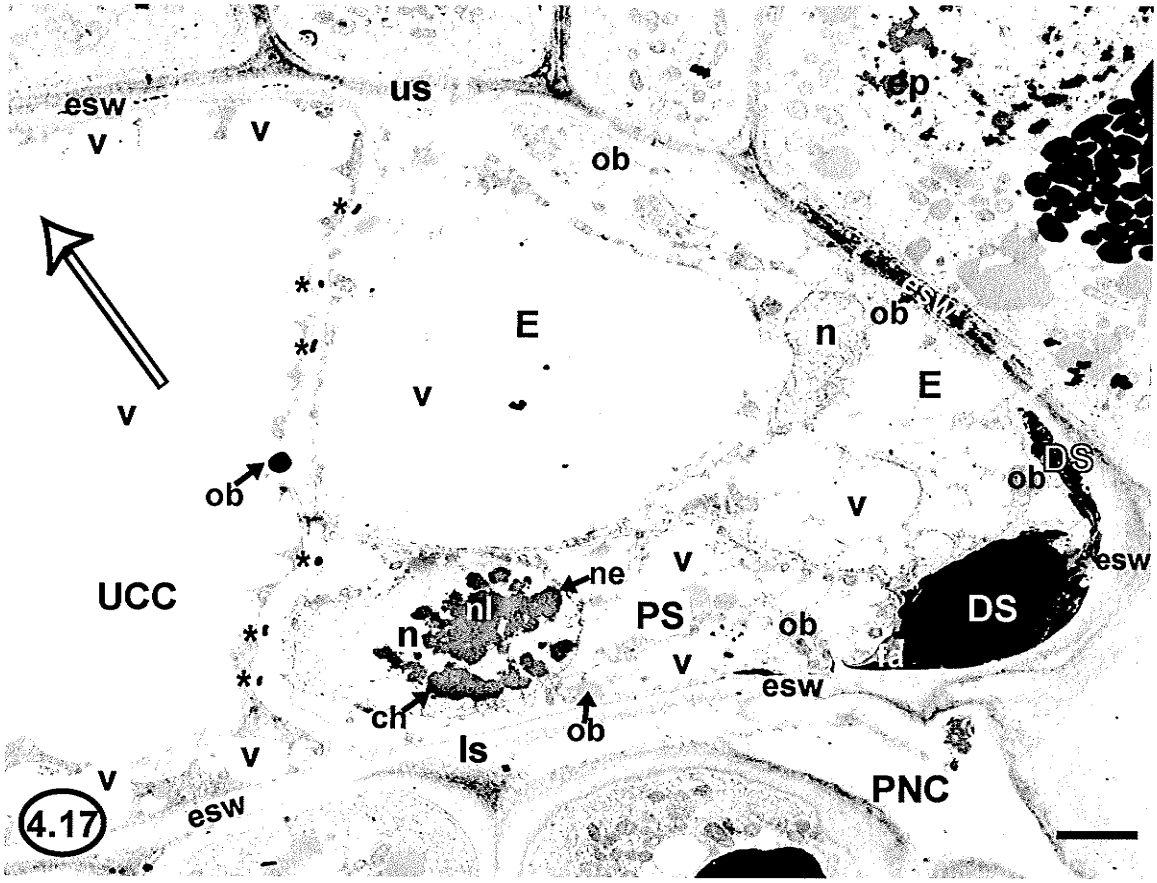
esw
us
ep
v
ob
E
n
DS
UCC
ne
nl
PS
ch
ls
PNC
4.17

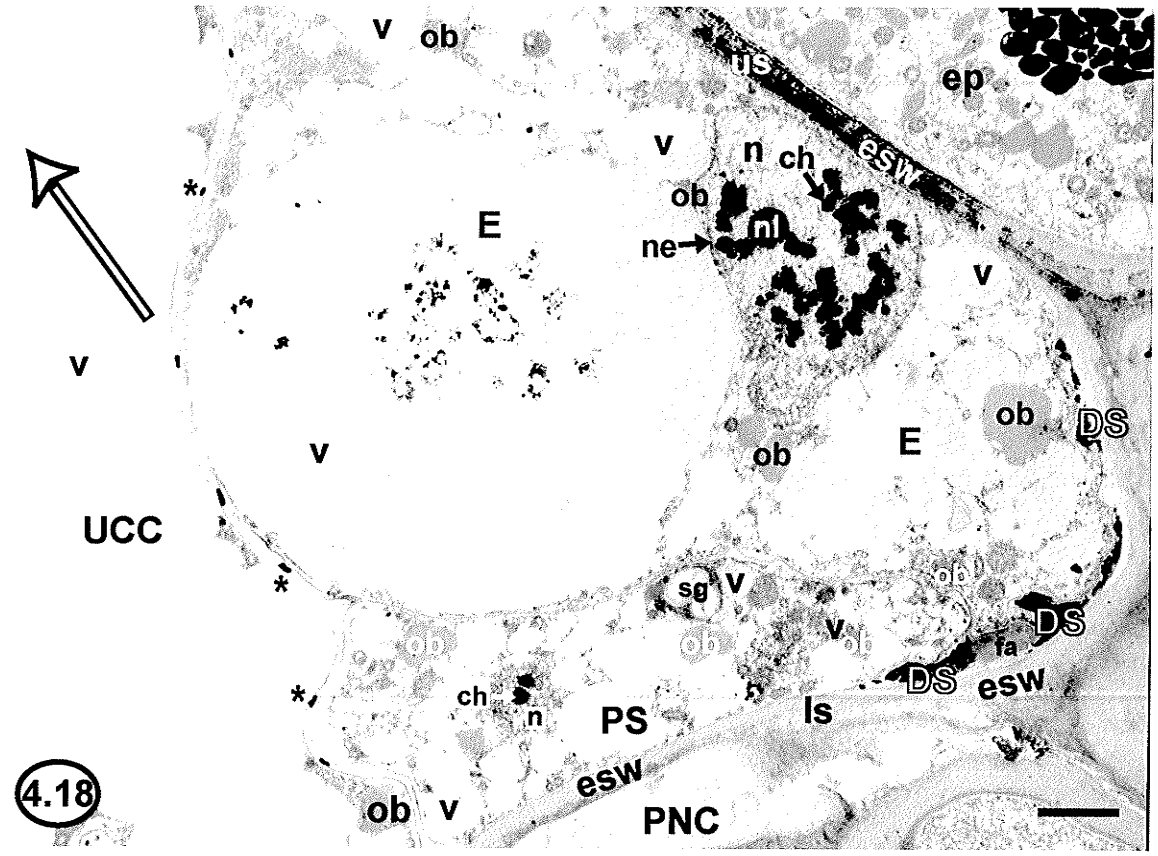
ls
ep
esw
ch
ne
nl
E
ob
DS
UCC
sg
fa
PS
n
PNC
4.18

Figure 4.19 Figure 4.19 is an electron micrograph depicting a magnified view of the egg apparatus seen in Figure 4.18, sampled from late May in the first spring of development (circa May 25). This particular figure highlights the interfaces of the egg cell (E) and the persistent synergid (PS) in the vicinity of the unfertilized central cell (UCC). Small closed arrowheads indicate the interface of the unfertilized central cell (UCC) with these two cells of the egg apparatus. Large open arrowheads indicate the interface of the egg cell with the persistent synergid in these upper regions. The degenerating synergid was not captured in this view. The unfertilized central cell was bounded by its plasma membrane (uccpm), as was the egg cell (epm), and the persistent synergid (pspm). The interface of the unfertilized central cell and the egg cell was a contact of the unfertilized central cell plasma membrane and the egg cell plasma membrane, and no cell wall material was present between the two membranes. However, electron opaque deposits (*) were found between the unfertilized central cell plasma membrane and the egg cell plasma membrane. Likewise, the interface of the unfertilized central cell and the persistent synergid was a contact of two plasma membranes. No cell wall material was present between these two membranes, although electron opaque deposits were. The interface of the egg cell with the persistent synergid in the vicinity of the unfertilized central cell (large open arrowheads) was primarily a contact of the egg cell plasma membrane with the persistent synergid plasma membrane. At this interface, some very scant cell wall material (!) could be observed, but no electron opaque deposits were seen. The degenerating synergid was not captured in these regions near the unfertilized central cell. However, serial sections showed that the degenerating synergid was no longer bounded by a plasma membrane, as the membrane had deteriorated, and thus the degenerating synergid boundary was represented by its cytoplasmic margin. Scant to negligible cell wall material was observed between the egg cell plasma membrane and the degenerating synergid cytoplasmic margin in the vicinity of the central cell; no electron opaque deposits were evident. Likewise, scant to negligible cell wall material was observed between the persistent synergid plasma membrane and the degenerating synergid cytoplasmic margin in the vicinity of the central cell; no electron opaque deposits were evident. ob = osmiophilic body. 1 cm scale bar = 1 μm.

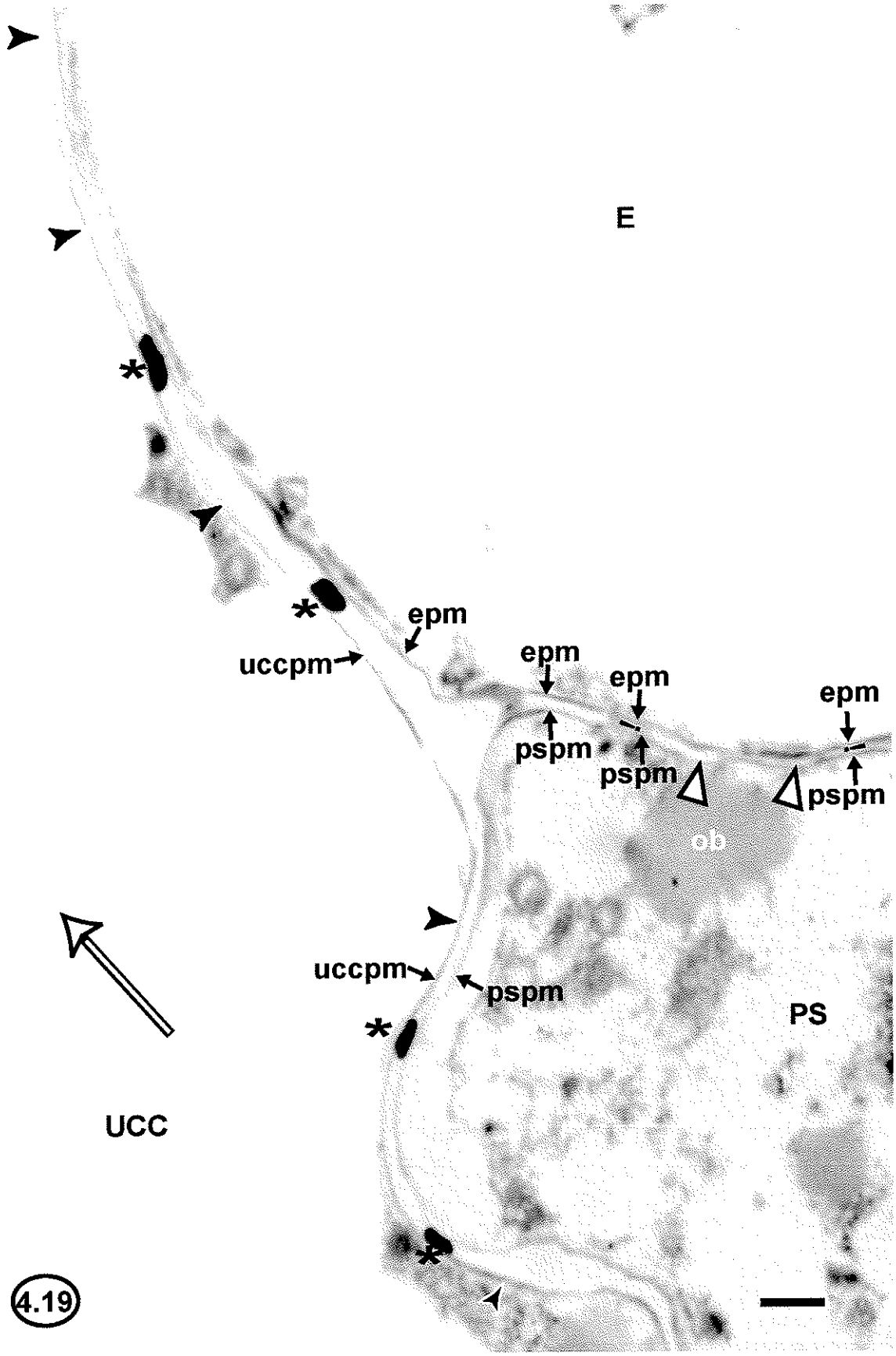

4.19

Figure 4.20 Figure 4.20 is an electron micrograph depicting a magnified view of the egg apparatus seen in Figure 4.18 and highlights the interfaces among the three cells of the egg apparatus in the regions near the lower pole of the embryo sac. The interface of the egg cell (E) with the persistent synergid (PS) is indicated by large open arrowheads; the interface of the egg cell with the degenerating synergid (DS) is indicated by small closed arrowheads; and the interface of the persistent synergid with the degenerating synergid is indicated by large closed arrowheads. The egg cell was bounded by its own plasma membrane (epm), as was the persistent synergid (pspm). The degenerating synergid boundary was represented by its cytoplasmic margin (dscm). Scant cell wall material (!) was present at the interfaces among the three cells of the egg apparatus. These interfaces in the regions proximal to the lower pole of the embryo sac contained more cell wall material than was observed at the regions distal to the lower pole of the embryo sac (seen in Figure 4.19). No electron opaque deposits were observed at the interfaces among the three cells of the egg apparatus. The filiform apparatus (fa) was present as a region where the cell wall material between the two synergids was particularly copious at the embryo sac wall, which was thickened. The filiform apparatus was mainly visible in the degenerating synergid, but a small portion of it was also caught in section within the persistent synergid. The filiform apparatus contorted the persistent synergid plasma membrane as well as the egg cell plasma membrane at the embryo sac wall where the three cells of the egg apparatus intersected with the embryo sac wall. Osmiophilic bodies (ob) and mitochondria (mt) were seen in both the egg cell cytoplasm and the persistent synergid cytoplasm, although they were found in greater abundance in the persistent synergid. Starch grains (sg) were observed only in the persistent synergid, and only rarely. The degenerating synergid cytoplasm was very dark. v = vacuole. 1 cm scale bar = 1 μm.

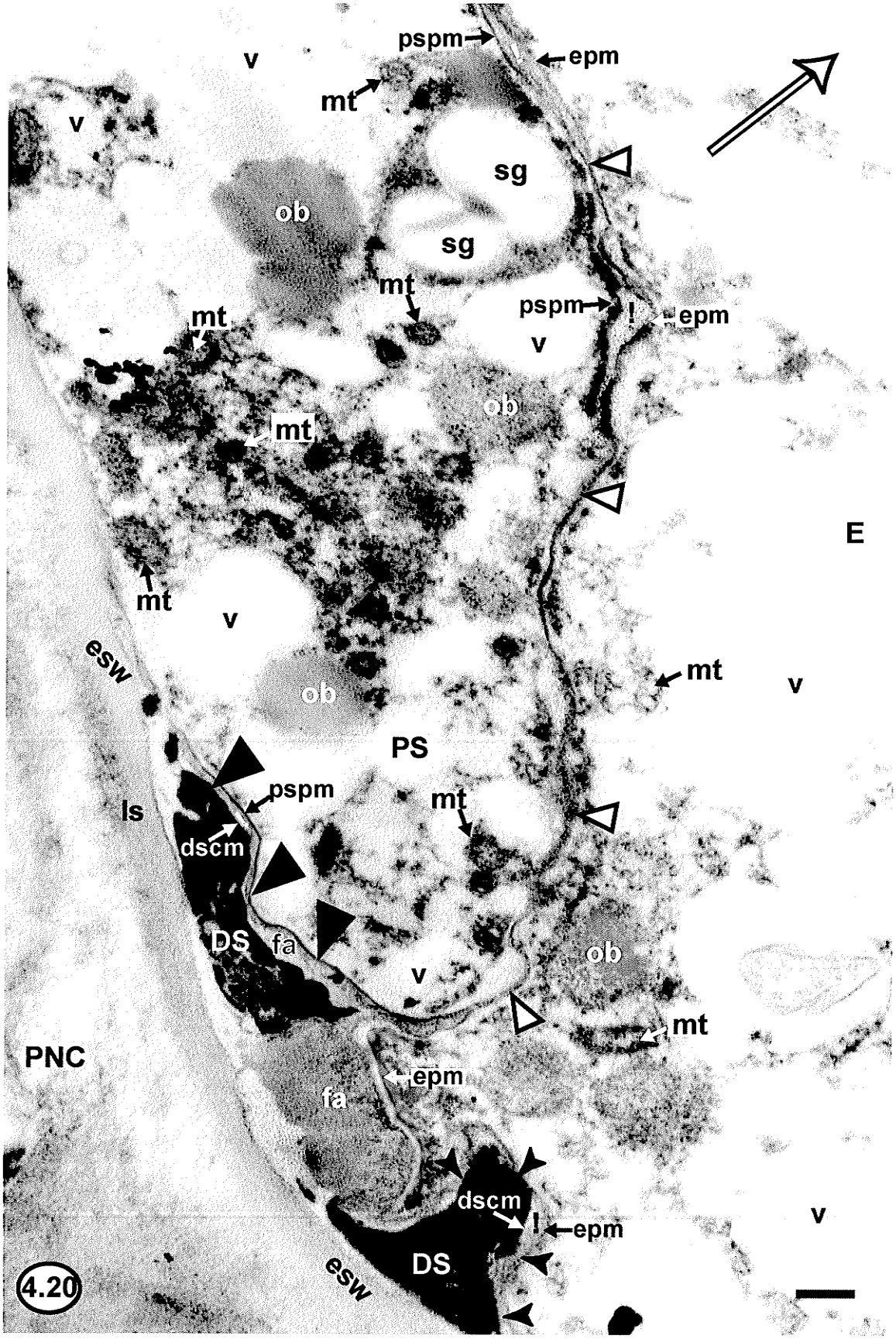
pspm
epm
v
mt
v
sg
ob
sg
mt
pspm
epm
mt
v
ob
mt
E
mt
v
esw
ob
mt
v
PS
pspm
mt
ls
dscm
DS
fa
v
ob
mt
PNC
epm
fa
dscm
epm
v
DS
esw
4.20

Figure 4.21 Figure 4.21 is an electron micrograph depicting a section of the lower pole of an unfertilized mature seven-celled embryo sac at approximately the same stage of development as seen in Figures 4.12 through 4.20. This figure features the two synergids. A lower portion of the persistent synergid (PS), a lower portion of the degenerating synergid (DS), and the unfertilized central cell (UCC) were visible. The egg cell and the filiform apparatus were out of the plane of section. Plasmolysis had occurred where the two synergids shared a common wall with the embryo sac. The persistent synergid was very cytoplasm-rich, and the cytoplasm was moderately darkly stained. It contained several small vacuoles (v) and osmiophilic bodies (ob). The degenerating synergid cytoplasm was very darkly stained. As in Figures 4.17, 4.18, and 4.20, the lack of membrane fragments within the degenerating synergid in Figure 4.21 suggested that it was at a slightly later stage of degeneration than seen in Figure 4.15. The organelles in the unfertilized central cell cytoplasm were particularly obvious in this figure. A large vacuole (v) was seen in the unfertilized central cell. The peripheral cytoplasm of the unfertilized central cell contained small vacuoles (v), osmiophilic bodies (ob), mitochondria (mt), and starch grains in amyloplasts (sg). * = electron opaque deposit. Stain = UA/LC. 1 cm scale bar = 2 μm.

Figure 4.22 Figure 4.22 is an electron micrograph depicting a section of the lower pole of an unfertilized mature seven-celled embryo sac. This embryo sac was at approximately the same stage of development as seen in Figures 4.12 though 4.21. As in Figure 4.21, the two synergids are featured. A lower portion of the persistent synergid (PS), a lower portion of the degenerating synergid (DS), and the unfertilized central cell (UCC) were visible (the egg cell was out of the plane of section). Some plasmolysis had occurred at the interface of the central cell and the persistent synergid. Of note, starch grains (sg) were seen in the darkly stained degenerating synergid cytoplasm. As in Figures 4.17, 4.18, 4.20, and 4.21, the degenerating synergid in Figure 4.22 was at a slightly later stage of degeneration than seen in Figure 4.15. * = electron opaque deposit, fa = filiform apparatus, mt = mitochondrion, ob = osmiophilic body, v = vacuole. Stain = UA/LC. 1 cm scale bar = 2 μm.

Figure 4.23 Figure 4.23 is an electron micrograph depicting a section of the lower pole of a mature seven-celled embryo sac. This embryo sac was at approximately the same stage of development as seen in Figures 4.12 through 4.22. Only the triangle-shaped degenerating synergid (DS) and the unfertilized central cell (UCC) were captured in the section. The interface at the unfertilized central cell and the degenerating synergid was a contact of unfertilized central cell plasma membrane (uccpm) with the degenerating synergid cytoplasmic margin (dscm). No detectable cell wall material was present at this interface, although electron opaque deposits (*) were seen at this interface. Mitochondria (mt) were observed in the unfertilized central cell peripheral cytoplasm. The degenerating synergid cytoplasm was very dark, although starch grains (sg) could still be seen. As in Figures 4.17, 4.18, 4.20, 4.21, and 4.22, the degenerating synergid in Figure 4.23 was at a slightly later stage of degeneration than seen in Figure 4.15. The degenerating nonfunctional dyad (nfd) could still be seen below the level of the degenerating synergid. This particular embryo sac may have just received a pollen tube (pt), as a spongiform cell wall, indicative of a pollen tube, could be seen between the embryo sac wall and the cytoplasmic margin of the degenerating synergid. v = vacuole. Stain = UA/LC. 1 cm scale bar = 1 μm.

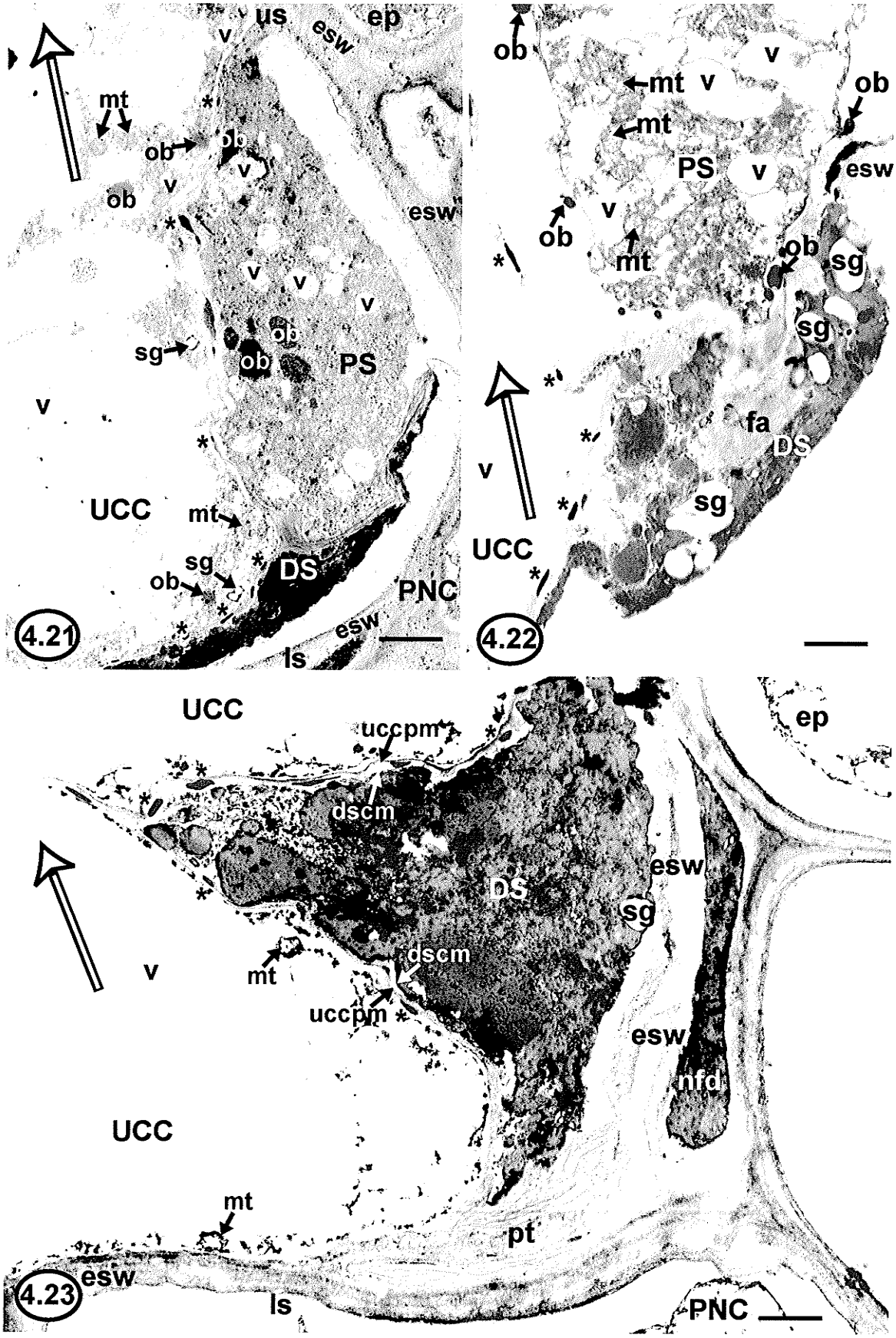
us
ep
esw
v
mt
ob
sg
PS
UCC
DS
PNC
ls
4.21
4.22
fa
uccpm
dscm
nfd
pt
4.23

Figure 4.24 Figure 4.24 is an electron micrograph depicting a section of the upper pole of an unfertilized mature seven-celled embryo sac. The embryo sac was at approximately the same stage of development as seen in Figures 4.12 through 4.23. The arrangement of the three oval- to triangle-shaped antipodals was as in Figures 4.12 and 4.13. Only two antipodals are visible, and only one of these two was in median section. Small closed arrowheads indicate the interface of the unfertilized central cell with the antipodals, and large open arrowheads indicate the interface between the two visible antipodals. Each antipodal was bounded by its plasma membrane (apm), as was the unfertilized central cell (uccpm). At the interface of the unfertilized central cell with the antipodals, cell wall material (!) and electron opaque deposits (*) were found between the unfertilized central cell plasma membrane and the antipodal plasma membranes. Similarly, at the interface between the two visible antipodals, cell wall material was found between the two antipodal plasma membranes. However, no electron opaque deposits were visible at the interface between the two visible antipodals. The cell wall material that partitioned the antipodals from each other and from the unfertilized central cell was uniform in thickness. A large vacuole (v) was seen in the unfertilized central cell. In the antipodals, a highly vacuolated (v) region was found adjacent to the unfertilized central cell. The majority of the antipodal cytoplasm along with the nucleus (n) was closer to the embryo sac wall at the upper pole of the embryo sac than to the unfertilized central cell. Antipodal cytoplasm was found in the perinuclear and peripheral regions. The antipodal nucleus possessed a particularly distinct nuclear envelope (ne) and moderately condensed chromosomal material (ch). The antipodal cytoplasm was dense with osmiophilic bodies (ob) and mitochondria (mt). Small vacuoles (v) were also found within the antipodal cytoplasm. Stain = UA/LC. 1 cm scale bar = 1.5 μm.

Figure 4.25 Figure 4.25 is an electron micrograph depicting a section containing a portion of the central cell within an unfertilized mature seven-celled embryo sac. The embryo sac was at approximately the same stage of development as seen in Figures 4.12 though 4.24. The direction of the lower pole (l) and the upper pole (u) is given. Some sterile PNC cells, including some in the epidermis (ep) of the PNC, were becoming crushed (arrowheads). The original embryo sac wall (esw), which was relatively thick, formed the major boundary of the central cell. There was, however, no evidence of transfer cell wall projections in the unfertilized central cell at the embryo sac wall. The central cell possessed a single fusion nucleus (n). The fusion nucleus was in closer proximity to the lower pole of the embryo sac (and the egg apparatus) than to the upper pole. Also, the fusion nucleus was in closer proximity to the lower side of the embryo sac than to the upper side. The fusion nucleus possessed a prominent nucleolus (nl), a distinct nuclear envelope (ne), a dense nucleoplasm, and moderately dispersed chromosomal material (ch). The unfertilized central cell was highly vacuolate and possessed very large vacuoles (v) that contained tannin-like debris (t) and threadlike materials (th). The central cell cytoplasm was found only as a thin layer along the periphery of the central cell and in a thin perinuclear layer; there was no difference in organelle content between the two regions of cytoplasm. The scant cytoplasm contained small vacuoles (v), starch grains (sg) and osmiophilic bodies (ob). Stain = UA/LC. 1 cm scale bar = 4 μm.

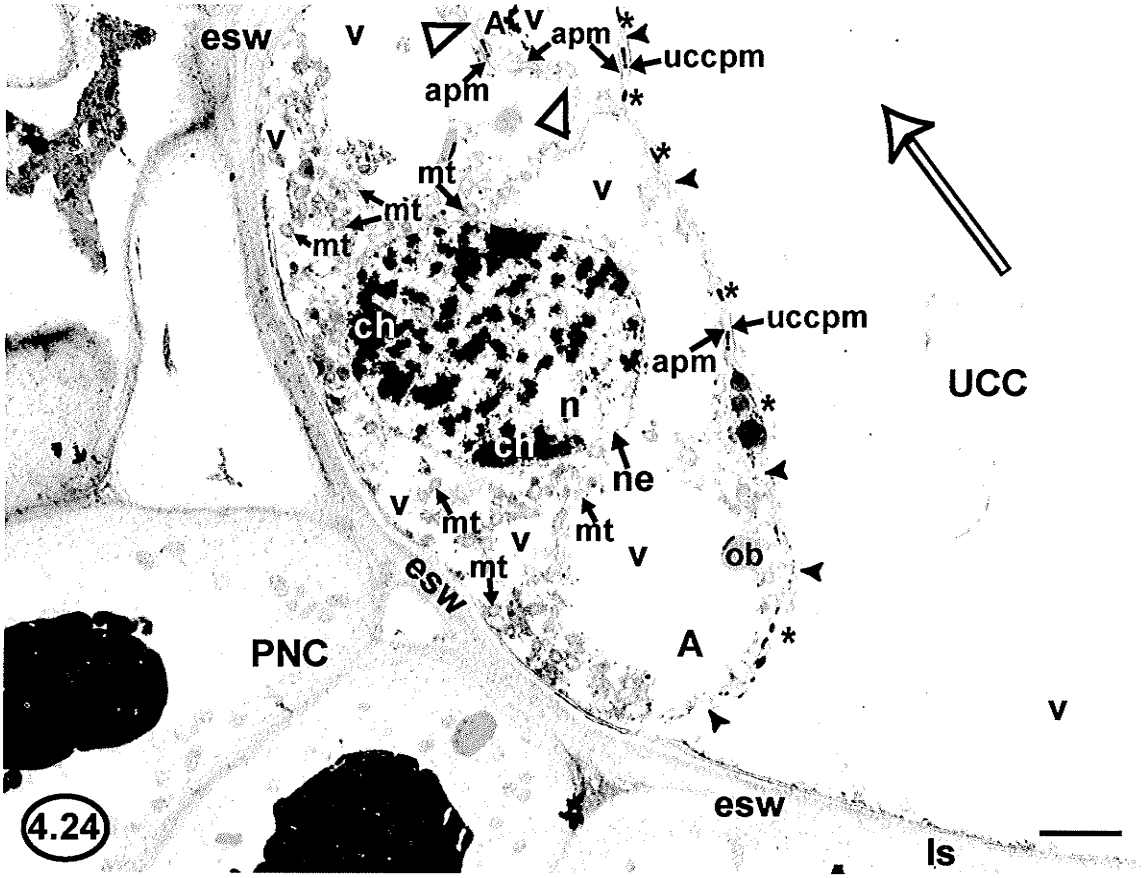
esw
v
A
v
apm
uccpm
apm
v
mt
mt
mt
v
ch
uccpm
apm
UCC
n
ne
ci
v
mt
v
mt
v
ob
esw
mt
PNC
A
v
esw
ls
4.24

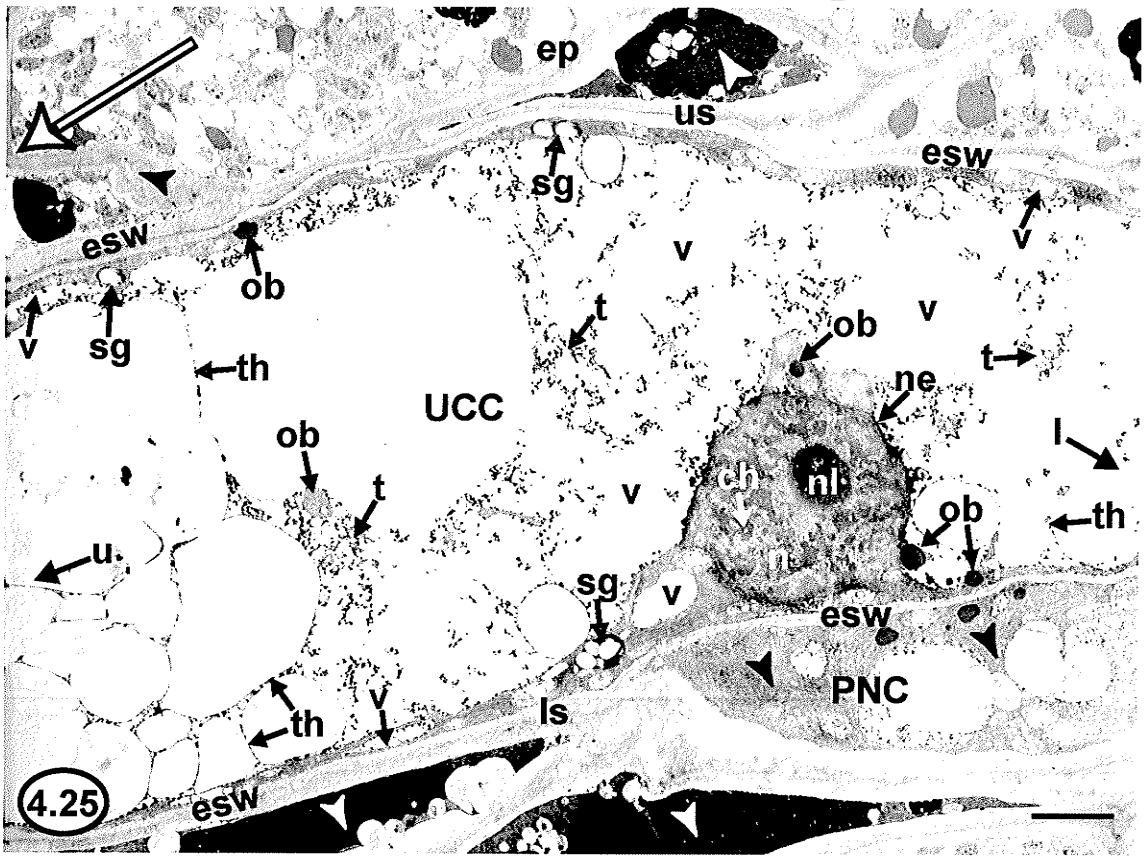
ep
us
sg
esw
esw
v
ob
v
sg
th
UCC
t
ob
v
t
ne
ob
t
u
v
cb
nl
ob
th
sg
v
esw
PNC
th
v
ls
esw
4.25

Figure 4.26 Figure 4.26 is a light micrograph depicting a near median longitudinal face view section of a female flower sampled from the end of May in the first spring of development (circa May 30). Double fertilization had occurred. A fertilized embryo sac was evident in the PNC, below the epidermis (ep) of the PNC. Only six of the seven cells of the fertilized embryo sac are visible in this section. The six visible cells were: three antipodals (A) at the upper pole of the embryo sac, the persistent synergid (PS) and the degenerating synergid (DS) at the lower pole of the embryo sac, and the fertilized central cell (FCC) residing in the centre of the embryo sac. The degenerating synergid shared an interface with the lower side of the embryo sac, whereas the persistent synergid shared an interface with the upper side of the embryo sac. The newly-formed zygote was out of the plane of section. Distinct cell walls partitioned the visible cells of the embryo sac. The filiform apparatus, however, was out of the plane of section. A nucleus (n) could be seen in two out of the three antipodals, in the persistent synergid, and in the fertilized central cell. All visible nuclei possessed discrete nuclear envelopes, distinct nucleoli, and dispersed chromosomal material. The nucleus within the fertilized central cell represented the primary endosperm nucleus. The fertilized central cell was basically non-vacuolate, although small vacuoles (v) could be seen. Small vacuoles could also be seen in the persistent synergid. The degenerating synergid possessed a darkly stained cytoplasm. esw = embryo sac wall, nfd = nonfunctional dyad. Stain = CV. 1 cm scale bar = 12 μm.

Figure 4.27 Figure 4.27 is a fluorescence micrograph of the same fertilized embryo sac that was seen in Figure 4.26. In Figure 4.27 the embryo sac was subjected to Calcofluor fluorescence microscopy. The location of the visible cells of the embryo sac is the same as in Figure 4.26. Strong blue fluorescence was seen at the cell walls of the PNC, the nonfunctional dyad (nfd), and the embryo sac. Additionally, blue fluorescence was seen at the interface of the fertilized central cell (FCC) with the three antipodals (A) (small closed arrowheads) as well as at the interfaces among the three antipodals (large open arrowheads). Also, blue fluorescence was seen at the interface of the fertilized central cell with the two synergids (small closed arrowheads), and at the interface between the two synergids (large open arrowhead). The filiform apparatus was out of the plane of section. DS = degenerating synergid, PS = persistent synergid. Stain = Calcofluor. 1 cm scale bar = 11.5 μm.

Figure 4.28 Figure 4.28 is an electron micrograph depicting a near median section of the lower pole of a fertilized seven-celled embryo sac at approximately the same stage of development as seen in Figures 4.26 and 4.27. The fertilized embryo sac was evident in the PNC, below the epidermis (ep) of the PNC. The zygote (Z), persistent synergid (PS), and fertilized central cell (FCC) were visible in the embryo sac. The three antipodals and the degenerating synergid were out of the plane of section. The zygote had a rounded-triangular appearance, was attached to the upper side of the embryo sac, and was found at a position that was above and to the side of the persistent synergid. The rounded persistent synergid shared an interface with the lower side of the embryo sac (compare to Figure 4.26 in which the degenerating synergid shared an interface with the lower side). The degenerating synergid, although not evident here, would have shared an interface with the upper side of the embryo sac, but it had become reduced as the zygote and persistent synergid enlarged. The interface of the fertilized central cell and the two visible cells of the fertilized egg apparatus is indicated by small closed arrowheads, and the interface between the zygote and the persistent synergid is indicated by large open arrowheads. Cell wall material had been deposited at these interfaces so that all partitioning cell walls were of uniform thickness and distinct. Aside from where the zygote shared a common cell wall with the upper side of the embryo sac, the cell walls bounding the zygote could be collectively referred to as the zygote wall. Electron opaque deposits were no longer visible at the interface of the fertilized central cell and cells of the egg apparatus (small closed arrowheads). The zygote and fertilized central had become less vacuolate than they had been prior to double fertilization, although many small vacuoles (v) could be observed in both cells. The zygote had lost the polarity of the large vacuole and cytoplasm that was evident prior to double fertilization. Following double fertilization, the persistent synergid remained cytoplasm-rich and darkly stained, although a few small vacuoles (v) could be seen. The persistent synergid contained a prominent nucleus (n), which possessed a very conspicuous nucleolus (nl), a distinct nuclear envelope (ne), and moderately dispersed chromosomal material (ch). The persistent synergid had lost the relative polarity of the nucleus, cytoplasm, and vacuoles that was evident prior to double fertilization, and the nucleus was found in a more central location. The amount of organelles had increased in the zygote, the persistent synergid, and the fertilized central cell following double fertilization. Mitochondria (mt) and starch grains in amyloplasts (sg) could be seen in the zygote, the persistent synergid, and the fertilized central cell, although these organelles were least frequent in the zygote. Notably, the fertilized central cell possessed peripheral clusters of mitochondria. Osmiophilic bodies (ob) were commonly observed in the zygote and the fertilized central cell, but they were relatively rare in the persistent synergid. The nonfunctional dyad (nfd) was visible below the lower pole of the fertilized embryo sac. fa = filiform apparatus. Stain = UA/LC. 1 cm scale bar = 5.5 μm.

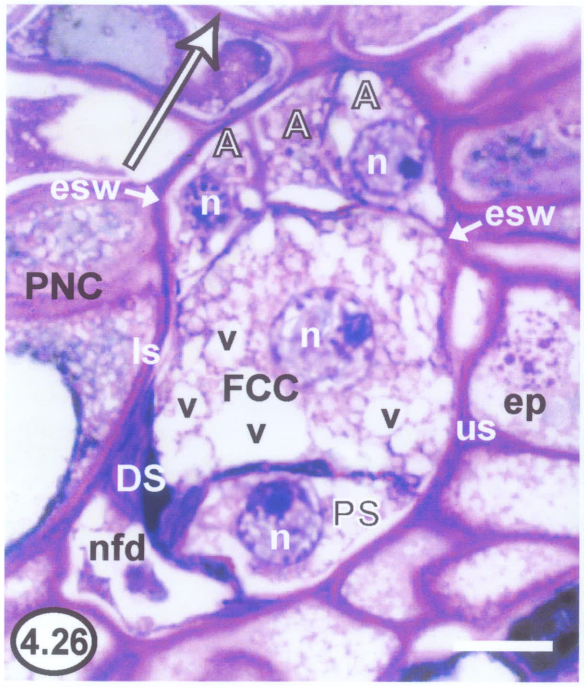
A
A
A
n
esw
n
esw
PNC
ls
v
n
v
FCC
v
v
ep
us
DS
PS
n
nfd
4.26

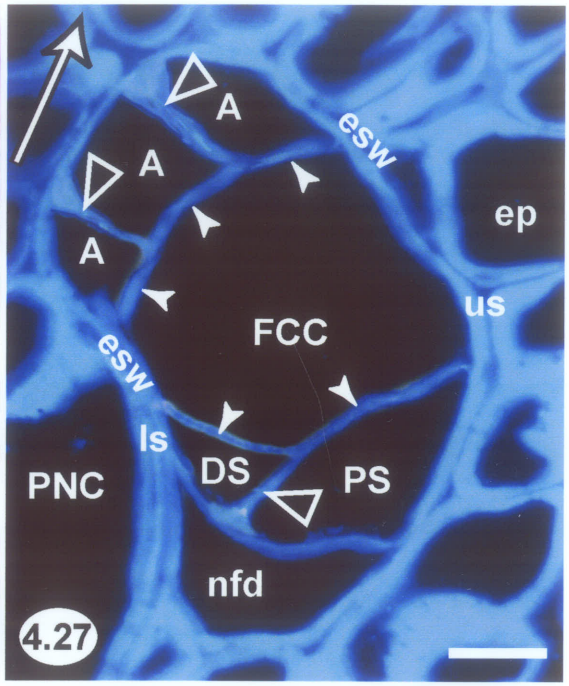
A
esw
A
A
ep
us
FCC
esw
ls
PNC
DS
PS
nfd
4.27

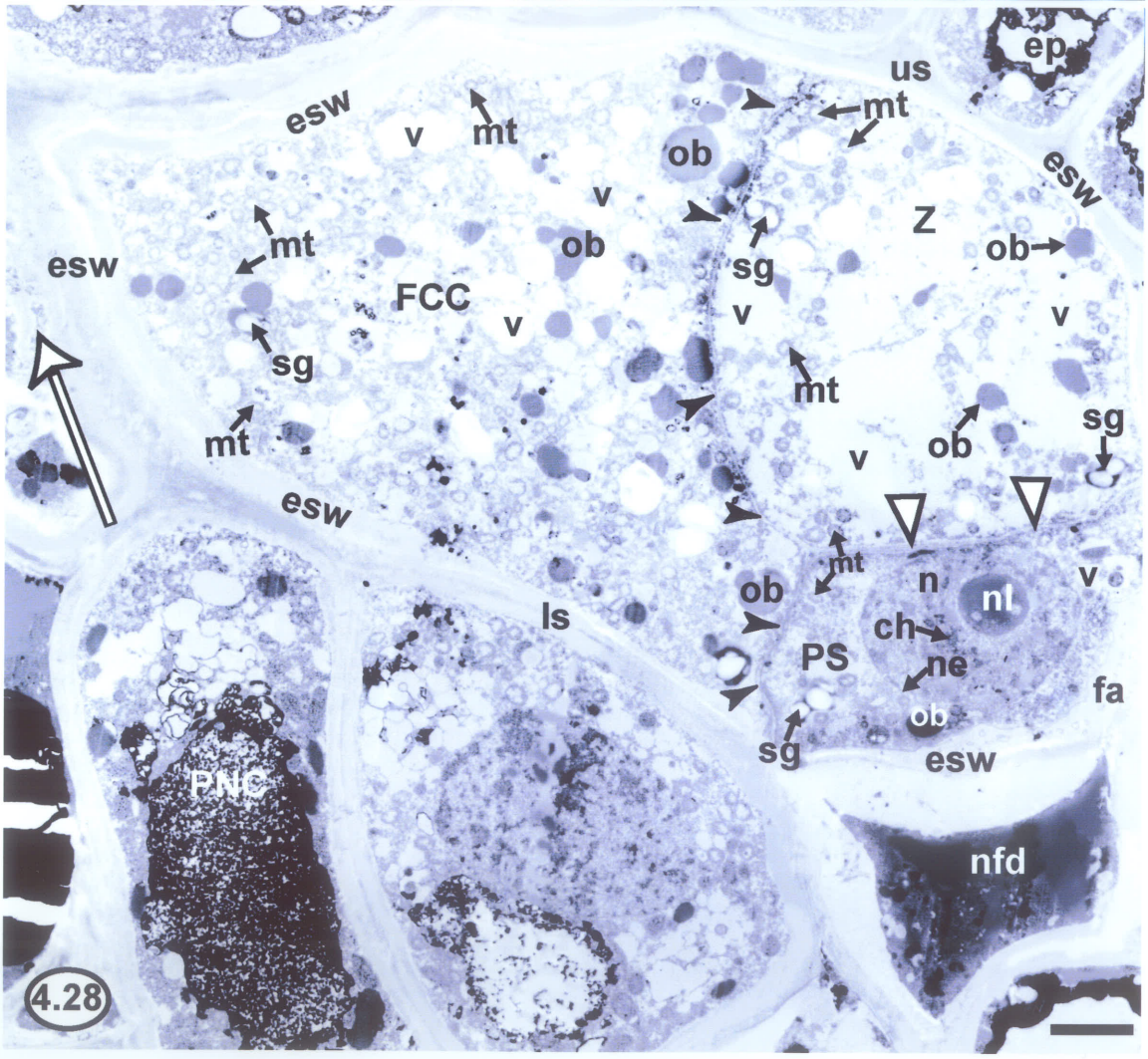
esw
v
mt
ob
us
mt
ep
esw
v
Z
esw
mt
ob
ob
sg
FCC
v
v
v
sg
mt
mt
sg
v
ob
esw
v
mt
n
nl
ob
ls
ch
PS
ne
fa
ob
sg
esw
PNC
nfd
4.28

Figures 4.29a and 4.29b Figures 4.29a and 4.29b are both computer-assisted composite drawings of the fertilized mature seven-celled embryo sacs seen in Figures 4.26, 4.27, and 4.28. The spatial organization of the seven cells bounded by the embryo sac wall (esw) is given in each figure. Hatched cellular interfaces indicate where another cell would obscure the interface. The zygote (Z) had attained a rounded-triangular appearance. The fertilized central cell (FCC) was at a morphologically higher position than the zygote. The persistent synergid (PS) and the degenerating synergid (DS) could occupy either synergid position. Grey shading within the degenerating synergid indicates that the cell has been crushed.

In Figure 4.29a, the persistent synergid is shown to share an interface with the lower side of the embryo sac, and the degenerating synergid is shown to share an interface with the upper side of the embryo sac.

In Figure 4.29b, the two synergids have the opposite configuration. Here, the degenerating synergid is shown to share an interface with the lower side of the embryo sac, whereas the persistent synergid is shown to share an interface with the upper side of the embryo sac.

In both Figures 4.29a and 4.29b, the persistent synergid could be seen to have attained a more rounded appearance following double fertilization. The filiform apparatus (fa) could be seen at the interface between the two synergids at the embryo sac wall. However, within the persistent synergid at the embryo sac wall, the filiform cell wall material had become more substantial following double fertilization. Digitate protuberances (dp) of the filiform apparatus were evident within the persistent synergid. The relative positioning of each nucleus (n) within each viable cell of the embryo sac is given, and the hatched portion of a nucleus indicates where another cell would obscure that portion of the nucleus. As the degenerating synergid had become reduced, no organelles (and thus no nucleus) were evident. The primary endosperm nucleus within the fertilized central cell was relatively larger than the nuclei of the other cells of the embryo sac and typically found at a position that was closer to the lower than to the upper pole of the embryo sac in the vicinity of the lower side of the embryo sac. A = antipodal. 1 cm scale bar = 5 μm.

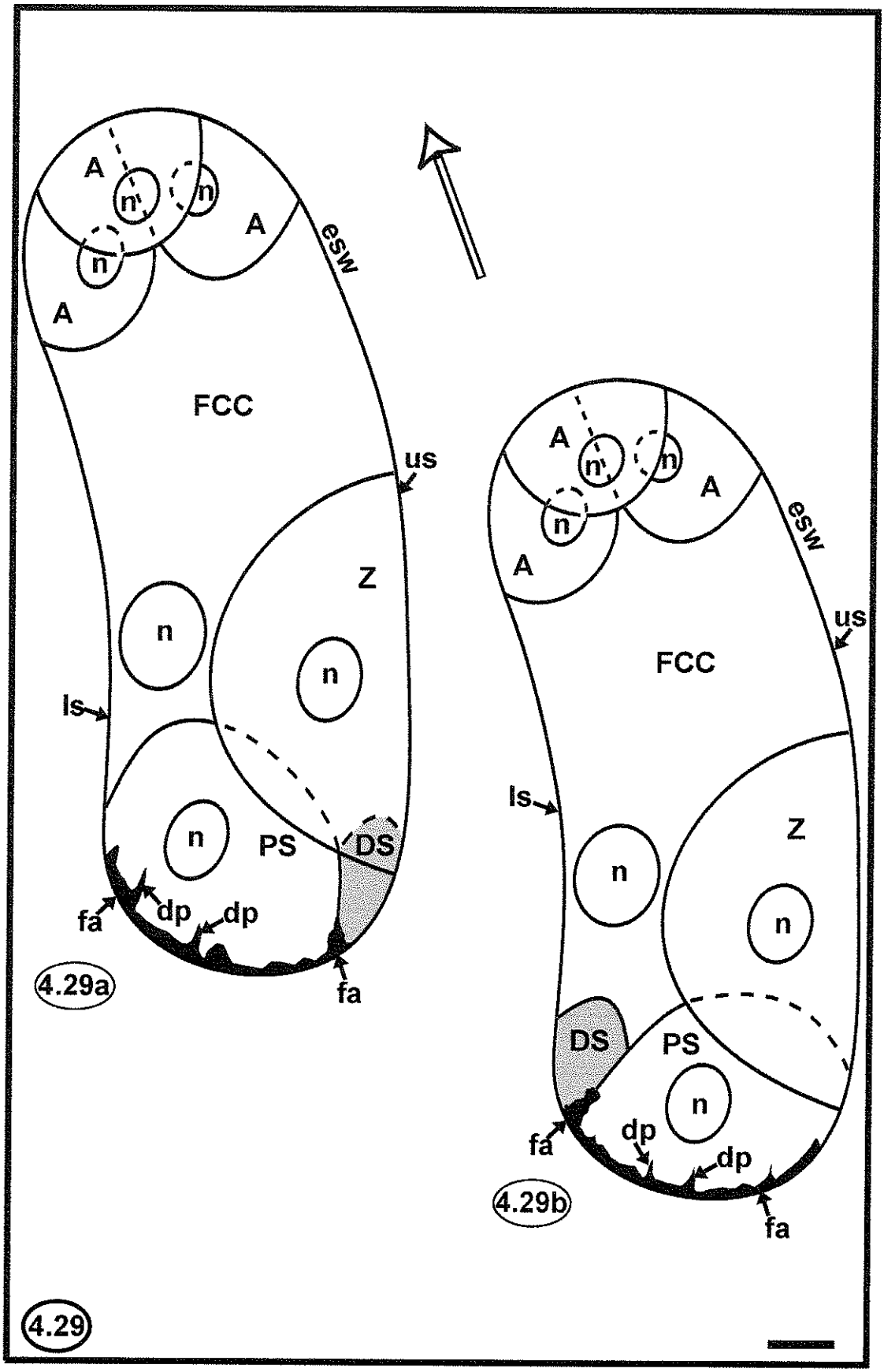
A
n'
n
A
n
A
esw
FCC
us
Z
n
ls
n
n
PS
DS
fa
dp
dp
fa
4.29a
A
n'
n
A
n
A
esw
us
FCC
ls
n
Z
n
DS
PS
n
fa
dp
dp
fa
4.29b
4.29

Figure 4.30 Figure 4.30 is an electron micrograph depicting a magnified serial section to the lower pole of the fertilized embryo sac seen in Figure 4.28. The zygote (Z), persistent synergid (PS), and fertilized central cell (FCC), each with their bounding plasma membrane (zpm, pspm, and fccpm, respectively) were visible in the embryo sac. Small closed arrowheads indicate the interface of the fertilized central cell with the two visible cells of the fertilized egg apparatus. Large open arrowheads indicate the interface of the zygote with the persistent synergid. Cell wall material (!) was now present at the interface of the fertilized central cell with the cells of the egg apparatus, and electron opaque deposits were no longer seen at this interface (small closed arrowheads). Also, the amount of cell wall material the interface of the zygote and the persistent synergid (large open arrowheads) was comparable to the amount seen at the interface with the fertilized central cell (small closed arrowheads). Moreover, there was no difference in the amount of cell wall material between the zygote with the persistent synergid in the regions near the fertilized central cell compared to the regions proximal to the embryo sac wall (esw) at the lower pole of the embryo sac. The filiform apparatus (fa) was visible at the embryo sac wall within the persistent synergid. Vesicles (ve) were seen within the cell wall material of the filiform apparatus. Also, vesicles could be seen in cytoplasm in the vicinity of the filiform apparatus. Notably, the filiform apparatus was fairly digitate, with digitate protuberances (dp) evident and apparently contorting the persistent synergid plasma membrane at the protuberance. A portion of the zygote nucleus (n) could be seen, and it occupied a more central position than the egg cell nucleus. In the persistent synergid, n = nucleus, nl = nucleolus, ne = nuclear envelope, and ch = chromosomal material. Other organelles were distributed as in Figure 4.28: mt = mitochondrion, ob = osmiophilic body, sg = starch grain, v = vacuole. Stain = UA/LC. 1 cm scale bar = 2.5 μm

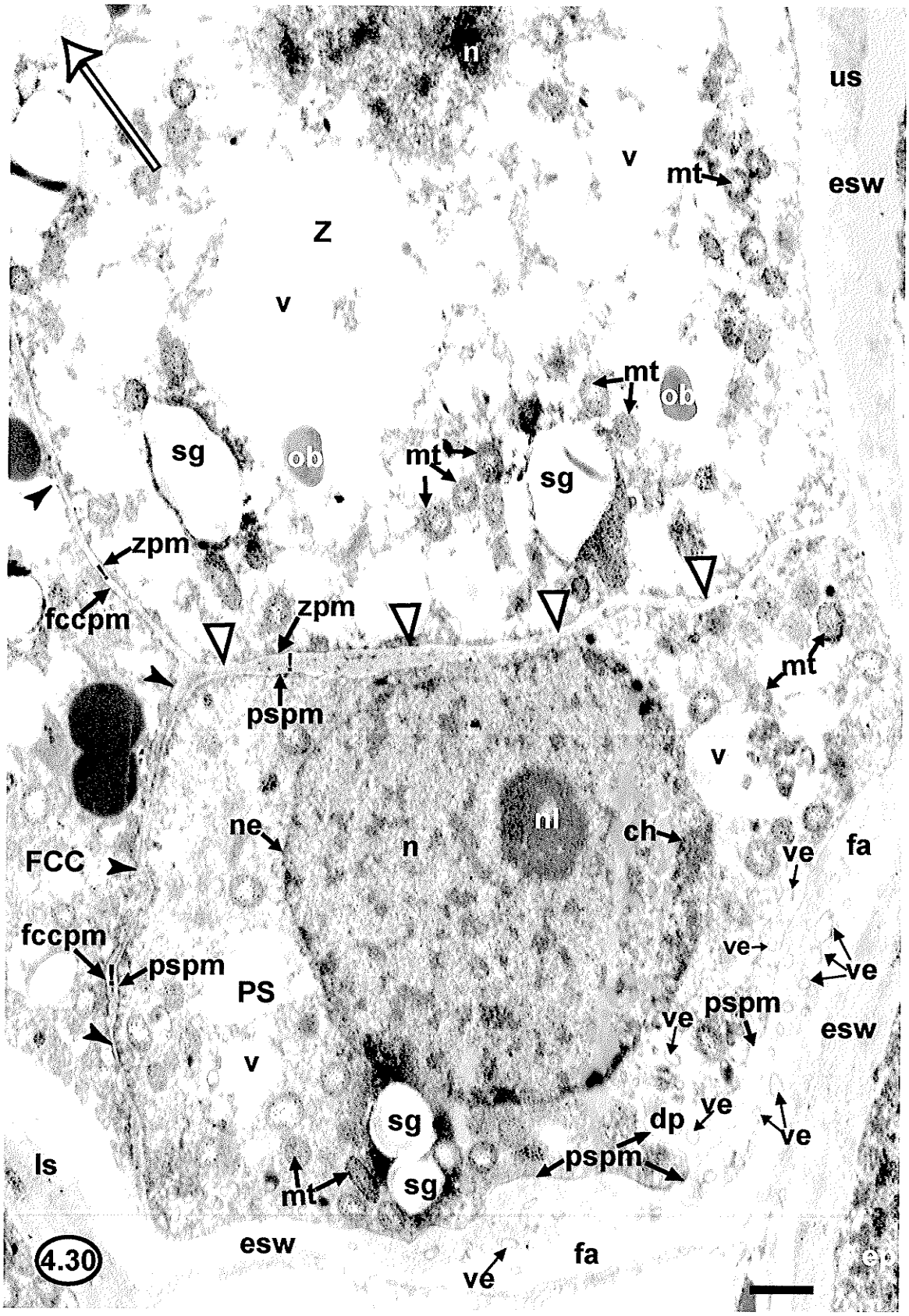
n
us
v
mt
esw
Z
v
mt
ob
sg
ob
mt
sg
zpm
fccpm
zpm
pspm
mt
v
ne
n
nl
ch
ve
fa
FCC
fccpm
pspm
PS
ve
ve
ve
pspm
esw
v
sg
dp
ve
ve
ls
mt
sg
pspm
esw
fa
ve
4.30

Figure 4.31 Figure 4.31 is an electron micrograph depicting a section containing the central portion of a fertilized embryo sac at approximately the same stage of development as seen in Figures 4.26 through 4.30. The fertilized central cell (FCC) was visible in the central region of the fertilized embryo sac, and the persistent synergid (PS) as well as the reduced degenerating synergid (DS) could be seen at the lower pole of the fertilized embryo sac. Here the persistent synergid interfaced with the lower side of the embryo sac. The three antipodals and the zygote were out of the plane of section. Small closed arrowheads indicate the interface between the fertilized central cell and the two synergids, where electron opaque deposits were no longer evident, although cell wall material (!) was. The interface between the persistent synergid and the degenerating synergid (large open arrowhead) was comparable in appearance and cell wall content to the interface of the two synergids with the fertilized central cell (small closed arrowheads) and thus the bounding cell walls of the two synergids had become uniformly thickened. The fertilized central cell had become more cytoplasm-rich and less vacuolate upon fertilization, although numerous small vacuoles (v) could be seen. The nucleus (n) of the fertilized central cell represented the primary endosperm nucleus. The primary endosperm nucleus possessed a very prominent nucleolus (nl), a distinct nuclear envelope (ne), and moderately dispersed chromosomal material (ch). The persistent synergid remained fairly cytoplasm-rich, although a few small vacuoles (v) could be seen. Numerous mitochondria (mt), and starch grains (sg) could be seen in the fertilized central cell. The persistent synergid also possessed many mitochondria. The fertilized central cell possessed peripheral and perinuclear clusters of mitochondria. Osmiophilic bodies (ob) were commonly observed in the fertilized central cell, but they were relatively rare in the persistent synergid. Starch grains (sg) could still be observed in the very dark cytoplasm of the degenerating synergid. fa = filiform apparatus. Stain = UA/LC. 1 cm scale bar = 5 μm.

Figure 4.32 Figure 4.32 is an electron micrograph depicting a section of the upper pole of a fertilized embryo sac at approximately the same stage of development as seen in Figures 4.26 through 4.31. Two of the three antipodals (A) were visible at the upper pole of the embryo sac, and the fertilized central cell (FCC) could be seen. Each antipodal was bounded by its plasma membrane (apm), as was the fertilized central cell (fccpm). The amount of cell wall material (!) at the interface of the antipodals and the fertilized central cell (small closed arrowheads) was slightly more obvious than it was prior to double fertilization, and electron opaque deposits could no longer be seen at this interface. The amount of cell wall material (!) at the interfaces among the antipodals (large open arrowheads) increased substantially following double fertilization and became filled with a fibrillar material (fb). Moreover, electron opaque deposits (*) were now evident within the thick cell walls among the antipodals. The antipodal plasma membranes were slightly contorted by these very thick partitioning walls. The antipodals had become cytoplasm-rich and therefore less vacuolate following double fertilization, although a few vacuoles (v) were remained in the cytoplasm. The cytoplasm was evenly distributed within each antipodal. Mitochondria (mt) increased in number following double fertilization, although there were no apparent osmiophilic bodies (ob) and no apparent starch grains (sg) in the antipodals following double fertilization. The antipodals showed no signs of degeneration. In the fertilized central cell, mt = mitochondrion, ob = osmiophilic body, sg = starch grain, v = vacuole. Stain = UA/LC. 1 cm scale bar = 2 μm.

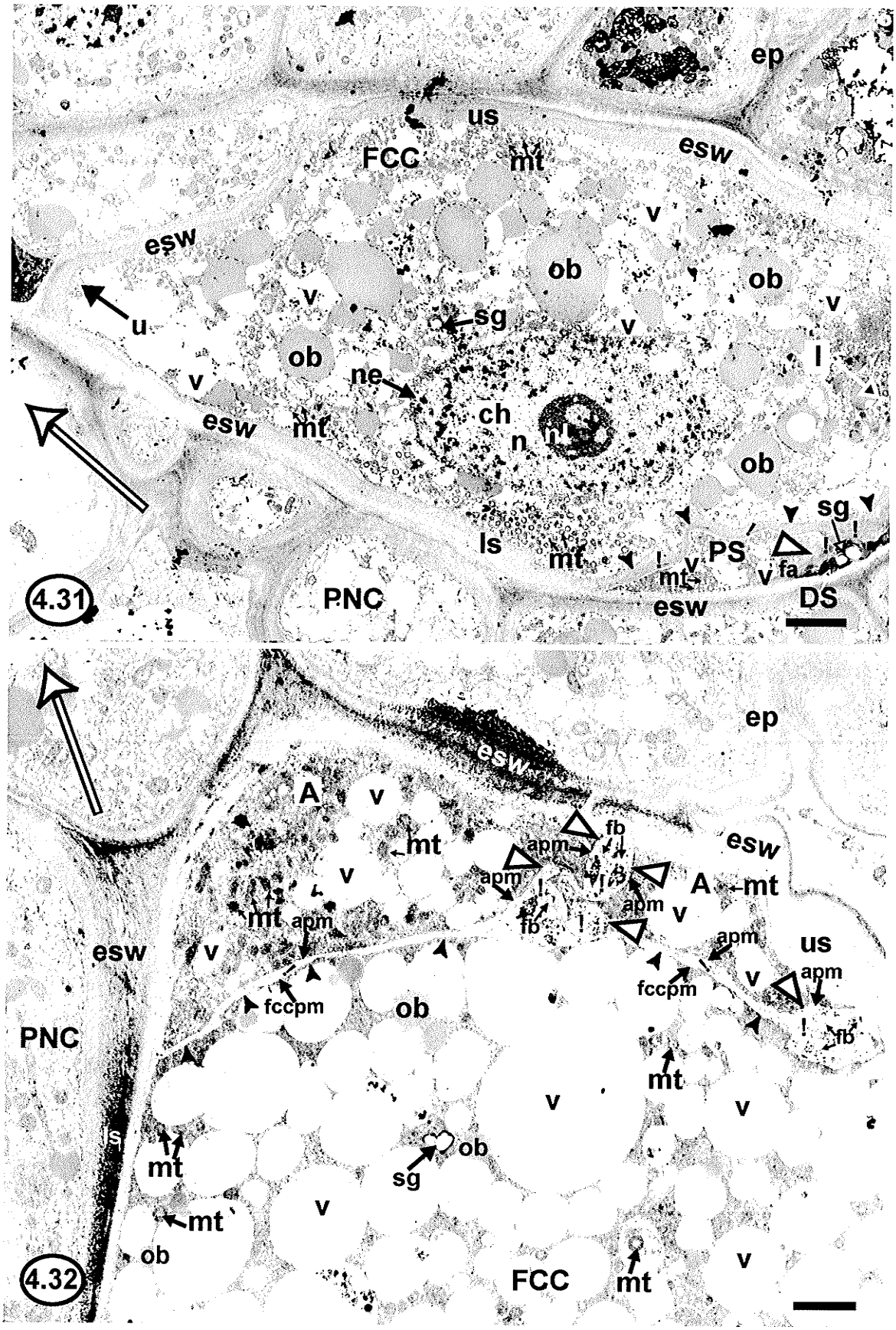
ep
us
FCC
mt
esw
v
esw
ob
ob
v
u
sg
v
l
ob
v
ne
esw
mt
ch
n
ob
sg
ls
mt
PS
v
fa
4.31
PNC
esw
DS
ep
esw
A
v
mt
fb
apm
esw
v
apm
A
mt
mt
apm
fb
v
apm
esw
v
us
apm
fccpm
v
apm
fccpm
ob
PNC
fb
mt
v
v
ls
ob
mt
sg
v
mt
ob
FCC
mt
v
4.32

Figure 4.33 Figure 4.33 is an electron micrograph depicting a section containing the lower portion of a fertilized embryo sac sampled from early June of the first summer (circa June 1) after double fertilization had occurred, but prior to division of the primary endosperm nucleus. The location of the lower pole and the direction of the upper pole of the embryo sac are given, although the majority of the upper pole of the embryo sac is out of the field of view. A caecum (c) protruded from the fertilized central cell (FCC) at the lower side of the embryo sac and was directed toward the base of the PNC. Large vacuoles (v) had formed within the lower region of the fertilized central cell near the caecum and within the caecum. There was no evidence of transfer cell wall outgrowths in the caecum. The fertilized central cell still possessed peripheral clusters of mitochondria (mt). The originally persistent synergid had become crushed, so it was no longer possible to differentiate between the two crushed synergids (SYa and SYb) found at the lower pole of the embryo sac. The crushed nonfunctional dyad (nfd) was seen below the two crushed synergids. Starch grains (sg) were present in all three crushed cells. The filiform apparatus could no longer be discerned. The zygote and primary endosperm nucleus were out of the plane of section. Sterile PNC cells showed a preponderance of mitochondria (mt) in the regions adjacent to the fertilized central cell and caecum. esw = embryo sac wall. Stain = UA/LC. 1 cm scale bar = 5 μm.

Figure 4.34 Figure 4.34 is an electron micrograph depicting the upper portion of the same fertilized embryo sac seen in Figure 4.33. The location of the upper pole and the direction of the lower pole of the embryo sac are given, although most of the lower pole of the embryo sac is out of the field of view. The initiating caecum is also out of the field of view. The three antipodals (A) and the upper region of the fertilized central cell (FCC) are evident. The upper region of the fertilized central cell in the vicinity of the antipodals remained relatively non-vacuolate, as it had been immediately post fertilization, prior to caecum formation. Organelles such as mitochondria (mt), osmiophilic bodies (ob), small vacuoles (v), and starch grains (sg), which were seen in the fertilized central cell prior to caecum formation, could still be observed in the upper portion of the fertilized central cell following caecum formation. The antipodals did not begin to degenerate during caecum initiation and early caecum growth. The antipodals maintained the same organellar composition they had possessed immediately following double fertilization, containing many mitochondria (mt) and relatively few osmiophilic bodies (ob). esw = embryo sac wall. Stain = UA/LC. 1 cm scale bar = 4 μm.

Figure 4.35 Figure 4.35 is a computer-assisted composite drawing of the lower portion of the embryo sac and caecum (c) shown in Figure 4.33 and the upper portion of the same embryo sac shown in Figure 4.34. The caecum began to develop from the fertilized central cell (FCC) on its lower side at the embryo sac wall (esw). Within the embryo sac, hatched cellular interfaces indicate where another cell would obscure the interface. The position of the zygote (Z) is indicated, as it was not captured in Figure 4.33. The zygote remained at the lower pole of the embryo sac, but attached to the upper side of the embryo sac. The originally persistent synergid could no longer be distinguished from the originally degenerating synergid (two synergids are labeled SYa and SYb). Grey shading within the synergids indicates that the cells have been crushed. The filiform apparatus could no longer be discerned. The relative positioning of each nucleus (n) within each viable cell of the embryo sac is given, and the hatched portion of a nucleus indicates where another cell would obscure that portion of the nucleus. The primary endosperm nucleus within the fertilized central cell, which was not captured in Figure 4.33, was found above the caecum, in the vicinity of the zygote and crushed synergids. The primary endosperm nucleus was also found near the point where the caecum had originated (the mouth of the caecum). The antipodals (A) did not begin to degenerate during early caecum growth. 1 cm scale bar = 5 μm.

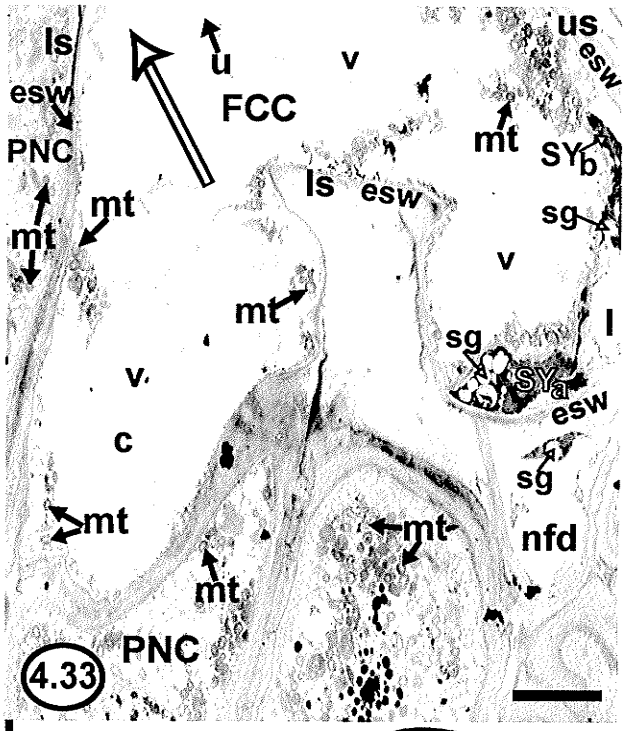
ls
esw
PNC
mt
mt
u
FCC
v
ls
esw
us
esw
mt
SYb
sg
v
mt
l
sg
SYa
esw
v
c
sg
mt
mt
nfd
mt
PNC
4.33

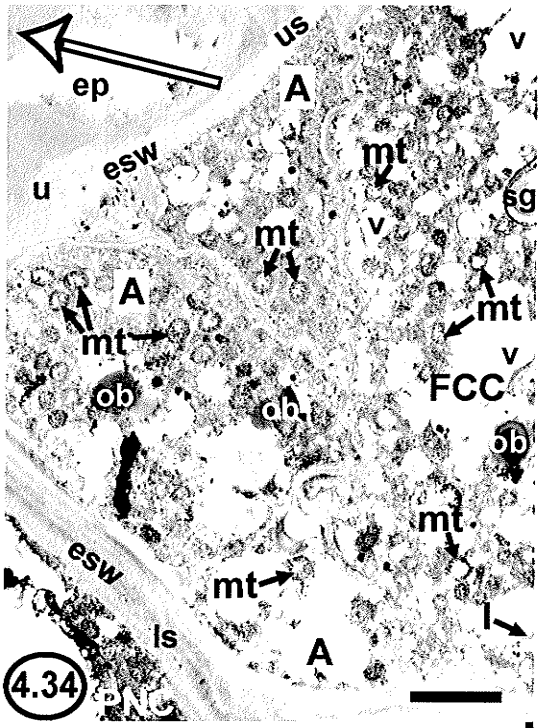
ep
us
A
v
esw
u
mt
v
sg
mt
A
mt
mt
v
ob
ob
FCC
ob
mt
esw
mt
ls
A
l
4.34

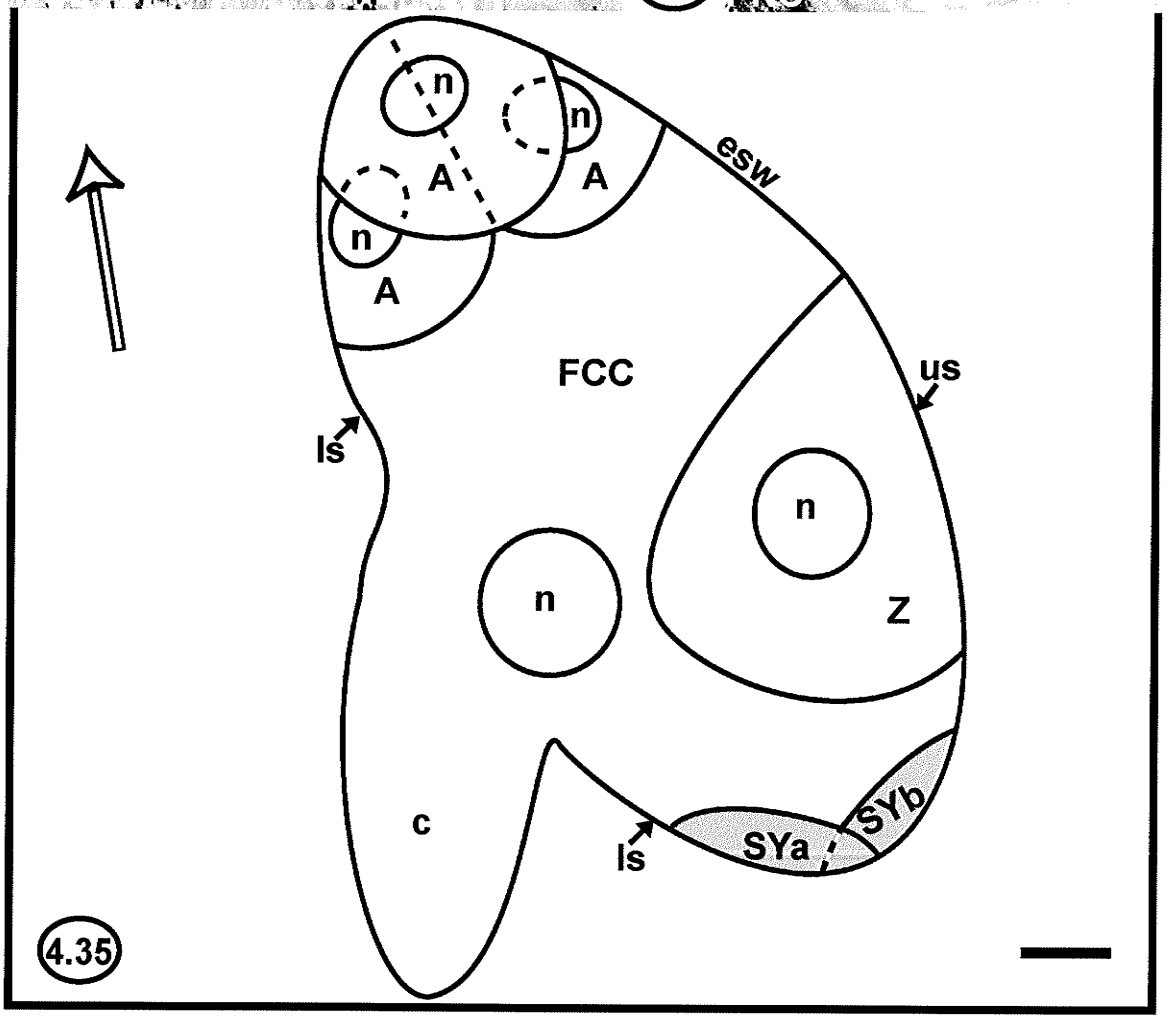
n
n
A
A
esw
n
A
FCC
us
ls
n
n
Z
c
ls
SYa
SYb
4.35

Figure 4.36 Figure 4.36 is a light micrograph depicting a section containing a fertilized embryo sac sampled from early June of the first summer of development (circa June 3) after the caecum (c) had reached the base of the PNC. The primary endosperm nucleus (n) had not divided. The antipodals (A) had become crushed at the upper pole of the embryo sac. Sterile PNC cells had become crushed (small closed arrowheads) as a result of the intercellular growth of the caecum. The thick-walled zygote (Z), however, was rounded and prominent at the lower pole of the embryo sac, where it still shared a common wall with the original embryo sac wall (esw) at the upper side of the embryo sac. The primary endosperm nucleus remained above the caecum, at the mouth of the caecum, in the vicinity of the zygote and crushed synergids (SYa and SYb). Remnants of the nonfunctional dyad (nfd) could be observed below the level of the crushed synergids. The primary endosperm nucleus remained at the mouth of the caecum, possessing a prominent nucleolus (nl), a discrete nuclear envelope (ne), and moderately dispersed chromosomal material (ch). v = vacuole. Stain = CV. 1 cm scale bar = 11 μm.

Figure 4.37 Figure 4.37 is a fluorescence micrograph of a section containing a fertilized embryo sac at approximately the same stage of development as seen in Figure 4.36. This section was subjected to aniline blue fluorescence microscopy. Only the cell wall on the lower side of the embryo sac showed a pale blue fluorescence. The caecum (c) cell wall did not fluoresce. Stain = aniline blue. 1 cm scale bar = 40 μm.

Figure 4.38 Figure 4.38 is a computer-assisted composite drawing of an embryo sac and caecum (c) at the same stage of development as seen in Figures 4.36 and 4.37. The caecum, developing in a downward direction, had reached the base of the PNC. Within the embryo sac, hatched cellular interfaces indicate where another cell would obscure the interface. The zygote (Z) shared a common wall with the original embryo sac wall (esw) at the upper side of the embryo sac. Grey shading within cells indicates that the cells have been crushed. The two synergids (SYa and SYb) remained at the lower pole of the embryo sac. The antipodals (A) had became crushed at the upper pole of the embryo sac. The zygote nucleus (n) remained in the centre of the zygote. The primary endosperm nucleus (n) of the fertilized central cell (FCC) remained undivided in the vicinity of the zygote and two crushed synergids at the mouth of the caecum, above the level of the caecum. 1 cm scale bar = 9 μm.

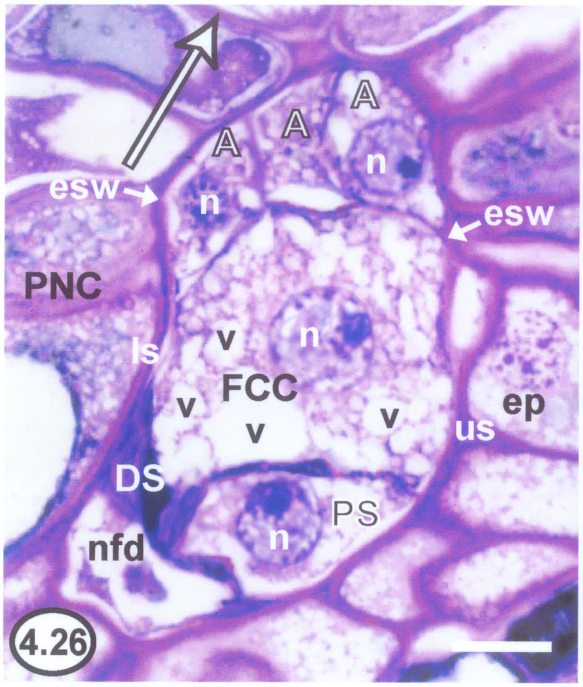
A
A
A
n
esw
n
esw
PNC
ls
v
n
v
FCC
v
v
ep
v
us
DS
PS
n
nfd
4.26

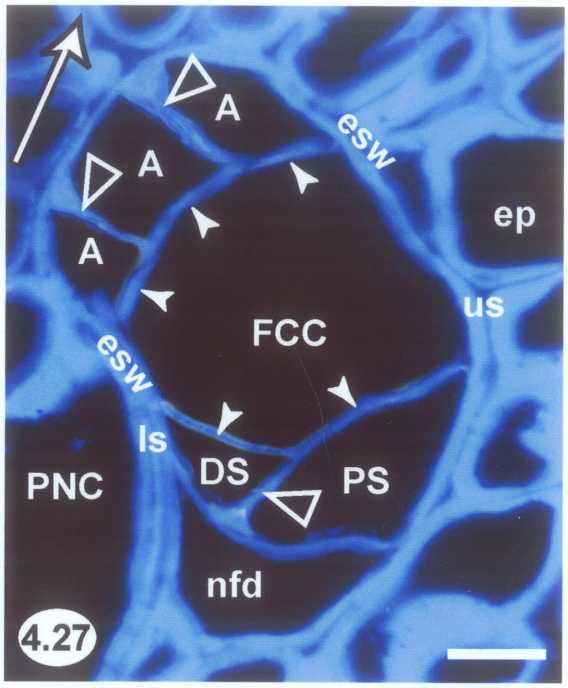
A
esw
A
A
ep
us
FCC
esw
ls
PNC
DS
PS
nfd
4.27

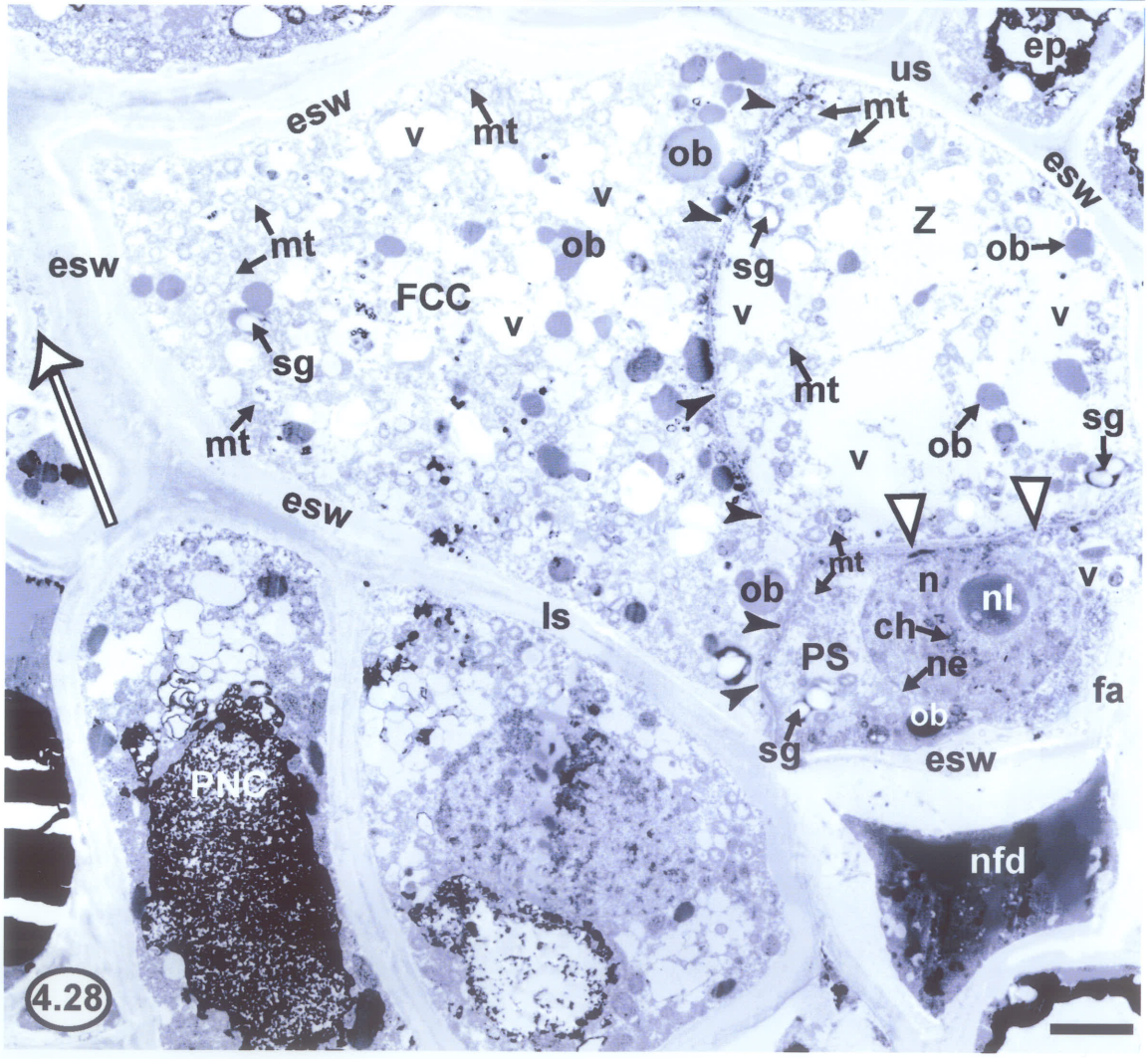
esw
v
mt
ob
us
mt
ep
esw
v
Z
esw
mt
ob
ob
sg
FCC
v
v
v
sg
mt
mt
sg
v
ob
esw
ls
ob
mt
n
nl
v
ch
PS
ne
fa
ob
sg
esw
PNC
nfd
4.28

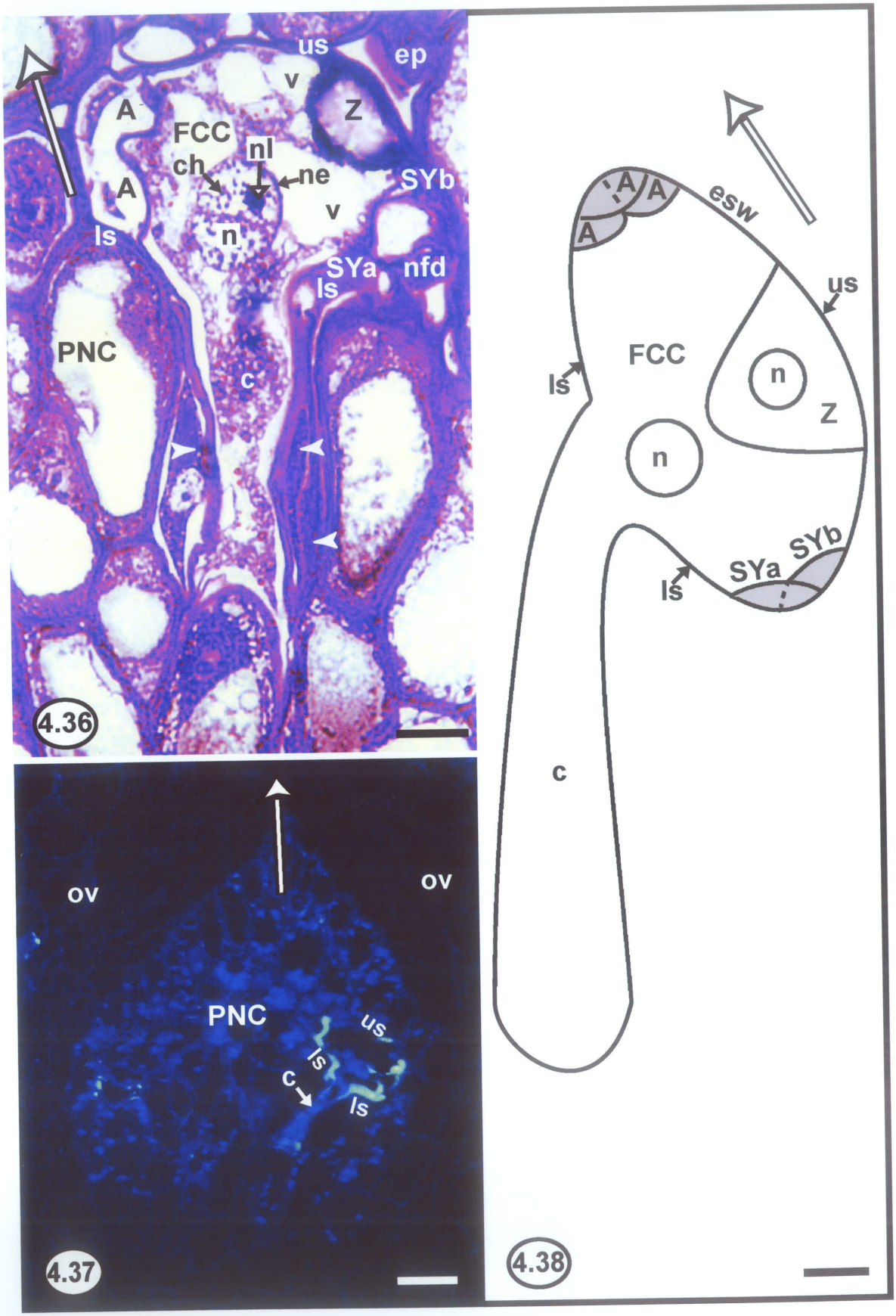
us
ep
v
Z
A
FCC
nl
ch
ne
SYb
A
v
ls
n
SYa
nfd
ls
PNC
c
4.36
ov
ov
PNC
us
ls
c
ls
4.37
A
A
A
esw
us
FCC
ls
n
Z
n
SYa
SYb
ls
c
4.38

Figure 4.39 Figure 4.39 is a light micrograph depicting a section containing a fertilized embryo sac sampled from mid June of the first summer of development (circa June 16). The caecum (c) had reached the base of the PNC, and the primary endosperm nucleus had divided. The crushed antipodals (A) were visible at the upper pole of the embryo sac, and the crushed synergids (collectively labeled SY) along with the crushed nonfunctional dyad (nfd) were visible at the lower pole of the embryo sac. The thick-walled zygote (Z) was rounded and prominent at the lower pole of the embryo sac, where it still shared a common wall with the upper side of the embryo sac. This section features the products of the division of the primary endosperm nucleus. One primary endosperm daughter nucleus (dn_z) remained in the same position that the primary endosperm nucleus had occupied, residing within the original confines of the fertilized central cell in the vicinity of the zygote and crushed synergids. The other primary endosperm daughter nucleus (dn_c) had migrated into the caecum. Cytokinesis had taken place immediately, and the two primary endosperm daughter nuclei were now separated by a slightly curved cell wall (cw), which formed at the mouth of the caecum. Cell wall formation effectively created the first two endosperm cells; one endosperm cell (ez) was delimited by the original confines of the fertilized central cell in the vicinity of the zygote. The other endosperm cell was the entire caecum (still labeled c). The primary endosperm daughter nucleus in the vicinity of the zygote (dn_z) was stained more darkly than the primary endosperm daughter nucleus in the caecum (dn_c). Like the undivided primary endosperm nucleus, the primary endosperm daughter nucleus in the vicinity of the zygote (dn_z) possessed a prominent nucleolus (nl) and moderately dispersed chromosomal material. However, the primary endosperm daughter nucleus in the caecum possessed moderately condensed chromosomal material. The endosperm cell in the vicinity of the zygote appeared to be moderately vacuolated (v) in its lower region, but was more cytoplasm-rich in its upper region, near the crushed antipodals. The caecum (endosperm cell) was highly vacuolated and possessed large vacuoles (v). The base of the caecum was distended (large open arrowhead). Crushed sterile PNC cells (small closed arrowheads) were evident at the periphery of the caecum. Stain = CV. 1 cm scale bar = 15 μm.

Figure 4.40 Figure 4.40 is a light micrograph depicting a section serial to the fertilized embryo sac seen in Figure 4.39. This section features the prominent, uniformly thick-walled zygote (Z), which was rounded and possessed several small vacuoles (v). The prominent zygote nucleus (n) possessed two distinct nucleoli (nl). The endosperm cell in the vicinity of the zygote is out of the plane of section. Only the lower portion of the caecum (c) (a uninucleate endosperm cell) is captured in section; the upper portion of the caecum (and its nucleus) is out of the plane of section. The caecum was highly vacuolate, possessing large vacuoles (v). The base of the caecum was distended (large open arrowhead). A = antipodals (crushed), nfd = non functional dyad (crushed), SY = synergids (crushed), small closed arrowheads = crushed sterile PNC cells. Stain = CV. 1 cm scale bar = 15 μm.

Figure 4.41 Figure 4.41 is a computer-assisted composite drawing of the serial sections of the embryo sac shown in Figures 4.39 and 4.40. The caecum (c) had reached the base of the PNC and the primary endosperm nucleus had divided. Within the embryo sac, hatched cellular interfaces indicate where another cell would obscure the interface. Grey shading within cells indicates that the cells have been crushed. The three crushed antipodals are collectively labeled A, and the two crushed synergids are collectively labeled SY. The round zygote (Z) predominated within the embryo sac and shared a common wall with the original embryo sac wall (esw) at the upper side of the embryo sac. One primary endosperm daughter nucleus (dn_z) remained in the same position that the primary endosperm nucleus had occupied, residing within the original confines of the fertilized central cell (FCC) in the vicinity of the zygote and crushed synergids. The other primary endosperm daughter nucleus (dn_c) was found in the caecum. The two primary endosperm daughter nuclei were separated by a slightly curved cell wall (cw) found at the mouth of the caecum. Thus, one endosperm cell (ez) was delimited by the original confines of the fertilized central cell in the vicinity of the zygote. The other endosperm cell was the entire caecum (still labeled c). The base of the caecum (endosperm cell) was distended (large open arrowhead). Development of the caecum in a downward direction coupled with the migration of a primary endosperm daughter nucleus into the caecum permitted cellular endosperm to develop below the level of the zygote. 1 cm scale bar = 15 μm.

Figure 4.42 Figure 4.42 is an electron micrograph depicting a section containing a fertilized embryo sac at approximately the same stage of development as seen in Figures 4.39, 4.40, and 4.41. The caecum (c) was a uninucleate endosperm cell. The lower portion of the caecum and the primary endosperm daughter nucleus (dn_c) that had migrated into the caecum are visible. The cell wall (cw) of the caecum is indicated. There was no evidence of transfer cell wall outgrowths in the cell wall of the caecum. The primary endosperm daughter nucleus in the caecum possessed a fairly distinct nuclear envelope (ne), as had the primary endosperm nucleus. However, the primary endosperm daughter nucleus in the caecum also possessed moderately condensed chromosomal material (ch), unlike the primary endosperm nucleus. Perinuclear cytoplasm was present and was rich in mitochondria (mt). The caecum was highly vacuolate, possessing large vacuoles (v). Stain = UA/LC. 1 cm scale bar = 3 μm.

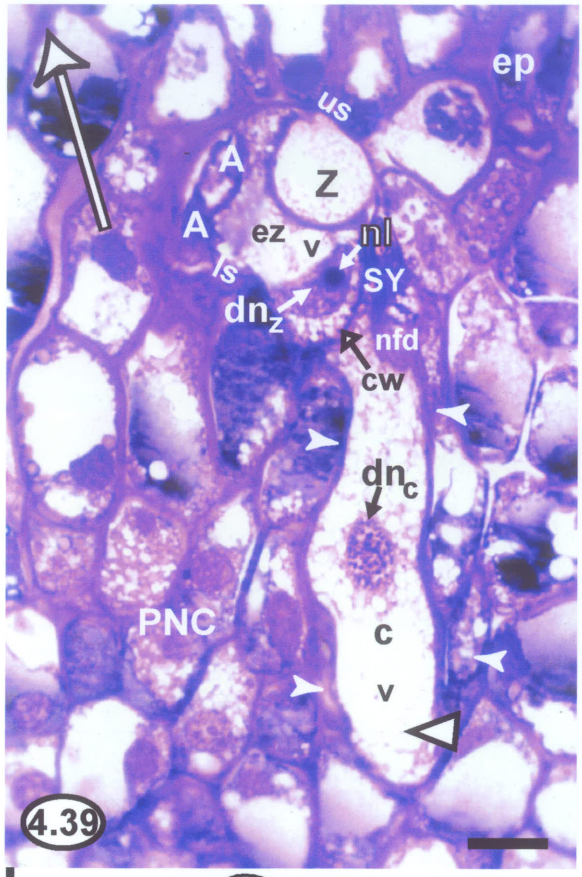
ep
us
A
Z
A
ez
v
nl
ls
SY
dnz
nfd
cw
dnc
PNC
c
v
4.39

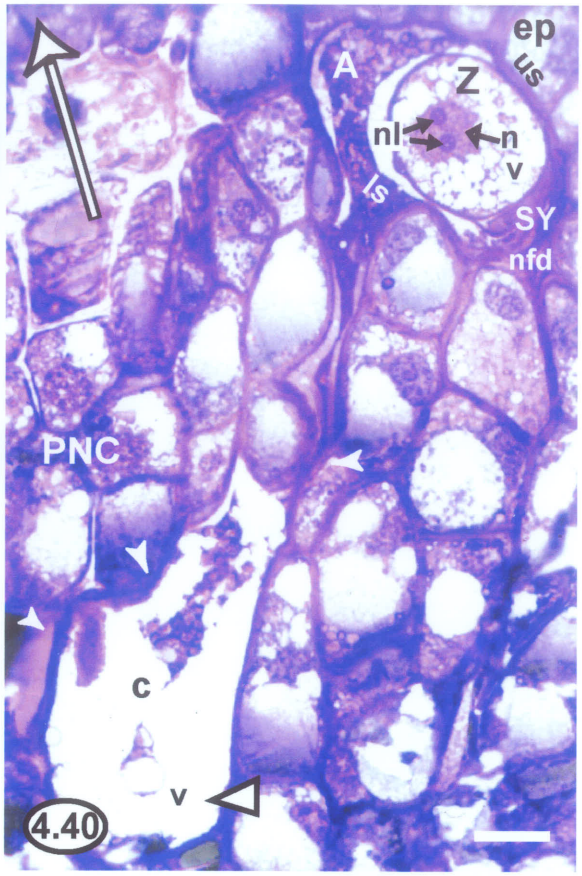
ep
us
A
Z
nl
n
v
ls
SY
nfd
PNC
c
v
4.40

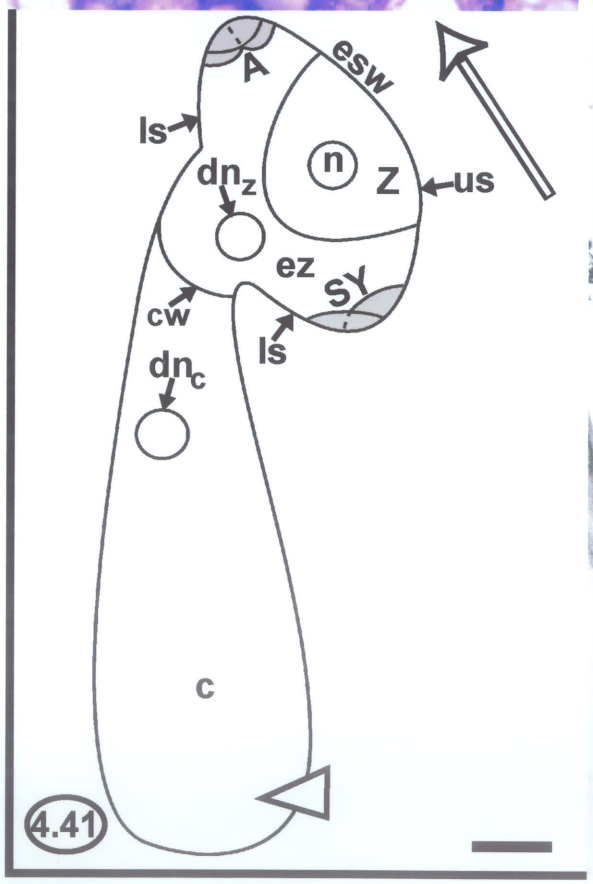
A
esw
ls
n
Z
us
dnz
ez
SY
cw
ls
dnc
c
4.41

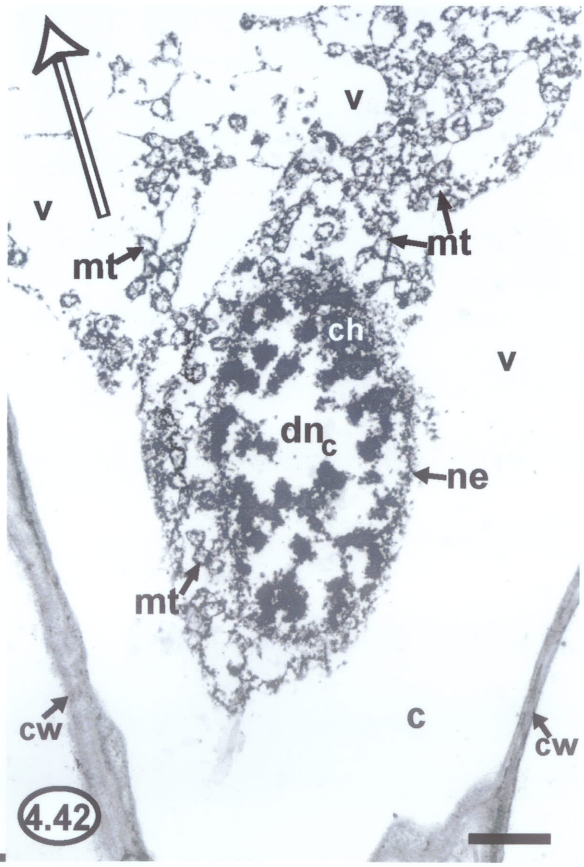
v
v
mt
mt
ch
v
dnc
ne
mt
cw
c
cw
4.42

Figure 4.43 Figure 4.43 is a light micrograph depicting a section containing a zygote along with cellular endosperm developing in one plane, sampled from late June of the first summer (circa June 26). The thick-walled zygote (Z) was prominent, contained several vacuoles (v), and shared a common wall with the upper side of the embryo sac. The endosperm cell in the vicinity of the zygote (seen in Figure 4.39) and the caecum endosperm cell (seen in Figures 4.39, 4.40, and 4.42) had each undergone two or three cellular divisions in one plane. Divisions of the endosperm cell(s) in the vicinity of the zygote were anticlinal to the lower surface of the zygote and accordingly, three triangular endosperm cells (ez) had developed in the vicinity of the zygote, below the level of the zygote. Note how these endosperm cells had been displaced downward. The endosperm cells in the vicinity of the zygote were in the same plane as the zygote, were held within the original but expanded confines of the fertilized central cell, and possessed prominent vacuoles (v). Concurrently, cellular division(s) of the caecum endosperm cell, transverse to the long axis of the caecum, had resulted in the formation of four distinctly rectangular-shaped endosperm cells (ec) in a uniseriate file within the caecum. These four endosperm cells remained within the original but expanded confines of the caecum. Nuclei (n) were observed in the caecum endosperm cells. The caecum endosperm cells possessed large vacuoles (v), although the lowermost caecum endosperm cells possessed particularly large vacuoles. Small closed arrowheads = crushed sterile PNC cells. A = (crushed) antipodals, nfd = (crushed) nonfunctional dyad, SY = (crushed) synergids. Stain = TB, pH 4.4. 1 cm scale bar = 8 μm.

Figure 4.44 Figure 4.44 is an electron micrograph depicting a section containing cellular endosperm at approximately the same stage of development as seen in Figures 4.42 and 4.43. Figure 4.44 features the lowermost two caecum endosperm cells (ec). The original caecum boundary as delimited by its cell wall (cw) is indicated. No transfer cell wall outgrowths were evident in this cell wall. The two caecum endosperm cells possessed large vacuoles (v). A nucleus (n) could be observed in the lowermost endosperm cell of the caecum and it appeared to be in a state of degeneration. Cytoplasm was found in peripheral and perinuclear locations. Stain = UA/LC. 1 cm scale bar = 4.5 μm.

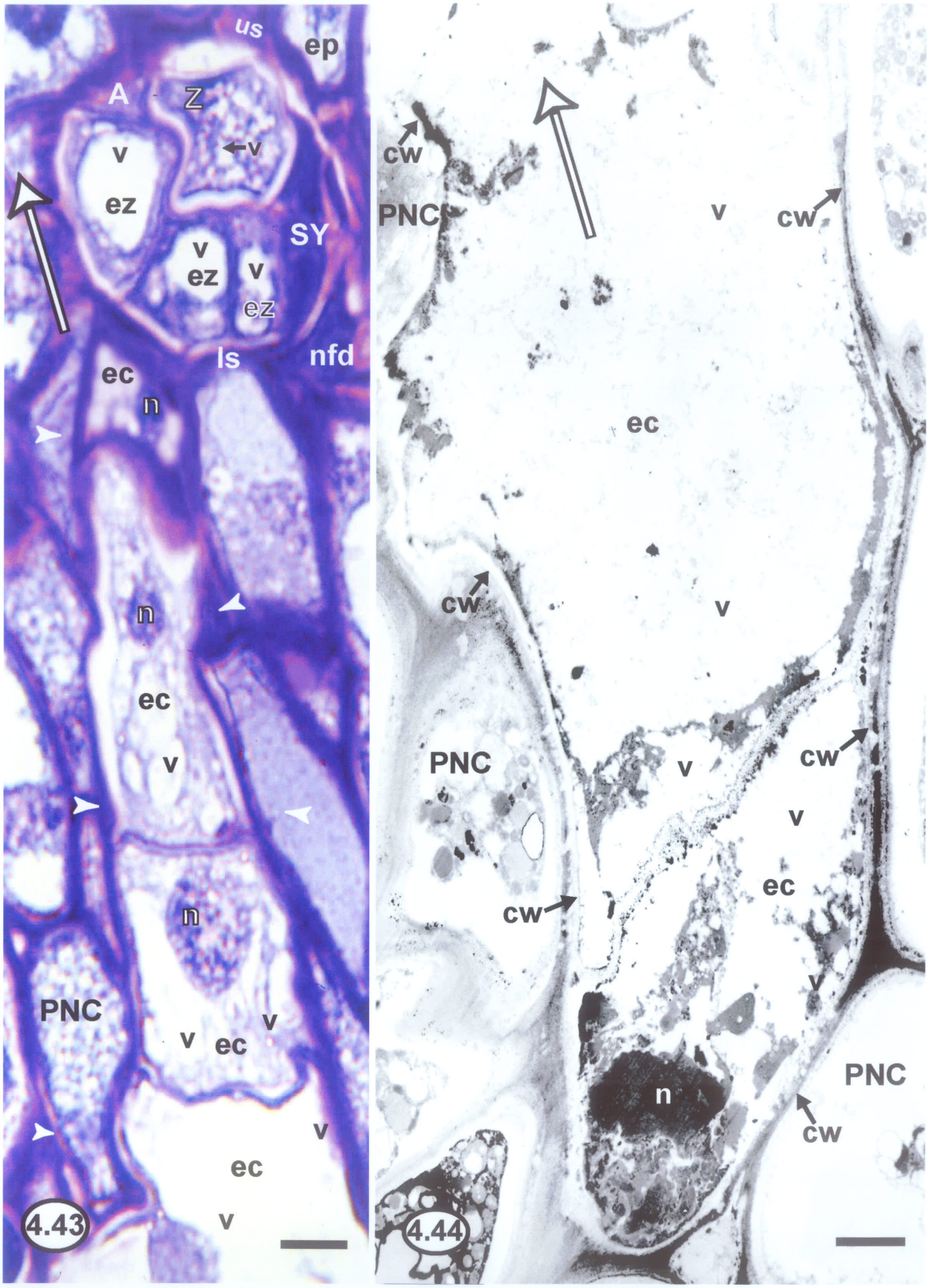
us
ep
A
Z
v
v
ez
SY
v
ez
v
ez
ls
nfd
ec
n
n
ec
v
n
PNC
v
v
ec
v
ec
v
4.43
cw
PNC
v
cw
ec
cw
v
PNC
v
cw
v
ec
cw
v
n
PNC
cw
4.44

Figure 4.45 Figure 4.45 is a light micrograph depicting a section containing a zygote along with cellular endosperm developing in more than one plane, sampled from mid July of the first summer (circa July 12). Only the zygote (Z) and endosperm cells in the vicinity of the zygote (ez - representative cells labeled) are captured in section; the caecum endosperm cells are out of the plane of section. The thick-walled zygote was rounded and prominent, sharing a common wall with the upper side of the embryo sac. The endosperm cells in the vicinity of the zygote were dividing in all planes below the level of the zygote, and thus had proliferated in a cup that enveloped the lower portion of the zygote. No endosperm cells were found above the level of the zygote, as the upper part of the zygote remained attached to the embryo sac wall. Note the presence of a cell wall (cw) between two endosperm cells that had arisen from a division that was periclinal (as opposed to anticlinal) to the surface of the zygote. Portions of the crushed synergids (SY) were visible at the lower pole of the embryo sac. Stain = CV. 1 cm scale bar = 13 μm.

Figure 4.46 Figure 4.46 is an electron micrograph depicting a section serial to that shown in Figure 4.45. Only the endosperm cells in the vicinity of the zygote (ez - representative cells labeled) were captured in section; the zygote was not. The caecum endosperm cells were out of the field of view, although their direction is indicated (ec). The fact that the endosperm cells in the vicinity of the zygote could still be captured in section when the zygote could no longer be captured provides evidence that these endosperm cells were dividing in all planes below the level of the zygote. No endosperm cells were found above the level of the zygote, as the zygote remained attached to the upper side of the embryo sac. These endosperm cells in the vicinity of the zygote had well-defined cell walls and the cytoplasm contained an assortment of subcellular structures including mitochondria, (mt) osmiophilic bodies (ob), and starch grains (sg) in amyloplasts. Small to medium-sized vacuoles (v), some of which appeared to be filled with tannin-like substances (t), were common to these endosperm cells. The prominent nuclei (n) possessed distinct nucleoli (nl). The crushed antipodals (A) were visible at the upper pole of the embryo sac, and the crushed synergids (SY) were visible at the lower pole of the embryo sac. Stain = UA/LC. 1 cm scale bar = 3 μm.

Figure 4.47 Figure 4.47 is a light micrograph depicting a section serial to those shown in Figures 4.45 and 4.46. Only the endosperm cells of the caecum (ec) were captured in section, and they had also begun to divide in all planes like the endosperm cells in the vicinity of the zygote (further verified by serial sectioning - not shown). Note the presence of a cell plate (cp) between two recently-divided caecum endosperm nuclei (n) that was longitudinally rather than transversely oriented to the axis of the caecum. The lowermost two or three cells at the base of the caecum, however, remained in a uniseriate file (further verified by serial sectioning - not shown). Small closed arrowheads = crushed sterile PNC cells. Stain = CV. 1 cm scale bar = 13 μm.

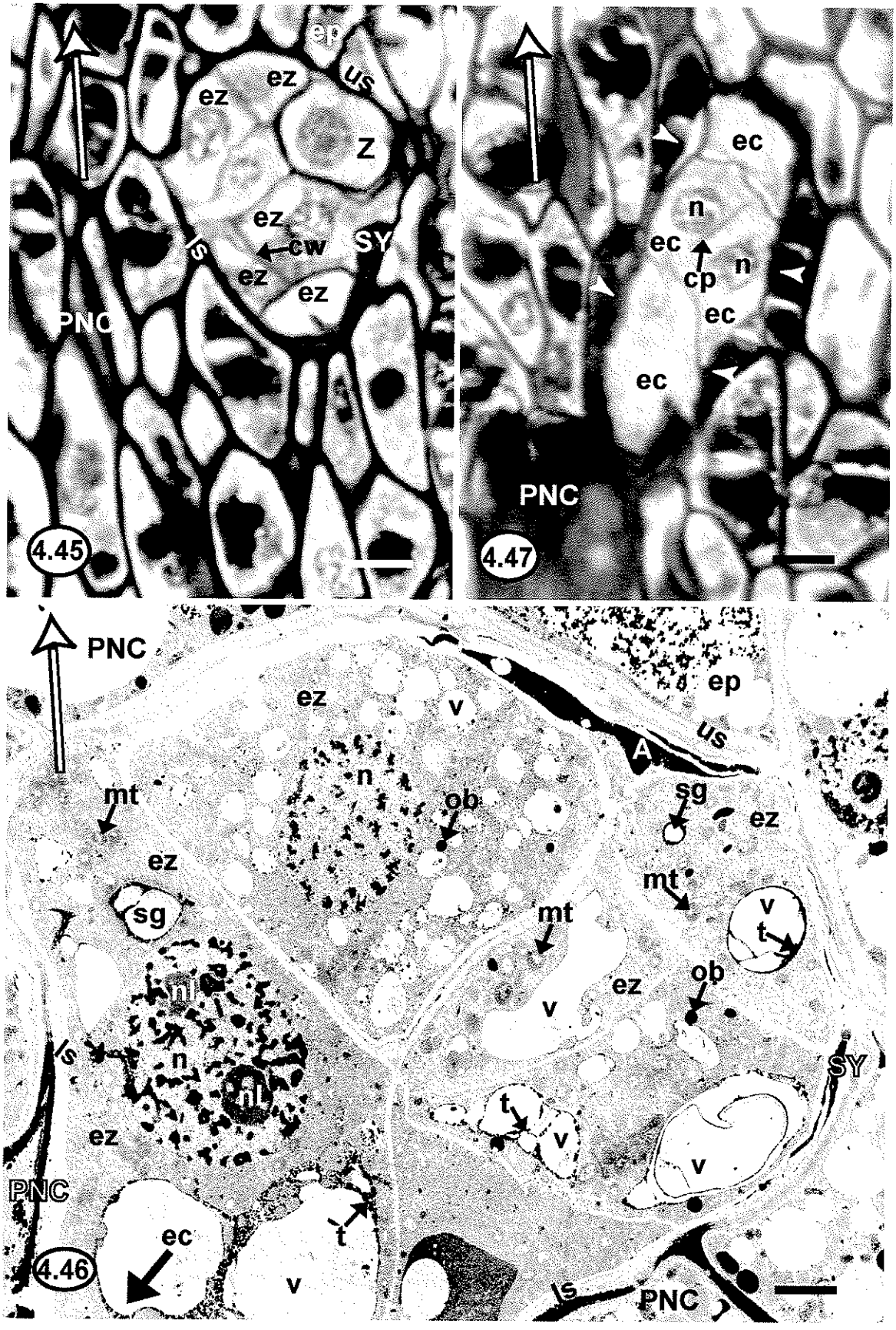
ep
ez
us
ez
Z
ez
cw
SY
ls
ez
ez
PNC
4.45
ec
n
ec
cp
n
ec
ec
PNC
4.47
PNC
ez
v
ep
us
A
n
mt
ob
sg
ez
ez
mt
v
t
sg
mt
ob
ez
nl
v
ls
n
nl
SY
ez
t
v
v
PNC
t
ec
4.46
v
ls
PNC

Figure 4.48 Figure 4.48 is an electron micrograph depicting a section containing a zygote (Z) at the same stage of development as the zygote shown in Figure 4.45. Although the zygote still shared a common cell wall with the upper side of the embryo sac, the zygote was seen to be in the process of dislodging from the embryo sac wall (esw). Where the zygote shared a common cell wall with the embryo sac, the zygote plasma membrane (zpm) could be seen to be pulling away from the embryo sac wall. In the region between the zygote cell plasma membrane and the embryo sac cell wall (the periplasmic space), vesicles (ve) lined with electron dense materials could be seen. The zygote cytoplasm still contained clusters of mitochondria (mt), as well as several small vacuoles (v). The zygote nucleus (n) contained regions of both condensed and dispersed chromosomal material (ch). A small portion of an endosperm cell in the vicinity of the zygote (ez) was captured, as was the zygote wall (zw) between that portion of the endosperm cell and the zygote. The zygote plasma membrane at that part of the zygote wall was not captured in section, and neither was the plasma membrane of the endosperm cell. Stain = UA/LC. 1 cm scale bar = 2 μm.

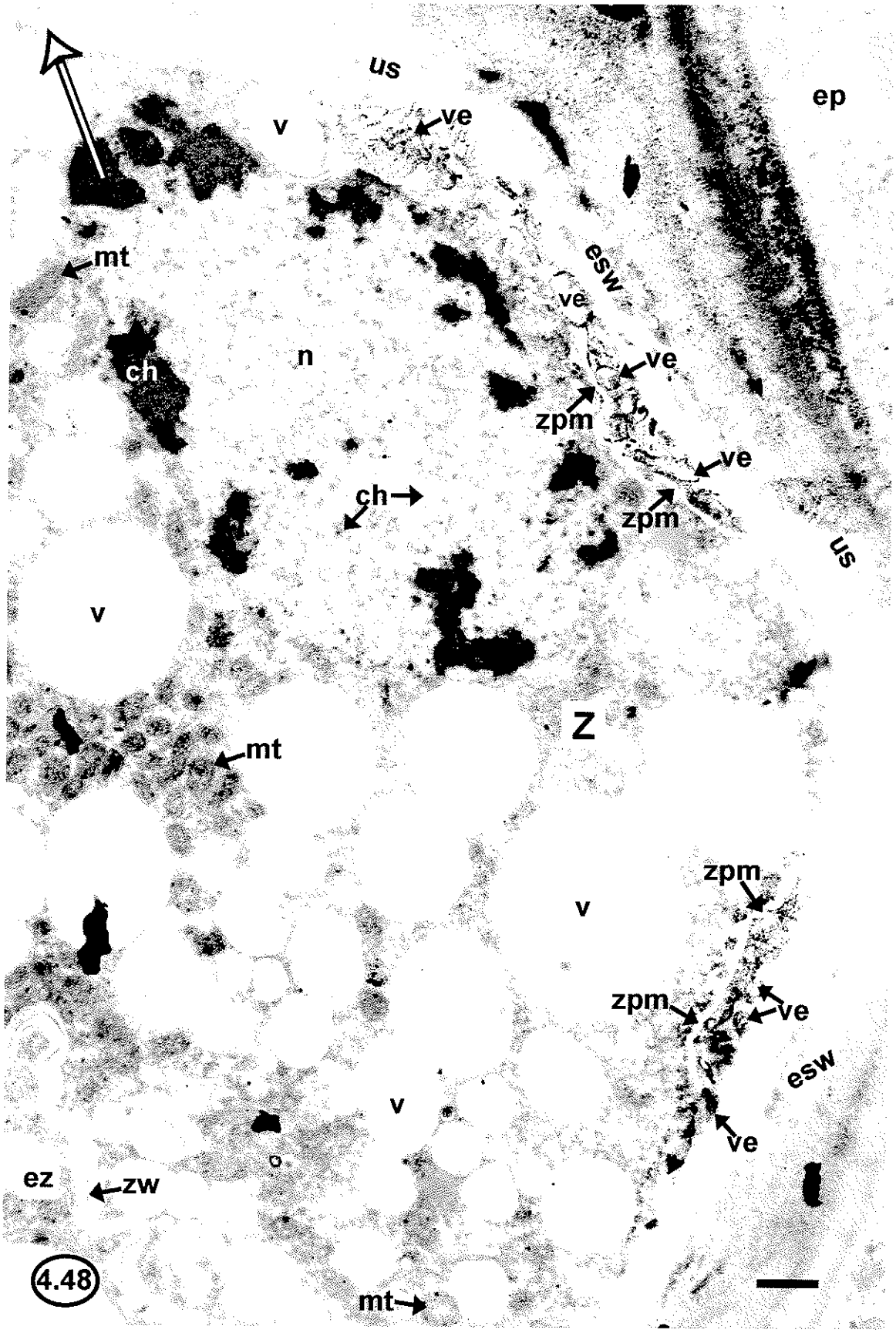
us
ep
v
ve
mt
esw
ve
n
ch
ve
zpm
ve
ch
zpm
us
v
Z
mt
zpm
v
zpm
ve
esw
v
ve
ez
zw
4.48
mt

Figure 4.49 Figure 4.49 is a light micrograph depicting a section containing a two-celled embryo (each cell of the embryo labeled ey), sampled from late July of the first summer, circa July 20. Zygotic division had recently occurred (more detail in Figure 4.50). The second, abortive, degenerative embryo sac (des) could still be seen within the PNC. Tiers of dividing endosperm cells (ez - representative cells labeled) originally derived from endosperm cells in the vicinity of the undivided zygote began to encircle the two-celled embryo above the level of the embryo. One tier of primarily anticlinally-dividing endosperm cells began to encircle the two-celled embryo in a upward clockwise direction (indicated by an arrow labeled cwt) and a second tier of primarily anticlinally-dividing endosperm cells began to encircle the embryo in an upward counterclockwise direction (indicated by an arrow labeled cct). These two encircling tiers were in the same plane as the two-celled embryo. Below the level of the embryo, other endosperm cells that had also been derived from endosperm cells in the vicinity of the zygote continued to divide in all planes. The majority of the caecum endosperm cells, which were also continuing to divide in all planes, were out of the plane of section, although two distended caecum endosperm cells (ec) could be seen at the very base of the PNC. However, these two lowermost caecum endosperm cells remained in a uniseriate file at the base of the caecum. PNC cells were becoming crushed and displaced on all sides of the expanding endosperm. In addition, the epidermis of the PNC adjacent to the embryo and endosperm became crushed (cep). Thus, the embryo and endosperm had come to lie outside of the PNC and in direct contact with the ovarian tissue on that side. Stain = CV. 1 cm scale bar = 20 μm.

Figure 4.50 Figure 4.50 is a light micrograph depicting a magnified view a serial section of the two-celled embryo (each cell of the embryo labeled ey) shown in Figure 4.49. Details of the two-celled embryo are featured. Relative to the point where the two-celled embryo was anchored to (although dislodging from) the embryo sac wall (esw), the cell wall (cw_1) that resulted from zygotic division and separated the two embryonic cells appeared to be transverse. The two embryonic cells were equal in size and were held within the boundary of the original zygote wall (zw), which was thicker than the newly formed transverse cell wall separating the two embryonic cells. The two embryonic cells possessed prominent nuclei (n) that each contained a distinct nucleolus (nl). Dividing endosperm cells (ez - representative cells labeled) originally derived from endosperm cells in the vicinity of the undivided zygote were also visible. Observations regarding division of these endosperm cells and their participation in the initiation of encirclement of the embryo were as in Figure 4.49. Notably though, two endosperm cells below the level of the embryo, originally derived from cells in the vicinity of the zygote, were only caught in partial section (large open arrowheads), verifying that endosperm cells below the level of the embryo were continuing to divide in all planes. The caecum endosperm cells cannot be observed in this figure. Arrow labeled cwt = clockwise encircling tier of anticlinally-dividing endosperm cells, arrow labeled cct = counterclockwise tier of anticlinally-dividing endosperm cells, cep = crushed epidermal cells of the PNC. Stain = CV. 1 cm scale bar = 10 μm.

Figure 4.51 Figure 4.51 is a light micrograph depicting a section containing a round, recently formed four-celled embryo (each cell of the embryo labeled ey), sampled from the end of July of the first summer, circa July 31. Division of each cell in the two-celled embryo seen in Figures 4.49 and 4.50 was accompanied by formation of a longitudinal cell wall (cw_2) that was perpendicular to the transverse cell wall (cw_1) derived from zygotic division. The resulting four embryonic cells were all in the same plane and similar in appearance. The original zygote wall (zw) remained thicker than the newly formed partitioning cell walls (cw_1) and (cw_2). The primarily anticlinally dividing clockwise tier (arrow labeled cwt) and counterclockwise tier (arrow labeled cct) of endosperm cells (ez) originally derived from endosperm cells in the vicinity of the zygote had completely encircled the four-celled embryo. Thus, endosperm cells were now found above the embryo in primarily one plane, effectively separating the embryo from the embryo sac wall. In this example, the counterclockwise-advancing tier predominately aided encirclement, whereas the clockwise tier was less defined. Most endosperm cell divisions in the endosperm cell tiers above the embryo were in the plane of the embryo. However, occasional endosperm cell divisions outside of the plane of the embryo took place above the embryo, as endosperm cells that lay outside of the plane of the encircling tiers could be seen in partial section above the embryo (small closed arrowheads). Below the embryo, other endosperm cells originally derived from endosperm cells in the vicinity of the zygote continued to regularly divide in all planes, as endosperm cells that lay outside of the plane of the embryo could often be seen in partial section (large open arrowheads). Caecum endosperm cells were not captured in this figure, but they continued to divide in all planes except at the uniseriate base. cep = crushed epidermal cells of the PNC. Stain = CV. 1 cm scale bar = 14 μm.

Figure 4.52 Figure 4.52 is a light micrograph depicting a section of a young fruit sampled from early August (circa August 5). The embryo (ey) was still four-celled. Notably, however, the endosperm cells above the embryo (ez - only representative cells labeled), which had ultimately been derived from endosperm cells in the vicinity of the zygote via the two encircling tiers, had begun to regularly proliferate in all planes. This mass of endosperm cells residing above the level of the embryo was called the cap (cap). It was no longer possible to distinguish the presence of a caecum, except at the uniseriate base (not shown). Moreover, aside from the cap cells, endosperm cells that had originated in the vicinity of the zygote could no longer be distinguished from those that had originated in the caecum. Thus, all endosperm cells below the level of the embryo will be referred to as endosperm cells (en) without further reference to their origin, excepting cells representing caecum endosperm cells at the uniseriate base (not shown). As endosperm cells divided, more of the PNC cells were crushed and displaced to the side containing remnants of the second, abortive, degenerative embryo sac (des). No PNC cells remained above the cap or where the endosperm had come into direct contact with the ovarian tissue, as the epidermis of the PNC that had been in contact with the endosperm had been crushed and obliterated. The ovarian tissue displayed the first signs of cell division and cell enlargement. Stain = TB, pH 4.4. 1 cm scale bar = 35 μm.

Figure 4.53 Figure 4.53 is a light micrograph depicting a section containing a young fruit sampled from mid August (circa August 14). The embryo (ey) had reached the globular stage, and was a small, undifferentiated globe of about eight to sixteen cells. No suspensor was evident. The dividing cells of the endosperm (en) had displaced almost all of the PNC to the side containing the degenerative embryo sac (des), and the endosperm was proceeding to downwardly crush the sterile PNC cells. The base of the endosperm (the original base of the caecum) still contained dilated caecum endosperm cells (ec) persisting in a uniseriate file. The ovarian cells continued to divide and enlarge, but there was no differentiation into specific fruit zones. cap = cap of endosperm cells. Stain = TB, pH 4.4. 1 cm scale bar = 40 μm.

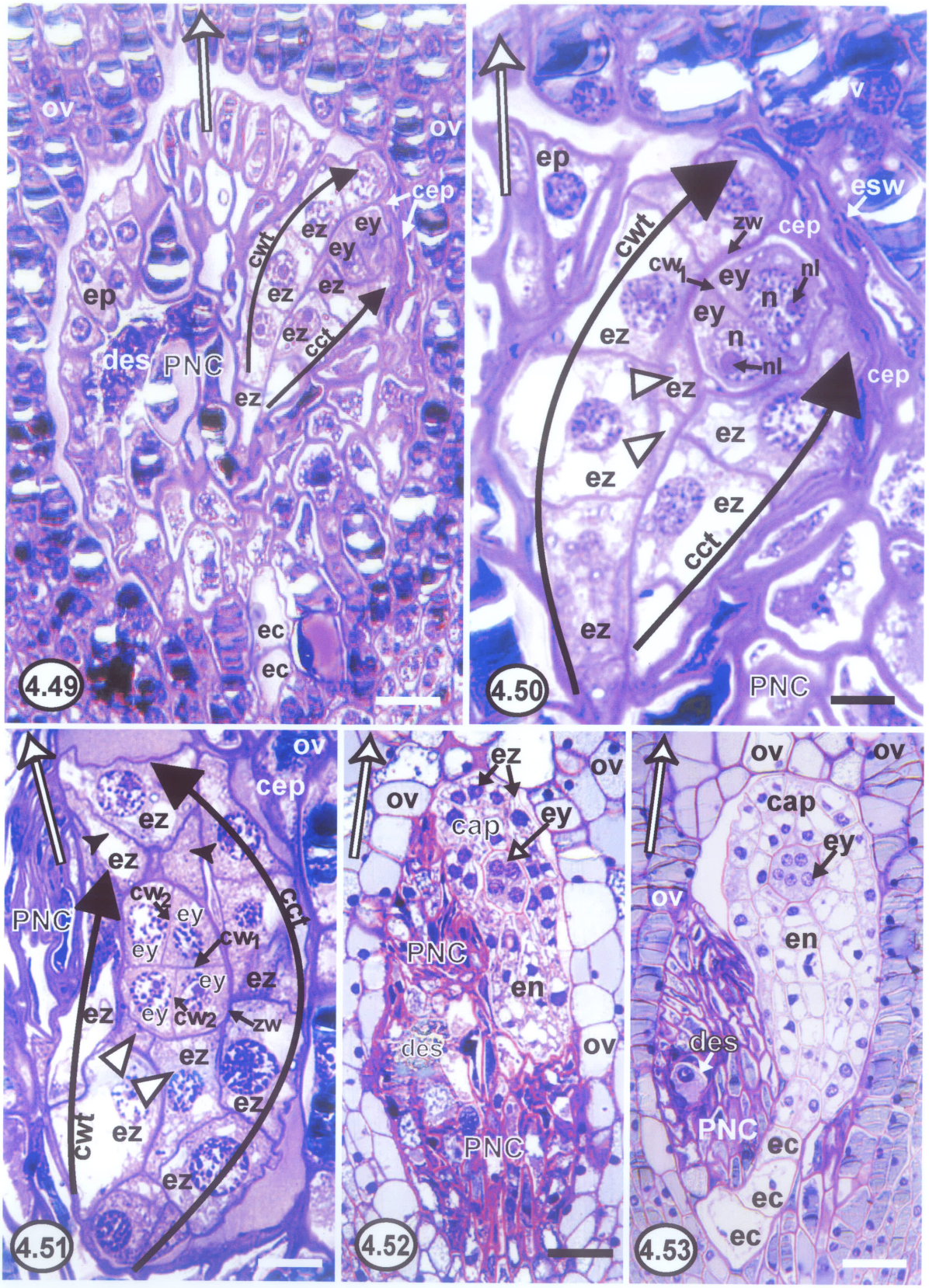
ov
ov
cep
ep
cwt
ez
ey
ey
ez
ez
ez
cct
des
PNC
ez
ec
ec
4.49
ep
v
esw
zw
cep
cwt
cw1
ey
nl
ey
n
n
ez
nl
ez
cep
ez
ez
ez
cct
ez
PNC
4.50
ov
cep
ez
ez
PNC
cw2
ey
ey
cw1
ey
ez
ez
ey
cw2
zw
ez
ez
cwt
ez
ez
cct
4.51
ez
ov
ov
cap
ey
PNC
en
des
ov
PNC
4.52
ov
ov
cap
ey
ov
en
des
PNC
ec
ec
ec
4.53

Figure 4.54 Figure 4.54 is a macro lens photograph of the young fruit (yfr) on the female inflorescences as they would appear on jack pine (*Pinus banksiana*) in late August at the end of the first summer of development, circa August 20. The young fruit now had a more rounded appearance and had lost the bilateral flattening that characterized the unfertilized flower. The lower three-quarters of each fruit, proximal to the pedicel within the bract (br), were dark green, and the upper quarter was yellowish-green. Each stigma (s) had turned red. 1 cm scale bar = 5 mm.

Figure 4.55 Figure 4.55 is a light micrograph depicting a section of a young fruit at the same stage of development as seen in Figure 4.54. The globular embryo (ey) was comprised of about sixty to one-hundred cells, although specific tissues had not differentiated. The endosperm (en), growing by cell divisions and cell enlargement, had completely crushed all of the cells of the PNC, and these crushed cells could be seen at the base of the endosperm. The base of the endosperm, which had previously represented the uniseriate base of the original caecum, finally became multiseriate as those endosperm cells at the base underwent cell divisions in all planes (large open arrowhead). Three fruit zones could be distinguished within the young fruit. The innermost zone, or endocarp (ed), was immediately adjacent to the endosperm, and completely enveloped the endosperm on all sides. Most cells of the endocarp were isodiametric and had an empty appearance, as they were highly vacuolate. However, tannin-like materials (t) were present in the vacuoles in some of these endocarp cells, although the cells with tannin-like materials had a rather sporadic distribution within the endocarp. The endocarp was about five to ten cell layers in thickness. The mesocarp (me) was the next fruit zone immediately outside of the endocarp, and the mesocarp completely enveloped the endocarp on all sides. The mesocarp was about four to five cell layers in thickness, but the cells of the mesocarp were much smaller in median diameter than the cells of the endocarp. The cells of the mesocarp were slightly elongated and had prominent nuclei (small closed arrowheads), which were large relative to the volume of a mesocarp cell. Outside of the mesocarp was the outermost fruit zone, or exocarp, which was divided into an inner region of exocarp (exi) and an outer region of exocarp (exo). The inner exocarp was immediately adjacent to the mesocarp, possessed five to seven layers of vacuolate cells, and embedded the vascular tissues (not shown). The outer exocarp (the outer layer of the fruit) possessed five to seven layers of darkly stained cells. The cells of the exocarp were similar in median diameter to the cells of the endocarp. The two regions of exocarp enveloped nearly all of the mesocarp except for where the exocarp became confluent with the tissue of the pedicel (p) below the level of the endosperm. cap = cap of endosperm cells. Stain = TB, pH 4.4. 1 cm scale bar = 100 μm.

Figure 4.56 Figure 4.56 is a light micrograph depicting a magnified view of a section of a young fruit at approximately the same stage of development as seen in Figures 4.54 and 4.55. The embryo (ey) was as described in Figure 4.55, although it could be seen here that cells of the embryo were less vacuolate than the cells of the endosperm (en). Due to the increased size of the embryo, some of the endosperm cells adjacent to the expanding embryo had become compressed (large closed arrowheads). The endosperm had also increased in size, and in order to keep pace with the expanding mass of endosperm, outer peripheral endosperm cells (small closed arrowheads) adjacent to the endocarp (ed) were undergoing predominantly anticlinal divisions. Many of these outer peripheral endosperm cells became slightly compressed due to the pressure of the continued overall growth of the endosperm. The base of the endosperm was multiseriate (large open arrowhead). The crushed PNC was visible at the base of the endosperm. The endocarp was as described in Figure 4.55. The mesocarp and exocarp were out of the field of view. cap = cap of endosperm cells, t = tannin-like material, v = vacuole. Stain = CV. 1 cm scale bar = 25 μm.

Figure 4.57 Figure 4.57 is a light micrograph depicting a section of a young fruit sampled from the mid winter resting period (circa December 20), between the first summer and the second spring of development. The fruit had a similar internal appearance to fruits sampled in late summer, circa August 20 (see Figures 4.55 and 4.56 for details). Cells with tannin-like materials (t) were still sporadically distributed within the endocarp (ed) as they had been prior to the winter period. Notably, however, tannin-like materials (t) had apparently accumulated in the upper peripheral cells of the endocarp. cap = cap of endosperm cells, en = endosperm, ey = embryo, me = mesocarp, exi = inner exocarp, exo = outer exocarp. Stain = CV. 1 cm scale bar = 150 μm.


br
s
yfr
yfr
br
4.54

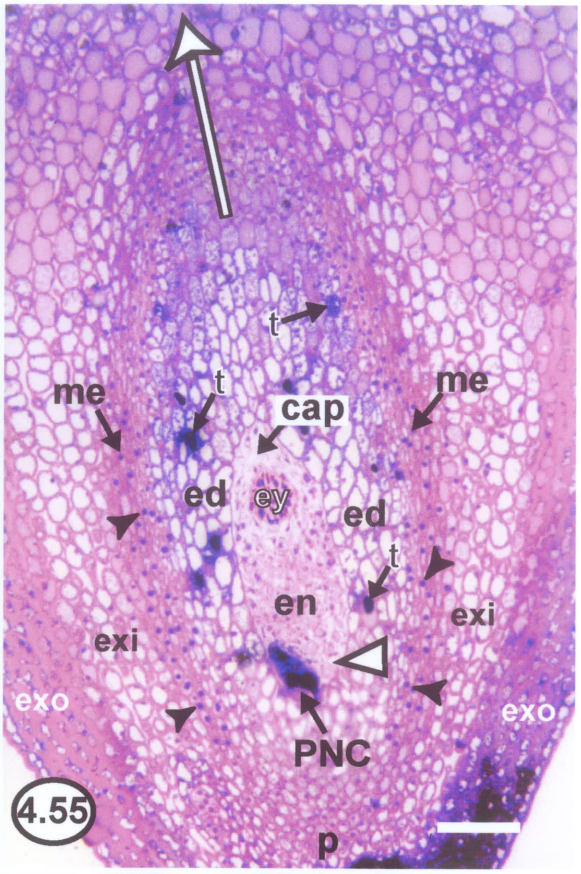
t
me
t
cap
me
ed
ey
ed
t
en
exi
exi
exo
exo
PNC
4.55
p

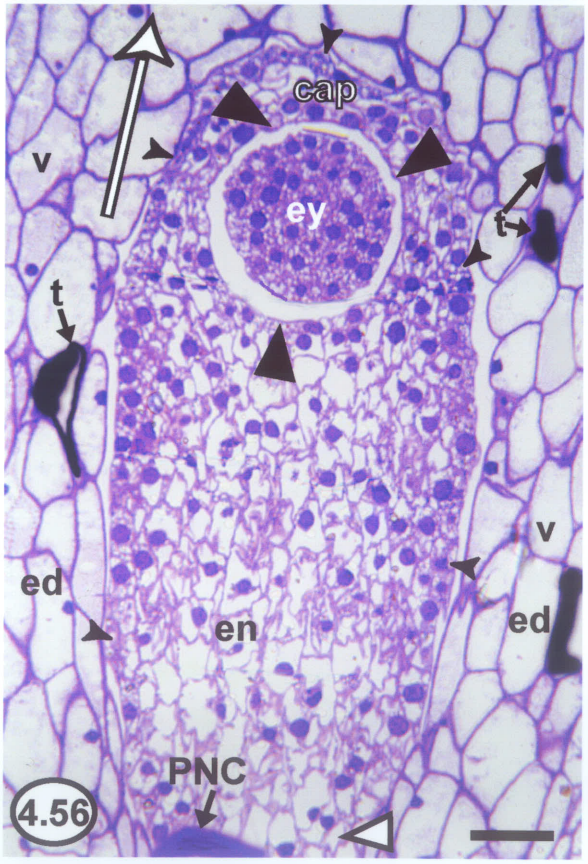
cap
v
ey
t
t
v
ed
ed
en
PNC
4.56

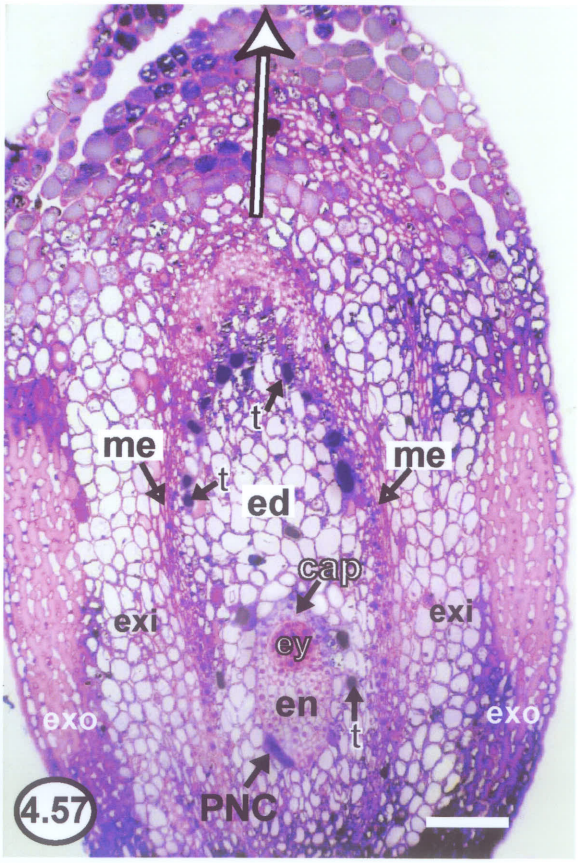
t
me
me
t
ed
cap
exi
exi
cy
en
t
exo
exo
PNC
4.57

Figure 4.58 Figure 4.58 is a light micrograph depicting a section of a young fruit sampled from mid May (circa May 17) of the second spring of development. The appearance and size of the embryo (ey) and endosperm (en) had not changed since late in the first summer, circa August 20. Development in the fruit had resumed, as changes were occurring in the mesocarp (me). Specifically, the innermost uniseriate layer of mesocarp to one side of the endocarp (ed) in the upper quarter of the fruit was beginning to differentiate into viscin cells (vi), which were beginning to elongate and secrete a mucilage. The elongation process was beginning to compress cells of both the endocarp and the inner exocarp (exi) in the vicinity of the elongating viscin cells (endocarp and inner exocarp cells compressed by elongating viscin cells are indicated by small closed arrowheads). Tannin-like materials (t) had now accumulated in most of the upper endocarp cells. Endocarp cells compressed by the elongating viscin cells were prone to accumulate tannin-like materials in their vacuoles. However, endocarp cells containing tannin-like materials in their vacuoles were still found in a sporadic distribution among the entire endocarp. Tannin-like materials were also beginning to accumulate within the vacuoles of both the inner exocarp cells and the outer exocarp cells (exo), particularly in the compressed cells of the inner exocarp. Remnants of the crushed PNC could still be seen at the base of the endosperm. cap = cap of endosperm cells. Stain = CV. 1 cm scale bar = 100 μm.

Figure 4.59 Figure 4.59 is a light micrograph depicting a section of a young fruit sampled from mid June of the second summer (circa June 16). Both the embryo (ey) and the endosperm (en) had increased in size. The embryo had increased in cell number to approximately two hundred cells and was still globular. The general appearance of the embryo had not changed, and no embryonic differentiation had occurred. The endosperm had more than doubled in length via cell divisions and cell enlargement. Two different zones could now be distinguished within the endosperm with regard to cell size and appearance. The first zone was essentially the base of the endosperm, and contained large cells with large vacuoles. These cells were designated Type 1 endosperm cells (tp_1). The second zone comprised the remainder of the endosperm and contained smaller, cytoplasm-rich cells with small vacuoles. These cells were designated Type 2 endosperm cells (tp_2). At this time, the second zone also included the cells of the cap (cap). More of the endosperm cells adjacent to the embryo had become compressed to accommodate the growth of the embryo (not indicated). Remnants of the crushed PNC could still be seen at the base of the endosperm. To account for endosperm growth, the endocarp cells (ed) adjacent to the expanded endosperm had become compressed (endocarp cells compressed by the expanded endosperm are indicated by large open arrowheads). Below the level of the endosperm, all endocarp cells became completely compressed and confluent with the mesocarp (confluent area indicated by ed+me). The cells of the confluent endocarp and mesocarp below the endosperm became tannin-filled (t). In the mesocarp (me), the innermost uniseriate mesocarp layer on all sides of the endocarp in the upper half of the fruit had developed into viscin cells (vi). Tannin-like material could be seen within some of the viscin cells. The elongation process continued to compress the cells of both the endocarp and the inner exocarp (exi) in the vicinity of the elongating viscin cells (endocarp and inner exocarp cells compressed by elongating viscin cells are indicated by small closed arrowheads). Thus, the endocarp cells were being compressed in one direction by the expanding endosperm, and in the opposite direction by the elongating viscin cells. Tannin-like materials continued to accumulate in the vacuoles of more cells of the endocarp, inner exocarp, and outer exocarp (exo) particularly in those cells that had been compressed. Stain = CV. 1 cm scale bar = 160 μm.

Figure 4.60 Figure 4.60 is a light micrograph depicting a section of a fruit at approximately the same stage of development as seen in Figure 4.59. This section was treated with aniline blue black (ABB) stain. All nuclei and cell walls stained blue. Cytoplasmic regions had a tendency to stain blue, whereas vacuolar contents tended to be negative for blue staining with ABB. The cells of the young, undifferentiated, globular embryo (ey) acquired more stain than the cells of the endosperm (en). Blue stained globules (small closed arrowheads) represented protein bodies. Protein bodies could be seen within the embryo, although there was no pattern to their location. Protein bodies were also seen in the endosperm cells, but they were more common in Type 2 endosperm cells (tp_2), including the cells of the cap (cap), than in Type 1 endosperm cells (tp_1). Protein bodies were rare but present within the cells of the endocarp (ed), inner exocarp (exi), and outer exocarp (exo). Overall though, the contents of the highly vacuolate endocarp and exocarp cells were essentially negative for blue staining with ABB. These cells appeared colourless if there were no tannin-like materials in the vacuoles, or greyish-black if tannin-like materials (t) were present. Viscin cell (vi) mucilage stained blue, whereas viscin cell contents were negative for blue staining with ABB. Most viscin cell contents were colourless, but sometimes the viscin cell contents stained greyish-black, indicating the presence of tannin-like materials in the vacuoles. The cells of the mesocarp (me) that had not differentiated into viscin tissue of either cell type contained relatively large nuclei, and because the proteinaceous nuclei were stained blue, these undifferentiated cells appeared quite blue relative to the cells of the endocarp and exocarp. Stain = ABB. 1 cm scale bar = 75 μm.

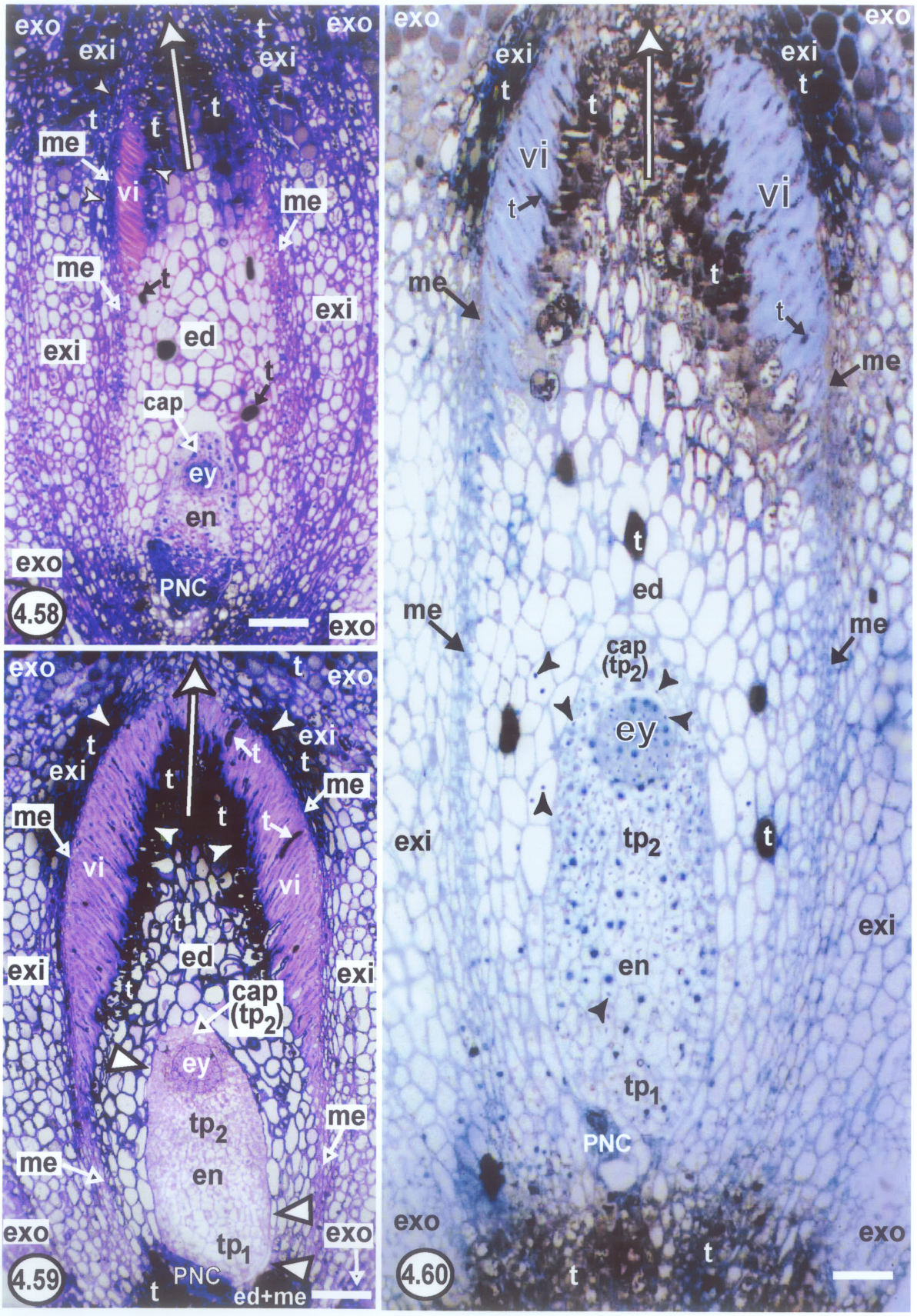
exo
exi
t
me
vi
ed
cap
ey
en
PNC
4.58
4.59
4.60
cap (tp2)
tp2
tp1
ed+me

Figure 4.61 Figure 4.61 is a light micrograph depicting a section of a young fruit sampled from late July (circa July 20) of the second summer of development. The embryo (ey) was at an undefined post-globular stage of embryo development. The size of the endosperm (en) had increased to a certain extent, but it was apparent that the rate of endosperm growth was slowing relative to that of the embryo. Endosperm cells in the cap (cap) had changed from Type 2 (tp_2) cells (cytoplasm-rich and small) to Type 1 (tp_1) cells (vacuolate and large). Type 2 endosperm cells could be observed in the central region of the endosperm. The growing endosperm, as well as the enlarging embryo, continued to compress endocarp cells (ed) adjacent to the endosperm (endocarp cells compressed by the enlarging embryo and endosperm are indicated by large open arrowheads). Changes continued in the mesocarp (me). Specifically, the innermost uniseriate mesocarp layer on all sides of the endocarp in the upper two-thirds of the fruit had developed into elongated, mucilaginous viscin cells (vi). Tannin-like material (t) could be seen within some of the viscin cells. The elongation process had continued to compress the cells of the endocarp and inner exocarp (exi) in the vicinity of the elongating viscin cells (endocarp and inner exocarp cells compressed by elongating viscin cells are indicated by small closed arrowheads). Thus, the endocarp continued to be compressed from all directions. Tannin-like materials continued to accumulate in the vacuoles of even more cells of the endocarp, inner exocarp, and outer exocarp (exo) particularly in those cells that had been compressed. Stain = CV. 1 cm scale bar = 115 μm.

Figure 4.62 Figure 4.62 is a light micrograph depicting a magnified view of the embryo (ey), endosperm (en), and endocarp (ed) seen in Figure 4.61. Cells in the inner region of the embryo had also become slightly vacuolate (v) and enlarged. The outer layer of embryonic cells was still very cytoplasm-rich, and had undergone anticlinal divisions to form the uniseriate protoderm (pd). Compressed endosperm cells continued to be observed adjacent to expanding embryo (endosperm cells compressed by the expanding embryo are indicated by large closed arrowheads). cap = cap, t = tannin-like materials, tp_1 = Type 1 endosperm cells, tp_2 = Type 2 endosperm cells, v = vacuole. Stain = CV. 1 cm scale bar = 50 μm.

Figure 4.63 Figure 4.63 is a light micrograph depicting a section of a fruit at approximately the same stage of development as seen in Figures 4.61 and 4.62. The section was subjected to the Periodic Acid - Schiff's (PAS) treatment. All cell walls stained pink, indicating the presence of carbohydrates in the cell walls. Pink stained granules represented starch grains in amyloplasts (small closed arrowheads). Starch grains could be seen within the embryo (ey), where they appeared to be limited to the lower peripheral regions of the embryo. In the endosperm (en), starch grains were common only in the Type 2 endosperm cells (tp_2), although starch grains appeared to be lacking in Type 2 endosperm cells enveloping the lower two-thirds of the embryo. Endosperm cells in the cap (cap) and at the base of the endosperm, which were all Type 1 cells (tp_1), contained only a few starch grains. Notably, all of the peripheral cells of the entire endosperm appeared to be completely devoid of starch grains (peripheral endosperm cells indicated by large open arrowheads). A few endocarp cells (ed) also contained starch grains. Nonetheless, the contents of the highly vacuolate endocarp, inner exocarp (exi), and outer exocarp cells (not shown) were essentially negative for the PAS treatment. These cells appeared colourless if there were no tannin-like materials in the vacuoles, or greyish if tannin-like materials (t) were present. The viscin cell (vi) mucilage stained pink, and there were apparently a few starch grains in the viscin cells. Overall, the cell contents of most viscin cells were colourless and thus also negative for the PAS treatment. However, tannin-like materials in a few of the viscin cells stained greyish. The contents of the undifferentiated mesocarp cells (me) were colourless. The PNC could be observed below the endosperm. Stain = PAS. 1 cm scale bar = 85 μm.

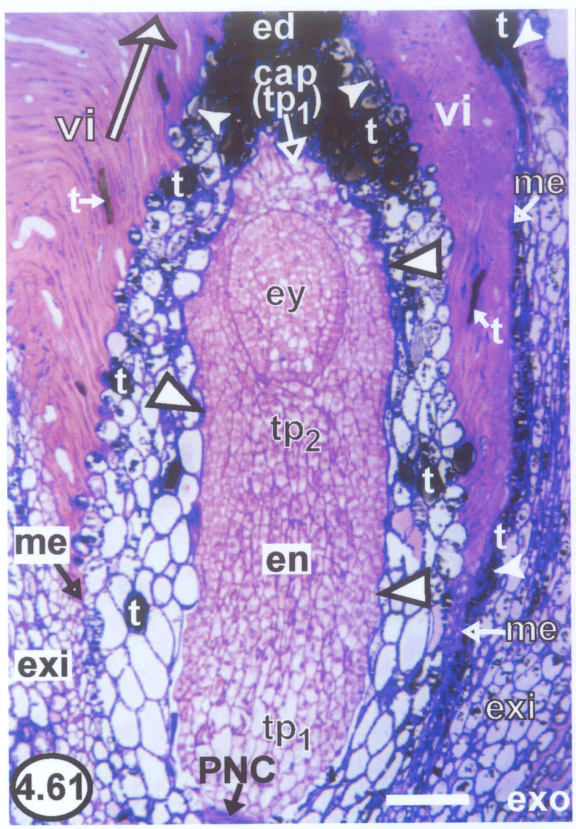
ed
cap
(tp1)
t
vi
vi
t
t
me
ey
t
t
tp2
t
me
en
t
t
me
exi
t
me
exi
tp1
PNC
4.61
exo

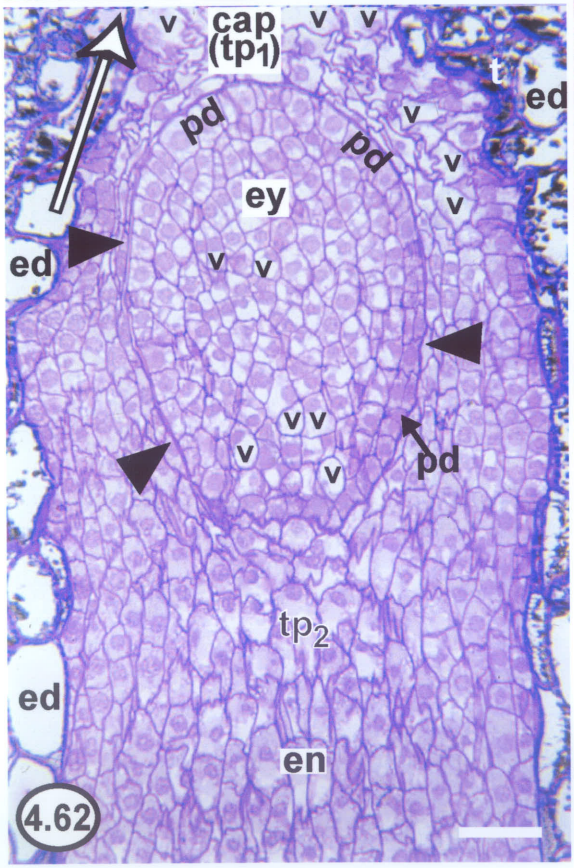
v
cap
(tp1)
v
v
t
ed
pd
pd
v
v
ey
v
ed
v
v
v
v
pd
v
v
tp2
ed
en
4.62

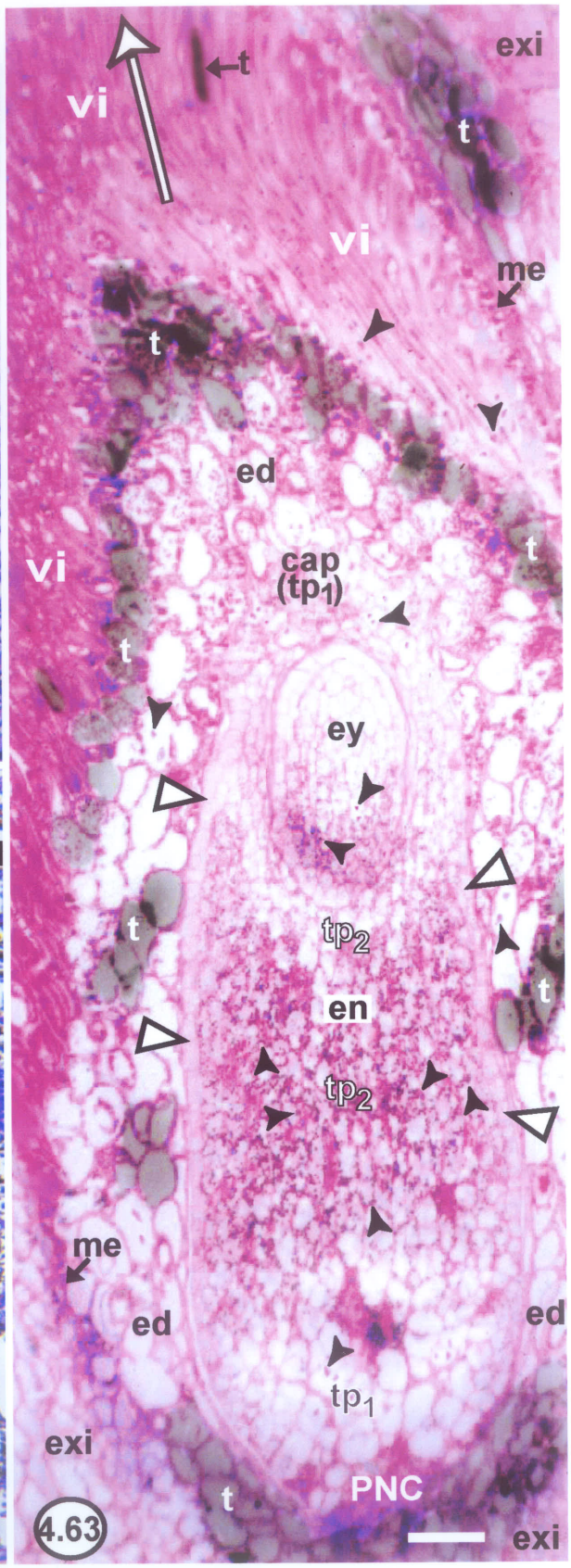
exi
vi
t
t
vi
me
t
ed
vi
t
cap
(tp1)
t
t
ey
tp2
t
en
t
tp2
me
ed
ed
tp1
exi
t
PNC
4.63
exi

Figure 4.64 Figure 4.64 is a light micrograph depicting a section of a young fruit sampled from early August of the second summer (circa August 5). The embryo (ey) had reached its maximum girth, but had continued to expand in an upward longitudinal direction, thus obtaining an elongated ovoid appearance. The endosperm (en) acquired a vase-like appearance because the vacuolate Type 1 endosperm cells (tp_1) both at the base of the endosperm and in the cap (cap) had enlarged to an even greater extent via their expanding vacuoles (v). Type 2 endosperm cells (tp_2) could be seen in the central region of the endosperm. The crushed remnants of the PNC could still be observed at the base of the endosperm. The mesocarp no longer existed as such, as changes had occurred in all mesocarp cells. Specifically, all of the cells in the innermost uniseriate layer of mesocarp in the upper three-quarters of the fruit had now developed into viscin cells (vi). The viscin cells had elongated to their fullest extent but continued to secrete mucilage. Tannin-like material (t) could still be seen within some of the viscin cells. Also, the remaining outer three to four cell layers in the upper three-quarters of the mesocarp had differentiated into enlarged, isodiametric vesicular cells (vc). The lower quarter of the mesocarp would not differentiate into viscin tissue of either cell type, but would instead become completely tannin-filled and a part of the pseudoseed coat (psc). All of the endocarp cells, which had now become compressed and tannin-filled, would comprise the remainder and majority of the pseudoseed coat. Cells of the inner exocarp (exi) immediately adjacent to the now evident vesicular cells had all been fully compressed and their vacuoles had all become filled with tannin-like materials (compressed cells of the inner exocarp cells are indicated by small closed arrowheads). Additionally, more cells of both the inner exocarp and the outer exocarp (exo) were continuing to accumulate tannin-like materials in their vacuoles, although not to the extent of the compressed cells of the inner exocarp. Stain = CV. 1 cm scale bar = 215 μm.

Figure 4.65 Figure 4.65 is a light micrograph depicting a PAS-treated section of an embryo (ey), portion of endosperm (en), and portion of the pseudoseed coat (psc) at approximately the same stage of development as seen in Figure 4.64. Small closed arrowheads indicate starch grains. Starch grains could be seen within the embryo, where they were still limited to the lower peripheral regions of the embryo. The majority of the cells in the inner region of the embryo still possessed large vacuoles (v). However, the radicular apex (ra) was now evident and represented by a cluster of cytoplasm-rich cells at the upper pole of the embryo. The cells of the protoderm (pd) maintained their cytoplasm-rich appearance. The Type 2 endosperm cells (tp_2) enveloping the lower two-thirds of the embryo had now accumulated starch grains. As was previously observed, Type 1 endosperm cells (tp_1) of the cap region (cap) contained only a few starch grains and large vacuoles (v). All peripheral cells of the endosperm now appeared to contain a few starch grains (peripheral cells indicated by large open arrowheads). The starch grains of the endosperm were relatively larger than the starch grains in the embryo. Cells of the endosperm, notably those cells in the cap immediately adjacent to the radicular apex of the embryo, continued to be compressed in order to accommodate the upward growth of the embryo (endosperm cells compressed by the expanding embryo are indicated by large closed arrowheads). t = tannin-like materials. Stain = PAS. 1 cm scale bar = 50 μm.

Figure 4.66 Figure 4.66 is a light micrograph depicting a non-median section of a fruit at approximately the same stage of development as seen in Figures 4.64 and 4.65. The section was treated with ABB. There was no change in the general distribution of the ABB stain in the embryo (ey), endosperm (en), and viscin cells (vi) from what was seen earlier in development in mid June of the second summer, circa June 16 (review details in Figure 4.60). Protein bodies cannot be clearly seen here, but their distribution in the embryo and endosperm (see details in the following Figure 4.67) remained basically the same as what was seen previously (review details in Figure 4.60). However, the endosperm cells of the cap (cap), having developed from Type 2 (tp_2) endosperm cells into Type 1 (tp_1) endosperm cells, now possessed fewer protein bodies (review Figure 4.60 and see the following Figure 4.67 for details). This was because protein bodies were typically more common in Type 2 endosperm cells than in Type 1 endosperm cells (review Figure 4.60). The vesicular cells (vc) were negative for blue staining with ABB. Tannin-like materials (t) had a tendency to appear greyish-black in the presence of the ABB stain, although they were still negative for the blue staining of ABB. Tannin-like materials had accumulated in the vacuoles of all cells of the pseudoseed coat (psc). Also, tannin-like materials had accumulated in the vacuoles of many cells of the inner exocarp (exi) and outer exocarp (exo), especially within the compressed cells of the inner exocarp (compressed cells of the inner exocarp are indicated by small closed arrowheads). These areas that had accumulated tannin-like materials in their vacuoles had a tendency to appear greyish-black overall. If protein bodies remained in the exocarp or endocarp (now the majority of the pseudoseed coat), the greyish-black staining obscured them. Stain = ABB. 1 cm scale bar = 280 μm.

Figure 4.67 Figure 4.67 is a light micrograph depicting a magnified view of the embryo (ey), portion of the endosperm (en), and portion of the pseudoseed coat (psc) seen in Figure 4.66. The non-median section was treated with ABB. There was no change in distribution of the ABB stain in the embryo and endosperm cells from what was seen previously (review details in Figure 4.60). Small closed arrowheads indicate protein bodies. Protein bodies could be seen within the embryo and endosperm. The cap cells (cap) were now Type 1 cells (tp_1), and possessed fewer protein bodies than when the cap cells were Type 2 endosperm cells (review Figure 4.60). Because all cells of the pseudoseed coat had accumulated tannin-like materials (t) in their vacuoles, these areas had a tendency to appear greyish-black overall and thus remained negative for blue staining with ABB. If protein bodies still remained in the endocarp (the majority of the pseudoseed coat), the greyish-black staining obscured them. tp_2 = Type 2 endosperm cells. Stain = ABB. 1 cm scale bar = 50 μm.

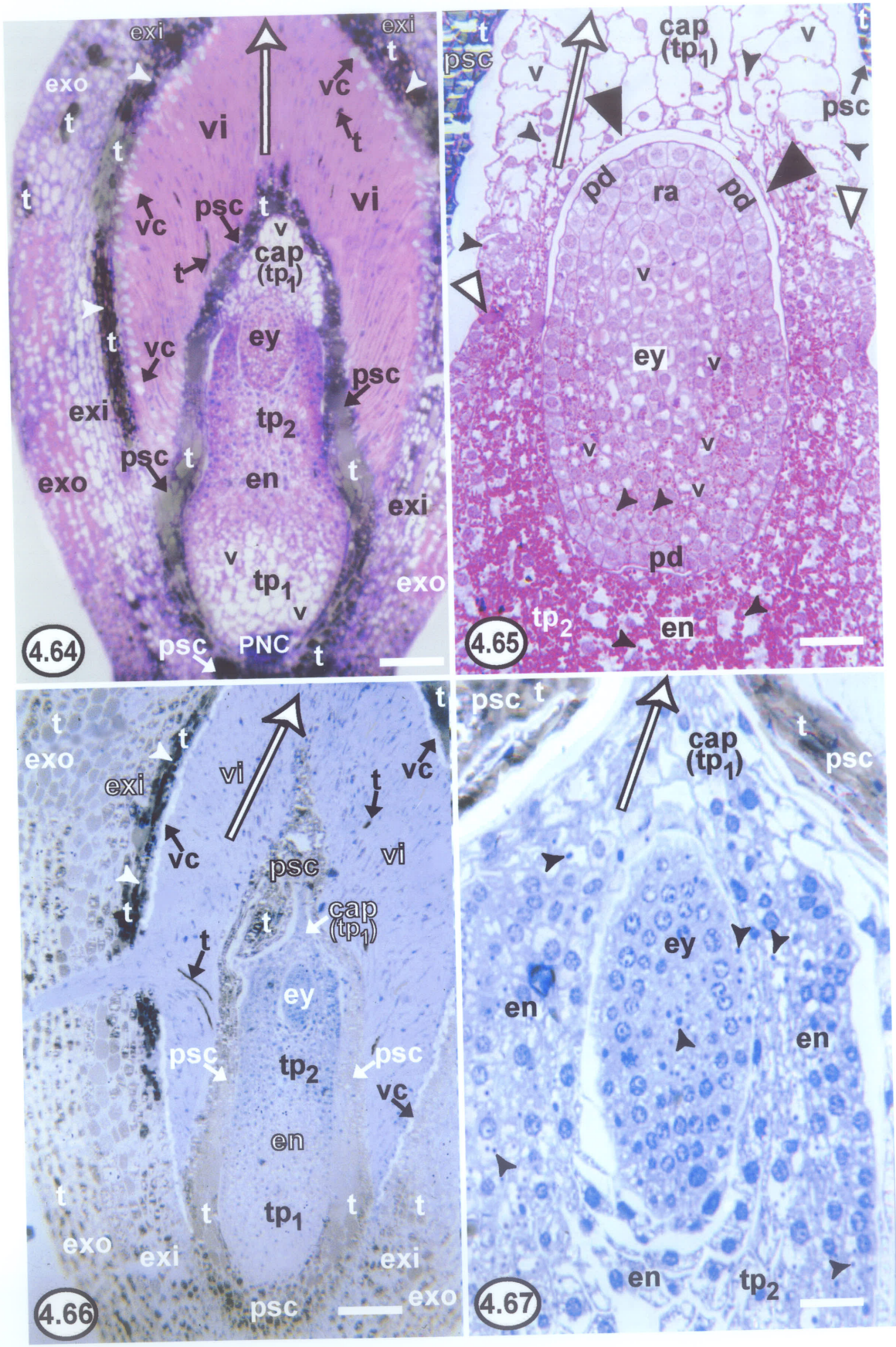
exi
exo
t
vi
vc
psc
v
cap
(tp1)
ey
tp2
en
PNC
4.64
cap
(tp1)
pd
ra
tp2
4.65
4.66
4.67

Figure 4.68 Figure 4.68 is a light micrograph depicting a non-median section of a fruit at approximately the same stage of development as seen in Figures 4.64, 4.65, 4.66, and 4.67. The section was treated with the metachromatic stain Toluidine blue O (TB) at a pH of 4.4, and the cytochemistry of the various regions within the fruit was of interest. The embryo (ey) as a whole stained purple. There was no particular staining pattern in the endosperm (en), although the vacuolate Type 1 endosperm cells (tp_1), including those in the cap (cap), acquired less stain than the cytoplasm-rich Type 2 (tp_2) endosperm cells. All peripheral cells of the endosperm (comprised of both Type 1 and Type 2 cells and including the peripheral cells of the cap) also stained purple (peripheral endosperm cells are indicated by large open arrowheads). Tannin-like materials (t) that had accumulated in vacuoles of the pseudoseed coat (psc) cells, the inner exocarp cells (exi), and outer exocarp cells (exo) stained greenish-blue. The viscin cell (vi) mucilage stained pink, whereas the majority of the viscin cell contents did not take up the TB stain. However, the few tannin-like materials in the viscin cells stained greenish-blue. Starch grains (small closed arrowheads) were also observable in the viscin cells, although the starch grains were unstained and thus recognizable only by their shape and appearance. The enlarged vesicular cells (vc) were essentially negative for the TB stain. The PNC was visible at the base of the endosperm. Stain = TB, pH 4.4. 1 cm scale bar = 140 μm.

Figure 4.69 Figure 4.69 is a light micrograph depicting a section of a fruit at approximately the same stage of development as seen in Figures 4.64 through 4.68 was sectioned, and showed the presence of two embryos, or "twins". Each embryo was found in its own endosperm. One embryo (ey_t) and its endosperm (en_t) had a similar appearance to the typical embryo and endosperm found at this developmental time period circa August 5 (review Figure 4.64). The typical embryo (ey_t) possessed a radicular apex (ra) with cytoplasm-rich cells, a protoderm (pd) with cytoplasm-rich cells, and an inner region with relatively vacuolate (v) cells, as would be expected in an embryo observed circa August 5 of the second summer. The endosperm (en_t) associated with the typical embryo possessed Type 1 endosperm cells (tp_1) at the endosperm base, and Type 2 endosperm cells (tp_2) in the central region of the endosperm, as would also be expected. The cap cells (cap_t) of this typical endosperm had developed from cytoplasmic Type 2 endosperm cells into vacuolate Type 1 endosperm cells, as would be expected. However, the second embryo (ey_l) and its endosperm (en_l), were lagging in development. They were smaller than the typical embryo and endosperm. No obvious differentiation was evident in the embryo. Although the two types of endosperm cells were visible in the endosperm, the cap (cap_l) of the lagging endosperm had not become vacuolate and thus had not developed from Type 2 cells into Type 1 cells. The fruit tissues, including the pseudoseed coat (psc), viscin cells (vi), vesicular cells (not shown), and exocarp (not shown) enveloping the two embryos and endosperms had a similar appearance to the typical fruit tissues sampled at this time in early August, circa August 5 (review Figures 4.64, 4.66, and 4.68). There was only one region where crushed PNC cells could be observed. t = tannin-like material. Stain = CV. 1 cm scale bar = 100 μm.

Figure 4.70 Figure 4.70 is a macro lens photograph of the ripe, mature fruit (fr) on the female inflorescences as they would appear on jack pine (*Pinus banksiana*) in late August in the second summer (circa August 20). The fruits had reached their maximum size. Along with the ripe fruit ready to discharge their contents, young first year fruits (yfr) were also evident on the same shoot. Additionally, incipient, pre-meiotic, pre-anthesis flowers (paf) developing in the summer prior to the predefined first spring of development (when anthesis occurs) could also be observed. In the ripe fruit, the yellow pedicels (p) had elongated to about 2 mm in length, and could be seen outside of the cup-like bract (br). The pedicels were recurved, and thus the fruits were somewhat droopy. The lower three-quarters of each fruit, proximal to the pedicel, were still dark green, and the upper quarter was still yellowish-green. Each stigma (s) was still reddish. There were typically up to three ripe fruits in a cyme, although it was not uncommon to see aborted individuals (ai) in the cyme alongside ripe fruit. Sometimes it was apparent that a fruit had prematurely dropped out of the cyme, as there were some bracts where the pedicel could no longer be observed (small closed arrowhead). 1 cm scale bar = 4 mm.

Figure 4.71 Figure 4.71 is a light micrograph depicting a section of a ripe fruit of a similar stage in development as seen in Figure 4.70). The section was stained with the Yeung procedure. Most of the main components of the pseudoseed held within the fruit can be seen. The embryo (ey) had elongated at its radicular pole and had crushed but not obliterated the cells of the cap (cap). Within the embryo, the cells of the previously differentiated protoderm (pd) and radicular apex (ra) remained cytoplasm-rich. The procambium (pc) had differentiated, and was represented by three to four files of highly cytoplasmic cells in the central column of the upper two-thirds of the embryo. The remainder of the embryonic cells lying between the procambium and the protoderm represented the differentiating cells of the ground meristem (gm), which still contained vacuoles (v). Starch grains stained pink with the Yeung procedure (starch grains are represented by small closed arrowheads). The ground meristem possessed most of the starch grains of the embryo. Rudimentary cotyledons (ct) could be seen at the lower pole of the embryo, which represented the rudimentary shoot apex. Starch grains were now extremely abundant in the Type 2 endosperm cells (tp_2) surrounding the lower two-thirds of the embryo. The crushed cells of the cap (cap) stained pink from the Yeung procedure. Similarly, the viscin cell (vi) mucilage stained pink. For the most part, the viscin cell contents remained colourless after treatment with the Yeung procedure. However, the tannin-like materials (t) within a few of the viscin cells stained greenish-blue. The tannin-filled cells of the pseudoseed coat (psc) also stained greenish-blue with the Yeung procedure. en = endosperm. Stain = Yeung procedure. 1 cm scale bar = 90 μm.

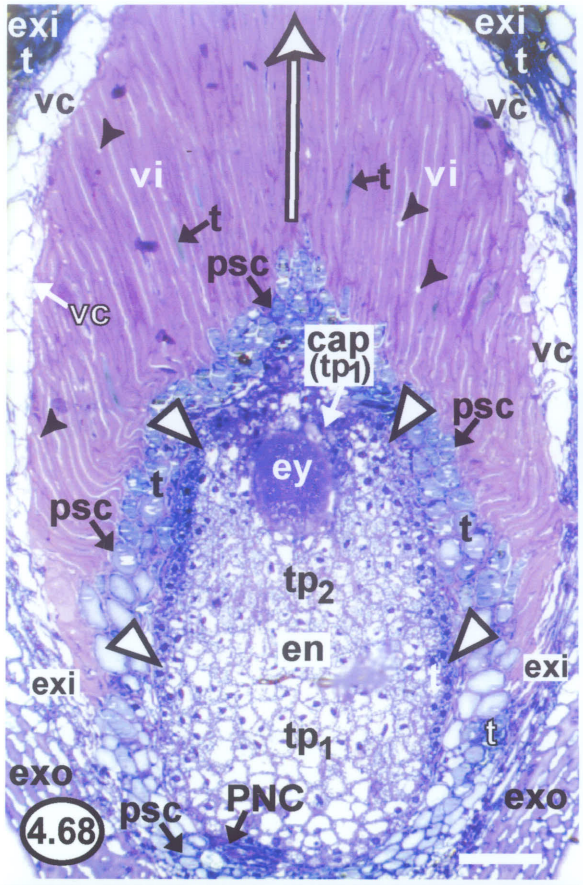
exi
t
vc
vi
t
psc
vc
cap
(tp1)
psc
ey
t
psc
t
tp2
en
exi
exi
tp1
t
exo
psc
PNC
exo
4.68

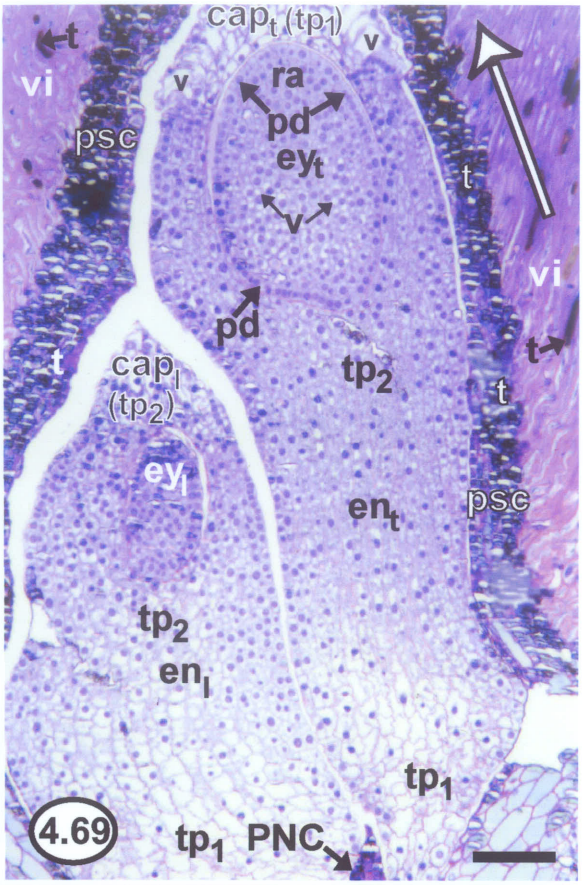
t
vi
v
capt (tp1)
v
ra
pd
eyt
v
t
vi
psc
pd
t
capl
(tp2)
tp2
t
t
eyl
entpsc
tp2
enl
tp1
tp1
PNC
4.69

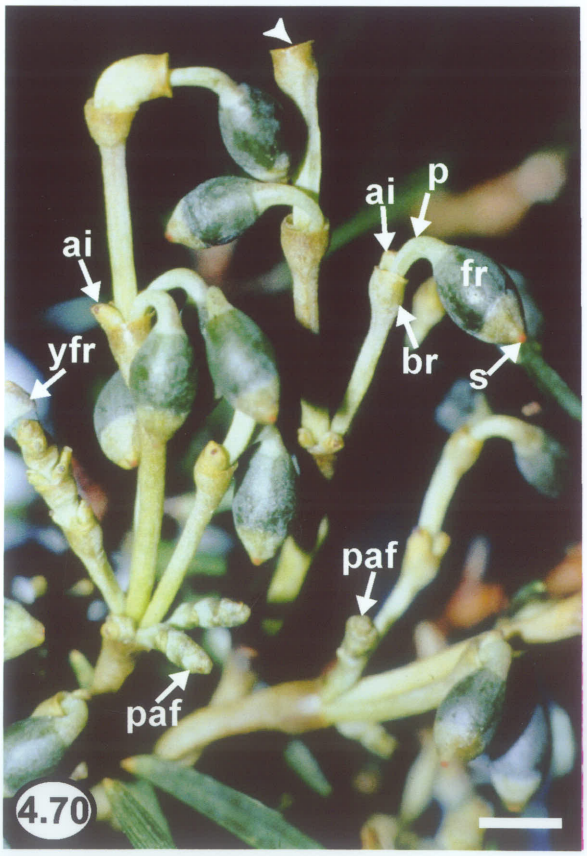
ai
p
ai
fr
yfr
br
s
paf
paf
4.70

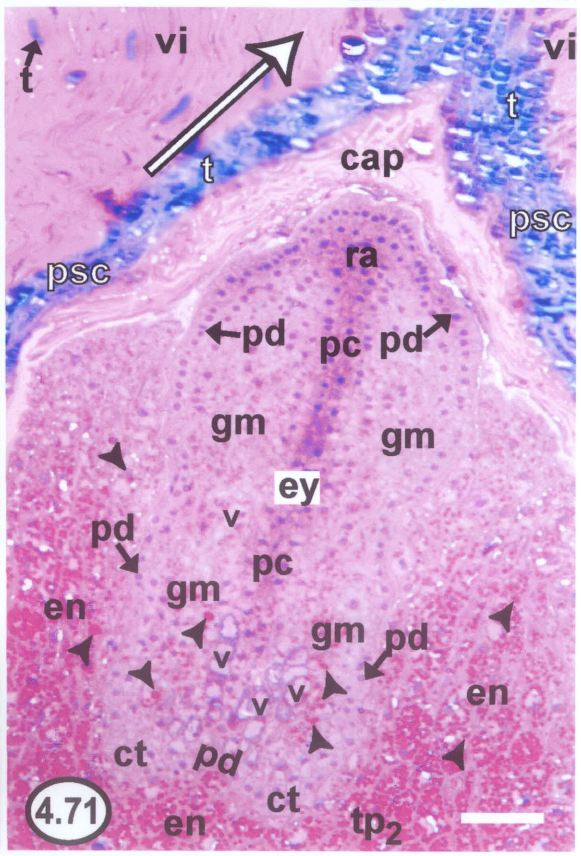
t
vi
vi
t
t
cap
psc
psc
ra
pd
pc
pd
gm
gm
ey
v
pd
pc
gm
en
gm
pd
v
v
v
en
ct
pd
ct
en
tp2
4.71

Figure 4.72 Figure 4.72 is a montage of two light micrographs depicting sections of a ripe fruit at a similar stage in development as seen in Figures 4.70 and 4.71. The sections were treated with Sudan Black B (SBB) stain. Most of the main components of the pseudoseed held within the fruit can be seen. Cell walls, nuclei, and starch grains were essentially negative for staining with SBB, although the cell wall boundary (large open arrowheads) around the radicular apex (ra) of the embryo (ey) appeared to be stained quite black, indicating a lipid component. In the embryo, most procambium (pc) cells as well as a few ground meristem (gm) cells in the area of the cotyledons (ct) were completely filled with a very darkly stained material representative of lipid components (small closed arrowheads in the embryo). Type 2 endosperm cells (tp_2) enveloping the lower two-thirds of the embryo also contained a few black globules, which were representative of lipid bodies (small closed arrowheads in the endosperm). The compressed endosperm cells in the cap (cap) were negative for the SBB stain. The cells of the pseudoseed coat (psc) were positive for the stain, especially in the regions adjacent to the crushed cap, but the positive staining reaction was most likely a reaction with the tannin-like materials (t). en = endosperm, pd = embryonic protoderm. Stain = SBB. 1 cm scale bar = 35 μm.

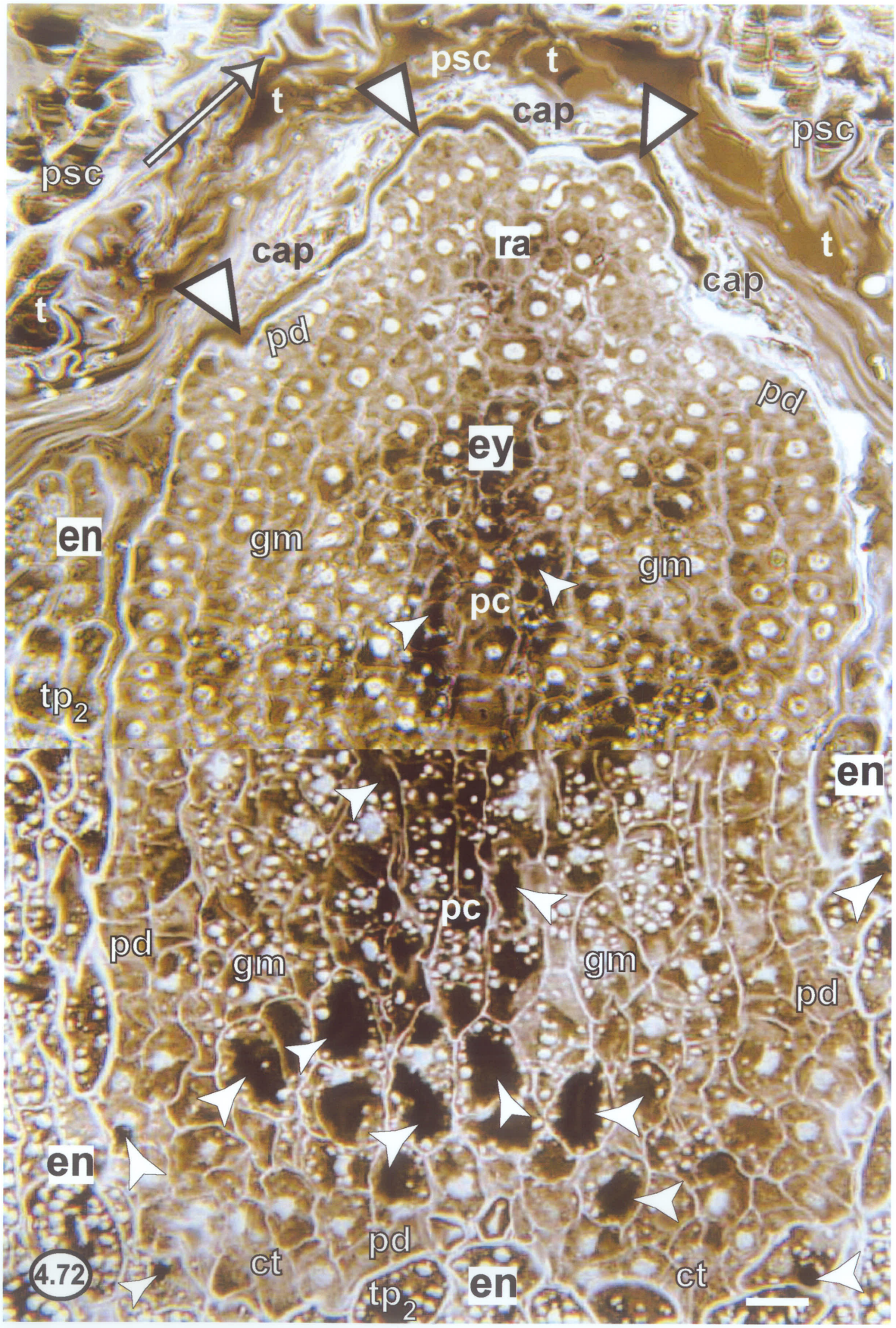
psc
t
cap
psc
t
psc
t
cap
ra
t
cap
t
pd
pd
ey
en
gm
gm
pc
tp2
en
pc
pd
gm
gm
pd
en
4.72
ct
pd
tp2
en
ct

Figure 4.73 Figure 4.73 is a light micrograph depicting a cross section of a ripe fruit of a similar stage in development as seen in Figure 4.70, 4.71, and 4.72. Most of the main components of the pseudoseed held within the fruit can be seen. This particular section features the vascular traces, which appeared to be comprised entirely of xylem tissue (x) (including parenchyma), as no obvious phloem tissue was observed. Two vascular traces could be seen within the inner exocarp (exi), just outside of the compressed cells of the inner exocarp (compressed cells of the inner exocarp are indicated by small closed arrowheads). The vascular traces were only about five to eight cells in diameter. The cell walls of the xylem vessel elements (not indicated) stained purplish. en = endosperm, exo = outer exocarp, ey = embryo, psc = pseudoseed coat, t = tannin, tp_2 = type 2 endosperm cells, vc = vesicular cells, vi -= viscin cells. Stain = CV. 1 cm scale bar = 150 μm.

Figure 4.74 Figure 4.74 is an electron micrograph depicting a section of a ripe fruit of a similar stage in development as seen in Figure 4.70 through 4.73. A xylem vessel element (xve) in a vascular trace could be seen in longitudinal section and was embedded among cells of the inner exocarp (exi). The cell wall (cw) of the vessel element displayed helical type secondary wall thickenings (h). Commonly, vessel elements in the fruit possessed cytoplasm as well as organelles, and thus appeared viable. The elongated nucleus (n) of the vessel element could be seen and it possessed fairly condensed chromosomal material (ch). The cytoplasm of the vessel element was relatively dark staining, and contained a large number of mitochondria (mt) as well as a few osmiophilic bodies (ob). No obvious phloem tissue was seen in the vicinity of the xylem vessel element. Stain = UA/LC. 1 cm scale bar = 3 μm.

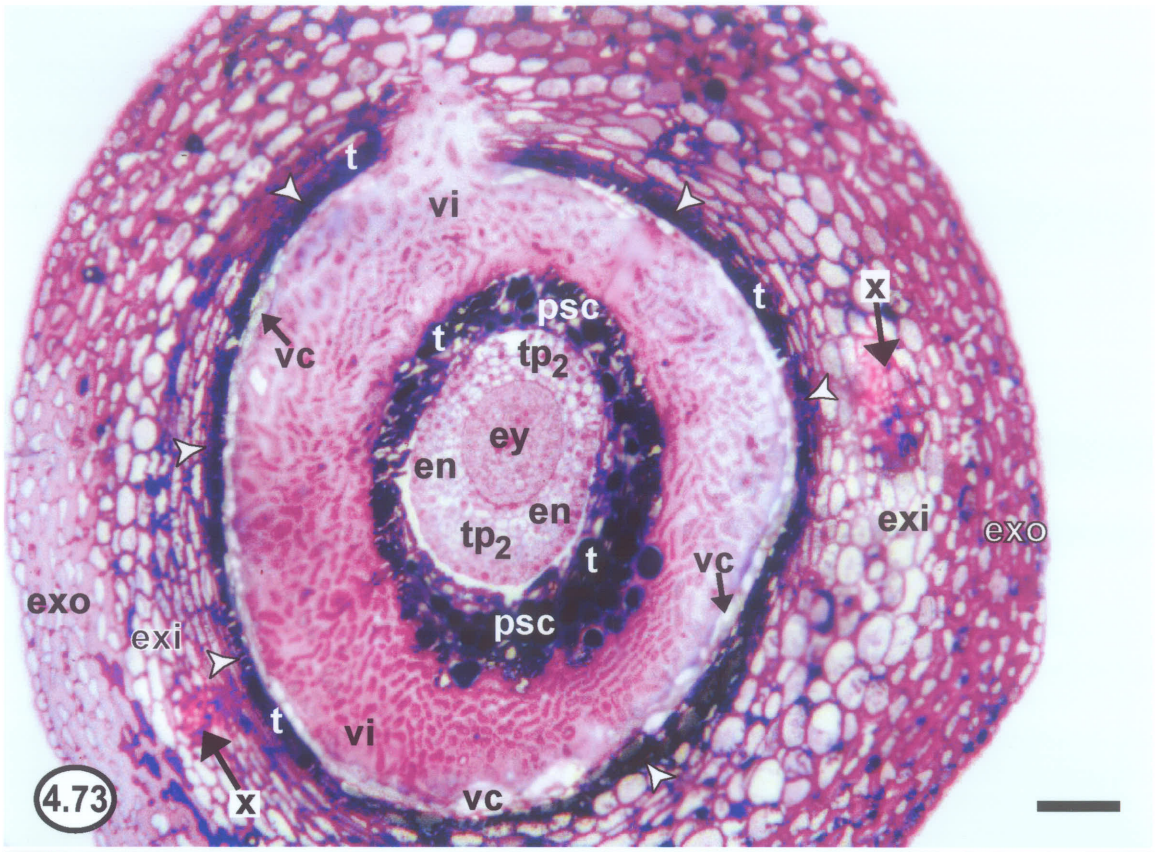
t
vi
t
x
psc
vc
t
tp2
ey
en
en
tp2
t
vc
exi
exo
exo
exi
psc
t
vi
x
vc
4.73

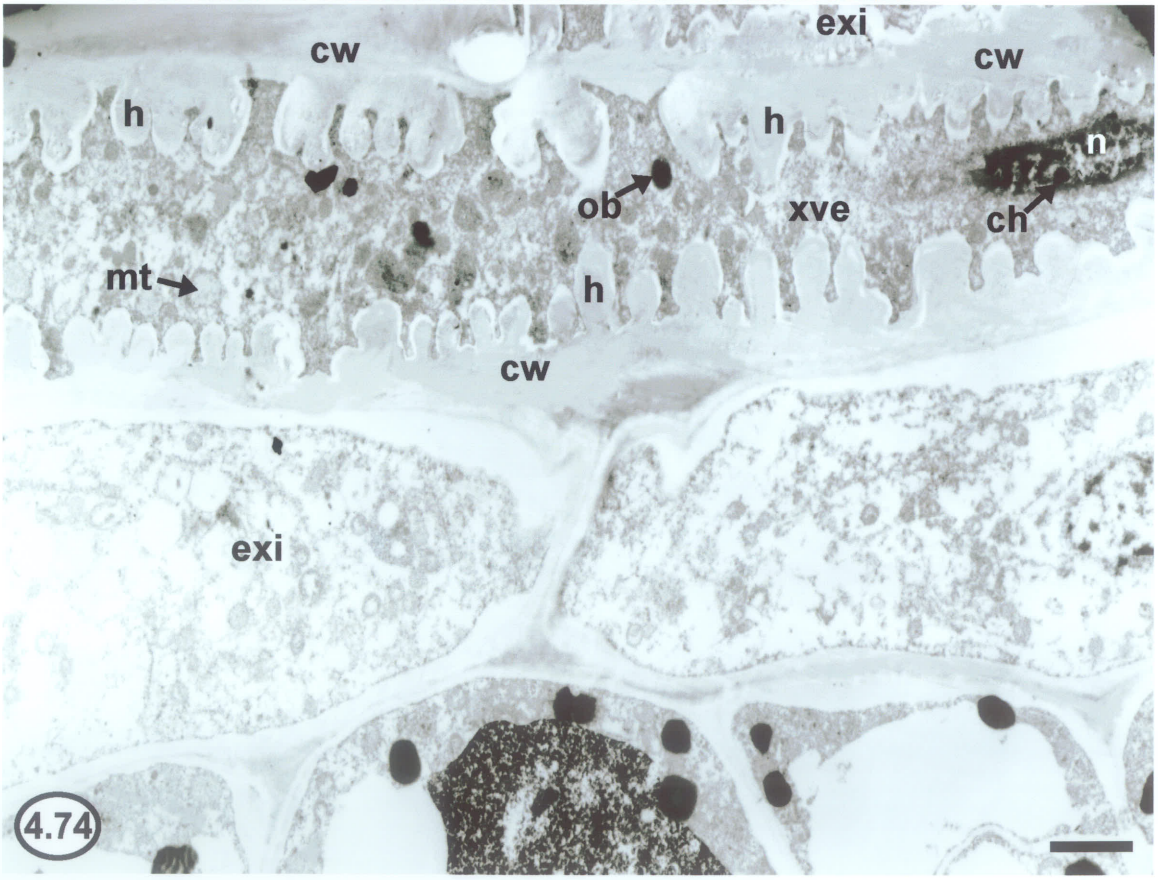
exi
cw
cw
h
h
n
ob
xve
ch
mt
h
cw
exi
4.74

Figure 4.75 Figure 4.75 is a micrograph of a whole, naturally discharged pseudoseed photographed through a dissecting light microscope. The pseudoseed was sampled from a cheesecloth wrap collected in the last week of August (circa August 25). Discharged pseudoseeds captured in cheesecloth wraps all had the same external appearance regardless of when the wraps were collected from the last week of August to the first week of October. Although the stigma was not a part of the discharged pseudoseed, its direction is still given by the large arrow in order to preserve the original orientation defined earlier. Mucilaginous, nacreous but slightly green viscin cells (vi) enveloped the tanniferous, brown pseudoseed coat (psc). This specimen was preserved in modified Karnovsky's fixative, but unfixed material had the same appearance (not shown). As vesicular cells were not part of the discharged pseudoseed, no vesicular cells were observed. t = tannin-like materials. 1 cm scale bar = 250 μm.

Figure 4.76 Figure 4.76 is a light micrograph depicting a section of a discharged pseudoseed. This pseudoseed was sampled from a cheesecloth wrap collected in the last week of August (August 25) and was at approximately the same stage of development as seen in Figure 4.75. Discharged pseudoseeds had similar internal appearances regardless of the cheesecloth wrap collection time. A discharged pseudoseed had nearly the same appearance as it did when it was still inside the exocarp of the fruit prior to explosive discharge. The large arrow indicates the original direction of the stigma. Most of the main components of the discharged pseudoseed can be seen. Within the embryo (ey), the cells of the procambium (pc) and radicular apex (ra) remained cytoplasm-rich, and the ground meristem (gm) still contained vacuoles (v). However, the cells of the embryonic protoderm (pd) found above the radicular apex had now developed vacuoles (v), despite the fact that these protodermal cells had previously been cytoplasm-rich. The rudimentary cotyledons of the rudimentary shoot apex were just out of the plane of section, although their location is indicated (ct). In the endosperm (en), Type 1 (tp_1) and Type 2 endosperm cells (tp_2) could be seen. The entire endosperm had contracted so that the endosperm had lost some length and gained some width. Moreover, the endosperm tissue also appeared to possess more intercellular spaces (large open arrowheads) especially in the region of the Type 2 endosperm cells. The vacuolate Type 1 endosperm cells now appeared to be filled with a tannin-like material (t). The PNC at the base of the endosperm was out of the plane of section. cap = endosperm cells of the cap, psc = pseudoseed coat, vi = viscin. Stain = CV. 1 cm scale bar = 150 μm.

Figure 4.77 Figure 4.77 is a micrograph of a discharged pseudoseed photographed through a dissecting light microscope. This pseudoseed was sampled from a cheesecloth wrap collected in the last week of August (August 25) and was at approximately the same stage of development as seen in Figures 4.75 and 4.76. The pseudoseed had been treated with 2, 3, 5-triphenyl tetrazolium chloride (2, 3, 5-TTC). The results of 2, 3, 5-TTC staining on discharged pseudoseeds were similar regardless of the cheesecloth wrap collection time. The large arrow indicates the original direction of the stigma. This embryo (ey) had stained red. The viscin cells (vi) had a faint red tinge after staining. The pseudoseed coat cells (psc), which were filled with tannin-like materials (t), were not red stained. Only the upper portion of the endosperm (en) in the regions that were adjacent to the embryo were red stained and thus only Type 2 (tp_2) endosperm cells were potentially viable. Due to the dissection process, cells in the cap could not be readily observed. There were no changes in the results regarding the viability of the various pseudoseed components over three cheesecloth wrap collection times in August, September and October at the end of the second summer of development. tp_1 = type 1 endosperm cells. Stain = 2, 3, 5-TTC. 1 cm scale bar = 260 μm.

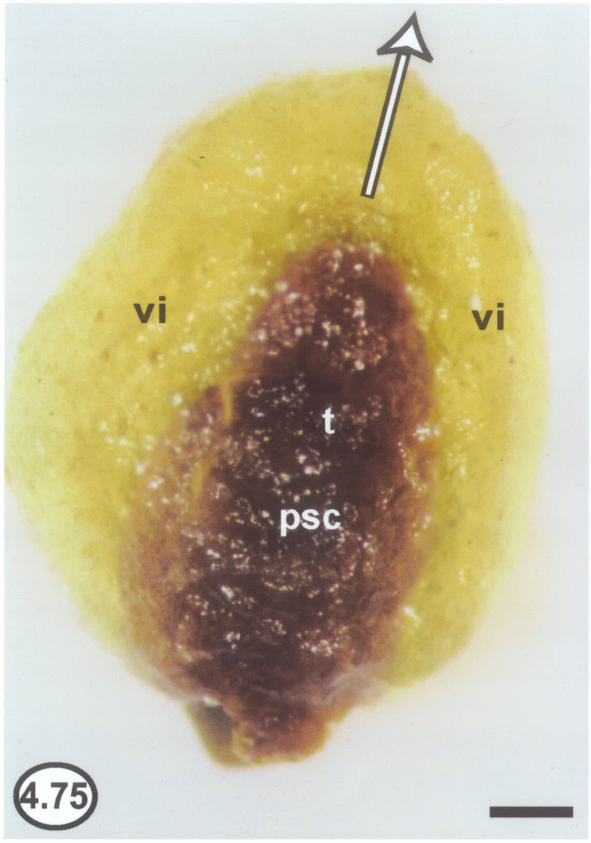
vi
vi
t
psc
4.75

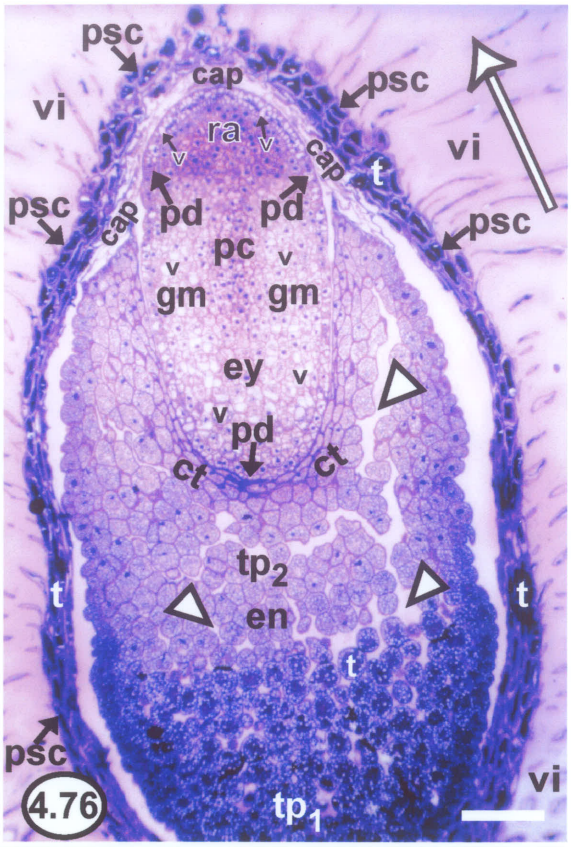
psc
cap
psc
vi
ra
v
v
cap
t
vi
psc
cap
pd
pd
psc
pc
v
v
gm
gm
ey
v
v
pd
ct
ct
tp2
t
en
t
t
psc
vi
4.76
tp1

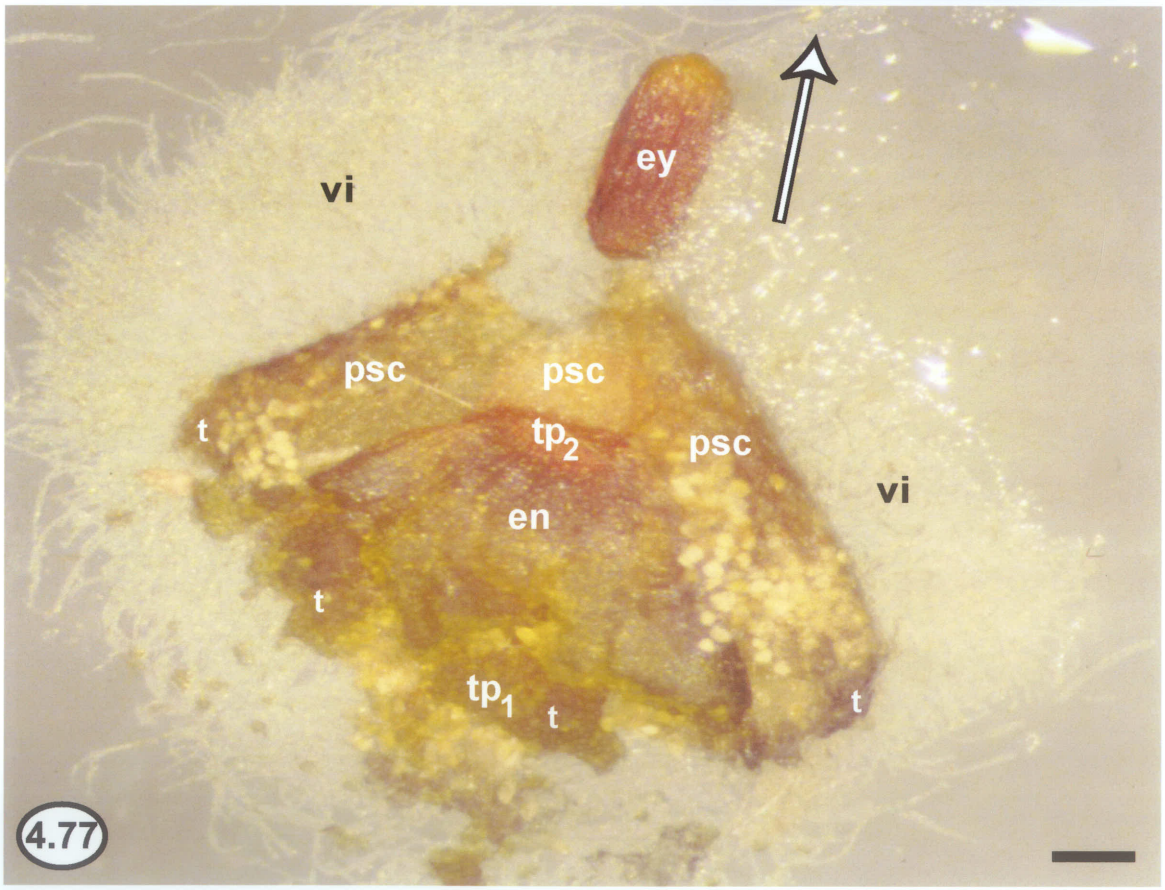
ey
vi
psc
psc
t
tp2
psc
vi
en
t
tp1
t
t
4.77

III. DISCUSSION

1. Similarities between *Arceuthobium americanum* and its Host (*Pinus banksiana*) regarding Development in the Female Structures and Pollination

1A. Synchrony between reproductive development in female flowers/fruit of *Arceuthobium americanum* and female cones of *Pinus*

Reproductive development in a female flower/fruit of *Arceuthobium americanum* (including megasporocyte initiation, megasporogenesis, embryogenesis, endosperm development, and pseudoseed maturation) is notable for its long duration. It takes about seventeen months from anthesis to explosive discharge of a mature pseudoseed. Moreover, as female flower bud initiation in *A. americanum* takes place in the fall preceding anthesis, it takes a full twenty-four months for an incipient female flower (if fertilized) to produce a viable pseudoseed. Similarly, reproductive development in a female cone of the host *Pinus banksiana* and other *Pinus* species (including megasporocyte initiation, megasporogenesis, megagametogenesis, embryogenesis, megagametophyte development, and seed maturation) takes twenty-four months from female cone initiation in the fall to the production of viable seeds (Raven *et al.*, 1999). Thus, not only are the time periods for reproductive development in the respective female structures of *A. americanum* and *P. banksiana* nearly identical, but the timing of both initiation and seed maturation is similar in the two species.

It is extremely common for the life cycle of a parasite to be synchronized with the life cycle of its host. Not only is reproductive development in female structures of *Arceuthobium americanum* and its host in synchrony, but so is development in male structures (K.Y. Sereda, pers. comm., 2001). Life cycle synchrony has been reported for fungal parasites and their plant hosts (Desprez and Dupuis, 1994), insect parasites and their plant hosts (Udayagiri *et al.*, 1997), and nematode parasites and their plant hosts (Jones *et al.*, 1997). In these cases, host factors are believed to be directly involved in the synchronization, although the host factors have not been characterized. Unfortunately, the relationships of parasitic plants with their plant hosts have not been well studied with regard to the synchrony of parasite and host life cycles, although, some host-derived factor(s) is probably involved in the synchronization.

It is highly likely that a hormone or combination of hormones dictating the progression of reproductive development in pine cones may also be dictating a parallel progression of reproductive development in the flowers of the parasite. Regarding reproductive development in the female pine cones, hormones such as abscisic acid, indole-3-acetic acid, and gibberellins have been implicated in controlling the processes of megagametogenesis and embryogenesis in many conifers (Kong *et al.*, 1997). Host-synthesized hormones are commonly translocated into the dwarf mistletoe (Hawksworth and Wiens, 1996), and could govern reproductive development in both host and parasite. It takes only twelve months for an incipient female flower of the related *Arceuthobium pusillum* (if fertilized) to produce a viable pseudoseed (Hawksworth and Wiens, 1996). *Picea mariana* (black spruce), the principal host of *A. pusillum*, similarly takes only twelve months from the initiation of female cones to the maturation of the cones and production of viable seeds (Viereck and Johnston, 1990). This synchrony provides further evidence to suggest that the same systems control reproductive development in both the host and the dwarf mistletoe.

Although it is unlikely that the dwarf mistletoe is exerting any substantial control over the host reproductive development, it would certainly be of interest to compare specific reproductive events in the female (and male) cones of infected and uninfected hosts. If different, this may suggest that the dwarf mistletoe has some control over the development of the host. However, it would provide more meaningful information to examine reproductive development in the flowers of dwarf mistletoes parasitizing non-principal hosts. For example, *Arceuthobium americanum* can sometimes, if only rarely, parasitize *Picea mariana* (Hawksworth and Wiens, 1996). As described, reproductive development in the female cones of *P. mariana* is essentially twelve months faster than reproductive development in the female cones of *Pinus banksiana*, the principal host of *A. americanum*. If reproductive development in the female flowers of *A. americanum* found on *Picea mariana* has an altered duration, very strong proof would be put forward suggesting that the host plays a paramount role in the dictation of reproductive development in the female flowers of dwarf mistletoe. Similar examinations and comparisons should be made regarding male development in *A. americanum* parasitizing principal and non-principal hosts.

1B. Congruencies in the timing of pollination as well as the interval between pollination and fertilization in *Arceuthobium americanum* and its host

A similarity between pollination in *Arceuthobium americanum* and its host *Pinus banksiana* (as well as other *Pinus* species) is the fact that pollination takes place at the megasporocyte stage in both organisms, prior to megasporogenesis and megagametogenesis (Hawksworth and Wiens, 1996). In the flowering plants, this is highly unusual, as both megasporogenesis and megagametogenesis have typically already occurred at the time of pollination (Mauseth, 1988). However, as there may be some host-controlled synchrony with regard to reproductive development in the two organisms, it is not surprising that the pollination process in both organisms should occur at a similar time relative to female developmental events. At the megasporocyte stage in both organisms, the female tissue produces an exudate that aids in pollination; this implies that the stage of female development has a role in the timing of pollination. In *A. americanum*, the exudate was present on the stigma (Figure 4.1), and this exudate likely aids in the entrapment of pollen, regardless of whether pollination is by wind or insect. Similarly, in *Pinus* species, the exudate is present in the vicinity of the nucellus, micropyle, and pollen chamber at the time of pollination, and aids in the entrapment of the wind-dispersed pollen (Raven *et al.*, 1999). The stigmatic exudate of *A. americanum* in Manitoba disappeared just before the onset of megasporogenesis, when pollen tubes would already have reached the base of the PNC (Figure 4.11). As in *A. americanum*, the exudate in *Pinus* disappears after pollen entrapment. Furthermore, the loss of the exudate in *Pinus* is said to be due to evaporation, and the evaporation process is believed to draw the pollen grain into the nucellus (Raven *et al.*, 1999). In a similar fashion, then, the loss of the stigmatic exudate in *A. americanum* may also result from evaporation, and the evaporation may help to draw the pollen grain deeper into the stigmatic surface where germination can take place.

A relatively long interval between pollination and double fertilization occurs in both *Arceuthobium americanum* and its host, which coincides with the long process of reproductive development in the two organisms. Pollination of *A. americanum* occurs in late March of the first spring (Hudson, 1966; Gilbert. 1988; D.A.R. McQueen, pers. comm., 1995), but double fertilization does not occur until the end of May of the first spring (D.A.R. McQueen, pers. comm., 1995; section II. Results - 9 of this chapter) or as late as mid June of

the second spring (Hudson, 1966). The slight discrepancy in the observations regarding the timing of double fertilization in *A. americanum* might exist due to climate differences, site differences, host differences, or annual variation. D.A.R. McQueen (pers. comm., 1995) and this thesis examined *A. americanum* on *Pinus banksiana* in southern Manitoba, whereas Hudson (1966) examined *A. americanum* on *P. contorta* in Montana, U.S.A. Regardless of these slight discrepancies, the interval between pollination and fertilization in *A. americanum* is over two months long. Similarly, a long delay exists between pollination and fertilization in the host *Pinus banksiana* and other *Pinus* species as well (Raven *et al.*, 1999). In most flowering plants, the time between pollination and double fertilization is usually less than 48 hours (Maheshwari, 1950). Yet, very long intervals between pollination and fertilization are characteristic of the gymnosperms (Raven *et al.*, 1999). Thus, it seems as if the host gymnosperm is at least partially responsible for the long interval between pollination and fertilization in *A. americanum*.

Part of the delay between pollination and fertilization in both *Arceuthobium americanum* and its host is the time it takes the pollen tube to grow through the style and the placental-nucellar complex (PNC) in *A. americanum* and the nucellar tissues of *Pinus*. D.A.R. McQueen (pers. comm., 1995) found that an *A. americanum* pollen tube did not reach the base of the PNC until mid April of the first spring (almost one month following pollination), and Hudson (1966) believed that an *A. americanum* pollen tube did not reach the base of the PNC until two months following pollination. The slight discrepancy in the timing of pollen tube growth of *A. americanum* likely reflects aforementioned climate, host, and site differences as well as general variation. It also takes several months for the pollen tube of *Pinus* to growth through the nucellar tissue (Raven *et al.*, 1999).

The remainder of the delay between pollination and fertilization in both *Arceuthobium americanum* and *Pinus* is attributable to the fact that after the pollen tubes reach the proper location, the tubes must wait until an egg cell is formed. D.A.R. McQueen (pers. comm., 1995) found that the growing pollen tubes of *A. americanum* encounter the base of a megasporocyte as opposed to a fully formed embryo sac (megagametophyte) with an unfertilized egg cell. Hudson (1966) believed that megasporogenesis of *A. americanum* takes place during pollen tube growth so that the pollen tubes encounter the base of a functional megaspore (Hudson, 1966). In either case, the pollen tubes must wait until a

mature embryo sac is formed before double fertilization can occur. Similarly, in *Pinus*, although the pollen tube does reach a megagametophyte, the megagametophyte is not fully formed, for archegonia with unfertilized egg cells do not typically develop until some time after the pollen tube has reached the *Pinus* megagametophyte (Konar and Oberoi, 1969). Thus, the pollen tube in *Pinus* must wait for megagametogenesis to be completed before fertilization can take place.

It is likely that slow pollen tube growth and delayed formation of an egg cell may be partially related to early female developmental events. Firstly, in typical flowering plants, strong chemical signals (possibly calcium) emitted from the filiform apparatus between the synergids in a fully developed embryo sac likely ensure that the pollen tubes have a target towards which they rapidly grow (Coe, 1954; Reiser and Fischer, 1993; Herrero, 2001). In *Arceuthobium americanum*, however, megasporogenesis has not even started at the time of pollination, and the pollen tubes may not be receiving a chemical signal due to the absence of synergids; consequently, the tube growth may be slow. The hormonal balance of the host may be delaying both megasporogenesis and megagametogenesis in *A. americanum*, and may be responsible for slow pollen tube growth. Secondly, it may be that if female development were slowed in the parasite and host so that the pollen tube reaches the proper region of female tissue before an egg is present, fertilization would obviously be delayed in both organisms. Again, then, as the hormonal balance of the host may be delaying megasporogenesis and megagametogenesis in *A. americanum*, the host would thus be responsible for the fact that the fully elongated pollen tubes have to wait at the base of the megasporocyte. Therefore, the host may be ultimately responsible for the long interval between pollination and fertilization in *A. americanum*.

1C. Pollen tube growth in *Arceuthobium americanum* and its host

The fact that pollen tubes of *Arceuthobium americanum* begin to elongate before a mature seven-celled unfertilized embryo sac (megagametophyte) is formed contradicts much of the literature regarding pollen tube growth in flowering plants. In typical flowering plants, chemical signals emitted from the filiform apparatus potentially elicit a conformational change to the apical actin in the growing pollen tube tip, which in turn influences the direction of tip growth (Geitmann and Emons, 2000; Heath and Geitmann,

2000). Yet, a pollen tube will reach a megasporocyte of *A. americanum* at the precise location of the future egg apparatus prior to synergid formation and even before the process of megasporogenesis has initiated. This suggests that the synergids do not play a role in guiding the pollen tube in *A. americanum*. Furthermore, pollen tubes are found below both megasporocytes/functional megaspores of *A. americanum* (Figure 4.11), even though one megasporocyte/functional megaspore typically does not proceed beyond the four-celled stage and thus never produces synergids (see section II. Results - 7 of this chapter). This further establishes that synergids are not needed for pollen tube guidance in *A. americanum*. Similarly, pollen tube growth in the host *Pinus banksiana* and in all gymnosperms is obviously not guided by synergids, as synergids do not form in the gymnosperms (Raven *et al.*, 1999). Yet, the pollen tube reaches the immature gymnosperm megagametophyte at the precise location of the future egg cell. Therefore, some agent other than a chemotropic factor from the synergids must be directing the growth of the pollen tube in both *A. americanum* and the gymnosperms, and as the tube growth is slow in both organisms, the agent may not be as efficient as the synergid factor.

It is likely that the growing pollen tube tip employs environmental sensing systems to aid in tube growth (Heath and Geitmann, 2000). Firstly, the pollen tube may thigmotropically detect and respond to intercellular structure of the style (flowering plants) and/or nucellus (flowering plants and gymnosperms), as the style/nucellus structure likely provides a directed pathway that guides the pollen tube through the female tissues (Herrero, 2001). However, although a thigmotropic response of the pollen tube to style/nucellus structure could play a role in rough guidance, it is unlikely that this alone could direct the pollen tube to the precise proper location of the egg cell (or future egg cell, as in *Arceuthobium americanum* and gymnosperms). Secondly, it is possible that a general negative phototropic response in the elongating pollen tube could ensure that the pollen tube grows into the female tissues. This has not been specifically suggested in any of the literature, although Campbell *et al.* (2001) noted that significantly more pollen tubes reached the nucellus in *Triticum aestivum* X *Zea mays* crosses performed at high light intensity than that at low light intensity. However, as in the case of style/nucellus structure, it is unlikely that a general negative phototropic response in the pollen tube alone could direct the pollen tube to a precise location.

Therefore, in both *Arceuthobium americanum* and gymnosperms, chemotropic factors may be involved in pollen tube guidance. However, the chemotropic factor(s) would be secreted by the megasporocyte(s), which are present at the time of pollination in both organisms, not synergids, which are absent at the time of pollination in either organism. The chemotropic factors produced by the megasporocyte(s) would create a chemical gradient that could be sensed by the growing pollen tube tip. The detection of the gradient by the pollen tube would in turn elicit a conformational change in the apical actin and direct the growing pollen tube to the source of the chemical emission (Geitmann and Emons, 2000; Heath and Geitmann, 2000). As pollen tube growth in both *A. americanum* and its host is slow, the megasporocyte(s) may not be able to secrete as much of the chemotropic factor(s) as the synergids of typical flowering plants are able to secrete. Alternatively, a chemotropic factor(s) potentially emitted from the megasporocyte(s) may not be as potent as the putative chemotropic factor (calcium) emitted from the synergids. The engagement of a non-calcium chemotropic factor for pollen tube guidance in *A. americanum* and gymnosperms is supported by the fact that Heslop-Harrison (1986) suggested other molecules besides calcium are involved in pollen tube attraction. In addition, Feijó *et al.* (1999) believed that anions such as chloride might play a role in pollen tube direction. Conceivably, an anion such as chloride may be secreted by the megasporocyte(s) in *A. americanum* and gymnosperms where it could act as a chemotropic factor for pollen tube guidance in these organisms.

In addition to responding to stylar/nucellar structure via thigmotropism, light via a general negative phototropism, and chemical gradients, the pollen tube of *Arceuthobium americanum* and its host may somehow be responsive to callose produced by the megasporocyte(s). This would not be a chemotropic response, as callose is an insoluble material (to be discussed shortly). As demonstrated for *A. americanum*, pale blue fluorescence in the presence of aniline blue indicated that callose was present in the megasporocyte wall (the embryo sac and nonfunctional dyad wall) throughout megasporogenesis (Figure 4.11). The presence of megasporocyte callose during the process of megasporogenesis is typical for most flowering plants undergoing monosporic or bisporic megasporogenesis and sexual reproduction (Mauseth, 1988; Peel *et al.*, 1997). The heaviest accumulation of callose was along the lower side of the functional megaspore and in the

vicinity of the future location of the egg apparatus in *A. americanum* (Figure 4.11). This callose was likely present in the megasporocyte wall prior to megasporogenesis (Peel *et al.*, 1997). Although there are no examples in the literature describing the presence of callose in megasporocytes of gymnosperms, no literature explicitly states that callose is not formed in these. As callose is often present in the megasporocytes of flowering plants, it is possible that callose may be found in the megasporocytes of gymnosperms, and may persist throughout megasporogenesis and megagametogenesis. This is likely, considering that gymnosperm megasporocytes appear to undergo a type of monosporic megasporogenesis (Mauseth, 1988); the presence of callose in the megasporocytes of gymnosperms needs to be investigated. Callose tends to be synthesized in the presence of calcium (Dyachok *et al.*, 1997), so perhaps the calcium gradient thought to be crucial in directly guiding pollen tube growth in typical flowering plants also exists as a result of its necessity for megasporocyte callose induction.

While it is relatively easy to understand pollen tube response to a gradient of a soluble chemotropic factor such as calcium or chloride, it is difficult to comprehend how a pollen tube could grow in response to an insoluble material such as callose. However, it may be possible that the pollen tube tips of *Arceuthobium americanum* and gymnosperms are able to "see" the callose in the megasporocyte(s). Specifically, perhaps the tips of the pollen tube possess plasma membrane photoreceptors that are able to perceive the distinct spectral emissions from megasporocyte callose. One of the most typical features of a plant is its ability to detect light, but more importantly, most plants can respond to specific wavelengths of light including blue, red, and far red via appropriate photoreceptors (Salisbury and Ross, 1992). Thus, it is conceivable that the pollen tube tip might possess the ability to respond to a specific wavelength of light. Perhaps a photoreceptor such as rhodopsin, a common photoreceptor in algae, fungi, and animals (Raven *et al.*, 1999) is present in the pollen tube tip plasma membrane. Transmission of spectral information from megasporocyte callose could be readily detected by pollen tube tip membrane photoreceptors (pollen tube callose would not interfere with reception, as the young growing tip possesses no cell wall callose - Ferguson *et al.*, 1998). Reception of the proper wavelength by the pollen tube tip photoreceptor could elicit the changes in pollen tube tip actin conformation that are needed to direct pollen tip growth. Moreover, regarding *A.*

americanum, there is a large deposition of callose on the lower side of the functional megaspore (and likely the lower side of the pre-meiotic megasporocyte as well), which would ensure that the growing pollen tube does not stray beyond the nearest path to the future egg apparatus. The largest deposition of megasporocyte callose in *A. americanum* is in the region of the future egg apparatus, and so the pollen tube in this organism would be drawn to a fairly specific location.

It is possible that enough light enters the small region of the young *Arceuthobium americanum* PNC and gymnosperm nucellus to allow reflectance from the megasporocyte callose to be detected by pollen tube tip receptors. In the young flowers, tannin-like materials are absent from the region of the PNC as well as the carpel, and so the tissues are fairly hyaline, potentially allowing light transmission (Figures 4.3 and 4.4). Fibre optic properties of mesophyll cells allowed light to migrate into the deeper tissues of etiolated oat seedlings (Mandoli and Briggs, 1982). Likewise, Fineran (1995) suggested that fibre optic properties of host bark might be involved in the transmission of light to the embedded *Korthalsella* sucker. Therefore, fibre optic properties of PNC/nucellar tissue may allow for the illumination of megasporocyte callose as well as for the transmission of callosic reflectance back to photoreceptors in the pollen tube tip plasma membrane. The perception and response of a pollen tube to reflectance from megasporocyte callose may not be as rapid as the response of a pollen tube to a chemical gradient, which might explain why pollen tube growth would be slow in *A. americanum* and gymnosperms. It should be noted that even though light could potentially illuminate megasporocyte callose, a general negative phototropic response is still possible for rough pollen tube guidance, as any light penetrating the PNC/nucellar tissues would attenuate as it reaches deeper tissues. Other potential roles of callose during megasporogenesis will be further discussed in part 3B of this discussion.

Since synergids are not necessary for pollen tube growth in either *Arceuthobium americanum* (likely most Viscaceae and Loranthaceae as well) or gymnosperms, it might follow that synergids are not essential for pollen tube growth in any flowering plant. Rather, the putative chemotropic factors secreted from synergids may merely increase the rate of pollen tube growth. The concept that megasporocytes may be able to secrete pollen tube attractants and that callose may be an attractant needs to be further investigated in other flowering plants and gymnosperms.

Yet another similarity between *Arceuthobium americanum* (Figure 4.11) and its host pine is the fact that multiple pollen tubes can enter the PNC/nucellar tissue (Konar and Oberoi, 1969). In *A. americanum*, multiple tubes likely enter the PNC as multiple (two) megasporocytes are present, although each megasporocyte apparently has the ability to attract more than one pollen tube. Similarly, the megasporocyte in *Pinus* can attract multiple pollen tubes. In both organisms, the growing pollen tubes might possess very similar abilities to compete for the attractant, and subsequently, all tubes grow equally slowly in response to the attractant. The multiple tubes may also interfere with each other, contributing to an overall slow growth rate. In addition, some host-derived hormone (or other host-derived factor) facilitating multiple tube growth in the nucellus of the host *Pinus* may also permit multiple tube growth in the PNC of *A. americanum*. In typical flowering plants, usually only one pollen tube reaches an embryo sac. Although a greater amount or more efficacious pollen tube attractant has been posited to direct tube growth in typical flowering plants, there is likely a greater disparity among the competitive abilities of the growing pollen tubes, and hence the fittest pollen tube is the first to reach the typical flowering plant embryo sac (Stephenson and Winsor, 1986).

In both *Arceuthobium americanum* (Figure 4.11) and its host pine (Konar and Oberoi, 1969), pollen tubes are bifurcated. Bifurcated pollen tubes are believed to be a characteristic of wind-pollinated species including gymnosperms (Mauseth, 1988), although the reason behind the branching has not been explained in the literature. It may be that wind-dispersed pollen needs to be lighter than pollen dispersed by other vectors. Subsequently, the nutritive load in a light, wind-dispersed pollen may not adequately supply a growing pollen tube with enough energy to elongate autonomously and so a growing pollen tube must branch in order to absorb nutrients from the surrounding maternal tissue. More evidence is put forward suggesting that pollination in *A. americanum* is via the wind. Again, some host-derived hormone (or other host-derived factor) dictating pollen tube branching within the pine cone might also govern pollen tube branching within the PNC of *A. americanum*.

1D. Potential for polyembryony in *Arceuthobium americanum* and its host

A final similarity regarding reproductive development in the female structures of both *Arceuthobium americanum* and its host *Pinus banksiana* should be addressed. In both organisms, there is potential for polyembryony. In *A. americanum*, the PNC contains two megasporocytes, each of which could potentially produce an embryo sac with an egg cell. Relative to the typical flowering plant, this represents an increased potential for polyembryony, as typical flowering plants only possess one megasporocyte per nucellus. As demonstrated, however, polyembryony does not typically occur in *A. americanum*, as only one of the two megasporocytes usually proceeds through megagametogenesis to a four-celled embryo sac (megagametophyte) stage. In *Pinus*, a single megagametophyte has the ability to produce as many as six egg cells that are each fertilized (Foster and Gifford, 1974). Thus, like *A. americanum*, the potential for polyembryony is increased in *Pinus* species, and this potential is realized during the early stages of embryo development. However, as in a pseudoseed of *A. americanum*, typically only one embryo is found in the mature *Pinus* seed. In both *A. americanum* and *Pinus*, the potential for polyembryony likely increases the probability that a given PNC/nucellus will produce a vigorous embryo, as intranucellar competition potentially selects the fitter megasporocyte/embryo sac (*A. americanum*) or fittest egg/embryo (*Pinus*) to succeed.

It is unlikely that the potential for polyembryony in *Arceuthobium americanum* and *Pinus* are co-evolutionarily or physiologically correlated, as the potential for polyembryony exists in all mistletoes (Bhatnagar and Johri, 1983; Bhandari and Vohra, 1983). Moreover, whereas *Pinus* species (and gymnosperms in general) represent evolutionarily primitive organisms (Raven *et al.*, 1999), *Arceuthobium* species (and mistletoes in general) are advanced organisms (Bhatnagar and Johri, 1983; Bhandari and Vohra, 1983), and thus the potential for polyembryony in *Arceuthobium* and *Pinus* likely arose in very different ways. Although the potential for polyembryony is probably a useful feature in mistletoes and gymnosperms like *Pinus*, the potential for polyembryony was likely lost in the evolution from gymnosperms toward typical flowering plants because the ability of a given ovule to produce multiple embryos probably demanded a great deal of energy. However, in the likely evolution of mistletoes from typical flowering plants, the useful feature of potential polyembryony might have reappeared concomitantly with the feature of ovular reduction.

As less energy would be directed in the formation of a complicated ovular structure, more energy could be initially directed toward the maintenance of multiple egg cells/embryos (Loranthaceae) or megasporocytes (*Arceuthobium*). The reduced nucellar tissues of mistletoes may even potentially act as the limiting factor that selected for the healthiest megasporocyte/egg. The mechanisms by which potential polyembryony likely arose in *Arceuthobium* (and other mistletoes) is further discussed in parts 2B and 2C of this discussion, and the differences in potential versus realized polyembryony among the different mistletoe groups will be addressed in part 3C of this discussion.

2. Ovular Reduction in *Arceuthobium* and Relevant Taxa

2A. The Placental-Nucellar Complex (PNC)

The "ovule" of *Arceuthobium americanum* was called a placental-nucellar complex (PNC) because the ovular structure lacked integuments and a discrete funiculus, and also because the base of the nucellus was continuous with the ovarian placenta (Figures 4.2b and 4.3). The term "PNC" should be extended to all *Arceuthobium* species as well as to most Viscaceae, Loranthaceae, and Eremolepidaceae displaying a protuberant, erect, orthotropous, ategmic, reduced ovular structure with basal placentation. However, caution should be used in applying the term to the ovular structures of the Viscaceous mistletoes *Viscum* and *Notothixos* and the Loranthaceous mistletoes *Helixanthera*, *Barathranthus*, *Dendrophthoe falcata*, *Scurrula*, *Moquiniella*, *Tapinanthus*, *Taxillus*, and *Tupeia*, as these species lack protuberant structures.

As parasitic plants tend to have unitegmic or ategmic ovules (Bouman, 1984; Judd *et al.*, 1999), and as parasitism tends to be a feature of advanced species (Judd *et al.*, 1999), it follows that integumentary reduction is a feature of advanced species. In many cases, the integumentary reduction is likely a result of convergent evolution, since unrelated groups of parasitic plants, such as the Santalales and the Balanophorales, share the feature of ategmic ovules. Regardless of the manner of evolution, integumentary reduction, along with the concomitant nucellar and funicular reduction, perhaps allow for a simplification in development that permits less energy to be given to the formation of a complicated ovular structure, as implied earlier. This simplification would indicate a more advanced system, and could have a role in the establishment of potential polyembryony, as described

previously (see part 1D of this discussion). As the embryos of most parasitic plants are reduced at maturity compared to the embryos of typical flowering plants (Kuijt, 1969), it might follow that these reduced embryos do not require a highly complicated ovular structure in which to mature.

2B. Derivation of *Arceuthobium* via ancestors common to the Santalaceae: Fagerlind's (1945a) series

Progressive ovular reduction that is reflective of evolutionary derivation as opposed to evolutionary convergence is convincingly demonstrable in the order Santalales. Fagerlind (1945a) presented a series of illustrations showing the stages by which integumentary reduction may have arisen in *Arceuthobium* via ancestors common to the Santalaceae (Figure 4.78, found on the following page). Fagerlind's (1945a) sequence begins with a hypothetical ovary (Figure 4.78a) containing two unitegmic, erect (funiculus directed upward), slightly anatropous (funiculus bent 180 degrees), out-turned ovules (funiculus lies between the placenta and the bulk of the ovule) displaying free central placentation. Although the somewhat reduced funiculus of each ovule is initially directed upward, the anatropous curvature causes the ovular apices to project toward the base of the hypothetical ovary. This particular hypothetical starting point is odd, as no members of the Santalaceae (or Santalales) have ovules that resemble those in Fagerlind's (1945a) hypothetical ovary. Nonetheless, Fagerlind (1945a) suggested that an ovary as seen in Figure 4.78a evolved toward an ovary with two ovules as seen in *Thesium* of the Santalaceae (Figure 4.78b). The ovules in *Thesium* are unitegmic, display free central placentation, are pendulous (funiculus directed downward), and orthotropous (funiculus and nucellus in a straight line) (Johri and Bhatnagar, 1960). As in the hypothetical ovary, the ovular apices in *Thesium* project toward the base of the ovary. The funicular and integumentary tissues of the ovules in *Thesium* are reduced compared to those of the ovules in the hypothetical ovary, although the single integument remains evident in *Thesium*. Thus, in the transition from the hypothetical ovary to that like *Thesium*, there was a loss of anatropous curvature in the ovules combined with a change to a pendulous state as well as a reduction of the funicular and integumentary tissues, but not a complete loss of single integumentation.

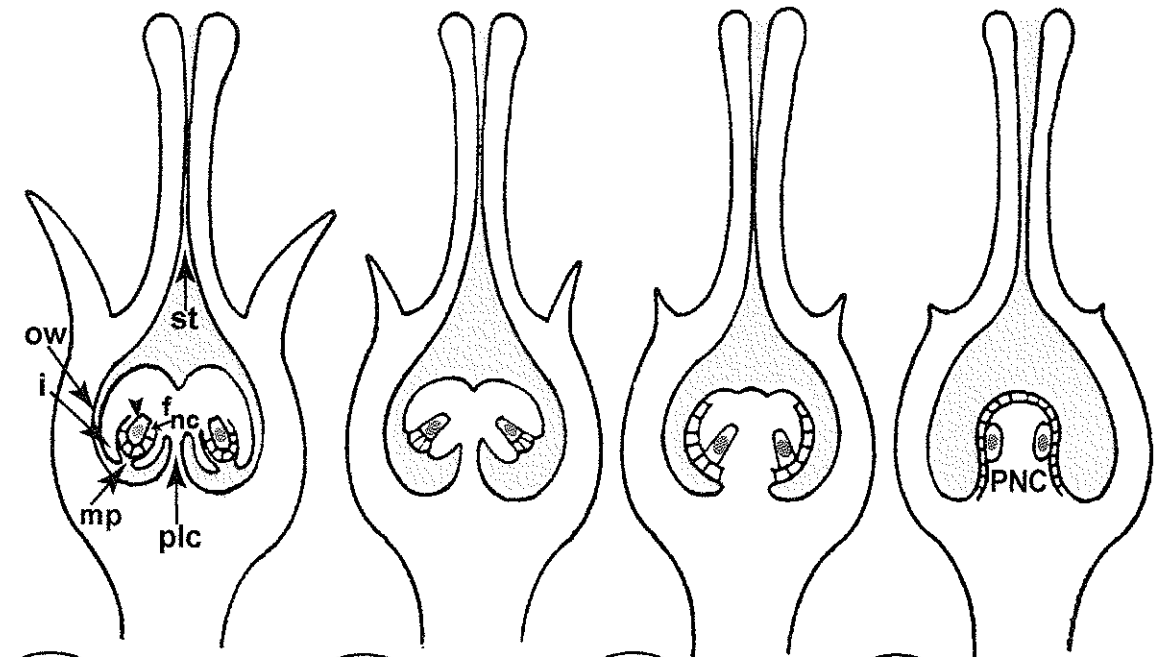

4.78 Fagerlind's (1945a) sequence showing the possible derivation of the "ovule" (PNC) as seen in *Arceuthobium* via a common ancestry with the Santalaceae. Integumentary reduction is a feature of this series. See text (Chapter Four, section III. Discussion - 2B) for more details. Figures are labeled only where necessary. The ovarian loculus is filled light grey. The uniseriate layer of rectangular cells represents the nucellar epidermis. Closed arrowhead = megasporocyte (the megasporocyte nucleus is indicated by a dark grey filled oval), f = funiculus, i = (single) integument, mp = micropyle, nc = nucellar tissue, ow = ovary wall (pericarp), plc = ovarian placenta, st = stylar canal (after Fagerlind, 1945a).

Subsequently, according to Fagerlind's (1945a) sequence, an ovary as seen in an ancestor like *Thesium* (Figure 4.78b) evolved toward an ovary with two ovules as observed in *Santalum* of the Santalaceae (Figure 4.78c)*. The ovules of *Santalum* display free central placentation, are pendulous and orthotropous, but are ategmic (Johri and Bhatnagar, 1960). Thus, there was complete loss of ovular integumentation in the trend from an ovary as in *Thesium* to an ovary as in *Santalum*. In addition, the funicular tissues of the ovules in *Santalum* are further reduced compared to those of *Thesium*, although two separate ovules are still discernible.

Finally, according to Fagerlind's (1945a) sequence, the two ovules as seen in an ancestor like *Santalum* (Figure 4.78c) merged into one ategmic, erect, orthotropous, "ovule" displaying basal placentation (the ovular apex projects away from the ovarian base), as seen in *Arceuthobium* of the Viscaceae (Figure 4.78d; i.e. a PNC). Thus, along with the merger, there was loss of a distinct placental column. Notably, Fagerlind's (1945a) sequence shows how an ovular structure with two rather than one megasporocyte can emerge.

The general theme to Fagerlind's (1945a) series is quite viable, particularly considering that more recent molecular data from nuclear small subunit (SSU) ribosomal (r) DNA and chloroplast ribulose-1,5-bisphosphate carboxylase large chain (rbcL) sequences (Nickrent and Malécot, 2001a, b) support the general trend (Figure 4.79, found on the following page). Specifically, it can be seen in Nickrent and Malécot's (2001a, b) phylogeny that *Arceuthobium* and *Santalum* share a more recent common ancestor than either does with *Thesium* (Figure 4.79). Furthermore, although Fagerlind (1945a) was not explicit, the series (Figure 4.78) illustrates why the functional megaspore from each megasporocyte in *Arceuthobium* arises from the morphologically upper dyad and why the egg apparatus arises at the morphologically lower pole of the embryo sac. The ancestral micropyle would have been present near the morphologically lower (but ancestrally upper) pole of each megasporocyte, so although the functional megaspore in *Arceuthobium* is morphologically higher, it is ancestrally lower (ancestrally chalazal). Similarly, although the egg apparatus of *Arceuthobium* arises at the morphologically lower pole of the embryo sac, it in fact arises at the ancestrally upper (ancestrally micropylar) pole of the embryo sac.

* "...ancestor like *Thesium* evolved toward...*Santalum*...": this statement is meant to indicate that *Thesium* and *Santalum* share a common ancestor that resembles *Thesium*. Phrases comparable to this are found throughout parts 2B and 2C of this discussion, and should be interpreted in a similar fashion.

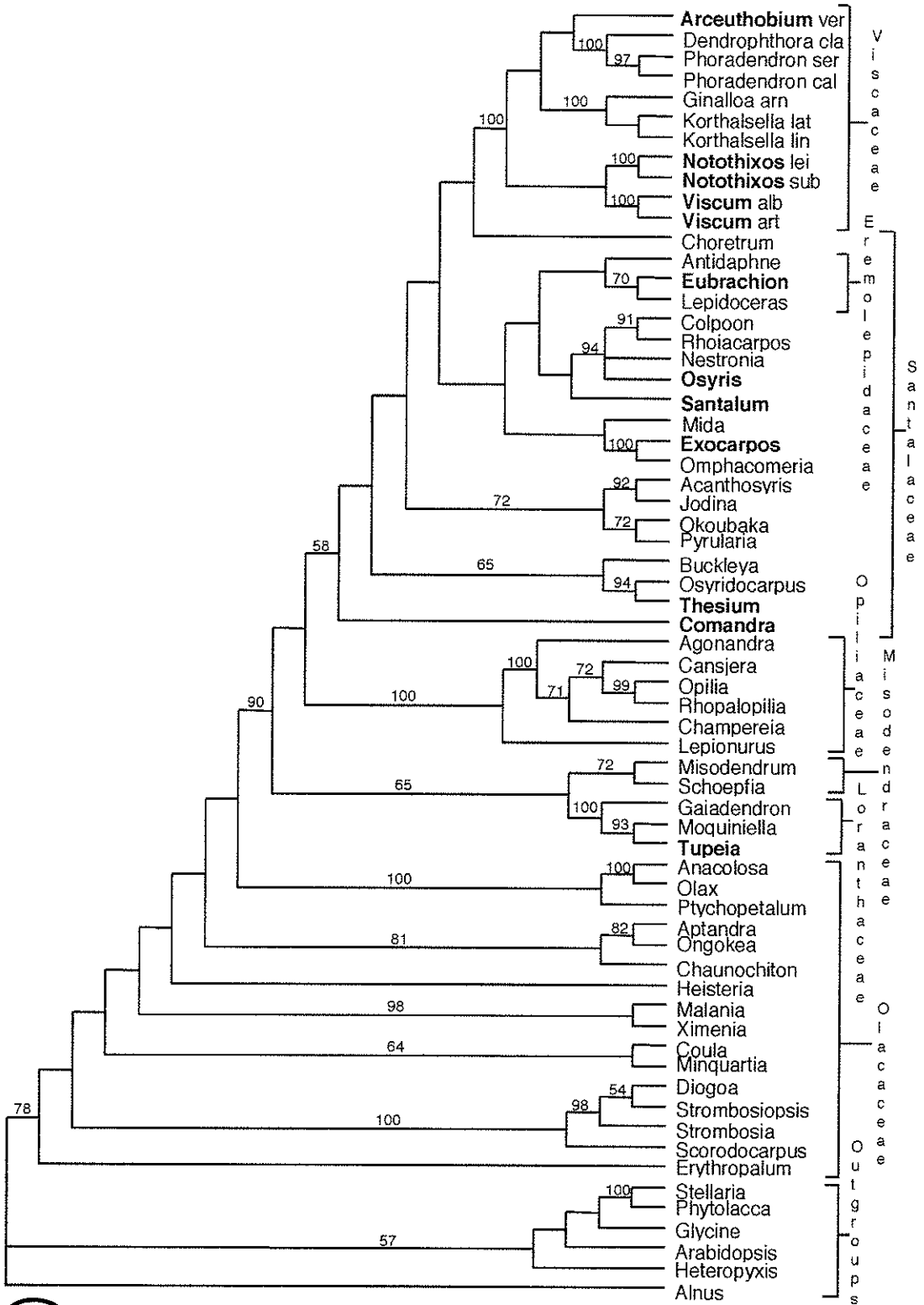

4.79 Phylogeny of the order Santalales. Data are from nuclear small subunit (SSU) ribosomal (r)DNA and chloroplast ribulose-1,5-bisphosphate carboxylase large chain (rbcL) sequences. Bootstrap values are indicated along the nodes. The Eremolepidaceae have been indicated. Genera specifically referred to are shown in **bold** (adapted and **reprinted with permission from Nickrent and Malécot, 2001b**). See text (Chapter Four, section III. Discussion - 2B).

Nonetheless, it is more useful to consider the PNC as an erect orthotropous structure with basal placentation and to use the morphological topography described in Chapter Two, section I. - 4B and in section II. Results - 3 of this chapter, in which regions near the apparent ovular apex are deemed higher.

2C. Extension of the principles from Fagerlind's (1945a) series to the order Santalales in conjunction with Nickrent and Malécot's (2001b) molecular phylogeny of the Santalales

Features of the extended series and their relationship to Nickrent and Malécot's (2001b) phylogeny of the Santalales

Principles from Fagerlind's (1945a) series can be extended to most families in the Santalales. This modified and extended series featuring ovular characteristics is shown in Figure 4.80 (found on the following page). The most important feature of this series is the explanation of why a given dyad or megaspore becomes functional in relation to the polarity of the ovule. The polarity of upper and lower in relation to the apparent ovular apex will be used as described in Chapter Two, section I. - 4B and section II. Results - 3 of this chapter. Several details regarding the Santalaceae needed to be included in order to elucidate the ultimate pathway toward *Arceuthobium* and the Viscaceae. The details regarding the Santalaceae also help to account for the fact that the members of the Loranthaceae, the Eremolepidaceae (*Eubrachion*), and *Viscum minimum* do not show the apparent inversion to the embryo sac organization that most Viscaceae do. For clarity, all megasporocytes were shown to produce a mature embryo sac with an egg cell, although it is realized that this is not always the case. Additional stages have been included in the series to account for the fact that several Santalacean tribes have pendulous, anatropous, out-turned ovules (review Chapter Two, section I. - 2B). Fagerlind's (1945a) series did not account for these ovules.

For the most part, the extended series shown in Figure 4.80 is largely supported by the molecular data of Nickrent and Malécot (2001b - Figure 4.79). Although the series shown in Figure 4.80 could have been made to be linear, this would not have made sense with respect to the phylogeny of Nickrent and Malécot (2001b - Figure 4.79), and would have introduced the confounding problems of convergent evolution. Nonetheless, obvious ovular trends were not ignored at the expense of the molecular phylogeny. The series in

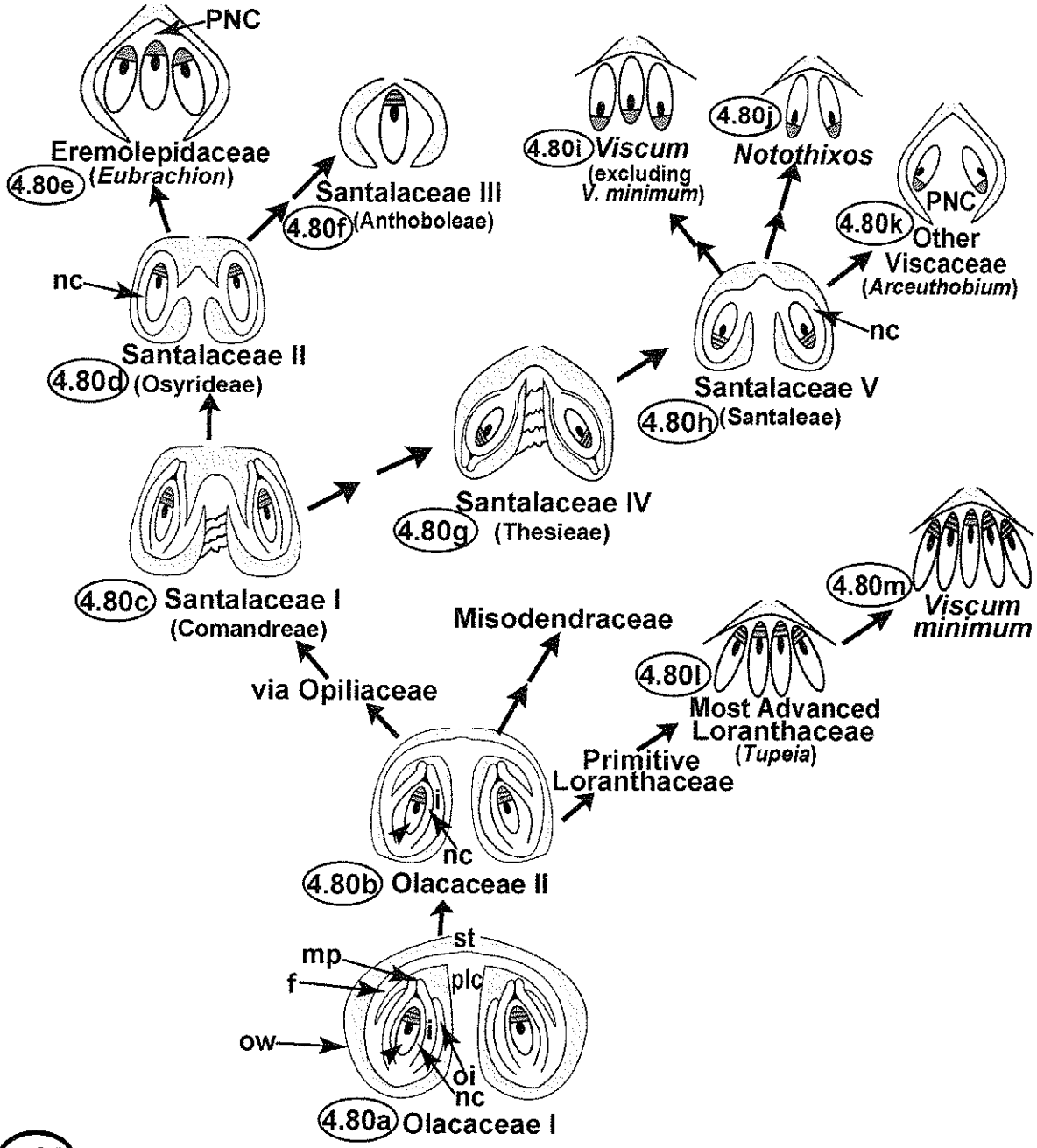

4.80 Possible sequence for the derivation of ovular structure in the order Santalales. More ancestral groups are shown at the bottom of the figure, whereas more derived groups are shown at the top of the figure. Unlabeled arrows show the direction of evolution; double arrows imply that several steps may have been necessary. See text (Chaper Four, section III. Discussion - 2C). Figures are labeled only where necessary. The ovarian loculus is filled light grey, degenerated nonfunctional megaspores and degenerated nonfunctional dyads are filled dark grey, and the egg cell is filled black. Closed arrowhead = embryo sac, f = funiculus, i = inner (or single) integument, mp = micropyle, nc = nucellar tissue, oi = outer integument, ow = ovary wall (pericarp), plc = ovarian placenta, PNC = placenta-nucellar complex, st = stylar canal. A twisted placenta is indicated by wavy lines.

Figure 4.80 shows groups with more recent common ancestors near the top of the figure, and groups with less recent common ancestors near the bottom of the figure. All families in the Santalales are encompassed in the extended series shown in Figure 4.80. The five major tribes of the Santalaceae defined by Johri and Bhatnagar (1960), excluding their sixth tribe Opilieae (since described as the family Opiliaceae; Watson and Dallwitz, 1992), will be illustrated as evolutionary stepping stones in the pathway toward the Eremolepidaceae and most Viscaceae.

With regard to Nickrent and Malécot's (2001b) phylogenetic tree of the Santalales (Figure 4.79), the labeling of clades delineated as Santalacean tribes by Nickrent and Malécot (2001b) have been omitted for visual clarity. In addition, whereas Nickrent and Malécot (2001b) had considered the Eremolepidaceae to be a tribe of the Santalaceae, the Eremolepidaceae has been re-labeled on the tree as a family, although its potential position within the Santalaceae is still displayed.

The Olacaceae

The molecular phylogeny of Nickrent and Malécot (2001b - Figure 4.79) shows that the Olacaceae was likely the first family to be derived in the order Santalales. There are two main groupings of the Olacaceae: the non-parasitic, bitegmic Olacaceae I (Figure 4.80a), and the primarily parasitic unitegmic or ategmic Olacaceae II (Figure 4.80b; Bouman, 1984; Johri and Bhatnagar, 1960). Members of the Olacaceae I (Figure 4.80a) possess two to five bitegmic, pendulous, anatropous, in-turned ovules showing central placentation (only two ovules are shown in Figure 4.80a). Due to the pendulous but anatropous condition, the ovular apices project away from the ovarian base. Only one megasporocyte develops in each ovule, and the single megasporocyte undergoes monosporic megasporogenesis with the lowest (chalazal) megaspore becoming functional, as is typical for flowering plants. The egg apparatus arises at the upper (micropylar) pole of the embryo sac, as is typical. Members of the Olacaceae II (Figure 4.80b) possess ovules that are extremely similar to the Olacaceae I (4.80a), aside from the fact that the ovules of the Olacaceae II are unitegmic and ategmic (two unitegmic ovules shown in Figure 4.80b). Thus, integumentary reduction via integumentary loss likely occurred in the derivation of Olacaceae II through an ancestor like Olacaceae I.

Three major trends leading away from the Olacaceae II

As all other families in the Santalales have unitegmic and ategmic ovules, it was extremely likely that the remaining families in the Santalales were derived from an ancestor like the Olacaceae II (Figure 4.80b). From the Olacaceae II (Figure 4.80b), there were likely three major trends of evolution (Figure 4.80): one progressing toward the Loranthaceae (and *Viscum minimum*), a second trend progressing toward the Misodendraceae, and a third trend progressing via the Opiliaceae toward the Santalaceae, Eremolepidaceae, and Viscaceae.

The basis for the delineation of the three major evolutionary trends will become further evident as each trend is discussed. The most complex trend, the trend from the Olacaceae II via the Opiliaceae toward the Santalaceae, Eremolepidaceae, and Viscaceae, will be discussed and illustrated first. The second most complex trend, the trend from the Olacaceae II toward the Loranthaceae (and *Viscum minimum*) will be the second trend described. The simplest trend, the trend from the Olacaceae II toward the Misodendraceae, will be discussed last.

Major trend from the Olacaceae II via the Opiliaceae toward the Santalaceae, Eremolepidaceae, and Viscaceae

Support for this sequence of derivation is provided by the molecular phylogeny of Nickrent and Malécot (2001b - Figure 4.79). Figure 4.79 shows that the Viscaceae and Eremolepidaceae share a more recent common ancestor than either family does with Santalaceae, and similarly, these families share a more recent common ancestor than they do with the Opiliaceae. However, the Opiliaceae will not be described further, as there is not very much information available regarding the ovules of this family, aside from the knowledge that the ovules of the Opiliaceae show some nucellar reduction when compared to the Olacaceae (Bouman, 1984).

Regarding the major trend from Olacaceae II via the Opiliaceae toward the Santalaceae, Eremolepidaceae, and Viscaceae, evolution likely engineered change from the ovules seen in an ancestor like Olacaceae II (Figure 4.80b) through the Opiliaceae toward the ovules seen in the first Santalacean category, the Santalaceae I (Figure 4.80c). The Santalaceae I represents members of the tribe Comandreae. Support for the concept that the Santalaceae I (Comandreae) was the first Santalacean tribe to evolve is provided by the

molecular phylogeny of Nickrent and Malécot (2001b - Figure 4.79). The ovules of the Santalaceae I (Comandreae - Figure 4.80c; Johri and Bhatnagar, 1960) are the same in number as the Olacaceae II (two to five; Figure 4.80b). Also, like many members of the Olacaceae II (Figure 4.80b), the ovules of the Santalaceae I (Comandreae- Figure 4.80c) are unitegmic and develop only one megasporocyte. Moreover, the Santalaceae I (Comandreae- Figure 4.80c) display similar patterns of megasporogenesis as well as embryo sac arrangement as the Olacaceae II (Figure 4.80b).

However, although the ovules of both the Santalaceae I (Comandreae - Figure 4.80c) and the Olacaceae II (Figure 4.80b) are pendulous and anatropous with ovular apices projecting away from the ovarian base, the ovules of the Comandreae are out-turned (Figure 4.80c), whereas the ovules of the Olacaceae are in-turned (Figure 4.80b). Moreover, the ovules of the Comandreae (Figure 4.80c) show nucellar, placental, and funicular reduction when compared to those of the Opiliaceae (Johri and Bhatnagar, 1960; Bouman, 1984) and the Olacaceae II (Figure 4.80b). Furthermore, the placenta of the Comandreae is twisted (Figure 4.80c) compared to the typical non-twisted placenta of the Olacaceae II (Figure 4.80b). Thus, an overall ovular tissue reduction along with a twisting of the placental tissues was likely derived in the evolution of the Santalaceae I (Comandreae) from an ancestor like Olacaceae II/Opiliaceae. The twisting of the placental tissues along with funicular reduction likely caused the ovules to become physically displaced from an in-turned state (Figure 4.80b) to an out-turned state (Figure 4.80c) during evolution. The twisting of the placental tissues likely occurred as the growth of some placental regions became suppressed during the early evolutionary stages of placental tissue reduction.

Two courses then likely led away from the unitegmic Santalaceae I (Comandreae - Figure 4.80c). The first of these courses involved evolution toward the Santalaceae II, which represents members of the tribe Osyrideae (Figure 4.80d). The molecular phylogeny of Nickrent and Malécot (2001b - Figure 4.79) partially supports this pathway, as the phylogeny shows that *Osyris* was derived more recently than *Comandra*. In the Santalaceae II (Osyrideae - Figure 4.80d), the ovules are nearly identical in number (two to five; only two shown), arrangement, and appearance to those of the Santalaceae I (Comandreae), except that the ovules of the Santalaceae II (Osyrideae - Figure 4.80d) have lost integumentation to become ategmic. Also, the placental tissues of the Santalaceae II

(Osyrideae - Figure 4.80d) are even more reduced than the placental tissues of the Santalaceae I (Comandreae - Figure 4.80c) and do not possess a twisted appearance. During possible evolution from an ancestor like Santalaceae I (Comandreae - Figure 4.80c) to the Santalaceae II (Osyrideae - Figure 2.80d), the placental tissues lost the twisted appearance as suppression of growth had become uniform during the later evolutionary stages of continued placental reduction.

From the Santalaceae II (Osyrideae), both the Eremolepidaceae (Figure 4.80e) and the Santalaceae III (representing members of the tribe Anthoboleae - Figure 4.80f) may have been independently derived. The Eremolepidaceae (Figure 4.80e) may have been derived from an ancestor like the Santalaceae II (Osyrideae - Figure 4.80d) if further placental reduction and ovular fusion in a member that possessed at least three ovules occurred along with a change from monosporic development to bisporic development. This is partially supported by the molecular phylogeny of Nickrent and Malécot (2001b - Figure 4.79), which shows that Eremolepidaceae (specifically *Eubrachion*) was derived more recently than *Osyris*. In the Eremolepidaceae represented by *Eubrachion* (Figure 4.80e), a single ategmic orthotropous ovule displays basal placentation (the "ovule" is a PNC) and the apex of the PNC projects away from the base of the ovary (Bhandari and Indira, 1969). The PNC often develops three megasporocytes (likely resulting from the fusion of the three ancestral ovules), and the megasporocytes undergo bisporic megasporogenesis with the lower dyad (near the ovular base) becoming the functional megaspore. The egg apparatus arises at the upper pole of each embryo sac (near the ovular apex). Note that the proposed evolutionary sequence from the Santalaceae I (Comandreae - Figure 4.80c) via the Santalaceae II (Osyrideae - Figure 4.80d) toward the Eremolepidaceae (Figure 4.80e) allowed for the functional dyad and egg apparatus to arise in the typical, non-inverted fashion observed in most flowering plants.

Conversely, if extreme placental reduction and ovular fusion in an ancestor like the Santalaceae II (Osyrideae - Figure 4.80d) that possessed two ovules occurred along with the loss of an archesporial cell/megasporocyte, the Santalaceae III (Anthoboleae - Figure 4.80f) may have been derived. This is partially supported by the molecular phylogeny of Nickrent and Malécot (2001b - Figure 4.79), which shows that *Exocarpus* of the Anthoboleae was derived more recently than *Osyris*. In the Anthoboleae (Figure 4.80f), a single ategmic

orthotropous ovule displays basal placentation and the ovular apex projects away from the base of the ovary (Johri and Bhatnagar, 1960). The ovule develops a single megasporocyte that undergoes monosporic megasporogenesis with the lowest megaspore (near the ovular base) becoming functional. The egg apparatus arises at the upper pole of the embryo sac (near the ovular apex). Again, the evolutionary sequence from the Santalaceae I (Comandreae - Figure 4.80c) via the Santalaceae II (Osyrideae - Figure 4.80d) toward the Santalaceae III (Anthoboleae - Figure 4.80f) allowed for the functional megaspore and egg apparatus to arise in the typical, non-inverted fashion.

The second course that led away from the Santalaceae I (Comandreae - Figure 4.80c) likely involved evolution toward more advanced Santalaceae (Santalaceae IV - Figure 4.80g and Santalaceae V - Figure 4.80h) and ultimately Viscaceae (Figure 4.80i, 4.80j, and 4.80k). Evolution likely initiated change from the Santalaceae I (Comandreae - Figure 4.80c) to the Santalaceae IV, which represents the tribe Thesieae (Figure 4.80g). The molecular phylogeny of Nickrent and Malécot (2001b - Figure 4.79) supports the derivation of the Thesieae from an ancestor like the Comandreae, as the phylogeny shows that Santalaceae I (Comandreae) was the first Santalacean tribe to evolve. The ovules of the Santalaceae IV (Thesieae - Figure 4.80g) are the same in number, general appearance, type of megasporogenesis, and embryo sac arrangement as the Santalaceae I (Comandreae - Figure 4.80c), except that the ovules of the Santalaceae IV (Thesieae - Figure 4.80g) are orthotropous, not anatropous. Thus, for the Santalaceae IV (Thesieae - Figure 4.80g) to have been derived from an ancestor like the Santalaceae I (Comandreae - Figure 4.80c), a loss of anatropous curvature likely occurred; this change to an orthotropous condition caused the ovular apices to project toward the ovarian base. In relation to the polarity of the ovule, note how there was no change in the positioning of the functional megaspore or polarity of the embryo sac in the Thesieae compared to the Comandreae. However, in relation to the polarity of the ovary, the positioning of the functional megaspore and polarity of the embryo sac would appear inverted in the Thesieae compared to the Comandreae. A moderate decrease in anticlinal cell divisions of the abaxial integuments could have caused the loss of anatropous curvature, which likely took several evolutionary steps. Interestingly, the Santalaceae IV (Thesieae - Figure 4.80g) do not show a notable decrease in the amount of placental tissue when compared to the Santalaceae I (Comandreae - Figure 4.80c), and

like the Santalaceae I (Comandreae - Figure 4.80c), the Santalaceae IV (Thesieae - Figure 4.80g) possess a twisted placenta. This further confirms that the two tribes are closely related, and, as the orthotropous state is believed to be a derived character (Bouman, 1984), the positioning of the Thesieae after the Comandreae in the sequence is validated.

The Santalaceae V, representing the tribe Santaleae (Figure 4.80h), were then potentially derived from an ancestor like the Santalaceae IV (Thesieae - Figure 4.80g). Fagerlind (1945a) also implied this derivation (see Figures 4.78c and 4.78d). Ovules of the Santalaceae V (Santaleae - Figure 4.80h) are identical in number, similar in appearance, and undergo the same pattern of megasporogenesis as ovules of Santalaceae IV (Thesieae - Figure 4.80g). However, the ovules of the Santalaceae V (Santaleae - Figure 4.80h) are ategmic, whereas the ovules of the Santalaceae IV (Thesieae - Figure 4.80g) are unitegmic. Also, the placenta of the Santalaceae V (Santaleae - Figure 4.80h) is reduced and not twisted compared to the placenta of the Santalaceae IV (Thesieae - Figure 4.80g). Thus, in the derivation of the Santalaceae V (Santaleae - Figure 4.80h) via the Santalaceae IV (Thesieae - Figure 4.80g), integumentary loss and further placental reduction likely occurred, similar to the probable derivation of the Santalaceae II (Osyrideae - Figure 4.80d) from the Santalaceae I (Comandreae - Figure 4.80c).

From an ancestor like the Santalaceae V (Santaleae - Figure 4.80h), three separate groups of Viscaceae were likely derived: *Viscum* species (Figure 4.80i - excluding *V. minimum*), *Notothixos* species (Figure 4.80j), and remaining non-*Viscum*, non-*Notothixos* Viscaceae (including *Arceuthobium* - Figure 4.80k). Again, these derivations are generally supported by Nickrent and Malécot's (2001b) phylogeny (Figure 4.79), which shows that the Viscaceae share a more recent common ancestor with the Santalaceae V (Santaleae) than they do with most other Santalaceae. *Viscum minimum*, however, is so exceptional that it is likely Loranthaceous and will be described shortly. If extreme placental reduction and ovular fusion in an ancestor like the Santalaceae V (Santaleae) that possessed at least three ovules occurred along with a change from monosporic development to bisporic development, *Viscum* species (not including *V. minimum* - Figure 4.80i) may have been derived. In these *Viscum* species (Figure 4.80i), neither the nucellus nor the ovarian cavity differentiates, and the multiple (generally three) megasporocytes develop hypodermally at the base of the ovary (Bhandari and Vohra, 1983). The multiple megasporocytes undergo

bisporic megasporogenesis with the morphologically upper (but ancestrally lower) dyad becoming the functional megaspore. The egg apparatus arises at the morphologically lower (but ancestrally upper) pole of each embryo sac.

Alternatively, if extreme placental reduction and ovular fusion in an ancestor like the Santalaceae V (Santaleae - Figure 4.80h) that possessed two ovules occurred along with a change from monosporic development to bisporic development, *Notothixos* species (Figure 4.80j) may have been derived. In *Notothixos* species (Figure 4.80j), neither the nucellus nor the ovarian cavity differentiates, and two megasporocytes develop hypodermally at the base of the ovary (Bhandari and Vohra, 1983). Patterns of megasporogenesis and embryo sac arrangement are as in *Viscum* (Figure 4.80i - excluding *V. minimum*).

Finally, if moderate placental reduction and ovular fusion in an ancestor like the Santalaceae V (Santaleae - Figure 4.80h) that possessed two ovules occurred along with a change from monosporic development to bisporic development, the remaining non-*Viscum*, non-*Notothixos* Viscaceae (including *Arceuthobium* - Figure 4.80k) may have been derived. In these non-*Viscum*, non-*Notothixos* Viscaceae (Figure 4.80k), a single ategmic orthotropous ovule showing basal placentation (a PNC) is present in which the ovular apex projects away from the base of the ovary (Bhandari and Vohra, 1983). Two megasporocytes develop within the PNC. Patterns of megasporogenesis and embryo sac arrangement are as in *Viscum* (Figure 4.80i - excluding *V. minimum*) and *Notothixos* (Figure 4.80j). For completeness, the *Arceuthobium* egg is shown attached to the morphologically upper side of each embryo sac in Figure 4.80k (it is realized that only one embryo sac reaches maturity).

Note how the change from the anatropous to the orthotropous condition first observed in the Santalaceae IV (Thesieae) along with the subsequent ovular fusion likely led to the apparent inversion in the positioning of the functional dyad and egg apparatus in these Viscaceae (Figures 4.80i, 4.80j, and 4.80k). As implied, the course from the Santalaceae I (Comandreae - Figure 4.80c) via the Santalaceae IV (Thesieae - Figure 4.80g) and Santalaceae V (Santaleae - Figure 4.80h) toward the Viscaceae (Figures 4.80i, 4.80j, and 4.80k) is similar to that proposed by Fagerlind (1945a) in Figure 4.78. However, Fagerlind's (1945a) series lacked important details regarding the positioning of the functional megaspore and the polarity of the embryo sac. Moreover, Fagerlind (1945a) did not describe *Comandra* or the Comandreae as being the starting point for the series, and

instead described a hypothetical ancestor that does not resemble any other member of the Santalaceae or even the Santalales. Thus, considering the evidence presented in Figure 4.80 and in the molecular phylogeny of Nickrent and Malécot (2001b - Figure 4.79), the hypothetical ancestor drawn in Fagerlind's (1945a) series (Figure 4.78a) is erroneous and would be better represented by a member of the Comandreae.

Major trend from the Olacaceae II toward the Loranthaceae (and Viscum minimum)

From the Olacaceae II (Figure 4.80b), another major trend likely progressed toward the Loranthaceae (and, as will be shown, possibly *Viscum minimum*). Nickrent and Malécot's (2001b) phylogeny (Figure 4.79) strongly implies that the Loranthaceae were directly derived from an ancestor that was also common to the some Olacaceae (not indicated, but Olacaceae II). Thus, evolution likely engineered a change from the ovules in an ancestor like the Olacaceae II (Figure 4.80b) toward the ovules seen in the Loranthaceae. The Olacaceae II possess two to five unitegmic or ategmic ovules (two unitegmic ovules shown in 4.80b). In the Loranthaceae, the ovules are either protuberant basal structures (PNCs) that are four-lobed, three-lobed, and unlobed, or represent an extremely reduced condition in which neither the nucellus nor the ovarian loculus fully differentiates and the megasporocytes develop hypodermally at the ovarian base (Bhatnagar and Johri, 1983). It is easy to envision the derivation of a four-lobed Loranthaceous PNC (such as seen in *Lysiana* - not shown, but see Maheshwari *et al.*, 1957) as occurring via fusion of four (ategmic) ovules (as possibly present in an ancestor like Olacaceae II) along with placental reduction. From the four-lobed Loranthaceous PNC, Maheshwari *et al.* (1957) elegantly showed the further derivation of the three-lobed Loranthaceous PNC (as in *Amylotheca*), the unlobed Loranthaceous PNC (as in *Helicanthes*), and the extremely reduced Loranthaceous condition (as in *Tupeia* where the megasporocytes develop hypodermally at the base of the ovary). The evolutionary series of Maheshwari *et al.* (1957) will not be shown here, although the most derived ovular structure (as seen in *Tupeia*) is shown in Figure 4.80l.

The fusion of the four ategmic ovules (possibly present in an ancestor like Olacaceae II) apparently established the tendency of the Loranthaceae to form four megasporocytes per ovary. Approximately four megasporocytes typically form in all Loranthaceous ovaries, regardless of the size of the archesporium or appearance of the ovular structure (Johri *et al.*,

1957; Maheshwari *et al*, 1957; Dixit, 1958, 1961; Narayana, 1958a, b; Prakash, 1960, 1963; Raj, 1970). The four or so megasporocytes undergo monosporic megasporogenesis with the morphologically and ancestrally lowest megaspore becoming functional. The egg apparatus arises at the morphologically and ancestrally upper pole of each embryo sac. The fusion of ategmic ovules via an ancestor like Olacaceae II would allow for the positioning of the functional megaspore and orientation of the embryo sacs in the Loranthaceae (Figure 4.80l) to maintain the same arrangement observed in typical flowering plants.

The extended series shows that *Viscum minimum* (Figure 4.80m) was likely derived from an ancestor like the most reduced Loranthaceae (4.80l). General ovular features of *V. minimum* are similar to those of other *Viscum* species as well as to those of the most reduced Loranthaceae. However, the number of megasporocytes, megasporogenesis, and (most importantly) the polarity of the embryo sac of *V. minimum* is notably more similar to the Loranthaceae than to other *Viscum* species. In most *Viscum* species studied, no more than three megasporocytes form, megasporogenesis is bisporic, the morphologically upper dyad becomes functional, the egg apparatus arises at the morphologically lower embryo sac pole, and polyembryony is moderately rare, as generally only one embryo sac reaches maturity (Bhandari and Vohra, 1983). However, in both *V. minimum* (Figure 4.80m) and Loranthaceae (Figure 4.80l), more than three megasporocytes form (as many as eight in *V. minimum*), megasporogenesis is monosporic, the morphologically lowest megaspore becomes functional, the egg apparatus arises at the morphologically upper embryo sac pole, and polyembryony is frequent, as all embryo sacs reach maturity (Bhatnagar and Johri, 1983; Zaki and Kuijt, 1994, 1995). Therefore, it is very likely that *V. minimum* is more closely related to the Loranthaceae than to the Viscaceae; any evolution from an ancestor like the Loranthaceae toward *V. minimum* would have been primarily non-ovular. The extra megasporocytes in *V. minimum* may have arisen via selection of ancestor like the Loranthaceae that occasionally had more than four megasporocytes. There have been no substantial studies on the phylogeny of *V. minimum* relative to the Viscaceae and other Santalales. Moreover, Nickrent and Malécot (2001a, b) did not include *V. minimum* in their analyses (Figure 4.79). Furthermore, there has been little work done on *V. minimum* in general. More work is needed on this interesting species. Alternatively, it is possible that *V. minimum* was derived through an ancestor like the Santalaceae II (Osyrideae - Figure 4.80d)

via extreme placental reduction, integumentary loss, and ovular fusion in an ancestor that possessed five ovules.

Major trend from the Olacaceae II toward the Misodendraceae

As mentioned in the Chapter Two, section I. - 2B, the ovules of the Misodendraceae have not been well studied, although they generally appear to resemble those of the Santalaceae V (the tribe Santaleae of the Santalaceae - Figure 4.80h) in appearance, integumentation, and number. It would be very tempting to show that the Misodendraceae were derived via an ancestor like the Santalaceae V (Santaleae - Figure 4.80h). However, Nickrent and Malécot's (2001b) phylogeny (Figure 4.79) clearly shows that the Misodendraceae are very distantly related to and derived earlier than *Santalum* of the Santaleae. Therefore, as only poor ovular data exists for the Misodendraceae, and as Nickrent and Malécot's (2001b) phylogeny (Figure 4.79) shows that the Misodendraceae might be closely related to the Olacaceae, a major trend of evolution from the Olacaceae II likely progressed via several steps toward the Misodendraceae. It is very important to realize that the Misodendraceae were probably not derived from the ancestors like Loranthaceae, since the ovules of the Misodendraceae, which resemble those of the tribe Santaleae (Figure 4.80h), are not as reduced as those in the Loranthaceae. It is unlikely that ovular structure would have enlarged during evolution (Bouman, 1984). Moreover, it is just as unlikely that the Loranthaceae were derived from ancestors like the Misodendraceae. Although it might be tempting to show that ovular reduction and fusion in an ancestor like the Misodendraceae led to the formation of the Loranthaceae, fusion of ovules such as those found in an ancestor like the Misodendraceae (resembling the Santaleae - Figure 4.80h) would have led to an inversion of the embryo sac. Such an inversion does not occur in the Loranthaceae. Thus, any proposed evolutionary pathway from the Misodendraceae to the Loranthaceae would be erroneous.

Contrary to the thesis that an evolutionary pathway from the Misodendraceae to the Loranthaceae (or vice versa) did not occur, Nickrent and Malécot (2001b) showed that the Misodendraceae are very closely related to the Loranthaceae (Figure 4.79). However, note that only three of the over sixty-five Loranthaceous genera (Barlow, 1983) were included in the phylogeny. It is doubtless that the inclusion of more Loranthaceous genera in a

phylogenetic molecular study of the Santalales such as performed by Nickrent and Malécot (2001b) would show that the Misodendraceae are very closely related to the Olacaceae but not so closely related to the Loranthaceae.

Conclusions regarding the extended series

Although Fagerlind and others like him have been criticized for emphasizing a single character, such as ovular reduction, to reconstruct phylogeny (D.L. Nickrent, pers. comm., 2002), it should also be recognized that a single character might have smaller sub-characters that are not necessarily correlated with each other. For example, ovular reduction is not necessarily correlated with change to bisporic development: all *Viscum* species have extremely reduced ovular structures, but *V. minimum* displays monosporic megasporogenesis, while all other *Viscum* species are bisporic. Similarly, both the Eremolepidaceae and *Arceuthobium* species have a PNC and display bisporic megasporogenesis, but the embryo sacs have opposite polarity in these two taxa. In other words, the ovule structure is not a single character, and can be mined for several characters that are useful in phylogeny.

The more characters that can be used for reconstructing phylogeny, the more accurate the phylogeny will be. As logical as the extended series shown in Figure 4.80 is, there is room for further interpretation and clarification. Yet, the series does point out possible groupings and taxa that should be examined further, with *Viscum minimum* as the most obvious species that should be re-investigated. Most importantly, the series displays how critical it is to clarify which megaspore/dyad becomes the functional megaspore; the categorization of the functional megaspore has never been well described for the mistletoes in general.

3. The Two Megasporocytes, Megasporogenesis, and Megagametogenesis in *Arceuthobium americanum*

3A. The two megasporocytes

As indicated in section II. Results - 5 of this chapter, each of the two megasporocytes in *Arceuthobium americanum* likely developed directly from an archesporial cell, as only the epidermis of the PNC separated each megasporocyte from the ovarian tissue on either side

of the PNC, resulting in the tenuinucellate condition (see Figure 4.4). This corresponds with the findings of Hudson (1966), which stated that the archesporium of *Arceuthobium americanum* was two-celled and that the tenuinucellate condition was achieved. Thus, the findings of Dowding (1931), which stated that the archesporium of *A. americanum* possessed more than two cells and that the crassinucellate condition was achieved, are erroneous. As the tenuinucellate condition befits the theme of nucellar reduction, the presence of the tenuinucellate condition in the advanced *A. americanum* is not surprising. Hudson (1966) observed no crushed sterile PNC cells in the vicinity of the relatively large megasporocytes of *A. americanum*. This implied that the sterile PNC cells underwent some cell divisions in order to keep pace with the enlargement of each of the two archesporial cells/megasporocytes.

The megasporocyte nuclei were also determined to be relatively large, occupying about 50% of the cell (Figure 4.4). At the stage depicted in Figure 4.4, each megasporocyte nucleus was in prophase I, since meiosis had begun in the unopened female flower buds during the fall preceding the first spring. Thus, a megasporocyte nucleus may have been relatively large because it needed to accumulate and accommodate all of the proteins required for the process of meiosis (Rothwell, 1988). Megasporocytes that have been halted at prophase I of meiosis are not unique to *A. americanum*, as Shamrov (1997) noted that the megasporocytes of *Paeonia* (peonies) are halted at prophase I. Like *A. americanum*, *Paeonia* and other members of the *Paeoniaceae* also have multicellular archesporia (Tilton, 1980). In addition, invertebrate and vertebrate females, including humans, produce many primary oöcytes that are halted at prophase I (Purves *et al.*, 1998). Thus, in organisms producing multiple female "germ" cells (including megasporocytes or oöcytes) there may be an advantage to premature initiation of meiosis and subsequent maintenance at prophase I. Perhaps too much energy would be required for multiple female germ cells to undergo all stages of meiosis at once, and so the temporal separation of prophase I from the remaining stages of meiosis might permit energy recovery during the hiatus.

3B. Megasporogenesis and selection of the functional megaspore in a given megasporocyte

Both megasporocytes of *Arceuthobium americanum* were capable of completing megasporogenesis (see section II. Results - 6 of this chapter), supporting the findings of Bhandari and Vohra (1983), and the two meiotic divisions of megasporogenesis were synchronous between the two megasporocytes. The synchrony was not surprising, for hormones or other diffusive controlling factors in the PNC could have worked to synchronize meiotic events between the two megasporocytes in the relatively small PNC in much the way mitotic events are synchronized in a free nuclear endosperm (Brown *et al.*, 1996). For each megasporocyte, megasporogenesis was bisporic. Bisporic megasporogenesis may represent an evolutionarily advanced state (Mauseth, 1988), and this would make sense, as *Arceuthobium* has been shown to be evolutionarily advanced. The bisporic state is advanced possibly because it allows the healthier, more vigorous nucleus to form the egg cell (Klekowski, 1988). Moreover, as an energy-requiring cell wall synthesis event occurring in monosporic development does not occur in bisporic development, the omission of the synthetic event might also represent an evolutionary advancement. In bisporic development, only one of the two dyads develops into the functional megaspore; in *A. americanum*, the upper. Thus, some agent was acting in the election of one dyad to become functional in favour of the other.

In the flowering plants undergoing monosporic or bisporic development, it has been stated that a gradient, either nutritional or in the distribution of growth factors, confines viability to one megaspore or dyad (Bell, 1996). However, in *Arceuthobium americanum* and possibly other flowering plants (Bell, 1996), the choice of the functional megaspore is likely a purely genetic selection. A genetic basis for the selection of the functional megaspore in *A. americanum* was supported by the fact that a change to the ovular structure during evolution of *Arceuthobium* did not affect which dyad became functional (Figure 4.80). Specifically, the morphologically upper but ancestrally lower ovular region became directly connected to tissues in contact with the pedicel during evolution, and as the pedicel may represent the source of nutrients and/or growth factors, it could be suspected that the morphologically lower dyad should have become functional. This, however, was not the

case, as the morphologically upper (ancestrally lower) dyad of *A. americanum* invariably remained functional, supporting the concept of genetic selection.

It is likely that apoptosis (programmed cell death), which has been shown to be under genetic control (Osborne and Schwartz, 1994), brings about the ordered degradation of the fated lower dyad in *Arceuthobium americanum* via the activation of genes coding for proteases and endonucleases (Osborne and Schwartz, 1994; Bell, 1996). Either apoptotic genes of the sporophytic tissue become activated to specifically target the lower dyad for degradation, or the apoptotic genes of the lower dyad itself become activated. Moreover, although segregation during meiosis is believed to be random, this is not always the case, for some alleles may preferentially segregate to certain poles, as has been observed during megasporogenesis of *Rosa* (Täckholm, 1922) and *Zea mays* (Rhoades, 1942). Thus, perhaps the lower dyad consistently attains specific genes that the upper does not (or vice versa).

The presence of megasporocyte callose must also be addressed in a discussion of functional megaspore selection. Although it has already been hypothesized that megasporocyte callose could play a role in pollen tube guidance, the megasporocyte callose may certainly have a role related to functional megaspore selection as well. Rodkiewicz (1970) suggested that callose may play some role in the selection of the functional megaspore in monosporic and bisporic species by ensuring that the proper megaspore/dyad becomes nonfunctional. In *Arceuthobium americanum*, this concept is supported, since the nonfunctional dyad from each megasporocyte acquires a larger buildup of callose than the functional megaspore (Figure 4.11). This large callose buildup may isolate the nonfunctional dyad from the PNC, inhibiting the transport of nutrients into that dyad. Thus, the potential aforementioned apoptotic genetic processes affecting the nonfunctional dyads may involve callose synthesis.

However, callose is also present in each functional megaspore, although not to the extent noted for each nonfunctional dyad (Figure 4.11). The presence of callose in each functional megaspore of *Arceuthobium americanum* may not only be involved in pollen tube guidance (described in part 1C of this discussion) but may also represent an incompatibility response. Following meiosis, all cell products formed (megaspores or dyads), regardless of whether they are destined to become functional or not, have acquired a genetic makeup that is different from the surrounding sporophytic tissue. Subsequently, the cell products may

initiate an incompatibility response that involves callose synthesis, for callose synthesis is known to be induced during incompatibility reactions (Dyachok *et al.*, 1997). The callose buildup in the nonfunctional dyad of *A. americanum* is substantially greater than that of the functional megaspore. As such, callose-synthesizing genes of the fated lower dyad are likely induced to a greater extent than those of the functional megaspore, and/or callose-synthesizing genes of the sporophyte target the lower dyad more heavily. As implied earlier, alleles related to callose synthesis, intensity of callose synthesis, or recognition by the sporophyte may have preferentially segregated to certain poles and thus dyads during megasporogenesis, or may have preferentially been activated. More work is needed on this phenomenon.

Tannin-like materials began to accumulate within vacuoles of the *Arceuthobium americanum* PNC during megasporogenesis (Figures 4.5 and 4.7). Similarly, tannin-like materials have been shown to accumulate within the vacuoles of nucellar tissues in flowering plants (Shamrov, 2000). If assimilates destined for the functional megaspore and embryo sac were not moved into the functional megaspore or embryo sac from the PNC at an adequate rate, the potentially osmotically-active assimilates would have begun to amass in the PNC. In order to neutralize the effects of an increased osmotic pressure, the excess assimilates might have been converted into less osmotically active tannins. Matsuki (1996) found that excess assimilates could be converted into polyphenolics (including tannins), and Fukushima *et al.* (1991) found that when the osmotic pressure within *Hiratanenashi kaki* fruits increased due to an increase in osmotically-active substances, these substances were converted into tannins. It is likely that the tannins in the *A. americanum* PNC were mobilized later in development to supply carbohydrates for the endosperm and embryo.

3C. Megagametogenesis: Of the two functional megaspores formed (one from each megasporocyte), which one succeeds?

Of the two functional megaspores formed in *Arceuthobium americanum*, (one from each megasporocyte) only one functional megaspore was capable of successfully completing megagametogenesis to form a mature seven-celled embryo sac (see section II. Results - 7 of this chapter). Development of the other functional megaspore was halted at the four-nucleate stage; Hudson (1966) and Calvin (1996) also observed this in *A. americanum.*

Therefore, aside from the "choice" of which dyad from a given megasporocyte formed the functional megaspore, there was also a choice with regard to which of the two functional megaspores from each megasporocyte formed the mature seven-celled embryo sac within a given PNC. As implied earlier, the presence of a choice with regard to which megasporocyte/functional megaspore develops into the successful embryo sac represents an evolutionary advancement, as selection for reproductive success can occur within a single PNC, and only the fitter megasporocyte/functional megaspore will form the successful embryo sac.

A choice at the megasporocyte/functional megaspore level as observed in *Arceuthobium americanum* represents an evolutionary advancement over Loranthaceous mistletoes (and *Viscum minimum*). In the Loranthaceae and *V. minimum*, all megasporocytes/functional megaspores produce successful embryo sacs that may all be fertilized, as polyembryony (and polyendospermy) is common in mature pseudoseeds (Bhatnagar and Johri, 1983; Zaki and Kuijt, 1994). However, as only one embryo succeeds during pseudoseed germination, selection for fitness occurs at the embryo level. This selection for the fittest embryo in the Loranthaceae and *V. minimum* likely requires more effort than selection for the fittest megasporocyte/functional megaspore in *A. americanum*, as the energy contributed to several growing embryos and endosperms would be greater than the energy contributed to two unicellular embryo sacs. Therefore, potential polyembryony as it exists in *A. americanum* is more efficient and advanced than the realized polyembryony of the Loranthaceae and *V. minimum*.

Ultimately, the fitter megasporocyte/functional megaspore of *Arceuthobium americanum* was likely able to undergo megagametogenesis more rapidly than the less fit functional megaspore, reaching the four-nucleate stage first. This concept is supported by work of Hudson (1966), Tainter (1968), and Bhandari and Nanda (1968a), which indicated that megagametogenesis is typically more rapid in one of the two functional megaspores in *Arceuthobium* species. The four-nucleate embryo sac from the fitter megasporocyte/functional megaspore of *A. americanum* would be more advanced and thus more capable of obtaining nutrients from the PNC than the lagging embryo sac from the less fit megasporocyte/functional megaspore. A similar concept regarding competition for nutrients or other resources has been put forward regarding choice of successful embryo sacs

(Bell, 1996) and embryos (Wiens *et al.*, 1987; Arathi *et al.*, 1996). Therefore, while selection of a functional megaspore from the two dyads of a given megasporocyte was likely primarily influenced by apoptotic genes, selection of a successful embryo sac from the two functional megaspores in a given PNC was likely mainly based on genes that contributed to fitness and competitive ability.

Whereas the hormones of the PNC and sporophyte may have synchronized the process of megasporogenesis, each functional megaspore likely independently underwent megagametogenesis under the control of its own new genetic system as opposed to under the hormonal control of the PNC. The fact that one embryo sac of *Arceuthobium americanum* was typically abortive verified that only one embryo sac was capable of undergoing double fertilization; this substantiated the findings of Hudson (1966) and Calvin (1996).

However, in very rare cases, both functional megaspores of *Arceuthobium americanum* (one from each megasporocyte) were able to complete megagametogenesis to produce a mature seven-celled, embryo sac. This is evidenced by that fact that twin embryos, each in its own endosperm, were found within an *A. americanum* pseudoseed (Figure 4.69). There was only one region where crushed PNC cells could be observed, indicating that each embryo and endosperm had been conceived in the same PNC, and the side-by-side placement of each embryo and its endosperm validated that both megasporocytes had successfully completed megasporogenesis and megagametogenesis. Of the several hundred *A. americanum* fruit examined, the example in Figure 4.69 displays the only case of polyembryony and polyendospermy observed, representing a rate of polyembryony and polyendospermy of less than 1%. Similarly, Hudson (1966) noted one instance in which two embryos were found within the same pseudoseed of *A. americanum*, and Tainter (1968) occasionally but rarely observed two embryos in the pseudoseed of *A. pusillum*. In addition, Hawksworth (1961) reported that only about 1% of the pseudoseeds of *A. americanum* and *A. vaginatum* subsp. *cryptopodum* contained two embryos and two endosperms. Weir (1914) found somewhat higher levels of polyembryony in *A. vaginatum* subsp. *cryptopodum* (15%) and *A. douglasii* (13%). This further verified that typically only one embryo sac was capable of being fertilized in *A. americanum*.

4. General Organization of the Unfertilized Mature Seven-Celled Embryo Sac of *Arceuthobium americanum*: Comparisons with Typical Flowering Plants, Implications for Pollination, and Preparation for Future Development

The successful unfertilized, mature embryo sac of *Arceuthobium americanum* is very similar to that observed in many typical flowering plants, possessing an egg cell, two synergids, three antipodals, and a central cell. However, there are some noteworthy differences between the two. The major difference regarding the fact that the egg apparatus of *A. americanum* arose at the lower embryo sac pole instead of the expected upper pole (and that the antipodals arose at the upper pole instead of the lower pole) was accounted for in the extended series of Figure 4.80. It was determined that while the egg apparatus of *A. americanum* arose at the morphologically lower pole of the embryo sac, the egg apparatus essentially arose at the ancestrally upper pole. The same is true with regard to the antipodals of *A. americanum* arising at the morphologically upper but ancestrally lower pole.

Although the egg cell in many flowering plants is at the same level as the synergids (Reiser and Fischer, 1993), the egg cell of *Arceuthobium americanum* was situated above and to the side of the two synergids; Hudson (1966) also noted this. Moreover, Hudson (1966) as well as Hawksworth and Wiens (1996) believed that this arrangement might have precluded the normal process of fertilization through the synergid. Yet, there are several flowering plant species, including *Gossypium* (Jensen, 1965) and *Brassica* (Sumner, 1988), in which the egg cell arises slightly above and to the side of the synergids, and in these species, pollination is through the degenerating synergid, as is typical. In addition, aniline blue staining clearly showed that the callose-walled pollen tubes of *A. americanum* (Figure 4.11) did not approach the upper side of the embryo sac where the egg cell was attached. Instead, the pollen tubes of *A. americanum* accumulated at the base of the megasporocyte/embryo sac, near the two synergids, and thus the pollen tubes likely entered a synergid. This was confirmed in Figure 4.23, which clearly showed the pollen tube in the immediate vicinity of the degenerating synergid. Furthermore, the egg cell and synergids of *A. americanum* shared common interfaces with each other (see section II. Results - 7A of this chapter), and so the sperm nuclei from the pollen tube could have easily reached the egg cell through a synergid, specifically the degenerating synergid.

The positioning of the egg cell above and to the side of the synergids in *Arceuthobium americanum* was crucial in ultimately enabling the embryo to develop at a morphologically higher position than the central cell. As such, the embryo would have become positioned near the apex to the mass of viscin cells when the viscin cells fully developed (see Figure 4.64). As the viscin cells will be firmly affixed to the host periderm after explosive discharge, the embryo will have become placed in a position near the host periderm. Conversely, if the egg cell had been positioned at the very base of the embryo sac at the same level as the synergids, the endosperm would have developed above the embryo. Subsequently, the embryo would have had to germinate through or around the endosperm in order to contact the host periderm. The precise achievement of the arrangement of the embryo and endosperm in *A. americanum* is further explained in part 9C of this discussion.

Another difference between the embryo sac of *Arceuthobium americanum* and a typical embryo sac is with regard to the polarity of the cytoplasm of the egg cell and the synergid. In typical flowering plants, the cytoplasm and nucleus of the egg cell is adjacent to the central cell, while the cytoplasm and nucleus of the synergids is adjacent to the embryo sac wall (Kapil and Bhatnagar, 1981). In *A. americanum*, however, the cytoplasm and nucleus of the egg cell was adjacent to the embryo sac wall, while the cytoplasm and nucleus of the synergids was adjacent to the central cell. It may be surmised that this reversed cytoplasmic polarity was related to the peculiar arrangement of the *A. americanum* embryo sac wherein the egg apparatus arises at the morphologically lower pole. Moreover, perhaps the reversed cytoplasmic polarity aided in the developmental progression by which the embryo arises at a morphologically higher position than the endosperm. This, however, cannot be the case, since *Viscum minimum*, which has the typical embryo sac arrangement wherein the egg apparatus arises at the morphologically upper pole, also displays a reversed cytoplasmic polarity in its egg cell and synergids (Zaki and Kuijt, 1994). As the embryo sac of *V. minimum* has the typical arrangement, its embryo will easily develop at a morphologically higher position than the endosperm, so the reversed cytoplasmic polarity was likely not related to the establishment of the embryo at morphologically higher position than the endosperm in either organism.

If the reversed cytoplasmic polarity within the egg cell and persistent synergid in *Arceuthobium americanum* was not related to the reversed polarity of the embryo sac,

perhaps the reversed cytoplasmic polarity was related to the central cell expansion that occurred (see section II. Results - 10 of this chapter). Notably, massive central cell expansion does not generally occur in flowering plants (Mauseth, 1988), but does occur in *V. minimum* (Zaki and Kuijt, 1994), which, as mentioned, possesses an egg cell and synergids that display a reversed cytoplasmic polarity. However, massive central cell expansion also occurs in members of the Loranthaceae, in which the egg cell and synergids show the typical cytoplasmic polarity and the embryo sac shows the typical arrangement. Thus, it is unlikely that the cytoplasmic reversal played a substantial role related to central cell expansion in any of these organisms.

If the reversed cytoplasmic polarity in the egg cell and synergids of *Arceuthobium americanum* was not related to the reversed arrangement of the embryo sac or to central cell expansion, perhaps the reversed cytoplasmic polarity was related to the absence of an embryo sac at pollination. In typical flowering plants, the seven cells of the embryo sac are well established at the time of pollination (Reiser and Fischer, 1993). The typical cytoplasmic polarity of the egg cell and synergids is likely established as well, or becomes established during the period in which the embryo sac waits for the pollen tube to grow close enough for fertilization to become physically possible. However in *A. americanum*, pollination takes place long before the embryo sac forms. Moreover, the pollen tube reaches the base of a megasporocyte, not an embryo sac. Thus, fertilization in *A. americanum* likely takes place almost immediately after the seven cells of the embryo sac form, since the pollen tube is already in the proper location. The results of this thesis supported a very rapid fertilization process (see section II. Results - 9 of this chapter). As such, there may not be time for the standard polarity to become established in the egg cell and synergids. Support for the concept that the presence or maturity level of the embryo sac at pollination affects the cytoplasmic polarity of the egg cells and synergids in *A. americanum* is partially provided by *Gasteria verrucosa*. In *G. verrucosa*, pollination takes place before the egg and synergids are formed (Franssen-Verheijen and Willemse, 1990). Moreover, the pollen tube reaches the egg apparatus of this species before the egg and synergids have fully developed; when the egg cell does become evident, it displays a reversed cytoplasmic polarity. Perhaps in *G. verrucosa*, as in *A. americanum*, the period between egg cell formation and fertilization is too brief to allow the typical cytoplasmic polarity to become established.

The state of the embryo sac at pollination has not been determined for *Viscum minimum*. However, one might expect to find a megasporocyte as opposed to an embryo sac at pollination, as the egg cell and synergids of *V. minimum* show the same reversed cytoplasmic polarity as *Arceuthobium americanum*. The similarity of *V. minimum* to *A. americanum* does not undermine the evolutionary series as seen in Figure 4.80, for the host may play a substantial role in determining aspects and timing of female development, pollination, and pollen tube growth (see part 1B of this discussion). The timing of female reproductive events relative to pollination in *Euphorbia*, a common host for *V. minimum* (Zaki and Kuijt, 1994), has not been documented in the literature. Observations regarding the Loranthaceae substantiate that the reversed cytoplasmic polarity in the egg cell and synergids of *A. americanum* was possibly related to the state of the embryo sac at pollination. Like typical flowering plants, members of the Loranthaceae do not display a cytoplasmic reversal in the egg cell and synergids, and possess embryo sacs that are fully developed at the time of pollination (Dixit, 1961).

The interface of the unfertilized egg apparatus with the unfertilized central cell of *Arceuthobium americanum* lacked cell wall material; this was also noted by Hudson (1966), and is typical for flowering plants. Likewise, among the interfaces of the three cells of the unfertilized *A. americanum* egg apparatus, interfacial regions near the central cell possessed scant cell wall material, while interfacial regions near the embryo sac wall possessed more substantial cell wall material (Figures 4.12, 4.14, and 4.20). This is also typical for flowering plants (Kapil and Bhatnagar, 1981; Russell, 1993). Wall-less areas between the degenerating synergid and the unfertilized central cell of *A. americanum* likely permitted the transfer of a sperm nucleus from the degenerating synergid into the central cell so that fertilization of the central cell could take place (Russell, 1993). Similarly, wall-less areas between the degenerating synergid and the egg cell of *A. americanum* likely permitted the transfer of a sperm nucleus from the degenerating synergid to the egg cell in order for egg cell fertilization to occur (Russell, 1993). The fact that wall-less areas among the interfaces of the egg apparatus were not limited to the interface of the degenerating synergid with the central cell and with the egg cell suggested that the three cells of the egg apparatus followed similar early patterns of development and cell wall deposition. All antipodal interfaces did possess cell wall material (Figures 4.12, 4.14, and 4.24), as is typical (Reiser and Fischer,

1993). As the sperm nuclei would not enter the antipodals, cell wall material would not interfere in the fertilization process, and could have instead provided structural integrity to the relatively large embryo sac.

In *Arceuthobium americanum*, electron opaque deposits were observed at the interface of the unfertilized central cell and the egg apparatus (Figures 4.19 and 4.23), as well as at the interface of the unfertilized central cell and the antipodals (Figure 4.24). The presence of electron opaque deposits at the interface of the unfertilized central cell with some or all cells of the egg apparatus has been documented before (Guo Feng, 1997; Sumner, 1986; Huang and Russell, 1994). However, the presence of electron opaque deposits at the interface of the central cell and the antipodals has not been reported. Guo Feng (1997) believed that the electron opaque deposits seen in at the interface of the central cell and the egg apparatus of *Pelargonium hortorum* represented cell wall precursor material. Thus, at least some of the electron opaque deposits that were observed at the interface of the unfertilized central cell with the egg apparatus of *A. americanum* could have represented cell wall precursor material, likely non cellulosic matrix materials that perhaps became deposited in anticipation of double fertilization. Moreover, the electron opaque deposits at the interface of the central cell and the antipodals of *A. americanum* were likely cell wall precursor materials, since the antipodals underwent some wall thickening throughout development.

However, some of the electron opaque deposits observed at the interface of the unfertilized central cell and the egg apparatus as well as at the interface of the unfertilized central cell and the antipodals in *Arceuthobium americanum* may have also represented glycocalyx-like materials (M.J. Sumner, pers. comm., 1999; Sumner, 1986). Animal cells, which lack cell walls, possess carbohydrate materials that are covalently bound to proteins and lipids on the outer plasma membrane surfaces (Purves *et al.*, 1998). The carbohydrate moieties of these glycoproteins and glycolipids represent the glycocalyx, a matrix that provides integrity to animal cells and holds them together. Similarly, in regions of the *A. americanum* embryo sac where cell wall material was lacking and only plasma membrane contacts existed, such as the interface of the central cell with the egg apparatus, some of the electron opaque deposits may have represented glycocalyx-like materials that provided integrity to the interface. While the interface of the central cell with the antipodals did

contain cell wall material, some of the electron opaque deposits could nonetheless have represented glycocalyx-like material in addition to cell wall precursor material. It may be difficult to determine a compositional difference between cell wall precursors (particularly non-cellulosic precursors) and glycocalyx materials, as both would have a large carbohydrate component. Functionally, cell wall precursors and glycocalyx materials would have a similar role, although precursors would presumably be separate from the plasma membrane, whereas glycocalyx material would be intricately bound to the plasma membrane. The roles of the plant cell glycocalyx should be examined further, especially since there are implications for transgenic experiments that use plant protoplasts.

Huang and Russell (1994), using anti-actin antibodies, determined that the electron opaque deposits at the interface of the central cell and the degenerating synergid in *Nicotiana tabacum* were actin and believed that the actin was involved in transfer of a male nucleus from the degenerating synergid to the central cell. Thus, some of the electron opaque deposits between the unfertilized central cell and the degenerating synergid of *A. americanum* might not only have represented cell wall precursors/glycocalyx materials but could also have represented actin that was involved in central cell fertilization. Moreover, if the cells of the egg apparatus followed similar early developmental patterns, some of the electron opaque deposits seen at the interface of the central cell with the egg cell and persistent synergid of *A. americanum* might have also represented actin (perhaps alongside wall precursors/glycocalyx materials). Furthermore, electron opaque deposits at the interface of the central cell with all egg apparatus cells in *Pelargonium hortorum* (Guo Feng, 1997) and *Brassica campestris* (Sumner, 1986) might have represented actin as well as wall precursors/glycocalyx materials. The potential presence of actin between the plasma membranes of viable cells is particularly noteworthy, as the presence of intercellular actin suggests a novel mechanism of intercellular actin synthesis.

Huang and Russell (1994) also localized electron opaque actin deposits at the interface of the degenerating synergid with the egg cell in wall-less regions near the *Nicotiana tabacum* central cell, believing that the actin deposits were involved in male nucleus transfer from the degenerating synergid to the egg cell. However, electron opaque deposits were not observed at this interface in *Arceuthobium americanum.* It would be useful to re-examine this interface in the *A. americanum* embryo sac with anti-actin

antibodies; actin was likely present at this interface but not evident, possibly because the dark degenerating synergid cytoplasm may have occluded the deposits. The electron opaque deposits seen at the interface of the central cell and the antipodals of *A. americanum* would not have a role in sperm nucleus transfer, and thus, as mentioned, the deposits at this interface very likely represented cell wall precursors or glycocalyx materials as opposed to actin. It would be useful to examine this interface with anti-actin antibodies as well.

Plasmodesmata were not observed in the embryo sac wall of *Arceuthobium americanum*. The absence of plasmodesmata in embryo sac walls is typical for most flowering plants (Willemse and van Went, 1984; Han *et al.*, 2000). As plasmodesmata in the *A. americanum* embryo sac wall were lacking, intake of materials into any cell of the embryo sac from the PNC was thus by diffusion across the plasma membranes or by active transport across the membranes via membrane pumps such as ATPase (Van Caeseele *et al.*, 1996). Therefore, only small solutes, including inorganic materials, simple carbohydrates, and amino acids originally transferred in to the PNC via the vascular tissues of the pedicel could have entered cells of the embryo sac (the nature of the vascular tissue will be further described in part 10F of this discussion). Although transfer cell wall ingrowths were not immediately evident in any cell of the unfertilized embryo sac, mitochondria were present in all viable cells of the unfertilized embryo sac (Figures 4.20, 4.21, and 4.23), and these mitochondria might have played a role in active transport. The lack of a direct cytoplasmic connection between the gametophyte and the maternal sporophyte structurally isolated the diploid and haploid genotypes. This possibly prevented incompatible recognition proteins or glycoproteins (Salisbury and Ross, 1992) from moving from the maternal sporophyte to the gametophyte (or vice versa), as the plasma membranes at the embryo sac wall would have prevented the transfer of protein. Similarly, virus transmission from the maternal sporophyte into the gametophyte (or vice versa) might have been prevented (Ding, 1998).

Among the cells of the embryo sac of *Arceuthobium americanum*, neither plasmodesmata (in the areas where some cell wall material was present) nor direct cytoplasmic connections (in the wall-less areas) were observed. This is more unusual, as plasmodesmata/cytoplasmic connections have been observed among the cells of the embryo sac in many species (Kapil and Bhatnagar, 1981; Liu *et al.*, 1998; Han *et al.*, 2000). However, the species in which plasmodesmata/cytoplasmic connections were seen among

the cells of the embryo sac were all monosporic. As such, the eight nuclei of the embryo sac would have all been derived from one nucleus, and therefore all eight nuclei would have had the same genetic makeup. Conversely, in a bisporic species such as *A. americanum*, the eight nuclei of the embryo sac would have been derived from two nuclei possessing different genetic constitutions (assuming crossing over had taken place). Therefore, perhaps the lack of plasmodesmata/cytoplasmic connections among the cells of the embryo sac in *A. americanum* also structurally isolated cells of slightly different genetic makeup. Alternatively, perhaps plasmodesmata/cytoplasmic connections were present among the cells of the embryo sac of *A. americanum* but simply not observed because they were rare.

5. Details Regarding the Cells of the Unfertilized Mature Seven-Celled Embryo Sac of *Arceuthobium americanum*

5A. Unfertilized egg cell

The egg cell of *Arceuthobium americanum* was the second largest cell of the embryo sac, after the central cell (Figure 4.12), as is typical for a flowering plant. This finding contradicts Bhandari and Vohra's (1983) claim that the egg cell in the Viscaceae is the largest cell of the embryo sac. Aside from the reversed cytoplasmic polarity in the unfertilized egg cell of *A. americanum* (Figure 4.20), the egg cell ultrastructure was fairly typical with regard to the flowering plants. There were few organelles in the *A. americanum* egg cell cytoplasm, which indicated a low level of metabolic activity typically noted for flowering plants. The presence of highly condensed chromosomal material in the egg cell nucleus also indicated that the egg cell was quiescent (Figure 4.18), as highly condensed chromatin is typically not being transcribed (Rothwell, 1988). Some mitochondria were present in the egg cell cytoplasm of *A. americanum*, as the egg cell must respire and fuel membrane pumps (Figure 4.20). The presence of mitochondria in the unfertilized egg cell suggested that the mitochondria were maternally inherited, at least in part.

A few osmiophilic bodies were also present in the egg cell cytoplasm of *Arceuthobium americanum* (Figure 4.20). As these osmiophilic bodies generally stained greyish-light blue with crystal violet (not shown), they very likely represented lipid bodies. Lipids treated with osmium tetroxide and Toluidine Blue (TB) often stain greyish-blue (Gahan, 1984; Yeung, 1990). Thus, as crystal violet and TB are in the same stain family

(Gahan, 1984), greyish-blue appearance of osmiophilic bodies that had been stained with crystal violet indicated that the bodies were likely lipid (M.J. Sumner, pers. comm., 2002). Zaki and Kuijt (1994) believed similar osmiophilic bodies in the egg cell cytoplasm of *Viscum minimum* represented lipid bodies and stated that these lipid bodies might represent a type of reserve for the developing egg cell. This may be true for the *A. americanum* egg cell as well, especially that starch grains, another potential reserve, were apparently absent from the *A. americanum* egg cell. Moreover, as lipid tends to represent a more long-term storage material than starch (Salisbury and Ross, 1992), the lipids would probably also be used after fertilization has taken place. Although fatty acids may be readily transported across plasma membranes, the fatty acids are too insoluble to be readily transported among cells, due to the polar nature of cytoplasm (Salisbury and Ross, 1992). Thus, the lipids present in the egg cell had to be synthesized within the cell from carbohydrates, and the carbohydrates either entered the egg cell directly from the PNC or via other cells of the embryo sac. The synthesis of lipids likely occurred in plastids or proplastids, as suggested by Ke *et al.* (2000), and proplastids were indeed seen within the egg cell of *A. americanum*. In addition, although starch grains were apparently absent from the *A. americanum* egg cell, the presence of proplastids implicated the potential for starch grains (or other plastids) to develop post-fertilization. Furthermore, the presence of proplastids also suggested that plastids were maternally inherited in *A. americanum* (at least in part).

5B. Pre-fertilization synergids

Aside from the reversed cytoplasmic polarity in the pre-fertilization synergids of *Arceuthobium americanum* (Figure 4.20), the ultrastructure of the two synergids was similar to that of typical flowering plant synergids. However, at no time were two non-degenerating, healthy synergids seen within the embryo sac, implying that one synergid began to degenerate almost immediately after it had formed. Synergid degeneration in typical flowering plants can be somewhat protracted, since degeneration can occur anytime after pollination but before the pollen tube reaches the embryo sac (Raven *et al.*, 1999). In *A. americanum*, there was no interval in which the embryo sac waited for the pollen tube to grow, and thus rapid synergid degeneration likely occurred as soon as the embryo sac was formed in order to enable waiting pollen tubes to promptly accomplish fertilization.

Although Zaki and Kuijt (1994) did not mention the presence of a degenerate synergid in *V. minimum*, it is apparent from their micrographs that one synergid was degenerate (Zaki and Kuijt, 1994; Figures 29 and 30). As such, degeneration was likely rapid in this species as well; perhaps the pollen tube(s) waited for an embryo sac to form as in *A. americanum*. Regardless of its position in the embryo sac, either synergid in *A. americanum* could degenerate (Figure 4.13). Perhaps the synergid that formed first or that was nearer to a waiting pollen tube degenerated. Although pollination has been suggested as the trigger for synergid degeneration in typical flowering plants (Xi and Luan, 2001), synergid degeneration in *A. americanum* could not be triggered by pollination, as synergids would not have formed at the time of pollination. However, signals from the pollen tube itself might have triggered synergid degeneration, regardless of whether the tube was distant from (typical flowering plants) or very near (*A. americanum* and possibly *V. minimum*) a synergid.

Ultrastructural characteristics of the pre-fertilization persistent synergid in *Arceuthobium americanum* indicated that the persistent synergid was metabolically active, more so than the egg cell, since the persistent synergid contained a wider range of organelles and was cytoplasm-rich (Figure 4.20). The organellar composition of the persistent synergid was similar to that described by Zaki and Kuijt (1994) for *Viscum minimum*. The persistent synergid of *A. americanum* may have played a role in accumulating reserves that could be accessed by the central cell, egg cell, and ultimately the endosperm and zygote (Zaki and Kuijt, 1994). The proximity of the persistent synergid to both the central cell and the egg cell in both organisms (and all in flowering plants) further suggested that the persistent synergid had a role related to support of both the central cell and egg cell. As in the egg cell of *A. americanum*, starch grains were rare in the persistent synergid while osmiophilic bodies were common (Figure 4.20). The osmiophilic bodies were likely lipid bodies, as they commonly stained greyish blue with crystal violet (not shown). Similarly, starch grains were apparently rare while lipid bodies were apparently common in a (likely persistent) synergid of *V. minimum* (Zaki and Kuijt, 1994; Figure 32). Again, as lipids represent fairly long-term means of storage (Salisbury and Ross, 1992), the synergid would likely persist for a while after fertilization had taken place so that metabolites derived from stored lipids

could be continually provided to the endosperm and zygote. Proplastids in the persistent synergid (not shown) represented the site of lipid synthesis as well as future amyloplasts.

There was a filiform apparatus in the unfertilized embryo sac of *Arceuthobium americanum*, which was found between the two synergids as a thick fibrillar pad of wall material that became gradually tapered in the region of the unfertilized central cell. The filiform apparatus lacked the typical transfer cell ingrowths: a filiform apparatus lacking transfer cell ingrowths was also described for *Viscum minimum* as well as for several other flowering plants (Raghavan, 1986). As the filiform apparatus formed after the pollen tube had reached the embryo sac in *A. americanum*, it did not have a role in long distance pollen tube attraction. However, the filiform apparatus may have had a role in directing the pollen tube to discharge into the degenerating synergid (see Figure 4.23) as well as in ensuring delivery of the male sperm cells to the degenerating synergid (Russell, 1993). Furthermore, as postulated for filiform apparati (even those that are merely pads of material; Raghavan, 1986), the filiform apparatus of *A. americanum* may have been involved in the short distance active transport of metabolites or other materials into the persistent synergid from the PNC. As implied earlier, mitochondria seen in the persistent synergid of *A. americanum* may have provided energy for membrane pumps involved in active transport. Moreover, the mitochondria may not only have fueled the apparently high metabolic rate of the synergid, but potentially provided energy to initiate and establish new membrane extensions around the filiform apparatus (Zaki and Kuijt, 1994).

The degenerating synergid of *Arceuthobium americanum* (Figures 4.22 and 4.23) displayed characteristics of a typical degenerating synergid and, for that matter, a typical degenerating cell (Mauseth, 1988), possessing very darkly stained cytoplasm and generally amorphous organelles. Starch was probably just as rare in the degenerating synergid as it was in the persistent synergid, but because starch is relatively inert (Salisbury and Ross, 1992), it was likely the only substance evident during degeneration. In Figure 4.23, which displays a degenerating synergid that had just received a pollen tube, some of the starch grains evident in the degenerating synergid may have been discharged by the pollen tube. Pollen tube discharge of starch grains into the degenerating synergid has been noted for *Oryza* (Dong and Yang, 1989).

5C. Pre-fertilization antipodals

Like the pre-fertilization persistent synergid of *Arceuthobium americanum* (Figure 4.20), but unlike the egg cell, the ultrastructural characteristics of the pre-fertilization antipodals indicated that the antipodals were metabolically active, as they contained a wide range of organelles (Figure 4.24). Thus, the antipodals (Figure 4.24), like the persistent synergid (Figure 4.20), may have had a role in accumulating reserves for the other cells of the embryo sac prior to and following double fertilization. The organellar composition of the antipodals was similar to that described for *Viscum minimum* (Zaki and Kuijt, 1994). However, as opposed to the condition in *V. minimum* in which one antipodal was healthier than the other two, the three antipodals of *A. americanum* were very similar to each other, and all appeared healthy. Although metabolically active, the pre-fertilization antipodals of *A. americanum* (Figure 4.24) were not quite as metabolically active as the persistent synergid (Figure 4.20), since the antipodals were not as cytoplasm-rich as the persistent synergid. Since the antipodals were not as close to the egg cell as the persistent synergid, the antipodals likely primarily supported only the central cell as opposed to both the central cell and the egg cell. Thus, the support of one cell might not have been as metabolically demanding as the support of two cells. Moreover, there were three antipodals and only one persistent synergid. While antipodal-type tasks might have been divided amongst the three antipodals, synergid-type tasks might have had to be carried out by the only viable synergid. This would have also likely increased the metabolic activity of the persistent synergid when compared to an antipodal. The same scarcity of starch grains and relative abundance of osmiophilic bodies (likely lipid bodies) noted for the egg cell and persistent synergid of *A. americanum* (Figure 4.20) existed for the antipodals as well (Figure 4.24). As in the egg cell and persistent synergid, the osmiophilic bodies in the antipodals were likely lipid bodies, as they stained greyish-blue with crystal violet (not shown).

5D. Unfertilized central cell

The unfertilized central cell was indisputably the largest cell of the *Arceuthobium americanum* embryo sac (Figure 4.12), as is typical for a flowering plant (Mauseth, 1988). However, only one nucleus was visible in the central cell, as opposed to the expected two, and thus the single nucleus likely represented the diploid fusion nucleus (Figure 4.12 and

4.25). Evidence that the single nucleus in the unfertilized central cell was the diploid fusion nucleus (and that there were originally two haploid polar nuclei) was provided by the fact that the single central cell nucleus was twice as large as any of the haploid nuclei in the unfertilized embryo sac. See Chapter Six, sections III. Results and IV. Discussion for confirmation of the various ploidy levels in *A. americanum.* Similarly, Dowding's (1931) observation of only seven nuclei in the embryo sac *A. americanum* likely resulted because the two polar nuclei had fused. Therefore, the two polar nuclei must have fused very soon after their formation.

The fusion nucleus in the unfertilized central cell of *Arceuthobium americanum* was found very close to the cells of the egg apparatus (Figure 4.25), as is typical for flowering plants (Mauseth, 1988). The *A. americanum* fusion nucleus was likely found in this location because the nucleus was readying to be fertilized by the sperm nucleus that enters the central cell via the degenerating synergid. As there was cytoplasm associated with the fusion nucleus, and as the fusion nucleus was found near the egg apparatus, the bulk of the central cell cytoplasm was thus also found near the egg apparatus (Figure 4.25), as is typical (Mauseth, 1988).

In general, the unfertilized central cell of *Arceuthobium americanum* possessed a greater variety of organelles than the egg cell, and was thus more metabolically active than the egg cell, as is typical (Mauseth, 1988). However, unlike typical flowering plants, the unfertilized central cell did not have an abundance of organelles. This is likely because organellar proliferation was not triggered until fertilization had taken place. Folsom and Cass (1992) noted a similar situation in the central cell of *Glycine max.* The delay of organellar proliferation in the central cell of both *A. americanum* and *G. max* likely represented an advantage, as needless energy would not have to go toward sustaining a central cell that might not become fertilized. Whereas the persistent synergid and antipodals of *A. americanum* did show pre-fertilization organellar proliferation, these cells were considerably smaller than the central cell. If organellar proliferation occurred in a large cell such as the central cell, a great loss of energy would have occurred if fertilization failed.

Organelles present in the unfertilized central cell of *Arceuthobium americanum* might have been involved in acquiring nutrients for immediate needs of the unfertilized central cell and unfertilized egg cell as well as for the needs of the future endosperm and

embryo. Peripheral mitochondria likely aided in the active transport of material into the *A. americanum* central cell (Figures 4.21 and 4.23) from the persistent synergid, antipodals, and PNC, even though the unfertilized central cell possessed no obvious transfer cell walls (Figure 4.25). The presence of mitochondria in the central cell implied that the mitochondria of the future endosperm were, at least in part, maternally inherited, as they were in the egg cell. In addition, starch grains in amyloplasts, present in the unfertilized central cell (Figure 4.25), may have been needed for immediate needs of the unfertilized central cell and unfertilized egg cell as well as for requirements of future endosperm and embryo development. The presence of amyloplasts supported the concept of maternal plastid inheritance in the endosperm. Osmiophilic bodies (likely lipid bodies, as they stained greyish-blue with crystal violet - not shown) might have also contributed to future endosperm and embryo development. Both types of reserves, starch and lipids, were likely required in the unfertilized central cell because the central cell would undergo massive development as endosperm, which in turn would support the embryo throughout all stages of development. Due to the large size of the central cell, its role in supporting the future embryo was likely greater than that of the persistent synergids or antipodals.

A large central vacuole was present in the unfertilized central cell of *Arceuthobium americanum* (Figure 4.25), as is typical for flowering plants. The large vacuole permitted the central cell to expand without having to expend energy for the synthesis of cytoplasm, as the vacuole could accumulate a few osmotically active solutes and water to accomplish expansion. In turn, the expanded central cell would have a large surface area by which to take in nutrients, particularly in the event of successful fertilization, and the nutrients could subsequently be used to support future endosperm and embryo development. Occasionally, smaller vacuoles of the peripheral cytoplasm were seen to be confluent with the large central vacuole, and these smaller vacuoles were presumably contributing materials including tonoplast membrane to the large vacuole. Tannin-like materials were also seen in the large vacuole of the unfertilized central cell; similar tannin-like materials were seen in the developing embryo sac of *Viscum minimum* (Zaki and Kuijt, 1994). Zaki and Kuijt (1994) as well as Sangwan and Camefort (1983) believed that tannin-like materials in the large vacuoles of plant gametophytes are involved in the reconditioning of the gametophytic cells during the final conversion from the (maternal) sporophytic stage to the gametophytic stage.

6. Further Comments Regarding Pollination and Pollen Tube Growth in *Arceuthobium americanum*

Many aspects of pollination and pollen tube growth in *Arceuthobium americanum* have already been discussed in concert with female development. Nonetheless, a few further concepts should be addressed. The change in stigma colour from yellow (Figure 4.1) to red (Figure 4.54) likely occurred soon after pollination was accomplished, and indicated that the stigma was no longer receptive to pollination. The colour change possibly occurred because new pigments and/or proteins inhibitory to pollen germination had been synthesized on the stigmatic surface, or simply because small particulates had accumulated on the stigma and occluded the yellow colour.

It has already been mentioned that multiple pollen tubes entered the PNC of *Arceuthobium americanum* (as would be expected due to the presence of two megasporocytes) and that multiple pollen tubes were found around each megasporocyte. As implied earlier, each megasporocyte likely produced enough chemotropic material (or perhaps also megasporocyte callose) to attract multiple pollen tubes, albeit slowly. However, an interesting question arises as to how many pollen tubes penetrated the embryo sac when it formed. Moreover, as the pollen tube tips were seen to be bifurcated (D.A.R. McQueen, pers. comm., 1995), one wonders how many tips penetrated the embryo sac. Evidence suggested that only one pollen tube tip penetrated the embryo sac, doing so via the degenerating synergid (Figure 4.23). Similarly, Compton (1912) noted two pollen tubes in the presence of an embryo sac of *Lychnis*, but noted that only one had penetrated the embryo sac. Thus, not only did the pollen tube tip nearest to the embryo sac likely induce one of the two synergids (the nearer one) to degenerate in *A. americanum*, but the filiform apparatus likely also specifically directed only the nearest pollen tube tip to discharge into the degenerating synergid. In other words, communication worked bidirectionally. Furthermore, even though synergids were not required for pollen tube growth in *A. americanum*, the synergids were needed to direct the final penetration of the embryo sac, likely by chemotropic methods. Other tips of a given bifurcated pollen tube in *A. americanum* were probably involved in nutrient foraging.

Although the PNC of *Arceuthobium americanum* was ategmic, penetration of the PNC could be theoretically considered to be porogamous for two reasons. Firstly, the pollen

tubes entered the morphological apex of the PNC, which represented the typical location of a micropyle (Figure 4.11). Secondly, and more significantly, the pollen tubes approached the base of the embryo sac in the region representing the ancestral micropyle (see Figure 4.80). Notably, the pollen tubes did not enter the upper pole of the embryo sac (where the antipodals were located), even though the upper pole was closer to the stigma. This suggested that specifically the base of the megasporocyte was the source of a putative factor for pollen tube guidance. Furthermore, as megasporocyte callose was deposited most heavily at the base of the megasporocyte, the potential role of megasporocyte callose in pollen tube guidance was further supported.

One final comment about pollen tube penetration of the embryo sac is needed. The pollen tube likely entered a degenerate cell so that the cytoplasm of that cell could not interfere with the fertilization process. Moreover, an analogy exists with regard to enucleate phloem sieve tube elements (Raven *et al.*, 1999). Removal of the major genetic control of a cell likely ensures that the cell, be it a degenerating synergid or a sieve tube element, does not try to modify or otherwise control the progression of an entity though its system. Additionally, as the plasma membrane would have disintegrated in the degenerating synergid, movement of the sperm cells into the synergid from the pollen tube and movement of sperm nuclei into the egg cell or central cell would have been facilitated (Russell, 1993). Furthermore, pollen tube entry into a synergid ensured that even if only one pollen grain was successful in reaching the stigma and subsequently germinating toward the megasporocyte/embryo sac, the pollen tube from that single pollen grain would only have to penetrate the embryo sac once to accomplish double fertilization. There would be no need for multiple tubes to penetrate an embryo sac (one at the egg cell, the other at the central cell) for successful double fertilization.

7. Double Fertilization and the Fertilized Embryo Sac of *Arceuthobium americanum*

7A. The process of double fertilization and overall changes to the embryo sac

Although double fertilization was not specifically observed, ploidy level analysis determined that double fertilization indeed takes place in *Arceuthobium americanum*, as the embryo was determined to be diploid and the endosperm was determined to be triploid (see Chapter Six, section IV. Discussion - 3). Moreover, ploidy level analysis along with the

observation of megasporocyte callose ruled out apomixis as a method of embryogenesis (Chapter Six, section IV. Discussion - 3; Carman *et al.*, 1991). Regarding fertilization of the central cell, it was noted that the two polar nuclei first fused with each other before being fertilized (Figure 4.25). Notably, the fact that the primary endosperm nucleus in the fertilized central cell was 1.5 times larger than the diploid fusion nucleus and larger than any other nucleus in the embryo sac confirmed that fertilization had unquestionably taken place (Figure 4.26).

Double fertilization in *Arceuthobium americanum* was very rapid, taking place in a single day (see section II. Results - 9 of this chapter). Double fertilization was likely rapid because the pollen tubes were properly positioned. As is typical for flowering plants following double fertilization (Maheshwari, 1950), the cytoplasmic polarity evident in the unfertilized egg cell of *Arceuthobium americanum* (Figure 4.18) was no longer evident in the zygote (Figure 4.30). Specifically, the fertilized nucleus had acquired a more central location, the large vacuole had disappeared, and the amount of cytoplasm had increased (Figure 4.30). The loss of the large vacuole likely permitted the newly diploid nucleus to move to a more central location where it could better control the amassing cytoplasm. The shift from a more vacuolate to a more cytoplasmic state indicated a shift to a more active metabolism, typical for zygotes (Maheshwari, 1950). A similar loss of cytoplasmic polarity, increase in cytoplasm, and loss of vacuole occurred in the post-fertilization persistent synergid as well. This has not been observed in flowering plants before, but, as in the zygote, the decrease in vacuole likely permitted the synergid nucleus to move to a more central location where it could better control the amassing cytoplasm. Notably, the fact that the post-fertilization persistent synergid amassed cytoplasm and that its nucleus became centered implied that this cell did not degenerate (as would be expected for typical flowering plants), but instead likely had a role in zygote and endosperm maintenance. Specific details regarding the ultrastructure of the zygote will be addressed in part 7B of this discussion, and details regarding the ultrastructure of the post-fertilization synergids will be addressed in part 7C of this discussion.

As observed in typical flowering plants following double fertilization (Mogensen and Suthar, 1979), cell wall material became deposited at the interface of the zygote in *Arceuthobium americanum* with the fertilized central cell (Figures 4.26, 4.27 and 4.30). At

this interface, cell wall material was previously absent (Figures 4.12, 4.14, and 4.19). The deposition of cell wall material at this interface likely followed the pattern of typical cell wall fortification that takes place during normal cell wall growth (Krishnamurthy, 1999). Cell wall formation at the interface of the fertilized central cell and the zygote created a more definite boundary between the triploid genome of the fertilized central cell and the diploid zygote. The structural isolation of the different genomes likely prevented incompatibility reactions that may have resulted as the two distinct genomes began to synthesize outer plasma membrane proteins with potentially incompatible surface sequences or glycosylations (Salisbury and Ross, 1992).

The absence of plasmodesmata between the fertilized central cell and the zygote further suggested that a structural isolation of the two genomes was ideal, as the intercellular movement of incompatible cytoplasmic proteins or transcription factors (Ding, 1998) from different genomes could be prevented. Even if plasmodesmata had been present but merely not observed between the egg cell and central cell prior to double fertilization (review part 4 of this discussion), there were very likely no plasmodesmata between the zygote and central cell following double fertilization. Han *et al.* (2000) used membrane-impermeable, plasmodesmata-transported fluorescent dye tracers to show that symplastic isolation between the zygote and central cell in *Torenia fournieri* occurs soon after double fertilization. Furthermore, Han *et al.* (2000) believed this early symplastic isolation occurs in most flowering plants, as plasmodesmata are not present between the embryo and endosperm of flowering plants (Dute *et al.*, 1989).

Cell wall material was also deposited at the remaining interfaces among all cells in the embryo sac of *Arceuthobium americanum* following double fertilization (Figures 4.26, 4.27, and 4.30), probably following a pattern of typical cell wall fortification (Krishnamurthy, 1999). The deposition of cell wall material at the remaining interfaces of all cells created cell walls where none existed before (such as the interface of the central cell with the persistent synergid) or thickened existing cell walls (Figures 4.27 and 4.30). Like the deposition of cell wall material at the interface of the zygote and the fertilized central cell, the deposition of cell wall material at remaining zygotic interfaces is typical for flowering plants (Mogensen and Suthar, 1979; Natesh and Rau, 1984). The deposition of cell wall material at all zygotic interfaces permitted the zygote wall to become uniformly

thickened, as noted for typical flowering plants (Natesh and Rau, 1984). This uniform cell wall thickening likely protected the *A. americanum* zygote from being crushed during caecum expansion and endosperm growth, which are events that generate considerable pressure within the embryo sac. The presence of a complete cell wall at the interface of the zygote and the degenerating synergid suggested that fertilization of the egg cell had undoubtedly taken place, as the cell wall would have otherwise blocked migration of the sperm nucleus from the degenerating synergid to the egg cell.

However, the deposition of cell wall materials at non-zygotic interfaces in the fertilized embryo sac of *Arceuthobium americanum* was unusual, and has not been described for typical flowering plants. Cell walls at the interfaces of the nonviable degenerating synergid of *A. americanum* were obviously laid down by the other viable cells bordering it (the persistent synergid, the fertilized central cell, and, as mentioned, the zygote). Moreover, the presence of cell wall material at non-zygotic interfaces permitted the other cells of the fertilized embryo sac, particularly the persistent synergid and the antipodals, to maintain integrity. As such, the persistent synergid and the antipodals of *A. americanum* could potentially play roles in early zygote and central cell/endosperm maintenance instead of immediately becoming crushed and ineffectual, as is typical for flowering plants. Notably, the antipodals of *A. americanum* had even thicker cell walls than the persistent synergid. Consequently, the antipodals persisted well into the period of caecum expansion, whereas the persistent synergid was crushed during early caecum expansion (the significance of this will be discussed in parts 7C and 7D of this discussion). Furthermore, cell walls at all interfaces within the embryo sac may also have provided general support for the embryo sac, especially during further expansion. This role may have been particularly applicable to the relatively thick antipodal cell walls as well as the zygote cell wall.

As postulated for the interface of the fertilized central cell and the zygote of *Arceuthobium americanum*, cell wall deposition at the remaining interfaces of all cells in the fertilized embryo sac create definite boundaries among the differing genomes. For example, cell wall deposition at the interface between the persistent synergid and the zygote created a barrier between the haploid genome of the synergid and the diploid genome of the zygote. Likewise, cell wall deposition at the interface between the antipodals and the fertilized central cell created a barrier between the haploid genotype of the antipodals and the triploid

genome of the fertilized central cell. Cell wall deposition among the haploid cells of the embryo sac (for example, among the antipodals or between the persistent synergid and the degenerating synergid) may have helped isolate haploid genotypes of slightly different genetic makeup. Different genetic constitutions are found among haploid nuclei derived from a bisporic embryo sac (see part 4 of this discussion). As was noted for the interface of the fertilized central cell and the zygote, plasmodesmata were apparently absent from all interfaces within the fertilized embryo sac, again suggesting that structural isolation of the differing genomes/cells of genetic makeup was desirable. Furthermore, as plasmodesmata were possibly absent, the many mitochondria seen within the post-fertilization persistent synergid (Figure 4.30), antipodals (Figure 4.32), and fertilized central cell (Figure 4.31) may have thus been crucial in permitting transport from one cell of the embryo sac to another via membrane pumps.

Electron opaque deposits present at the interface of the unfertilized central cell and the egg apparatus (Figure 4.19 and 4.23) as well as at the interface of the unfertilized central cell and the antipodals (Figure 4.24) of *Arceuthobium americanum* disappeared after fertilization (Figures 4.30, 4.31, and 4.32). Putative electron opaque cell wall precursors present at the interface of the unfertilized central cell and the egg apparatus as well as at the interface of the unfertilized central cell and the antipodals would have been replaced with true cell wall materials following fertilization. The covalent bonding of the precursors into cell walls might have either dispersed the materials and/or reduced their ability to take up stain, making them less electron opaque. Similarly, putative electron opaque glycocalyx materials present at the interface of the unfertilized central cell and the egg apparatus as well as at the interface of the unfertilized central cell and the antipodals would have been replaced with plant cell wall material following fertilization. The cell wall material would have either masked the glycocalyx materials or rendered them unnecessary so that they could break down. Putative electron opaque actin deposits present at the interface of the unfertilized central cell with the degenerating synergid, believed to aid in central cell fertilization, would no longer be necessary following fertilization, and could have dissipated. Similarly, if any of the electron opaque deposits present at the interface of the central cell with the persistent synergid or egg cell represented actin, the deposits could have also dissipated. The potential presence of actin at the interface of the unfertilized central cell

with the persistent synergid/egg cell would have likely been a product of early development that was probably not needed prior to fertilization (review part 4 of this discussion), and would thus not be needed following fertilization. Finally, if electron opaque deposits had been observed at the interface of the degenerating synergid and the unfertilized egg cell in regions near the central cell, and if those deposits represented actin, the actin deposits could also have dissipated. Actin at the interface of the degenerating synergid and the unfertilized egg cell in regions near the central cell would have played a role in egg cell fertilization, and would thus be unnecessary following egg cell fertilization.

7B. The zygote, its quiescence, and the ending of quiescence

Immediately following fertilization, the chromosomal material of the newly diploid zygote nucleus in the newly formed zygote of *Arceuthobium americanum* became more dispersed (Figure 4.30) than it was before fertilization (Figure 4.18). As dispersed chromatin is typically undergoing transcription (Rothwell, 1988), the diploid nucleus in the zygote was likely undergoing more transcriptional events than the haploid nucleus in the unfertilized egg cell. Thus, along with the loss of cytoplasmic polarity, increase in cytoplasmic volume, and loss of the large vacuole following fertilization of the egg cell, the more dispersed state of the chromosomal material further indicated that the zygote had become more metabolically active than the unfertilized egg cell. It should also be mentioned that dwarf mistletoe nuclei are chromocentric (Hawksworth and Wiens, 1996); chromocentric nuclei have fairly dispersed chromosomal material (Purves *et al.* 1998). Therefore, it is not surprising that the nucleus in the new sporophytic generation (represented by the zygote, as no suspensor will form) should have properties that are similar to those observed in a mature dwarf mistletoe plant. Nonetheless, an increase in number and variety of organelles in the newly formed zygote also indicated the shift to a higher metabolic state. Most notably, starch grains had accumulated in the zygote, indicating that some proplastids seen earlier had developed into amyloplasts and that the zygote had begun to manipulate its reserves. More osmiophilic bodies were present as well. These osmiophilic bodies likely represented lipid bodies, as they stained greyish-blue with crystal violet (not shown), and the increase in the amount of lipid bodies in the zygote

(Figure 4.30) compared to the unfertilized egg cell (review Figure 4.20) confirmed that a metabolic increase had occurred post-fertilization.

Also following fertilization, the newly formed zygote of *Arceuthobium americanum* became rounder (Figure 4.30) than the unfertilized egg cell (Figure 4.18). This rounding off is not necessarily typical for flowering plants, as most flowering plant zygotes retain the elongated shape of the unfertilized egg cell (Crété, 1963). The more rounded appearance of the *A. americanum* zygote was likely partially due to the fact that a suspensor does not form in *Arceuthobium*, and thus a suspensor pole and embryo proper pole did not need to be maintained within the *A. americanum* zygote. The more rounded appearance was partially attributable to the aforementioned uniform thickening of the zygote wall. However, as a uniformly thickened zygote wall typically forms in flowering plants (Natesh and Rau, 1984), the rounding evident in the *A. americanum* zygote must have been attributable to other factors as well. The many smaller vacuoles present in the zygote of *A. americanum* (Figure 4.30) possibly created an even pressure around the entire periphery of the zygote, rounding out the cell. Subsequently, the rounder zygote was probably better able to diffuse the pressures accumulating in the embryo sac due to caecum and endosperm development. A rounder surface resists forces better than a more planar surface, as rounded surfaces can counter force vectors from different planes, whereas a more planar surface is only effective in countering force vectors emanating perpendicular to its plane.

It is difficult to ascertain whether the zygote of *Arceuthobium americanum* achieved a true quiescent (non-dividing but metabolically active) stage. Granted, the zygote did not undergo its first division until two months after double fertilization, and the endosperm began to develop before the embryo divided (see section II. Results - 13A of this chapter). Yet, as it took two full summers for the embryo to develop to maturity, at which point the embryo was still relatively small compared to a typical mature flowering plant embryo, the delayed zygotic division in *A. americanum* may have simply represented an overall pattern of slow development. Nonetheless, a two-month quiescent period for *A. americanum* is in agreement with the findings of Pisek (1923), who believed that the quiescent period for the zygote of *Viscum album* was also about two months. However, Hudson (1966) said that the zygote of *A. americanum* divided once after being surrounded by the endosperm in all planes, forming a two-celled proembryo before entering the true quiescent period. Bhandari

and Nanda (1968a) made a similar finding with regard to *A. minutissimum*. Hudson (1966) further stated that the two-celled proembryo of *A. americanum* remained quiescent for three to six weeks before it begins to divide. Thus, the findings of Hudson (1966) as well as those of Bhandari and Nanda (1968a) are not supported by the findings in this thesis. The differences in these authors' findings and the findings of this thesis likely result from anomalous years in development in the work of Bhandari and Nanda (1968a) and Hudson (1966), site differences, climatic differences, host differences, and, in the case of *A. minutissimum*, species differences.

There were a few changes in the zygote of *Arceuthobium americanum* that indicated the zygote was preparing to divide. Firstly, the zygote wall became even thicker (Figure 4.45). This likely occurred in order to protect the zygote against the pressures accumulating from endosperm development, but also to provide the zygote with more cell material that could be stretched when one cell divided into two. Secondly, some of the chromosomal material in the zygote nucleus began to re-condense, which suggested that mitosis was imminent (Figure 4.48). Finally, just prior to division, the zygote initiated dislodgment from the embryo sac wall (Figure 4.48). Where the zygote shared a common cell wall with the embryo sac, the plasma membrane could be seen to be pulling away from the embryo sac wall. In the periplasmic space between the zygote cell plasma membrane and the embryo sac cell wall, vesicles lined with electron dense materials could be seen as the zygote synthesized its own cell wall that would allow for complete detachment of the zygote from the embryo sac wall. The method by which the *A. americanum* zygote synthesized a new cell wall represents a rare method for cell wall ontogeny in the flowering plants, as cell wall formation does not commonly occur without cell division and also because the plasma membrane does not typically bleb to form extracellular vesicles. However, extracellular vesicles are not unique, as they can occur during periods of rapid cell wall synthesis (Gedalovich and Kuijt, 1987). The vesicles enabling the zygote cell wall formation in *A. americanum* were likely Golgi-derived and contained non-cellulosic cell wall matrix substances (Carpita *et al,* 1996). Cellulosic components to the new zygote cell wall were most likely synthesized by cellulose synthetases found on the zygote plasma membrane.

It is actually fairly odd that the process of zygotic (or even embryonic) separation from the embryo sac wall has not previously been described in flowering plants. Many

micrographs of seeds clearly show embryos surrounded by endosperm (Mauseth, 1988; p 416). These micrographs imply that the zygote or embryo must have detached from the embryo sac wall and synthesized its own new wall at the point of detachment (although it is also possible that breakdown of embryonic cells at the point of attachment to the embryo sac wall may have occurred). There is an example of synthesis of a new zygotic wall in *Durvillaea potatorum* of the algal division Phaeophyta, in which part of the thick zygote wall is replaced by a new cell wall as the zygote begins to grow and divide (Kevekordes and Clayton, 1999).

7C. Post-fertilization synergids

Like the zygote, the persistent synergid assumed a more rounded appearance following double fertilization (Figures 4.28 and 4.30). The more rounded appearance was likely attributable to the fact that the persistent synergid acquired complete bounding walls following double fertilization. As the acquisition of complete bounding walls is atypical for post fertilization flowering plant synergids, it is not surprising that cell wall deposition alone could create the rounded appearance in the persistent synergid of *A. americanum*. As with the zygote, the rounded state of the persistent synergid likely endowed the synergid with more strength to resist accumulating pressures.

Also following double fertilization, the persistent synergid of *Arceuthobium americanum* became more metabolically active (Figures 4.28 and 4.30). Most notably, the chromosomal material became more dispersed, which indicated an increase in transcriptional activity. In addition, the filiform apparatus became even thicker and more prominent following double fertilization. Moreover, vesicles likely derived from the Golgi and probably containing non-cellulosic cell wall material (Carpita *et al.*, 1996) had apparently become trapped in the filiform apparatus wall during the massive wall synthesis event. A similar event occurs during the massive thickening of viscin cell walls (Gedalovich and Kuijt, 1987). The post-fertilization thickening of the filiform apparatus is extremely unusual, and implicated the *A. americanum* filiform apparatus in roles other than fertilization. Furthermore, the *A. americanum* filiform apparatus had become somewhat digitate, and had thus obtained the more typical appearance of a transfer cell wall (some of the apparent vesicles in the filiform apparatus may represent digitate protuberance captured

in cross section). As in the pre-fertilization persistent synergid, the many mitochondria in the vicinity of the filiform apparatus in the post-fertilization persistent synergid likely contributed energy to extend membranes and to fuel membrane pumps. Therefore, the filiform apparatus was likely critical for the import of nutrients from the sporophytic PNC, and in turn, these nutrients would very likely support development of the fertilized central cell and zygote.

There was also a buildup of starch grains in amyloplasts in the persistent synergid of *Arceuthobium americanum* (Figure 4.30). The amyloplasts would have developed from proplastids seen earlier, as well as from plastid division. Along with the buildup of starch, there was a concurrent loss of osmiophilic (likely lipid) bodies. Thus, the reserves in the lipid bodies had likely either been utilized by the synergid, converted to starch, exported to the fertilized central cell or, most likely, exported to the zygote.

Considering that the persistent synergid of *Arceuthobium americanum* showed a buildup of bounding wall material, development of the filiform apparatus, accumulation of starch, and an overall increase in size (Figure 4.30), the persistent synergid likely had a definite role following fertilization, unlike the persistent synergid in most flowering plants. The *A. americanum* persistent synergid was likely particularly effective in the transfer of nutrients to the fertilized central cell and the zygote because the synergid was not destined to divide, and could thus function almost exclusively in nutrient transfer. However, the fact that lipid bodies had virtually disappeared from the persistent synergid likely indicated that the persistent synergid did not continue to import and export metabolites for too long following double fertilization. Indeed, the persistent synergid became crushed during the early stage of fertilized central cell caecum formation (Figure 4.33), which occurred prior to fertilized central cell or zygotic division. Apoptotic genes of the persistent synergid likely also contributed to its ultimate demise. Thus, even though the persistent synergid potentially supported the fertilized central cell and zygote upon their formation, continued support of the future endosperm and embryo by the persistent synergid did not occur, and the embryo would likely derive more support from the endosperm. Meanwhile, the degenerating synergid fulfilled its function during fertilization, and consequently became obliterated following fertilization.

7D. Post-fertilization antipodals

Like the pre-fertilization antipodals of *Arceuthobium americanum*, the post-fertilization antipodals probably had a role in providing nutrients to the fertilized central cell (Figure 4.32). As with the persistent synergid, the antipodals did not divide, and thus were likely involved in providing nutritive support for the fertilized central cell, which did have to prepare for division as well as caecum expansion. As mentioned, the particularly thick antipodal cell walls likely helped maintain the integrity of the rounded antipodals so that they could continue to provide reserves to the fertilized central cell even under the physical pressures of early caecum formation (Figures 4.33 and 4.34). Notably, whereas both synergids became obliterated during early caecum growth, the antipodals persisted until the caecum reached the base of the PNC. At this time, the zygote was likely relying more heavily on the fertilized central cell for reserves, rendering the persistent synergid unnecessary, whereas the fertilized central cell likely still needed support from the antipodals. The antipodals may have been specifically required to provide nutrients to the fertilized central cell for the process of caecum formation. The thick antipodal walls might have acted as regions of apoplastic transport, playing a role similar to the filiform apparatus. The contortion to the antipodal plasma membrane by the thick walls lends support to this notion, as the contortion would have increased the membrane surface area available for transport from the antipodal symplast to the apoplast. The electron opaque deposits that appeared in the partitioning cell walls of the antipodals possibly represented degraded vesicles that had become trapped during the period of massive cell wall synthesis (Figure 4.32); a similar observation was also made regarding the post-fertilization filiform apparatus (Figure 4.30). Furthermore, due to caecum formation, the volume of the fertilized central cell possibly became too large for the single primary endosperm nucleus to maintain effectively. It is well known that a given nucleus can only maintain a finite volume (Rothwell, 1988). Thus, the antipodal nuclei might have acted as extra control centers for the enlarged fertilized central cell.

As was noted for the persistent synergid of *Arceuthobium americanum* (Figure 4.30), there was buildup of starch grains in amyloplasts in the post-fertilization antipodals (Figure 4.32). The amyloplasts would have developed from proplastids seen earlier, as well as from plastid division. Also as noted for the persistent synergid (Figure 4.30), a loss of

osmiophilic (likely lipid) bodies occurred in the post fertilization antipodals (Figure 4.32). The reserves in the lipid bodies had either been utilized by the antipodals, converted to starch, or exported to the fertilized central cell. As noted for the persistent synergid, the fact that lipid bodies had virtually disappeared from the antipodals likely indicated that the antipodals did not continue to transport metabolites for very long following fertilization, although, as mentioned, the antipodals did persist for a somewhat longer duration than the persistent synergid. When the caecum reached the base of the PNC, the antipodals finally degenerated (Figures 4.36 and 4.38), and the first cell division of the fertilized central cell was triggered (Figures 4.39, 4.40, and 4.41). Thus, primary endosperm nucleus division had provided a second nucleus to aid in the control of the two-celled endosperm, and rendered the antipodals unnecessary. As in the persistent synergid, apoptotic genes of the antipodals likely also contributed to antipodal degeneration.

7E. Fertilized central cell

Immediately following fertilization, the central cell of *Arceuthobium americanum* lost its large vacuole and became more cytoplasmic, indicating a change to a more metabolically active state (Figure 4.31) typical for flowering plants (Folsom and Cass, 1992). The chromosomal material in the triploid primary endosperm nucleus became more dispersed than that in the diploid fusion nucleus, indicating that more transcriptional events were likely occurring, which in turn corroborated that the central cell had become more active following fertilization. The primary endosperm nucleus could be found at the location where the caecum would arise, suggesting that the primary endosperm nucleus governed caecum initiation.

There was an increase in the amount of organelles in the central cell of *Arceuthobium americanum* following fertilization (Figure 4.31), as is fairly typical for flowering plants (Briarty *et al.*, 1979). However, as the unfertilized central cell of *A. americanum* did not have a great abundance of organelles (Figure 4.25), the increase in the overall amount of organelles present in the central cell following fertilization was considerable (Figure 4.31). This implied that successful fertilization had triggered an organellar proliferation, as was also observed by Folsom and Cass (1992).

Mitochondria in particular were quite abundant within the fertilized central cell of *Arceuthobium americanum* and were organized in peripheral clusters (Figure 4.31). As mitochondria tend to congregate at times when energy is required (Raven *et al.*, 1999), the clustering of mitochondria indicated a shift to an even higher state of metabolism. Although no transfer cell ingrowths were visible, the clusters of peripheral mitochondria were likely involved in fueling membrane pumps for nutrient intake from the PNC (as well as possibly from the persistent synergid and antipodals prior to their degeneration). It is well known that mitochondria are often arrayed in clusters along the inner plasma membrane surface of cells in which the plasma membrane is very active in transporting materials into the cell (Raven *et al.*, 1999). The mitochondria clustering in the fertilized central cell of *A. americanum* likely specifically aided in the efficiency of the mitochondrial processes, as it has been suggested that mitochondrial clusters can represent electrically united systems that facilitate energy delivery (Skulachev, 2001). Some central cell factors potentially coordinated the mitochondrial clustering via microtubules, as was suggested for the mitochondrial clustering observed in the oöcytes of *Xenopus laevis* (Tourte *et al.*, 1991).

The amount of starch grains in amyloplasts and osmiophilic bodies (likely lipid bodies, as they stained greyish-blue with crystal violet - not shown) increased in the fertilized central cell cytoplasm of *Arceuthobium americanum* following fertilization (Figure 4.31). The amyloplasts developed from pre-existing proplastids or by plastid division. As the fertilized central cell would develop into an endosperm tissue that persists for two summers (see section II. Results - 21 of this chapter), both starch and lipids present in the fertilized central cell were likely required for immediate and long-term needs of the endosperm. Moreover, the fertilized central cell needed to accumulate many reserves because the persistent synergid, antipodals, and the PNC would not provide long-term support for the growing endosperm, as they become crushed (Figure 4.55). The endosperm then would be the only source of external nutritive support for the growing embryo, and thus the accumulation of many large and varying reserves within the central cell immediately following fertilization was paramount.

8. Embryo Development in *Arceuthobium americanum*

8A. Zygotic division forming the two-celled embryo

After the *Arceuthobium americanum* zygote wall attained its thickest appearance (Figure 4.45), after the zygote chromosomal material re-condensed (Figure 4.48), and after the zygote initiated its dislodgment from the embryo sac wall (Figure 4.48), the zygote divided to form two cells (Figures 4.49 and 4.50). Since no suspensor formed, the term proembryo was not applied, and the two-celled unit was referred to as a two-celled embryo proper (or simply a two-celled embryo). At this time, the endosperm had begun to encircle the two-celled embryo in one plane. Thus, Hudson's (1966) assertions that zygotic division in *A. americanum* occurred when the zygote was surrounded in all planes by endosperm is erroneous or resulted from site, climate, and/or host differences.

It was difficult to ascribe an orientation to the zygotic division of *Arceuthobium americanum*, primarily due to the loss of a long axis to the zygote (Figure 4.45) and because the zygote had begun to dislodge from the embryo sac wall (Figure 4.48). In theory, the plane of division should be determined relative to the long axis of the zygote or to the original long axis of the unfertilized egg cell (Johansen, 1950). The long axis of the unfertilized egg cell would be perpendicular to the embryo sac wall where the egg cell is attached, even if the egg cell was somewhat curved. The unfertilized egg cell (Figure 4.12) and the zygote (Figure 4.45) of *A. americanum* was initially attached to the upper side of the embryo sac, and the two-celled embryo similarly appeared to be anchored to the upper side of the embryo sac (Figures 4.49 and 4.50). Thus, as the cell wall that divided the two cells of the embryo was parallel to the upper side of the embryo sac, this cell wall was thus transverse to the "long" axis of the unfertilized egg cell, and hence the zygotic division was transverse. However, the division of the zygote likely followed the principles of minimum surface area in which the incipient wall occupied the plane within the dividing cell that represented the position of minimum surface area (Errera, 1886; Kaplan and Cooke, 1997).

The difficulty in ascribing an orientation to the zygotic division in *Arceuthobium* species created differing opinions. For example, whereas Cohen (1963) believed the zygotic division in *A. douglasii*, *A. campylopodum*, and *A. pusillum* was transverse, Bhandari and Nanda (1968a) believed the zygotic division in *A. minutissimum* was longitudinal. Cohen (1963) apparently used the long axis of the flower to determine the orientation of zygotic

division. This method was incorrect, but since the unfertilized egg cell/zygote was attached to the upper side of the embryo sac, the long axis of the unfertilized egg cell/zygote was essentially the same as that of the flower, and thus Cohen (1963) was fortunate. Bhandari and Nanda (1968a), on the other hand, used the long axis of the embryo sac to represent the long axis of the unfertilized egg cell/zygote. If the egg cell had been attached to the base of the embryo sac, this interpretation would have been correct. However, as the egg cell was attached to the upper side of the embryo sac, at approximately a right angle to the cell wall at base of the embryo sac, Bhandari and Nanda's (1968a) interpretation was incorrect. Therefore, assignment of *Arceuthobium* to a Piperad-type of embryogeny was erroneous, as the first division was transverse, not longitudinal.

The two embryonic cells resulting from zygotic division in *Arceuthobium americanum* were equal in size and hemispherical; this was also noted for the two embryonic cells of *A. pusillum* (Tainter, 1968). The equal size of the two embryonic cells foreshadowed the fact that a suspensor does not form, since an unequal zygotic division usually leads to the formation of a suspensor from the larger (and basal) embryonic cell (Wardlaw, 1955). Similarly, the equally cytoplasmic condition of the two embryonic cells of *A. americanum* implied that no suspensor would form, as early embryonic cells destined to become suspensors are quite vacuolate (Wardlaw, 1955). Moreover, the fact that the two embryonic cells of *A. americanum* were similar in both size and appearance confirmed that they contributed equally to embryo development.

Since the *Arceuthobium americanum* zygote was attached to the upper side of the embryo sac, the basal embryonic cell arose at a morphologically higher position than the terminal embryonic cell (Figures 4.49 and 4.50). Review Chapter Two, section I - 10A for a description of terminal and basal embryonic cells. As the radicle of typical flowering plants arises from more basal embryonic cells (Crété, 1963), the radicular structure of *A. americanum* likely also arose from the basal embryo cells. Even though the radicle of *Arceuthobium* species is not a true radicle, it nonetheless is analogous to a radicle, and would originate in a similar fashion. The fact that the basal cell was morphologically higher than the terminal cell was likely very important in establishing the ultimate radicular/cotyledonary axis of the mature embryo (Figure 4.71). Specifically, because the radicle region would arise from the more basal embryonic cells, the radicular pole of the

embryo would acquire the morphologically highest position of the embryo. Therefore, the radicular pole could become positioned near the apex of the mass of viscin cells, which would in turn permit the radicle to be one of the first tissues to contact the host periderm upon explosive discharge.

8B. Formation of the four-celled embryo and assignment of an embryogeny type

Whereas division in the two embryonic cells of *Arceuthobium pusillum* was asynchronous, as the terminal cell divided before the basal cell (Tainter, 1968), division in the two embryonic cells of *A. americanum* was simultaneous. The difference regarding the synchrony of these divisions in *A. pusillum* and *A. americanum* may represent an intrageneric difference. Following division of each cell in the two-celled embryo of *A. americanum*, the resulting four cells were similar in size, which again verified that both the terminal and basal cell contributed equally to the embryo.

Regardless of the embryogeny type assigned to different *Arceuthobium* species, the division in each cell of the two-celled embryo in all *Arceuthobium* species was visibly perpendicular to the zygotic division (Jones and Gordon, 1965; Cohen, 1963; Tainter, 1968; Bhandari and Nanda, 1968a; Figure 5.51 of this thesis). As it has now been clarified that the zygotic division in *Arceuthobium* was transverse, the divisions perpendicular to the zygotic division were thus longitudinal. Moreover, as no suspensor forms, and as both the terminal and basal cell contribute equally to the development of the embryo (proper), the embryogeny type of all *Arceuthobium* species is undoubtedly of the Asterad-type, *Penaea* variation. Note how the Loranthaceae are quite different from *Arceuthobium*, as the embryogeny type of the Loranthaceae is of the Piperad-type, *Dendrophthoe* variation (Johansen, 1950; Bhatnagar and Johri, 1983). The difference in embryogeny between *Arceuthobium* and the Loranthaceae supports the notion that *Arceuthobium* is not directly evolutionarily related to Loranthaceae (see Figures 4.79 and 4.80). Interestingly, *Eubrachion*, which follows the Solanad-type of embryogeny (Bhandari and Indira, 1969), shows a transverse zygotic division like *Arceuthobium*, and this shared feature perhaps validates that *Eubrachion* is more closely related to *Arceuthobium* than the Loranthaceae are (Figures 4.79 and 4.80). However, since the division in the basal and terminal cell of *Arceuthobium* was longitudinal, whereas the division of the basal and terminal cell in

Eubrachion is transverse, there is likely an evolutionary division between *Arceuthobium* and *Eubrachion.* Although most Viscaceae probably display the Asterad-type of embryogeny, one may wish to study the unexplored embryogeny of *Viscum minimum.* If *V. minimum* is more closely related to the Loranthaceae than Viscaceae (see Figure 4.80), *V. minimum* could display a Piperad-type of embryogeny.

8C. Globular to torpedo stages of embryo development and concurrent tissue differentiation

As is typical for flowering plants (Maheshwari, 1950), division of each cell in the four-celled embryo of *Arceuthobium americanum* created an eight-celled ball-like globular embryo (Figure 4.53). A suspensor was likely not necessary because the *A. americanum* embryo would become surrounded by endosperm in all planes; no suspensor would be required to push the embryo deeper into the endosperm since the embryo would already have excellent access to the endosperm. Notably, long suspensors are formed in Loranthaceae (Bhatnagar and Johri, 1969) and *Eubrachion* (Bhandari and Indira, 1969), which further indicates that these taxa are not directly related to *Arceuthobium.* Although all Viscaceous species are believed to lack suspensors (Bhandari and Vohra, 1983), one may wish to specifically examine *Viscum minimum* for the presence of suspensors. *V. minimum* may show suspensors like Loranthaceae if *V. minimum* is as closely related to the Loranthaceae as suspected (Figure 4.80).

The protoderm was the first embryonic meristem to differentiate in *Arceuthobium americanum* (Figure 4.62), as is typical for flowering plants (Mauseth, 1988). However, a definite protoderm did not become evident until the embryo had become slightly elongated. Thus, while the typical flowering plant protoderm differentiates while the embryo is in the globular stage, the protoderm of *A. americanum* did not differentiate until the embryo reached a post-globular ovoid stage. This delay likely occurred because the development of the *A. americanum* embryo is extended over two summers, and is thus somewhat delayed overall. In *A. pusillum* (Tainter, 1968) and *A. minutissimum* (Bhandari and Nanda, 1968a), the protoderm did develop at the globular stage, but both of these species complete embryo development in a single summer.

The radicular apex was the second tissue region to become evident in the embryo of *Arceuthobium americanum* (Figure 4.65), differentiating when the embryo had become even more elongated but still ovoid. Early differentiation of a radicular apex is not typical for flowering plants, since the radicular apex is said to be one of the last regions to differentiate (Mauseth, 1988). Nonetheless, the radicular apex was also believed to be the second tissue region to develop in both *A. pusillum* (Tainter, 1968) and *A. minutissimum* (Bhandari and Nanda, 1968a). Furthermore, Tainter (1968) also agreed that the differentiation of the radicular apex took place when the embryo of *A. pusillum* was still ovoid. Bhandari and Nanda (1968a), on the other hand, thought that differentiation of the radicular apex of *A. minutissimum* occurred with a change to a more torpedo-like embryo. Bhandari and Nanda (1968a) were likely confounding radicular differentiation with radicular elongation, as some radicular elongation does occur in the *Arceuthobium* embryo. The *Arceuthobium* "radicle" is a hypocotyledonary extension (Hawksworth and Wiens, 1996), and would be anatomically complex compared to a true radicle (Johri and Ambegaokar, 1984), so perhaps the differentiation of this complex tissue must ensue as soon as possible. More importantly and unlike typical flowering plants, the embryonic radicle in *Arceuthobium* essentially represented the embryo, as the shoot apex would be rudimentary and insignificant. Therefore, early establishment of the radicular apex was inevitable, since the radicle would represent the only significant embryonic tissue.

The two rudimentary cotyledons, an insignificant shoot apex, ground meristem, and procambium differentiated within the *Arceuthobium americanum* embryo immediately prior to explosive discharge, endowing the embryo with a torpedo-like appearance (Figure 4.71). As the cotyledons and shoot apex of *A. americanum* were rudimentary (Figure 4.71), their delayed differentiation was not surprising, nor was the obvious absence of an embryonic heart stage. As the parasitic *Arceuthobium* "seedling" produces no shoot upon explosive discharge, there was obviously no need for an embryonic shoot. The anatomy of the two vestigial cotyledons and rudimentary shoot apex was similar to that observed for *A. pusillum* (Tainter, 1968) and *A. minutissimum* (Bhandari and Nanda, 1968a). The significance of reduced cotyledons with regard to assessing the activity of the shoot apical meristem will be discussed in part 8D of this discussion.

The differentiation of the ground meristem and procambium at a torpedo stage as observed in *Arceuthobium americanum* (Figure 4.71) is quite typical for a flowering plant (Mauseth, 1988). Likewise, Tainter (1968) noted that ground meristem and procambium differentiated in *A. pusillum* at a torpedo stage, specifying that the procambium was the very last tissue to differentiate. However, differences exist in the literature with regard to the degree of procambial development in *Arceuthobium* species. Bhandari and Nanda (1968a) did not believe procambium developed in the embryo of *A. minutissimum*, while Kuijt (1960) and Cohen (1963) reported that procambium and even vascular tissue differentiated in the adult embryo of *A. americanum*, *A. campylopodum* and *A. douglasii*. No differentiated vascular tissue was observed in any *A. americanum* embryos examined for this thesis, even in embryos that had been examined several weeks after explosive discharge. The differences in the reports regarding procambial development among the different *Arceuthobium* species were likely attributable to interspecific differences. However, the difference in the reports regarding the presence of vascular tissue in adult *A. americanum* embryos were likely due to climate, site, and host differences. As development of a functional vascular system is crucial to all *Arceuthobium* species, procambium and a complex vascular system does develop at the time of germination (Hawksworth and Wiens, 1996).

Even though no differentiated vascular tissue was observed in *Arceuthobium americanum* embryos examined for this thesis, the procambium often appeared to possess two distinct strands (section II. Results – 21B of this chapter). This makes sense, as the embryo does not develop a true radicle, which would have a solid procambium, but instead develops a hypocotyledonary extension (Johri and Ambegaokar, 1984), which would likely develop two vascular traces, one from each rudimentary cotyledon.

8D. The mature embryo and significance of its anatomy for germination and host periderm penetration

Whereas typical flowering plant embryos are well developed at the time of dispersal (Maheshwari, 1950), the *Arceuthobium* embryo is relatively small and reduced, possessing only rudimentary cotyledons, an insignificant shoot apex, and no differentiated vascular tissue (Figure 4.76). The presence of a reduced embryo appears to be associated in some

degree with a parasitic or saprophytic mode of life, as reduced embryos are found in many unrelated parasitic and saprophytic plant families (Okonkwo and Raghavan, 1982). For those species that do not produce shoots upon germination, such as Viscaceae and most Loranthaceae, there is no need for a superfluous embryonic shoot, and hence the embryo may effectively be reduced. Even those parasites that do produce shoots upon germination, such as some root parasites, have reduced shoot apices. The presence of a reduced shoot apex in those plants that do produce shoots implies how much more important the radicle/haustorium is for establishment and growth than the shoot.

The fact that a rudimentary shoot axis and cotyledons do form in most parasitic plants (including *Arceuthobium* species) suggests that (a) gene(s) for shoot apical meristem origin likely exists and is active in these parasites. The presence of cotyledons, even rudimentary ones, implies that a shoot apical meristem is present (Kaplan and Cooke, 1997). However, in the parasitic plants, (a) gene(s) for meristem continuation may be mutated or absent, and this likely gene mutation/absence causes the shoot apical meristem to abort development at an early stage. Notably, a mutation exists in *Arabidopsis* called shoot meristemless, smt (Barton and Poethig, 1993). The designation of this mutation as meristemless is not appropriate, since a shoot meristem is present because cotyledons do form. This stm mutation ensures that the *Arabidopsis* shoot meristem does not develop correctly, as an epicotyl will not form (Barton and Poethig, 1993). Thus, perhaps an analogue to the stm mutation exists in *A. americanum* and other parasitic plants. Examination for the presence and activation of certain shoot apical meristem genes and mutations will lead to new ways of assessing the activity of the shoot apical meristem. This is particularly pertinent with regard to the parasitic plants.

The presence of a reduced embryo in parasitic species may also be correlated with the type of endosperm. Embryos tend to be smaller in cellular endosperm and relatively larger in nuclear (coenocytic) endosperm (Maheshwari, 1950). Notably, cellular endosperms are present in many parasitic species including *Arceuthobium* (Kuijt, 1969). Embryos might be smaller in cellular endosperm compared to nuclear endosperm because the cellular partitions in a cellular endosperm might physically inhibit embryo expansion. Furthermore, albuminous seeds, which are produced in *Arceuthobium* and other parasitic plants (Kuijt, 1969), tend to have small embryos whereas exalbuminous seeds have

relatively larger embryos. Perhaps an embryo is smaller in an albuminous seed when compared to an exalbuminous seed because the embryo in an albuminous seed does not absorb all nutrients from the endosperm prior to dispersal. As such, the embryo from an albuminous seed would not be able to grow as well as an embryo that has absorbed much of the nutrients from the endosperm, and thus the embryo from the albuminous seed would essentially be underdeveloped and small. Moreover, if an embryo has not absorbed many nutrients, that embryo would not require a large volume in which to house nutrients. In addition, perhaps the embryo is smaller in an albuminous seed because embryo expansion becomes physically impeded by the presence of endosperm.

The mature radicular apex of the embryo in *Arceuthobium minutissimum* (Bhandari and Nanda, 1968a) and *A. americanum* (Figure 4.72) was apparently covered by a prominent cuticle. In *A. americanum*, the cuticle stained with Sudan Black B (SBB) and thus contained a lipid component (Figure 4.72). Prominent cuticles on radicular structures are not common for typical flowering plants, especially at radicular tips, since it is believed that the ability of water to osmotically move into the root structure following germination is paramount; a cuticle would impede osmosis (Mauseth, 1988). However, the cuticle on the radicular apex of *Arceuthobium* species might have played a role prior to dispersal by conserving moisture within the embryo and isolating the embryo from the other fruit tissues. A similar role has been postulated for the radicular cuticle of *Berteroa incana* (Szczuka, 1996). In addition, the radicle of mistletoes is actually hypocotyledonary tissue that would lack a true embryo-derived root cap (Johri and Ambegaokar, 1984). Shoot tissues frequently have protective cuticles (Mauseth, 1988), so the presence of a cuticle on the shoot-like tissue of the "radicular" apex of *Arceuthobium* was not surprising, and the cuticle might have functioned in conserving water during germination. Moreover, as the mistletoe radicle does not obtain water by osmotic absorption but rather by direct vascular connection with the host, a cuticle would not impede the ultimate ingress of water.

The anatomy of the mistletoe radicle is likely better suited to penetration and establishment on periderm than to penetration and establishment on soil. Firstly, as some degree of mechanical strength is required to achieve host penetration, the endarch pattern to the "radicle" of a mistletoe might provide a more effective distribution of the penetrative forces than the simple vascular stele of a typical root. As in the case of most aerial

mistletoes, the vascular tissues that will be contacted inside of the periderm are obviously shoot like, so the shoot-like anatomy of the mistletoe "radicle" might ensure better connection of its vascular tissue with that of the host.

Some comments regarding the structure and function of the *Arceuthobium americanum* radicle must be made with regard to its post-dispersal tropisms. The tropisms of the *A. americanum* radicle have features in common with both roots and shoots. This is likely owing to the fact that the radicle has general root function but shoot structure. The *A. americanum* radicle displays negative phototropism (Hawksworth and Wiens, 1996), as do many roots (Salisbury and Ross, 1992). However, the *A. americanum* radicle displays positive thigmotropism (Hawksworth and Wiens, 1996), as do many shoots (Salisbury and Ross, 1992). In addition, the *A. americanum* radicle displays neutral geotropism (Hawksworth and Wiens, 1996); this is unlike shoots, which display negative geotropism, and unlike roots, which display positive geotropism (Salisbury and Ross, 1992). The features of the *A. americanum* radicle are well suited to the specific penetration of host periderm, as negative phototropic properties would likely encourage growth toward the periderm, which is typically shaded, and positive thigmotropic properties would also encourage growth toward the periderm, which has a characteristically rough surface. Furthermore, the lack of geotropic response in the radicle ensures that the nearest section of host periderm, regardless of it is above or below the germinating radicle, could be penetrated. The lack of a typical root cap may permit this neutral geotropic response.

Polyembryonic mistletoe pseudoseeds have already been discussed to a certain extent with reference their genesis and to the evolutionary implications of their formation in the different mistletoe taxa (see part 3C of this discussion). It should be mentioned that while polyembryony is natural to Loranthaceae (Bhatnagar and Johri, 1983) and *Viscum minimum* (Zaki and Kuijt, 1994), it is generally atypical in the remaining Viscaceae (Bhandari and Vohra, 1983; Hawksworth and Wiens, 1996) and *Eubrachion* (Bhandari and Indira, 1969). Polyembryony is undeniably anomalous in *Arceuthobium* (Hawksworth and Wiens, 1996). Thus, when a polyembryonic pseudoseed forms in *Arceuthobium*, such as seen in Figure 4.69, it will likely not succeed.

8E. Nutrient reserves of the mature embryo

It was mentioned that no plasmodesmata occurred between the zygote and the fertilized central cell of *Arceuthobium americanum* (see part 7A of this discussion), as is typical for flowering plants (Dute *et al.*, 1989; Han *et al.*, 2000). This lack of plasmodesmata persisted throughout post-fertilization development of *A. americanum*, as no plasmodesmata were observed between the embryo and the endosperm. This is also typical for flowering plants (Dute *et al.*, 1989). Nutrients would thus enter the embryo from the endosperm via transport across the membrane, likely aided by ATPase, sucrose synthase, and invertase (Wittich and Willemse, 1999; Van Caeseele *et al.*, 1996). Antibodies for these proteins, isolated from other plant species, should be used to probe the embryo of *A. americanum* to determine how absorptive it is.

Typical for flowering plants (Bewley and Black, 1978), starch grains in amyloplasts (Figures 4.63 and 4.65) and protein bodies (Figures 4.60 and 4.67) were typical storage forms within the embryo of *Arceuthobium americanum*. The starch grains (Figure 4.65) and protein bodies (Figure 4.67) tended to accumulate in the lower portions of the embryo and in the ground meristem (when it differentiated). It is very common for embryos to accumulate reserves in the ground meristem, as the ground tissue is a region that is often dedicated to nutrient storage (Raven *et al.*, 1999). It was also not surprising that the lower portion of the embryo stored the majority of the nutrients, since the lower portion of the embryo was embedded in and closer to the bulk of the endosperm.

In addition, the ground meristem and procambium in the embryo of *Arceuthobium americanum* possessed many lipid bodies (Figure 4.72). Lipid bodies are also a common storage form in the embryo of many flowering plants (Bewley and Black, 1978). Lipids are very high-energy nutrient stores (Raven *et al.* 1999), and their presence along with starch grains and protein bodies suggested that the germination process in *A. americanum* would demand a very large amount of energy. A major portion of the energy would likely supplement the mechanical penetration of the host periderm. This is particularly probable considering that many lipids were found in the procambium. The procambium in particular would likely require a large energy input during germination in order to produce thrust for the penetration process via the timely differentiation and elongation of vascular tissue. The presence of lipids in the embryo likely also afforded the embryo some protection during the

winter between dissemination and germination. Firstly, as the freezing point of many lipids is relatively high (room temperature), lipid in the *A. americanum* embryo would likely not become violently distorted during very cold periods, as they would effectively be already frozen (Salisbury and Ross, 1992). Secondly, as lipids are hydrophobic, the presence of many lipids in the *A. americanum* embryo would ensure that there would be less free water in the embryo. Subsequently, the ability for ice and damaging ice crystals to form within the embryo would be diminished.

The mature embryo of *Arceuthobium americanum* contained chlorophyll, as it was entirely green (not shown). Chlorophyllous embryos are found in about one-third of all plant families (Dahlgren, 1980). Notably, the embryo of *A. americanum* was green while it was still within the fruit. As light is required for chlorophyll synthesis (Castelfranco and Beale, 1983), some light must have been able to reach the plastids in the embryo. The light was likely transmitted to the embryo before the endocarp became completely filled with potentially light-occluding tannin-like materials (i.e. before the pseudoseed coat fully differentiated; the role of the pseudoseed coat in light absorption and blockage will be discussed in part 10C of this discussion). As noted for the young PNC (review part 1C of this discussion), fibre optic properties of the exocarp, vesicular cells, and viscin cells might have permitted light to reach the embryo. The elongated, nacreous viscin cells may have been particularly well suited to light conductance. The fact that light was able to reach the embryo supports the earlier notion that light possibly illuminated megasporocyte callose. In addition, Fineran (1995) believed that a low level of light reaching sucker cells in *Korthalsella* was able to drive some level of photosynthesis in the suckers, even though the suckers were embedded in the host branch. Similarly, van Cleve *et al.* (1993) found that pith cells of poplar, which are buried deep within the stem, are photosynthetically active. Therefore, the embryo of *A. americanum* may have been able to undergo a low level of photosynthesis, even while it was still in the fruit. It would be interesting to note if there was a changeover from an absorptive state (in which plasma membrane pumps on the outer surface of the embryo were active) to a more autonomous, photosynthesizing state (in which plasma membrane pumps became less active) during embryo development within the fruit. There may have also been a final stage where the photosynthetic rate of the embryo within the fruit decreased after the endocarp became completely filled with tannin-like materials.

The presence of chlorophyll in the pre-dispersal embryo of *Arceuthobium americanum* likely allowed photosynthesis to resume very quickly during germination in the spring, as there would be no lag time between chlorophyll synthesis and photosynthesis. As the germinating embryo will not form a shoot, all of the post-germination photosynthesizing duties would be performed by the embryonic tissues (as well as the endosperm and possibly even the viscin cells; this will be described in part 9F of this discussion and in Chapter Five). The photosynthesis could likely begin in earnest as soon as the green embryonic radicle emerged from the tanniferous pseudoseed coat. The hypocotyledonary, shoot-like nature of the *A. americanum* "radicle" again demonstrates an advantage over a typical plant root, since a typical plant root would likely not be able to photosynthesize. Furthermore, as embryonic photosynthesis could likely occur during germination, more evidence is put toward the notion that much energy is necessary for the processes of germination and periderm penetration. One must wonder if the photosynthesis performed by the embryo is the most intensive photosynthesis performed by the parasite during its entire life cycle, since the photosynthetic rate likely drops considerably after vascular contact with the host is made.

9. Caecum and Endosperm Development in *Arceuthobium americanum*

9A. Caecum formation, expansion, and possible haustorial function

The embryo sac caecum of *Arceuthobium americanum* formed as a lateral outgrowth from the fertilized central cell (Figures 4.33 and 4.35), and eventually reached the base of the PNC/ovary (Figure 4.36). Double fertilization was required for caecum formation, as the caecum did not form until obvious post-fertilization changes had taken place in the embryo sac (review section II. Results - 9 of this chapter; also read Chapter Six for confirmation that double fertilization occurs in *A. americanum*). Thus, only one embryo sac in *A. americanum* was capable of forming a caecum, since the other embryo sac degenerated at the four-nucleate stage and obviously remained unfertilized. Similarly, double fertilization was believed to precede caecum formation in several other *Arceuthobium* species (Tainter, 1968; Hudson, 1966; Jones and Gordon, 1965, Bhandari and Nanda, a, b). The polarity of the embryo sac of *A. americanum* remained the same following fertilization and during caecum development, as the zygote remained below the level of the fertilized

central cell. Thus, there was no inexplicable reversal in embryo sac polarity immediately following double fertilization as was described for *A. pusillum* (Tainter, 1968) and *A. campylopodum* (Cohen, 1970). More importantly, the embryo sac did not become partitioned by a cell wall prior to primary endosperm nuclear division and caecum formation, as had been described for *A. pusillum* (Tainter, 1968), *A. campylopodum* (Cohen, 1970), *A. douglasii* (Jones and Gordon, 1965; Bhandari and Nanda, 1968b), and *A. americanum* (Hudson, 1966). These authors' observation of a partitioning cell wall was erroneous and attributable to the fact that the caecum does not necessarily lie on the exact same sectioned plane as the embryo sac, but can instead project slightly away from the plane of section. Consequently, as the lower side of the embryo sac or wall of the caecum could have come into the plane of section, these authors had probably confused the lower side of the embryo sac or wall of the caecum with a partitioning wall.

As is typical for any expanding cell (Salisbury and Ross, 1992), vacuoles aided the expansion of the caecum in *Arceuthobium americanum* (Figure 4.33, 4.35, and 4.37). As elaborated elsewhere, vacuole formation allows a cell to expand so that the cell does not need to synthesize energy-demanding cytoplasm. As the presence of an expanded caecum extends the surface area of the embryo sac, the *Arceuthobium* caecum has been postulated to possess haustorial function (Thoday and Johnson, 1930; Jones and Gordon, 1965; Tainter, 1968; Bhandari and Nanda, 1968a, b; Cohen, 1970); this has not been verified. Since the *A. americanum* caecum was an outgrowth of the fertilized central cell and thus the embryo sac wall, there were consequently no plasmodesmata between the caecum and the sterile cells of the PNC, and so any materials entering the caecum would have had to cross the plasma membrane. Thus, the presence of many plasma membrane pumps in the *A. americanum* caecum would have supported the concept that the caecum had a haustorial function. In the future, the caecum should be screened for ATPase activity or other membrane pump activity via biochemical tests or antibodies. If transfer cell ingrowths had been observed in the *A. americanum* caecum, evidence would be put toward an absorptive role for the caecum. However, the absence of these ingrowths did not negate a haustorial role for the caecum, since peripheral clusters of mitochondria were observed in the fertilized central cell (Figure 4.33) and caecum. These mitochondria were possibly fueling membrane pumps that drove the ingress of metabolites into the fertilized central cell and caecum from the PNC.

Notably, the sterile cells of the PNC also possessed a preponderance of mitochondria in regions adjacent to the fertilized central cell and caecum of *Arceuthobium americanum* (Figure 4.33). This suggested that the input of metabolites into the fertilized central cell and caecum was aided by cellular activity of sterile PNC cells. Furthermore, the dedicated input of metabolites into the fertilized central cell and caecum likely compromised the metabolism of the sterile PNC cells, contributing to their ultimate demise. The possibility that specific cellular activity of the nucellus could furnish the fertilized central cell (and endosperm) with metabolites has not been directly addressed in flowering plants. Therefore, activity of the nucellus should be examined more specifically. Nonetheless, as before, many metabolites supplied to the fertilized central cell (and caecum) likely aided in the future development of the endosperm and ultimately the embryo.

9B. Division of the primary endosperm nucleus and early endosperm development

As was observed in most *Arceuthobium* species except *A. pusillum* (Tainter, 1968), the primary endosperm nucleus of *A. americanum* did not migrate into the caecum prior to division but rather remained in the vicinity of the zygote. After division of the primary endosperm nucleus in *A. americanum* (and most *Arceuthobium* species except *A. pusillum*), one daughter nucleus migrated into the caecum and cytokinesis took place (Figures 4.39, 4.40, and 4.41). As was observed in (or at least implied for) most *Arceuthobium* species studied, cytokinesis following division of the primary endosperm nucleus in *A. americanum* created a two-celled endosperm (also see Chapter Two, section I - 11C). The caecum was one endosperm cell, while the second endosperm cell resided in the vicinity of the zygote. In this thesis, it was specified that the *A. americanum* endosperm cell in the vicinity of the zygote was housed in the confines of the original fertilized central cell. Regardless, in all *Arceuthobium* species studied, division of the primary endosperm nucleus occurred before zygotic division, substantiating that endosperm development occurred before embryo development, as is typical for flowering plants (Maheshwari, 1950). Further endosperm divisions in *A. americanum* involved mitosis and cytokinesis, confirming cellular endosperm development for this species; cellular development is typical for bisporic species (Mauseth, 1988; Bhandari and Vohra, 1983). Notably, there was no point in which the caecum was free-nuclear, contradicting Hudson's (1966) observation of a free-nuclear caecum in *A.*

americanum. Moreover, the caecum was multicellular during early growth, in contrast to Bhandari and Nanda's (1968a) observation that the caecum of *A. minutissimum* remained uninucleate throughout development.

In this thesis, development of the endosperm "proper" (the endosperm cells in the vicinity of the zygote) in *Arceuthobium americanum* was similar to that described for *A. americanum* by Hudson (1966) as well as to that described for *A. pusillum* (Tainter, 1968). Essentially, development of the endosperm cells in the vicinity of the zygote was initially in one plane (the plane of the zygote) and occurred via divisions that were anticlinal to the surface of the zygote. However, whereas Hudson (1966) implied that the zygote became completely enveloped by endosperm cells in one plane before endosperm divisions could ensue in all planes, this thesis showed that endosperm cells immediately below the zygote could undergo divisions in all planes (Figures 4.45, 4.46, and 4.50) before complete encirclement occurred. Nonetheless, as noted by Hudson (1966), two upwardly advancing tiers of endosperm cells achieved encirclement of the zygote in *A. americanum* by dividing in primarily one plane. The triangular shape of the encircling endosperm cells likely aided the endosperm cells in maintaining the anticlinal plane required for complete encirclement. Furthermore, the direct pressure applied by endosperm cells that were dividing in only one plane above the zygote likely ultimately effected the complete dislodgment of the two-celled embryo from the embryo sac wall. If the endosperm cells had instead initially begun to encircle the zygote/embryo in more than one plane above the level of the zygote, the pressure may have been too diffuse to effectively achieve dislodgment and encirclement.

Endosperm cells above the level of the embryo of *Arceuthobium americanum* would eventually proliferate in all planes, forming the cap (Figure 4.52). Thus, the cap described for *A. minutissimum* (Bhandari and Nanda, 1968a) and *Eubrachion* (Bhandari and Indira, 1969) did not represent endocarp, as had been suggested by these authors, but instead represented endosperm. This will be addressed in parts 9E and 10C of this discussion. Moreover, see Chapter Six, sections III. Results and IV. Discussion for further verification that the cap cells were indeed endosperm cells, not persistent endocarp.

9C. Explanation for the phenomenon of the embryo arising at a morphologically higher position than the endosperm in *Arceuthobium* (and related taxa)

Although the central cell was initially at a morphologically higher position than the egg cell in a young flower of *Arceuthobium americanum* (see Figures 4.12 and 4.13), the embryo was found at a higher position than the bulk of the endosperm in the more developed fruit (Figure 4.64). Several developmental features were responsible for this phenomenon of reorientation in *A. americanum*. Firstly, the formation of a downwardly-directed caecum and the movement of an endosperm daughter nucleus into the caecum permitted endosperm cells to become established below the level of the zygote (Figures 4.46, 4.47, and 4.50). In addition, the first few divisions of endosperm cells in the vicinity of the zygote were directed downward: space was provided for these endosperm cells to develop below the zygote because the zygote was initially attached to the upper side of the embryo sac (Figure 4.43). Thus, although the encircling tiers of endosperm cells were upwardly displaced, the net downward displacement of endosperm cells developing in the vicinity of the zygote and in the caecum essentially allowed the bulk of endosperm to proliferate below the level of the embryo. Furthermore, complete detachment of the zygote/embryo from the embryo sac wall and establishment of cap cells permitted the developing endosperm to easily convey the embryo upward as the endosperm developed, since the embryo was no longer anchored to the embryo sac wall and could be entirely buoyed by endosperm. Hudson (1966) noted a similar passive conveyance of the embryo of *A. americanum* by the endosperm, although he never specified how the endosperm achieved its lower position. The manner of embryo and endosperm reorientation described for *A. americanum* in this thesis was likely similar for all *Arceuthobium* species as well, and thus the caecum had a primary role in the reorientation of developing endosperm relative to the embryo. The importance of the embryo arising at a morphologically higher position than the endosperm was previously discussed in parts 4 and 8A of this discussion.

A similar phenomenon of reorientation occurred in the Viscaceous members *Korthalsella* (Rutishauser, 1935, 1937), *Dendrophthora* (York, 1913), *Ginalloa* (Rutishauser, 1937), *Phoradendron* (Billings, 1933), *Viscum album*, and *V. articulatum* (Steindl, 1935). Specifically, a reexamination of the figures in these publications showed that, as in *Arceuthobium*, the egg cell arose at a lower position than the central cell, but the

embryo developed at a higher position than the endosperm. In these aforementioned (non-*Arceuthobium*) Viscaceous taxa, caecum formation and endosperm development did not achieve the reorientation. Instead, a slow but steady curvature of the immature embryo sac caused the lower end of the embryo sac (containing the egg cell) to obtain a morphologically higher position than the central cell. However, a reorientation did not occur in *Eubrachion* (Bhandari and Indira, 1969), *V. minimum* (Zaki and Kuijt, 1974), and Loranthaceae (Bhatnagar and Johri, 1983), further indicating that these taxa may not be directly related to *Arceuthobium*, but also again implying that *V. minimum* is potentially related to the Loranthaceae.

9D. Continued endosperm development and further comments regarding the caecum and the endosperm cap

During the stages of endosperm development in *Arceuthobium americanum* when the caecum represented a distinct entity, all caecum endosperm cells were notably more vacuolate than those in the vicinity of the zygote/embryo (Figures 4.43, 4.44, and 4.53). The caecum, being a distinct vacuolate structure, was likely still primarily involved with expansion, absorption, and reorientation, whereas the endosperm cells in the vicinity of the zygote/embryo, being more cytoplasmic, were likely functioning more specifically in shunting metabolites to the zygote/embryo. However, when the nucleus in the lowermost caecum endosperm cell degenerated, as it frequently did (Figure 4.44), the onset of endosperm caecum proliferation was likely signaled so that the caecum could become entirely multiseriate (and consequently no longer readily distinguishable from endosperm cells in the vicinity of the zygote/embryo). With careful observation, vacuolate caecum-derived endosperm cells could have likely still been distinguished from more cytoplasmic endosperm cells derived from the vicinity of the zygote, although the caecum was certainly no longer a distinct entity. The caecum was probably no longer needed as a defined structure because its primary roles in expansion and reorientation had been achieved. Thus, contrary to Hudson's (1966) assertions, the caecum of *A. americanum* did not persist throughout embryogenesis.

The cap of endosperm cells in *Arceuthobium americanum* may have initially developed in order to aid in the detachment of the embryo from the embryo sac wall and to

concomitantly assist in the reorientation of the embryo and endosperm, but the cap likely also had other functions as well. Firstly, when endosperm development in *A. americanum* was complete by late July of the second summer, the endosperm cells in the cap changed from a cytoplasmic, Type 2 state (Figure 4.59) to a vacuolate, Type 1 state (Figure 4.62). Shortly after this change in the cap cells took place, the radicular apex of the embryo differentiated (Figure 4.65) and elongated (Figure 4.71), and thus it was likely that the change in the cap cells triggered the changes in the radicular apex of the *A. americanum* embryo. This is particularly likely if the endosperm cap had a role in controlling development of the radicle, as Serrato-Valenti *et al.* (2000) had suggested for *Phacelia tanacetifolia*. Furthermore, endosperm cells that surround the radicular apex of flowering plant embryos possibly aid in the prevention of premature germination (Serrato-Valenti *et al.*, 2000). A similar role is likely for the cap of endosperm cells in *A. americanum* as well. The change in the appearance of the *A. americanum* cap cells likely contributed to some confusion regarding the origin of the cap cells, as the vacuolate appearance of the fully developed cap cells was in sharp contrast to the majority of the endosperm cells found below the embryo.

Due to its position at the radicular apex, it is easy to postulate that the cap of endosperm in *Arceuthobium americanum* could have functioned in roles similar to that of a typical root cap following dispersal, especially considering that a true embryo-derived root cap was lacking (Figure 4.64). A typical root cap functions in negative phototropism (Evans *et al.*, 2001), lubrication (Salisbury and Ross, 1992; Raven *et al.*, 1999), and positive geotropism. As the germinating radicle of *A. americanum* displays negative phototropism (Hawksworth and Wiens, 1996), the endosperm cap of *A. americanum* (if the cap remained associated with the radicle during germination) could possibly direct the negative phototropism, hence assuming some root cap function. Moreover, if the endosperm cap of *A. americanum* remained associated with the growing radicle during host periderm penetration, the endosperm cap could possibly lubricate the penetration process, thus possibly performing another root cap function. However, as the germinating radicle of *A. americanum* displays neutral geotropism (Hawksworth and Wiens, 1996), it is unlikely that the endosperm cap of *A. americanum* functioned in any role regarding geotropism. The possibility that endosperm caps undertake root cap functions has not been examined in any

flowering plant. Furthermore, as the growing radicle of *A. americanum* displays positive thigmotropism, the endosperm cap of *A. americanum* could be involved in this tropism, even though positive thigmotropism is more of a shoot feature, and could be alternatively ascribed to the shoot characteristics of the *A. americanum* radicle. More work is needed.

9E. Apparent radicular protrusion from the endosperm

While endosperm cells surrounded the embryo of *Arceuthobium americanum* throughout most embryonic development (Figures 4.52 and 4.56), Sallé (1983) believed that the mature embryo of most Viscaceae protruded from the endosperm, as did Bhandari and Nanda (1968a), specifically referring to *A. minutissimum*. Images of ripe, mature fruit in this thesis also seem to depict the radicular pole lying outside of the endosperm (Figures 4.71, 4.72, and 4.76). Thus, one wonders what happened to the cap of endosperm cells, and could be tempted to discard the concept that the endosperm cap might have had root cap function. However, upon closer inspection of the images (Figures 4.71, 4.72, and 4.76), it is obvious that the radicular pole was covered by a compressed but distinct cap of cells. Therefore, elongation of the radicular apex had compressed but certainly not obliterated the cap of endosperm cells in the ripe, mature fruit. As mentioned, this elongation had likely been triggered by the earlier vacuolation of the cap cells (Figures 4.62 and 4.64). It is easy to see why Bhandari and Nanda (1968a) thought that this cap of cells represented endocarp, as the cells did not resemble the majority of the endosperm cells.

Compressed cap cells in the ripe, mature fruit of *Arceuthobium americanum* were positive for polysaccharides (Figure 4.71) but negative for lipid materials (Figure 4.72). Typical root caps also have a large polysaccharide component (Raven *et al*, 1999), and thus the concept that the endosperm cap cells of *A. americanum* may have functioned in roles similar to that of a typical polysaccharidic root cap is further supported. Moreover, as the cap was deemed to be viable even after it was compressed (see section II. Results - 22E of this chapter), the cap very likely played important roles during germination, as well as possibly host recognition and penetration. See Chapter Six for a further discussion of the cap.

9F. Maturing and mature endosperm

Various levels of endosperm zonation occurred in the maturing endosperm of *Arceuthobium americanum*. The first level of zonation was manifested in vacuolate Type 1 endosperm cells and cytoplasmic Type 2 endosperm cells (Figure 4.64). This level of zonation has already been discussed to a certain extent: the change in the cap cells likely occurred as a cue for differentiation of the embryonic radicular apex, while the vacuolate cells at the base of the endosperm possibly represented descendents of vacuolate caecum endosperm cells (Figure 4.53). The basal endosperm cells likely remained vacuolate throughout development in order to provide turgor and strength to the base of the endosperm, which was probably under considerable pressure due to the presence of hygroscopic viscin cells (Figure 4.64). The basal endosperm cells became even more vacuolate and enlarged as endosperm development progressed, likely in order to countervail the increasing pressures within the fruit. As a consequence of the enlarging vacuolate basal endosperm cells, the endosperm of *A. americanum* acquired a vase-shaped appearance. In contrast, endosperm cells that were closer to the embryo remained cytoplasmic, likely in order to deal specifically with nutrient sequestration and transfer to the embryo, deferring the problem of increasing pressure to the basal endosperm cells. It should also be noted that the cap cells and the basal endosperm cells were some of the first-formed and thus oldest endosperm cells created, and so their vacuolate appearance could also have represented a useful product of aging.

Storage reserves in the endosperm of *Arceuthobium americanum* were the same as those in the embryo, and included starch grains in amyloplasts (Figures 4.63 and 4.65), protein bodies (Figures 4.60 and 4.67), and lipid bodies (Figure 4.72). These types of reserves are fairly common in the endosperms of typical flowering plants (Bewley and Black, 1978). Vacuolate Type 1 endosperm cells apparently did not have enough cytoplasm to house a substantial amount of starch grains, protein bodies, and lipid bodies, as these reserves were all were relatively rare in the Type 1 endosperm cells. On the other hand, cytoplasmic Type 2 endosperm cells, dedicated to nutrient sequestration and delivery to the embryo, held a large amount of starch grains, protein bodies, and lipid bodies.

A level of zonation occurred with regard to the distribution of starch grains in the endosperm of *Arceuthobium americanum*. This level of zonation indicated assimilate

transfer zones as opposed to vacuolate and cytoplasmic zones. In the peripheral layer of endosperm cells, starch grains were initially absent, likely because the peripheral cells were actively shunting metabolites from the maternal tissues to the inner endosperm cells (Figure 4.63). Therefore, no starch initially accumulated in this peripheral transfer zone because the cytoplasm was specifically dedicated to translocation, not storage. A similar starch-free peripheral endosperm zone was noted for Loranthaceae (Bhatnagar and Johri, 1983). Likewise, there was initially a starch-free zone in the immediate vicinity of the embryo, suggesting that this region of endosperm was also a region of transfer that dealt with the conveyance of assimilates from the endosperm into the embryo (Figure 4.63).

However, when the endosperm of *Arceuthobium americanum* reached maturity, the starch-free endosperm zone at the periphery of the endosperm was no longer evident, as starch had accumulated in this area (Figures 4.65 and 4.71). As the maternal tissues had fully differentiated, they were likely no longer capable of supplying metabolites to the endosperm. Thus, the peripheral endosperm zone was no longer needed for assimilate transfer, and assimilates remaining in the peripheral endosperm had likely been converted into starch grains. Nonetheless, even in the nearly mature fruit, purple staining with TB indicated that the peripheral endosperm cells contained an abundance of proteins and/or nucleic acids (Sumner, 1988). Thus, some continued transfer of metabolites from the maternal tissues to the endosperm might have still been ongoing. The proteins may have represented ATPases as well as cytoplasmic enzymes involved in nutrient transfer and metabolism, whereas nucleic acids may have represented mRNA required for the translation of these enzymes. Alternatively, if transport into the endosperm had truly ceased in the nearly mature fruit, the purple staining of the peripheral endosperm cells could have represented proteinaceous masses of degraded transfer enzymes as well as proteinases that aided in the degradation of the transfer enzymes.

Similarly, when the endosperm of *Arceuthobium americanum* reached maturity, the starch-free endosperm zone in the immediate vicinity of the embryo was no longer evident, as starch had also accumulated in this area (Figures 4.65 and 4.71). As the mature embryo would be entering the winter period, the embryo was likely no longer taking in metabolites from the endosperm, and so the endosperm in the immediate vicinity of the embryo was not

immediately required for transfer. Thus, some assimilates remaining in the endosperm near the embryo were likely converted into starch grains.

The persistent endosperm in the albuminous pseudoseed of *Arceuthobium americanum* would likely be used during germination in the following spring. Jacobsen (1984) stated that the endosperm of albuminous seeds is preferentially used for germination. The starch grains, protein bodies, and lipid bodies present in the *A. americanum* endosperm upon explosive discharge would have persisted until the spring, as the embryo would likely not have used any of these reserves during the intervening winter. The endosperm in the immediate vicinity of the embryo would likely become starch free again when transfer from the endosperm to the embryo resumed during germination. The presence of many and varied nutrient stores in the endosperm suggested that the process of germination requires a great input of energy. As in the embryo, the lipid bodies in the endosperm possibly acted as protective overwintering materials (see rationale given in part 8E of this discussion and Salisbury and Ross, 1992). Also as noted for the embryo, the specific presence of high-energy lipid bodies in the endosperm further validated that the germination process required an extreme energy input. Notably, lipid bodies are also present in the endosperm of Loranthaceous species (Bhatnagar and Johri, 1983), as the germination process in those mistletoes is likely energy-intensive as well (although avian disseminators of Loranthaceous taxa would also benefit from a fatty endosperm).

The endosperm of *Arceuthobium americanum*, like the embryo, was green and chlorophyllous, even when still within the fruit. The endosperm likely became green and photosynthesized in a manner similar to the embryo (see part 8E of this discussion). Although the endosperm may have accumulated chlorophyll and potentially photosynthesized within the fruit, any photosynthesis likely became ineffective when the endocarp became filled with potentially light-blocking tannins (i.e. when the pseudoseed coat differentiated). Thus, in order for photosynthesis to resume in the spring, the cracking of the pseudoseed coat during embryo germination likely also permitted the endosperm to rapidly resume photosynthesis. When photosynthesis in the endosperm resumed in the spring, assimilates could be used to support the intensive process of germination. Of course, any assimilates or reserves contained in the endosperm would have to be translocated to the

embryo via membrane pumps, and so the endosperm likely persisted throughout most of the germination process.

Chlorophyll has been observed in the endosperm of most Viscaceae (Bhandari and Vohra, 1983), whereas chlorophyll is not typical in the endosperm of Loranthaceae (Bhatnagar and Johri, 1983). Overall, Viscaceous pseudoseeds are smaller than Loranthaceous ones (Bhandari and Vohra, 1983; Bhatnagar and Johri, 1983). As such, the large Loranthaceous seeds likely carry more nutrient reserves than smaller Viscaceous pseudoseeds, and thus the larger, highly nutritious Loranthaceous pseudoseeds would probably not require photosynthesis to supplement germination. On the other hand, the smaller Viscaceous pseudoseeds, particularly the explosively discharged *Arceuthobium* pseudoseeds, could not carry quite as many nutrients as Loranthaceous seeds, and thus would have to supplement the germination process with photosynthesis.

Tannin-like materials could be seen in the vacuoles of some *Arceuthobium americanum* endosperm cells following explosive discharge (Figure 4.76). Tannin-like materials in the endosperm may have accumulated due to the presence of excess assimilates, as was noted for early development of the PNC (see part 2A of this discussion and Matsuki, 1996). If assimilates were not moved into the embryo fast enough, or if they were not readily converted into typical storage products, the assimilates could have been converted into tannins. It is possible that tannins could be mobilized during germination to supply nutrients for the embryo. However, as previously described for lipid bodies, the hydrophobic tannin-like materials (Gahan, 1984) might also have acted as protective overwintering materials. The role of tannins as materials that can impart cold tolerance/hardiness to plant tissues has not been very well explored in the literature. However, there has been some preliminary evidence indicating that polyphenolics, which comprise tannins and other compounds, accumulate to a greater extent in the leaves of cold-tolerant genotypes compared to cold-stressed genotypes (Solecka *et al.*, 1999; Priyanka and Mishra, 2001). Chalker (1992) specifically thought that phenolic-rich areas represented ice nucleating barriers in cold-tolerant *Azalea* buds. More work is required in this area, and perhaps *A. americanum* could be used as a test subject.

The apparent loss in length and gain in width to the mass of endosperm of *Arceuthobium americanum* following explosive discharge likely occurred because the viscin

cells had become freed from the vesicular cells, permitting the endosperm to adjust its shape to ambient pressure. During the adjustment, some intercellular spaces formed in the endosperm as endosperm cells became detached from each other at their middle lamellae and slid by each other. Although the formation of intercellular spaces in the endosperm was a result of discharge and adjustment to ambient pressure, the intercellular spaces likely also benefited the chlorophyllous endosperm by enhancing gas exchange and photosynthesis.

While occurrences of polyembryony have been mentioned in studies of *Arceuthobium* species (Weir, 1914; Hawksworth, 1961; Hudson, 1966; Tainter, 1968), occurrences of polyendospermy in *Arceuthobium* have not been well documented. In this thesis, two endosperms were once found in a single fruit of *A. americanum* (Figure 4.69), and the side-by-side positioning of the endosperms implied that the two embryo sacs in a single PNC each produced an endosperm. The two endosperms remained separate entities, and did not form a composite endosperm. This is unlike Loranthaceous mistletoes, in which a composite endosperm is typical, and forms from the fusion of multiple endosperms that originated from multiple embryo sacs (Bhatnagar and Johri, 1983). The rarity of polyendospermy in *A. americanum* and the fact that a composite endosperm did not form when polyendospermy did occur further confirmed that polyembryony and polyendospermy is anomalous in *Arceuthobium*.

In this thesis, an attempt might have been made to use features of endosperm development in order to help clarify some of the phylogenetic relationships in the Santalales. However, in all Santalales, endosperm development has merely been described as being cellular and has not been categorized further. As such, it was difficult to find characters by which to assemble similarities and differences. The lack of detail in endosperm categorization was also a problem encountered by Floyd and Friedman (2000), who found the categorizations of free-nuclear, cellular, and helobial endosperm development were similarly limiting for phylogenetic reconstruction. In recognition of these limitations, Floyd and Friedman (2000) outlined a more precise system for endosperm categorization. Therefore, it would be very useful for someone to go through literature regarding various families in the Santalales and categorize the endosperm development according to the system of Floyd and Friedman (2000).

However, certain changes would have to be made to the system of Floyd and Friedman (2000) before it could be used to categorize endosperm and consequently reconstruct phylogeny in the Santalales. Firstly, the presence of embryo sac/endosperm caeca as well as the manner of caeca formation should be included as categories in the system, since many Santalalean members form caeca (Johri and Bhatnagar, 1960). Secondly, Floyd and Friedman (2000) relied heavily on the concept of micropylar/chalazal polarity for their categorizations. This polarity is fairly meaningless in most Santalales, as integuments and thus a micropyle are typically lacking. Presuming the ancestral location of a Santalalean micropyle would not necessarily be helpful in establishing polarity, since it more sensible to use a real as opposed to a hypothetical point of reference for establishing polarity. Therefore, a different denotation of polarity should be used in the system of Floyd and Friedman (2000); perhaps the polarity could be based on the location of the egg apparatus and antipodals. With modifications and more precise definitions, the system of Floyd and Friedman (2000) could likely be used to help elucidate phylogeny in the Santalales, especially if the system was used in conjunction with other anatomical and molecular measures.

10. Fruit (Pericarp) Development in *Arceuthobium americanum* and Comments about the Vascular Tissue

10A. Early fruit ontogeny

The number and size of cells in the ovarian tissues of *Arceuthobium americanum* had increased by end of the first summer of development (Figure 4.55). As a result, the three fundamental fruit zones (endocarp, mesocarp, and exocarp) became evident: the mesocarp could be distinguished by its slightly more elongated cells, whereas endocarp and exocarp could be distinguished by their slightly larger and more isodiametric cells. Early identification of the three fruit zones made it extremely easy to detect the exact zone from which the more differentiated cells (viscin cells, vesicular cells, pseudoseed coat cells) arose. Early identification of the three fruit zones provided a much simpler method of tracing ontogeny than the overcomplicated designations created by Bhandari and Nanda (1968a) and Bhandari and Indira (1969).

10B. Accumulation and evidence of tannins in the fruit tissues

Before describing the ontogeny of the major fruit tissues of *Arceuthobium americanum* in more detail, some mention should be made to the occurrence of tannin-like materials, which accumulated within vacuoles of certain fruit tissues throughout fruit development. In the mature fruit (Figure 4.64), tannin-like materials could be found within vacuoles of the pseudoseed coat cells, viscin cells, and many inner exocarp cells. If a pseudoseed coat cell or inner exocarp cell accumulated tannin-like materials in its vacuole, the vacuole essentially expanded to occupy the entire volume of the cell. Conversely, tanniferous vacuoles of viscin cells usually did not expand to occupy the entire volume of a viscin cell. As the tannin-like materials were visibly brown in the pseudoseed coat (Figure 4.75), the materials very likely represented polyphenolic phlobapenes. Phlobapenes are the anhydrous derivatives of tannins and are brown, amorphous substances (Gahan, 1984). All tannin-like materials observed (including those in the PNC, viscin cells, inner exocarp, and endosperm) were also likely phlobapenes. Moreover, when stained with TB (Figure 4.68) and the Yeung procedure (Figure 4.71), suspected tannin-like materials in the pseudoseed coat, viscin cells, and inner exocarp stained greenish-blue. The greenish-blue staining confirmed the presence of tannins, as tannins stain bright green-blue when stained with TB (Kinzel and Bolay, 1961; O'Brien *et al.*, 1964) and the Yeung procedure (Yeung, 1990) due to the presence of polyphenols.

The accumulation of tannins within vacuoles of the pseudoseed coat, inner exocarp cells, and viscin cells of *Arceuthobium americanum* likely occurred in the manner previously described for the accumulation of tannins within vacuoles of the PNC (see part 3B of this discussion and Matsuki, 1996) and the endosperm (see part 9F of this discussion and Matsuki, 1996). However, excess assimilates that were converted into tannins within the pseudoseed coat, viscin cells, and inner exocarp might not be have been required for nutrition, but might have instead represented viscin mucilage precursors (see Chapter Five, section III. Discussion - 10 and Fukushima *et al.*, 1991). A more detailed description of each tissue and its ontogeny as well as the role of the tannins in each fruit tissue follows.

10C. The endocarp, the pseudoseed coat and usage of the term "pseudoseed"

As the endocarp of *Arceuthobium americanum* was recognized early in its development, it was easy to determine that the endocarp became entirely compressed and completely filled with tannin-like materials. Thus, the entire endocarp formed the majority of the tannin-filled pseudoseed coat (Figures 4.55, 4.59, 4.61, and 4.64). More importantly, although it was postulated that the endocarp of *A. minutissimum* (Bhandari and Nanda, 1968a) and *Eubrachion* (Bhandari and Indira, 1969) became completely obliterated except for a persistent cap at the radicular end of the embryo, this was not the case for *A. americanum*. As stated in part 9B of this discussion and verified in Chapter Six, the cap of *A. americanum* represented endosperm, and the same is likely true for *A. minutissimum* and *Eubrachion*.

The tanniferous pseudoseed coat of *Arceuthobium americanum* was analogous to the tanniferous crest described for *A. minutissimum* by Bhandari and Nanda (1968a) and for *Eubrachion* by Bhandari and Indira (1969), since the pseudoseed coat/crest was immediately adjacent to and enveloped the endosperm and embryo in all species. However, as only the lower mesocarp cells contributed to the pseudoseed coat of *A. americanum*, the crest described by Bhandari and Nanda (1968a) and Bhandari and Indira (1969) was likely not primarily mesocarpic, as these authors had suggested, but was instead primarily endocarpic, as in *A. americanum*.

One may question the use of the term "pseudoseed coat" for describing the tannin-filled compressed endocarp and lower mesocarp cells of *Arceuthobium americanum*. One may be tempted to describe the compressed endocarp and lower mesocarp as simply pericarp. However, to describe the compressed endocarp/lower mesocarp as pericarp becomes confusing, because the viscin cells are also pericarp: thus, stating that the embryo and endosperm of the dispersal unit are enveloped in "pericarp surrounded by viscin cells" erroneously implies that the viscin cells are not pericarp. Stating that the embryo and endosperm are merely "enveloped in pericarp" neglects to adequately draw attention to two distinct pericarp layers (the tannin filled endocarp/lower mesocarp and the viscin cells). Referring to the endocarp/lower mesocarp as simply "endocarp" would be erroneous, as this neglects the fact that some mesocarp contributes to the layer. Bhandari and Nanda's (1968a) term "crest" may have been used to describe the endocarp/lower mesocarp, with the

clarification that the crest is primarily endocarpic, not mesocarpic, as these authors had suggested. Yet, the term "crest" neglects to encompass the obvious seed coat function that the layer possesses. Therefore, the term "pseudoseed coat" is the most useful to describe the endocarp/lower mesocarp, as the term infers seed coat function without implying integumentary derivation.

Most of the seed coat function attributable to the pseudoseed coat of *Arceuthobium americanum* is derived from its extremely tanniferous nature. Tannins are extremely common in the typical flowering plant seed coat, functioning as anti herbivory agents and as materials that can absorb harmful ultraviolet rays (Mauseth, 1988; Epiñosa and Engelman, 1994; Krishnamurthy, 1999). Upon looking at the structure of some mammalian melanins known to absorb ultraviolet radiation (Goodwin, 1983), it is apparent that the structure of the melanins is extremely similar to that of anhydrous phlobapene tannins (Goodwin, 1983). The ability to protectively absorb ultraviolet radiation is important for the discharged pseudoseed, which must typically lie exposed to the sunlight in the daylight hours from September though May. Although there is not much ultraviolet radiation during this time, over the long period, exposure could be cumulatively damaging, as it is in humans (Rothwell, 1988). The tannins in the pseudoseed coat may have restricted water loss from the embryo and endosperm both prior to and following explosive discharge. Specifically, as the vacuoles containing tannin-like materials were essentially as big as a given pseudoseed coat cell, movement of water through the symplast would be restricted; also, as the tannins are hydrophobic (Gahan, 1984), transvacuolar movement would be inhibited. It has been shown that when vacuoles containing tannin-like materials occupy the major portion of a cell, symplastic transport is severely restricted or impeded (Gross and Koch, 1991; Algan and Buyukkartal, 2000). In a similar fashion, water loss from the viscin cell mucilage to the embryo and endosperm of *A. americanum* may also have been restricted by the pseudoseed coat during the time when the pseudoseed was still within the fruit. Additionally, the tannins in the pseudoseed coat may have protected the pseudoseed against winter cold damage, as was earlier suggested for tannins in the endosperm of the discharged pseudoseed (see part 9F of this discussion). Tannins first appeared to accumulate within vacuoles of the endocarp/differentiating pseudoseed coat during the winter "resting" period between the first summer and the second spring of development (Figure 4.57). As it was unlikely that any

metabolism was ongoing during the winter, perhaps the extreme conditions and possible ice crystal formation in non-tanniferous regions caused the passive amalgamation of smaller tannin particles into larger particles. While this obviously did not represent a true accumulation of tannin, it nonetheless represented a reorganization of tannin that may have aided in cold hardiness. More work is required on this subject (Chalker, 1992; Solecka *et al.*, 1999; Priyanka and Mishra, 2001).

10D. The viscin tissue

Both the viscin cells and vesicular cells developed from the upper three-quarters of the mesocarp in *Arceuthobium americanum* (Figures 4.58 and 4.64). It makes sense to have referred to the differentiated mesocarp as being viscin tissue, a complex tissue of two cell types, as had been described for *Viscum album* (Sallé, 1983). The innermost layer of the mesocarp in the upper three-quarters of the *A. americanum* fruit became the uniseriate layer of elongated, mucilaginous viscin cells, and the outer three to four layers in the upper three-quarters of the fruit had become enlarged, isodiametric vesicular cells. As explained in Chapter Five, section III. Discussion - 7, the small diameter of the outer mesocarp cells likely allowed them to resist the accumulating pressures in the fruit so that they could differentiate into the vesicular cells. The ontogeny, cytochemistry, and functions of the viscin tissue are described fully in Chapter Five.

10E. The exocarp

From its inception, the exocarp of *Arceuthobium americanum* was visibly partitioned into an outer exocarp and an inner exocarp (Figure 4.55). Cells of the outer exocarp had thickened walls (especially in regions proximal to the pedicel), whereas cells of the inner exocarp had relatively thinner walls: thus, the two regions likely had different roles. The fruit of *Arceuthobium* species is generally believed to have a visible but thin outer hydrophobic cuticle (Bhandari and Nanda, 1968a; Fisher, 1983); the presence of this thin cuticle may have contributed to the leathery appearance described for the Viscaceous fruit exterior (Bhandari and Vohra, 1983). However, as the cuticle on the *Arceuthobium* fruit is rather thin, the fruit has been postulated to permit a large surface area for evaporation (Fisher, 1983). Yet, hydrophobic materials might not have merely existed on the surface of the fruit as a cuticle proper (Mauseth, 1988). The thickened nature of the outer exocarp cell

walls and their tendency to react positively with Sudan Black B (SBB), particularly in regions proximal to the pedicel (not shown), implied that hydrophobic materials might have also existed throughout the outer exocarp cell walls in a fashion typically described for suberized walls (Mauseth, 1988). The suberized nature of the outer exocarp likely restricted water loss, which in turn permitted the viscin cell mucilage to retain water necessary for explosive discharge, and permitted the embryo and endosperm to remain hydrated.

In contrast, the thinner, SBB-negative inner exocarp cell walls of the *Arceuthobium americanum* fruit likely facilitated apoplastic movement of water and other materials. Apoplastic movement of water and other materials throughout the inner exocarp was particularly likely, as the vascular tissues were found in this region. Even when vacuoles of inner exocarp cells immediately adjacent to the mesocarp/vesicular cells became filled with hydrophobic tannins, apoplastic movement of water away from its vascular source would likely not be greatly impeded. Gross and Koch (1991) found that the apoplastic water content and apoplastic water movement away from a vascular source did not change significantly when tannin-like materials accumulated in the vacuoles of cells in the shoots of Norway spruce. However, when the inner exocarp cells of *A. americanum* became tannin-filled, water entering the inner exocarp apoplast via the vascular tissues could likely not enter the symplast or vacuoles of inner exocarp cells (see part 10C of this discussion as well as Gross and Koch, 1991; Algan and Buyukkartal, 2000). Similarly, water entering the apoplast of the inner exocarp of *A. americanum* via the vascular tissues could likely not readily enter the region of the suberized outer exocarp cells (particularly in regions proximal to the pedicel). Thus, most water entering the thin-walled region of the inner exocarp cells in a nearly mature *A. americanum* fruit via the vascular tissues would likely be directed apoplastically to the viscin cells and possibly to the embryo and endosperm. Moreover, when tannin-like materials accumulated in the inner exocarp, water would likely be conserved in the viscin cell mucilage as well as possibly the embryo and endosperm, since symplastic and transvacuolar water movement through the inner exocarp cells would be impeded due to the presence of the tannin-filled vacuoles. In order to elicit a transpiration pull, some water entering the inner exocarp via the vascular tissues was likely able to exit the distal regions of the fruit where the cell walls of the outer exocarp were thinner and less

obviously suberized. The fact that stomata only exist in the distal regions of the *Arceuthobium* fruit (Wilson and Calvin, 1996) supported this concept.

The tannin-filled inner exocarp layer also likely acted to provide a counter force to the pressure accumulating in the viscin cell mucilage (this is described further in Chapter Five, section III. Discussion - 10). Notably, the degenerate outer layer of mesocarp described for *Eubrachion* (Bhandari and Indira, 1969) may have actually been a tannin-filled inner exocarp region as seen in *A. americanum.*

10F. The vascular tissue

As in *Arceuthobium minutissimum* (Bhandari and Nanda, 1968a) and *Eubrachion* (Bhandari and Indira, 1969), the mature exocarp of *A. americanum* (specifically the inner exocarp) possessed two vascular traces (Figure 4.73). This number of vascular traces is fairly typical for flowering plants (Mauseth, 1988). Also, as in *A. minutissimum* (Bhandari and Nanda, 1968a) and *Eubrachion* (Bhandari and Indira, 1969), the vascular traces of *A. americanum* first became evident in the young ovarian (carpellary) tissues of the unfertilized female flower (Figure 4.2b and 4.3); this is also typical for flowering plants. The vascular tissue in the *A. americanum* flower/fruit was apparently comprised solely of xylem tissue that consisted of vessel elements and xylem parenchyma; phloem tissue was apparently absent from the vascular tissue (Figures 4.3, 4.73, and 4.74). The absence of phloem from the vascular tissues is not typical for flowering plants. However, the vascular tissues of *Arceuthobium* species frequently lack phloem (usually specifically sieve elements), especially in the haustorial structures (Lamont, 1983; Calvin and Wilson, 1996). Thus, the absence of phloem in the fruit of *A. americanum*, while not specifically detailed elsewhere, was not surprising. Upon a very close inspection, it might be shown that phloem parenchyma and/or phloem fibers existed in the fruit, as these cell types are often found in the stem tissue of *Arceuthobium* species (Wilson and Calvin, 1996). Nonetheless, phloem sieve tube elements were completely lacking in the fruit of *A. americanum*, and thus transport of organics would likely be dependent on the xylem tissue. The notion that xylem vessel elements and the apoplast have the ability to conduct organics in addition to water and mineral nutrients has been supported by many workers (Lamont and Southall, 1983;

Coetzee and Fineran, 1989). Thus, the potential for organics to reach the flower/fruit via xylem tissues was great.

The vessel elements in the xylem tissues of the *Arceuthobium americanum* flower/fruit possessed helical secondary wall thickenings (Figures 4.3 and 4.74). The presence of xylem vessels with helical thickenings was not unusual, as Bhandari and Vohra (1983) noted vessel elements with helical thickenings in several Viscaceous fruits. The helical thickenings would have provided strength to vessel elements under the tension of the transpiration pull (and perhaps under the hygroscopic pull of the viscin cell mucilage in older fruit). Although helical thickenings would have provided strength, the helical thickenings would have also permitted the vessel elements to elongate (become passively stretched) in the growing flower/fruit. Passive elongation of the vessel elements likely occurred even in older fruit, since fruit continued to gradually increase in size until explosive discharge was imminent.

The (helical) cell walls of *Arceuthobium americanum* xylem vessel elements in both young flowers (Figure 4.3) and ripe, mature fruit (Figure 4.73) stained purplish with crystal violet. This implied that the thickenings were not lignified during any stage of development, as lignin treated with osmium tetroxide and TB stains green (Gahan, 1984; Yeung, 1990). As mentioned in part 5A of this discussion, because crystal violet is in the same stain family as TB (Gahan, 1984), lignified walls treated with osmium tetroxide and crystal violet would have also stained greenish (M.J. Sumner, pers. comm., 2002). While it was not too surprising to find differentiating and thus non-lignified vessel elements in young flowers, the presence of non-lignified vessel elements in more mature fruit was somewhat unusual, as vessel elements in typical flowering plants are usually lignified at maturity (Mauseth, 1988). Although the presence of non-lignified vessel elements of ripe, mature *A. americanum* fruit might be attributable to a long vessel differentiation time, it is more likely that the vessel elements remained non-lignified at fruit and vessel maturity, since lignified vessel elements were never observed. The absence of lignin in the vessel elements in ripe, mature *A. americanum* fruit is in agreement with the concept that the vessel elements possibly continued to passively elongate during late stages of fruit development. Lignin would have otherwise made the vessel element cell walls non-plastic and incapable of stretching (Mauseth, 1988). The absence of lignin in the vessel element cell walls of *A. americanum*

fruit might have been attributable to the concept that organics are transported by the vessel elements in mistletoes (Lamont and Southall, 1983; Coetzee and Fineran, 1989). If the vessel elements had become lignified, the lignin could have reduced the apoplastic transport of organic materials out of the vessel elements and into the parenchyma of the fruit (Fineran, 1996). Thus, the absence of lignin in the vessel elements of the *A. americanum* flowers/fruit likely facilitated apoplastic unloading of organics in these regions.

Occasionally, the vessel elements in the flower/fruit of *Arceuthobium americanum* possessed cytoplasm, a single nucleus, and organelles, and were thus viable (Figure 4.74). The fruit containing the vessel element shown in Figure 4.74 was mature, and thus even older fruit possessed vessel elements with cytoplasm and organelles. The presence of cytoplasmic vessel elements was probably directly correlated with the absence of lignin in the vessel cell walls. In typical flowering plants, lignification of the developing vessel elements often directly contributes to the death of the cytoplasm due to isolation of the symplast (Mauseth, 1988). The absence of lignin in the mature vessel elements of *A. americanum* fruit, which was unusual for a flowering plant, likely permitted the cytoplasm of those *A. americanum* vessel elements to remain viable at maturity. Nonetheless, many vessel elements did lack cytoplasm, as would be expected (Figure 4.3).

The absence of lignin and presence of cytoplasm in some mature vessel elements of *A. americanum* flowers/fruit might be related to the fact that phloem sieve elements/tube members were absent from the vascular tissue. As phloem sieve elements/tube members (Mauseth, 1988) as well as assimilate-conducting cells of mosses (Ligrone *et al.*, 2000) are non-lignified and possess cytoplasm (although not a nucleus) at maturity, cytoplasm may be specifically needed for the transport of organics. It is believed that microtubules present in the viable cytoplasm of assimilate-conducting cells in mosses are necessary for the long distance symplastic transport of organics (Ligrone *et al.*, 2000). Similarly, as the xylem tissues of mistletoes, specifically the vessel elements, are believed to transport organics, the cytoplasm of vessel elements in *A. americanum* may have needed to be retained for assimilate transport. In addition, Salisbury and Ross (1992) stated that the symplastic route is more efficient for solute transfer than the apoplastic route. Thus, the presence of cytoplasm in vessel elements may have provided a more effective method of transferring

dissolved assimilates to the flower/fruit than if transport was through the apoplastic dead lumena of typical vessel elements.

The cytoplasmic vessel elements in the flowers/fruit of *Arceuthobium americanum* had characteristics of both tracheary elements and phloem sieve elements/tube members. A potential xylem-phloem hybrid cell type had initially been identified in the haustorium of certain root parasitic Santalaceae (Benson, 1910). However, Fineran *et al.* (1978) determined that this potential hybrid was actually a specialized type of tracheary element that Fineran *et al.* (1978) called a graniferous tracheary element. Wilson and Calvin (1996) showed the presence of what appeared to be graniferous tracheary elements in the fruit of *A. americanum*. Thus, the few osmiophilic bodies present in the cytoplasmic vessels from *A. americanum* fruit in this study (Figure 4.74) might have represented granules similar to those observed by Wilson and Calvin (1996). However, although initially highly cytoplasmic, true graniferous tracheary elements become lignified and dead at maturity (Fineran *et al.*, 1978; Fineran, 1996). Even when true graniferous tracheary elements are in a cytoplasmic stage of development, they are enucleate (Fineran *et al.*, 1978; Fineran, 1996). The cytoplasmic vessel elements seen in the flowers/fruit of *A. americanum* in this study, although possibly granular, were nucleated, living, and non-lignified at maturity. Thus, the cytoplasmic vessel elements that were observed in this study might have represented novel graniferous elements as opposed to strictly defined graniferous tracheary elements. The graniferous tracheary elements observed by Wilson and Calvin (1996) would therefore also potentially represent novel graniferous elements.

Fineran *et al.* (1978) believed that because granules were found in the dead lumena of graniferous tracheary elements, the granules played a structural or supportive role. Although the so-called vessel elements containing putative granules in the *Arceuthobium americanum* fruit were cytoplasmic, the presence of cytoplasm did not rule out a supportive role for the granules. Fineran (1985) also added that the granules observed in graniferous tracheary elements of haustorial regions might have played a role in controlling the flow of sap in those regions. A similar role of cytoplasmic flow control could be postulated for the granules in the cytoplasmic vessel elements of the *A. americanum* fruit, especially considering that the fruit represents the opposite pole of the parasitic transpiration stream, and would likely mirror or possibly control flow rates occurring in the haustorium.

However, granules in graniferous tracheary elements and in cytoplasmic elements of *Arceuthobium* closely resemble phloem sieve P-protein bodies (Salisbury and Ross, 1992 as well as Fineran, 1985). P-proteins play a role in phloem sieve wounding protection (Salisbury and Ross, 1992). If the granules in cytoplasmic vessel elements of the *A. americanum* fruit represented wound-protecting P-proteins, the analogy of these vessel elements to cytoplasm-containing phloem sieve elements would be extended further, and the argument that some of the cytoplasmic vessels had characteristics of phloem would be strengthened.

The potential that some of these so-called cytoplasmic vessel elements in the flowers/fruit of *Arceuthobium americanum* represented flange-type parenchyma (or simply flange) cells (Fineran, 1996) should also be discussed. Flange cells are elongated parenchyma cells possessing an open reticulate pattern of secondary wall thickenings called flanges and a viable, nucleated cytoplasm (Fineran, 1996). These unusual cells have only been reported in a few flowering plants (Fineran, 1998), and in mistletoes, flange cells have only been observed in the haustorial tissues of the mistletoes *Korthalsella* (Fineran 1996, 1998) and *Phoradendron* (Fineran and Calvin, 2000). Although the pattern of the secondary wall thickenings in the so-called cytoplasmic vessel elements in the flowers/fruit of *A. americanum* were typically helical and not reticulate, this does not rule out the possibility that at least some of these cytoplasmic elements were actually flange cells. Likewise, although the presence of granules has not been described for flange cells (Fineran, 1996), their potential presence in the cytoplasmic vessel elements in the *A. americanum* flowers/fruit does not eliminate the possibility that some of the cytoplasmic elements represented flange cells.

However, whereas Fineran (1996) noted the presence of lignin in the flange cell walls of *Korthalsella*, lignin did not exist in the cytoplasmic vessel elements in the flowers/fruit of *Arceuthobium americanum* (Figure 4.73). If some of the cytoplasmic vessels seen in the *A. americanum* fruit were flange cells, the differing observations regarding lignification in the two organisms may either represent an intergeneric difference or a difference between haustorial flange cells and fruit tissue flange cells. The flanges of a flange cell are layered and possess a broad base attached to the primary wall (Fineran, 1996). In contrast, secondary wall thickenings of vessel elements in *Korthalsella* were said

to possess a narrow base supporting a wide distal portion. Using these criteria, it was difficult to state whether the cytoplasmic vessels seen in the *A. americanum* flowers/fruit were flange cells or true vessel elements, because the magnification used to examine *A. americanum* flowers/fruits was too low (Figures 4.3 and 4.74) and the preservation was inadequate (Figure 4.74). The flowers and especially the more mature fruit of *A. americanum* should be examined for the presence of flange cells.

Flange cells in the haustoria of *Korthalsella* (Fineran, 1996) and *Phoradendron* (Fineran and Calvin, 2000) are likely involved in uptake. The cell wall flanges may allow the flange cell to function as a transfer cell by increasing membrane surface area. As the flower/fruit of *A. americanum* would represent a strong sink and also a transport region not unlike a haustorium, flange cells potentially present in the flower/fruit could have been involved in unloading. As Fineran (1996) suggested that the presence of lignin in the flange cells of the *Korthalsella* haustorium might reduce apoplastic transport, the absence of lignin in the possible flange cells of the *A. americanum* fruit might have enhanced apoplastic unloading within the fruit. More work is needed.

However, the presence of cytoplasmic vessel elements (Figure 4.73) as well as typical (non-cytoplasmic) vessel elements (Figure 4.3) in female flowers/fruit of *Arceuthobium americanum* suggests that the flowers/fruit may have a role in controlling the transpiration flow through the parasite and host (Wilson and Calvin, 1996). This role is also likely, considering that the *A. americanum* fruit has numerous stomata.

10G. The mature fruit and use of the "pseudoberry" and "pseudoseed" terminology

Before considering the usage of the words "pseudoberry" and "pseudoseed" in the terminology of *Arceuthobium*, one must consider if the fruit truly is a berry, as stated by Calder (1983). A berry would have an endocarp that is fleshy (Mauseth, 1983), but the endocarp of *A. americanum* could hardly be described as fleshy. Inherent in the definition of a fleshy tissue is the notion that the tissue is moist. The endocarp of *A. americanum*, becoming filled with hydrophobic tannins, could not be moist. Therefore, the fruit of *A. americanum* is likely not a berry. Perhaps the term drupe better describes the *A. americanum* fruit. A drupe is one-seeded, as is the fruit of *A. americanum*. Moreover, the endocarp of a drupe is often adherent to the dehisced seed; similarly, the endocarp of *A.*

americanum is adherent to the dehisced endosperm/embryo. However, the endocarp of a drupe is typically described as being hard (Mauseth, 1988), whereas the endocarp of *A. americanum* is not hard or sclerotic. Nonetheless, the endocarp of *A. americanum* is certainly closer to being hard than it is to being fleshy. Therefore, as the fruit of *A. americanum* is one seeded with an endocarp that is adherent to the endosperm, and as the endocarp is not fleshy, the fruit of *A. americanum* would be better described as a drupe than as a berry. Similarly, the fruit of Santalaceae and Olacaceae are considered (pseudo)drupes (Ram, 1959). The fruit of other Viscaceae, though, may still be better described as berries.

The usage of the term "pseudo" in describing the Viscaceous fruit must be addressed. Calder (1983) called the Viscaceous fruit a pseudoberry because it lacks a seed coat derived from integuments. Likewise, the fruit of *Arceuthobium americanum* could be called a pseudodrupe. The "pseudo" terminology is actually quite useful, for it immediately implies how unique the fruit is. More importantly, calling the fruit of *A. americanum* a "pseudodrupe" is much more concise than calling it a "drupe that lacks a seed coat derived from integuments". Workers involved in parasitic plant research are likely already familiar with the usage of the pseudoberry and pseudodrupe terminology, and thus it makes sense to continue to use this terminology. As the pseudoberry and pseudodrupe terminology is in common usage, it would not be difficult to implement the term "pseudoseed" to describe the dispersal unit of *A. americanum*. This term is also much more concise than describing the embryo and endosperm as "lacking a seed coat derived from integuments but enveloped in two layers of pericarp". As the term "pseudoseed coat" was already illustrated to be the best term to describe the tanniferous endocarp/lower mesocarp (see part 10C of this discussion), it only makes sense for the pseudoseed coat to be a part of a pseudoseed.

Regardless of what the fruit of *Arceuthobium americanum* is called, its ripe, mature structure is extremely well designed for explosive discharge. The role of the vesicular cells, tannin filled inner exocarp, and viscin cells in explosive discharge will be described in Chapter Five, section III. Discussion - 10. However, it will be mentioned that the recurved nature of the pedicel in the ripe fruit probably helped to angle the discharging pseudoseed so that it would not be shot down toward the same host (or the ground) but would instead be shot upward and outward to a new host. The precise differentiation of an abscission layer at the base of the fruit (just below the pseudoseed coat) also helped the pedicel separate from

the fruit so that the pedicel did not obstruct the discharging pseudoseed. As suggested by Gilbert (1988), pseudoseed discharge from a fully ripe fruit was likely triggered by mechanical action of rain and by rising temperatures encountered in the early morning.

11. The Discharged Pseudoseed and Viability

11A. Discharged pseudoseed

Upon explosive discharge, the *Arceuthobium americanum* endosperm changed dimensions (Figure 4.76). As mentioned, this likely occurred as the discharged pseudoseed adjusted to the ambient pressure (see part 8F of this discussion). However, a point to make is that the discharge process must cause some stress to the embryo and endosperm, and could perhaps even limit viability. As effective as explosive discharge is as a dispersal mechanism, it may have detrimental effects as well. Perhaps in order to countervail the detrimental effects of explosive discharge, shoots from a single dwarf mistletoe infection synthesize hundreds of fruit (Hawksworth and Wiens, 1996).

Immediately following explosive discharge, the protoderm of the *Arceuthobium americanum* radicular apex became more vacuolate (Figure 4.76). Perhaps the discharge process triggered the vacuolation of the embryonic protoderm; in turn, a more vacuolate protoderm at the radicular apex might have provided the embryonic radicle the turgor and strength it would need to penetrate the pseudoseed coat and viscin cells during the germination process in the following spring.

The viscin cells of the discharged pseudoseed of *Arceuthobium americanum* were slightly green, indicating the presence of chlorophyll (Figure 4.75). This was verified and will be further discussed in Chapter Five, section III. Discussion - 9. Nonetheless, the possibility that the viscin cells were able to photosynthesize, potentially at germination, again suggested that germination requires a large energy input. The presence of chlorophyll in the embryo and endosperm as well as the potential role of this chlorophyll in germination has already been described in parts 8E and 9F of this discussion.

Regarding germination in *Arceuthobium americanum*, light might not have been a strong cue for germination, as tannins in the pseudoseed coat would likely have blocked most light from reaching the embryo. Similarly, moisture or humidity might not have been a strong cue for germination, as the tannins in the pseudoseed coat are hydrophobic (Gahan,

1984). Thus, temperature is very likely the cue for germination in *A. americanum* (Gilbert, 1988). Germination likely takes place as quickly as physically possible in order to avoid possible ultraviolet light damage to the uncovered embryo and endosperm. The negative phototropic response of the germinating *A. americanum* radicle may represent a mechanism of light evasion so that damage to the radicle from ultraviolet radiation might be avoided.

11B. Viability

Embryo

The embryos of discharged pseudoseeds of *Arceuthobium americanum* collected in August, September, and October were examined for viability with 2, 3, 5-TTC. The percentage of red-stained embryos was used to indicate germination potential (Scharpf and Parmeter, 1962). The germination potential did not change significantly over the three collection periods (see section II. Results - 22C of this chapter), and the average viability/germination potential (58%) was encompassed in the general range determined with 2, 3, 5-TTC by Scharpf and Parmeter (1962), Robinson (1995), and Jerome (2001). However, whereas the viability of pseudoseeds brought into storage by these authors invariably declined (regardless of the storage temperature), the viability of pseudoseeds left in the field during the fall for this study was constant. Perhaps to best preserve *Arceuthobium* pseudoseeds in storage for longer periods, fall day/night temperature cycling as opposed to constant temperatures should be used for storage conditions. Additionally, because the pseudoseed coat likely impedes light transmission, light is likely not necessary for maintaining viability; moreover, the fact that the pseudoseeds were wrapped in cheesecloth probably did not affect viability (admittedly, other cheesecloth factors are unknown). Different species and different hosts may have effects on pseudoseed viability, so one must be careful in comparing viability among different *Arceuthobium* species on different hosts, as Jerome (2001) indicated. Although germination was not specifically examined in this thesis, actual germination rates of *Arceuthobium* pseudoseeds that have been stored (at fall day/night temperatures) could possibly be improved with a cold treatment (C.A. Jerome, pers. comm., 2001).

Other pseudoseed components

Absent from the studies of pseudoseed viability in *Arceuthobium* were references to the viability of other pseudoseed components stained with 2, 3, 5-TTC. Notably, the endosperm in the vicinity of the embryo of *A. americanum* stained red, as did the viscin cells (Figure 4.77). Moreover, these observations of red staining did not change over time. Thus, workers wishing to determine the germination potential of embryos should probably not ignore the viability of these other components. The endosperm in the vicinity of the embryo likely maintained viability throughout the fall (and winter) so that transport into the embryo could be rapidly resumed during germination in the following spring. While the lower part of the endosperm did not show a positive reaction for viability, the lower endosperm probably merely possessed a low metabolic rate. The entire endosperm would very likely increase its metabolic rate in the spring of germination in order to begin photosynthesizing as well as in order to mobilize reserves for the germinating embryo.

The slight red staining of the viscin cells implied that some viscin cell component was viable (Figure 4.77). Thus, the viscin cells may have had other important roles following discharge and potentially even during the spring of germination (more detail in Chapter Five, Section III. Discussion - 8C). Finally, although not specifically noted for a discharged pseudoseed, the cap cells in the mature, ripe fruit of *A. americanum* also stained red, even when the cap cells had been compressed. This too implied that the cap cells, even when they became compressed, likely maintained viability following explosive discharge, and may be important in germination. Viability of the cap and potential cap roles are discussed further in Chapter Six, IV. Discussion - 4B).

12. Conclusions

The present study was undertaken in order to outline reproductive development in the female flowers/fruit of *Arceuthobium americanum*. Therefore, the four major objectives outlined at the beginning of this chapter have been accomplished. Firstly, reproductive events in the female flowers/fruit were described in detail using modern ultrastructural and cytochemical techniques, and some of the reproductive events were found to be unique with regard to the flowering plants. Many of the unique features of reproductive development were likely related to the parasitic habit. The reduction of nucellar tissues, possible

competition between embryo sacs, and reduction of embryos allowed less energy to be put toward the processes of fertilization and embryogenesis. However, the accumulation of large and varied nutrient stores in both the embryo and endosperm along with the potential for these tissues (and perhaps the viscin cells) to photosynthesize indicated that energy was instead being allocated to the germination process.

Secondly, many of the controversies regarding development in *Arceuthobium* were resolved. A major factor contributing to the controversies was a lack of clarification to the general polarity and organization of the reproductive structures. Moreover, the role that the embryo sac caecum played in the reorientation of embryo sac growth was not realized in earlier studies. Notably, the functioning of the caecum in the reorientation of embryo sac growth has not previously been recorded for flowering plants.

Thirdly, the term placental-nucellar complex (PNC) was coined in order to describe the ovular structure of *Arceuthobium*. This term is better suited to describing the ovular structure of *Arceuthobium* than other terms used previously, such as "mamelon" and "papilla": whereas the older terms merely described the shape of the ovular structure, the new term "PNC" describes the tissue composition of the ovular structure. Similarly, the term "pseudoberry" was realized as an acceptable term, with the stipulation that the fruit in *Arceuthobium* was more likely a pseudodrupe than a pseudoberry. Likewise, the terms pseudoseed and pseudoseed coat were created in order to accurately characterize the appearance as well as the function of the *Arceuthobium* dispersal unit and its fruit-derived, tanniferous coat through which germination occurs. Viability of the dispersed pseudoseed was examined and it was determined that viability easily persisted in the field. Moreover, it was concluded that the scoring of pseudoseed viability should encompass not only the viability of the embryo, but also the viability of other pseudoseed components.

Finally, relationships among the various families of the Santalales, between *Arceuthobium* and its host, and between *Arceuthobium* and other flowering plants were explored. By compiling and categorizing ovular characteristics of the Santalales that have been described in the literature and ovular characteristics of *Arceuthobium* that were elucidated in this thesis, major phylogenetic trends in the order were exposed. One major phylogenetic trend showed that *Arceuthobium* arose via a common ancestor to the

Santalaceae (likely a common ancestor to the tribe Santaleae). Furthermore, areas for phylogenetic reinvestigation were highlighted.

The relationship between the parasite and the host was shown to be synchronized in many respects. The synchrony not only represented a result of shared translocated materials, but also likely represented the many thousands of years of co-evolution between the two organisms. Other researchers are beginning to examine the phenomena of co-evolution. Finally, the many comparisons and references made between *Arceuthobium* and typical flowering plants will hopefully be useful to any worker pursuing studies regarding reproductive development in any flowering plant.